Introduction to Radar Target Recognition

P. Tait

Introduction to Radar Target Recognition

Other volumes in this series:

Introduction to Radar Target Recognition

P. Tait

Contents

5   Frequency and time domain analysis   **183**

6   Other high-resolution techniques   **221**

Foreword

One of the most serious problems in today's military capability is the lack of rapid and reliable identification of objects in the battle space. Developments in cooperative identification techniques, such as improved identification of friend or foe (IFF) systems for air targets, may greatly increase the probability of correct identification of a friend. Such systems, however, will never be able to positively identify non-aligned or hostile targets. This results in reduced mission effectiveness – even worse, a friendly target that fails to cooperate could easily be regarded as hostile. This may lead to fratricide, the tragic killing of one's own forces. Public opinion has, rightly so, become ever more reluctant to accept such human losses. Therefore, there is an urgent need to extend military capability with options for quick and accurate target recognition at long ranges, whatever the target's allegiance.

In the civil world, demand for non-cooperative target recognition is expanding as well, in particular in the defence against terrorism where hijackers may tamper with cooperative systems on aircraft or ships.

There is no single solution to fulfil these needs. Radar, however, is one of the primary contributors to this capability. Radar has already proven to be the tool of choice for the detection and tracking of targets since the Second World War. For several decades the use of radar for target recognition has been coming onto the horizon, mainly due to the development of microwave components and the ever-increasing speed of computer processing. Indeed, radar is emerging as an outstanding tool for the acquisition of signatures for recognition at very long range, and in all-weather and night and day circumstances.

For these reasons, Peter Tait's outstanding book is of high value – and timely.

The volume covers the entire spectrum of target recognition using radar. Laying the foundation of radar technology – including high-resolution and signal modulation techniques – the book discusses radar system topics, operational issues and the actual recognition process. It also deals with the important topic of the fusion of radar target recognition results with other sources of information.

The applications of radar target recognition cover a tremendous scope, too. Military uses range from airborne, naval and land-based systems and include missile defence. Civil applications deal with the detection of buried landmines, and the defence against terrorism. All techniques are carefully weighed to expose their

relative advantages and disadvantages. This truly is the most complete work available on the subject.

Peter Tait uses his long experience in the field to strike a fine balance between the book's pedagogical purpose and its presentation of current research. This also makes the book accessible at different levels, for both engineering and non-engineering readers.

The quality of this book will ensure that its goal – improving the knowledge of target recognition with radar – will be achieved. This will no doubt stimulate further research and development, contribute to better and more effective radar systems and, ultimately, a safer world.

Dr René van der Heiden
NATO Consultation Command and Control Agency

List of acronyms

ADC	Analogue to digital converter
ATR	Automatic target recognition
AWACS	Airborne warning and control system
BMEWS	Ballistic missile early warning system
BVRAAM	Beyond visual range air-to-air missile
CFAR	Constant false alarm rate
CW	Continuous wave
DAC	Digital to analogue converter
dB	Decibel
dBc	Power level (in dB) below carrier frequency
DSP	Digital signal processor
FDTD	Finite difference time domain
FM	Frequency modulation
FPGA	Field programmable gate arrays
GHz	Giga hertz
GMTI	Ground moving target indication
HERM	Helicopter engine rotor modulation
HF	High frequency
HRRP	High-resolution range profile
HPD	High-power discriminator
I	In-phase
IF	Intermediate frequency
IFF	Identification of friend or foe
INS	Inertial navigation system
ipp	Inter pulse period
ISAR	Inverse synthetic aperture radar
JEM	Jet engine modulation
LFM	Linear frequency modulation
LNA	Low noise amplifier
LO	Local oscillator
MHz	Mega hertz

MFR	Multi-function radar
NCTR	Non-cooperative target recognition
NF	Noise figure
PC	Personal computer
prf	Pulse repetition frequency
Q	Quadrature
rcs	Radar cross-section
RF	Radio frequency
rpm	Revolutions per minute
SAR	Synthetic aperture radar
SSR	Secondary surveillance radar
STALO	Stable local oscillator
TDU	Time delay unit
TRM	Transmit/receive module
TWTA	Travelling wave tube amplifier
VCO	Voltage controlled oscillator

Preface

Radar is becoming a progressively more sophisticated sensor. It is evolving from a system which detects and tracks targets, to one providing imaging and recognition capabilities. At present, the techniques being developed have not been widely disseminated beyond the laboratories of the radar specialists working in their specific fields. This book has been written to provide an introduction to radar target recognition for the non-specialists, who will have future needs to understand the topic in the course of their professional work, and for the general reader, who has an interest in technical topics.

No prior knowledge of radar has been assumed and a tutorial on radar is included. The techniques used for recognising ground, naval, airborne and ballistic missile targets are presented. These include high-resolution range profiling, SAR, ISAR, JEM, helicopter blade flash and HERM. The operational needs for the development of radar target recognition functions for both military and civil systems are discussed. The issues associated with the radar system and component designs needed to support target recognition and the integration of these new functions with conventional radar modes are presented. Radar systems using dish antennas and phased arrays are covered. The techniques used for the assembly of databases of target signature characteristics are discussed. Classification methods used for recognising targets from the measured radar data and from other available information are presented.

The target recognition techniques are derived from first principles and relatively simple explanations are provided, which are aimed to inform the reader of the essence of the techniques, without the need to understand complex mathematics. For those wishing to develop a deeper knowledge of target recognition, references are provided for further reading. Books are available that cover some of the topics in depth, and other topics are accessible in specialist technical papers.

Acknowledgements

Chapter 1

Introduction

1.1 Background to radar

Radar was first patented in Germany in 1904 by Christian Hülsmeyer [1,2], following pioneering work by James Clerk Maxwell on electromagnetic theory [3,4] in the United Kingdom and by Heinrich Hertz in Germany. Radar has been technically refined continuously, as new innovations have been practically proven, developed and integrated into operational systems. Developments from radar's beginning to advanced techniques are summarised in References 5–8. Fundamentally, a radar system sends out pulses of electromagnetic energy, which travel almost unimpeded through the air or space until they encounter an object in their path. The interaction with the object involves some of the energy being reflected from the object, some being absorbed by the object and some being transmitted through the object. The proportion of the incident energy that is reflected is dependent on the wavelength of the radar signal and the size, shape and material composition of the object. The reflected energy can potentially go in any direction, so the energy reflected back to the radar is very small and is detected using a specially designed receiver. Objects of interest, such as aircraft, are called targets, and objects, which can potentially get confused with targets such as reflections from the ground, buildings or the sea, are called 'clutter'. Great efforts are made by radar designers to filter out clutter returns from those of targets.

Technology has become available that can detect targets on the land, on the sea, in the air and outside the earth's atmosphere. These include aircraft, land vehicles, ships, air breathing and ballistic missiles, all of which are the main points of interest for the topic of this book, radar target recognition. Radar has also been used to detect targets ranging from buried ordnance [9], to weather systems [10], to being the cruise control and collision avoidance sensor in luxury cars [11], to measure the distances and rotational speeds of our planetary neighbours in the solar system [12]. Although these applications are not specifically addressed in this book, many of the techniques and technologies needed for military target recognition are based on those employed in this wide range of radar applications.

As the technology has developed, smaller targets have been able to be detected with progressively more reliability at longer ranges. Hardware and algorithmic techniques have been developed, which enable targets to be detected and tracked in the presence of ground, sea and weather clutter and jamming [13]. Continuous advances have been made in the field of semi-conductor technology, allowing the development of progressively higher performance solid-state microwave components and high-speed low-cost computers. The availability of more and cheaper computing power progressively enables more targets to be reliably and simultaneously tracked in more difficult environments.

1.2   Typical radar functions

Until relatively recently, radar has been used primarily as a sensor to detect and track targets, as only limited information has been available to be extracted from the radar signal reflected back from the target. A 'blip' or 'plot' was conventionally obtained and displayed representing a radar reflection from the target. It lacked resolution on target features and could not be called a target signature by any standards. For example, the Martello radar, which was in production in the 1990s, was typical of the general class of long-range air defence surveillance radars, and is shown in Figure 1.1.

This type of radar would have the ability to detect and track airborne targets in the range of several hundreds of kilometres. Typical advertised performance parameters for this class of radar are shown in Table 1.1.

The range resolution specified for these systems was normally several tens of metres, which was in excess of the target dimensions, so clearly there was no specified high-resolution mode capability for the standard production models of
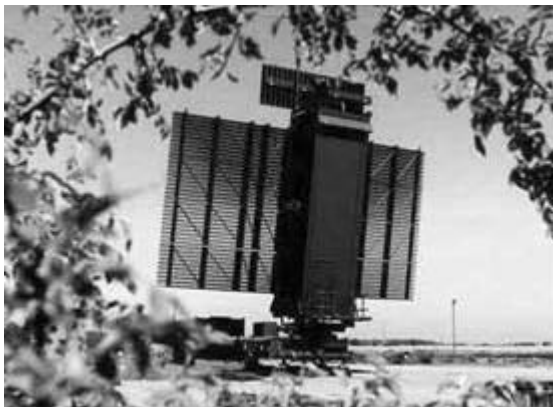
Figure 1.1   *Martello long-range surveillance radar (Courtesy of BAE Systems Integrated System Technologies Ltd)*

Table 1.1 *Typical long-range air defence radar performance specification*

Instrumented range	470 km
Operating frequency bands	1–2 GHz
Scanning period	10 s
Altitude coverage	Horizon to 100000 ft
Range resolution	150 m
Range accuracy	30 m
Azimuth accuracy	0.2 degrees
Height accuracy	1500 ft

this generation of air defence radars. More modern radars of this general class are the Raytheon Thales Master [14] and the BAE Systems Integrated System Technologies Ltd (Insyte) AR327 [15] radars. Details on how radars measure various parameters associated with the target are discussed in Chapter 2 and are also covered in Reference 16, so will only be summarised in this chapter.

Radars of this type were traditionally able to measure the range to and the velocity of the target. Its position in azimuth and elevation could also be measured, so that its altitude could then be estimated. From the strength of the signal reflected from the target, an estimate could be made of its radar cross-section, which provided a rough measure of its size. However, these parameters which had been measured and estimated only gave a rough assessment of the possible general category of the class of target and made little contribution for providing a more detailed assessment of the actual target type. From this relatively low-resolution primary surveillance radar data alone, an assessment of whether it was likely to be a friend, foe or neutral could not be reliably made. (The use of secondary surveillance radar (SSR) data is discussed later in this chapter.)

1.3   The need for target recognition

1.3.1   *Target recognition definitions*

Before discussing target recognition, some of the terms used are discussed. Various words are used for classifying targets from measured radar data. Target recognition, classification, categorisation and identification tend to be used fairly loosely and often interchangeably, with no universally agreed definition. Different defence agencies, universities, defence contractors and also individuals mean different things when they use these terms. For the purposes of this book, target classification and categorisation mean isolating the target to a general class. For example, missiles, fixed wing or rotary wing aircraft would be three general categories of air targets. Other categories could be military or civil aircraft, or manned or unmanned aircraft, friend, foe or neutral, threatening or non-threatening. Other levels of categorisation could be

supersonic or sub-sonic missile, helicopter, fighter aircraft, military transport, civil airliner or light aircraft. Hence, when the terms target categorisation and classification are used, supporting statements are needed to define the actual type of classification that is meant. Target identification is used here to define the target in more precise terms. If a target can be identified as an F-16 with reasonable confidence, this would be target identification. If a target could be identified as possibly being a Tornado, MIG-29 or F-15, this would be considered to be very precise classification, but not full identification. Target recognition is used here to encompass all of the above levels of recognising targets and covers target classification and target identification. The words 'Non-Cooperative Target Recognition' (NCTR) cover the techniques and technologies that provide high-resolution target signatures and use them to make some decisions about the type of target that has been detected. Clearly, this function is performed with no cooperation from the target concerned and it may even not be aware that its signature is being measured for recognition purposes.

The phrase 'Raid Assessment' should also be included with the definitions, as it is used to mean the counting of the number of military targets clustered together. In particular it is employed in air-to-air and air defence applications for the assessment of the number of threatening aircraft that would be grouped together in a raid. Clearly, it is necessary to know how many targets are being engaged, so as to provide an appropriate and effective response. A raid assessment function could be considered as an intermediate radar function with higher resolution than traditional radar modes, which is sufficient to isolate the individual targets, but less precise than that needed for obtaining high-resolution signature data for the recognition functions described in the previous paragraph.

1.3.2   Current and future military requirements

Future military combat systems will have requirements for their sensor systems to identify threatening targets with high reliability beyond visual ranges in order to perform to their full potential and to achieve high levels of operational effectiveness. On 9 April 2002 Rear Admiral Philip Balisle, the US Director of the Navy Surface Warfare Division, made a statement to the Seapower Sub-committee of the Senate Armed Surface Committee on surface weapon systems [17]. He said that the multi-function radar (MFR) for the fleet must detect hostile aircraft and missiles before they can be engaged with the weapon systems. Among its functions will be to conduct automatic detection, identification and tracking of targets. It will also provide NCTR and kill assessment capabilities. The Rear Admiral was making a very strong statement that the radar was a key sensor to support the protection of the US fleet and that radar NCTR was now of a high priority.

Missiles are now being developed with ranges well beyond visual identification ranges, to provide a performance edge against potential adversaries. In air-to-air combat, for example, it is clearly a major advantage to have longer range missiles than the adversarial aircraft. An example is the beyond visual range air-to-air missile (BVRAAM) [18] developed for the Typhoon aircraft, as shown in Figure 1.2.

Figure 1.2   Beyond visual range air-to-air missile developed for Typhoon aircraft (Courtesy MBDA)

The identification of threatening adversaries beyond visual range will be necessary to utilise the full benefit of the missile's range. Currently, the rules of engagement of many armed forces are such that positive visual identification is required, prior to launching a missile, until reliable non-visual target recognition technology becomes available.

The Brimstone missile developed for the UK's Royal Air Force can detect, identify and destroy targets at a range of many kilometres. A millimetric wave radar seeker provides the NCTR function of ground targets [19].

Long-range target identification functions are considered to be essential for future combat defence systems. In future conflicts, there are expected to be a combination of friendly, hostile and neutral targets. These could be land, naval or air vehicles, with a mix of civil and military targets, so target recognition functions will have to be effective in different environments with a significant variety of targets.

From the military viewpoint, it is absolutely essential to minimise, or preferably to eliminate, fratricide, also known as blue on blue engagements or friendly fire incidents, in which allies attack their own forces by mistake. It is also politically extremely difficult to sustain blue on blue casualties without public morale being damaged and pressure being exerted on the government to withdraw from the conflict. This is particularly true with the 'CNN effect', whereby the media rapidly report any incidents. These events also sap the morale of the combatants and degrade operational

Figure 1.3   An Airbus 300. A similar aircraft was shot down by USS Vincennes in 1988 (Photograph courtesy of Airbus)

effectiveness. Historically, in human conflicts there have consistently been significant numbers of casualties arising from friendly fire and a very conservative figure would be about ten per cent of all battlefield casualties up to recent times [20].

1.3.3   Tragic incidents

In order to illustrate the results of military systems operating without an effective target recognition capability, a few examples from recent history are now provided of incidents in which civil and friendly targets were engaged with tragic consequences.

On 1 September 1983, a Korean Airlines Boeing 747, flight KAL 007 flying from Anchorage, Alaska to Seoul, South Korea, was shot down by a Soviet missile and all on-board perished. There have been suggestions that it had been confused with a US military aircraft operating in the area.

On 3 July 1988, an Iranian Airlines Airbus A-300, flight IR655, en route from Bandar Abbas in Iran to Dubai was shot down by two missiles launched from the USS Vincennes, which was on patrol in the Persian Gulf. All 290 passengers and crew were killed. This tragedy is commemorated in Iran every year on the anniversary, and it is clearly an event that the Iranians will not forget for many years. It has even been speculated that the Pan Am jet destroyed over Lockerbie in Scotland in 1988 was in retaliation for the shooting down of the Iranian Airbus.

In the 1991 Gulf War, of the 148 US fatalities, 35 were caused by friendly fire. Of the 16 British killed, 9 were caused by the allies. On 5 October 2001, a Russian Sibir Tu-154 Airliner flying from Israel to Russia was thought to have been shot down by a missile fired by Ukrainian troops in a military exercise. All on-board perished. In both the 2002 war in Afghanistan and the 2003 Iraq war there were several incidents of ground troops being killed by friendly fire from the air. In the latter conflict a UK Tornado aircraft was shot down by a Patriot missile, apparently being mistaken for a Scud ballistic missile. In another incident a US F-16 fighter jet reportedly fired on an allied Patriot missile battery after the Patriot's fire control radar mistakenly locked on to the plane [21]. The jet fired a high-speed anti-radiation missile which damaged the battery's radar before it could launch a missile. In the same conflict two British

Figure 1.4   Challenger tank. In 2003 Iraq war two UK Challenger tanks engaged each other in combat, with tragic consequences (Photograph courtesy of UK MoD)

soldiers were killed apparently in an exchange of fire between two British Challenger tanks (Figure 1.4).

If an effective target recognition capability had been operating many of these events may well have never occurred. It can be seen that apart from the terrible effects to all those concerned in these tragedies, there can be long-term political, diplomatic and international implications for the various countries involved.

1.3.4   Other military and civil considerations

Besides not engaging an unidentified target too rapidly, it is equally essential to minimise the number of hostile targets penetrating defences. It is necessary for the early detection and identification of the threat and to then counter it with appropriate means, to prevent its infiltration through the defences, to prevent casualties being sustained and damage to assets. Unconventional approaches from the adversary would also be expected, so the ability to detect and identify potential threats in order to maintain situational awareness is essential. Other recent developments to be considered include terrorism and associated asymmetric warfare. The use of decoys and the disguising of targets by various physical and electronic means also have to be addressed. A hostile target could be masquerading as benign but with lethal intentions.

Also in the military field, target recognition will be required to improve the assessment of potential threats, particularly to positively identify a foe. It also will be needed to provide a major contribution to situational awareness and control of the battle area. There will be requirements to provide an accurate and up-to-date local air picture. Effective target recognition over a wide range of military targets and large area will contribute to information superiority over potential and actual adversaries. The early identification of a threat provides more time to react. It enables the defence to take appropriate defensive action, which can involve the use of the optimum weapon systems, countermeasures or evasive action. If the threat can be precisely classified to its actual target type, such as a particular type of fighter or missile, the optimum weapon can be allocated to maximise the chance of its destruction. Also if the threat is a light aircraft, for example, the use of cannon fire may be sufficient to neutralise the threat rather than using expensive missiles, which may be limited in supply.

Another associated issue is that of kill assessment and debris characterisation. If an engagement of, for example, a close in weapons system has taken place by launching a missile against a threatening air target, it is necessary to know whether the engagement was successful and whether further launches of missiles would be required. A high-resolution sensor would be needed to measure the characteristics of any engagement debris and to assess whether the target or its remnants still posed a threat.

Although the military requirements will be the driver for the development of the target recognition technology, civil systems will also be able to benefit. For policing the entry of illegal immigrants, smugglers or terrorists into a country by land or sea, the availability of a reliable target recognition capability in coastal surveillance and air traffic control systems would enhance these systems and provide more information to enable the appropriate response to be made.

1.4   Non-cooperative target recognition

1.4.1   Identification of friend or foe systems

From the above considerations it is clear that a target recognition capability is required. There are operational SSR that both civil and military airspace control authorities use and IFF used by the military. Modern IFF is a cooperative two-channel system, with one frequency used for the interrogating signals and another for the response. Modes of operation exist for both civil and military aircraft use and for military aircraft exclusively [22,23]. However, there are weaknesses in the IFF system in conflict environments. IFF systems can fail, can be jammed, can be damaged in combat or can be turned off. The latter would occur in the case of operations being conducted under conditions of radio silence, which are required in certain military situations such as when going into combat or during covert operations with special forces involved. Military codes can be broken or compromised by espionage.

In the age of unconventional tactics, terrorists or adversaries could incorporate civil aircraft IFF transponders on missiles or combat aircraft and masquerade as passenger airliners in civil airlanes. Although IFF can make a good contribution to target recognition, it is clearly not infallible, from the tragic examples presented above, and other sensors are required to provide higher levels of confidence of the target identity.

1.4.2   Radar for NCTR

Radar is the key sensor for the provision of a NCTR function and other tasks such as kill assessment. It is long range, it propagates to and is reflected from the target at the speed of light, which is almost instantaneous, it has no dependence on target emissions and it has an all weather capability, which includes rain, fog, mist and cloud. It can operate in the day or night, in any season and in the presence of smoke. No other sensors can fulfil these requirements for surface and air-based sensor platforms. Sensors operating in the infrared and optical parts of the electromagnetic spectrum degrade in poor weather conditions and generally have a significantly shorter range than radar. Electronic warfare and electronic support measure systems rely on the emissions from the target for locating and possibly identifying it. Acoustical systems are limited by the speed of sound, which is about 330 m/s, so are only considered for very short-range applications.

Although radar is the key sensor for providing the NCTR function, any other information available from cooperative or non-cooperative active or passive sensing techniques should also be utilised to establish the target's identity. This topic is covered in Chapter 13, which addresses the combining or high-resolution radar signature data with other data.

Examples of radars with high-resolution target recognition modes are the Captor for the Typhoon aircraft (formerly Eurofighter) [24], shown in Figure 1.5, and the AN/APG-77 radar for the United States F-22 Raptor aircraft [25].

1.5   Radar target recognition applications

1.5.1   Airborne military platforms

The various applications for an operational NCTR capability are now discussed. As we have seen earlier, fighter aircraft will need a NCTR technology incorporated in the fire control radar for air-to-air engagements. This sensor is normally housed in the nose of the aircraft. Radars installed in fighters have previously been used to detect and track airborne targets in both look up and look down modes. Fighter aircraft with air-to-surface modes will need to engage land targets in combat, such as tanks and armoured military vehicles, so these will be required to be detected and recognised. NCTR capabilities will also be required for engaging naval targets. Combat aircraft, which will be required to cover all these types of missions, will need multi-mode radar functions for supporting detection, tracking and NCTR.
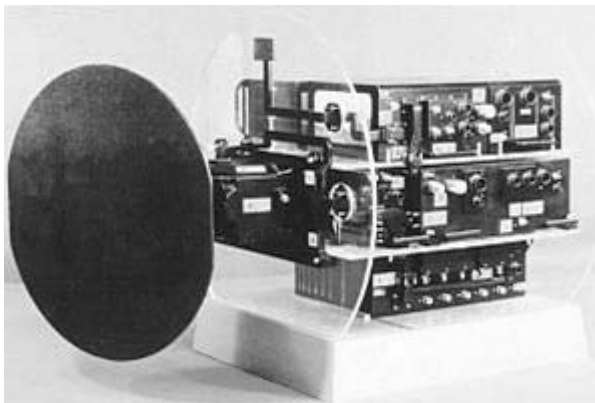
Figure 1.5   Captor radar for Typhoon aircraft, which utilises high-resolution air-to-air combat modes (Courtesy of Selex Sensors Ltd)

Missiles carried on aircraft are expected to have a target recognition capability for situations in which the missile is directed or cued towards the required target, but which may need to be selected from neighbouring non-hostile, civil or neutral targets. The missile sensor is often a small radar housed in the nose cone, so a NCTR function should be included. For air-to-air engagements the missile would need to acquire and recognise the target assigned to it by the fire control radar. In addition, in order to optimise the lethality probability when the missile strikes the target, it may be necessary for the radar to actually image the target to hit the vulnerable 'soft spot'. For air-to-surface missiles the ability to recognise land and naval targets and to distinguish them from non-threatening civil targets and background 'clutter' is clearly important.

Airborne early warning radar systems, such as the US AWACS [26] (Airborne Warning and Control System) E-3 Sentry aircraft and the Swedish Erieye [27] system for patrolling over the land and sea, are expected to employ aircraft target recognition techniques in their radars. The US carrier-based E-2C Hawkeye aircraft [28] provides airborne surveillance for the carrier battle group is stated to have a radar target recognition capability [29].

An example of an air-to-surface surveillance radar system is that incorporated in the US E-8C JSTARS aircraft [30]. The Federation of American Scientists state that 'Joint STARS Automatic Target Recognition (ATR) provides Joint STARS operators with automated surface target recognition/identification using radar data'. In the UK, the Astor platform [31] would be expected to have an air-to-surface target recognition capability. High-resolution radar imaging modes that utilise synthetic aperture and inverse synthetic aperture techniques would be employed for recognising features on the ground and for imaging land vehicles and ships for targeting.

Maritime surveillance systems include the UK Sea King [32] helicopter with its Searchwater radar. This would be expected to have high-resolution modes for the detection and recognition of different types of ships and small boats. This function is

Figure 1.6   Seawolf weapons system. This type of close-in weapons system is expected to have future requirements for its sensors to support target recognition functions (Courtesy of UK MoD)

performed for the US by the Lockheed Martin Aeronautics P3-C Orion [33] and this reference states that it has a 'special imaging radar'.

1.5.2   Naval military platforms

Close in weapons systems, such as the Seawolf missile system [34], shown in Figure 1.6, used by the UK's Royal Navy, are expected to employ a target recognition function to enable threatening targets to be identified before missiles are launched.

Long-range naval air surveillance is provided by systems such as the BAE Systems Insyte/Thales S1850M Long-Range Radar [35], the US Aegis radar [36], the French M3R [37] and the UK's Sampson [38] phased array radars. The integration of high-resolution target recognition modes to support the surveillance and tracking functions of these types of systems would clearly be beneficial in peacekeeping operations and in times of combat.

On the US Navy's Aegis class cruisers the AN/UPX-34(V) radar track discrimination system provides target identification of the SPY-1 radar tracks of air-borne targets. The target of interest is illuminated by the ship's fire control radar and

the reflected radar returns are processed to provide a list of candidate aircraft [39]. Israel is also developing an E/F band active array MFR for air defence applications, which includes a target classification capability. The system is being designed to be installed in ships as small as corvettes [40].

Future navies operating from the deep sea to littoral environments, in support of amphibious landings for example, will need recognition capabilities for a wide range of military and civil targets. Ships from the sizes of large naval vessels to small patrol boats and rubber inflatable boats could be encountered. Civil and military aircraft, missiles and land vehicles would also need be to detected and recognised in various scenarios.

1.5.3 Land-based military platforms

As discussed earlier, long-range air defence radars will need target recognition capabilities. They cover hundreds of thousands of square kilometres of air space and provide early detection of aircraft and missiles. It is expected that future generations of long-range air surveillance radars, such as the BAE Systems Insyte Commander [41], would include target recognition capabilities.

For the shorter range air defence missile systems, such as the UK Rapier missile system [42], which employs both a surveillance radar [43] and a tracker radar, as shown in Figure 1.7 [44], the incorporation of target recognition functions is expected to provide final confirmation of the target's identity, to avoid friendly fire incidents or engaging civil targets.

Military land vehicles would also be expected to incorporate a target recognition capability to avoid friendly fire incidents. Radar systems would provide benefits in supplying this function when optical or thermal sensing systems' performance is impaired in situations of poor visibility.

Figure 1.7   Blindfire tracker radar used with the Rapier Missile System. Future radars of this type are expected to incorporate target recognition functions (Courtesy of BAE Systems Integrated System Technologies Ltd)

1.5.4   Civil applications

For civil and homeland defence agencies in the age of terrorist threats, it is likely that coastal surveillance radar systems and civil air traffic control systems will need NCTR capabilities against ships and aircraft targets, to supplement the existing cooperative target recognition systems. The ability to make good estimates of the type or class of aircraft or ship that has been detected can provide confirmation of whether it is the expected target, or whether it is masquerading as the expected target.

The availability of this information on the target enables the appropriate resources to be allocated to counter the threat. There are close parallels here with the military situation, in providing a timely and measured reaction to the potential threat, by allocating resources to check it out, and allowing decisions on further actions to be taken including the use of force. More conventional activities such as the detection of the smuggling of contraband and illegal immigrants would also benefit from target recognition. The policing of economic exclusion zones, involving fishing and mineral exploitation, for example, would also benefit from a capability of recognising what type of ship or aircraft is intruding into the protected zone. Again, decisions can be made on what action has to be taken, when an estimate of the type of target detected has been made.

Another application is the enhancement of terminal area surveillance and precision approach control at airports, which utilise radar sensors [45]. The high precision measurement capabilities of radar and the use of other sensors, allow the position and speed of fixed-wing aircraft and helicopters to be measured very accurately, as well as having the capability to potentially confirm the aircraft type. On occasion, manoeuvring aircraft on the ground have been confused by the controllers at airports, so the ability to separate and identify individual aircraft can enhance safety. It is also necessary to locate airport vehicles, whose movements also have to be controlled.

1.5.5   Ballistic missile defence

Another military application in which it is necessary to have a target recognition capability is in ballistic missile defence [46]. If the incoming ballistic missile is to be intercepted by a missile launched by the defence, this is called active defence. To achieve this, it is first necessary for the defence to detect and track the threatening missile. It is necessary to determine the ballistic trajectory of the missile very accurately and to provide an estimate of where and when it can be intercepted on its trajectory. The vital issue is to establish which object in the threat cloud is carrying the warhead, so that it can be tracked and intercepted. In some cases, the threat is unitary, which means that the warhead and booster stay attached for the entire 'flight'.

Examples of unitary missiles are the German V2 of the Second World War and the current family of Scud missiles. In other cases the threat cloud would contain the re-entry vehicle, the booster and any debris generated as a result of the separation of the re-entry vehicle from the booster. In addition it is expected that the more sophisticated

threats would include countermeasures, which may be decoys and chaff [47]. As the radar is the key sensor for tracking the threat from the ground, it would also be required to have high-resolution modes appropriate to separating the re-entry vehicle from all the other objects and discriminating it with high reliability and rapidly. The predicted location of the re-entry vehicle would then be used by the interceptor for targeting.

The US is developing the four-face SPY-1E radar, which is envisaged to be part of a dual-band theatre ballistic missile defence radar suite, operating in concert with a tracking I/J-band (X-band) High-Power Discriminator (HPD) radar [48]. The latter would be used to discriminate the re-entry vehicle for interception. For the long-range intercontinental ballistic missile threat, the US is developing the Sea-based X-band radar to provide the mid-course solution to precision discrimination and interceptor support. Its functions include searching, acquisition, tracking and kill assessment [49]. High-resolution techniques for ballistic missile defence are discussed in Chapter 11.

1.6   Technical challenges

To achieve an acceptable level of target recognition performance is a challenge to the radar designer, the authority responsible for specifying and procuring the radar equipment and to some extent the operator of the radar, who is faced with new and a different type of information. Past and current radar systems have been specified to detect a target of a certain radar cross-section (or size), under defined environmental conditions, with a particular probability and false alarm rate. Radars have been required to initiate and maintain tracks to certain measurable accuracies. However, requirements for specifying target recognition functions are expected to be quite different for all those involved in the procurement and development process. These issues are discussed later in Chapter 14.

1.7   Summary of book contents

In the following chapters, the radar technology employed for providing high-resolution target signatures for recognition purposes is presented. Of particular importance are the practical implementation issues for incorporating the techniques into real systems. Although some mathematics has inevitably had to be used to explain the concepts presented, emphasis has been placed on providing the reader with their physical interpretation. Both the technological and operational aspects of integrating NCTR modes are discussed.

Initially, a tutorial on the basic radar principles is presented in Chapter 2 within the context of providing the foundations for the subsequent chapters on the target recognition techniques. The main functional elements of a radar are discussed and the process of detecting and tracking targets is addressed. References are provided for readers who may wish to study some of the radar topics in more detail. As a prerequisite to the description of the high-resolution radar techniques required for target

recognition, the background to radar measurements is presented. As an introduction to target recognition, the basic functions in the process are discussed.

In Chapter 3, the main techniques for providing a high-range resolution (down-range) capability are presented. Included are the advantages of each technique and any associated limitations. These methods used on their own provide a one-dimensional high-range resolution target image.

In Chapter 4, techniques for providing both high down-range and high cross-range resolution are presented. This covers Doppler beam sharpening, synthetic aperture radar (SAR) and inverse synthetic aperture radar (ISAR) techniques. These techniques are used to provide two-dimensional images of targets.

In Chapter 5, techniques are discussed, which do not use high-range resolution, but frequency and time domain analysis. The first of these is Jet Engine Modulation (JEM), which measures the frequency characteristics of jet engines from their radar signatures, as the basis for recognition. The other techniques used for helicopters detect the reflections of the main rotor's blades, and from the rotor itself, as the basis for the recognition of helicopters.

In Chapter 6, other high-resolution radar techniques are presented, which can supplement the methods previously described. These are monopulse target imaging, polarisation, combined high-range and resolution techniques, impulse and ultra high-resolution radars.

In Chapter 7, the system design issues associated with incorporating high-resolution modes into radars are discussed. Key aspects are sensitivity and dynamic range for the receiver. Another issue of importance is calibration of the radar's high-resolution mode and compensating for system distortion.

The implications on component design are addressed in Chapter 8. The waveform generator, up-converter, transmitter, receiver, digitiser and signal processor are discussed.

Antenna design configurations have significant implications on the supporting of high-range resolution functions and the key issues are presented in Chapter 9 and cover dishes and phased arrays.

The implications of using NCTR in operational systems are discussed in Chapter 10. Passive- and active-phased arrays and tracker radars using mechanically scanning antennas are discussed.

The applications to real targets of the radar recognition techniques previously presented in the earlier chapters of the book are addressed in Chapter 11. The various types of targets are discussed with respect to the different techniques for generating high-resolution target images. The advantages and disadvantages of each technique are summarised and recommendations are provided for the optimum approach, taking into account the target, the environment, time lines and operational aspects.

Chapter 12 describes the target recognition process and involves radar measurements, target signature modelling and databases, recognition algorithms and data processing. This brings together all the elements needed in a radar system to support target recognition. The processes and techniques needed for using radar data and converting it into estimates of target type are discussed. This also includes image processing technology for recognising signatures.

Chapter 13 provides a framework for combining radar data with data available from other sensors. Bayesian networks are presented, target classifiers are discussed and a simulation example is provided.

The summary and conclusions are presented in Chapter 14.

The Appendix covers the theory of the classical stepped frequency technique, the derivation of the JEM spectrum and Bayes' Theorem.

Some of the references provided in this book are internet web addresses, which should be readily available for most readers. As websites are amended regularly, the information referenced may not be immediately accessible. It is advised that the reader then contacts the webmaster for the site, who should be able to retrieve earlier information presented.

References

1   HÜLSMEYER, C.: '*Verfarhen, um entfernte metalische Gegenstandemittels electrische Wellen einem Beobachter zu melden*'. German Patent Office no. 165546, 30th April 1904

2   PRITCHARD, D.: 'The Radar War'. Patrick Stephens Limited, 1989, p. 25

3   PUGH, E.M. and PUGH, E.W.: 'Principles of Electricity and Magnetism' (Addison-Wesley Publishing Company, Reading, MA, 1965)

4   REITZ, J.R. and MILFORD, F.J.: 'Foundations of Electromagnetic Theory' (Addison-Wesley Publishing Company, Reading, MA, 1967)

5   BURNS, R. (Ed.): 'Radar Development to 1945' (The Institution of Electrical Engineers, London, 1988)

6   BARTON, D.K.: 'Historical Perspective on Radar', *Microwave Journal,* 1980, **38**, pp. 21–9

7   GALATI, G. (Ed.): 'Advanced Radar Techniques and Systems' (The Institution of Electrical Engineers, London, 1993)

8   SWORDS, S.S.: 'Technical History of the Beginnings of Radar' (The Institution of Electrical Engineers, London, 1985)

9   DANIELS, D.J., GUNTON, D.J., and SCOTT, H.F.: 'Introduction to Subsurface radar', *IEE Radar and Signal processing proceedings* Vol. 135, pp. 278–320, London

10 MAHAPATRA, P.R.: 'Aviation Weather Surveillance Systems: advanced radar and surface sensors for flight safety and air traffic management' (The Institution of Electrical Engineers, London, 1998)

11 ERIKSSON, L.H. and BRODEN, S.: 'High Performance Automotive Radar' *Microwave Journal*, 1996, pp 24–38

12 ARICEBO NATIONAL ASTRONOMY AND IONOSPHERE CENTER: www.naic.edu/~nolan/radar/

13 FARINA, A. (Ed.) 'Optimised Radar Processors' (The Institution of Electrical Engineers, London, 1987)

14 THALES RAYTHEON SYSTEMS.: www.thalesraytheon.com. Master M Long Range Infrastructure 3-D Surveillance Radar

15 BAE SYSTEMS INTEGRATED SYSTEM TECHNOLOGIES LTD WEBSITE: www.baesystems.com/insyte AR327 Commander

16 SKOLNIK, M.: 'Introduction to Radar Systems' (McGraw Hill, New York, 1970)

17 US NAVY WEBSITE. www.navy/mil

18 UK DEFENCE PROCUREMENT AGENCY: www.mod.uk/dpa/projects/bvraam/contractor.htm

19 FEDERATION OF AMERICAN SCIENTISTS WEBSITE: www.fas.org/man/dod-01/sys/missile/row/brimstone.htm

20 SHOCKLEY, D.A.: 'Friendly Fire: Reducing The Risk Of Future Battlefield Tragedies', www.globalsecurity.org/military/library/report/1992/SDA.htm

21 SKY NEWS, March 25, 2003 – 17:15 (UK)

22 INTEGRATED PUBLISHING. 'IFF System Overview' www.tpub.com/content/combat/14308/css/14308_102.htm

23 STEVENS, M.C.: 'Secondary Surveillance Radar' (Artech House, Boston, MA, 1998)

24 www.airpower.at/flugzeuge/eurofighter/sensorik.htm#captor

25 www.globalsecurity.org/military/systems/aircraft/f-22-avionics.htm

26 BOEING WEBSITE: www.boeing.com/defense-space/infoelect/e3awacs/

27 ERICSSON WEBSITE: www.ericsson.com/microwave/products_sensors_erieye.shtml

28 www.globalsecurity.org/military/systems/aircraft/e-2.htm

29 FEDERATION OF AMERICAN SCIENTISTS' WEBSITE: www.fas.org/man/dod-101/sys/ac/e-2.htm

30 FEDERATION OF AMERICAN SCIENTISTS' WEBSITE: www.fas.org/irp/program/collect/jstars.htm

31 RAYTHEON WEBSITE: www.raytheon.com/products/astor/

32 THALES GROUP UK WEBSITE: www-v3.thalesgroup.com/all/pdf/searchwater2000aew.pdf

33 LOCKHEED MARTIN AERONAUTICS COMPANY WEBSITE: www.lmaeronautics.com/products/recon/p3/

34 UK ROYAL NAVY WEBSITE: www.royal-navy.mod.uk/static/pages/1989.html

35 BAE SYSTEMS INTEGRATED SYSTEMS TECHNOLOGY LTD WEBSITE: www.baesystems.com/insyte S1850M

36 LOCKHEED MARTIN AERONAUTICS COMPANY WEBSITE: www.lockheedmartin.com/wms/findPage.do?dsp=fec&ci=13584&rsbci=13197&fti=0&ti=0&sc=400

37 THALES RAYTHEON SYSTEMS WEBSITE: www.thalesraytheon.com M3R Extended air defence

38 BAE SYSTEMS INTEGRATED SYSTEM TECHNOLOGIES LTD WEBSITE: www.baesystems.com/insyte Sampson

39 FEDERATION OF AMERICAN SCIENTISTS WEBSITE. www.fas.org/man/dod-101/sys/ship/docs/cg_14-93.html

40 *International Defence Review*. 13 January 2004

41   BAE SYSTEMS INTEGRATED SYSTEM TECHNOLOGIES LTD WEBSITE:
      www.baesystems.com/insyte Commander
42   UK ROYAL AIR FORCE WEBSITE: www.raf.mod.uk/equipment/surfacetoair.
      html#rapier
43   BAE SYSTEMS INTEGRATED SYSTEM TECHNOLOGIES LTD WEBSITE:
      www.baesystems.com/insyte Dagger
44   BAE SYSTEMS INTEGRATED SYSTEM TECHNOLOGIES LTD WEBSITE:
      www.baesystems.com/insyte Blindfire
45   SELEX WEBSITE: www.airport-technology.com/contractors/traffic/ams/
46   UNITED STATES MISSILE DEFENSE AGENCY WEBSITE: www.acq.osd.
      mil/bmdo/bmdolink/html/midcrse.html
47   UNION OF CONCERNED SCIENTISTS WEBSITE: www.ucsusa.org/
      global_security/index.cfm
48   *International Defence Review*. 13 January 2004
49   RAYTHEON WEBSITE:
      www.raytheon.com/businesses/rids/docs/SBX_03.pdf

Radar principles

2.1 Tutorial

2.1.1 Introduction

The main objective of this chapter is to provide the reader who is not a radar specialist, with a tutorial on the main aspects of radar design architectures and techniques, which support conventional radar modes. It is aimed to provide the reader with a general understanding of how current radars are designed and how they function by presenting some typical designs, without covering all the detailed techniques available. More information can be obtained from References 1–3. Radars which employ mechanically scanning antennas such as parabolic reflectors and phased array radars which utilise electronic scanning techniques are presented. The main functional components employed and the basic principles of radar signal processing are also discussed.

Radars which can support target recognition functions follow the basic principles of conventional radar design and build on these foundations to provide the high-resolution target signature measurement capability. In some cases existing radar designs are also compatible with, or could be upgraded to support, target recognition functions. These issues are discussed in the later chapters of the book.

2.1.2 Basic concept

Radar stands for Radio Detection and Ranging. Radars use the electromagnetic spectrum for transmitting and receiving signals. In free space electromagnetic waves propagate at the speed of light, which is 299,792 km/s. This was first estimated with an accuracy of 1 per cent by Römer in 1676, by observing the intervals between eclipses of the planet Jupiter's innermost satellite [4].

The basic concept of a radar transmitting a signal and receiving a return from a target is shown in Figure 2.1.
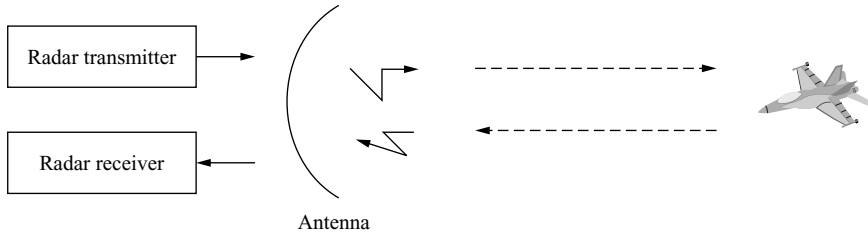
Figure 2.1   Transmitting and receiving a signal from a target

The radar generates a signal, which is transmitted through an antenna into free space. The antenna is designed to concentrate the radar energy in a particular direction, which in this case is towards the aircraft target. Only a small proportion of the transmitted radar energy reaches the target, with the rest missing it or illuminating other nearby objects, including the earth's surface or going off into space, as the radar beam is normally much wider than the angular dimensions of the target. The radar beam broadens as the wave propagates from the radar, so is reduced in strength with distance and the energy incident upon the target also reduces with distance. For a metallic aircraft target, most of the incident energy is reflected and a small amount is absorbed. The energy reflected from the target tends to propagate in all directions and the amount directed back towards the radar is dependent upon the wavelength of the signal, the size, shape and the materials of the aircraft. Hence, only a small proportion of the energy actually illuminating the aircraft, or any other target, is reflected back in the direction of the radar. The reflected energy then propagates through free space and is incident upon the radar's antenna and is directed into the radar receiver and is processed to detect the target. Of all the energy transmitted by the radar, perhaps one part in 10^9 (one billionth) or 10^{12} (one trillionth) is detected after being reflected by the target, so radars need high-power transmitters and very sensitive receivers.

2.1.3   Radar waves

There is no fundamental difference between radar waves travelling through the air and conventional radio waves, which are used to broadcast radio programmes and television pictures. The electromagnetic wave carries energy in the form of electric and magnetic fields, which are oscillating at the wave's frequency [5–7] and are mutually orthogonal (or at 90°) to the direction of propagation. Energy is stored in these fields and is continually transferring between them at the wave's vibration frequency as the wave propagates at the speed of light. These concepts are illustrated in Figure 2.2. By convention, the electric field tends to be used to represent the wave in explanations rather than the magnetic field. The electric field has physical units of volts per metre and is a measure of the strength of the signal. In addition, by integrating the value of the electric field over a portion of space at right angles to the direction of propagation of the radar wave, a voltage is obtained. This voltage associated with an electromagnetic wave propagating through free space is the same physical phenomenon as voltages associated with signals being conducted in the electrical

Electric field vector, *E*

Energy flows in direction of propagation
of radar wave

The radar energy is carried in the wave's
electric and magnetic fields and propagates
at the speed of light in free space

90°

90°

90°

90°

In a radar wave the electric field, magnetic field and
direction of propagation are mutually orthogonal

Magnetic field vector, *H*
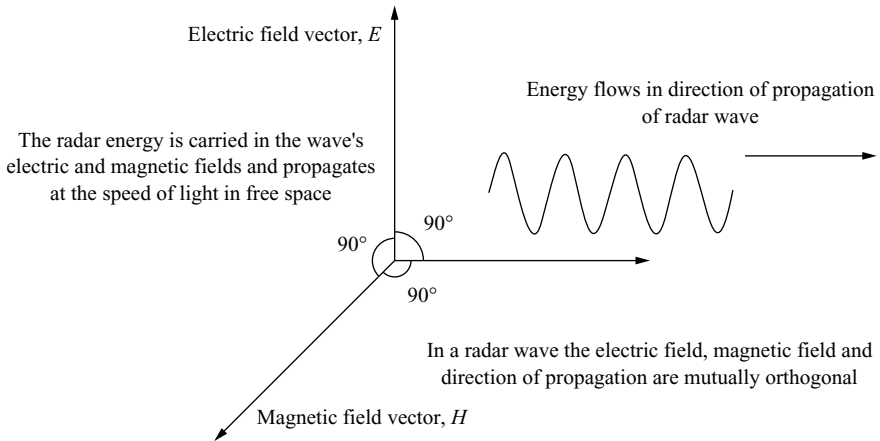
*Figure 2.2   Electromagnetic wave with direction of propagation, electric and
magnetic field vectors being mutually orthogonal*

circuits. Interestingly, free space actually has an impedance [8], which is about 377 Ω
and is the value of the electric field divided by the magnetic field. This is not resistive in
the same way as a resistor in an electrical circuit, which dissipates electrical energy in
the form of heat, but is a means of facilitating the propagation of the wave. The
impedance of free space is reactive and has no resistive component, so no energy is
dissipated as the wave propagates.

The power density or power flux, P_f, of an electromagnetic wave travelling
through space, is measured in watts per square metre, and is the average value of the
voltage squared, $\overline{V^2}$, divided by the impedance of free space, Z, per unit area:

$$P_f = \frac{\overline{V^2}}{Z} \tag{2.1}$$

This is analogous to Ohm's Law for electrical circuits in which the power dissipated in
a resistive component is equal to the root-mean-square voltage divided by its electrical
resistance.

The most basic radar signal propagating through free space is a sinusoidal wave of
the form shown in Figure 2.3. The 'x-axis' is the distance measured in the direction of
propagation of the wave and the 'y-axis' represents the amplitude variations appro-
priate to the strength of the instantaneous electric field along the wave. The radar
wave as shown in the figure is effectively frozen in time. The distance between the
two adjacent troughs of the wave is defined as one wavelength, λ. The relationship
between the velocity of the wave, *c*, the wavelength and the frequency of vibration
of the wave, *f*, is given by:

$$c = \lambda f \tag{2.2}$$

Maximum amplitude
of wave *a*

Direction of propagation of
radar signal

One wavelength λ

Distance
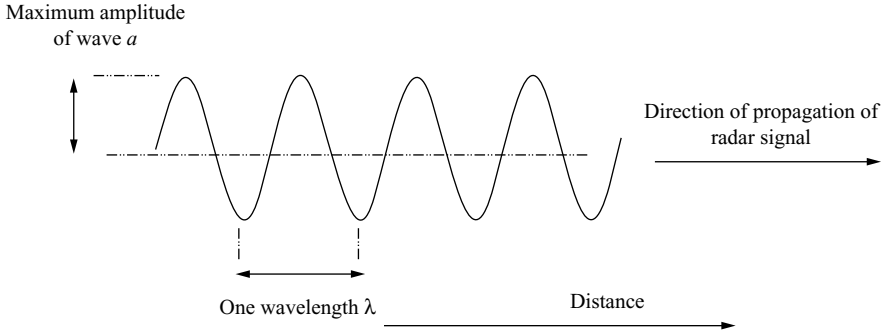
Figure 2.3   Sinusoidal radar wave

For an electromagnetic wave propagating from a radar transmitter, the signal is a high-frequency sinusoid varying in both time and space and is of the form:

$$a = \frac{A}{r} \sin 2\pi f \left\{ t - \frac{r}{c} \right\} \tag{2.3}$$

where *a* is the instantaneous value of the electric field, *A* is a constant, *t* is the time and *r* is the range from the radar transmitter.

It can also be seen that the amplitude of the radar signal's electric field varies as the inverse of the distance from the radar from the $1/r$ term. This will be discussed below. The instantaneous phase, φ, of the wave is:

$$\varphi = 2\pi f \left\{ t - \frac{r}{c} \right\} \tag{2.4}$$

On studying Equation (2.3) it can be seen that at constant range, at a given position in space, the electric field varies with time as:

$$a = \frac{A}{r} \sin(2\pi f t + \varphi_{Const}) \tag{2.5}$$

$$\text{where } \varphi_{Const} = -\frac{2\pi f r}{c}$$

This variation of amplitude of the electric field with time, at a fixed position, is shown in Figure 2.4.

The time between the two adjacent troughs represents a complete cycle of vibration of the electromagnetic wave.

The period of the wave, *T*, is given by the inverse of the frequency, *f*:

$$T = \frac{1}{f} \tag{2.6}$$

In Equation (2.3) it can be seen that the strength of the radar signal's electric field varies as the inverse of the range from the source. This is represented in Figure 2.5. The radar waves can also be considered to be like the ripples formed in a pond, when a stone has been dropped into the water. Close to the centre of the disturbance the

Maximum amplitude
of wave *a*

One cycle *T*
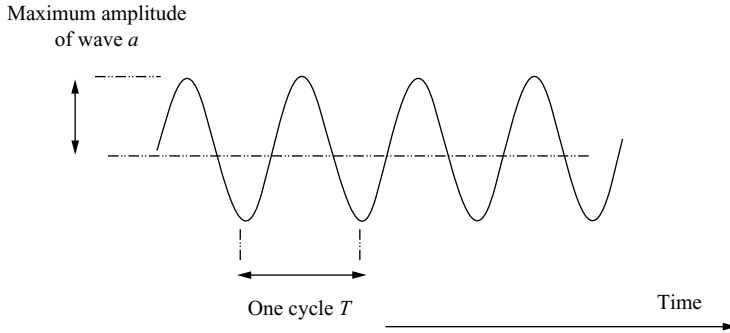
Time

Figure 2.4   Variation in electric field of radar wave with time at a fixed position

Direction of propagation of
radar waves

Radar beam
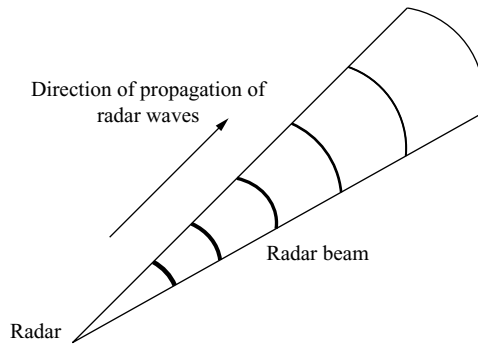
Radar

Figure 2.5   Signal weakens as it gets further from radar

waves are largest and as the ripples move away towards the edge of the pond they lose their strength. The major difference with the analogy of the stone dropped into the pond and a radar signal is that the radar signal is concentrated in a beam, as shown in Figure 2.5. From electromagnetic theory, the power density or flux of the wave propagating through space, $P_f(r)$, varies inversely with the square of the distance from the source [9], that is, $P_f(r)\alpha(1/r^2)$. This means that the power density of the radar signal varies as the inverse of the square of the distance to the target, so if the range to the target doubles, the power density of the signal illuminating the target reduces by a factor of four.

   The reflected signal from the target tends to propagate in all directions as shown in Figure 2.6 and the associated power density also reduces as a factor of the square of the distance from the target. The actual power illuminating the radar is already reduced by a factor of the square of the range of the target and there is this additional factor of the square of the range for reducing the power density of the signal propagating back from the target to the radar. The overall loss of signal is therefore proportional to the range of the target to the power of four. Hence, by doubling the range of the target,
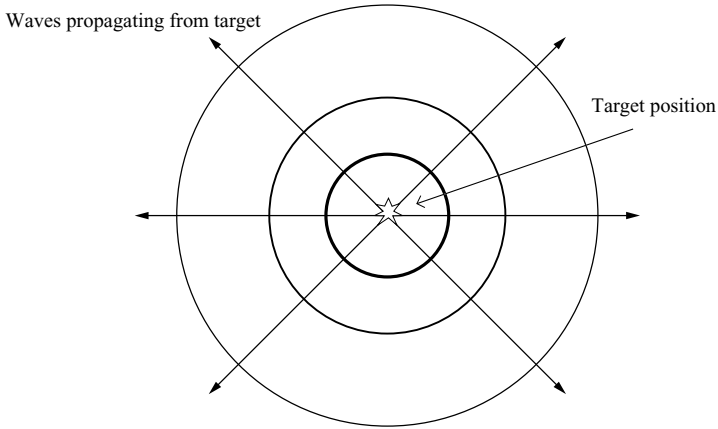
Figure 2.6   Reflection of radar signal from target: energy reflected from target tends to propagate in all directions

the received signal is reduced by a factor of 2^4 which is 16. This will be used later in the chapter for the calculation of range, using the 'Radar range equation'.

2.1.4   Radar wavelengths

The actual wavelength employed by a radar is dependent upon the application. The wavelengths used vary from several tens of metres in the so-called high frequency (HF) part of the radio spectrum to extremely short wavelengths of below 1 mm [10,11]. The corresponding frequencies of operation vary from a few megahertz (MHz) to over one hundred gigahertz (GHz), respectively (1 GHz is 1000 MHz or 1000 million cycles/s). This range of frequencies is used as favourable transmission, propagation and reception of signals can be achieved in the vicinity of the earth's surface and in the atmosphere. Using wavelengths longer than 100 m is not very practical, as range, angle and velocity measurements of targets are poor, as will be seen later in this chapter. In addition the spectrum is congested with radio broadcasting stations. For wavelengths from tens of metres to a few centimetres, electromagnetic energy readily propagates through the atmosphere with little attenuation due to the air, water vapour or dust. At wavelengths shorter than a few centimetres the attenuation of radar signals in the atmosphere progressively rises, mostly due to the effects of water vapour and droplets in the atmosphere. There are also effects due to oxygen resonance lines in the millimetre wave bands that limit radar range [12].

In Table 2.1, is a very general summary of the applications of the various radar bands used. The types of radar function will be described later in the chapter.

2.1.5   Range to target

Using Figure 2.7, the range or distance from the radar to a particular target is shown to be R metres. The radar signal has to make a two-way journey to the target and back,

Table 2.1   *Typical applications of various radar bands*

Radar wavelength	Frequency	Application
3–100 m	1–30 MHz	Over the horizon HF sky wave and surface wave
10 cm–150 m	1–3000 MHz	Ground penetrating radar
1 m	400–600 MHz	Long-range surveillance; Ballistic missile detection
20 cm	1–2 GHz	Land and naval long-range surveillance; Air traffic control
5–10 cm	3–6 GHz	Land and naval surveillance; Multi-function radar Airborne early warning
3 cm	8–10 GHz	Airborne interceptor fire control Land and naval fire control Ballistic missile defence fire control
1.5 cm	15–20 GHz	Battlefield surveillance
3 mm–1 cm	35, 94 GHz	Missile seekers
2 mm	70–80 GHz	Vehicle collision avoidance and cruise control
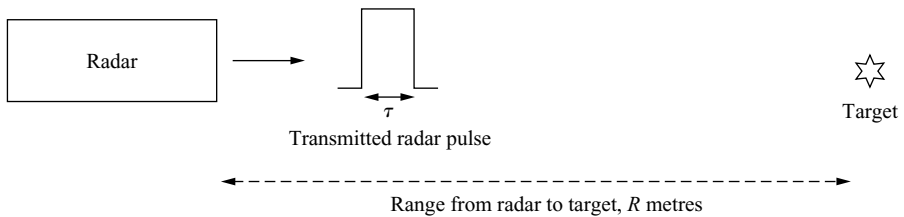
Figure 2.7   *Range to target*

so it travels a total distance of $2R$ metres. The velocity of electromagnetic wave, c, has almost the same value in air as in a vacuum and is constant with the wavelength of the signal. Hence, if the time, T, for the signal to travel from the radar to the target and back can be measured, then the range to the target can be calculated. Hence,

$$R = \frac{cT}{2} \qquad (2.7)$$

Fortunately, the technology is available to measure the time, T, with good accuracy, so the range to the target can easily be determined. It should be noted that the radar signal has been represented as a short pulse and its time duration, τ, must be short in relation to the delay to the target, otherwise uncertainties in the timing of the
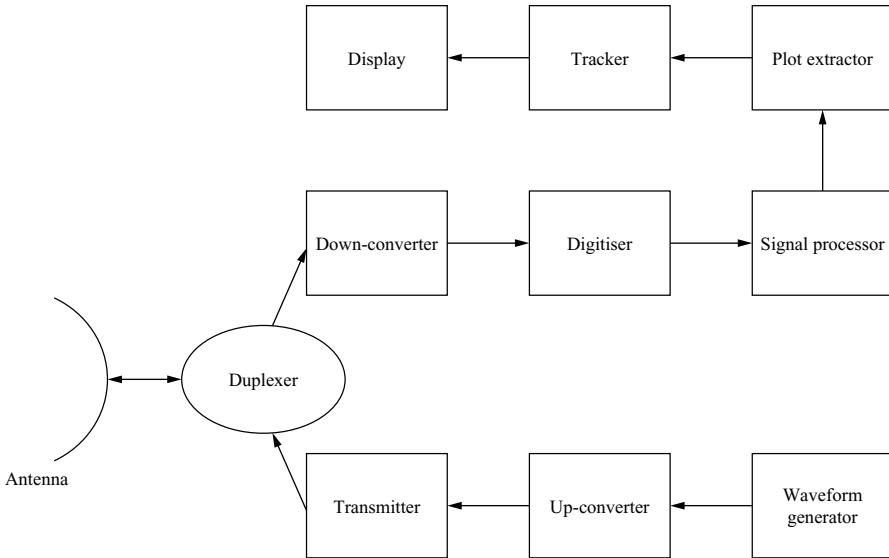
Figure 2.8   Functional block diagram of typical radar system

received signal degrade the range measurement. This will be discussed in more detail later in this chapter.

2.1.6   Functional components of radar

In Figure 2.8 the main functional components of a typical radar system are shown. The boxes are functions that the radar performs and do not all necessarily represent real individual physical components. An overview of the overall function of the radar system is provided here. More details on the individual elements are presented in the later sections.

The radar pulses are generally synthesised in the waveform generator at a low frequency. They are then up-converted using mixers operating in the microwave frequency range to generate the signal at the required transmission frequency. The signal then is amplified in stages to the full transmitter output power. Between the transmitter and antenna is a device called a duplexer, which directs the transmitter power to the antenna, while at the same time preventing significant leakage into the receiver. The signal is then transmitted from the antenna. If the antenna is mechanically rotating it transmits energy in accordance with the direction in which it is instantaneously pointing.

The signal reflected from targets or clutter back in the direction of the radar is collected by the antenna. The signal then passes into the duplexer, which is a non-reciprocal device, and this time directs it into the first stage of the receiver. It is amplified and normally down-converted to a low baseband frequency. This analogue signal is then digitised in an analogue to digital converter (ADC) and can

now be processed in a digital computer. The main functions of the signal processor are filtering, integration of pulses and possibly pulse compression.

This data is then passed to the plot extractor, which identifies possible alarms generated by detected targets, which are called plots. These plots are normally recorded using range, azimuth, elevation and possibly velocity as labels. The plots are passed to the target tracker, which compares plots coming into the radar with time. Plots which appear to be associated with the same target are used to generate a tentative track, which gives an estimate of the position and direction along which the target is moving. It also provides a prediction of where the target is expected to be during the next scan of the antenna, when it is again expected to be illuminated by the radar. When the target track has been satisfactorily established, it is stated to be a confirmed track. The stage after this is called track maintenance, when new plot data is received and is used to maintain the previously established track. Targets that are being tracked are presented to the radar operator on a display.

In the following sections these radar functions are discussed in more detail.

2.1.7   Waveform generation

2.1.7.1   Introduction

In this section typical radar waveforms and techniques for generating them are presented. The actual reasons why the particular types of waveforms are used are discussed in Section 2.1.18, the section on signal processing. It is generally not practical to generate the radar signal directly at the operating frequency, so the design route taken is to generate the signals at a much lower frequency band and apply frequency mixing to the signal in one or two stages. The centre frequency of the waveform is then raised to the operating frequency band. High-purity sinusoidal signals are used throughout the radar to contribute to the generation and receiving of the radar waveform. The reference sinusoidal signals are also used to provide the timing and synchronisation functions within the radar. Various combinations of the techniques presented below can be used together and are dependent upon the detailed application.

2.1.7.2   Pulse train

The function of the waveform generator is to provide the modulation envelope of the radar signal at a low power level. At this stage of signal generation there is generally no carrier frequency. A typical pulse burst synthesised by the waveform generator is shown in Figure 2.9. The main features of the waveform can be seen. Each pulse has a particular time duration, which is known as the pulse width. The time between the end of one pulse and the start of the next is called the inter-pulse period. The time taken from the generation of one pulse to the generation of the next one is the pulse repetition period and is almost always constant over a burst of radar pulses. The inverse of the pulse repetition period is called the pulse repetition frequency (prf) and is measured in hertz. The timing signals, which are used to generate the pulse lengths and prfs, are provided by electronic 'counting' circuits, which use the reference signals discussed above as clock pulses.
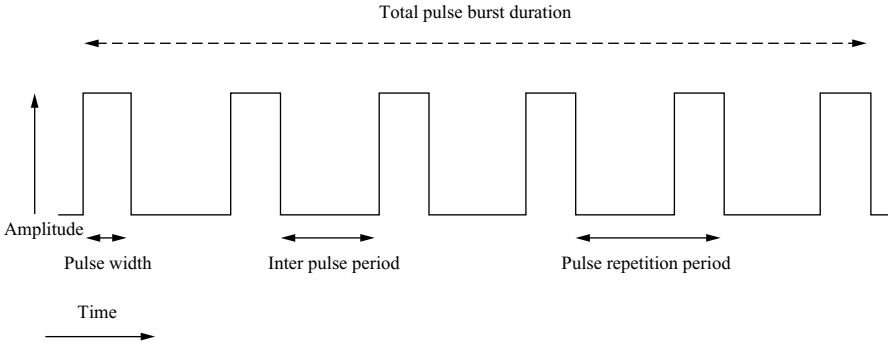
Figure 2.9   Waveform generator output is modulation envelope of signal
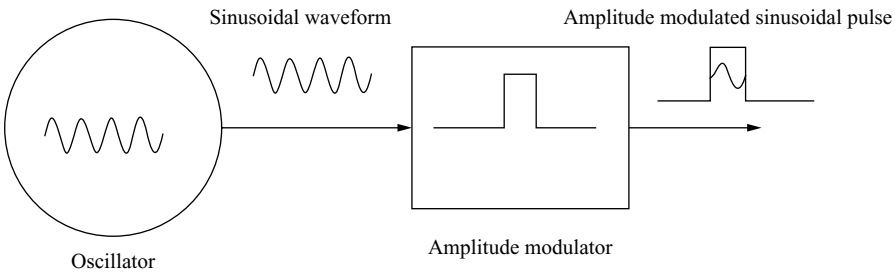
Figure 2.10   Generating the modulated pulse

The radar integration period is the period over which returns are received from a single burst of transmitted pulses. The target returns from transmitting several pulses are processed together as the information associated with a particular pulse is not often used on its own. The signal shown above is the envelope of the transmitted signal. The methods of generating the modulation of a signal are discussed in the next sections.

2.1.7.3   Modulation envelope

One method of generating the modulated radar pulse is shown in Figure 2.10. A high-quality oscillator generates a sinusoidal signal, which then undergoes amplitude modulation to provide the required pulse length. Timing signals are sent to the modulator from the radar controller for the start time and stop time of each pulse and for the commencement and completion of each burst of pulses. The modulator [13] provides a low-loss path when the pulse envelope is required. For the interpulse period when no signal is needed, the modulator is set to be highly lossy or resistive, so that virtually none of the incident sinusoidal signal is transmitted. A PIN diode is a type of device that can be used as a programmable modulator [14].
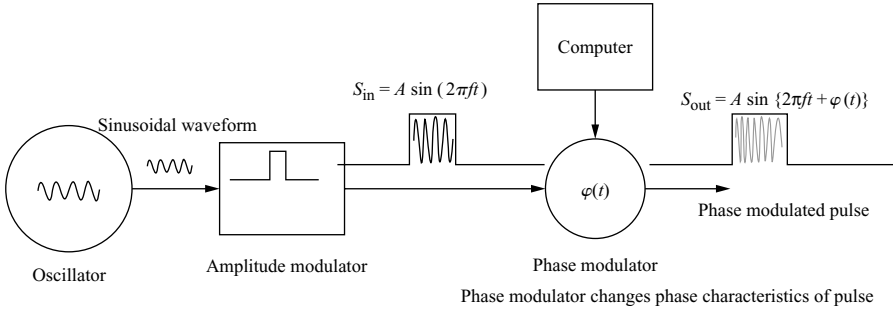
Figure 2.11   Generating the phase modulated pulse

2.1.7.4   Phase modulation

Some radar waveforms are coded using phase or frequency modulation (FM) [15] which is a form of pulse compression and is used for improving the range resolution of the transmitted signal and will be discussed in more detail later.

Figure 2.11 shows a technique for phase modulating the pulse using a phase shifter [16]. Using the same technique for amplitude modulating the pulse, as in Figure 2.10 to provide its envelope, it is then applied to the phase shifter. The characteristics required for the phase modulation are stored in a digital computer as time varying phase coefficients across the pulse, $\varphi(t)$. The phase shifter changes the phase of the sinusoidal waveform applied, so for an input signal, S_{in} of the form:

$$S_{in} = A\sin(2\pi ft) \tag{2.8}$$

where A is the amplitude, or voltage, of the signal, f its frequency and t is time. At the output of the phase shifter, the signal S_{out} is of the form:

$$S_{out} = A\sin\{2\pi ft + \varphi(t)\} \tag{2.9}$$

The phase modulation $\varphi(t)$ provides the required phase characteristics of the modulated pulse.

2.1.7.5   Vector modulation

Vector modulation is a technique used for simultaneously modulating a signal in amplitude and phase and is used to generate waveforms with large bandwidths [17]. A vector modulator [18,19] is shown in Figure 2.12 and uses three input signals.

The first input signal is:

$$S_{in} = A\sin(2\pi ft) \tag{2.10}$$

Vector modulation uses 'In-Phase' and 'Quadrature' components of the modulating waveform in the form of cosine and sine coefficients, which comprise the other two input signals. These are synthesised in a digital to analogue converter (DAC). For the instantaneous frequency, f_1, for the waveform of amplitude, B, the 'In-Phase'
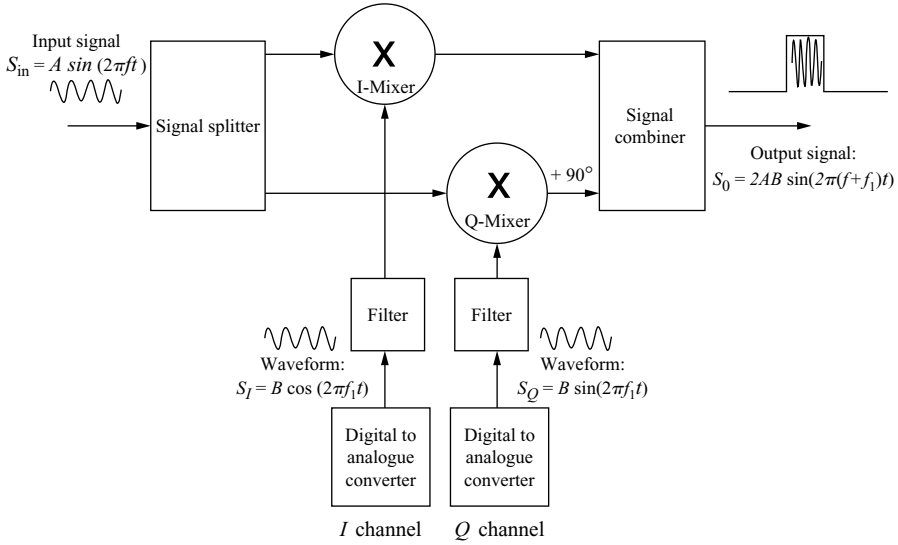
Figure 2.12   Generation of signal using vector modulator

or I term is:

$$S_I = B\cos(2\pi f_1 t) \tag{2.11}$$

and the 'Quadrature' or Q term is:

$$S_Q = B\sin(2\pi f_1 t) \tag{2.12}$$

As the Q channel sine wave lags the I channel cosine wave by 90° they are said to be in quadrature. Two well-matched frequency mixers are used for combining the various frequency components. The input signal, S_{in} is divided equally into two channels by the splitter, which then applies the signals to the respective mixers. A mixer is a non-linear device [20,21] that combines signals at different frequencies. The output of the mixer is in the form:

$$S_{Mixer} = (A + B)m_1 + (A + B)^2 m_2 + \cdots + (A + B)^N m_N \tag{2.13}$$

The values m_n represent the transfer function coefficients of the mixer, with the m_1 term being the linear component. The m_2 term is of interest here, as it provides the non-linearity required for mixing the two input frequencies. The output of the in-phase mixer is:

$$S_{Mixer\,I} = (S_{in} + S_I)^2 = \{A^2\sin^2(2\pi ft) + 2AB\sin(2\pi ft)$$
$$\times \cos(2\pi f_1 t) + B^2\cos^2(2\pi f_1 t)\} \tag{2.14}$$

Similarly for the quadrature channel:

$$S_{\text{Mixer } Q} = (S_{\text{in}} + S_Q)^2 = \{A^2 \sin^2(2\pi ft) + 2AB \sin(2\pi ft)$$
$$\times \sin(2\pi f_1 t) + B^2 \sin^2(2\pi f_1 t)\} \tag{2.15}$$

Theses two outputs, $S_{\text{Mixer } I}$ and $S_{\text{Mixer } Q}$ are combined with a relative phase shift of 90° applied to the quadrature channel. The output signal, S_0 of interest is:

$$S_0 = S_{\text{Mixer } I} + S_{\text{Mixer } Q} = 2AB \sin\{2\pi t(f + f_1)\} \tag{2.16}$$

This is the signal required, which is the frequency sum of the input signal and the modulation signal. Other frequency multiples and harmonics would normally be filtered out. Vector modulation can provide considerable flexibility in waveform generation, as it can combine both amplitude and phase modulation functions. The value of f_1 can be a continuously varying frequency, so this technique is appropriate to many modulation schemes.

A critical design issue for the vector modulator is to provide good in-phase and quadrature balance between the two channels. Otherwise an 'image' of the intended signal is also generated, which can appear to be a false target, if it is not corrected. Local oscillator (LO) breakthrough and unwanted mixing products can also distort the radar signal and degrade performance.

2.1.7.6   Synthesis of reference frequencies and timing signals

The basic reference signals, which are used in the radar, include base-band and various LO frequencies. These comprise all the signal sources for generating and modulating the radar signal, which were presented above. They also include the LO signals used for up- and down-conversion and the reference frequency for the digitiser. Crystal oscillators are usually used as the reference sources for these radar signals as they provide highly stable signals. A typical crystal oscillator frequency is 10 MHz. This signal source is also used to provide the timing signals for the radar for pulse lengths and prfs using counter circuits. Various techniques involving phase locked loops, voltage-controlled oscillators (VCOs) and frequency multiplying and dividing circuits are used to generate the radar reference signals required [22–25].

The use of a phased locked loop [26] to generate the various frequencies required in the radar is an indirect synthesis technique, as shown in Figure 2.13. The crystal oscillator output feeds into a phase detector, which is connected to a VCO. The output of the VCO is fed into a frequency divider, which is also connected to the phase detector. A fairly simple way to consider the function of this circuit is to view it as a control system. With a properly designed loop bandwidth and transfer characteristic, under stable conditions there is very little 'error' signal fed back to the phase detector. This means that the VCO output frequency must be a factor of N higher than that of the crystal oscillator. Within the constraints set by the loop bandwidth, the VCO also takes on the crystal oscillator's stability characteristics.

The high-quality crystal oscillator performance is utilised by the radar via the VCO, which boosts the signal power level and multiplies the frequency. In order
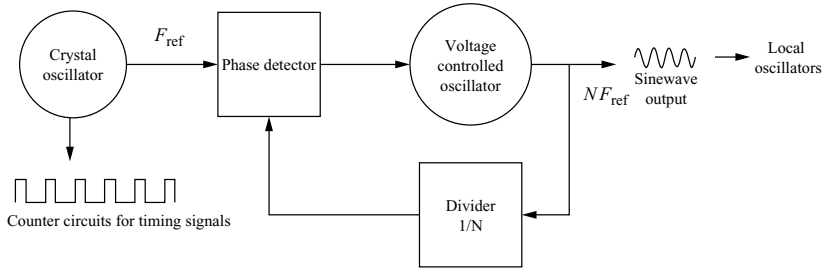
Figure 2.13   Frequency synthesis using a phased locked loop
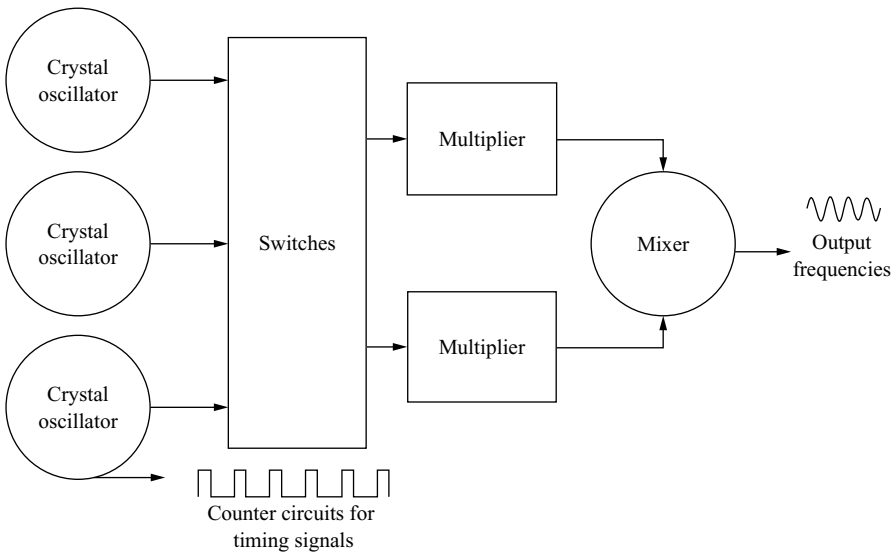
Figure 2.14   Direct frequency synthesis

to provide different values of VCO output frequency, the divider ratio can be programmable, but is generally too slow for very fast switching radar applications.

The technique, which has been widely used in radar to generate the required frequencies, is direct frequency synthesis [27]. The outputs of a bank of crystal oscillators are multiplied up and mixed together to provide a wide variety of frequencies.

This can be seen in Figure 2.14. The crystal oscillators run continuously and the frequencies are selected using the electronic switches, which are usually pin diodes. These signals are multiplied in frequency and combined in a microwave mixer. The advantage of this method is that switching between frequencies can be achieved rapidly, in about 1 µs. The disadvantage is that the crystal oscillator frequencies are not mathematically related to each other, so it is not suitable in applications requiring
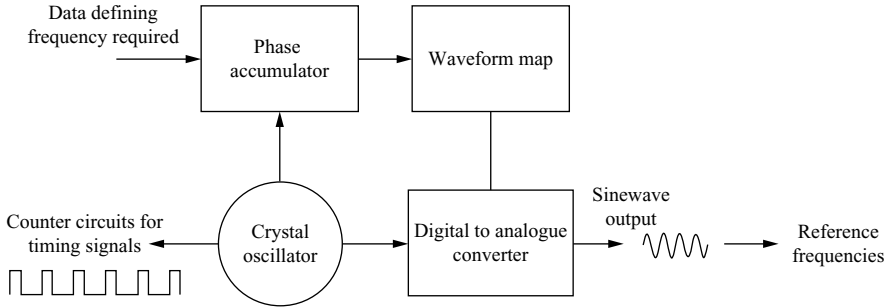
Figure 2.15   Direct digital synthesis

numerically related output frequencies or oscillators linked to the same reference source.

Another technique used for frequency generation, but which can tune the frequency rapidly, is direct digital synthesis [28] and is shown in Figure 2.15. The basis of this technique is to provide a digital representation of the sinusoidal signal to be synthesised and to use a DAC to generate the signal. Data are provided to the phase accumulator, which defines the output frequency required. The crystal oscillator is used by the accumulator as a reference clock. The accumulator's output is a digital word, which represents the instantaneous phase of the output signal. This value of phase is then used by the waveform map, which is a look-up table of waveform data, to generate a digital signal, which is then converted to analogue output sinusoid in the DAC. The output must be filtered to reject any clock related spurious signals.

An advantage of this technique is the ability to generate a wide range of waveforms [29], which are stored in the memory map. The upper frequency limit is determined by the availability of DACs.

2.1.8   Up-conversion

After the radar waveform has been generated at a relatively low frequency, it has to undergo further frequency conversions to be elevated to the operational frequency band of the radar.

The up-conversion process is shown in Figure 2.16. After being modulated in the waveform generator the signal is filtered to avoid any extraneous mixer products re-mixing with the signal or local oscillators, which would generate further spurious signals and degrade radar performance. Two up-conversions are shown in the diagram, which is typical. After the first mixing process, the centre frequency of the signal is raised from the value of f to $f + f_{LO1}$. It is increased exactly by the frequency of the first LO, f_{LO}. After the second up-conversion, the signal's centre frequency is raised to $f + f_{LO1} + f_{LO2}$. These frequencies are called intermediate frequencies (IFs), as these are intermediate frequency stages on the way to the final transmitted radio frequency (RF) signal.
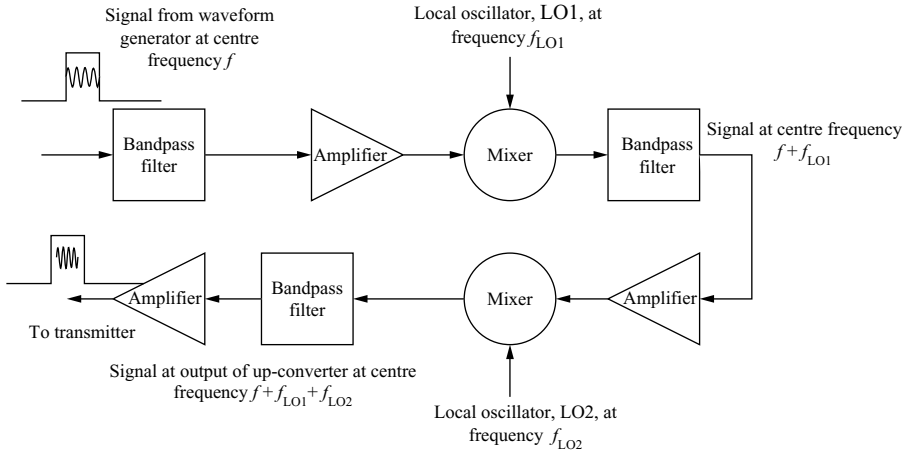
Figure 2.16   Up-conversion

Amplifiers are included to increase the power of the signal to compensate for the mixers' attenuation of the signal and to provide the appropriate drive level for the transmitter. The mixing process is not efficient for maintaining the energy in the signal and directs most of it into various mixing products and heat. Attenuation or loss of signal level through a component is defined as the ratio of the power at the input to the component, to the power at the output and is expressed in decibels (dB) as follows:

$$L = 10 \log_{10} \left\{ \frac{P_{\text{in}}}{P_{\text{out}}} \right\} \tag{2.17}$$

where L = loss, P_{in} = input power, P_{out} = output power.

For a typical mixer, the loss is about a factor of four or five in power ratio terms, which translates to about 6–7 dB.

As can be seen from the above discussions a variety of sinusoidal signals is needed in the radar for actually generating the waveform, for providing the LOs and timing clocks. For many modern radar applications these signals are synthesised from a single reference oscillator.

2.1.9   Transmitter

2.1.9.1   Introduction

For high performance, there are two main classes of radar transmitter currently used, travelling wave tube amplifiers (TWTAs) [30–32] and solid-state amplifiers [33–35]. For the systems employing mechanically scanning antennas, TWTAs are the most popular design used.
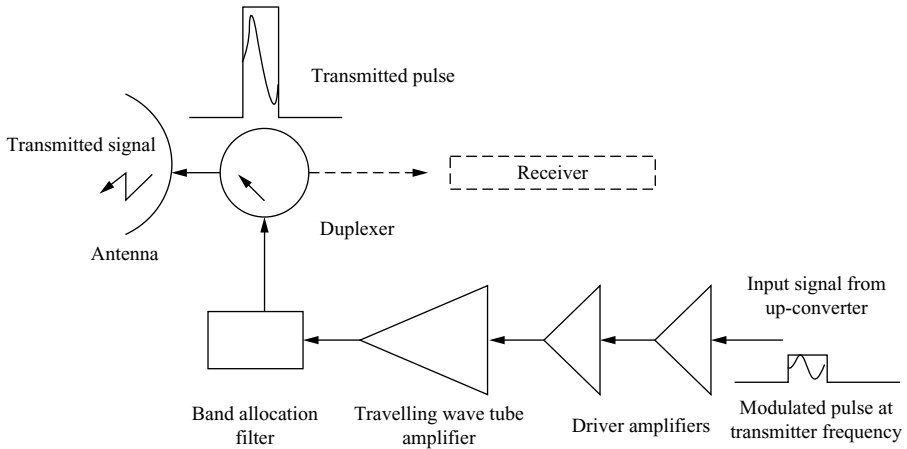
Figure 2.17   Typical transmitter components

2.1.9.2   Travelling wave tube amplifier

The physics of the TWTA's operation is based on modulating electrons emitted from a cathode, which then interact with the RF signal, which is to be amplified [36]. Energy is effectively extracted from the electrons by the RF signal, which absorbs their energy, so is amplified. The TWTA is a device with a large bandwidth, so it is a good candidate for supporting high-range resolution target recognition modes. TWTAs operate over most of the radar bands and can provide many tens of kilowatts output power. They are used in land, naval, airborne and space radar applications. The range and the performance of any radar are constrained by the amount of output power the transmitter is able to provide and radiate via the antenna. A typical block diagram of a radar transmitter is shown in Figure 2.17. The signal from the up-converter is first amplified in solid-state power amplifiers to the optimum drive level and is then amplified by the TWTA. It is important that spurious signals at the input to the TWTA are minimised as this amplifier tends to be run into saturation to maximise the output power. Under these conditions third-order mixing products from signals within the amplifier passband are generated and also appear within the TWTA's band and would degrade radar performance.

Prior to transmission the output of the amplifier is filtered to ensure that no out of band or harmonic spurious signals generated in the radar are transmitted into neighbouring frequency bands. The signal then passes through the duplexer into the antenna for radiating into free space.

2.1.9.3   Solid-state amplifiers

The output powers of solid-state transistor amplifiers are typically a few watts or tens of watts, so individually generate far less power than TWTAs. They are being incorporated into phased arrays, which can utilise thousands of the devices in a single radar.

All 'rays' from focus are reflected in
same direction in parallel to axis of
symmetry of dish

Feed horn

Feed horn is positioned
at focus of dish

Antenna aperture shown in
two dimensions and is
circularly symmetric for
parabolic dish

Antenna aperture
shown in one dimension

Radar signal from feed horn illuminating
antenna aperture
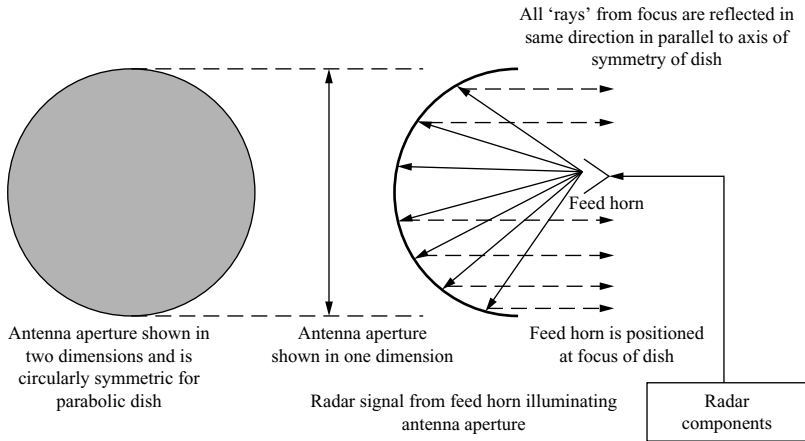
Radar
components

*Figure 2.18   Aperture of dish antenna illuminated by feed horn for transmitting
radar signal*

They do not have the same design complexities associated with vacuum tubes, but
cooling of the modules and mutual interference between them are often critical issues.

2.1.10   Antenna

2.1.10.1   Introduction

The first function of the antenna is to act as a transducer that transforms the microwave
signal generated in the radar's electronic circuitry to an electromagnetic wave propa-
gating in free space. It gives directionality to the transmitted signal and concentrates
the energy appropriately. The second and equally important function is to collect the
reflected energy from targets and to transform the received electromagnetic wave into
a microwave signal and direct it into the radar receiver.

The essence of antenna design is based upon the application of electromagnetic
theory and Maxwell's equations [37]. In Figure 2.18, the function of the antenna
is shown for transmitting the radar signal using a parabolic dish antenna, which is
discussed in Section 2.1.10.8. After the signal is generated by the radar's electronic
components, it is transmitted through a device, such as a feed horn, which is designed
to illuminate the antenna aperture with the electromagnetic signal. In this process
the electromagnetic signal has been transferred from propagating through wires and
cables in electrical circuits to a wave in free space.

The feed horn is designed to generate electric (and magnetic) fields, which prop-
agate to the antenna aperture, so that the aperture is given the amplitude and phase
distribrution across it necessary to provide the propagated radar beam. These ampli-
tude and phase values are designed to provide a well-formed radar beam in the 'far
field' at ranges appropriate to detect targets of interest. At every position on the
antenna aperture, which for the case shown is every position on the parabolic dish,
the values of the amplitude and the phase are defined.
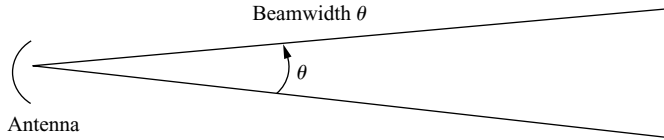
Figure 2.19　Main beam of antenna: energy is concentrated in one direction
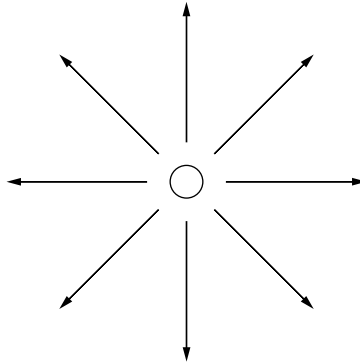
Figure 2.20　'Reference' antenna transmitting power uniformly in all directions

The beam shape generated by the antenna is the Fourier transform [38–42] of the electric field distribution across the aperture. This means that the physical dimensions of the antenna aperture and the amplitude and phase values of the electric field across it define the shape of the radar beam that transmits the radar signal.

In Figure 2.19, the main beam of the antenna is shown and represents the angle in which most of the transmitted energy is directed. If any energy is transmitted in other directions they are called the antenna sidelobes.

The main antenna design parameters are discussed in this section and a parabolic dish antenna is presented as an example of a popular design. Phased array antennas are presented later in the chapter after the fundamentals of radar have been covered.

2.1.10.2　Antenna gain

The antenna is said to have 'gain' or directivity in that it concentrates the majority of the transmitter power in one direction. It does this at the expense of all the other directions. The normal measure of antenna gain is to calculate the ratio of the total power transmitted in the main beam using the directional antenna, as shown in Figure 2.19, to the total power that would appear in that same angle if it were all transmitted uniformly in all directions as shown in Figure 2.20.

If the directional antenna has angular dimensions, or beamwidths of θ_A and θ_E in azimuth and elevation, respectively, as shown in Figure 2.21, the actual solid angle of the beam is approximately θ_E multiplied by θ_A or $\theta_E\theta_A$.
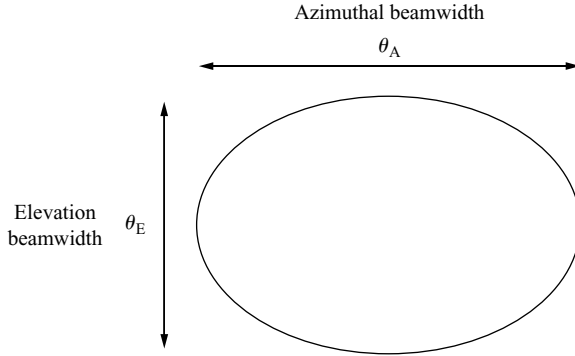
Figure 2.21   Antenna main-beam shape

In the case of the uniform transmission of power in all directions, which is a solid angle of 4π steradians, the power transmitted per steradian is $P/4\pi$. For the directive beam, the power density is the transmitted power divided by the azimuth and elevation beamwidths. Hence, the gain of the antenna is the ratio of the power density of the directive antenna divided by the power density of the reference antenna which is:

$$G_a = \frac{(P/\theta_E\theta_A)}{(P/4\pi)} = \frac{4\pi}{\theta_E\theta_A} \tag{2.18}$$

where G_a = average antenna gain in beam and P = transmitter power

The gain is therefore inversely proportional to the antenna beamwidths and is now derived in the next sections

2.1.10.3   Antenna pattern for uniformly illuminated linear aperture

The antenna pattern for an aperture, which is uniformly illuminated, in one dimension is given by integrating all the contributions to the wavefront from across the aperture. In Figure 2.22, the contribution to the wavefront at an angle α to a line perpendicular to the aperture, from the electric field at position X, at a distance x from the centre of the aperture at position C, is shown. The relative path length to the wavefront is $x\sin\alpha$ and represents a phase contribution of $(2\pi x \sin\alpha)/\lambda$ measured in radians to the wavefront in direction α. The integration for all values of x between $+a/2$ and $-a/2$ gives the strength of the electric field, in the far field at angle, α.

The expression for calculating the strength of the electric field is shown in Equation (2.19), using complex notation:

$$f(\alpha) = \int_{-a/2}^{a/2} Ee^{(2\pi ix \sin\alpha)/\lambda}dx \tag{2.19}$$

where α = angle, x = position along aperture, E = electric field amplitude and $f(\alpha)$ = signal as a function of angle in far field.
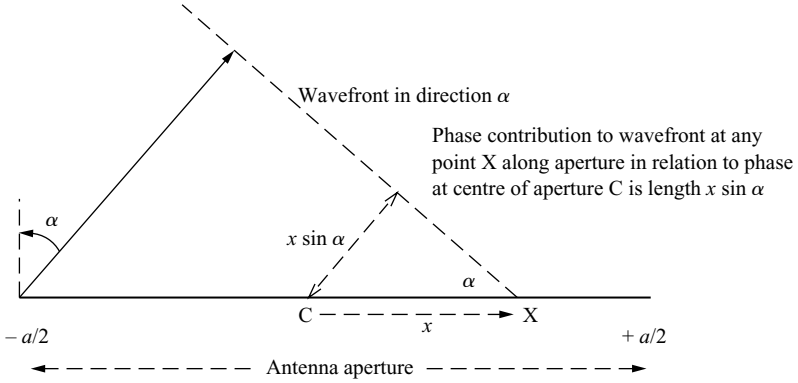
Figure 2.22   Contribution to wavefront at angle α to antenna bore-sight for uniformly illuminated aperture
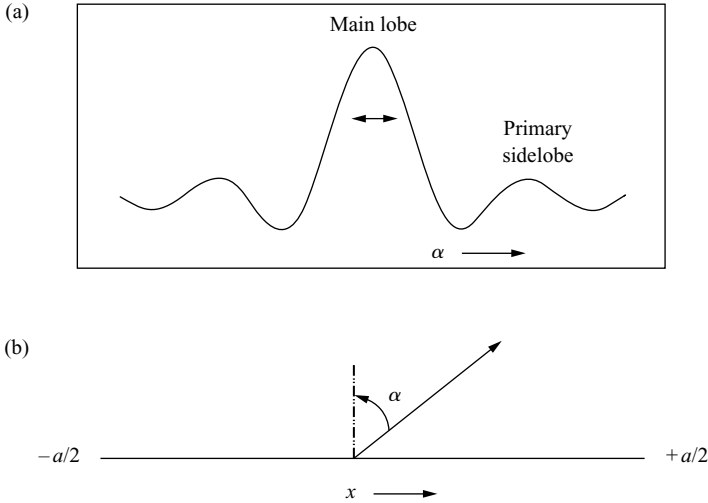
Figure 2.23   Antenna pattern for uniform aperture: (a) electric field strength variation with angle and (b) antenna aperture

This is evaluated as:

$$f(\alpha) = Ea \left\{ \frac{[\sin \pi (a/\lambda) \sin \alpha]}{(\pi \alpha/\lambda) \sin \alpha} \right\} \tag{2.20a}$$

Normalising this function to have a value of unity at $\alpha = 0°$, gives:

$$f(\alpha) = \left\{ \frac{[\sin \pi (a/\lambda) \sin \alpha]}{(\pi \alpha/\lambda) \sin \alpha} \right\} \tag{2.20b}$$

This is shown in Figure 2.23.

The antenna's main lobe can be seen with sidelobes also appearing. In order to reduce the level of the antenna sidelobes, a weighting function is normally applied [43], which is the subject of Section 2.1.10.5. The power function, $P(\alpha)$, is the square of the $f(\alpha)$.

$$P(\alpha) = f(\alpha)^2 = \left\{ \frac{\sin^2\left[(\pi a/\lambda)\sin\alpha\right]}{(\pi\alpha/\lambda)^2\sin^2\alpha} \right\} \tag{2.21a}$$

The half power beamwidth, $\theta \approx 0.84\lambda/a$ \hfill (2.21b)

From (2.21b) the half power beamwidth, θ, of a uniformly illuminated antenna has a value of approximately λ/a. The relationship between the antenna length, the wavelength and the beamwidth is typically as follows:

$$\theta = \frac{k\lambda}{a} \tag{2.22}$$

where $a =$ length of antenna aperture in plane of angle θ and $k =$ constant (typically has value between 1 and 2 and is dependent upon weighting function used).

2.1.10.4   Antenna gain and aperture

Equation (2.22) relates the antenna aperture length required at a particular frequency to obtain a specified beamwidth. Hence, for a square aperture of area A and using a value of $k = 1$, then $\theta^2 \approx \lambda^2/A$.

Applying (2.18) and taking into account the antenna efficiency η gives:

$$G_p = \frac{4\pi\eta}{\theta^2} = \frac{4\pi A\eta}{\lambda^2} \tag{2.23a}$$

where $G_p =$ peak antenna gain, $A =$ area of antenna aperture, $\lambda =$ wavelength of transmitted signal and $\eta =$ antenna efficiency.

$$A_e = \eta A \tag{2.23b}$$

where $A_e =$ effective antenna area.

The actual peak gain of an antenna is wave length dependent [44] as is shown in Equation (2.23a). However, the theoretical value of gain stated is not achieved in practice, due to various losses in the antenna and feed network. The gain is reduced by an efficiency factor, η, which is included, and has a value less than unity. It is the ratio of the antenna gain actually obtained to the theoretical gain achieved by a perfect antenna of the same physical aperture. As the gain is proportional to the antenna aperture, the effective antenna aperture is defined as the physical aperture multiplied by the antenna efficiency, as shown in (2.23b). The factor $A\eta$ appearing in (2.23a) can be replaced by A_e.

For a given antenna aperture the gain increases as the square of the wavelength. Also at a constant wavelength, the gain is proportional to the size of the aperture.
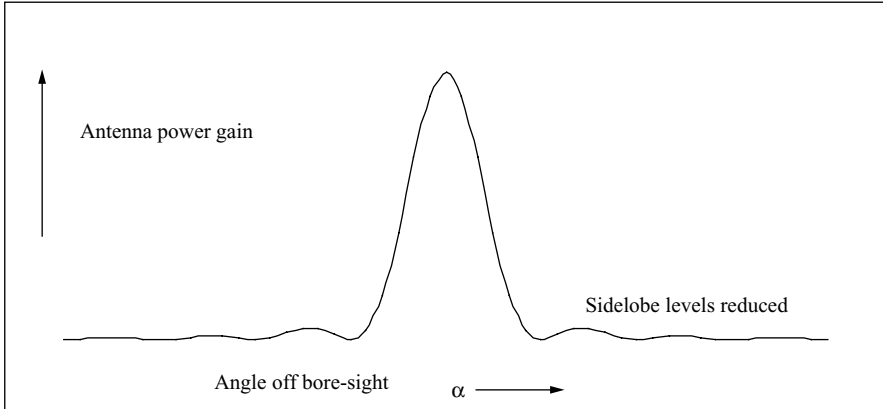
Figure 2.24 Antenna beam pattern with reduced sidelobe levels using weighting function

2.1.10.5 Antenna sidelobe reduction

The primary sidelobes shown in Figure 2.23(a) are about 13 dB down from the peak antenna gain. This is not good enough for most applications, so weighting functions are used to reduce the levels to typically well below 30 dB. In order to reduce the level of the energy transmitted in the antenna sidelobes, a weighting function is applied across the aperture, so there is no longer a uniform electric field across it. This can be achieved by modifying the design of the horn, which illuminates the aperture, to provide specific non-uniform electric field values at the aperture.

Figure 2.24 shows qualitatively the result of applying a weighting function across the aperture. It can be seen that the sidelobe levels are reduced, but the antenna gain also tends to be reduced, but to a much lesser extent. The beamwidth also increases.

Some examples of many possible weighting functions are shown in Table 2.2. The values of associated antenna gain reduction, broadening of the beamwidth and the relative intensity of the first antenna sidelobe compared with employing no weighting function are presented and have been derived from Reference 45.

It can be seen that the various values of the performance parameters can be optimised and traded with others. As the level of the peak sidelobe is reduced, the value of the peak antenna gain tends to reduce and the beamwidth increases. The weighting function selected is application dependent.

2.1.10.6 Collecting area of antenna aperture on receiving signals

The antenna has been discussed from the transmitting point of view so far. For receiving the signal, it is the aperture's collecting area and beam pattern that are important (Figure 2.25).

Interestingly the antenna beamshape pattern is the same on transmitting as receiving for most conventional dish-type antennas, as a consequence of Maxwell's equations. This means that the sidelobe levels are exactly the same in both cases.

Table 2.2   Effects of weighting functions on antenna performance parameters

Weighting function	Gain loss (dB)	Beamwidth broadening (%)	Intensity of first sidelobe relative to peak gain (dB)
None	0	0	−13
$\cos^2$	1.7	62.7	−32
Triangular	1.25	43.1	−26.4
Circular	0.63	14.7	−17.6

Radar waves reflected from target

Collecting area of antenna aperture
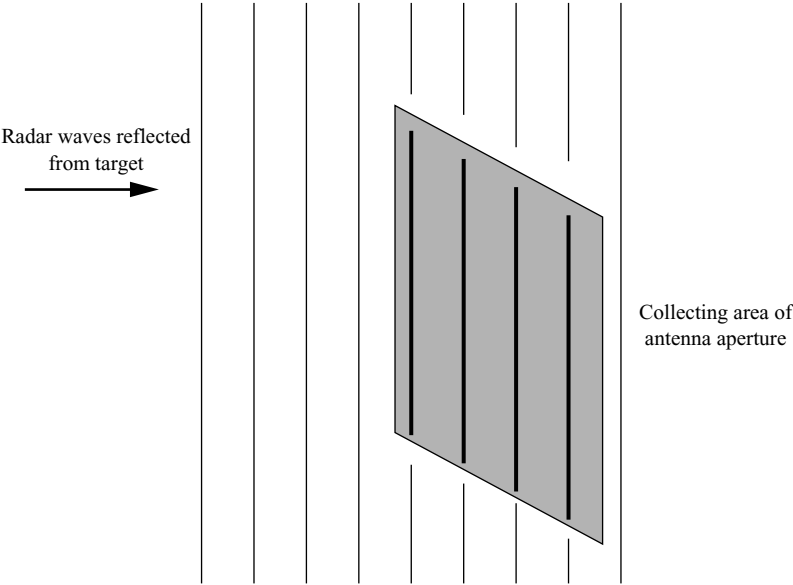
Figure 2.25   Antenna using its aperture to collect signal reflected from target

However, the sidelobe performance is critical for receiving the signal as it determines how much extraneous interference can enter the antenna through the sidelobes. The principles outlined in this section are general for all antennas. However, phased array radars are a type of radar which use a special antenna design and are discussed later in this chapter.

2.1.10.7   Rotating radar antenna to detect targets

The most simple radar antenna that scans searching for targets, rotates at a constant rate and has a single radar beam that has a constant elevation angle coverage. This
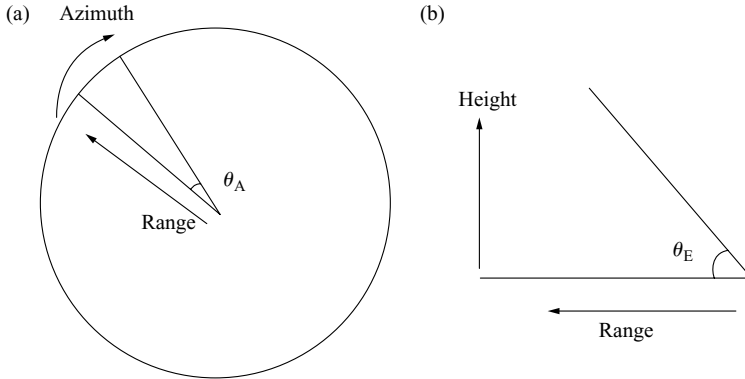
Figure 2.26   Antenna scanning: (a) radar antenna viewed from above: antenna is rotating clockwise and (b) antenna's elevation coverage

is shown in Figure 2.26 and can be compared to a searchlight. In Figure 2.26(a), the radar antenna is at the centre of the circle and is viewed from above. It is rotating its antenna beam of width, θ_A, in a horizontal plane. The beam coverage in elevation is shown in Figure 2.26(b). As the radar antenna rotates, the beam continuously sweeps round covering 360° in azimuth in typically a few seconds. Clearly, it cannot detect targets above its elevation beam coverage. Hence the antenna angular coverage is 360° in azimuth by θ_E in elevation and is able to detect targets to a maximum range appropriate to its sensitivity. It is not absolutely necessary for the elevation coverage to start from the horizon, so the minimum elevation angle could be at least several degrees.

Although the antenna is constantly rotating and it may be typically pointing in a given direction for only a few thousandths or hundredths of a second, this time slot would be sufficient for pulses to be transmitted by the radar and received, allowing targets to be detected. Some designs of antenna allow the beam to scan in elevation also, which increases the elevation angular coverage.

The antenna beam illuminates the target for a time T_{dwell} which is equal to the rotational period of the antenna, T_p, multiplied by the antenna azimuthal beamwidth, θ_A, divided by 360°, that is, $T_{dwell} = T_p \theta_A / 360$.

2.1.10.8   Parabolic dish antenna

A very well-known antenna design is the parabolic dish. An example is shown in Figure 2.27, which has different azimuthal and elevation beamwidths and hence different respective linear dimensions. A very useful property of the parabola is that all rays parallel to its axis of symmetry are reflected from the dish and pass through the focus. In addition, all the path lengths for the rays are exactly the same, so all the phases are correct. Designs based on these principles are advantageous for supporting high-range resolution modes and are discussed in Section 9.2.

Figure 2.27   Parabolic dish antenna (Courtesy of BAE Systems Insyte)

All 'rays' parallel to axis of symmetry of
dish are brought to a focus

Feed horn is positioned
at focus of dish
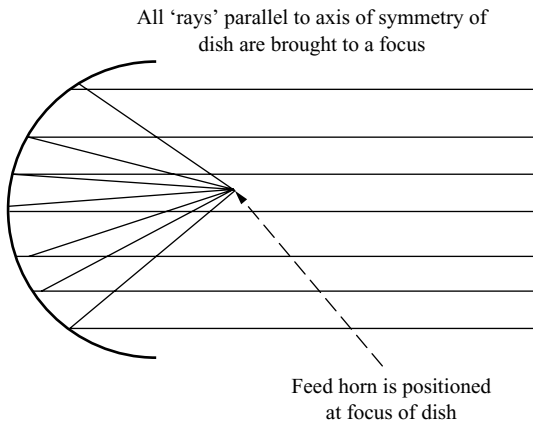
Figure 2.28   Theory of operation of parabolic dish antenna

In order to illuminate the dish a small feed horn is installed at the focus. This normally has an associated weighting function for minimising antenna sidelobes. On receiving the radar signal, the horn collects the radar wave after being reflected from the dish. One small disadvantage is that the feed horn partially obscures the aperture, which is called blockage, but this generally has only a small effect on the antenna gain and beamwidth.

Phased array antennas are discussed in Section 2.1.23, as their theory of operation can be best appreciated after other aspects of radar are covered first.

2.1.11   Doppler effect

2.1.11.1   Doppler frequency derivation

The Doppler effect [46] is illustrated in Figure 2.29. The transmitted radar signal propagates through space and is reflected from the target, at range, R, which is moving
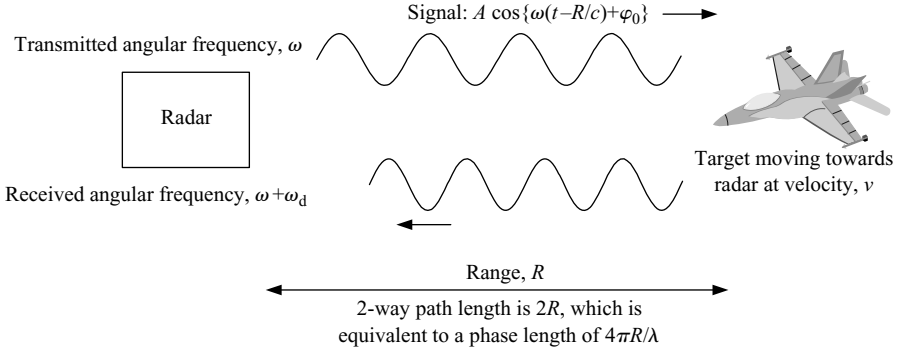
Figure 2.29   Doppler effect: the signal is shifted by angular frequency ω_d

towards the radar with a radial velocity component v. In the radar, a reference oscillator is used for phase comparison purposes with the received signal. This type of modern radar design is called a 'coherent pulse Doppler radar' and is most important for target recognition applications.

An electromagnetic wave propagating from the radar to the target [47], is given by:

$$x = A(R)\cos\{\omega(t - R/c) + \varphi_0\} \tag{2.24}$$

where x is the instantaneous amplitude of the wave, R is the range, $A(R)$ is the peak amplitude of the wave, which is range dependent, φ_0 is the starting phase on leaving the radar, t is the time with respect to a reference, c is the speed of light and ω is the angular frequency $= 2\pi f$

The electromagnetic wave is reflected from the target at range, R, and the two-way path length for the signal is a distance, $2R$. The signal received at the radar from a target at range R has a phase, which is given by:

$$\varphi = \omega\left(t - \frac{2R}{c}\right) + \varphi_0 + \varphi_t \tag{2.25}$$

where φ_t is the phase change of the signal at the target.

Frequency is defined as the rate of change of phase with time. The angular frequency of the returned signal measured at the radar is the rate of change of phase, φ, in Equation (2.25) and has units of radians:

$$\frac{d\varphi}{dt} = \frac{d\{\omega(t - 2R/c) + \varphi_0 + \varphi_t\}}{dt}$$

$$= \omega + \frac{d(-2R\omega/c)}{dt}$$
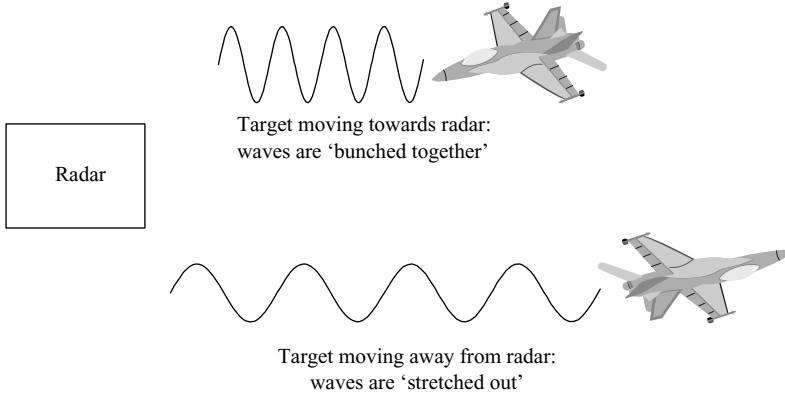
Figure 2.30   Illustration of Doppler effect

As the target is approaching, the rate of change of range with time is a negative quantity, so:

$$\frac{d\varphi}{dt} = \omega + \frac{2v\omega}{c} \text{ (in radians per second)}$$

$$f_r = f + \frac{2vf}{c} \text{ (in hertz)} \tag{2.26}$$

where velocity, $v = -dR/dt$ for closing target, f_r = received frequency and f_d = Doppler frequency = $2vf/c$.

With reference to Equation (2.26), there are two terms. The first is the electromagnetic wave's frequency. The second is the dependence on the target's radial velocity vector, which gives rise to the Doppler term associated with the change of range of a moving target.

Equation (2.26) is for the well-known Doppler effect and the term $2vf/c$ is a constant rate of change of phase with time, which is a frequency, known as the Doppler frequency, f_d. The radar receiver effectively detects a received radar pulse with a shifted frequency. This is similar to the experience of hearing the change of frequency of a police car siren, which has an increased frequency when it is closing and a decreased frequency on receding. The Doppler effect is most important in radar and is used very widely for detecting moving targets in the presence of background clutter.

The Doppler effect is illustrated in Figure 2.30. For a closing target, the aircraft is effectively shortening the wavelength of the incident wave by moving towards it. The time between two wavefront peaks or troughs, reflected from the target, is reduced by virtue of the closing motion. As the wavelength is defined by the distance between two peaks (or troughs) of the wavefront, it is shortened by this effect and the frequency correspondingly increases. The opposite effect happens for a receding target. The aircraft is moving away and the peaks and troughs of the wave are slightly more spread out than for a stationary target, and the wavelength is extended by the
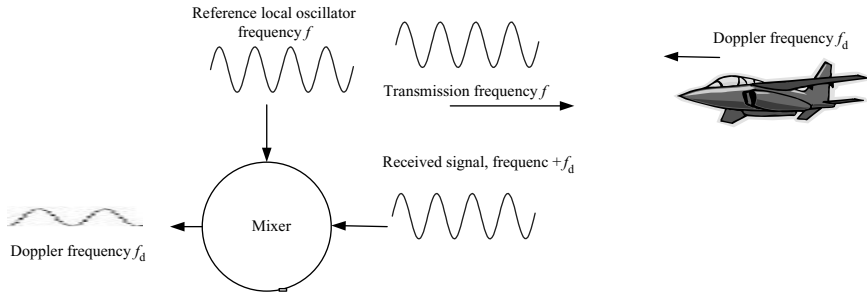
Figure 2.31   Doppler radar concept

target's motion. As the frequency is inversely proportional to the wavelength, the frequency due to a closing target increases.

2.1.11.2   Pulse Doppler radar concept

For coherent pulse Doppler radars [48–50], phase is a key parameter that the radar measures and is important for the high-resolution target recognition modes. As well as measuring the time delay to the target, the phase of the returned signal relative to that transmitted is also measured.

Conceptually, the operation of a coherent Doppler radar is shown in Figure 2.31 for a single pulse and a single receiver channel. In-phase and quadrature channels would normally be used and are discussed Section 2.1.15.2.

It is necessary to utilise the reference frequency, f, which should be the same as the transmitted frequency. In the receiver the mixer subtracts the reference signal and the received signal with the Doppler shift, to obtain the Doppler shifted signal. Doppler frequencies ranging from tens of hertz to tens of kilohertz are typically measured by radars, which have operating frequencies of thousands of millions of hertz. The ratio of the Doppler frequency to the radar frequency is typically about one million, so extremely small relative changes in frequency have to be measured by the radar to detect the Doppler frequency due to the target.

It can be seen that it is necessary to have a stable local oscillator (STALO), which does not drift in frequency in the time taken to transmit and receive the signal, otherwise it would not be possible to detect or measure the Doppler frequency with any reliability. This topic will be discussed in more detail later in the chapter under the heading of phase noise.

2.1.11.3   Pulse Doppler burst

The concept just described demonstrates how the Doppler frequency may be extracted from a single pulse. For normal pulsed radars, the Doppler frequency is detected over the whole radar pulse train, rather than on the basis of a single pulse. The measurement of the Doppler frequency over a pulse train is illustrated in Figure 2.32. The received signal Figure 2.32(b) is mixed with the reference of the transmitted signal Figure 2.32(a) to generate the signal shown in Figure 2.32(c). In this case the Doppler
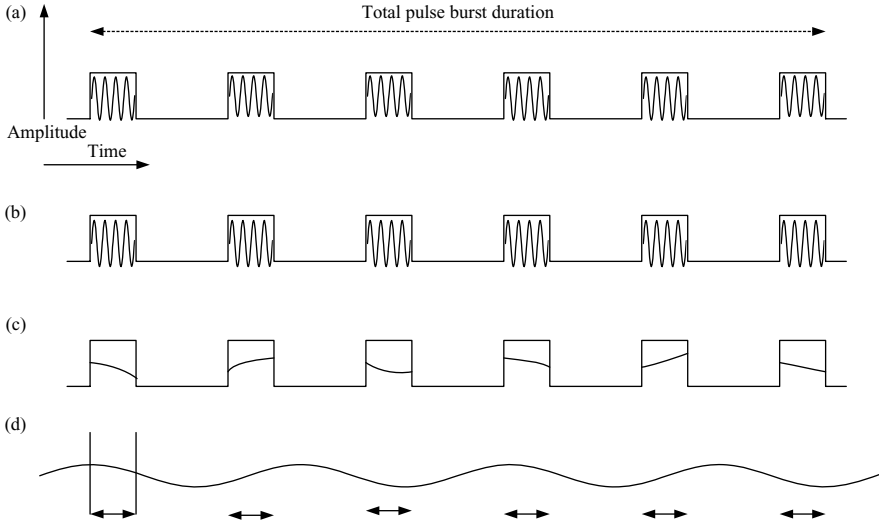
Figure 2.32   *Measuring Doppler frequency across pulse train: (a) transmission fre-*
quency f ; (b) received signal frequency f + f_d; (c) sampled Doppler
frequency f_d and (d) full Doppler frequency signal f_d

frequency is relatively low and only a fraction of a cycle appears across any one
pulse. In order to detect and measure the Doppler signal, it is necessary to combine
the contributions from each pulse in the pulse train.

In a coherent pulse Doppler radar the amplitude and phase of each pulse Figure
2.32(d) are measured in the radar receiver, so one complex data sample is obtained
from each pulse. Effectively the radar receiver measures the average values of these
parameters over the pulse's duration. The analogue signals described above will be
digitised in an ADC and digital representations of the signal will be operated on in
the radar signal processor, which will be described later in this chapter. This data
obtained is the time domain representation, $f_{\text{sig}}(t_n)$, of the N received Doppler signal
pulses and is of the form:

$$f_{\text{sig}}(t_0), f_{\text{sig}}(t_1), f_{\text{sig}}(t_2), \ldots, f_{\text{sig}}(t_{N-1}) \text{ for } N \text{ radar pulses}$$

In order to establish the frequency of samples of a signal that are not continuous, but
are discrete, it is necessary to perform a discrete Fourier transform [51–55] on the
data, which will transform this time domain data into frequency domain components.
This transform effectively takes the discontinuous signal sampled in Figure 2.32(c)
and converts it into a frequency representing the full signal shown in Figure 2.32(d).
The discrete Fourier transform of the N complex data samples is:

$$f_{\text{sig}}(f_k) = \sum_{n=0}^{N-1} f \, \text{sig}(t_n) e^{-2\pi i f_k t_n} \tag{2.27}$$

where f_k = discrete frequency component, k, t_n = time of measurement of sample, n and $f_{sig}(f_k)$ = frequency transform of time domain signal $f_{sig}(t_n)$.

This Fourier transformation process is taking time domain information from the radar signal and converting it into frequency domain information to provide the Doppler frequency. This enables the individual frequency components to be detected and for the Doppler effect to be measured. This has a loose analogy to the operation of a radio or television receiver. Signals are sent out by the transmitter at different frequencies, associated with different programmes being broadcast, in time sequence, and are detected by the receiver. When a radio receiver is being tuned manually, an electrical circuit is filtering the incoming signals and selecting the one of interest. The Fourier transform effectively takes all the signals from different targets with different velocities, and hence Doppler frequencies at once, into parallel receivers tuned to the different filter channels representing the different frequencies of the signals and assesses the strength of the signal in each receiver. The large signals are due to the strongest returns from radar targets.

2.1.12   Thermal noise

2.1.12.1   Noise temperature

Before discussing the radar receiver, thermal noise is presented, which is very often the key factor in determining the sensitivity of a radar and its associated target detection performance. From the theory of thermodynamics [56,57], in every conductor of electricity, electrons are in continuous random motion and are in thermal equilibrium with the molecules of the conductor. For a resistor at a temperature, T, relative to absolute zero ($-273°C$ or 0K) which is not connected to any source of power, such as a battery, is producing electrical noise as follows:

$$P_r = kTB \tag{2.28}$$

where P_r has units of W/Hz, k = Boltzmann's constant = 1.38×10^{-23} joules/K and B = bandwidth of system.

The energy that the resistor is producing is due to its thermal equilibrium with the environment. If it is connected to an electrical circuit, it is losing this noise energy to the circuit, in accordance with Equation (2.28), but from the laws of thermodynamics, this lost energy is being continuously replaced by being transferred via thermal agitation of molecules. As an example, at a temperature of $17°C$, or 290 K, the power generated by the resistor is of the order of 4×10^{-23} W/Hz. The power available is proportional to the bandwidth of the circuit. A resistor, which is at a physical temperature, T, is defined to have an effective noise temperature T. As the noise power available from a source of noise is directly proportional to the absolute temperature of the noise source, it is stated to have a noise temperature in Kelvin.

The statistics of thermal noise are Gaussian [58] and this distribution is shown in Figure 2.33.

$$P(V_N) = \frac{1}{\sigma\sqrt{2\pi}}e^{-V_N^2/2\sigma^2} \tag{2.29}$$
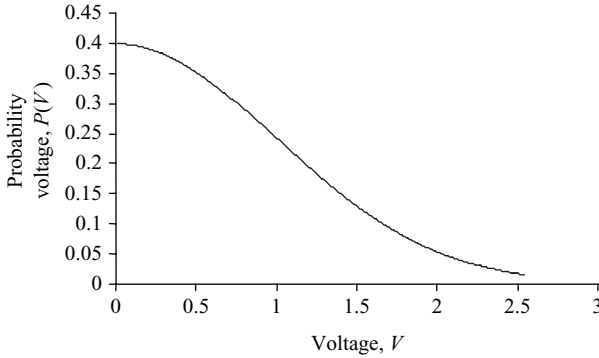
Figure 2.33   Noise has a Gaussian probability density function: standard deviation of noise voltage, σ, chosen to have value 1

where $P(V_N)$ = probability of noise voltage, V_N and σ = standard deviation of noise probability distribution.

The noise generated by a source is dependent upon its temperature T and follows these statistics. The mean level value of the noise voltage is also its standard deviation. As noise is generated by random processes, there is a finite, albeit a small, probability that it can have values significantly larger than its mean value, which could be mistaken for a target and would then be called a false alarm. In radar, the detection of small signals is critically dependent upon understanding the level of noise present and its statistics. This will be discussed in more detail in the section on signal processing and target detection.

2.1.12.2   Noise figure

The term noise figure (NF) [59] is used for radar and communication receivers as a means of expressing a measure of their sensitivity. As receivers are constructed from materials that have some resistive characteristics, which absorb and radiate thermal noise, they exhibit noise effects similar to the resistor discussed above. The NF of a receiver is defined as the ratio of the noise output of the receiver divided by the noise measured at the output of an ideal receiver. The ideal receiver contributes no noise of its own and any noise measured is due to external sources.

This statement is interpreted to mean the ratio of:

- The power at the output of the receiver, due to the receiver's own noise plus the amplified value of the reference input noise.
- To the amplified value of the reference input noise alone.

All these measurements are made in the receiver's bandwidth of interest.

Consider an amplifier with an effective noise temperature of T_E and a power gain of G, as shown in Figure 2.34. The noise contribution, due to the amplifier, is defined as being equivalent to a resistor at temperature, T_E, its effective temperature.
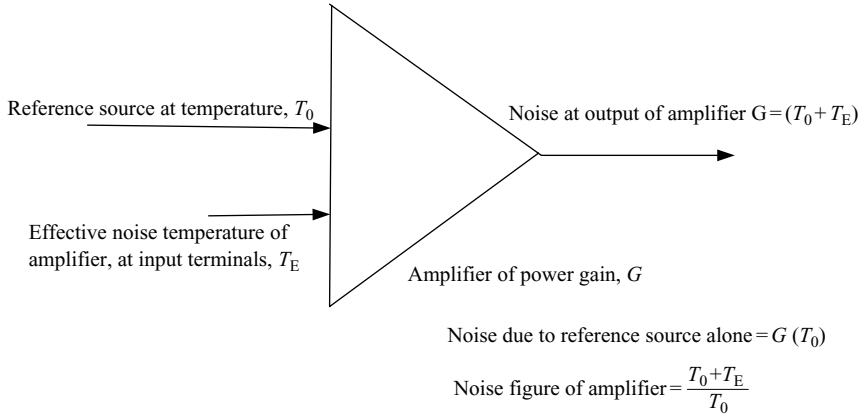
Figure 2.34   Noise figure of an amplifier

From the definition and using Equation (2.28), the total noise power at the output is:

$$P_{\text{out}} = Gk(T_0 + T_{\text{E}})B \tag{2.30}$$

where G = amplifier power gain.

The power at the output due to the reference source at T_0 is:

$$P_o = GkT_0B \tag{2.31}$$

The NF of the amplifier is given as the ratio of P_{out} to P_o:

$$NF = \frac{Gk(T_0 + T_{\text{E}})B}{Gk(T_0)B} = \frac{T_0 + T_{\text{E}}}{T_0} \tag{2.32a}$$

where NF = noise figure of amplifier, and $T_0 = 290$ K. It is normally expresssed in dB, as $10 \log_{10}(NF)$.

Also total noise $= T_0 + T_{\text{E}} = (NF)T_0$ (2.32b)

2.1.12.3   Passive component noise

In addition to amplifiers having noise figures or effective noise temperatures, passive components, such as antennas and filters, do also. Antennas have an effective NF due to thermal effects in the antenna and due to the environment. Within the antenna there are resistive effects due to currents flowing, which lead to attenuation of the signal and the generation of noise. The direction in which the antenna, and in some circumstances the antenna sidelobes, are pointing is important. Any ground or sea, which the antenna is illuminating, is at the ambient temperature and has some conductivity, so generates noise. This noise enters the antenna in the same way that a signal would and contributes to the effective noise temperature of the antenna. When it

Antenna noise
temperature, T_A

Gain, G_{LNA}

Gain, G_2
T_2

Gain, G_3
T_3

LNA noise temperature T_{LNA}

Noise temperature $= T = T_A + T_{LNA} + T_2/G_{LNA} + T_3/(G_{LNA} G_2)$
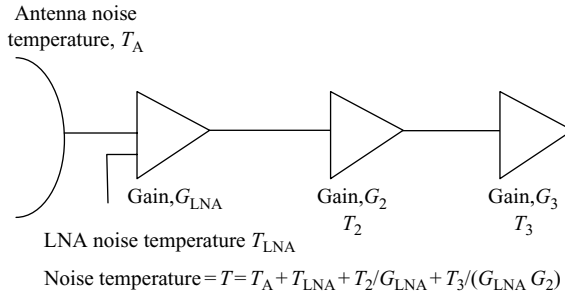
Figure 2.35   Noise temperature calculation for radar receiver with several amplifier stages

is pointing towards the sky and outer space, which are generally cooler, there is less noise generated and the antenna's effective noise temperature is less. Hence, the level of noise entering the radar through the antenna varies with the direction in which it is pointing and also with the time of day and season.

The NF of a lossy passive component, which reduces the level of the radar signal, is actually equal to the value of loss. For example, a component which attenuates the signal by a factor of 2 in power or 3 dB, has a 3 dB NF.

2.1.12.4   Cascaded noise figure

The noise temperature, T, of a radar system is dependent on all the components in the receiver chain. However, the most important factors are the resistive losses at the front end of the receiver and the NF of the first amplifier in the receiver chain. Losses and the NFs of the components further back in the receiver chain have little effect on the overall NF. As a result of the front end amplification, the signal levels in these back end components are much greater than the noise they generate. This can be seen in Figure 2.35. The second and third amplifiers have signal levels well above the system noise floor. Effectively the noise temperatures of these components are divided by the amount of amplifier gain preceding them [60]. The noise temperature is dominated by the low noise amplifier (LNA) and the antenna. The total receiver noise with respect to the antenna is given by the receiver noise temperature multiplied by Boltzmann's constant and the receiver bandwidth.

2.1.13   Phase noise

Phase noise is generated in radar components and is dependent on the physics and designs of the actual devices. The main components exhibiting phase noise characteristics, which are of most interest to the radar designer, are solid state and TWTAs, oscillators, frequency multipliers and frequency sources.

Phase noise [61–63] is any deviation of the phase of a signal from a perfect sine wave. It is a modulation on the phase of the signal. Phase noise is defined as the power that is measured in a 1 Hz bandwidth, at a particular offset frequency from the carrier,

For sinusoidal signal phase increments constantly: phase noise causes deviations

A

Phase noise is any modulation on phase, θ, which is deviation from constant phase change with time

θ

Figure 2.36   Phase noise

Relative power to carrier, dBc/Hz

Frequency offset from carrier, Hz
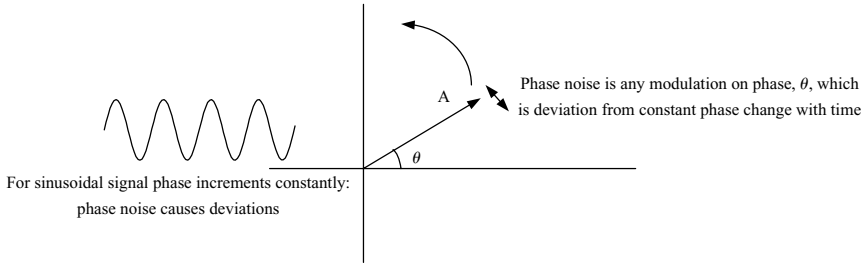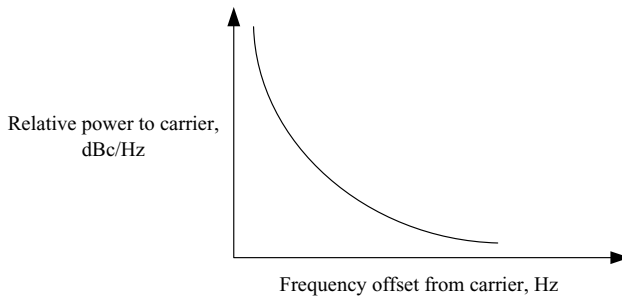
Figure 2.37   Representing phase noise as a noise power level versus frequency plot

relative to the full power of the signal. It has units of dB below the carrier, dBc/Hz. A typical value for a crystal oscillator is $-100 \, dBc/Hz$ at 1 kHz offset from the carrier.

Phase noise can occur due to random collisions between electrons and in semiconductors [64] due to random movements of electrons across potential barriers, such as diode or transistor junctions (Figure 2.36).

Figure 2.37 illustrates how phase noise can be represented for a component or system. At any particular frequency offset from the radar carrier frequency, there is a value of noise power that is relative to all the power in the signal.

In Section 2.1.11, the Doppler effect was presented. It was stated that a very small change in frequency of the signal had to be measured to detect moving targets using the Doppler effect. The challenge to radar engineers is to ensure that in the presence of large returns, such as ground clutter, the target can be seen.

The effects of phase noise on detecting a small target in the presence of clutter are shown in Figure 2.38. In Figure 2.38(a) the target and clutter are shown and can be differentiated by their Doppler frequencies for the case of a radar exhibiting no phase noise. In Figure 2.38(b) is the case in which the radar has phase noise and this manifests itself effectively by spreading the clutter out in the frequency domain and obscuring the target. The actual value of the frequency spreading is dependent on the level of the clutter signal, the radar's phase noise characteristics and the target range [65]. This is particularly important for high-resolution radars, which dissect the target into small elements with small radar cross-sections (rcs).
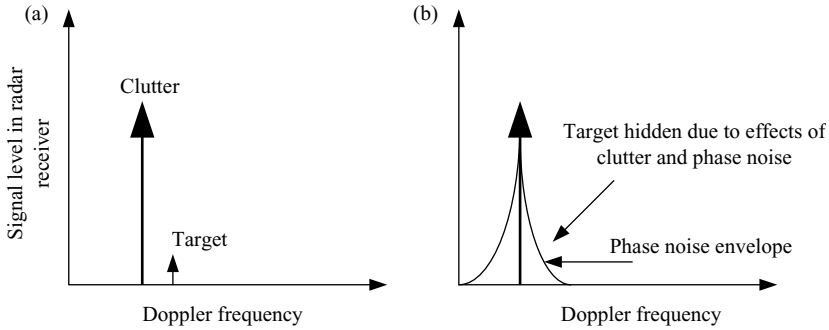
Figure 2.38   In the presence of phase noise, small targets can be obscured by clutter: (a) clutter and signal levels with no phase noise present and (b) clutter and signal levels with phase noise present
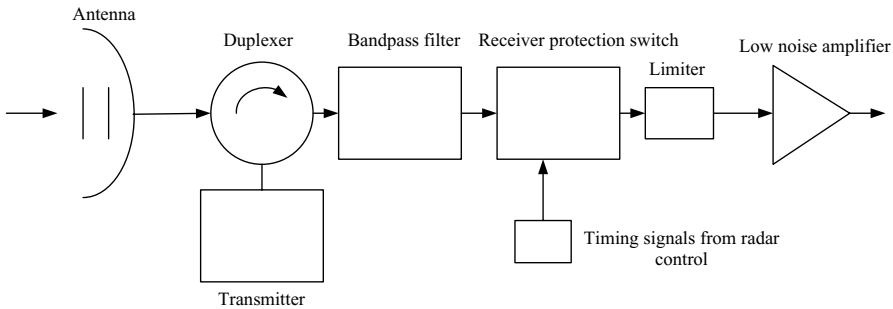
Figure 2.39   Receiver front end

2.1.14   Receiver front end

The main components comprising the front end of the radar receiver are shown in Figure 2.39. After receiving the signal in the antenna, it is directed through the duplexer into the receiver. Initially, signals, which are outside of the radar's frequency band of operation, are filtered out. This is to avoid either damaging the radar receiver due to overload or saturation effects, which would degrade operation. In contrast, the receiver protection switch [66] is designed to protect the radar receiver from its own transmitted signals. This type of switch is normally based on PIN diode technology [67,68]. It is switched into two attenuation states by timing signals from the radar's timing and control circuits. When the radar is transmitting, the switch is set in a high attenuation mode, so that any residual signal, which has not been transmitted and leaks through the duplexer towards the receiver, can be attenuated, to avoid damaging the receiver. Also, if there are any large nearby targets, which are generally of no interest for radar detection, they could reflect high-level radar returns into the receiver. For this reason the receiver protection switch is usually on longer than the duration of the radar pulse, so that the time taken for the radar signal to be reflected from nearby
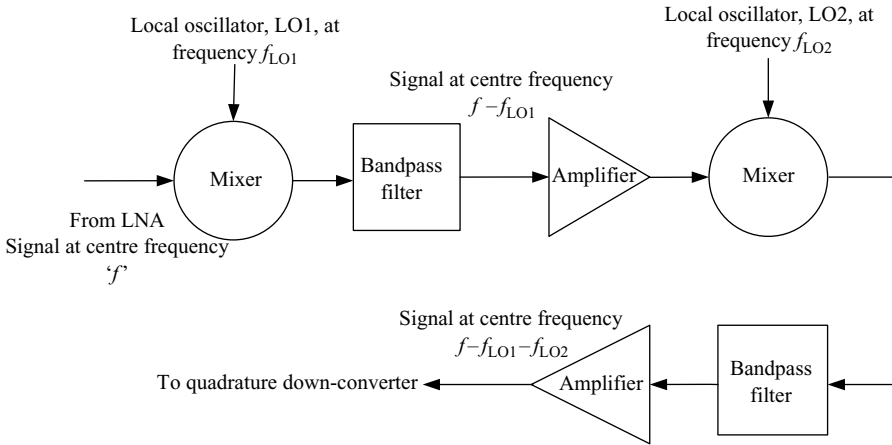
Figure 2.40   Two down-conversion stages

targets is added to the pulse duration. During the radar reception period the switch is set to its low attenuation mode, to allow the receiver to operate with maximum sensitivity.

In high-power radars the PIN diode switches normally are designed to attenuate the highest level signals to relatively low residual power levels entering the LNA. However, LNAs are very sensitive devices and have semi-conductor junctions made of various materials, which include silicon and gallium arsenide [69,70] and have dimensions of the order of microns (one micron is one thousandth of a millimetre). This means that it is prudent to have another layer of defence, to protect the LNA, which is called a limiter [71]. PIN diodes are again used, but are designed to attenuate these lower power leakage signals to safe levels. The limiter circuit is normally incorporated into the LNA, but does not have timing signals controlling the PIN diode's attenuation level. Limiter circuits are designed to react rapidly to signal overloads, by detecting the high-power signal. One method of achieving this is to use a Shottky diode [72] detector, which detects the signal and in so doing, biases the PIN diode into its attenuation mode.

The LNA provides the first stage of amplification in the receiver, prior to the signal being down-converted.

2.1.15   Down-conversion

2.1.15.1   Two-stage conversion

Two stages of down-conversion are shown in Figure 2.40. The signal frequency is reduced in two sequential mixers. After mixing the signal undergoes bandpass filtering to reject unwanted out of band mixing products. It is then amplified to boost the level of the signal, including compensating for the several dB of loss occurring in each mixer. The LO frequencies are both derived from, and coherent with, the master reference oscillator discussed in the section on frequency generation earlier.
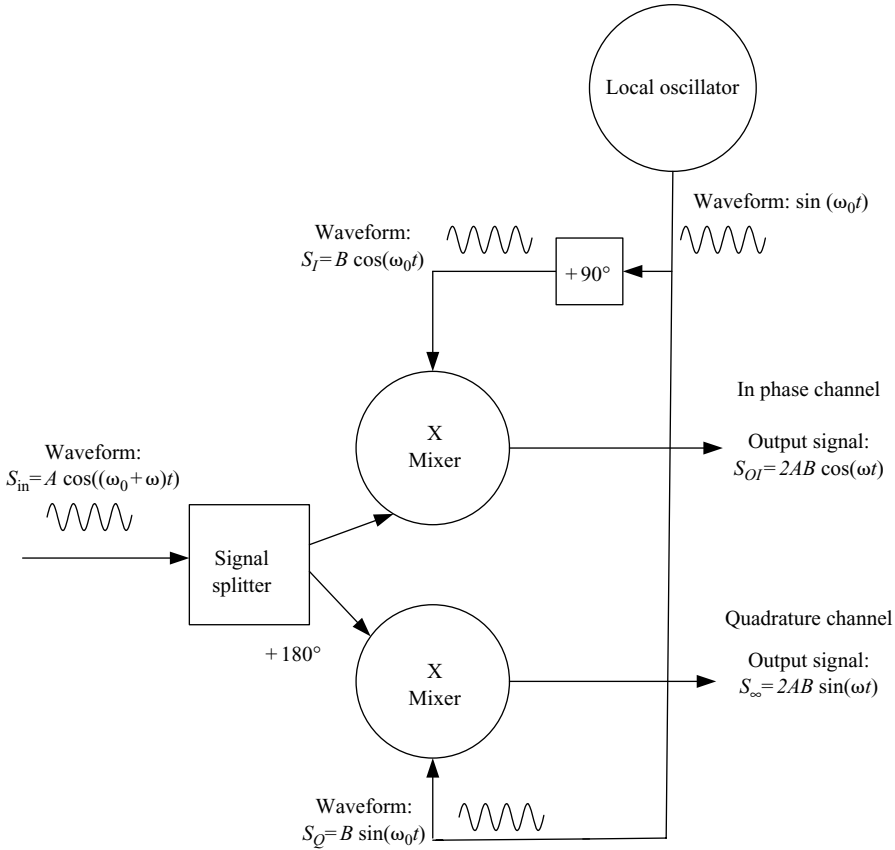
Figure 2.41   Quadrature down-conversion

In some cases, depending on system design constraints and operating frequencies there may be more or fewer mixing stages. Clearly, more mixing stages would be expected for radars, which are operating in the millimetre wavebands for example, at frequencies of several tens of gigahertz.

2.1.15.2   Quadrature down-conversion

The output of the second mixer normally would feed into a quadrature down-converter, which is shown in Figure 2.41, and effectively performs the inverse function of the vector modulator presented earlier. The objective is to convert the signal into in-phase and quadrature channels, enabling the phase information to be extracted, particularly for coherent pulse Doppler signal processing for the detection of moving targets.

The input signal is $S_{in} = A \cos(\omega + \omega_0)t$, which is to undergo the final stage of down conversion, by mixing it with the signal of frequency, ω_0. For the upper mixer

in the diagram, the in-phase component of the LO is used, $S_I = B\cos(\omega_0 t)$. For the lower mixer, the quadrature component of the LO, $S_Q = B\sin(\omega_0 t)$ is used.

Two well-matched frequency mixers are used for the down conversion process. The input signal, S_{in}, is divided equally into two channels by the splitter, with 180° phase change applied to the quadrature channel, and is then applied to the signals to the respective mixers. The LO signals are derived from a reference source to provide radar coherence. In order to provide the correct phase in the mixers, it is necessary to insert 90° phase shift in the in-phase channel in relation to the quadrature channel. After the mixing process, the outputs are low pass filtered, so all signals of frequencies of ω_0 and above are rejected. The non-linear action of the mixer combines the signals at the different frequencies. The output of the mixers is in the form:

$$S_{\text{Mixer}} = (A + B)m_1 + (A + B)^2 m_2 + \cdots + (A + B)^n m_n \tag{2.33}$$

The values 'm_n' represent the transfer function coefficients of the mixer, with the 'm_1' term being the linear component. The 'm_2' term is of interest here, as it provides the non-linearity required for mixing the two input frequencies. The output of the in-phase and quadrature mixers are

$$\begin{aligned}
S_{\text{OI}} &= (S_{in} + S_I)^2 = (A\cos((\omega + \omega_0)t) + B\cos(\omega_0 t))^2 \\
&= AB\cos\omega t \tag{2.34a}
\end{aligned}$$

$$\begin{aligned}
S_{\text{OQ}} &= (S_{in} + S_Q)^2 = (-A\cos((\omega + \omega_0)t) + B\cos(\omega_0 t))^2 \\
&= AB\sin\omega t \quad \text{(after filtering)} \tag{2.34b}
\end{aligned}$$

Hence the in-phase and quadrature components of the signal are generated at the base-band frequency. The critical design parameter for the quadrature down-converter is the in-phase and quadrature balance between the two channels. This means that for input signals for equal in-phase and quadrature components, the two respective output amplitudes are equal. Also for input signals with only one in-phase or quadrature component, there should be no output signal in the other channel. If these are not balanced, after signal processing, an 'image' signal can appear which is the inverse of the velocity of the real target causing possible false alarms in the radar.

The quadrature down-converter is effectively a 'synchronous video detector', for detecting the Doppler signal. The receiver synchronises the LO waveform to that of the carrier frequency of the incoming signal to extract the Doppler frequency.

2.1.16   Receiver dynamic range

2.1.16.1   Sensitivity limit

As was seen in Section 2.1.12, the lower limit of the radar receiver's dynamic range is determined by thermal noise considerations and can also be affected by phase noise generated by various radar components.
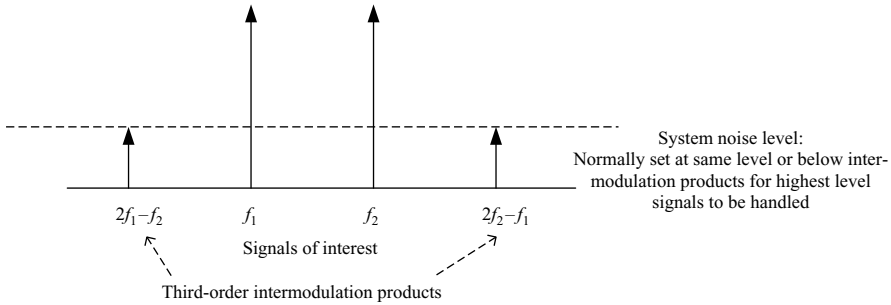
Figure 2.42   Third-order intermodulation products

2.1.16.2   Upper signal level limit

At the other extreme, the receiver performance is limited by too large signals. The main factor limiting high-level signal handling in the analogue part of the radar receiver prior to digitisation is its third-order intercept point [73].

The third-order intermodulation products, $2f_1 - f_2$ and $2f_2 - f_1$, are shown with two radar signals, f_1 and f_2 (Figure 2.42). The third-order signals are significant in that they appear in the radar signal's passband. Consider the following equation representing non-linearity in the radar receiver:

$$V_{Out} = A\{V_1 \cos(\omega_1 t) \text{ and } V_2 \cos(\omega_2 t)\} + B\{V_1 \cos(\omega_1 t) + V_2 \cos(\omega_2 t)\}^2$$

$$+ C\{V_1 \cos(\omega_1 t) + V_2 \cos(\omega_2 t)\}^3 \tag{2.35}$$

where V_{Out} is the output signal, $V_1 \cos(\omega_1 t)$ and $V_2 \cos(\omega_2 t)$ are the input signals

The first '*A*' term is the linear coefficient and provides the frequencies of interest f_1 and f_2. The second-order intercept term, '*B*', produces frequencies at $2f_1, 2f_2, f_1 - f_2$ and $f_2 + f_1$, which are outside of the passband for most radars. The '*C*' term, produces the third-order intercept products at $2f_1 - f_2$ and $2f_2 - f_1$, which are in the radar passband. The main concern about these spurious signals is that they are generated when the Doppler frequencies from two targets mix together in the receiver and can appear to be true targets.

The dynamic range of the analogue parts of the radar receiver is set such that, for the maximum level of signals the radar has to handle, the associated third-order intercept products are at or below the radar noise level, after taking into account the integration of several pulses over a transmission burst.

2.1.17   Analogue to digital converter

2.1.17.1   Digitisation of analogue signal

The radar signal has been analogue since before it was transmitted. In the ADC or digitiser [74,75], it is translated into a digital number enabling it to be rapidly processed using high-speed computers.
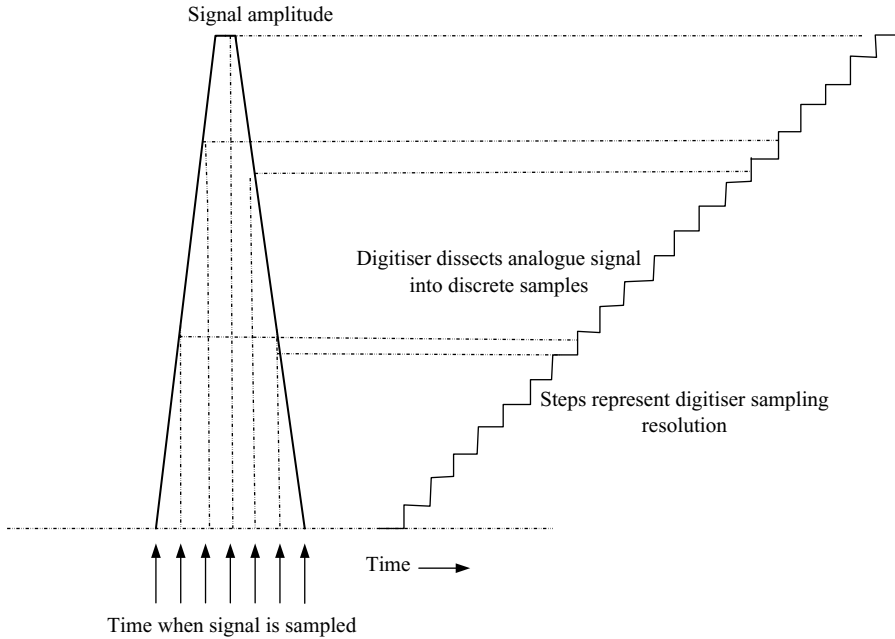
Figure 2.43 Analogue to digital conversion

The basic performance parameter of an ADC is its number of bits, n, which represents 2^n possible signal levels, using the binary system.

The digitisation of a signal is represented in Figure 2.43. The digitiser samples the voltage of the signal, including its polarity, at regular intervals, as shown on the time axis. The steps in the diagram represent the resolution capability of the digitiser. At each time sample point, the analogue signal is partitioned and a number is generated equivalent to the number of virtual steps measured.

2.1.17.2 Number of digitiser bits

For a n-bit digitiser, a binary number with n digits is generated at the ADC sample rate. The largest signal that can be measured using all the bits is a factor of 2^n higher than the smallest possible signal.

As voltage is being measured in a maximum of 2^n states, this corresponds to a dynamic range, DR, which is by convention always specified as a power:

$$DR = 20 \log_{10}(2^n) \tag{2.36}$$

For example, for a 10-bit ADC, the theoretical dynamic range is 60 dB. However, in practice, the theoretical value is not usually achievable and a quantity called the effective number of bits is defined. Hence, a 10-bit digitiser may only have 8 effective bits, so would perform closer to a theoretically perfect 8-bit digitiser. For the radar application, the two digitiser channels are shown in Figure 2.44.
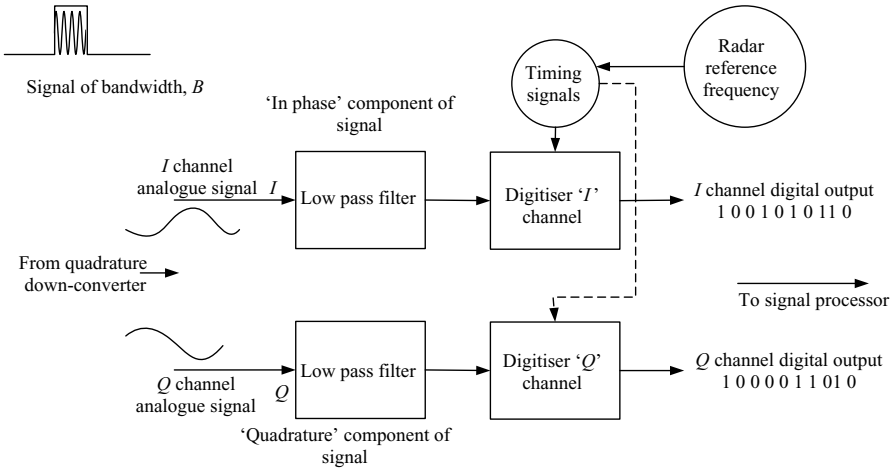
Figure 2.44   In phase and quadrature digitiser channels: Sampling rate must exceed B per second in each channel to meet Nyquist sampling criterion

2.1.17.3   Sampling rate

Before digitisation the signal is low pass filtered appropriate to its bandwidth. This minimises the noise and any extraneous signals entering the digitiser. It is necessary for the two digitiser channels to be balanced so that minimal distortion to the signal occurs. The digitiser samples at a minimum speed appropriate to the Nyquist sampling [76] criterion. It is necessary that the sampling rate of the signal is at least twice as high as the highest frequency signal present. For in phase and quadrature sampling, as presented here, it means that both of the two channels must sample at a rate that is as high as the bandwidth of the analogue signal, prior to quadrature down-conversion. For example, for a radar system with 5 MHz bandwidth, both digitisers must sample at a minimum rate of five million data points per second. It can be seen that at the output, there are two streams of digital radar data, which are at the digitiser sampling rate. The timing of the digitiser samples is governed by the radar's reference frequency and must be synchronised with the other timing functions of the radar. If sampling has met the Nyquist sampling criterion, then the 'I' and 'Q' data stream is a high-fidelity representation of the radar signal, so all the analogue information is held in the digital form.

2.1.17.4   Spurious free dynamic range

In radar applications it is usual to coherently integrate several pulses over a transmission burst. It is necessary for the digitiser to accommodate coherent pulse integration without distortion to the signal. Interestingly, it is possible, and very frequently implemented, to detect signals below the least significant bit of the digitiser. The finite resolution of the ADC produces quantisation levels of plus or minus the lowest significant bit. This means that within a certain range all analogue signals are represented

Pulse length $\Delta\tau$
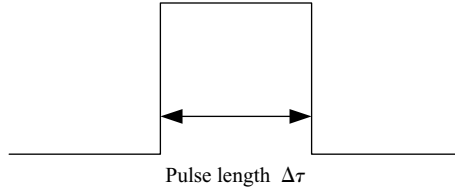
Figure 2.45   Radar pulse of duration $\Delta\tau$

by the same digital number. However, if the sensitivity limit of the digitiser is set such that the white noise entering it from the radar receiver is of the order of one bit, then this noise has the effect of randomising the position of the least significant bit and, less frequently, the other low bits, due to the statistical nature of noise. This means that for random noise plus a small signal entering the ADC, the signal 'biases' the random noise and over a period of time there is a bias towards the low-level ADC bits having non-random values and representing the effects of the small signal [77]. If the ADC were operating with no noise to randomise the bits, then integration of signals of level below one bit would not be possible, as the output would remain at zero.

Hence, by integrating over either long radar pulses or over a train of pulses, which are individually below the lowest significant bit sensitivity, these very small signals can be detected. The low power limit at which pulses can be integrated is set by the spurious free dynamic range of the digitiser. At this point spurious signals are generated and are at the limit of detectable signals. The spurious free dynamic range of a digitiser can be 20–30 dB more than the single pulse dynamic range stated in Equation (2.36).

2.1.18   Signal processing

2.1.18.1   Spectrum of radar pulse

In Section 2.1.11, pulse Doppler signal processing [78] was discussed for extracting the Doppler frequency and hence the velocity of the target from the radar returns. Consider a radar pulse of time duration, $\Delta\tau$, at a carrier frequency, f (Figure 2.45).

In the frequency domain the pulse is represented by its frequency transform [79], which is a way of constructing the signal using sine wave functions.

$$f_{\text{sig}}(f) = \int_{-\infty}^{\infty} f_{\text{sig}}(t)e^{-2\pi \iota ft} dt \qquad (2.37)$$

where f = frequency, $f_{\text{sig}}(f)$ = frequency transform of time domain signal $f_{\text{sig}}(t)$ and is evaluated as:

$$f_{\text{sig}}(f) = -\Delta\tau \left\{ \frac{\sin(\pi f \Delta\tau)}{\pi f \Delta\tau} \right\} \qquad (2.38)$$
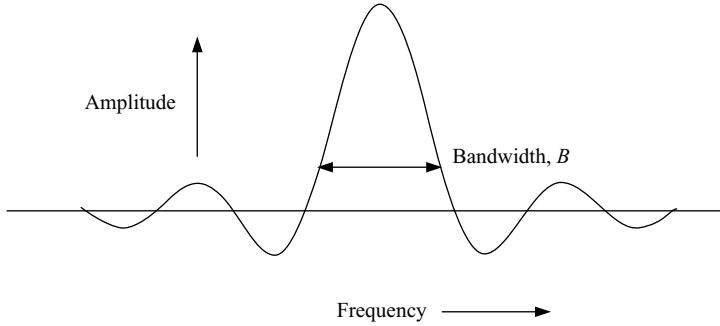
Figure 2.46   Spectrum of rectangular radar pulse of duration $\Delta\tau$ ($B = 1/\Delta\tau$)

This is a 'sin x/x' function and is shown in Figure 2.46. The power spectrum is:

$$\{f_{\text{sig}}(f)\}^2 = (\Delta\tau)^2 \left\{ \frac{\sin^2(\pi f \Delta\tau)}{(\pi f \Delta\tau)^2} \right\} \tag{2.39}$$

The bandwidth of the transmitted pulse of duration $\Delta\tau$ can be defined as its reciprocal, $1/(\Delta\tau)$ or B, when measured at the 3.9 dB points relative to the peak value of the power spectrum, or approximately 40 per cent of the peak value. It corresponds to frequency values of $+\Delta B/2$ and $-\Delta B/2$, (or $\pm 1/2\Delta\tau$).

$$B = \frac{1}{\Delta\tau} \tag{2.40}$$

for a rectangular pulse measured at -3.9 dB from peak.

The spectrum in Figure 2.46 is made up of sine waves with most of the energy concentrated in a continuum of frequencies between $+\Delta B/2$ and $-\Delta B/2$, or $+1/(2\Delta\tau)$ and $-1/(2\Delta\tau)$.

2.1.18.2   Range resolution of pulse

Figure 2.47 shows two targets separated by the limit of the range resolution, Δr, of the radar pulse of duration, $\Delta\tau$. In the diagram, two point targets are shown. A point target is theoretical for the purpose of demonstration and it can be considered to be an 'ideal' reference target. It has no range extent and when illuminated by a radar reflects the signal back to the radar with no distortion. The two point targets have been separated such that, on being illuminated by the radar, the reflected returns have a relative time delay, which is the duration of a single pulse and is the limit of the radar's range resolution. This differential time delay of the radar returns from the two targets, $\Delta\tau$, is the time taken for the radar wave to travel the distance between the two targets and back, which is $2\Delta r$. Hence, $2\Delta r$ divided by $\Delta\tau$ equals the speed of light, c. The range resolution of the pulse is then given by:

$$\Delta r = \frac{c\Delta\tau}{2} \tag{2.41}$$
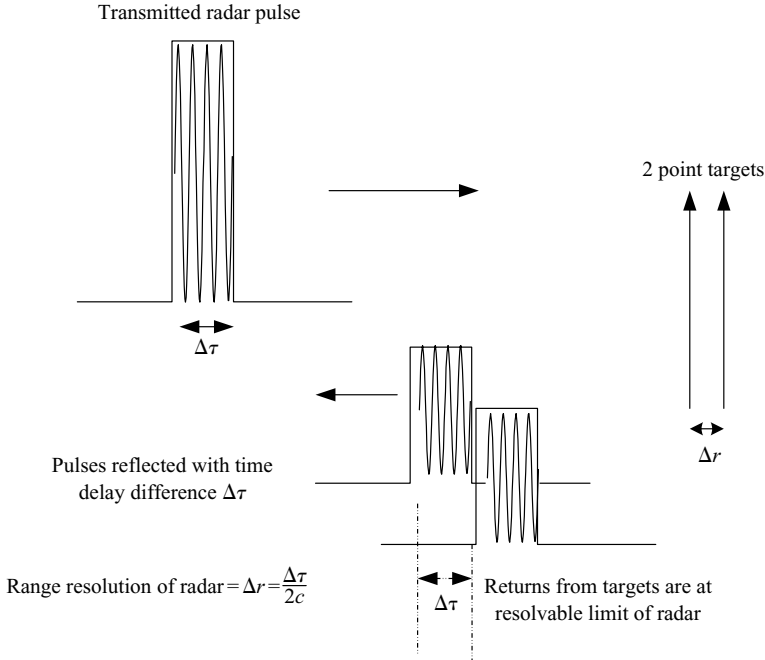
Figure 2.47   Range resolution of a radar pulse

Using (2.41), the range resolution of the pulse is given by:

$$\Delta r = \frac{c}{2B} = \frac{c\Delta\tau}{2} \tag{2.42}$$

This is also consistent with the Rayleigh criterion [80] for resolving objects.

2.1.18.3   Range gates

In addition, from the Nyquist criterion, as discussed in Section 2.1.17, when sampling a radar signal of bandwidth, B, in the digitiser , 'I' and 'Q' samples are each needed at a minimum rate of B per second. This also equates to a sampling time interval of $1/B$ or $\Delta\tau$, which is a pair of 'I' and 'Q' samples for every time interval, $\Delta\tau$. Hence, by digitising at a time interval appropriate to a radar pulse length, $\Delta\tau$, the criterion is met for obtaining the available information from the signal. This time interval or the equivalent range interval, Δr, is called a radar range gate and is used as the basic timing interval in radar receivers. It is illustrated in Figure 2.48.

The range gates cover a distance from close to the radar, to the maximum detection range of the radar, taking into account range ambiguities, which are discussed in the next sections. For a point target, which is illuminated by an ideal radar pulse, and located at the centre of a range gate, only a return for a single range gate is obtained. For a point target straddling two range gates, returns will be in both. This will be discussed more in Section 2.1.20 on matched filters.
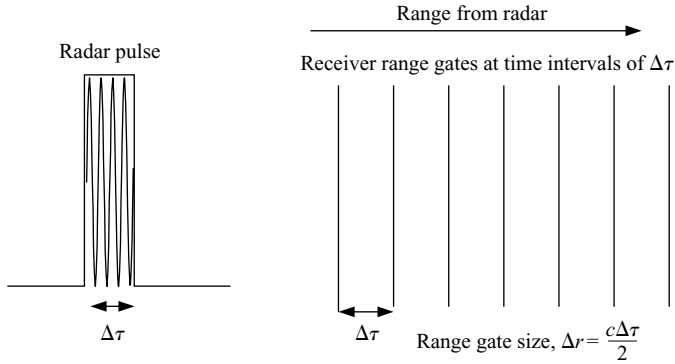
Figure 2.48   Range gates for a simple pulse

2.1.18.4   Blind range zones

When a radar pulse is being transmitted, the radar receiver is normally isolated for protection purposes and is effectively switched off. The radar cannot detect any targets for the duration, $\Delta\tau$, of the pulse. The receiver is able to detect targets again after the pulse has been transmitted. As the radar pulse is being transmitted, the returns from targets or clutter at short ranges close to the radar cannot be detected, as the receiver is inactive. The ranges at which targets cannot be detected, due to this 'eclipsing' effect, as it is known, are called 'blind zones'. Figure 2.49 shows this effect for ranges very close to the radar.

After a time corresponding to half the duration of the transmitted pulse, $\Delta\tau/2$, the front of the pulse has reached a range of $c\Delta\tau/2$. Any returns from targets entering the radar at shorter ranges are not detected, as the radar receiver is off until time, τ, as the two-way transit time at these ranges is less than τ. Hence, the radar has a blind zone from range zero, at the radar, to range $c\Delta\tau/2$, and is dependent on the length of pulse, $\Delta\tau$, employed by the radar.

It also means that over this time, with the radar receiver off, any signals entering the radar from longer ranges associated with pulses transmitted earlier are also not detected. The ranges at which target detection is not possible are shown in Figure 2.50 and are dependent upon both the pulse length and the pulse repetition interval. Beyond the first blind zone, the additional blind zones occur at ranges such that the pulses are returning to the radar at the same time as the pulse described in the previous diagram. The condition for this to occur is that the round trip of the pulse to the longer range targets is equal to an integral number of pulse repetition periods, τ_{prp}, of the radar. The pulse train parameters are shown in Figure 2.50(a) and the blind zones are shown in Figure 2.50(b). The blind zones occur for every pulse repetition period, at ranges of multiples of $c\tau_{prp}/2$ and each corresponds to lost range coverage of $c\Delta\tau/2$. Theoretically these blind ranges extend indefinitely, but in practice radars are limited in range, so it is only over the operating ranges of interest that blind zones are significant.

(a)

At ranges of less than $c\Delta\tau/2$ returns
reach radar when receiver is off:
Corresponds to radar receiver being
off for period $\Delta\tau$

Front of pulse is at range of $c\Delta\tau/2$ at time $\Delta\tau/2$
Remaining half of pulse not yet transmitted

$\Delta\tau/2$

(b)

$\Delta\tau$ Radar receiver is off for period $\Delta\tau$

Range

Radar

Front of pulse is at range of $c\Delta\tau$ when receiver is switched on again
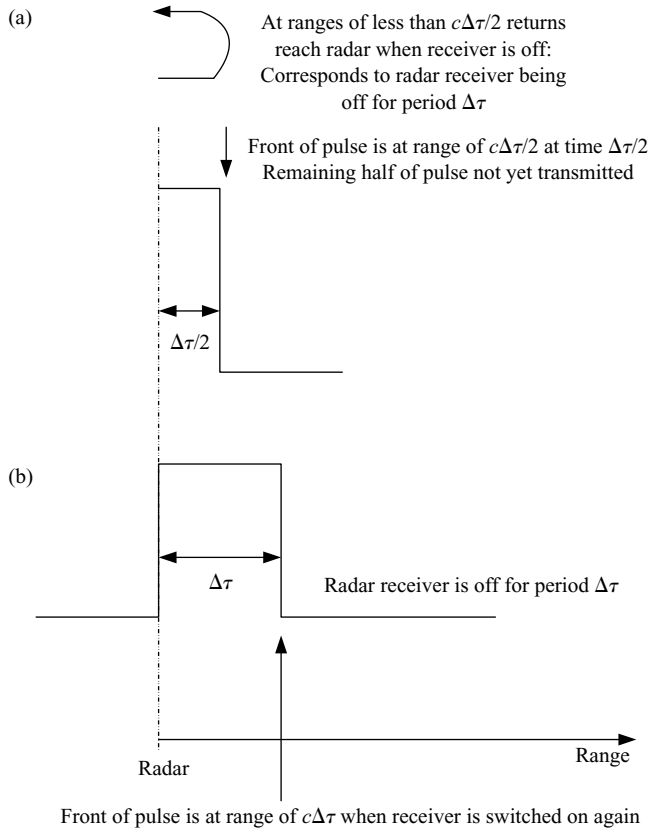
*Figure 2.49   Blind range zone in vicinity of radar: position of pulse (a) at time $\Delta\tau/2$
and (b) at time $\Delta\tau$*

2.1.18.5   Unambiguous range

After a radar pulse has been transmitted, the time delay to the target and back is used
to determine its range. However, under certain circumstances it is not possible to
determine the range to the target *unambiguously* from a single train of radar pulses.
With reference to Figure 2.51, consider a radar operating with a pulse repetition period
of τ_{prp}. The equivalent range corresponding to this time delay of τ_{prp} is $c\tau_{prp}/2$, so
this is the maximum range the pulse can reach and be reflected back from a target to
the radar, before the next pulse is transmitted. If the maximum range of the radar is
less than $c\tau_{prp}/2$, then all the detectable targets have ranges less than $c\tau_{prp}/2$. The
radar is then said to be operating unambiguously in range, at this prf.

2.1.18.6   Range ambiguities

If the maximum range of the radar is more than $c\tau_{prp}/2$, then the radar is said to be
operating ambiguously in range. Under these conditions returns entering the radar

(a)

(b)
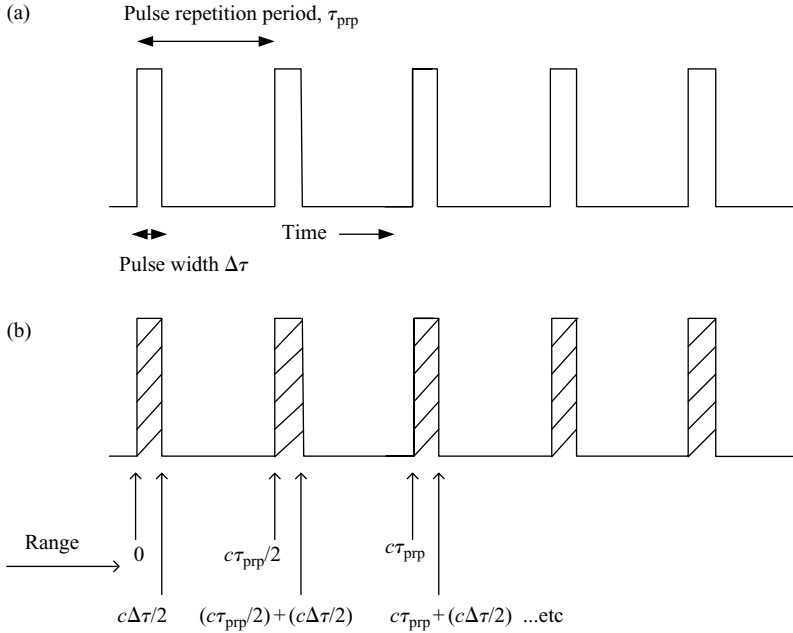
Figure 2.50   Blind zones for a transmitted pulse train: (a) transmitted pulse train and (b) blind zones are shaded
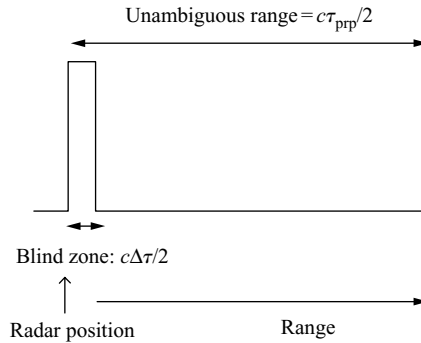
Figure 2.51   Unambiguous range for radar with pulse repetition period t_{prp} is $c\tau_{prp}/2$

receiver could come from targets and clutter at different ranges, which are separated by two-way time delays of integral multiples of pulse repetition periods. On the basis of a single train of pulses, the true range to the target cannot then be determined using current radar signal processing techniques. For a radar operating ambiguously,
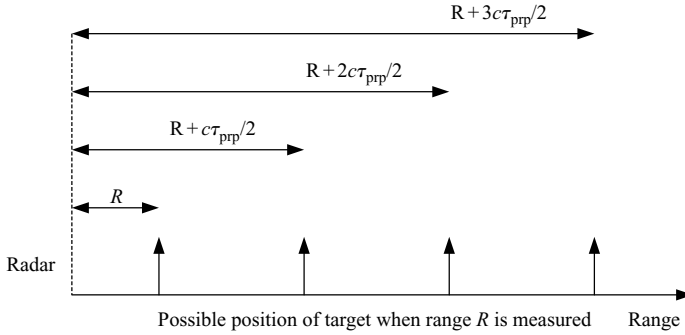
Figure 2.52   Target range is ambiguous

the true range is given by the following possibilities:

$$R_{\text{true}} = R_{\text{amb}} + \frac{nc\tau_{\text{prp}}}{2}$$

(2.43)

where R_{true} is the true target range, R_{amb} is the ambiguous range measured, n is an integer and is dependent upon which ambiguity the target resides in and τ_{prp} is the pulse repetition period. This is illustrated in Figure 2.52.

In Figure 2.52 is an example of the possible ranges of a target, when the radar is operating ambiguously. There are four different possibilities for the correct range of the target at this particular prf. They are at intervals of $c\tau_{\text{prp}}/2$ and the total number of ambiguities present is dependent upon the radar's maximum range.

If a radar is operating ambiguously in range, it is necessary to resolve the ambiguity and determine the true range to the target, otherwise it is not possible to establish the target track. The normal technique used to resolve range ambiguities is to use multiple prfs and then solve algebraic equations from the ambiguous ranges measured in the different prfs [81]. As will be seen later in the book, range ambiguities are significant for target recognition applications.

2.1.18.7   Ambiguous range gates

The radar receiver is normally 'on' during the interpulse period. For a simple pulsed radar, with no other modulation, the number of range gates available for target detections over one burst of pulses, is the inter pulse period, τ_{ipp}, of the radar divided by the radar pulse width. This is illustrated in Figure 2.53 with parameters expressed as both time and range. When the range to any target is measured, it appears in one of the range gates shown. The number of range gates is determined by the radar pulse parameters.

2.1.18.8   Doppler ambiguities

It was shown in Section 2.1.11 that the Doppler frequency, and hence the target radial velocity vector, is normally measured over a train of coherent radar pulses. Each radar pulse contains amplitude and phase information on the target, which is extracted by signal processing.

(a)

Inter pulse period = τ_{ipp}

$\Delta\tau$

Range gate coverage = τ_{ipp}(or = $c\tau_{ipp}/2$, as range)

(b)

Range gate width = pulse width = $\Delta\tau(=c\Delta\tau/2$ as range)
Number of range gates = $\tau_{ipp}/\Delta\tau$
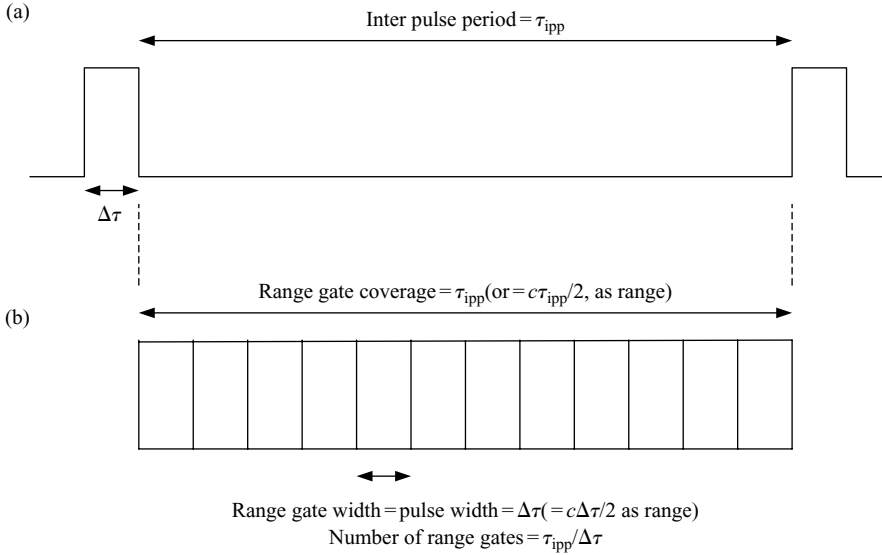
Figure 2.53   Range gate parameters: (a) pulse parameters and (b) range gates

The transmission frequency of the radar determines the Doppler frequency obtained from a moving target. The Nyquist [82] criterion determines the pulse repetition frequency of the radar needed to measure Doppler frequency unambiguously. A radar pulse train with a pulse repetition frequency of f_{prf} samples the signal at this rate. From the Nyquist criterion, it is necessary to sample a signal at twice the rate of the highest signal frequency present to unambiguously capture all the information in the signal. Hence, the highest frequency signal that can be extracted from the radar pulse train sampling at f_{prf} is the $\pm f_{prf}/2$. The maximum Doppler frequency the radar can measure unambiguously with this prf is $f_{prf}/2$. An example of ambiguous Doppler measurement is shown in Figure 2.54.

The two waveforms in the figure have two quite different Doppler frequencies, but the measurements of the values of voltage are exactly the same for both. For explanatory purposes only a single sampling channel is shown, rather than 'I' and 'Q' channels. When this time history data is Fourier transformed, the resulting Doppler frequency is exactly the same for both waveforms. f_{prf} is sufficiently high to unambiguously measure the frequency of waveform Figure 2.54(a), as the highest frequency component in the waveform is less than half the sampling frequency of the pulse train. In fact there are about two cycles of this waveform for six sampled pulses, which meets the Nyquist criterion. However, for waveform Figure 2.54(b) there are about seven cycles and the prf is too low to measure it unambiguously. The prf would have to be raised to almost two and a half times its current value to measure this signal unambiguously. This waveform is also said to be aliased, as the measurement is not providing its true value [83].

At each sample point both waveforms have same voltage, so appear to be same waveform
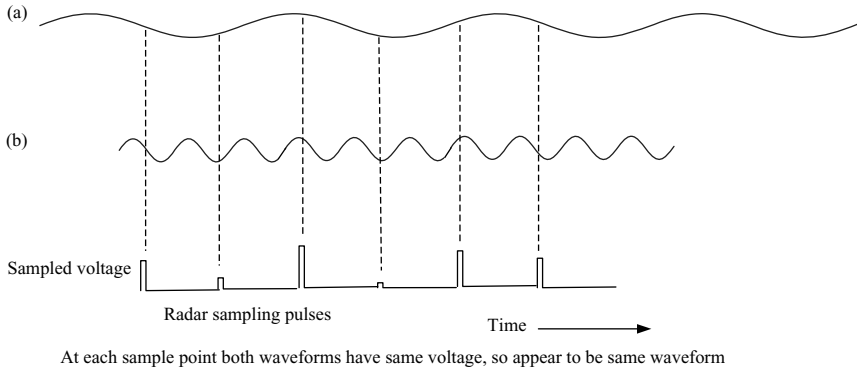
Figure 2.54   Ambiguous Doppler measurement: waveform voltage against time characteristic is measured (a) unambiguously and (b) ambiguously
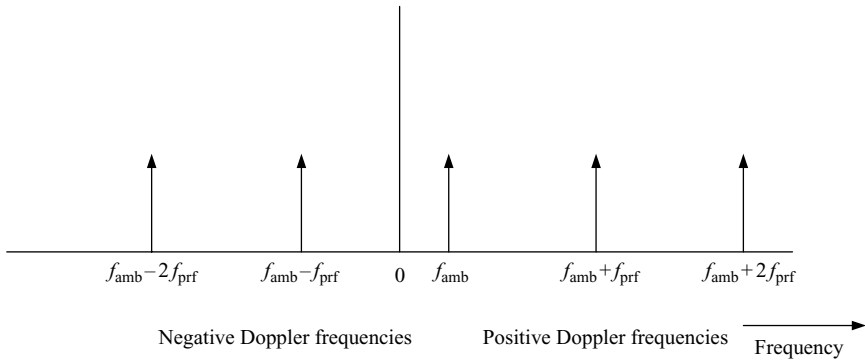
Figure 2.55   Doppler ambiguities. f_{amb} is the ambiguous value of Doppler frequency which has been measured

The measured value of a Doppler frequency, which is aliased, is given by the following:

$$f_{true} = f_{amb} + nf_{prf} \tag{2.44}$$

where f_{true} is the true Doppler frequency, f_{amb}, is the ambiguous frequency measured and n is an integer, which can be postive or negative. This is illustrated in Figure 2.55.

The Doppler frequency measured, f_{amb}, can have a real value of f_{amb} plus or minus an integral value of the prf. Interestingly, if a positive value of Doppler frequency is measured, it does not necessarily mean it is a closing target. It can be seen in Figure 2.55 that f_{amb} could actually be a receding target, with its Doppler 'folded round' to appear to be approaching.

The main way in which Doppler ambiguities are resolved is to use bursts of different pulse repetition frequencies and compare the apparent frequencies in each
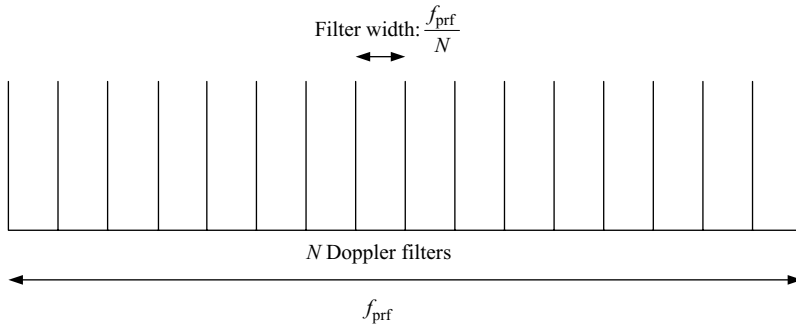
Figure 2.56   *Doppler filters*

of them [84]. The frequency that is common to the various prfs is the true Doppler frequency. Another way to resolve the ambiguity is from the radar track. By effectively comparing the target range and angular position over several radar measurement periods, the distance and the direction in which the target is moving can be established and related to the ambiguous Doppler frequency candidates.

As discussed in Section 2.1.11, the time series of pulses is Fourier transformed into the frequency domain to a set of Doppler filters. From the symmetry of the digital Fourier transform, the number of Doppler filters obtained is the same as the number of pulses in the burst, which are processed in the radar. The N Doppler filters are shown in Figure 2.56 and occupy a frequency span of f_{prf}. The bandwidth of each filter is nominally f_{prf}/N. The integration time on target is approximately the number of pulses transmitted, N, multiplied by the inverse of f_{prf}, which is N/f_{prf} and is approximately the same value as the inverse of the frequency resolution f_{prf}/N.

Whatever the target or clutter's velocity, it will appear in at least one Doppler cell (or sometimes called a bin). If the Doppler frequency straddles two bins, the energy is distributed between the two. In each of the Doppler filters is either a signal, with some noise, or just noise. The contents of each cell are represented by an amplitude and phase.

2.1.18.9   Receiving radar data

In Figure 2.57(a) a radar antenna is represented rotating in azimuth. At each beam position at least one burst of radar pulses is transmitted and reflected returns enter the radar receiver. Figure 2.57(b) shows the data being assembled, prior to signal processing. For each transmitted pulse data is collected for each range gate. The data in each range gate would be an amplitude and a phase component, which would normally reside in the in-phase and quadrature channels. The number of range gates is given by the inter-pulse period, τ_{ipp}, divided by the pulse length, $\Delta\tau$. In the figure the returns from each transmitted pulse are shown as a set of range gates arranged horizontally. As further pulses are transmitted, received data is again assembled into respective horizontal sets. A matrix is progressively built up consisting of a set of

Range gate coverage $= \tau_{ipp}$ (or $= c\tau_{ipp}/2$, as range)
Number of range gates $= \tau_{ipp}/\Delta\tau$

Range gate width $=$ pulse width
$= \Delta\tau (= c\Delta\tau/2$ as range)
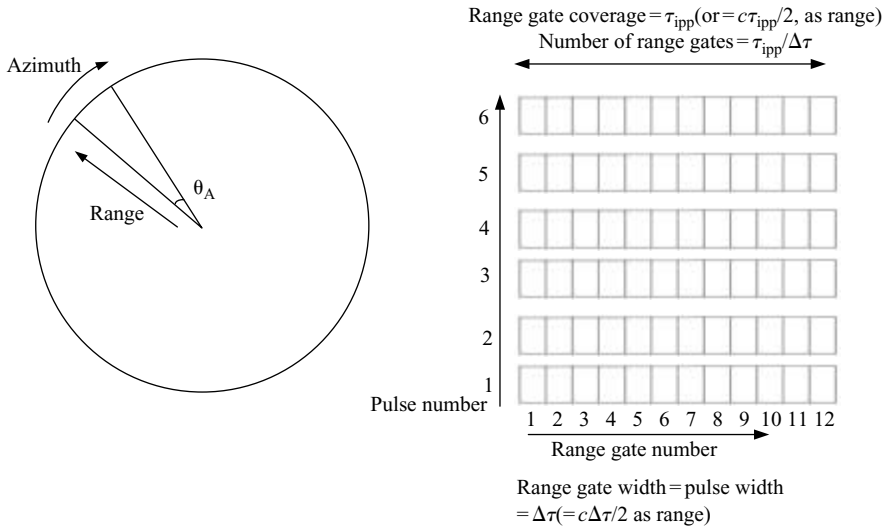
Figure 2.57   *Formation of a pulse-range gate matrix: (a) radar is at centre of cir-*
cle and is rotating clockwise. At each angular position radar data is
received sequentially after each pulse is transmitted for each range
gate and (b) radar pulse-range gate matrix

range cells in one direction against pulse number in the orthogonal direction. The data is arranged in this format at the output of the ADC.

2.1.18.10   Corner turning data

In order to process this data, it must be re-arranged. The data undergoes an operation called 'corner turning', so that the Doppler filtering operation can take place. From being arranged on the basis of each pulse transmitted, it is arranged on the basis of range gate number. This operation effectively brings together the data from each range gate. The data from each range gate is now assembled sequentially from the first to the last pulse then Fourier transformed into the frequency domain to provide the Doppler frequency components.

Figure 2.58 shows the re-arranged data, so that the Fourier transform can be performed for each range gate over the sequence of pulses received. The shaded cells are an example of data at the same range for each of the pulses, which is then transformed in the frequency domain for determining the Doppler frequency of targets.

2.1.18.11   Range-Doppler map

The output of the Fourier transform is shown in Figure 2.59 in the form of the range-Doppler map.

In each range gate the signal has been transformed from the time domain to frequency domain. The amplitude is represented by the shade in each cell. Although it is

Data *corner turned* from being arranged horizontally to vertically in diagram, so that it
can be processed by range gate number over sequence of pulses transmitted
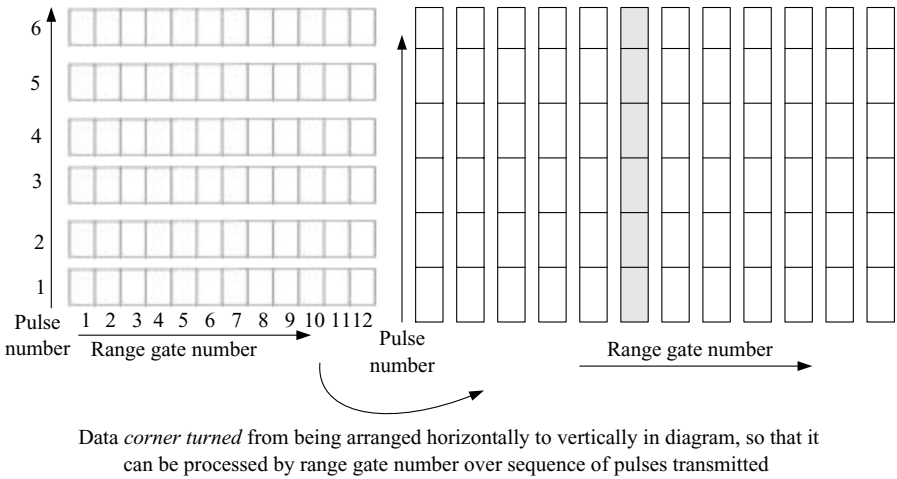
Figure 2.58   Corner turned range gate-pulse data for performing Fourier transform
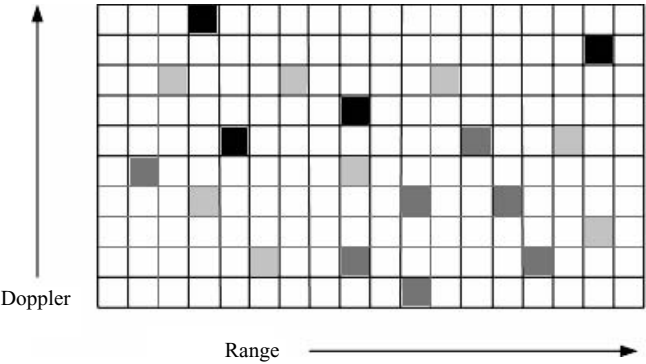
*Figure 2.59   Range-Doppler map: the shade of the colour represents the amplitude
detected in each cell*

not explicitly shown, every range-Doppler cell actually has some level of amplitude,
as the signal has not yet been thresholded and noise is present. In many of the cells
there are just noise contributions, with no target or clutter returns. From this data it is
not yet possible to identify the presence of targets. Depending upon the radar and also
the target position and velocity, this data could be either ambiguous or unambiguous
in range or ambiguous or unambiguous in Doppler. A range-Doppler map is formed
for every burst of pulses transmitted, which are processed together. These maps are
formed for the direction in which the antenna beam is instantaneously pointing. As it
rotates to a new angular position, a new map is generated. For each time the antenna
completes a full rotation cycle, many range-Doppler maps are formed.

Length of vectors shown represents amplitude of signal

Signal   Noise   Signal + Noise   Detection threshold
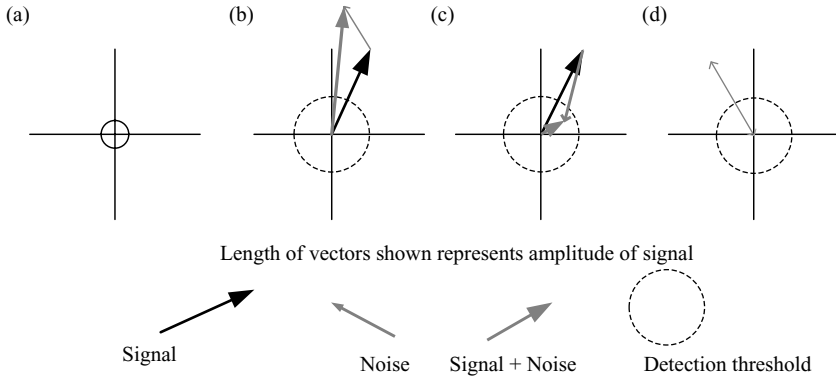
Figure 2.60   Combining signal and noise using a vectoral representation: (a) circle represents mean level of noise; (b) signal and noise vectors combine to still provide large amplitude; (c) large noise amplitude destructively combines with signal to give small net amplitude and (d) noise on its own provides large amplitude

2.1.18.12   Thresholding signal against noise

From the statistics of Gaussian noise, which were discussed in Section 2.1.12, there is a mathematical method for establishing the probability that a particular return is likely to be due to signal or noise [85]. There is a finite probability that noise can have any value and the probability that noise can reach a particular level can be precisely determined. Also in the presence of the target, the noise and target signals add up vectorially and hence both contribute to the value of amplitude and phase measured in each range-Doppler cell of Figure 2.59. The combination of these vectors is shown in Figure 2.60.

Various levels of noise are shown to combine with the signal in different ways to illustrate the key design aspects of setting threshold levels in the radar. The signal and noise are represented by vectors, which have amplitude and phase components. The amplitude is represented by the length of the vector and the phase by its direction. Figure 2.60(a) shows the mean amplitude level of the Gaussian noise, which is small compared to the signal in this example. The circle shows that it can have any random phase. Typically in radar receivers the signal-to-noise ratio is set to be between 12 and 15 dB measured in power terms or about a factor of 4 or 5 as a voltage ratio. In Figure 2.60(b) the signal and a value of noise, which is close to the mean, are shown combining, which results in a large vector, so the resulting signal is easily detected with reference to the threshold level indicated as the broken circle. In Figure 2.60(c) a large noise vector is seen to be destructively cancelling the signal, resulting in only a small combined amplitude, so that detection of the signal is below threshold and is not possible. In Figure 2.60(d) there is no signal, but the large noise amplitude would be mistaken for one, as it exceeds the detection threshold level, which would then be called a false alarm.

Threshold is set such that noise
has very low probability of having
high value and exceeding
threshold level

Threshold level is often set with signal having
0.5 probability of being detected

Threshold level

Threshold level is set in dB
relative to mean noise level

Signal + Noise

Power level of:
Signal plus noise
or noise

Noise

Very low threshold level would
guarantee target detections, but
also very large numbers of false
alarms due to noise

0   0.5   1

Probability of exceeding threshold level

Normal threshold level

Very low threshold level

Figure 2.61   Threshold setting for target detection

The decision that the radar engineer has to make is where to set the threshold for deciding when a target has been detected. As noise is of a statistical nature, threshold setting has to be carefully done in order not to miss required detections or to experience too many false alarms.

Threshold setting [86] is shown qualitatively in Figure 2.61. The curves show the probability of exceeding the detection threshold value, which is set to be normally 12 to 15 dB relative to the mean noise power level. Any value in a range-Doppler cell exceeding the threshold is a potential target detection and any value lying below it is rejected. For the noise on its own, for the higher threshold level shown, there is a very low probability that it can exceed this value and appear as a detection. The power level from the signal plus the noise is shown to cross this threshold level at a detection probability of 0.5, which is a typical value set.

The typical false alarm rates for the noise power to exceed the detection threshold are 10^{-6}–10^{-9}. It can be seen that lowering the detection threshold level increases the probability of detection, but also increases the probability of noise exceeding the threshold and causing false alarms. At the very low threshold level also shown, all target detections would be made, but the false alarm rate would be unacceptably high using conventional track initiation techniques.

In order to establish the actual noise level in each range-Doppler cell, to be able to set the detection threshold, it is normally measured. The setting of the threshold level can have quite significant effects on radar performance, as modest changes can result
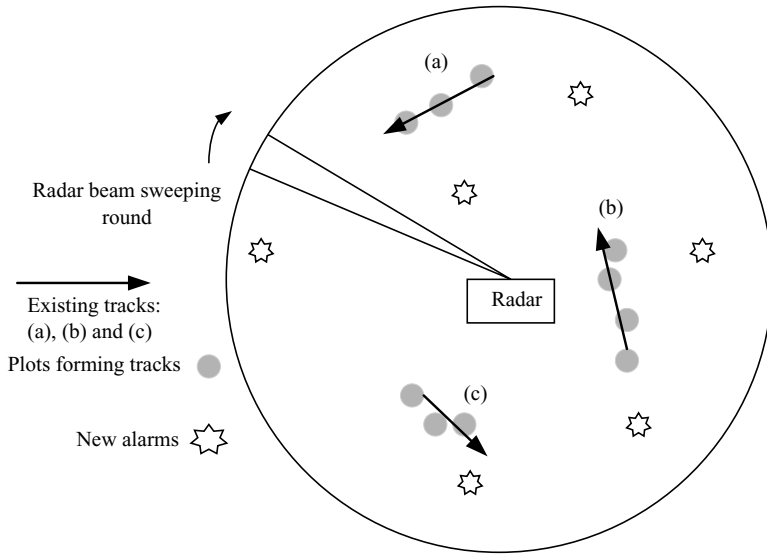
Figure 2.62   Existing target tracks and initial detection of potential targets: 'alarms' have range, velocity and angular parameters

in large changes to detection probability and false alarm rate. A technique known as 'Constant False Alarm Rate' (CFAR) [87] processing is used in which area averaging of the noise in neighbouring cells is calculated. The actual level of the threshold set then varies over the range-Doppler map, but the noise statistics remain consistent for target detection. This technique can also take into account the effects of clutter returns in setting the threshold.

2.1.19   Target tracking

From the thresholding function, potential targets are detected and are called alarms. Thresholding is applied to every range-Doppler map generated and the range, frequency and angular parameters for each alarm are then used for the next operation, which is tracking. If ambiguous prfs are being used, it is necessary to resolve range and/or Doppler ambiguities, particularly for airborne radars [88]. This is usually performed using multiple prfs during the dwell period on the target, before the antenna points to another angle. The ambiguous range-Doppler map is then resolved into unambiguous range-Doppler cells, so the correct range and radial velocity vector of each detected target should be obtained. The set of data now being held has typical range, velocity and angular parameters and an example is shown in Figure 2.62.

In some cases the angular information may be more precise than to within a radar beamwidth. Techniques such as monopulse comparators are used to obtain more precise angle estimation and will be discussed later in Chapter 6. Also more than one radar beam can be used in elevation to obtain a more accurate estimate of target altitude. The alarms shown are the first step towards initiating target tracks. Also

Figure based on axes labelled "Distance, *y*-axis" (vertical) and "Distance, *x*-axis" (horizontal).

Three alarms are consistent with association gates, so track is initiated

Three isolated alarms outside respective association gates, so track is not initiated

The alarms are shown in a two-dimensional coordinate system
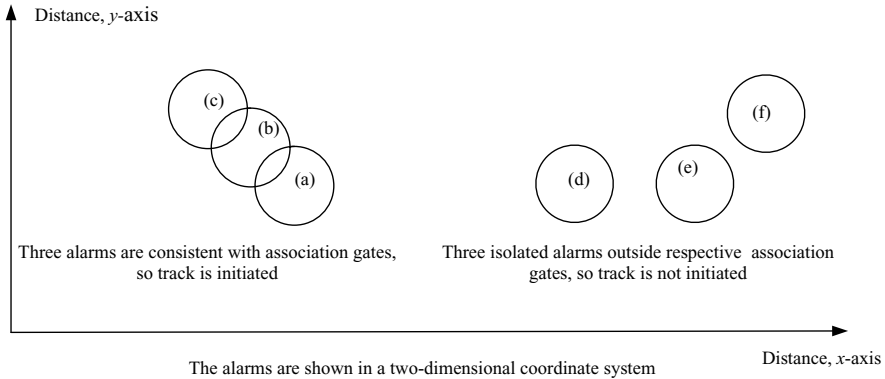
Figure 2.63   Alarms tested for track initiation

shown in Figure 2.62 are established tracks with the constituting alarms or plots. The tracking function can be considered to be applying the best straight line through the plot data for an assumed straight line track. The effects of noise cause the plots to deviate from their *true* positions, so averaging the data tends to provide the best estimate of the track. It is necessary for each new plot to be tested for being associated with an existing track or whether it is likely to be a new unrelated plot. It could be noise or a newly detected target. Track (c) has a candidate alarm nearby, which needs to be checked for its likelihood of being part of this track. In order to either maintain existing tracks or to initiate new tracks it is necessary that the alarms or plots for each target to be related. This is illustrated in Figure 2.63 for the initiation of a track for one target. The six circles represent the size of the association gates. The sizes of the association gates are dependent upon the resolution measurement capabilities of the radar, the signal-to-noise ratio and the velocity bracket for the targets of interest. They would normally use range for the association parameter, but velocity and altitude could also be included. So multi-dimensional association gates could be used, rather than the simple case shown, which just has two distance dimensions.

The alarms are at the centre of the association gates and are located in accordance with the radar's range and azimuth measurements. For (a), (b) and (c), these alarms could have arisen on sequential scans of the radar antenna. It can be seen that they are all consistent with their respective association gates, so a track is established. For (d), (e) and (f), these three plots are outside their neighbours' respective association gates, so no track is formed yet. At least one of these may have been a false alarm, due to noise in the receiver. Plots are held for a few scans for possible future association, then are dropped. The criteria employed for all these track initiation processes are application dependent.

After tracks are established, they are maintained on similar lines, but with progressively smaller association gates as the track matures and more measurements are made. They use tracking filters to perform this function [89–91]. They can also have parallel filters operating to detect manoeuvres, for example. Otherwise the tracking
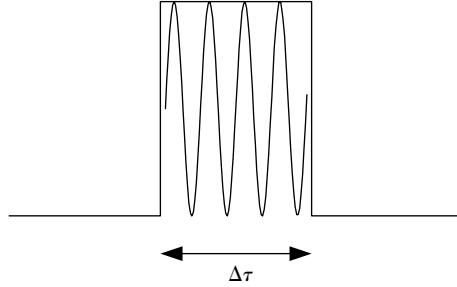
Figure 2.64   *A sinusoidal signal of frequency, f_c, modulated by a pulse of duration $\Delta\tau$: this is optimally detected using a filter of bandwidth $1/\Delta\tau$*

would fail if the target suddenly changed speed or direction. Other factors that can confuse trackers, as this whole tracking process is called, are multiple targets in close proximity and crossing targets, whereby their tracks can get confused. Target tracking involves continuous plotting of new target alarms, track initiation, track maintenance and dropping failed tracks as simultaneous functions. High-resolution modes and radar target recognition capabilities have the potential to improve target tracking and to resolve clusters of targets into separate objects.

2.1.20   Auto-correlation function of a pulse and matched filtering

When a radar transmits a pulse it is detected optimally in what is referred to as a matched filter [92,93]. It is necessary to evaluate the output of the matched filter for any type of waveform used, as it is a measure of the usefulness of a waveform for performing various measurements in particular situations. Effects such as clutter and multiple targets have to be considered. Interestingly in Section 2.1.17 the various signal processing operations that were performed were consistent with matched filtering for providing optimum detection of a single point source signal. The filtering and digitiser parameters selected and used were also appropriate for matched filtering, as both functions extract information from received signals for optimum detection performance.

A typical radar pulse is shown in Figure 2.64 and the optimum detection of this signal to maximise the signal-to-noise ratio is now discussed. The output of the matched filter is the auto-correlation of the time domain signal of Figure 2.64 and this will now be examined.

Mathematically this is stated as:

$$C(t) = \int_{-\infty}^{\infty} f_{\text{sig}}(\tau)^* f_{\text{sig}}(t + \tau) d\tau \tag{2.45}$$

where $C(t)$ is the waveform's auto-correlation function, $f_{\text{sig}}(\tau)^*$ is the complex conjugate of the signal and $f_{\text{sig}}(t + \tau)$ is the signal shifted in time by t.

Auto-correlation is effectively the multiplication of the signal by a replica of itself for all time delays. This has a peak value when it completely overlaps itself, which is when it is *matched* and provides the maximum output value. In the time domain this can be understood as a signal passing through a filter, with the auto-correlation function being the filter's output. The complex conjugate is used to take into account the phase contribution of the signal.

In Figure 2.65 the pulse is shown with a time shifted version of itself. The time shifted signal, $f_{sig}(t+\tau)$, is shown at six different time delays to demonstrate how the auto-correlation function is built up. In reality one signal is mathematically shifted from minus infinity to plus infinity. The illustration shows how Equation (2.45) works. The other signal, $f_{sig}(\tau)^*$, is shown with constant time delay. In practice, the 'moving' pulse slides past the fixed pulse and the amount of instantaneous overlap of the two pulses represents the value of their correlation for the time, t. The values of overlap obtained for different values of time, t, all contribute to the pulse's auto-correlation function. The area of overlap between the two functions, shown in grey, is the correlation value between them for time offset values, t. The correlation value is taken as the fractional overlap of the areas of the two functions.

It can be seen that for differential time delays of greater than $\Delta\tau$, there is no correlation. For values of t between $-\Delta\tau$ and $+\Delta\tau$ correlation occurs, with 50 per cent overlap occurring at $\Delta\tau/2$. The auto-correlation peak is at the point when $t = 0$ when the two pulses overlap completely.

The actual correlation function for the pulse of duration, $\Delta\tau$, is shown in Figure 2.66. It is a triangular function with a base of $2\Delta\tau$. Consider a point target, which is the most simple target that can be imagined, that reflects back energy, but has no range extent itself. For a radar using this type of pulse, it means that when the radar receiver is optimised to detect the pulse, the output of the matched filter for a point target gives rise to this triangular response.

The width of this response equates to the pulse's range resolution ($\Delta r = c/2\Delta B$). It should also be noted that there are no range ambiguities and that a single point target only gives a response at the output of the matched filter with a single peak. When other waveforms are examined later in this book, for target recognition purposes, it will be seen that there are cases when range ambiguities arise and have implications on the radar performance.

Figure 2.66 shows how the integral Equation (2.45) is being performed. The $f_{sig}(\tau)^*$ signal is held in the same position, while the other version of itself, $f_{sig}(t+\tau)$, is 'slid' through it. This is done by applying values of t from minus infinity to plus infinity. The result is the function shown in Figure 2.66. The integral performs the multiplying function at each time, t. The peak of the response in Figure 2.66 occurs when the two pulses absolutely overlap. The matched filter is effectively a replica of the transmitted pulse with the phase inverted. The auto-correlation can be seen as multiplying two signals with identical amplitudes together. In summary, the filter is matched as it replicates the amplitude/time profile of the actual signal of interest. In Section 2.1.18, it is shown that the spectrum of a pulse of duration, τ, has a bandwidth of $1/\tau$. Another way of considering a matched filter is to imagine a signal passing
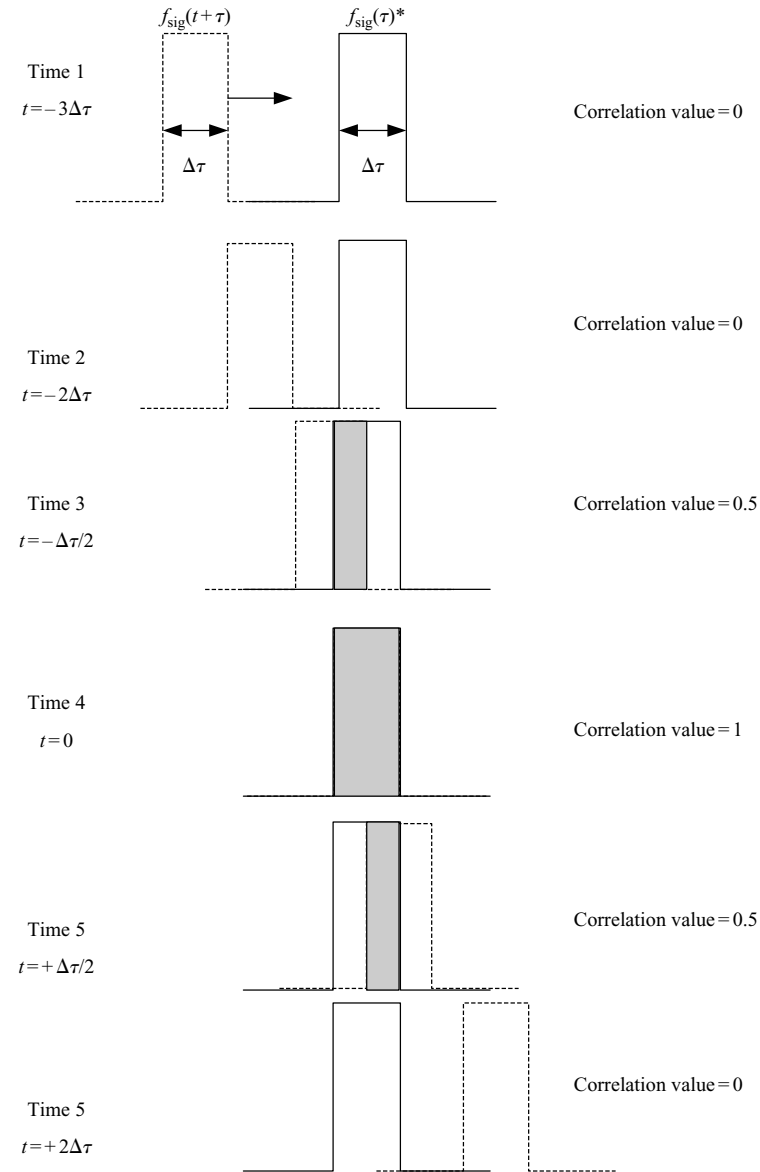
Figure 2.65   Illustrating the auto-correlation of a pulse of width $\Delta\tau$

through a physical filter of this bandwidth. The auto-correlation function is exactly the same as in Figure 2.66.

This means that the effective bandwidth of the receiver for a single pulse is the inverse of its time duration, which is $1/\Delta\tau$. This is also consistent with the digitisation

$$2\Delta\tau$$
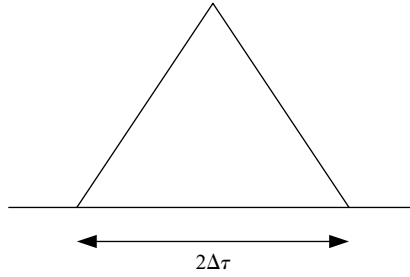
Figure 2.66   The auto-correlation function of a pulse of width $\Delta\tau$

shown in Figure 2.43 in Section 2.1.17. The filter is matched to the bandwidth of the signal to reject noise outside the signal's bandwidth and also acts to integrate the pulse's energy. The signal is then digitised at a rate appropriate to its bandwidth for high integrity sampling. The sampling points of the digitiser in time are performing a practically realisable version of the matched filtering function. (It is not quite a perfect matched filter, as it depends on its sampling point relative to the beginning and end of the pulse [94].)

2.1.21   Radar cross-section of a target

When a radar signal is incident on a target, one of the most important parameters for detection is how much energy is reflected back to the radar. The measure of the 'size' of the radar target is called its radar cross-section. Consider the radar illuminating a target in Figure 2.67.

Assuming the radar has a power flux, P_f, measured in watts per square metre, at the target. The rcs of the target appropriate to the direction of the radar is defined as σ. This means that the total power, P_{re}, reflected from the target is:

$$P_{re} = P_f\sigma \tag{2.46}$$

However, this power is radiated in all directions and by convention it is assumed that it is uniformly distributed in each direction. The flux, or power density at the radar, P_{rr}, is the total power reflected divided by the surface area of a sphere having a radius equal to the distance from the radar to the target, R:

$$P_{rr} = \frac{P_f\sigma}{4\pi R^2} \tag{2.47}$$

The value of σ has units of area and represents a cross-sectional area of the radar wavefront intercepted by the target and re-radiated in all directions. In reality there are great variations in the amount of power reflected in the different directions. There are dependencies, which include target shape, materials, size, aspect angle to the radar and wavelength. The actual physical dimensions of the target do not generally equate to the rcs. The rcs of a target for a particular set of conditions can be calculated using (2.47). If the transmitted radar power density, P_f, the distance to the target, R, and
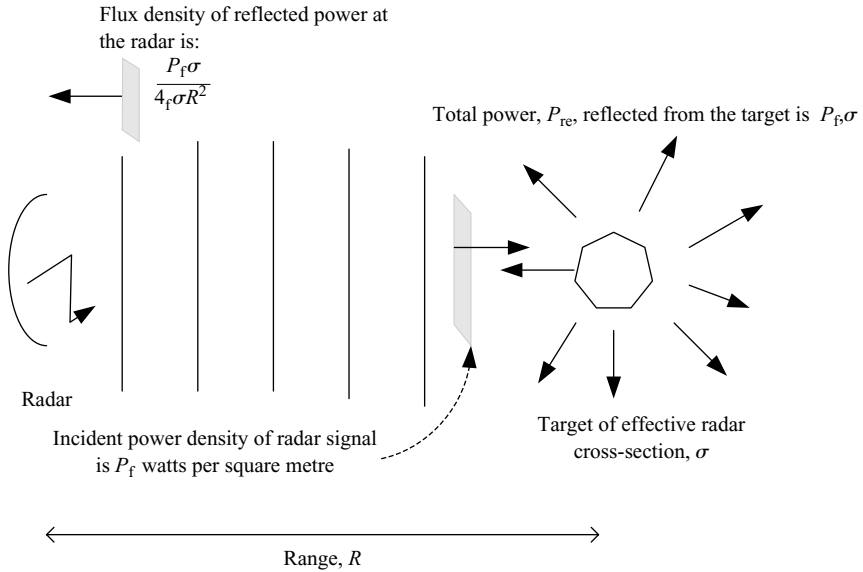
Figure 2.67   Radar signal incident on target and radiated in all directions

the received power flux returned to the radar, P_{rr}, are known, the unknown quantity σ can be determined.

The rcs of an object can be physically understood as a cross-section of area, which intercepts the transmitted signal and radiates it in all directions. Radar cross-sections of land vehicles are typically a few square metres in normal surveillance radar bands (5–20 cm wavelength). Civil airliners are in the range tens to hundreds of square metres and ships can be thousands of square metres. Land clutter reflections from large objects, such as mountains or cliffs, can be greater than tens of thousands of square metres.

2.1.22   Radar range equation

All the elements have now been covered to enable the range of a radar to be calculated. Figure 2.68 shows the contributing factors, which determine the range of the radar. The peak transmitter power is first considered. This has a value, P, but is reduced by losses, L_t, in the transmission chain and antenna. Losses are expressed as ratios here and are numbers larger than one. The loss is defined as the ratio of the input signal level to the output signal level of a component. Hence, the actual power transmitted is P/L_t. The antenna gain is G, and using Equation (2.23a), the power flux, P_f, at the target is given by:

$$P_f = \frac{PG}{4\pi R^2 L_t} = \frac{PA\eta}{R^2 \lambda^2 L_t} \tag{2.48}$$

where λ is the wavelength.
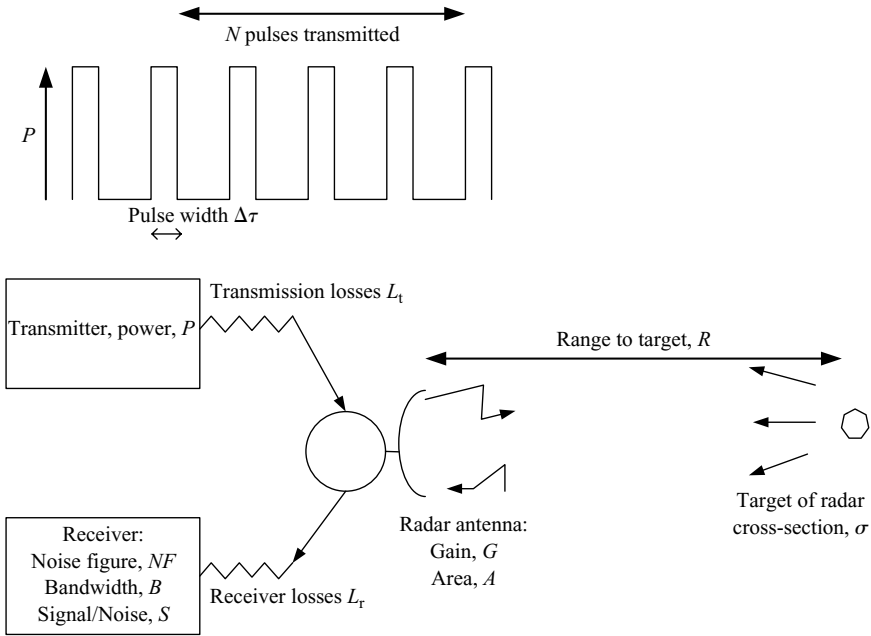
Figure 2.68   Factors affecting radar range

The power intercepted by the target of rcs, σ, is given by:

$$P_f = \frac{PA\eta\sigma}{R^2\lambda^2 L_t} \tag{2.49}$$

and using Equation (2.47), the power flux, P_{rr}, at the radar is:

$$P_{rr} = \frac{PA\eta\sigma}{(4\pi R^2)} \frac{1}{(R^2\lambda^2 L_t)} \tag{2.50}$$

The power received by the radar is:

$$\frac{A\eta P_{rr}}{L_r} = \frac{PA^2\eta^2\sigma}{(4\pi R^4\lambda^2)L_t L_r} \tag{2.51}$$

Taking into account the receiver losses, L_r.

The radar detects the target when the received signal is above the threshold level set with respect to the receiver noise. From Section 2.1.12, the receiver noise, N_f, is given by:

$$N_f = kT_0 B(NF) \tag{2.52}$$

The threshold level is a factor, S, above the noise floor:

$$SN_f = SkT_0 B(NF) \tag{2.53}$$

The noise is measured in units of power. The threshold level is set in accordance with the performance trade-offs shown in Figure 2.61. The level selected is a compromise between detecting as many targets as possible and minimising the false alarm rate. For matched filtering the receiver bandwidth is the inverse of the pulse width, $\Delta\tau$, and is reduced by a factor equal to the number of pulses coherently [95] integrated, N. Coherently integrating N pulses of width, $\Delta\tau$, can be considered in detection terms of being equivalent to having one long pulse of duration $N\Delta\tau$, which has a bandwidth of $1/N\Delta\tau$. Hence the receiver threshold is:

$$\text{S}N_{\text{f}} = \frac{SkT_0(NF)}{N\Delta\tau} \tag{2.54}$$

Equating the threshold level (2.54) with the received power from (2.51) gives the maximum radar range:

$$R^4 = \frac{PA^2\eta^2\sigma\,\Delta\tau N}{4\pi\lambda^2 L_{\text{t}}L_{\text{r}}SkT_0(NF)} \tag{2.55}$$

This is the well-known radar range equation and can be used to determine the range of many types of radar providing the parameters are known. As the range is dependent on the fourth root of the parameters on the right side of the equation, it can be seen that in order to double the range of a radar, the transmitter power has to be increased by a factor of 16, if all the other parameters' values are maintained. The range is clearly dependent upon the target rcs, σ. The losses on transmitting and receiving, and the NF of the receiver contribute to reducing the range. It can be seen that increasing the size of the radar antenna increases range.

It can also be seen that the range is inversely proportional to the square root of the wavelength, if all the other parameters remain the same. For coherently integrating pulses the received signal is proportional to the number of pulses transmitted.

2.1.23 Phased array radars

2.1.23.1 Introduction

The radars presented to date have been based on dish antennas with a single transmitter. The main waveform generation, up-conversion, receiver and digitiser functions generally use one main channel. The antenna dish physically rotates and targets are detected when illuminated by the main beam as it sweeps past them. The dish is typically illuminated by a single horn that provides the appropriate amplitude and phase distribution across its aperture for generating the radar beam.

Phased array radars are very different. The beam is synthesised in space by providing the appropriate amplitude and phase distribution of the electric field across the face of the phased array, which is generated and controlled by electronic components. Antenna elements are used for radiating the contributions to the wavefront. By changing the amplitude and phase values of the electric field generated by each element, the beam can be synthesised to point in a different direction. Electronic scanning can be in both azimuth and elevation and also allows the shape and rate of change of the direction of the beam to vary. These techniques are generally used

(a)

Normal to aperture
face

Direction of wavefront

θ

Phased array elements

Spacing '*d*'

Phase difference between
elements, *ϕ*

(b)

θ

d sin θ

A   B

Spacing '*d*' and phase difference
between elements A and B is *ϕ*
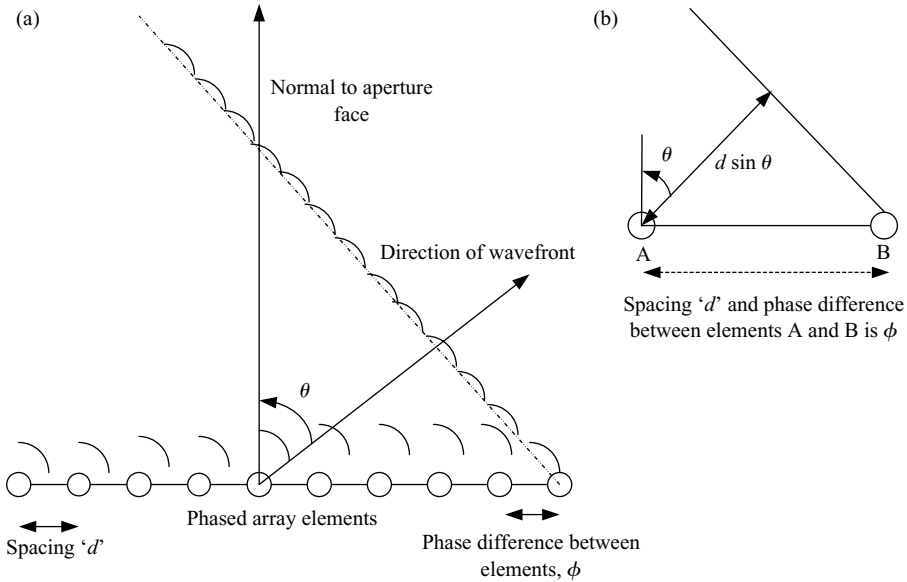
Figure 2.69   *Phased array basics: (a) element on array face and (b) expanded view*
of two phased array elements from beamframing when contributions
from two elements A and B are in phase on wavefront

when the radar system requirements do not enable these functions to be performed
rapidly or flexibly enough using mechanical scanning. In some designs electronic
and mechanical scanning can be used simultaneously. There are two general types of
phased arrays, passive and active, which are discussed in the next section.

2.1.23.2   Phased array concept

The basic theory of phased array radar is shown in Figure 2.69 and the example of
a one-dimensional linear array is provided. *d* is the element spacing along the array
and *ϕ* is the phase difference, which has been set between any two elements.

The phase difference between the first element and last element, number *n*, is
therefore $(n - 1)\phi$. The physical path length difference between any two neighbour-
ing elements' contributions to the wavefront is $d \sin \theta$, as is shown in Figure 2.69(b),
for two of the elements, A and B. When this physical length is measured as a phase,
it is $2\pi d \sin \theta / \lambda$. When the phase difference, *ϕ*, which is set between any two neigh-
bouring elements, is equal to the latter phase, all the elements' contributions on the
wavefront formed are in phase, hence:

$$\phi = \frac{2\pi d \sin \theta}{\lambda} \qquad (2.56)$$
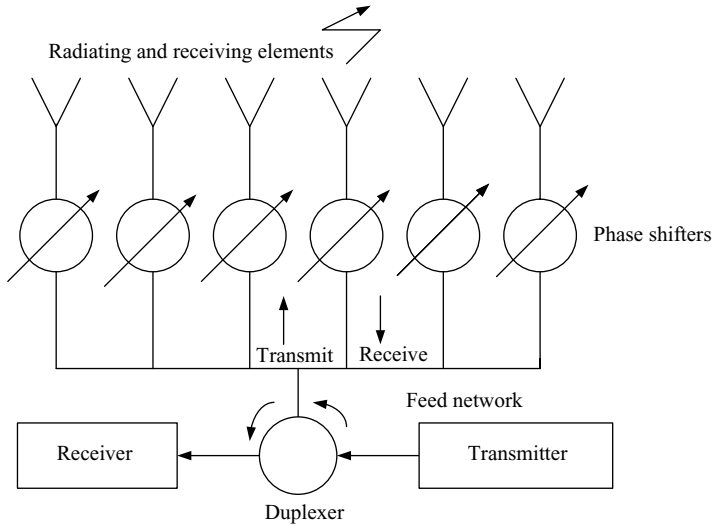
Figure 2.70   Basic passive-phased array architecture

By adjusting the value of ϕ, the value of θ changes, which changes the direction of propagation of the wavefront. The phased array's beam direction is therefore controlled by changing the relative phase shifts between elements. By changing the relative phases between the elements the beam shape can also be altered. The speed of changing beamwidth and beam direction is dependent on the rapidity with which the phase shifter settings can be changed.

2.1.23.3   Passive-phased array radars

A very basic design architecture for a passive-phased array radar is shown in Figure 2.70. The radiating elements are shown, which are situated on the face of the antenna array, and they also act as receiving elements. The key components, which change the phase of the signal, are the phase shifters, which are connected directly to the radiating elements in passive-phased array designs [96]. The signal can be generated via a single transmitter, such as a travelling wave tube, as shown in the figure, or can be distributed amongst a number of solid-state amplifiers. The single transmitter may use a single duplexer or divide the signal and direct it into different parts of the array, using several duplexers. Similarly, the architecture for receiving the signal could involve different numbers of receiver channels.

   The signal passes through the phase shifters after the final amplification stage before transmission. On receiving the signal it undergoes phase shifting before encountering any amplification in the receiver LNA. Phase shifting is needed for beamforming on transmission and reception. There are many possible variations on this basic architecture [97], which can include complex distribution networks and digital beamforming.
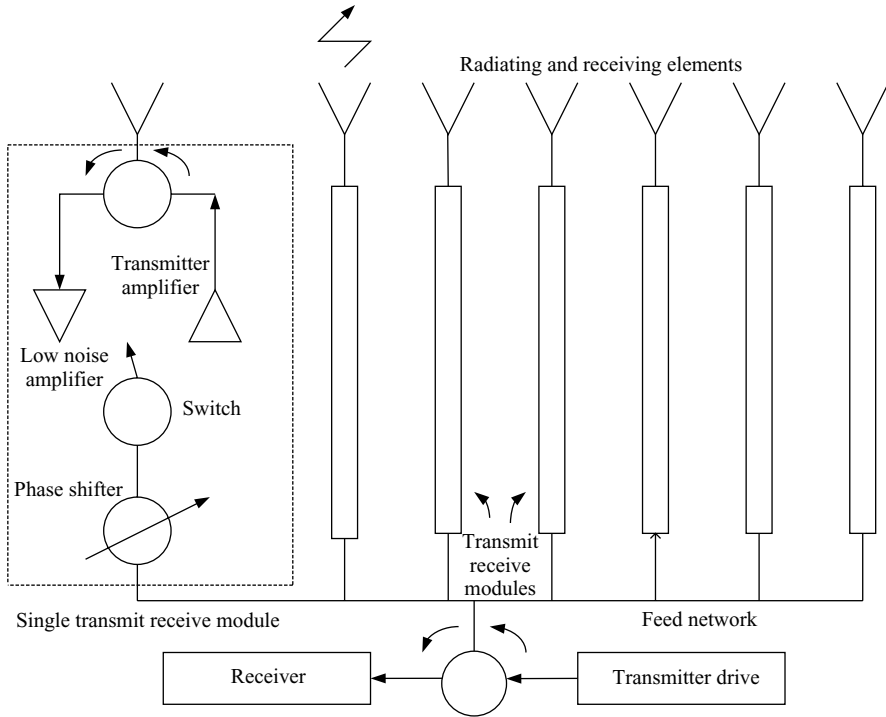
Figure 2.71   Basic active-phased array architecture

2.1.23.4   Active-phased array radars

A basic active-phased array design is shown in Figure 2.71 [98]. The design characteristic identifying an active-phased array is the use of transmit/receive modules (TRM) close to the radiating elements. In modern designs all the main IF and microwave components are solid state. The signal is conventionally generated and up-converted via various IF stages and amplified at RF within the box functionally labelled 'transmitter drive'. The signal then is divided into separate channels and goes through the microwave feed network.

The phase required at each radiating element is adjusted using the phase shifters shown, with one corresponding to each TRM. In the figure one TRM is shown in detail. In actual phased arrays there can be between hundreds and tens of thousands of TRMs, being dependent upon the physical size of the array and the transmission frequency. The same phase shifter is used on transmitting and receiving for beamforming and, if required, can be adjusted in the time interval between the radar pulse being transmitted and signal returns being received. An electronic switch is used to select the path of the signal for either the transmit or receive route. On transmitting, the signal is amplified before being radiated at the array face. A circulator is used to direct the signal to the array on transmit and to the LNA on receive. The LNA establishes the NF of the receiver.

The received signal is then switched into the phase shifter and directed into the main part of the receiver, via the feed network for down-conversion and signal processing. In some active-phased array designs down-conversion and digitisation can be performed at the level of the sub-array. A sub-array is a subset of TRMs, with several sub-arrays making up the full array.

Each of the TRMs is nominally matched in amplitude and phase, in particular so that phase errors do not distort the beam shape being generated. There are also normally elaborate procedures for calibrating the array face to ensure that the required wavefront is provided. In order to control antenna sidelobes, amplitude weighting can be performed by adjusting the gains of the TRMs, with the modules towards the outside of the array having less gain than the central units.

When the phased array is operating, the phase shifters are being continually adjusted on a pulse burst to pulse burst basis, so that the beam shape and direction can be rapidly controlled.

2.2 Radar measurements

2.2.1 Introduction

Within this section radar measurements are reviewed prior to discussing radar target recognition. The basic radar measurements have been presented in the preceding part of Chapter 2 from the point of view of detecting and tracking targets. For target recognition these same types of measurements are used, but are adapted and refined and methods for enhancing and achieving the higher resolution measurements are required.

For detecting targets, normally the highest range resolution used is much greater than the target's physical size. Typically range resolutions from tens to hundreds of metres are used in long-range air defence radars. The main criteria employed for the range resolution used for target detection and tracking are for the target's energy to be confined to one range gate and to provide sufficient range measurement accuracy for the required target tracking precision.

Similarly for the measurements in the frequency domain, the resolution required depends on the requirements for target tracking accuracy. The angular resolution requirements are dependent on the target detection and tracking accuracies needed. In contrast to detection and tracking, high-resolution radar functions are designed to divide the target into small elements, so the design criteria are very different from the conventional radar modes. However, higher-resolution modes are also governed by the basic radar range equation, but it has to be adapted. This section provides a general introduction to high-resolution measurements, which are discussed in more detail later in the context of specific high-resolution target recognition techniques.

2.2.2 Range measurements

As was seen earlier in the chapter, in Equation (2.42), the range resolution obtainable is $c/2\Delta B$. The pulse lengths used for conventional detection and tracking

(a) Conventional radar pulse for target detection

(b) High-range resolution radar pulse
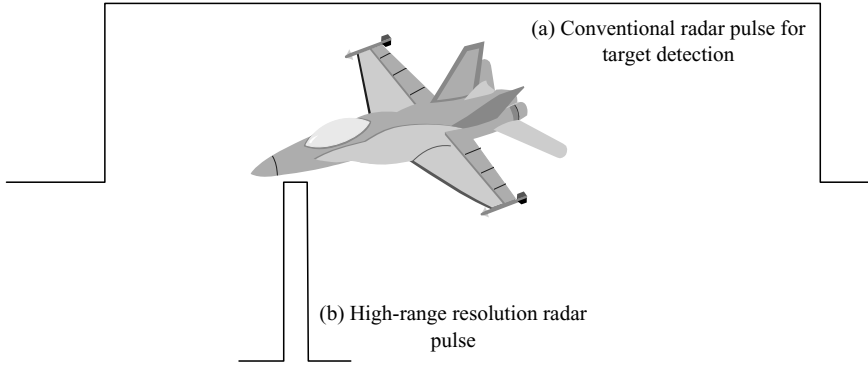
Figure 2.72   Radar pulse lengths for conventional and high-range resolution modes
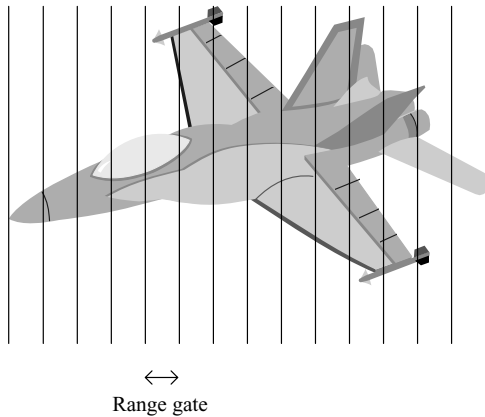
Range gate

Figure 2.73   High-resolution range gates

modes in contrast to the high-range resolution mode are shown qualitatively in Figure 2.72.

The normal pulse is much longer than the target and the high-resolution pulse is a small fraction of the target length. In order to achieve a range resolution of 1 m, a pulse with a bandwidth of 150 MHz is needed. In contrast to detection and tracking modes, range gates for high-resolution modes are designed to dissect the target into small elements, as shown in Figure 2.73.

In the same way that the lower resolution modes measure the range to the target by its time delay for the round trip to the radar, the high-resolution mode also measures the time delay to each range gate. For a range resolution of 150 m, there is a time delay of one microsecond (1 μs) between the centre of two neighbouring range gates. For a radar with 1 m range resolution, the delay between two neighbouring range

gates is $(1/150)\,\mu s$, which is about $7\,ns$ ($1\,ns$, or one nanosecond, is one thousand millionth of a second). It can be seen that much greater timing accuracy is required for the higher resolution mode.

The amplitude of the radar return in each range gate results from reflections of the radar signal from the target at that time delay. The amplitude of the radar return represents the strength of the reflection of the signal from a particular region of the target determined by the time delay. With reference to the figure, it can be seen that all the returns in one range cell are collected together to provide a single amplitude contribution. For the range gate marked with the arrows, returns from various parts of the wing, some of the fuselage and parts of the cockpit contribute to the overall amplitude measured by the radar. This simple explanation assumes that no complex scattering mechanisms or multiple reflections are present, which can place reflections in the 'wrong' range gate.

The integration of radar pulses improves the signal-to-noise ratio of the return in each range gate, so as more pulses are integrated smaller elements of the target can be detected, within the constraints of the radar's range resolution and dynamic range.

2.2.3   Frequency measurements

The measurement of the Doppler frequency of targets was presented earlier. The frequency resolution obtained is the inverse of the radar integration period, T. The frequency measured was used to determine the radial velocity of moving targets. However, high-resolution frequency measurements can be used to measure the relative velocities of parts of targets with high precision, which can then be used for target recognition purposes. There are two types of frequency measurements, which can be used for target recognition. The first is the relative Doppler frequency of parts of the same nominally rigid mechanical structure, such as an aircraft or ship. The second is FM imparted to the radar signal, as a consequence of interacting with moving machinery of parts of the target, such engines.

Figure 2.74 shows a ship rolling about its centre of gravity, due to rough seas. For rotating objects, the Doppler vector measured by the radar varies with the different parts of the ship. If a radar were to measure the frequencies returned from this ship it would detect a range of frequencies around the radial velocity vector, V, associated with its bulk translational motion. The spread of the frequencies is determined by the positive and negative Doppler frequencies due to the rotational motion. It can be seen that at the angle of roll, θ, the three parts of the ship identified have different rotational components and different respective Doppler components, as measured by the radar.

A radar with sufficient velocity resolution can measure the velocity spread of returns from a particular target over a single dwell period and over several dwell periods for analysis. The bulk Doppler provides the radial velocity component of the target and the spread of Doppler frequencies provides the spread of velocities of the target. Also, over a number of dwell periods the rotational period of the ship can be determined. All of this information can be used to determine certain characteristics of the target for recognition purposes. In particular, if the radar also has a high range
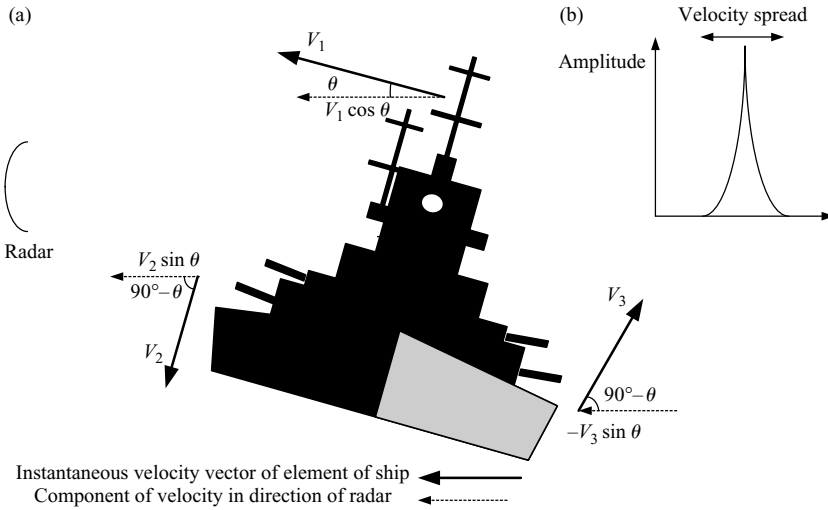
Figure 2.74   Rolling ship with different parts having different Doppler frequencies: (a) rolling ship and (b) radial velocity components of ship's motion

resolution capability, high-resolution imaging is possible, as will be discussed later.

Interestingly, if the platform on which the radar is installed is moving and the target is stationary, it is also possible to measure different Doppler frequencies from different parts of the target. The radial velocity vector component from the radar to the target varies slightly with aspect angle. This effect is utilised in synthetic aperture radar (SAR), will be presented in more detail later and can be used for the imaging and recognition of stationary ground targets and features on the ground. Differentiation of Doppler frequencies and cross-range resolution, which is introduced in the next section, are closely linked topics.

The second type of technique, which uses high-resolution frequency measurements, is associated with moving parts of targets, such as the turbine blades of jet engines, aircraft propellers and the rotor blades of helicopters. When the radar wave encounters these rotating objects, it is reflected and modulation is imparted to it. The frequency characteristics are dependent on the speed of rotation of the object, its mechanics and the number of blades or rotors it possesses. The modulation appears as frequency components of the Doppler spectrum of the object and can be used as discriminants for target recognition. This subject will be discussed later with jet engine modulation (JEM) and helicopter engine rotor modulation (HERM) being examples of associated target recognition techniques.

2.2.4   Cross-range resolution

As was seen in Equation (2.22), the beamwidth of an antenna is given by $k\lambda/a$, where k is a constant of typical value 1–2, λ is the wavelength and a is the antenna
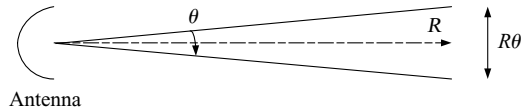
Figure 2.75   Cross-range resolution is dependent on the antenna aperture and range to the target
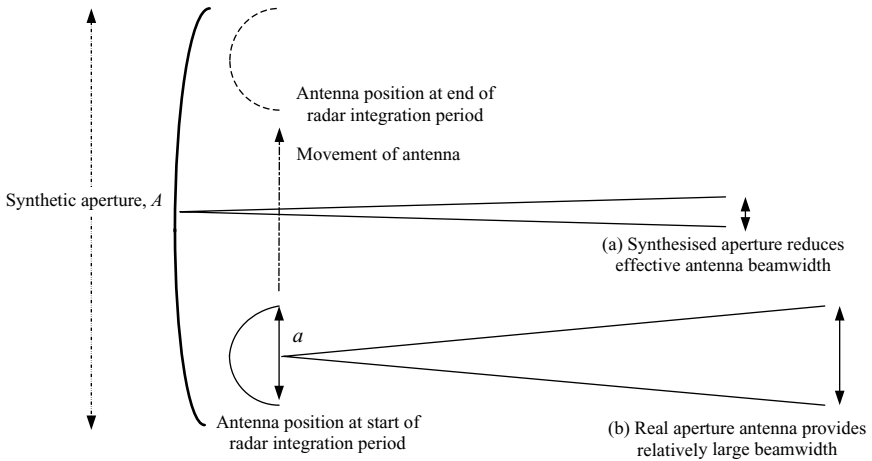
Figure 2.76   Synthesising a large antenna aperture to provide high cross-range resolution

aperture. The basic cross-range resolution of the radar is the beamwidth multiplied by the range of interest, as is shown in Figure 2.75.

The cross-range resolution of the radar is quite coarse compared to its down-range resolution. Various techniques are available to improve cross-range resolution. Monopulse techniques are used in many conventional radars and use two receiving beams for comparing the respective signals to provide a more precise estimation of the position within the beam. However, for most radar targets of interest and operational ranges, the improvement obtained is not normally sufficient to provide cross-range resolution appropriate to target dimensions, so does not contribute much to target recognition. These techniques, including super resolution, are discussed in Chapter 6.

The main technique for improving cross-range resolution is called synthetic aperture radar (SAR). The basis of the technique is to move the antenna along a baseline in order to *synthesise* an aperture, which is much larger than the antenna dimensions. This is illustrated in Figure 2.76. It is necessary to integrate coherently over the synthesised antenna baseline. To achieve this the target has nominally to travel in a straight line continuously illuminating the target over the integration period.

Synthetic aperture radar will be discussed in more detail in Chapter 4 and will be seen to utilise high-resolution frequency measurements as discussed in Section 2.2.3.

2.2.5   Summary

In this introductory section to high-range resolution radar, the main types of radar measurements have been presented. The measurement of high down-range resolution is dependent upon transmitting a large bandwidth signal and measuring the time delays appropriate to the high-resolution range gates. High-resolution frequency measurements provide the ability to measure differences in Doppler frequencies across individual targets, which can be moving or can be stationary objects on the ground, which can then be used for synthetic radar imaging. The measurement of radar returns from rotating objects or machinery provides discriminants for recognising propulsion systems of vehicles. These techniques will be discussed in detail in Chapter 5.

2.3   Introduction to target recognition

2.3.1   Introduction

The main processes involved in the target recognition function are introduced in this section from transmitting the radar signals to providing estimates of the type of target detected, prior to more detailed discussion in the later chapters. The basic scattering mechanisms from targets are discussed, as these are the link between the electromagnetic wave illuminating the target and the physical size, shape, orientation and material composition of the target, which then result in the signature measured by the radar. The shapes of objects determine their relative rcs and the variation with aspect angle to the radar, so hence the amount of signal reflected towards and detected by the radar. For objects composed of component parts of different shapes, as is generally the case with man-made objects, each component contributes to the target signature. Also the relative contributions will vary with aspect angle to the radar. The radar cross-sections of some standard object shapes are presented.

2.3.2   The target recognition process

2.3.2.1   Introduction

The target recognition process is summarised in Figure 2.77.

It is clearly necessary to design the radar appropriate to the type of measurement that has to be performed, to provide the type of target signature required. In order to obtain signatures of high integrity, the waveform must be carefully designed and the radar must support the transmission and reception of the signal without distortion. The waveform, the associated signal processing, radar phase noise and dynamic range performance also have to be designed to minimise the effects of clutter. There must also be sufficient energy radiating from the target to ensure that the smallest contributions to the target signature, which are needed for the recognition process, are detected reliably.
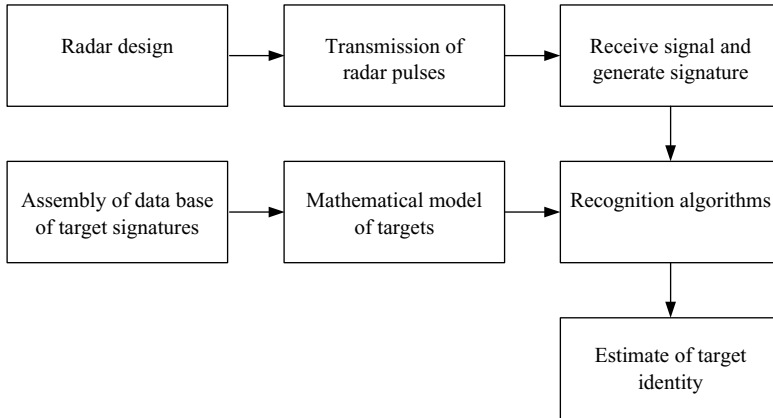
Figure 2.77   Target recognition process

2.3.2.2   Main functions

After the radar has transmitted the high-resolution pulse train, detected and processed the return from the target of interest, the signature is conditioned ready for the recognition process. In order to perform target recognition, a good deal needs to be known about the targets, which are to be recognised. High-integrity high-resolution reference signatures of all targets of potential interest, at aspect angles of interest and possibly with different stores, flight or assembly configurations are needed. It is necessary to mathematically predict the signatures of the targets to be encountered, or to physically measure the high-resolution signatures of the targets. A combination of these techniques can also be used. When the many measurements and/or signature modelling computer runs have been performed, it is necessary to assembly them into a database. The type of target recognition technique being utilised and the type of recognition algorithm employed determine how this data is subsequently used. It can be averaged in various ways and it is then translated into some form of mathematical model representing the targets' characteristics.

Recognition algorithms are mathematical techniques or formulae that compare the signatures which have been measured with the mathematical models of targets which have been assembled. The algorithms are designed to perform this function and are required to assess how close a match a particular signature is to its mathematical model reference and if any other targets also have a likelihood of being the same target. This is illustrated in Figure 2.78 for a measured range profile of an aircraft target.

The signature shown is a typical range profile of an aircraft. The recognition algorithm compares the signature obtained with the three reference signatures shown and provides an estimate of the best candidate for the unknown target's identity. In this example target 'C' is the best match as can be seen by comparing the shapes and sizes of the references with the measurement. There are many techniques available for recognition images or patterns. The main methods used in radar target recognition

Measured signature

Reference signature:
Target A

Reference signature:
Target B

Reference signature:
Target C
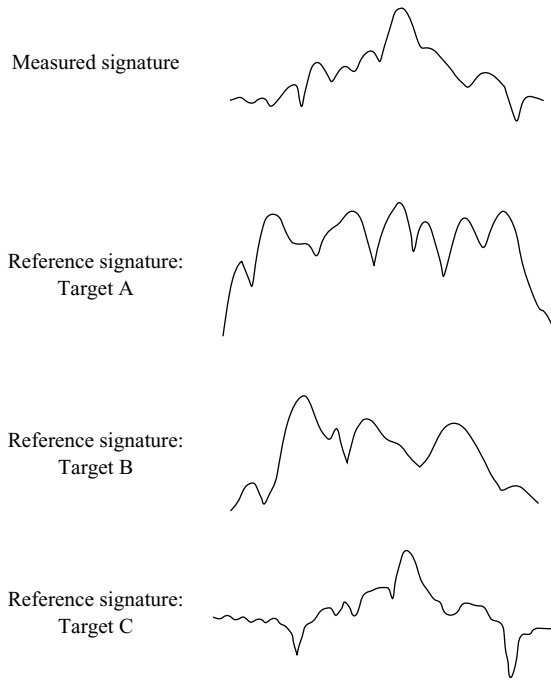
Figure 2.78   Measurement of a high-resolution target signature and comparison with reference signatures (Courtesy BAE Systems Insyte)

are discussed in Chapter 12. The algorithm would provide a measure of confidence in the decision made. It could be a probability or could be the number of target features that matched.

It can be seen that as in the detection of targets, the recognition of targets has a probability of correct assignment and a probability of wrong assignment to target type. These probabilities depend upon the quality of the radar measurement, the similarity of the two targets, the quality of the mathematical model of the targets and the effectiveness of the recognition algorithm. The quality of the radar measurement depends on the signal-to-noise ratio, whether clutter, interference or jamming are present and in some cases, whether the target is changing aspect angle or accelerating during the measurement. For high-range resolution measurements, for example, in certain circumstances a manoeuvring or accelerating target can blur the high-resolution image and thereby degrade the recognition process.

2.3.3   Electromagnetic scattering

2.3.3.1   Introduction

The electromagnetic scattering mechanisms occurring when the radar wave encounters any object determine how much energy is reflected back in the direction of the
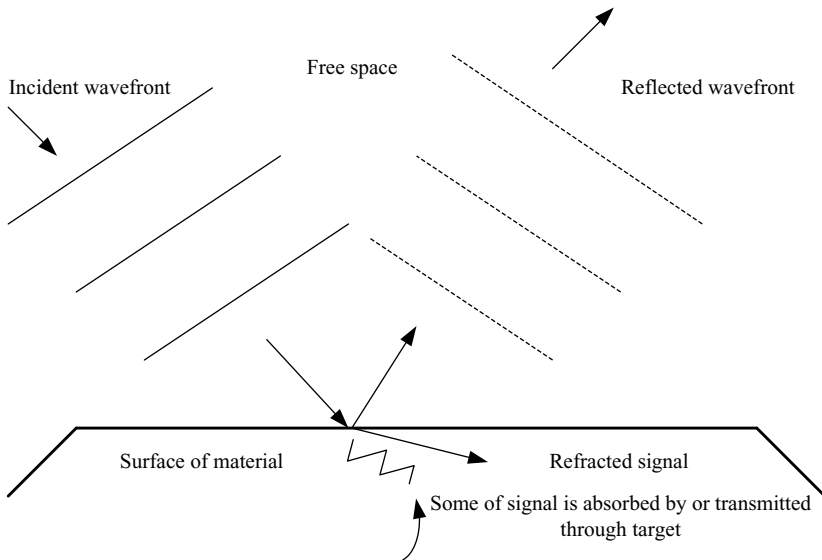
Figure 2.79   Interaction of radar wave when encountering object

radar. For the low-resolution radar used for detection and tracking all the energy associated with the returns from a single long pulse in the direction of the radar is integrated together and only a single amplitude and phase measurement are effectively made per pulse. For high-range resolution radar, for example, one type of target recognition method, the target is effectively divided into small elements, which are the high-resolution range gates. The scattering mechanisms at the time delay of the respective range gates determine the amplitudes and phases of the returned signals. The high-resolution range gates are effectively independent, whereby each integrates the energy at its respective time delay for reflection back to the radar. The net result of all the scattering is the target signature. For the frequency analysis and high cross-range resolution techniques and combination of these high-resolution methods, the elements of the target are again divided in various ways by the high-resolution radar waveform and signal processing. The signatures obtained are again determined by the scattering effects occurring for each constituent of the target.

2.3.3.2   Target interactions

The main interactions of the electromagnetic wave with the target are reflection, absorption, refraction, diffraction and creeping surface waves. In Figure 2.79 reflection, refraction and absorption are illustrated. A geometrical object model has been used to show the waveform interaction effects. The incident waveform is reflected at the boundary between free space and the object, but at reduced amplitude as some of the energy is absorbed and some is refracted through the object. The absorption is due to resistive losses in the material, which would be due to a non-perfectly
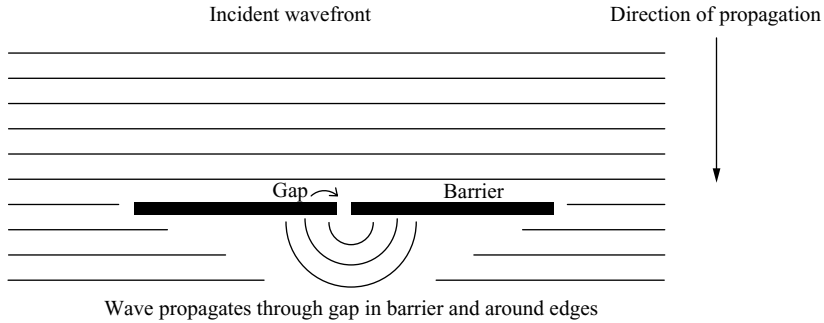
Figure 2.80   *Diffraction of radar wave*

conducting metal, for example. If there is a non-metallic component of the material, which is a non-conducting insulator, the signal can be refracted through it in the same way as light is refracted through a piece of glass. It can be seen that little energy is reflected back towards the radar, as the angle of incidence to the flat surface shown is not perpendicular to it. For flat surfaces, only at a narrow range of angles is energy reflected back towards the radar.

Diffraction occurs as another manifestation of the radar signal's electromagnetic wave characteristics. It is an effect such that signals are not constrained to travel in straight lines and can propagate around corners [99]. It is illustrated in Figure 2.80. The wave propagates through the gap in the barrier shown and also around it. This means that when the signal is interacting with the target it can propagate to locations that would be precluded from the geometrical optics model. Diffraction effects occur at wavelengths that are similar to the dimensions of target features. It enables waves to bend around the edges of targets and to be reflected from parts of the target that would be inaccessible at other wavelengths. It also allows propagation into the target through gaps in its structure.

The final effect to be mentioned is creeping surface waves [100,101]. This is a surface wave mode, whereby the signal can propagate along the surface of an object, to reach locations which would be completely inaccessible from the geometrical optical viewpoint.

2.3.3.3   Summary

It can be seen that the interaction of the radar wave with the target involves a number of different effects, which are dependent upon wavelength, target dimensions and material properties. The shapes of objects have very significant effects on the signal reflected back to the radar. The wavelength and the polarisation of the radar signal being employed and the dimensions and orientation of the object all contribute to a variation of rcs with aspect angle of the radar. For some targets, there can be orders of magnitude variations in rcs over a hemisphere of look angles. A summary of the maximum radar cross-sections of a number of commonly shaped objects, which are assumed to be conductors of electricity, appears in Table 2.3.
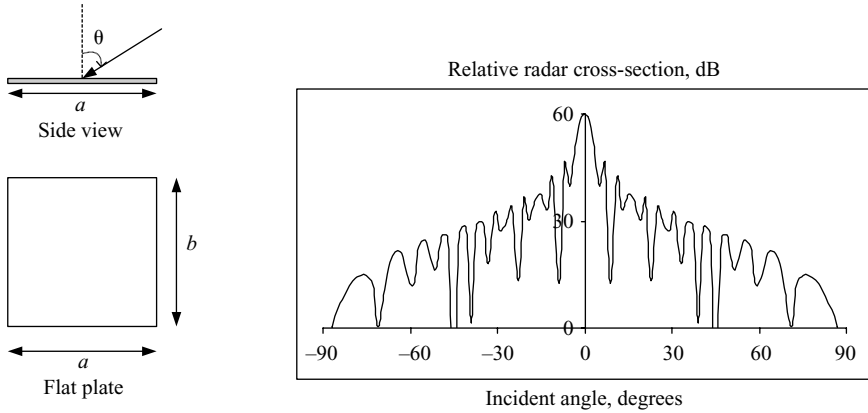
Figure 2.81   Variation of rcs of flat plate with incident angle

2.3.4   Radar cross-sections of simple objects

The radar cross-sections of a few conducting objects are now presented [102] in order to illustrate how variations occur with wavelength, aspect angle and size. The rcs, σ, of a flat plate of sides 'a' and 'b', as a function of incident angle, θ, and wavelength is given by:

$$\sigma = \frac{4\pi a^2 b^2}{\lambda^2} \left[\frac{\sin((2\pi/\lambda)a\sin\theta)}{((2\pi/\lambda)a\sin\theta)} \right]^2 \cos^2\theta \qquad (2.57)$$

The rcs as a function of incident angle is shown in Figure 2.81. It can be seen that the rcs of the flat plate varies by several orders of magnitude over a change in aspect angle of 90° for the incident signal.

For a sphere, as it is symmetric for every aspect angle of incidence, its rcs is clearly the same from every direction. There are actually three scattering regions for spheres, which are wavelength dependent and are shown in Figure 2.82.

At the longer wavelengths defined when $2\pi a/\lambda$ is less than unity, where a is the radius of the sphere, this is called the Rayleigh scattering region. The rcs is inversely proportional to the fourth power of the wavelength. The next region is called the 'resonance' or Mie region, when the value of $2\pi a/\lambda$ is between one and ten. Under these conditions a creeping wave is formed and travels right around the sphere and depending on the size of the sphere compared to the radar wavelength, can either constructively interfere with the part of the wave being reflected directly from the sphere's surface or destructively interfere with it. The final region occurs for short wavelengths when the value of $2\pi a/\lambda$ is greater than ten. Scattering can then be treated as an optical phenomenon and the rcs is close to the physical cross-section of the sphere, which is πa^2. The rcs of various objects appears in Table 2.3.

It can be seen that the rcs of the various objects varies considerably, clearly being dependent upon the wavelength and object size. The trihedral is composed of

Radar cross-section
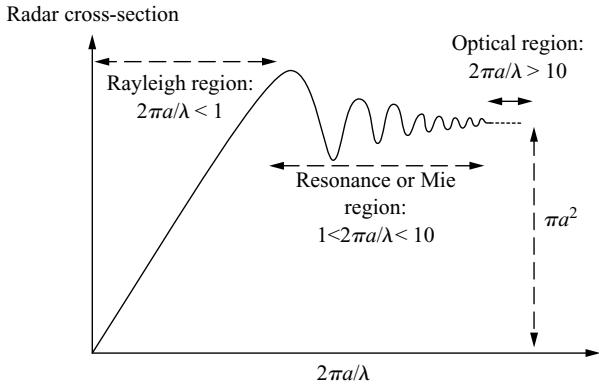
Figure 2.82   Variation of rcs of sphere of radius a with wavelength, λ

three flat plates mutually orthogonal (at 90°) to one another. Over several tens of degrees about the axis of symmetry the rcs is quite large, as any incident wave is reflected sequentially from the three faces and is reflected back to the radar. This is a consequence of the geometry and the fact that at each face the incident angle is equal to the reflected angle. This is the same principle as 'cat's eyes', which are used on road surfaces and posts and reflect car headlights back in the direction of the car to improve visibility at night. Reflections from mutually orthogonal plates forming part of a target are important in target recognition, as they provide a large rcs over a wide range of aspect angles and can be used as a discriminating feature. A real target, such as a ship or an aircraft, is made up of generally complex shapes, each of which has elements contributing to the rcs. In a high-resolution range gate there are usually several contributors to the associated radar return from that time delay.
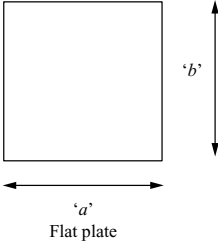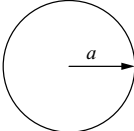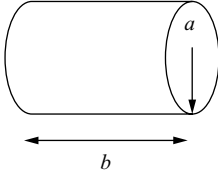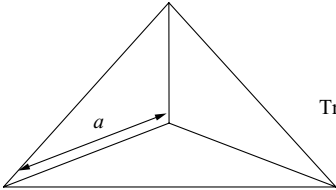
2.4   Summary

In Chapter 2, a summary of the main components constituting a radar system, the system design and some basic theory on radar performance has been provided. Radar measurements have been discussed, which form the basis of providing high-resolution modes.

The main functions involved in the provision of a radar target recognition mode have been outlined. High-resolution radar signatures are used for recognising targets and are dependent upon the target's shape, size, constituting materials, aspect angle and radar wavelength. The fundamental scattering mechanisms from targets have been presented.

The following chapters build on the basic information provided in this chapter and explain the concepts involved in designing and implementing radar target recognition modes.

Table 2.3 *Radar cross-sections of geometrical objects*

Object	rcs/comment

'b'
'a'
Flat plate

$$\frac{4\pi a^2 b^2}{\lambda^2} \left[\frac{\sin((2\pi/\lambda)a\sin\theta)}{((2\pi/\lambda)a\sin\theta)} \right]^2 \cos^2\theta \qquad \text{Max rcs} = \frac{4\pi a^2 b^2}{\lambda^2}$$

Where θ = incident angle

a
Sphere

For $2\pi a/\lambda < 1$: rcs $< \pi a^2$ and proportional to $1/\lambda^4$
(Rayleigh scattering region)

For $1 > 2\pi a/\lambda < 10$. Max rcs $\approx 4\pi a^2$
(Resonance or Mie region)

For $2\pi a/\lambda > 10$, rcs $= \pi a^2$
(Optical region)

a
Right circular cylinder
b

Max rcs $= 2ab^2/\lambda$

a
Triangular trihedral

Max rcs $= 4\pi a^4/3\lambda^2$
Large rcs over wide
range of angles

References

1 BARTON, D.K. *et al.*: 'Radar Technology Encyclopedia' (Artech House, Boston, MA, 1997)
2 HOVANESSIAN, S.A.: 'Radar System Design and Analysis' (Artech House, Boston, MA, 1984)
3 GALATI, G. (Ed.): 'Advanced Radar Techniques and Systems' (IEE, Stevenage, 1993)

 4 LONGHURST, R.S.: 'Geometrical and Physical Optics' (Longmans, London, 2nd edn, 1968), Chapter XXIV
 5 WILSON, T.: 'How Radio Signals Work' (McGraw Hill, New York, 1998)
 6 PUGH, E.M., and PUGH, E.W.: 'Principles of Electricity and Magnetism' (Addison-Wesley, Reading, MA, 1965) Chapter 11.2
 7 FEYMAN, R.P., LEIGHTON, R.D., and SANDS, M.: 'Lectures on Physics' (Addison-Wesley, Reading, MA, 1969) Chapter 27
 8 PUGH, E.M., and PUGH, E.W.: 'Principles of Electricity and Magnetism' (Addison-Wesley, Reading, MA, 1965) Chapter 11.2–11.5
 9 PUGH, E.M., and PUGH, E.W.: 'Principles of Electricity and Magnetism' (Addison-Wesley, Reading, MA, 1965) Chapter 11.6
10 LIVINGSTON, D.C.: 'The Physics of Microwave Propagation' (Prentice Hall, New York)
11 SAUNDERS S.: 'Antennas and Propagation for Wireless Communication Systems' (John Wiley & Sons, New York, 1999)
12 SKOLNIK, M.I.: 'An Introduction to Radar Systems' (McGraw-Hill, New York, 1970) Chapter 12
13 BEDARD, B.: 'Control High Speed Circuits with PIN Diode Switches', *Microwaves,* 1982, May, pp. 152–3
14 HOMER, G.M.: 'PIN Diode Driver Allows Linear RF Attenuation', *Microwaves*, 1983, April, pp. 83–4
15 LEVANON, N.: 'Radar Signals' (John Wiley & Sons, New York, 2004) Chapters 5 and 6
16 SPROUL, R.: 'The Working Man's Phase Shift Primer', *Microwaves and RF*, 1984, November, pp. 91–6
17 GENTILE, K.: 'Fundamentals of Digital Quadrature Modulation', *RF Design*, 2003, February, (www.rfdesign.com)
18 JOSWICK, W.: 'I/Q networks Deliver Various Modulation Formats', *Microwaves & RF*, 1994, March, p. 81
19 CURTIS J.: 'Complex Phasor Modulators Control Amplitude and Phase Simultaneously', *Microwaves and RF*, 1983, July, p. 123
20 MATTACH R.J., CROWE T.W., and BISHOP W.L.:'Frequency and Noise Limits of Scottky Barrier Mixer Diodes', *Microwave Journal,* 1985, March, p. 101
21 HALLFORD, B.R.: 'Trace Phase States to Check Mixer Designs', *Microwaves,* 1980, June, p. 52
22 BREWERTON, B., and URBANETA, N.: 'Synthesizer Primer Defining the Elements of Good Design', *Microwaves*, June, 1984, p. 79
23 DRISCOLL, M.M., JELEN, R.A., and MATTHEWS, N.: 'Extremely Low Phase Noise UHF Oscillators Utilising High Overtone Bulk Acoustic Resonators', *IEEE Transactions on Ultrasonics, Ferroelectrics and Frequency Control*, 1992, **39** (6), pp. 774–9
24 SULLIVAN, W.: 'High Speed Synthesizer Spans 2.25 to 18 GHz', *Microwaves and RF*, 2003, December

25 ALESSIO, G.: 'PLL Synthesiser enhances STALO radar performance', *Microwaves and RF*, 1996, May

26 KROUPA, V.F.: 'Phase Lock Loops and Frequency Synthesis' (John Wiley & Sons Ltd, New York, 2003)

27 GOLDBERG, B.-G.: 'Digital Frequency Synthesis Demystified' (Butterworth-Heinemann, Oxford, 1999)

28 KROUPA, V.F.: 'Direct Digital Frequency Synthesizers' (John Wiley & Sons Ltd, New York, 1998)

29 JIMENEZ, J.L., GISMERO, J., RAMIREZ, D., and PARDO, J.M.: 'Large Time-Bandwidth Product DDS Chirp Waveform Generator for High-Resolution Radars', Radar 2004, Toulouse, France, Paper no. 168

30 BENFORD, J., and SWEGLE, J.: 'An Introduction to High Power Microwaves', *Microwave Journal,* 1992, February, pp. 105–116

31 GILMOUR, A.S.: 'Principles of Traveling Wave Tubes' (Artech House, Boston, MA, 1994)

32 GILMOUR, A.S.: 'Microwave Tubes' (Artech House, Boston, MA, 1986)

33 GREBENNIKOV, A.: 'RF and Power Amplifier Design' (McGraw-Hill, New York, 2004)

34 CRIPPS, S.C.: 'Advanced Techniques in RF Power Amplifier Design' (Artech House, Boston, MA, 2002)

35 'Power Amplifier Design: A Collection from "Applied Microwave and Wireless" ' (Noble, Ashland, OH, 2002)

36 SMITH, B.L.: 'High Power Microwave Electron Tubes Designed for Modern Microwave Systems', *Microwave Systems News and Communications Technology*, 1985, June, pp. 68–81

37 FEYNMAN, R.P., LEIGHTON , R.B., and SANDS, M.: 'The Feynman Lectures on Physics', vol. 2 (Addison-Wesley, Reading, MA, 1969)

38 SKOLNIK, M.I.: 'An Introduction to Radar Systems' (McGraw-Hill, New York, 1970) Chapter 2-7

39 SPIEGEL, M.: 'Outline of Theory and Problems of Fourier Analysis' (Schaum, 1974)

40 KORNER, T.W.: 'Fourier Analysis' (Cambridge University Press, London, 1989)

41 SNEDDON, I.N.: 'Fourier Transforms' (Dover Publications, Mineola, New York, 1995)

42 JAMES, J.F.: 'A Student's Guide to Fourier Transforms: With Applications in Physics and Engineering' (Cambridge University Press, London, 2002)

43 SKOLNIK, M.I.: 'An Introduction to Radar Systems' (McGraw-Hill, New York, 1970), Chapter 2-7

44 SKOLNIK, M.I.: 'An Introduction to Radar Systems' (McGraw-Hill, New York, 1970) Chapter 7-1

45 SKOLNIK, M.I.: 'An Introduction to Radar Systems' (McGraw-Hill, New York, 1970) Table 7.1

46 FEYNMAN, R.P., LEIGHTON, R.B., and SANDS, M.: 'The Feynman Lectures on Physics' vol. 1 (Addison-Wesley, Reading, MA, 1969) Chapter 34.6

47 FEYNMAN, R.P., LEIGHTON , R.B., and SANDS, M.: 'The Feynman Lectures on Physics', vol. 2-21 (Addison-Wesley, Reading, MA, 1969)

48 BARTON, D.K.: 'C.W. and Doppler Radar' (Artech House, Boston, MA, 1978)

49 SCHLEHER, D.C.: 'Moving Target Indication and Pulsed Doppler Radar' (Artech House, Boston, MA, 1991)

50 MORRIS, G.V. *et al*.: 'Airborne Pulsed Doppler Radar' (Artech House, Boston, MA, 1996)

51 BRIGGS, W.L.: 'The DFT; Owner's Manual for the Discrete Fourier Transform' (Society of Industrial & Applied Mathematics, Philadelphia, PA, 1995)

52 TOLIMIERI, R. *et al*.: 'Algorithms for Discrete Fourier Transform and Convolution' (Springer-Verlag, New York, 1997)

53 CIZEK, V.: 'Discrete Fourier Transforms and Their Applications' (UK Institute of Physics, London, 1986)

54 SUNDARARJAN, D.: 'The Discrete Fourier Transform: Theory, Algorithms and Applications' (World Scientific Publishing, Hackensack, NJ, 2001)

55 STANFORD UNIVERSITY WEBSITE: Discrete Fourier transform. http://ccrma-www.stanford.edu/~jos/mdft/DFT_Definition.html

56 FEYNMAN, R.P., LEIGHTON, R.B., and SANDS, M.: 'The Feynman Lectures on Physics' vol. 1-41 (Addison-Wesley, Reading, MA, 1969)

57 SEARS, F.W.: 'Thermodynamics' (Addison-Wesley, Reading, MA, 1969) Chapter 17

58 SKOLNIK, M.I.: 'An Introduction to Radar Systems' (McGraw-Hill, New York, 1970) Chapter 2-4

59 MEER, D.E.: 'Noise figures (linear transducer)', *IEEE Transaction on Education*, 1989, **32** (2), pp. 66–72

60 FRIIS, F.: 'Noise Figure of Radar Receivers', *Proceedings of IRE*, 1944, **32**, pp. 419–22

61 ROBINS, W.P.: 'Phase Noise in Signal Sources' IEE Telecommunications Series (Peter Peregrinus, London, 1982)

62 FRUEHAUF, H.: 'SSB Phase Noise: A Key Specification', *Microwaves & RF Magazine,* 1984, June, p. 100

63 GOLDMAN, S.J.: 'Phase Noise Analysis in Radar Systems Using Personal Computers' (John Wiley & Sons, New York, 1989)

64 GOLDMAN, S.: 'Oscillator Phase Noise Proves Important to Pulse Doppler Radar Systems', *Microwave Systems News*, 1984, February, pp. 88–100

65 NEZAMI, M.K.: 'Evaluate Impact of Phase Noise on Receiver Performance', *Microwaves and RF*, May, 1998, pp. 165–180

66 ROBERTS: 'A Review of Solid-State Radar Receiver Protection Devices', *Microwave Journal*, 1999, February, pp. 121–2

67 JABLONSKI, W.: 'A new Method of the Design and Technology of PIN Diodes'. Proceedings of the 12th International Conference *Microwaves and Radar*, 1998, MIKON, May 1998, pp. 69–73

68 JANG, B.-J.: 'Voltage Controlled PIN Diode Attenuator with Temperature-Compensation Circuit', *Microwave and Wireless Components Letters*, 2003, **13** (1), pp. 7–9

69 LUDWIG, J. *et al.*: 'Gallium Arsenide and Related Compounds: Proceedings of the Third International Workshop' (World Scientific Publishing, Hackensack, NJ, 1995)

70 PENGELLY, R.S., and HAMMOND, C.: 'Microwave Field Effect Transistors: Theory, Design and Applications' (Noble Publishing, Ashland, OH, 2001)

71 NIEHENKE, E.C., STEIGERWALD, T.E., and LISENBARDT, A.E.: 'New limiters protect low noise FET amplifiers', *Microwaves*, 1984, February, pp. 89–96

72 DROZDOVSKI, N.V., and DROZDOVSKAIA, L.M.: 'Microstrip and Wave-guide Passive Power Limiters with Simplified Construction', *Journal of Microwaves and Optoelectronics*, 1999, **1** (5)

73 HOWARD, A.: 'Efficiently Simulating the Third-order Intercept Point of a Direct Conversion Receiver', *RF Design*, 2004, May

74 DEMLER, M.: 'High Speed Analogue to Digital Conversion' (Academic Press, New York, 1991)

75 HNATEK, E.R.: 'A User's Guide to Digital to Analogue and Analogue to Digital Converters' (John Wiley & Sons, New York, 1976)

76 LYONS, R.: 'Understanding digital signal processing's frequency domain', *RF Design*, 2001, November, pp. 36–48

77 BARTZ, M.: 'Large scale dithering enhances ADC dynamic range', *Microwaves and RF*, 1993, May, pp. 192–8

78 LYNN, P.A.: 'Digital Signals, Processors and Noise' (Palgrave Macmillan, New York, 1992)

79 BRACEWELL, R.N.: 'The Fourier transform and its Applications', Amazon.com

80 LONGHURST, R.S.: 'Geometrical and Physical Optics' (Longmans, Green and Co Ltd, London, 1969) pp. 218–9, 301–2

81 http://mathworld.wolfram.com/ChineseRemainderTheorem.html

82 http://mathworld.wolfram.com/SamplingTheorem.html

83 LYONS, R.: 'Understanding digital signal processing's frequency domain,' *RF Design*, 2001, November, pp. 36–7

84 KINGSLEY, S., and QUEGAN, S.: 'Understanding Radar Systems' (McGraw-Hill, New York, 1992) Chapter 2-3

85 SKOLNIK, M.I.: 'An Introduction to Radar Systems' (McGraw-Hill, New York, 1970) Chapter 2-5

86 KINGSLEY, S., and QUEGAN, S.: 'Understanding Radar Systems' (McGraw-Hill, New York, 1992) Chapter 5.5

87 MINKLER, G.: 'CFAR: The Principles of Automatic Radar Detection in Clutter' Available from Amazon.com

88 STIMSON, G.W.: ' Introduction to Airborne Radar' (Scitech Publishing Inc., 2nd edn) Chapter 25

89 KINGSLEY, S., and QUEGAN, S.: 'Understanding Radar Systems' (McGraw-Hill, New York, 1992) Chapter 3

90 BLACKMAN, S., and POPOLI, R.: 'Design and Analysis of Modern Tracking Systems' (Artech House, Boston, MA, 1999)

91 RISTIC, B., ARULAMPALAM, S., and GORDON, N.: 'Beyond the Kalman Filter: Particle Filters for Tracking Applications' (Artech House, Boston, MA, 2004)

92 KINGSLEY, S., and QUEGAN, S.: 'Understanding Radar Systems' (McGraw-Hill, New York, 1992) Chapter 4.8

93 LEVANON, N.: 'Radar Signals' (John Wiley & Sons, New York, 2004) Chapter 2

94 CANN, A.J.: 'Range Gate Straddling Loss and Joint Probability with Partial Correlation', *IEEE Transactions on Aerospace and Electronic Systems*, 2002, **38**, pp. 1054–1058

95 SKOLNIK, M.: 'An Introduction to Radar Systems' (McGraw-Hill, New York, 1970) Chapter 2-6

96 FELDLE, H., and SOLBACH, K.: 'Passive and Active Phased Arrays using Solid State Technologies'. UK IEE Colloquium. December 1991

97 BROOKNER, E.: 'Phased Array Radars, Past, Present and Future'. IEE Conference Radar, October 2002, Edinburgh

98 BROOKNER, E.: 'Phased Array Radars for the New Millenium'. CIE International Conference, 15–18 October 2001, Beijing, China, pp. 34–41

99 FEYNMAN, R.P., LEIGHTON, R.B., and SANDS, M.: 'The Feynman Lectures on Physics' vol. 1–30 (Addison-Wesley, Reading, MA, 1969)

100 HERMANN, G.F.: 'Empirical-Computational Methods in the Study of Creeping Waves', *IEEE Transactions on antennas and propagation*, 1990, **38** (1), pp. 51–91

101 YAN, J., XU., C., and XU, D.: 'Time Domain Analysis of Creeping Wave'. *Microwave Conference Proceedings*, APMC '97, 1997 Asia-Pacific, vol. 3, 2–5 December, 1997

102 SKOLNIK, M.I.: 'Radar Handbook' (McGraw-Hill, New York 1990, 2nd edn) Chapter 11

Chapter 3

High-resolution range profile

3.1 Introduction

3.1.1 Range profile signature

In this chapter high-range resolution radar is presented. A high-resolution range profile (HRRP) is a one-dimensional signature of an object. It is a representation of the time domain response of the target to a high-range resolution radar pulse. An example of the range profile of an aircraft in flight is provided in Figure 3.1. In each high-resolution range cell the amplitude of the signal is measured giving the strength of the return at that time delay. The main parts of the aircraft which contribute to the range profile are shown. It should be noted that most targets do not appear to have the same 'radar' length as their physical length due to two effects. Rather than the signal being reflected back towards the radar directly, it can bounce between different scatterers comprising the target, so the time delay is increased, which is manifested in the radar range profile signature being longer than the target. The other effect, which can occur, is the 'shadowing' of one part of the target by another part. This occurs when part of the target is obscured by a large part of the same target located between it and the radar, significantly reducing the energy in the wave reaching it and being reflected back to the radar. When this occurs at a particular aspect angle, a certain part of the target may not contribute to the range profile. For example, the fuselage and wings of a civil airliner can obscure the tail at certain aspect angles to the radar resulting in an apparently shorter aircraft.

3.1.2 Aspect angle effects

The range profile of the target is aspect angle dependent and the component parts of the aircraft contributing to the high-resolution range gates vary accordingly. This is illustrated in Figure 3.2. For the head on aspect angle, (a), the range gates are distributed along the axis of symmetry of the fuselage. It can be relatively clearly
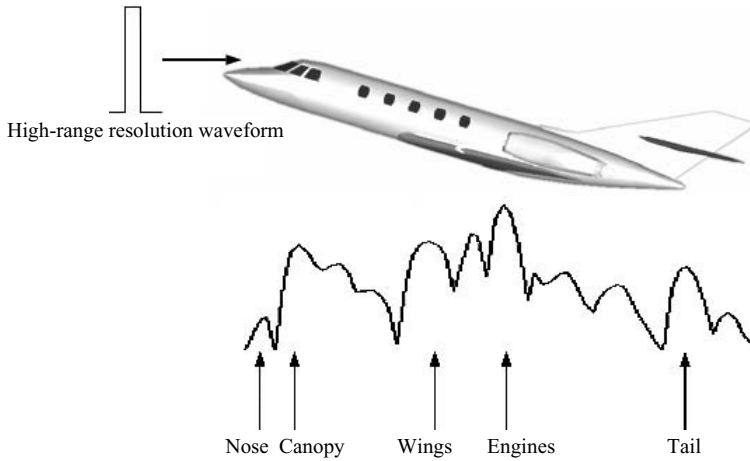
Figure 3.1   Typical high-resolution range profile of aircraft target (Courtesy of BAE Systems Insyte)
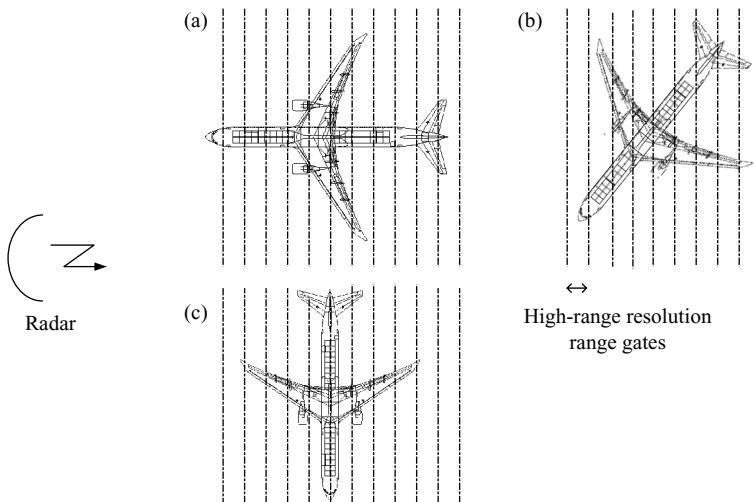
Figure 3.2   Different parts of the aircraft appear in each range gate as the aspect angle to the radar changes

envisaged which parts of the aircraft contribute to each range gate. In contrast with (b), parts of the wing would be expected to contribute to the returns in most of the range gates with returns from parts of the fuselage. With reference to (c), it can be seen that the fuselage is confined to a few range gates in comparison to (a), in which the fuselage returns would contribute to range gates all along the aircraft.

Hence, at each aspect angle, a unique set of contributions to the range profile combines from different parts of the aircraft. As the aspect angle changes, a different range profile is expected. Also, for each variant of the design of a particular target, such as Boeing 737-100 or 737-200, the range profile will differ. The level of difference in range profile between the two is clearly dependent on the mechanical, and to a lesser extent, the material differences between the two designs. The amount of similarity or correlation between the range profiles varies with aspect angle and it is not possible to generalise how closely they would match, being dependent on the actual type of target, so each case has to be treated individually.

In the next section target scatterers are discussed, followed by a summary of the range profiling process. In the remainder of the chapter the various radar techniques employed to generate high-range resolution waveforms are presented.

3.2   Target scatterers

3.2.1   *Individual scatterers*

The range profile of a target can be approximated to being made up by a number of individual scatterers, each of which corresponds to a mechanical feature of the target. An aircraft target may have typically 30 main scatterers. In Figure 3.3 can be seen that the engines, the nose, the main and tail wing roots and pylons on the wings have been identified as main scatterers. Each scatterer reflects back the signal towards the radar
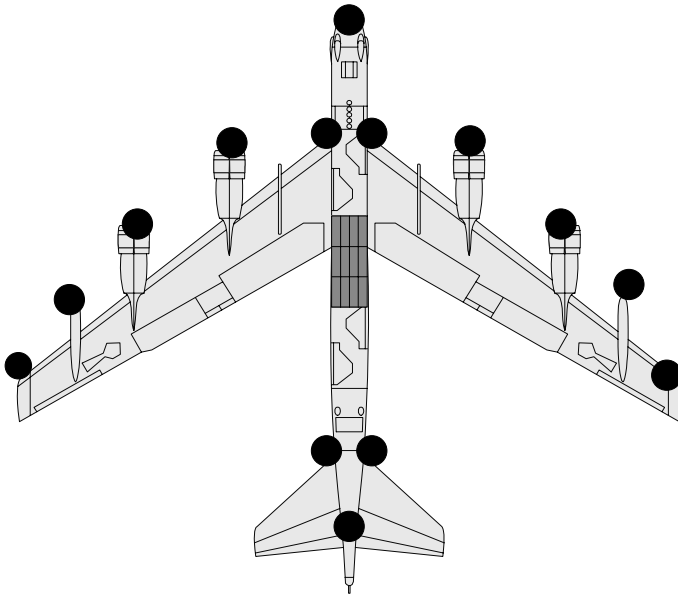
Figure 3.3   Aircraft target showing some of the main scatterers
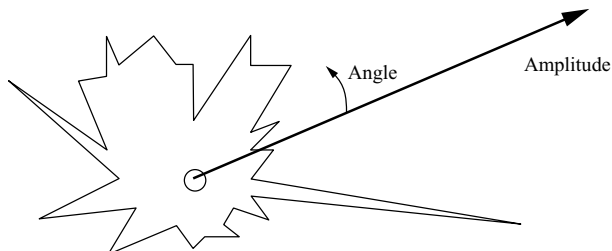
Figure 3.4   Representation of polar diagram of a single scatterer of a target over 360° in a single plane

as a function of the aspect angle to the radar. The characteristics of each individual scatterer can be represented as a 'polar' diagram of reflected amplitude versus azimuth and elevation angles. Figure 3.4 shows a two-dimensional representation of the polar diagram of a single scatterer.

The amplitude of a scatterer can vary by at least one or two orders of magnitude over 360°.

3.2.2   Scatterer interference effects

The reflections from the scatterers are from different physical parts of the target, which are usually separated by many wavelengths of the radar signal. As a result, there are various constructive and destructive interference effects occurring from the constituent scatterers when they are located within the same high-resolution range gate, but across range to the radar. Each scatterer has its own amplitude and phase characteristics and these combine as vectors to provide a net amplitude and phase return in the associated high-range resolution range gate. These interference effects between scatterers can give rise to rapid changes of the range profile of a target with aspect angle. The combining of the contributions of the scattering areas to a high-resolution range gate is illustrated in Figure 3.5.

However, the interference effects between scatterers tend to be far less for high-resolution waveforms than for low-resolution waveforms which effectively integrate the returns from the whole target. (The rcs of targets measured with low-resolution waveforms can fluctuate rapidly from look to look and various levels of fluctuation have been defined by Swerling [1].)

3.2.3   Range profile complexity

The combination of individual scatterer's characteristics varying with aspect angle and the interference effects between scatterers leads to rapid variations in range profile characteristics with aspect angle. In addition some reflection mechanisms cannot be easily represented as individual scatterers, such as cavities and discontinuities on the target's structure. In most cases the target scattering effects are very complex, making it difficult to predict the range profile accurately from simple scattering
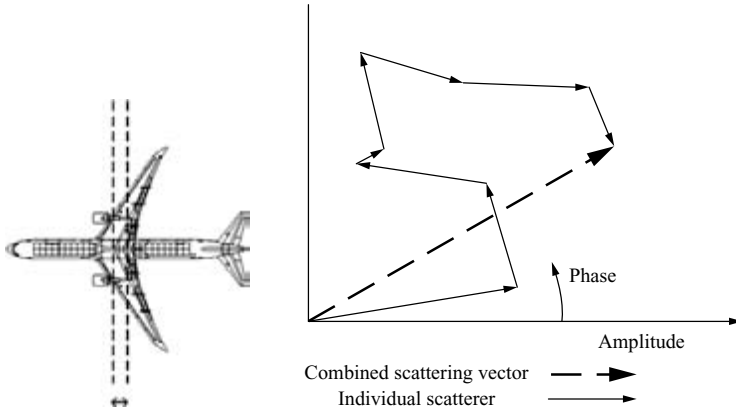
Figure 3.5   Combining of scatterers in each high-resolution range gate: (a) all scatterers in high-resolution range gate contribute to net amplitude and phase of resulting return and (b) combining scatterer contributions

models. More details on the range profiles of air targets and the robustness of target scatterers are discussed extensively in Reference 2. The modelling of the high-range resolution characteristics of targets is presented in Chapter 12.

3.2.4   Comparison of range profiles and optical images

Range profiles of targets cannot generally be considered to have features which are easily related to the optical images of targets that we can readily recognise. The range profiles of targets are one-dimensional images obtained using a signal wavelength of a few centimetres and a resolution of perhaps tens of centimetres. Optical images appear to us as three-dimensional and utilise wavelengths of a fraction of a millimetre. Range profiles contain amplitude information from the larger target scatterers, whereas optical images provide brightness and colour of each element of a three-dimensional image. In comparison to optical images range profiles are far more abstract.

However, features can be obtained from range profiles and recognition is achievable. Some of the techniques employed are presented in Chapter 12.

3.3   Overview of range profiling process

3.3.1   Introduction

In Chapter 2, the general process for measuring and processing high-resolution radar data for target recognition purposes was introduced. In this section aspects more specific to high-resolution range profiling are introduced and these concepts are developed in Chapter 12, which covers the whole target recognition process in more detail. High-resolution range profiling is applied to airborne, ground, sea and even ballistic missile targets.

+/− δθ

Target's track with angular uncertainty
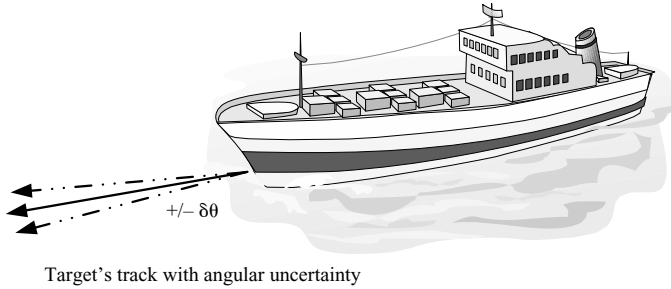
Figure 3.6   Establishing   target   track   prior   to   performing   range   profiling   measurements

3.3.2   Measurement of target signature

The conventional approach to obtaining high-range resolution target signatures is to initially detect and track the target. If it is in a military situation and the unknown target has a speed, altitude and direction that are potentially threatening to the defence, it would then be assessed as being a high-priority target, which should be rapidly classified and, if possible, identified. Similarly, if an unknown ship or aircraft target is detected by a coastal surveillance radar and appears to be infiltrating the territorial rights of the country, it could be either smuggling goods, illegally fishing, a terrorist threat or landing illegal immigrants. As the range profiles of targets vary very considerably with aspect angle, it is necessary to obtain a good track on them, prior to performing the range profile measurement or measurements. This is illustrated in Figure 3.6, where the target track is shown for the ship, with its angular uncertainty. Under most conditions, for non-manoeuvring targets, the direction in which the target is pointing is the same as the target track. However, for a ship in fast ocean currents or an aircraft subjected to a fast jet stream, this would not be the case. The higher the accuracy of the target track, the narrower the number of aspect angles that have to be accessed in the target database for potential matches and the faster that these operations are performed.

3.3.3   Target signature database

The concept of the database of range profiles for a particular set of targets is shown in Table 3.1. A two-dimensional database is shown, but it could also be extended to three-dimensions to cover elevation angles of the target, as well as azimuth. In each box is a representation of the range profile of the target at that aspect angle. Eleven potential target types are shown. The values P_{xy} can be either a sort of 'average' of the range profiles covering the respective aspect angle bracket or a set of range profile features.

There is a conflict between the number of range profiles stored in the database and the time taken to perform the recognition processing operations. The larger the number of range profiles that are stored in the database, intuitively the higher the probability

Table 3.1   Representation of a database of range profiles for 11 target types at n aspect angles

Target type	Target aspect angle, degrees										
	θ_1	θ_2	θ_3	θ_4	θ_5	θ_6	θ_7	θ_8	θ_9	$\ldots$	θ_n
1	$P_{1\,1}$	$P_{2\,1}$	$P_{3\,1}$	$P_{4\,1}$	$P_{5\,1}$	$P_{6\,1}$	$P_{7\,1}$	$P_{8\,1}$	$P_{9\,1}$	$\ldots$	$P_{n\,1}$
2	$P_{1\,2}$	$P_{2\,2}$	$P_{3\,2}$	$P_{4\,2}$	$P_{5\,2}$	$P_{6\,2}$	$P_{7\,2}$	$P_{8\,2}$	$P_{9\,2}$	$\ldots$	$P_{n\,2}$
3	$P_{1\,3}$	$P_{2\,3}$	$P_{3\,3}$	$P_{4\,3}$	$P_{5\,3}$	$P_{6\,3}$	$P_{7\,3}$	$P_{8\,3}$	$P_{9\,3}$	$\ldots$	$P_{n\,3}$
4	$P_{1\,4}$	$P_{2\,4}$	$P_{3\,4}$	$P_{4\,4}$	$P_{5\,4}$	$P_{6\,4}$	$P_{7\,4}$	$P_{8\,4}$	$P_{9\,4}$	$\ldots$	$P_{n\,4}$
5	$P_{1\,5}$	$P_{2\,5}$	$P_{3\,5}$	$P_{4\,5}$	$P_{5\,5}$	$P_{6\,5}$	$P_{7\,5}$	$P_{8\,5}$	$P_{9\,5}$	$\ldots$	$P_{n\,5}$
6	$P_{1\,6}$	$P_{2\,6}$	$P_{3\,6}$	$P_{4\,6}$	$P_{5\,6}$	$P_{6\,6}$	$P_{7\,6}$	$P_{8\,6}$	$P_{9\,6}$	$\ldots$	$P_{n\,6}$
7	$P_{1\,7}$	$P_{2\,7}$	$P_{3\,7}$	$P_{4\,7}$	$P_{5\,7}$	$P_{6\,7}$	$P_{7\,7}$	$P_{8\,7}$	$P_{9\,7}$	$\ldots$	$P_{n\,7}$
8	$P_{1\,8}$	$P_{2\,8}$	$P_{3\,8}$	$P_{4\,8}$	$P_{5\,8}$	$P_{6\,8}$	$P_{7\,8}$	$P_{8\,8}$	$P_{9\,8}$	$\ldots$	$P_{n\,8}$
9	$P_{1\,9}$	$P_{2\,9}$	$P_{3\,9}$	$P_{4\,9}$	$P_{5\,9}$	$P_{6\,9}$	$P_{7\,9}$	$P_{8\,9}$	$P_{9\,9}$	$\ldots$	$P_{n\,9}$
10	$P_{1\,10}$	$P_{2\,10}$	$P_{3\,10}$	$P_{4\,10}$	$P_{5\,10}$	$P_{6\,10}$	$P_{7\,10}$	$P_{8\,10}$	$P_{9\,10}$	$\ldots$	$P_{n\,10}$
11	$P_{1\,11}$	$P_{2\,11}$	$P_{3\,11}$	$P_{4\,11}$	$P_{5\,11}$	$P_{6\,11}$	$P_{7\,11}$	$P_{8\,11}$	$P_{9\,11}$	$\ldots$	$P_{n\,11}$

there is of obtaining a more precise match of the measured signature with reference data and hence the higher the probability of correctly assigning the target to its correct category. However, the time taken to perform these processing operations increases with the number of candidate range profiles to check.

An example is provided in Figure 3.7, which illustrates two methods of populating the signature database. A range profile is shown, which consists of a set of amplitudes covering the whole length of the target. One of these data sets would be needed for each target, for each set of elevation and azimuth angles held in the database. The alternative approach of holding a representative set of the target's main scatterers' positions is also shown. They would also be assembled for each target, for sets of elevation and azimuth aspect angles. The number of angles required would depend upon the robustness of the features employed. The drawing of the aircraft in the figure is compared with its measured range profile and also with extracted features from the range profile, namely the main scatterer positions. It can be seen that to reduce the size and complexity of the database, only the main scatterers are stored, which could be their relative positions only, with no amplitude data. In the example, the features identified include positions of the canopy, wings, engines and tail. This is only one type of feature, which could be used. Other target features could be the amplitudes and positions of the ten largest scatterers, for example. The nature of the database employed is dependent upon the complexity and confidence level required in the target recognition process. If only a simple determination of approximate target length and the positions of the main scatterers are required, a fairly simple database can be constructed, in terms of the data held for each range profile and the number of range profiles held per target. However, to differentiate two targets, which have very

(a)

(b)

(c)
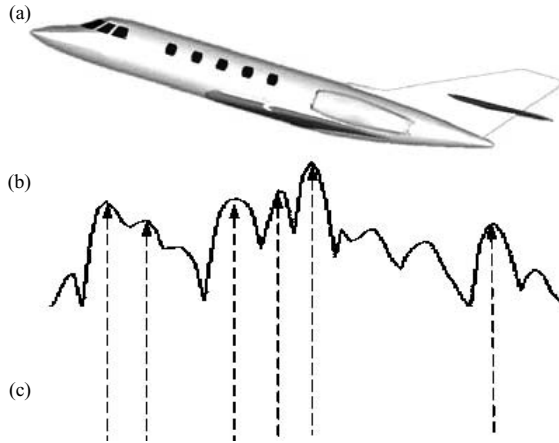
Figure 3.7 *Two examples of holding range profile data in target signature database (Courtesy of BAE Systems Insyte): (a) aircraft being imaged, (b) range profile and (c) positions of main scatterers along range profile as target features*

similar shapes and sizes, would require a far more complex range profile database, held at a large number of aspect angles, coupled with as accurate track information as possible.

3.3.4 Signature conditioning and recognition algorithms

The signature obtained is then conditioned for the next process, which also depends on the type of recognition algorithm being employed and the target's environment. Operations such as determining the range extent of the signature data, thresholding for the rejection of noise, clutter and interference and the extraction of the largest scatterer returns in the profile would then be performed. Normalisation would normally be applied to the data to enable range profiles measured at different ranges to be compared on a consistent basis. The conditioned range profile data is then compared with the database and the best match or matches of range profile are assigned with various levels of confidence.

3.4 High-range resolution radar pulse

The most simple high-range resolution radar waveform to understand is a single short pulse, as shown in Figure 3.8 and was discussed in Chapter 2, Section 2.15. The effective range resolution spread of the pulse is its auto-correlation function, as shown in Figure 2.66. This has a triangular shape and covers twice the length of the pulse. From the theoretical point of view, this is close to being the ideal radar pulse in terms of minimising the distortion of high-range resolution data captured from the
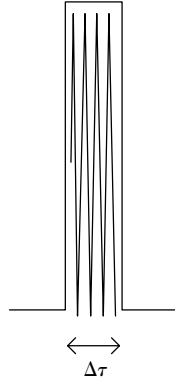
Figure 3.8   A short narrow pulse is the ideal theoretical waveform for high-range resolution applications, but its use is limited by practical constraints

target. The 'smearing' effect of this pulse is never beyond the overall confines of twice its length. When other types of modulation are presented later in this chapter, it will be seen that there are certain spreading effects, called time sidelobes, which can degrade the range resolution of the radar and specific measures have to be taken to overcome them.

Short radar pulses are also Doppler tolerant. This means that fast-moving targets with high Doppler frequencies can be efficiently processed with low levels of loss. They are also readily compatible with coherent pulse Doppler operation, enabling the pulses to be integrated to increase the sensitivity and range of the high-resolution mode. There are no inherent range coverage limitations due to the use of a short pulse. It will be seen that other waveforms have constraints associated with range coverage and Doppler tolerance. From the theoretical viewpoint, a short radar pulse has considerable advantages over other high-range resolution waveforms. However, it is practical implementation issues which severely limit this waveform's applicability to radar target recognition. It tends to be very inefficient and costly to transmit a series of very short high-power pulses in current transmitters, in comparison to other techniques employed, despite some performance compromises. This topic is covered in more detail in Chapter 8 on the practical implementation of high-resolution radar techniques.

3.5   Stepped frequency radar

3.5.1   Synthesing a wideband pulse

3.5.1.1   Spectrum of wideband pulse

For practical reasons most radars are not designed to generate very short duration pulses and support their transmission, reception and digitisation. The spectrum of a radar pulse was discussed in Section 2.1.18.1 and it was shown that for a pulse

Spectrum of a pulse sampled at constant
frequency increments
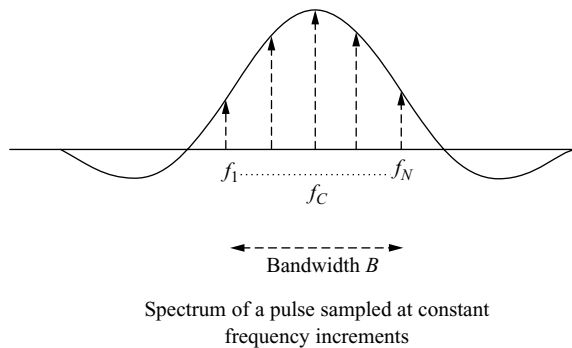
Figure 3.9   *Pulse of bandwidth, B, of signal is sampled at N frequencies, spaced at intervals of $B/(N-1)$*

of duration, $\Delta\tau$, the associated bandwidth occupied by the signal is approximately $1/\Delta\tau$ and also that the associated range resolution obtained is given by $c\Delta\tau/2$. For example, in order to provide a signal with one and a half metres' range resolution, a pulse of duration 10 ns or a one hundred millionth of a second would be needed. It would also be necessary to provide IF bandwidths of 100 MHz throughout the transmitter and receiver chain and to digitise the signal at the rate of 100 MHz in the in-phase and quadrature receiver channels. These are not practically implementable design parameters in most current radars.

The basis of the stepped frequency high-range resolution technique is to synthesise a very short pulse from a knowledge of its frequency components. It is first necessary to establish the frequency spectrum of a short pulse. A pulse of duration $\Delta\tau$ can also be represented by the reciprocal of its bandwidth, as $1/B$. Figure 3.9 shows a pulse of bandwidth, B. The objective is to synthesise the original high-resolution pulse in increments of low bandwidth signals. Consider providing a set of sampled frequencies to cover the bandwidth of the original pulse as shown in the figure. The signal to be synthesised is a pulse of duration, $\Delta\tau$, with carrier frequency, f_c. The bandwidth, B, of the signal is being constructed using N frequencies, spaced at intervals of $B/(N-1)$. These frequency components are each sinewaves of duration, τ, and are low bandwidth. In the figure each of these low bandwidth signals can be seen as a very sharp dotted line, as indicated by the arrow heads.

3.5.1.2   Combining sinusoids

Figure 3.10 illustrates how a set of the spectral components, which are sinewaves, combine to synthesise an approximation to a rectangular pulse.

The frequency components, f_1–f_5, are shown as individual sinewaves in (a) varying in amplitude against time. When these are combined they make up the time varying signal shown in (b), which is an approximation to the pulse shown in (c). It can also be seen that there are three pulses being synthesised in total. These are called 'ambiguities', which are a consequence of synthesising the pulse in discrete
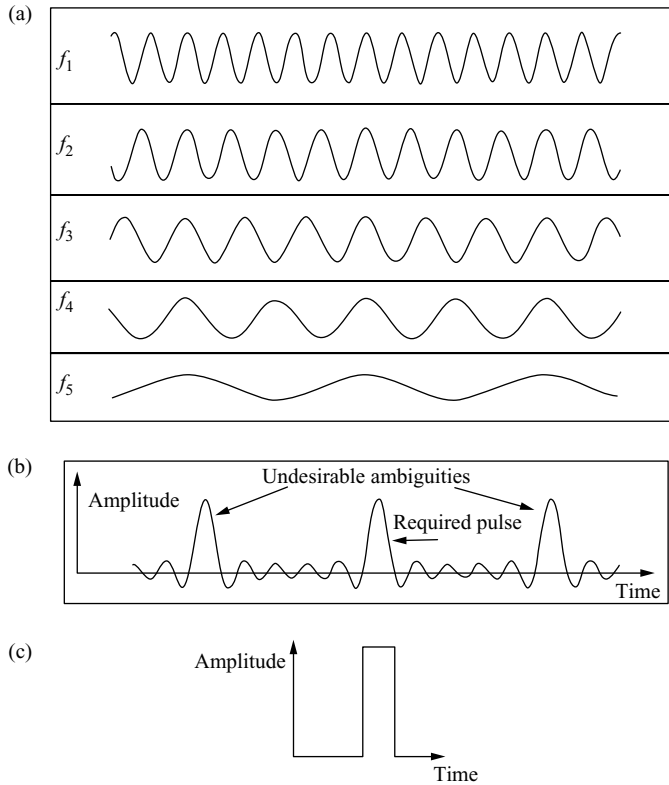
Figure 3.10 *The combining of a set of sinewaves to synthesise a rectangular pulse:*
(a) individual frequency components, (b) sum of frequency components
in (a) and (c) ideal pulse

frequencies, rather than by using an infinite set of frequencies, which is described by
the continuous function's shown in Figure 3.10. Clearly it is not practical to generate
an infinite set of frequency steps. Ambiguities can cause significant problems in try-
ing to generate a high-integrity range profile of a target and are discussed later in this
section. Also it can be seen that the 'pulse' being synthesised is not really rectangu-
lar, but is distorted. In practice when a rectangular pulse is synthesised using more
frequency components, a more precise result is obtained.

3.5.2 Measuring target signature

3.5.2.1 Applying stepped frequency waveform

This technique is implemented in a radar by stepping the transmission frequency of the
radar in increments of Δf from f_1 to f_N on a pulse to pulse basis. The increments Δf
also correspond to the total bandwidth divided by the number of frequency increments,
which is $B/(N-1)$.

(a)

(b)
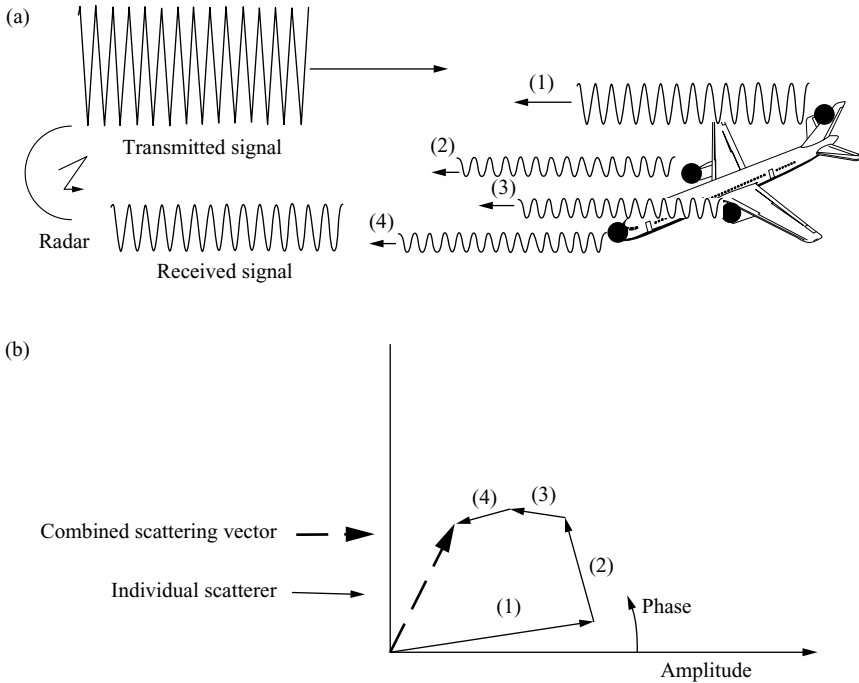
*Figure 3.11   Each stepped frequency signal measures a single amplitude and phase
component from a target combining individual scatterer contributions:
(a) signals reflected from four scatterers and (b) reflected signals
combine to form received signal*

The way this works is shown in Figure 3.11. At each transmission frequency
the long sinusoidal pulse illuminates the target. In the example provided four scat-
terers are shown, which each individually reflect their own amplitude and phase
contributions.

As the signal is a long sinusoidal pulse with negligible bandwidth, the individual
amplitude and phase components from the four scatterers combine as shown in
Figure 3.11(b). The result is a single sinusoidal signal with an amplitude and phase,
which represent the reflected signal of the target at the frequency of illumination.
Effectively the radar has integrated the energy received from the target and defines it
as two numbers, the amplitude and phase.

This is repeated for each frequency component, which is being used to synthesise
the wideband rectangular pulse. Each frequency is sequentially transmitted, with pulse
length $\Delta\tau$, and a single measurement of amplitude and phase is made, as illustrated
in Figure 3.12. If N frequency steps are utilised, N sets of amplitude and phase
measurements are made, which are then used to generate the range profile.

Hence, the frequency spectrum components of the target at the frequencies of the
measurements have been obtained.

Frequency stepping sequence	Amplitude and phase measured
f_1	$A_1\varphi_1$
f_2	$A_2\varphi_2$
f_3	$A_3\varphi_3$
f_4	$A_4\varphi_4$
f_5	$A_5\varphi_5$
$\downarrow$	$\downarrow$
f_N	$A_n\varphi_n$

Figure 3.12   Stepped frequency measurements: amplitude, A_n, and phase, ϕ_n, of target are measured at each frequency step

3.5.2.2   Generating range profile

The normal method of converting discrete frequency domain data to discrete time domain data is by use of the Fourier transform as discussed in Chapter 2. Equation (2.27) is the discrete Fourier transform, which converts time series data to frequency data. The inverse Fourier transform converts frequency domain data to time domain data, which is of interest here.

$$f_{\text{sig}}(t_k) = \sum_{n=1}^{N} f_{\text{sig}}(f_n)e^{2\pi i f_n t_k} \tag{3.1}$$

where t_k = discrete time component, k, f_n = frequency measurement of sample, n and $f_{\text{sig}}(t_k)$ = transform of frequency domain signal $f_{\text{sig}}(f_n)$.

By applying this equation to the measured frequency components, we then obtain a time series of data, which is the range profile of the target. Another way of viewing this process of measuring the target's scattering response at specific frequencies to obtain the range profile, is to imagine the N sinusoids as shown in Figure 3.12 to be summed together in the same way as the frequency components of Figure 3.10. The output is again the range profile. The Fourier tranform is a mathematical way of expressing this process and the implementation is well known. This process is illustrated in Figure 3.13 for the very simple representation of the aircraft target with four main scatterers as shown in Figure 3.11. The number of independent components of the range profile is actually equal to the number of frequency steps utilised. This can also be seen from the symmetry of the Fourier transform operation of Equation (3.1) in which N complex measurements at the respective frequencies transform to N complex
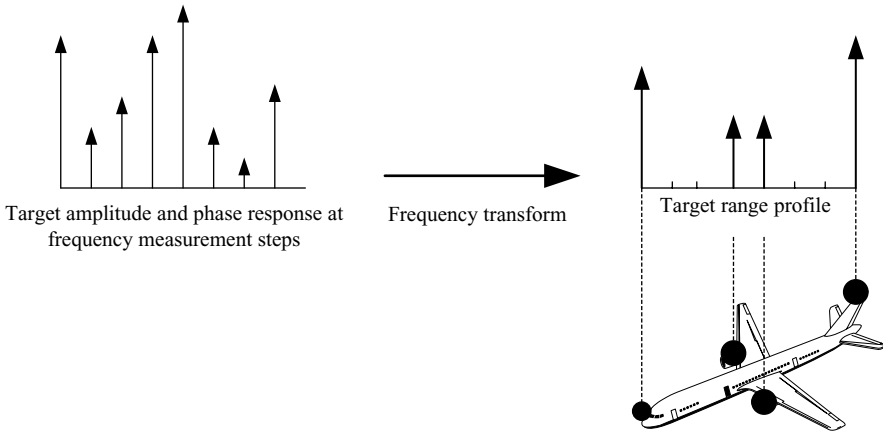
*Figure 3.13   Obtaining target range profile from stepped frequency measurements –
             four scatterers shown as an example*
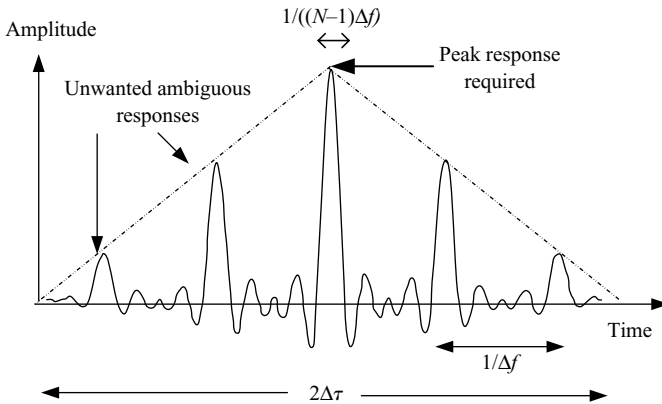
*Figure 3.14   Output of matched filter with weighting function for stepped frequency
             waveform*

components of the target's range profile. It can be seen that to obtain a specfic range
resolution for a target of a certain range extent, it is necessary to have at least a number
of frequency steps equal to the target length divided by the required range resolution.
It can also be noticed that phase as well as amplitude information is also obtained
along the range profile. This is useful in some high-range resolution applications.

    In order to establish the effects of this stepped frequency waveform on a target,
the output of the matched filter, which is the auto-correlation function of the input
signal, has to be calculated [3]. This is derived in the Appendix and is shown in
Figure 3.14.

3.5.3 Stepped frequency signature characteristics

3.5.3.1 Range ambiguities

Figure 3.14 is important for high-range resolution applications of stepped frequency techniques and its implications will now be discussed. The diagram shows the amplitude against time of the output of the matched filter. A series of pulses of duration, $\Delta\tau$, are transmitted at frequencies f_1–f_N in frequency increments of Δf. The range resolution achieved can be seen from the sharpness of the peak of the auto-correlation function, which is $1/((N-1)\Delta f)$ expressed as time or $c/(2(N-1)\Delta f)$ as a range. This also is $c/2B$, which is precisely the duration of the pulse being synthesised in Figure 3.9. This is the inverse of the bandwidth extent, which is covered by the waveform. The range resolution of the stepped frequency waveform, ΔR, is given by:

$$\Delta R = \frac{c}{2\Delta f(N-1)} \tag{3.2}$$

The effective bandwidth of the stepped frequency waveform is the size of the frequency step multiplied by the number of frequency increments used in the sequence. A weighting function would normally be applied over the amplitudes of the stepped frequency components [4] to reduce close in time sidelobes.

It can also be seen that ambiguites or main peaks in the output are also present. These occur at intervals of $1/\Delta f$, which is the inverse of the frequency stepping interval and correspond to range intervals, R_I, of $c/2\Delta f$. These are the same as the ambiguities arising in Figure 3.10(b), in which a high-resolution pulse is being synthesised in increments.

$$R_I = \frac{c}{2\Delta f} \tag{3.3}$$

Hence, with reference to the auto-correlation peak of the waveform, range ambiguities occur at relative ranges of R_m, given by:

$$R_m = \frac{cm}{2\Delta f} \tag{3.4}$$

where m is a whole number.

It can also be seen that the envelope of the output is a triangular function of base, $c\Delta\tau$. This is actually the auto-correlation function of a single pulse of width, $\Delta\tau$ and also equates to the range extent of $c\Delta\tau$. This means that range ambiguities only occur within the confines of the pulse length, which is intuitive. The approximate number of range ambiguities present, n_A, is obtained by dividing $c\Delta\tau$ by R_I:

$$n_A \approx 2\Delta\tau\Delta f \tag{3.5}$$

This is an approximation as $2\Delta\tau$ multiplied by Δf is not necessarily a whole number. This is basically twice the value of the step size divided by the bandwidth, $1/\Delta\tau$, of each pulse. This is interesting, in that it tells us that the number of ambiguities present is proportional to the ratio of the bandwidth associated with a single pulse to the bandwidth being stepped between pulses. Hence, we gain range resolution by stepping in frequency, but the price we pay is ambiguous range returns occurring

in the vicinity of the target. It can be seen that in high-resolution radar, as in many other engineering designs, we do not get something for nothing and there are trade-offs in design parameters. Substituting the value of the range resolution, ΔR, from Equation (3.2), the approximate number of ambiguities can be written as:

$$n_A \approx \frac{\Delta\tau c}{(N-1)\Delta R} \quad \text{for } N > 1 \tag{3.6}$$

For a required range resolution, ΔR, and for a given pulse length, $\Delta\tau$, the number of range ambiguities is inversely proportional to the number of frequency increments. Hence, in order to reduce the number of ambiguities present, it is necessary to increase the number of frequency steps used. We will now explore the meaning of these range ambiguities.

3.5.3.2   Multiple targets

Figure 3.15 illustrates the effects of the stepped frequency range ambiguities on several targets, which are within the sampling gate of the pulse of length, $c\Delta\tau$. For example, if pulses of 1 μs duration are used, the value of $c\Delta\tau$ is 300 m. Also assume four targets are within this 300 m range slot. If a bandwidth of 100 MHz is being synthesised using 20 frequency increments in 5 MHz increments, from Equation (3.3) the ambiguities occur at 30 m intervals, corresponding to the unambiguous range interval. Hence, there are 10 ambiguities over 300 m. As one complex sample is obtained for all targets within the $c/2\Delta f$ (or 300 m) range bracket, at each frequency step, all information from all the four targets is folded together into a 30 m range slot. Hence, all the range extent information from the targets, which is present, is mixed together, so a composite range profile of all the targets collapsed together is obtained. Generally, it is not possible to extract the high-range resolution data of the individual targets. It is not possible to determine the position of any of the targets
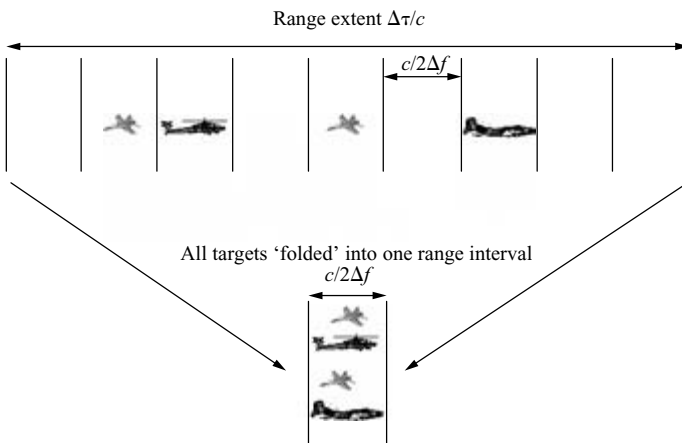
Figure 3.15   Effects of stepped frequency range ambiguities on multiple targets

within the range extent of $c\Delta\tau$, using this stepped frequency waveform sequence on its own. It can be seen that these range ambiguities mean that the actual position of each target is uncertain and that it is not even possible to establish with any confidence how many targets are present.

Although dependent on actual waveform parameters that are used and on the effective range extent of the individual targets, this technique is not recommended for situations in which multiple targets with similar velocities are located within a range slot appropriate to the length of the transmitted pulse. It will be seen later in the applications chapter that some differentiation between closely spaced targets is feasible if their radial velocities are sufficiently different.

3.5.3.3   Extended targets

Figure 3.16 shows the case of an extended target, which is larger than the unambiguous range of $c/2\Delta f$. The aircraft shown effectively occupies three ambiguous range intervals. Using the example of synthesising 300 MHz bandwidth in 10 steps of 30 MHz, which would give ambiguities at a range of 5 m from Equation (3.3). For an aircraft of 15 m radial range extent, it would straddle more than the 5 m unambiguous range interval. As the target occupies more than the unambiguous range interval of the stepped frequency waveform, it 'folds in' on itself causing a distortion of the high-range resolution data obtained. The range profile of the aircraft is severely corrupted and the 15 m of range profile data is shrunk into 5 m of range extent. It effectively provides little useful information for recognition purposes. It is not generally possible to resolve these distortions, so waveform parameters appropriate to the target's range extent have to be carefully chosen.
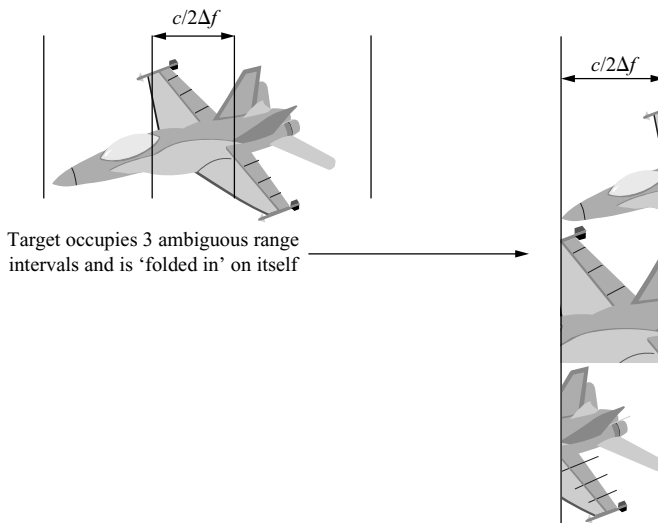
Figure 3.16   Effects of stepped frequency waveforms on targets extended in range
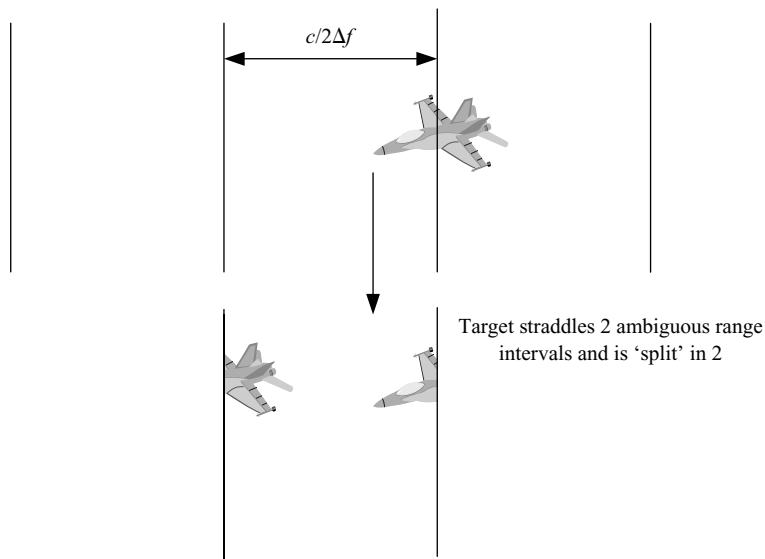
Figure 3.17   Effects of target straddling ambiguous range intervals

3.5.3.4   Range interval straddle

Another feature of this waveform is shown in Figure 3.17. It can be seen that if a target is positioned straddling two range intervals, it can be split into two, with one half at one side of the range interval and the remaining part at the other side. If there is only one target present, it is possible to re-construct the target signature from the two parts. However, it may not be possible to determine whether one or two targets are present until the whole recognition process has been implemented on the individual and composite parts of the divided target. However, if there is more than one target present, confusion arises as was shown in Figures 3.15 and 3.16.

3.5.4   *Operation in clutter*

If stepped frequency waveforms are employed with clutter present, the transmitting of a single pulse at each step does not reject clutter. The range profiles from the target and the clutter would overlap and would not provide any useful information on the target's characteristics for recognition purposes.

Pulse-Doppler waveforms reject clutter by transmitting the same waveform every pulse and by using the target's phase information to measure Doppler and hence filter returns with different Doppler frequencies.

Stepped frequency techniques can reject clutter by transmitting a number of pulses at each frequency and filtering the contributions from targets with different veloc-ities. After filtering, the respective amplitude and phase components are measured in each Doppler filter and these are equivalent to the amplitude and phase samples

measured with a single pulse as discussed in Section 3.5.2. The contributions from the various frequency steps are then combined to generate a range profile by applying a Fourier transform to the respective amplitude and phase samples from each step for the appropriate Doppler filter containing the target's energy. This is discussed further in Chapter 8.

3.5.5   Motion compensation

A critical issue with high-resolution radar and in particular for the stepped frequency technique is compensation for the motion of the target during the radar integration period. The basis of the stepped frequency technique is to effectively measure the phase of the target at each step as discussed in Sections 3.5.1 and 3.5.2. If the target is moving it is changing its relative phase to the radar at a rate proportional to its velocity vector in the direction of the radar. If this phase is not corrected for, an error is made in the measured phase to the target at each step and the resulting range profile can be severely degraded particularly for non-constant velocity.

Hence, it is necessary to compensate for the motion of the target over the radar integration period by effectively 'freezing' it in space. This can be performed by measuring the target's velocity over the radar integration period and compensating for the phase of each pulse individually. The velocity can be measured using the pulse Doppler waveform at each step as described in the previous section.

3.5.6   Technology for supporting stepped frequency applications

The critical design element needed to enable a radar to operate with a stepped frequency mode is a local oscillator, which can generate all the signal frequencies needed to synthesise the wideband pulse and is able to switch between these frequencies rapidly. As the stepped frequency technique is effectively counting the number of degrees of phase to the target scatterers each at frequency transmitted, the frequency has to be accurate and has to be rapidly reached and maintain its value over the measurement period. Any deviations from the required performance degrade the range profile of the target. The technological and implementation aspects are discussed in more detail in Chapter 8.

3.5.7   Stepped frequency conclusions

Stepped frequency techniques have played their part and will continue to contribute to target recognition in systems, which have limited bandwidth. However, the weaknesses in the technique have to be carefully understood in order to implement a high-integrity high-range resolution mode. Stepped frequency techniques are best suited to isolated single targets, such that the range ambiguities at the inverse of the stepping rate, $c/2\Delta f$, are not affected by other nearby targets. It is necessary that all the frequency steps have to be transmitted before the target changes aspect angle significantly, otherwise the target effectively de-correlates over the radar integration period and a distorted range profile results. Hence, targets with low aspect angle

changes over the radar measurement period are required. The radar length of the target must also be shorter than the value of $c/2\Delta f$, so that the target is not folded in on itself.

An example of a scenario in which stepped frequency techniques could be applied would be for an isolated land vehicle travelling on even road. However, for most practical applications, a variant of the stepped frequency technique, such as bandwidth segmentation discussed in Section 3.8 would be recommended, as it can overcome many of the difficulties associated with the classical technique described here.

3.6   Wideband pulse compression

3.6.1   Introduction

3.6.1.1   Objective

The main objective of using pulse compression [5] in high-resolution radar systems is to utilise the detection benefits of transmitting a long duration pulse, whilst at the same time obtaining the range resolution associated with a short pulse. Pulse compression involves coding the long pulse, such that when it is processed in the radar receiver, it provides the range resolution of a short pulse. Pulse compression is employed in radars to maximise the power transmitted and hence the radar range and sensitivity by maximising the mean power of the transmitter and energy on the target. Solid state and most vacuum tube transmitters tend to operate more efficiently with lower peak powers.

3.6.1.2   Concept

The concept of pulse compression is shown in Figure 3.18. In Figure 3.18(a) is a long unmodulated pulse of duration τ which has a bandwidth of $1/\tau$, and corresponds to a range resolution of $c/(2\tau)$. In Figure 3.18(b) is a short pulse of duration $\Delta\tau$ with an associated bandwidth of $1/\Delta\tau$ and a range resolution of $c/(2\Delta\tau)$, which has the same peak power, P, as (a), but contains far less energy, which is the product of peak power and pulse duration. It can be seen that (a) has the detection benefits of a long duration pulse, but has a relatively coarse range resolution. (b) has good range resolution, but is limited in range and sensitivity by having a low mean power for the same prf as (a). Generally it is not possible to re-gain the sensitivity lost due to having a short pulse by increasing the prf. The value of the prf is selected for optimum ambiguous range and ambiguous Doppler performance in the radar, which is application dependent. Also most transmitters have physical constraints on the maximum prf, which can be employed.

However, in using pulse compression, (c) has the benefits of both (a) and (b), enabling the same peak power to be used with a long pulse and also obtaining high-range resolution. This is achieved by using the same pulse length as (a), but by modulating it with a coded waveform, which has a bandwidth of pulse (b). The coding of the waveform produces a transmitted spectrum of bandwidth $1/\Delta\tau$, which is then processed in the radar receiver to produce a high-range resolution pulse of

(a)

Power ↕

Pulse length$=\tau$
(Bandwidth$=1/\tau$)

Time →

Peak power, P

(b)

Peak power, P

Pulse length$=\Delta\tau$
(Bandwidth$=1/\Delta\tau$)

(c)

Pulse length$=\tau$

| 1 | 2 | 3 | 4 | 5 | 6 | 7 | 8 | 9 |

Peak power, P

Coded sub-pulses of length$=\Delta\tau$
(Bandwidth$=1/\Delta\tau$)
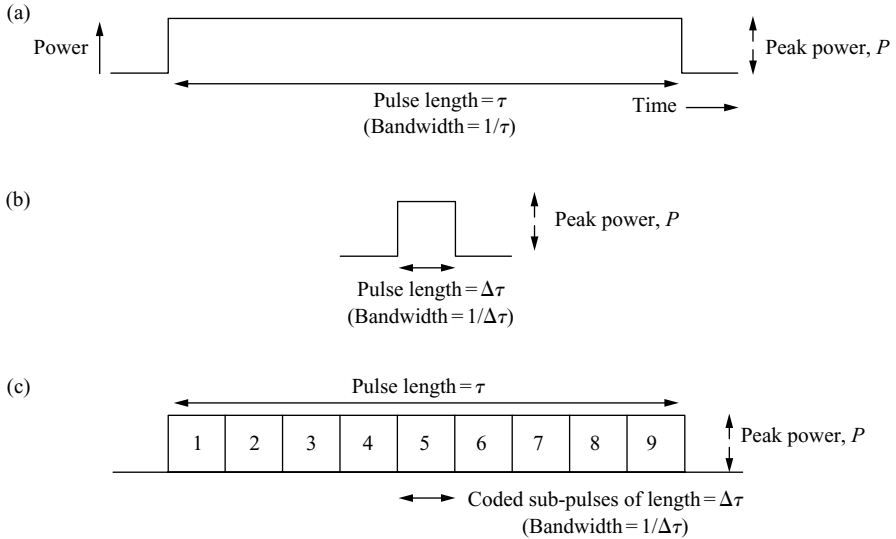
Figure 3.18   Maximising total energy transmitted and increasing bandwidth using pulse compression: (a) conventional long duration pulse with no coding giving: high total energy, but low bandwidth and low-range resolution, (b) short duration pulse giving: low total energy, but high-range resolution and (c) long duration pulse comprising coded sub-pulses giving: high total energy and high range resolution

duration $\Delta\tau$. The coding used is usually some form of phase or frequency modulation (FM), whereby the carrier frequency within the pulse is continuously modulated. The radar effectively synthesises a high-range resolution pulse and utilises the long duration pulse length available in the transmitter.

3.6.1.3   Pulse compression process

The ideal pulse compression process is illustrated in Figure 3.19. The transmitted pulse is represented by the 'expanded' pulse, which is made up of a number of short sub-pulses. Each of these sub-pulses can be considered to be individually coded. In the pulse compression receiver, the sub-pulses are compressed together to form the high-short pulse shown. For the eight sub-pulses shown, the relative length or duration of the expanded pulse to the compressed pulse is eight, which is called the pulse compression ratio. This is also the ratio of the amplitude of the compressed pulse to the expanded pulse. The range resolution of the waveform is determined by the width of the compressed pulse at the output of the compression receiver, which is also the width of each sub-pulse. The 'matched filter' theory for optimally detecting radar waveforms, which was discussed in Chapter 2, Section 2.1.20, is equally applicable to radars using pulse compression. The output of the matched filter is again the auto-correlation of the time domain waveform.
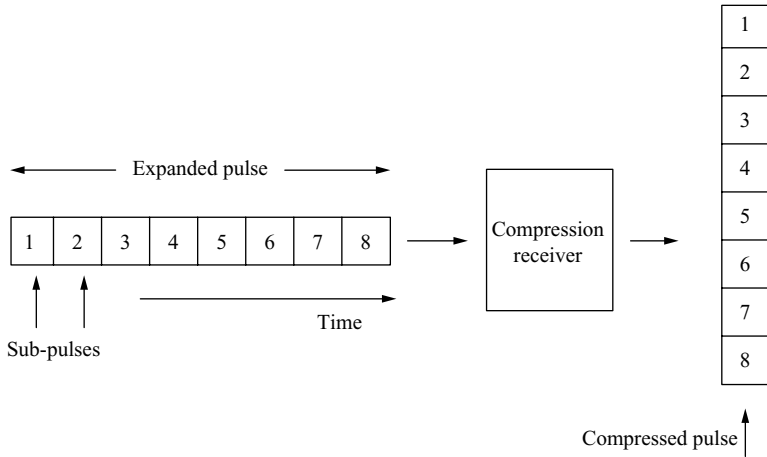
Figure 3.19   Ideal pulse compression process

The output of the pulse compression receiver shown in Figure 3.19 is ideal and is not achievable in practice. In real systems it is not possible to synthesise and compress a waveform, which compresses or integrates all the energy into a single high-resolution range gate.

3.6.1.4   Real pulse compression process

The compression process is not 100 per cent efficient and energy is 'spilt' into adjoining high-resolution range gates. The peak of the pulse compression receiver output can be considered to be the 'main lobe' and the other range gates occupied with the remaining energy are referred to as being the sidelobes. These are shown in Figure 3.20.

The main lobe energy for the actual compressed pulse is less than the ideal case. The difference represents a loss in signal energy and reduced radar sensitivity. This lost energy appears as the time sidelobes of the waveform used. These are generally at a low level compared to the main lobe response. However, the effect of the time sidelobes is to distort the HRRP of the target. For example, for a point scatterer, there would be a peak response of the main lobe with smaller responses at time intervals before and after the target. The target would appear as a large scatterer surrounded by small scatterers. Hence, there are two main effects, which degrade performance in real systems using pulse compression: losses reducing sensitivity and time sidelobes creating false scatterers. The level and position of the time sidelobes depend on the actual waveform chosen for a particular application. However, time sidelobes can be reduced by the application of a weighting function in the pulse compression receiver. This has the effect of reducing the 'ghost' point scatterers in the vicinity of the target, but also tends to increase the width of the main lobe response, so degrades the actual range resolution obtained.
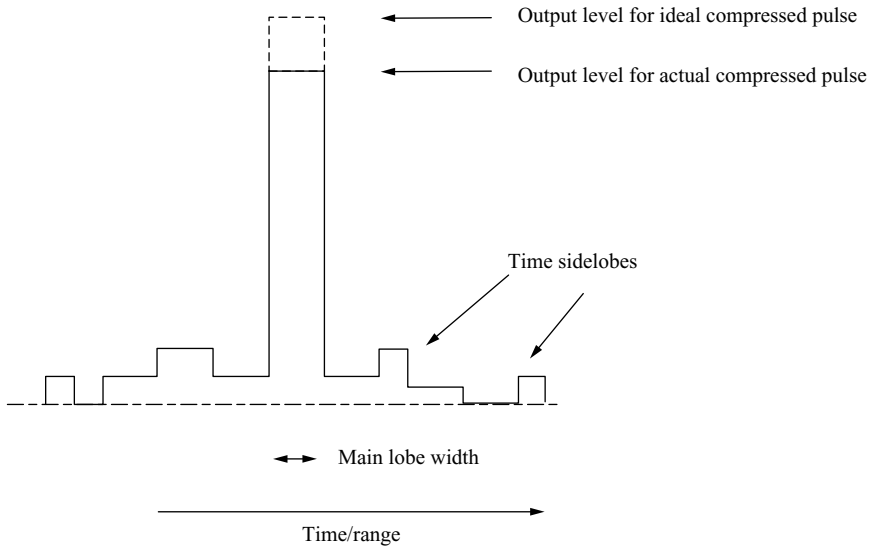
Figure 3.20   Output of pulse compression receiver with time sidelobes
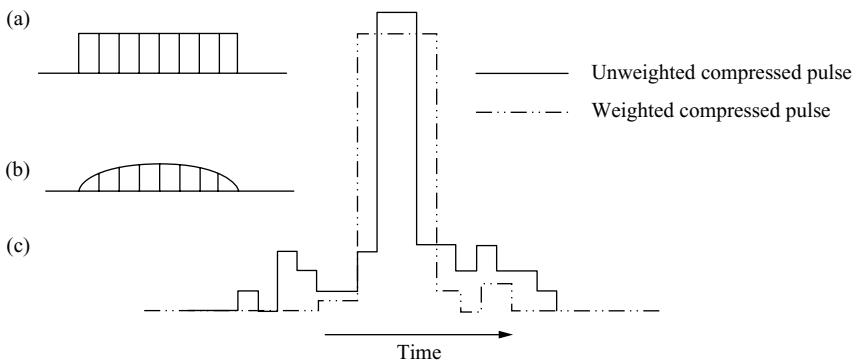
*Figure 3.21   Use of weighting function to reduce time sidelobes: (a) expanded pulse,
             (b) weighted expanded pulse and (c) output of compression receiver*

3.6.1.5   Application of weighting function

The application of the weighting function to the expanded waveform to reduce the
time sidelobes is illustrated in Figure 3.21. The waveform in (a) is the unweighted
expanded pulse with the wideband modulation. An amplitude weighting function is
applied to the pulse, as shown in (b). The output of the compression receiver is shown
in (c). The output for the unweighted pulse is shown as the filled in line and the output
for the weighted pulse is shown as the dotted line. It can be seen that the effects of

the weighting function are to reduce the level of the time sidelobes, to broaden the peak of the main lobe response and to reduce the level of the main lobe. The actual weighting function employed is application dependent, involving trade-offs in values of the aforementioned parameters.

3.6.1.6   Pulse compression waveforms

Different types of pulse compression techniques are used in radar systems and are dependent on the type of targets, on the associated clutter environment being encountered and on the wideband technology which can be supported in the host radar. In the latter part of this chapter chirp waveform and phase modulation techniques are presented. 'Stretch' and bandwidth segmentation techniques are also discussed, which are really variations on the main pulse compression theme.

3.6.2   Linear frequency modulation waveform

3.6.2.1   Frequency against time characteristic

A very popular form of pulse compression is linear frequency modulation (LFM). This is usually called a 'chirp' waveform, as it has a similarity with the chirp of birdsong. This name was given by the engineers who originally designed the technique and has remained ever since. The chirp waveform starts at the beginning of the pulse with a frequency f_1 and the frequency is changed at a constant rate during the pulse, ending at another frequency, f_2.

The chirp waveform is shown in Figure 3.22(a) as the amplitude of the signal against time and in (b) as the instantaneous frequency of the signal against time. The chirp can be expressed as:

$$V = V_A \cos(2\pi f_1(1 + kt)t) \tag{3.7}$$

where V is the instantaneous voltage of the chirp, V_A is the peak voltage of the wave, f_1 is the frequency at the start of the pulse, t is time with reference to start of pulse and k is a constant.

The term $f_1 t$ represents a signal of constant frequency. The constant k is determined by the rate of change of frequency required across the pulse, in order to provide the overall bandwidth required and has the units of frequency. At the end of the chirp the frequency f_2 is equal to $f_1 + k\tau^2$, where τ is the pulse width.
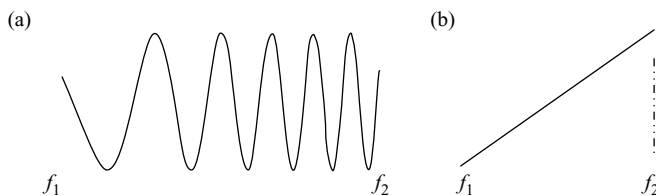
Figure 3.22   *LFM chirp waveform: (a) amplitude against time and (b) frequency against time*
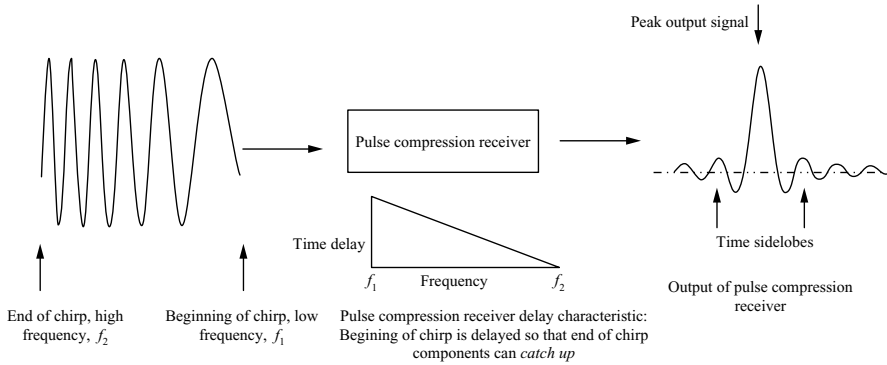
Figure 3.23 Compression of chirp waveform

3.6.2.2 Compression of LFM chirp

In order to compress this chirp it is necessary for all its frequency components to be brought together in a compression receiver in order to provide the sharp high-resolution pulse. One way of achieving this is to use a filter that provides a time delay that varies linearly with frequency. By employing a technique that enables the frequency components that arrive at the filter first to have a delayed transit through the filter, so that the later components all 'catch up' at the same time, achieves this objective. This is illustrated in Figure 3.23.

In Figure 3.23, it can be seen that the lower frequency f_1 of the chirp enters the pulse compression receiver (or filter) first. The higher frequency component f_2 enters the filter last and the time delay characteristics of the filter are such that all the frequency components exit from the filter at almost the same time. This then gives rise to the sharp peak of the output signal, which is then the high-resolution compressed waveform. The signal returning from a target would consist of a large number of slightly staggered chirps, which would not be discernible into individual high-resolution range cells until they had undergone the pulse compression process. In Figure 3.23, the time sidelobes of the chirp waveform can be seen. They actually extend for the duration of the expanded chirp pulse, but at a low level. The output of the compression filter has a sin x/x type of characteristic in amplitude, which corresponds to $(\sin x/x)^2$ if measured in power terms, which is normally more important to the radar system designer. The time, or also called range sidelobes, can be reduced with weighting functions, as discussed earlier, but at the expense of range resolution and signal processing loss [6–9].

3.6.2.3 Chirp characteristics

There are great advantages of using chirp waveforms for pulse compression. The peak time sidelobe level obtained can be below 40 dB with well-designed weighting functions, which is generally acceptable for most target recognition applications. The waveform is Doppler tolerant and is compatible with coherent pulse Doppler

signal processing, but there are also range-Doppler coupling effects. These topics are discussed in the next section.

The chirp pulse uses the available spectrum efficiently. The spectrum of the chirp has almost the shape of a 'top hat' for typical pulse compression ratios used. This means that the energy is spread almost evenly across the occupied spectrum with little spillage outside. This is important for high-range resolution applications, in which more and more bandwidth can be utilised, as requirements for higher and higher range resolution grow and the technology for supporting large bandwidth waveforms develops. There is also pressure on the use of the electromagnetic spectrum from many users. The radar community has to compete particularly with the telecoms industry for spectral resource.

3.6.2.4   Range-Doppler coupling

For the chirp of Figure 3.23, on detecting a target with a Doppler frequency of f_d, the frequency of the chirp is now starting at $f_1 + f_d$, and ends at frequency $f_2 + f_d$. This means that when it enters the pulse compression filter, each frequency component is effectively the value of the Doppler frequency, f_d, in advance of an equivalent chirp for a stationary target at the same range. The pulse compression filter then speeds up the transit of the pulse by the ratio of the Doppler frequency divided by difference in frequencies of the signal at the beginning and end of the pulse, which is the waveform's bandwidth. The signal at the output of the compression receiver for the frequency-shifted signal is therefore ahead of that of the stationary target. The relative range of the moving target, which is determined by the time delay to the target and back, is therefore apparently less than it should be, in this case, and gives rise to the moving target appearing to be closer in range. This is called range-Doppler coupling and can be significant in some target recognition applications. This effect is stated in Equation (3.8):

$$R_{dc} = \frac{c\tau f_d}{2B} \tag{3.8}$$

where R_{dc} = range-Doppler coupled distance, τ = pulse length and B = bandwidth of waveform.

This also means that for targets with low Doppler frequencies in comparison to the compression receiver bandwidth, there is very little loss of signal as most of the target's frequency spectrum is contained within the receiver's bandwidth. The waveform is therefore tolerant to Doppler shifts and even very fast targets having high Doppler frequency shifts are efficiently processed with little degradation in sensitivity and time sidelobe performance. This is illustrated in Figure 3.24, in which the chirps with and without Doppler frequencies are compared. The amplitudes are almost identical, with the moving target coupled in range.

If pulse-Doppler techniques are being used and pulses are being coherently integrated, the Doppler frequency can be determined on a pulse to pulse basis. The compression filter of Figure 3.23 would actually have in-phase and quadrature channels for measuring the amplitude and phase of the signal. Over the burst all the in-phase and quadrature samples would be obtained for each high-resolution range
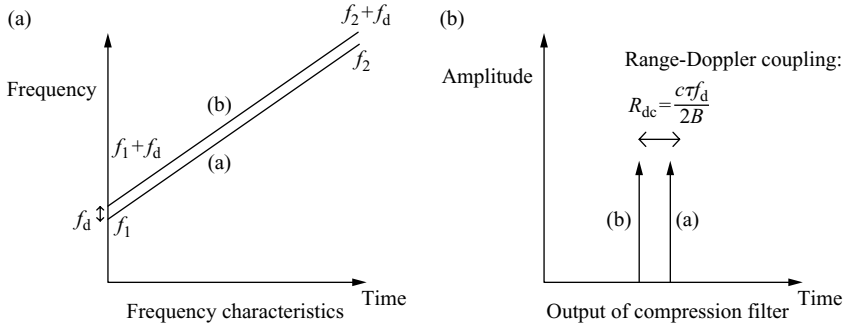
Figure 3.24   Effect of Doppler frequency on linear FM chirp: (a) stationary target and (b) moving target with Doppler frequency f_d

gate and transformed into the frequency components to establish the Doppler frequency. Hence, as the Doppler frequency can be measured, it is then possible to compensate for the range-Doppler coupling using Equation (3.8). This is an added complication in the signal processing, but it can be performed, if required.

3.6.2.5   Chirp filters

Chirps can be generated and compressed using pairs of filters [10,11], which are normally surface acoustic wave devices, as described in the references. Matched pairs of filters are used so that the characteristics of the expanded chirp correspond closely to those of the compression filter. The actual chirp signal is generated by applying an impulse to the filter, which has been designed to have the output response in accordance with the radar system's requirements of pulse length and chirp bandwidth. A more modern technique is to use a digital waveform generator for chirp synthesis and to perform the pulse compression after digitisation, as part of the digital signal processing functions. If this approach were used there would clearly be no visible filter generating or compressing the waveform in the traditional analogue sense, but would merge into the various computational operations. However, functionally there is no significant difference between the two approaches.

3.6.3   *Non-linear frequency modulation*

This is similar to the LFM technique discussed in the previous section, with the obvious difference being a non-linear frequency–time characteristic is used. The advantages are due to there being no requirement for a weighting function associated with the compression receiver. Low signal processing losses and a sharp compression peak are obtained. However, in practice, this technique has not been traditionally popular, due to the additional complexity of generating and compression of this more complex waveform. However, with the advent of digitally generated and compressed pulses, this technique may well come into favour.
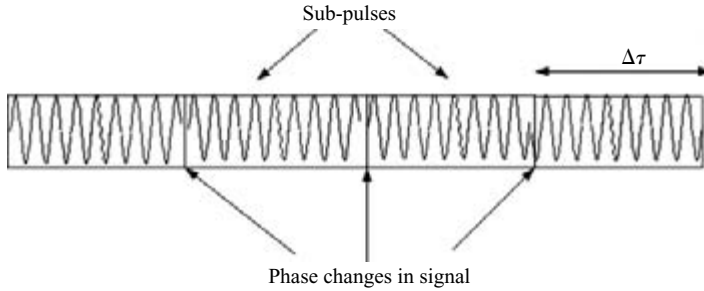
Figure 3.25   *Representation of phase coding a signal*

3.6.4   Phase coded waveforms

3.6.4.1   Introduction

Phase coded waveforms differ from the frequency modulated techniques discussed above in that they operate at a constant frequency. The required bandwidth is obtained by periodically changing the phase of the waveform as a discrete step. The radar pulse transmitted is effectively divided into a number of sub-pulses, as shown in Figure 3.25.

The frequency of the signal is seen to undergo a rapid change in phase at intervals of $\Delta\tau$. The rate at which the phase is changed corresponds to a modulation rate, which has an associated bandwidth. It is this bandwidth which provides the high-range resolution pulse characteristics. The number of degrees of phase change applied is dependent upon the phase modulation technique being used. If 180° phase changes are used, it is called a bi-phase code. If 90° phase steps are employed, it is called a quadriphase code. The general term for utilising any number of phase states is called polyphase coding. Different types of phase coded techniques are now described.

3.6.4.2   Barker codes

These are bi-phase codes, which provide an auto-correlation peak, which is the same number, N, as the value of sub-pulses in the code. The maximum level of the time sidelobes is less than or equal to one. However, no Barker codes have been discovered with lengths of more than 13, which represents the maximum pulse compression ratio available. Although they are useful for conventional radar modes, the pulse compression ratio is not sufficient for most target recognition applications [12].

3.6.4.3   Maximal length codes

Another set of codes is called maximal length. These are easy to implement, as they can be generated by using a digital shift register with a feedback circuit [13]. These have the advantage that they can be very long with up to millions of 'sub-pulses', so that very high pulse compression gains can be obtained. They can also be used in association with coherent pulse Doppler signal processing, if the same code is transmitted on every pulse. They can be used for high-resolution radar applications, but one disadvantage is that they are not particularly tolerant to target returns with high

Doppler frequencies, in comparison to chirp waveforms. Compensation techniques can be employed for Doppler, but this adds complications to the signal processing.

3.6.4.4 Polyphase codes

Unlike bi-phase codes, which can only take two states, quadriphase codes [14] can have four phases or states. Polyphase codes can have any number of phases [15,16] and states. Although some of these codes have interesting properties, they are not known to have been applied very frequently.

3.6.4.5 Implementation

Phase coded waveforms were originally compressed using various analogue mixing techniques. However, now they are normally compressed to provide the high-range resolution signal data after the signal has been digitised, as part of the computational operations.

3.6.5 Noise-like waveforms

Before the development of digital modulation techniques [17] to synthesise high-range resolution waveforms, various techniques were investigated using wideband noise sources [18,19]. These were able to provide a different random wideband wave-form for every pulse. Normally to maintain the peak output power of the radar, the waveform would be clipped or driven through a saturated amplifier. An example of a noise-like pulse is shown in Figure 3.26.

The main advantage of a noise-like transmission is that it is relatively covert, so it is more difficult to detect by a potential adversary, particularly if the pulses are long with only a short interpulse period. Nowadays if noise-like or pseudo-random wave-forms are required, they can be generated and compressed using digital techniques. Standard techniques are available to generate pseudo-random number sequences, which can then be modulated onto signals using DACs and frequency mixers. A dis-advantage of this sort of waveform is that it is not truly coherent pulse Doppler, so the advantages of coherent pulse filtering are not obtained [19]. The rejection of clutter [20], for example, is achieved as a result of having a high-pulse compression gain with a long code, rather than by filtering different velocities, using the Doppler effect. A noise-like waveform would not provide the same signal for every transmitted pulse, so the normal Doppler filtering of pulses would not be performed. For most current
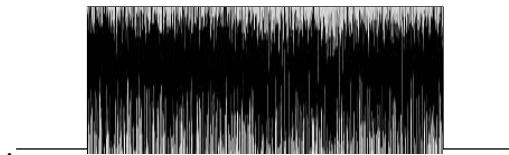
Figure 3.26   A noise-like radar pulse (Courtesy of BAE Systems)
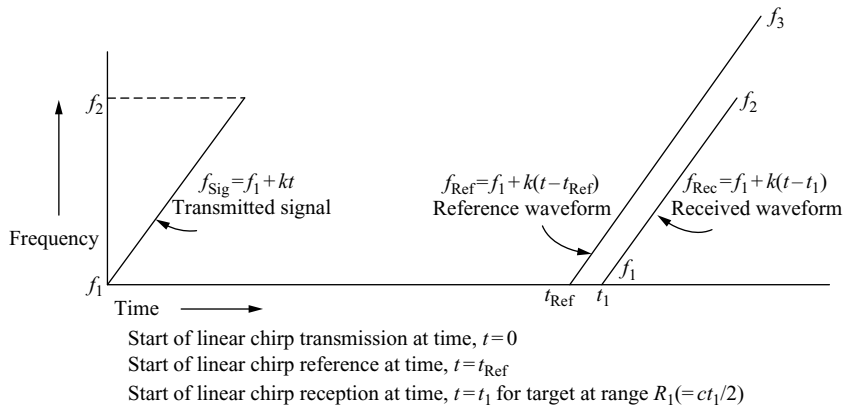
Figure 3.27   Waveforms used in stretch technique and timings

high-resolution radar and target recognition applications, this type of waveform would not be used.

3.7   Stretch

3.7.1   Stretch technique

This is a technique, which is based on linear chirp waveforms, for generating and compressing wideband waveforms, while minimising equipment. It is now one of the most popular and effective techniques used in high-resolution radar and target recognition [21,22]. The transmitted waveform is shown in Figure 3.27 and starts at time, $t = 0$, at frequency, f_1, and rises linearly with time at a rate of k hertz per second to frequency, f_2.

For a point target at range, R_1, which corresponds to a two-way time delay of t_1, the received chirp is shown again as a linear FM signal going from f_1 to f_2. Also shown is a reference chirp, which is used in the receiver, which starts at time t_{Ref} at frequency f_1 and also rises at the same rate as the transmitted signal, k hertz per second, but to a higher end frequency, f_3. These are shown in Figure 3.28.

The reference chirp is used in the receiver to mix with the received signal in order to produce a sinusoidal output signal. The reference and received signals are given by the following:

$$f_{\text{Ref}} = f_1 + k(t - t_{\text{Ref}}) \tag{3.9a}$$

$$f_{\text{Rec}} = f_1 + k(t - t_1) \tag{3.9b}$$

The difference frequency obtained from the output of the mixer is:

$$f_{\text{Out}} = f_{\text{Ref}} - f_{\text{Rec}} = k(t_1 - t_{\text{Ref}}) \tag{3.10}$$

(a)

(b)   Received signal from target
$f_{Rec}=f_1+k(t-t_1)$

f_1 ⋀⋁⋀⋁⋀⋁ f_2

Frequency

Frequency difference
$f_{Out}=k(t_1-t_{Ref})$

f_1 ⋀⋁⋀⋁⋀⋁ f_3

Reference
waveform   Received signal

$f_{Ref}=f_1+k(t-t_{Ref})$
Reference waveform

Mixer

t_{Ref} t_1 Time

Output signal
$f_{Out}=f_{Ref\text{-}Rec}=k(t_1-t_{Ref})$
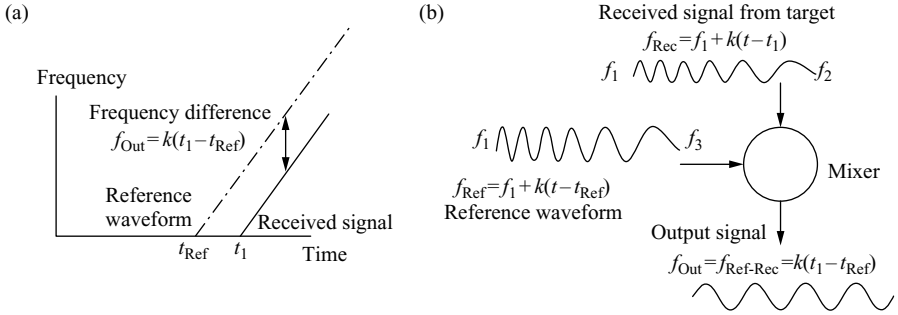
Figure 3.28   *Output frequency from stretch mixing process: (a) difference frequency between received and reference signal is constant for stationary target; (b) received signal is mixed with reference waveform to give sinusoidal output signal*

Substituting the range, $R_1 = ct_1/2$ and re-arranging (3.10):

$$R_1 = \frac{c}{2}\left(\frac{f_{Out}}{k} + t_{Ref}\right)$$ (3.11)

This equation provides the range from the measurement of the output frequency, f_{Out}, from the mixer. The values of c, k and t_{Ref} are known, enabling the range to be determined. The range of the target is proportional to the output frequency measured after subtracting the t_{Ref} term.

   At the output of the mixer the signal undergoes analogue to digital conversion and then is transformed into the frequency domain via a fast Fourier transform and expressed as a spectrum. These functions are illustrated in Figure 3.29. For a high-range resolution application the spectrum in the figure represents the HRRP of a target as the range position is proportional to frequency. It can be seen that the reference chirp has to be longer than the transmitted chirp in order to be able to efficiently mix the signal and to be able to provide reasonable range coverage. The Doppler frequencies of moving targets also have to be accommodated. If the time delay, or range, between two targets of interest is too long, only part of the received signal can be compressed. This reduces the range resolution, as not all the bandwidth of the signal is being used. The time sidelobe performance is degraded as a shorter non-optimum waveform is being used and the sensitivity of the radar is reduced because energy from the received signal is lost.

3.7.2   Range coverage

It can be seen that the range coverage for the stretch technique is proportional to the additional bandwidth provided by the reference signal in the receiver. Using the chirp frequency–time profile of k hertz per second and if the reference chirp is longer than the transmitted signal by a time duration of $\Delta\tau$, then the range coverage is given as
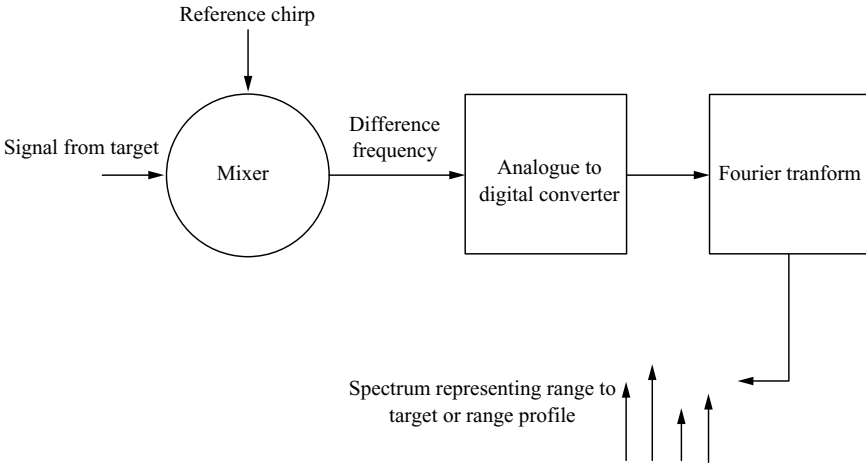
Figure 3.29   *Stretch processes within the radar receiver*
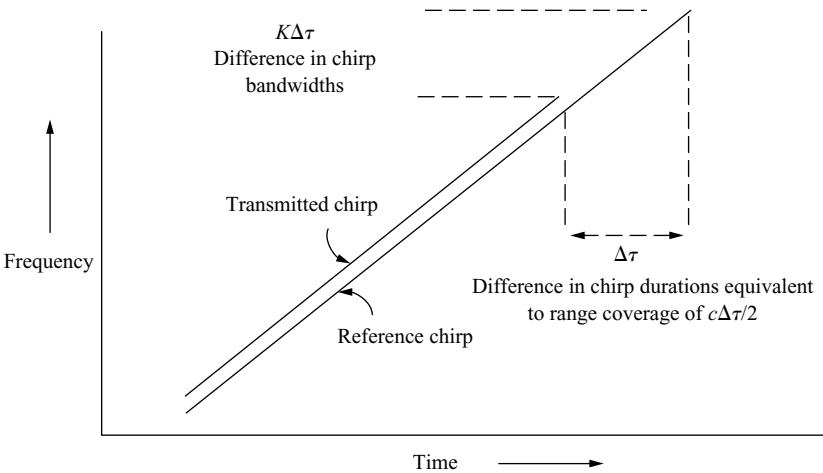
Figure 3.30   *Range coverage, $c\Delta\tau/2$, of stretch waveform is determined by difference in duration between reference and transmitted signals, $\Delta\tau$*

the time delay difference of $\Delta\tau$, which is $c\Delta\tau/2$, expressed in metres. This is shown in Figure 3.30. The extra bandwidth needed in the reference chirp is $k\Delta\tau$ Hz.

3.7.3   *Range-Doppler coupling*

The chirp waveform employed in stretch exhibits the same range-Doppler coupling effects as any other chirp waveform. A key advantage is that the waveform is Doppler

tolerant and that for most high-range resolution applications the Doppler frequency from the target is small in comparison with the bandwidth of the transmitted signal. Hence, there should be little associated loss with the pulse compression process. For the coherent pulse Doppler applications in which the stretch waveform is repeated on a pulse to pulse basis, for a target with a Doppler frequency, the stretch waveform's frequency is shifted slightly, as discussed in Section 3.6.2.

With reference to Equations (3.9) to (3.10) above, the Doppler frequency adds directly onto the received signal and hence to the output signal from the mixer. This frequency offset then gives a proportional offset to the range in (3.11), which is $cf_d/2k$ the range-Doppler coupling.

Again, the Doppler frequency can be measured from performing frequency analysis across the pulse train and compensated for after the signal is digitised. The coupled range component can then be corrected as part of the signal processing operations.

3.7.4   Digitiser bandwidth

The key advantage of using a stretch waveform is that the digitiser bandwidth requirements are far less stressing than if the chirp were digitised conventionally, as discussed in Section 3.6.2. The digitiser speed required is dependent on the bandwidth of the output signal that emerges from the mixer after multiplying the radar signal by the reference waveform. The total bandwidth of the transmitted chirp is $k\tau$ Hz, then the digitiser bandwidth required for conventional digitisation is $k\tau$ Hz. This is shown in Figure 3.31. It neglects the effects of Doppler, which increase the bandwidth requirements marginally.
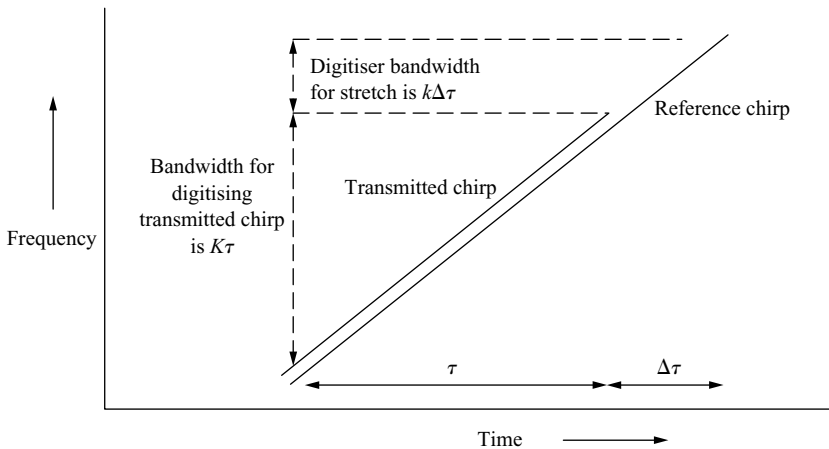
Figure 3.31   Digitiser bandwidth requirements for stretch are considerably reduced in comparison with conventional techniques

When employing stretch, the digitiser is only required to operate at a bandwidth appropriate to the required range coverage, which is $k\Delta\tau$ Hz. Hence, there is a bandwidth ratio between the two techniques of $\Delta\tau/\tau$ Hz.

The use of a lower bandwidth digitiser provides considerable performance advantages. In radar systems it is usually the digitiser that determines the dynamic range of the system. At the lower digitiser speed more effective bits are available and a higher spurious free dynamic range can generally be obtained. The dynamic range of the radar cross-sections (rcs) of whole targets and high-resolution elements of targets that can be simultaneously processed without distortion is improved. This is particularly important for target recognition applications in which small target elements are to be detected, which can be in the presence of large returns from other targets or clutter in the vicinity. If the dynamic range is limited, as it could be in the comparative case of digitising the whole chirp bandwidth, then the sensitivity level would be set by the largest rcs detected, so smaller objects would be missed. This is illustrated in Figure 3.32. The use of a lower speed digitiser also reduces the requirement for a high-speed interface to the signal processor at the digitiser output.

It can be seen that the requirements for a low bandwidth digitiser to achieve high dynamic range performance conflict directly with providing large-range coverage for the high-range resolution function.

In comparing Figure 3.30 and Figure 3.31, it can be seen that the longer the reference chirp and the larger its bandwidth, increased range coverage is obtained. However, as the reference chirp bandwidth increases, so the output signal's bandwidth from the mixing process increases, increasing the digitiser bandwidth requirements. This is a good example of radar parameter trade-offs that have to be assessed, taking into account performance requirements and constraints associated with the available technology. It can be appreciated that the advantages of the stretch technique can be
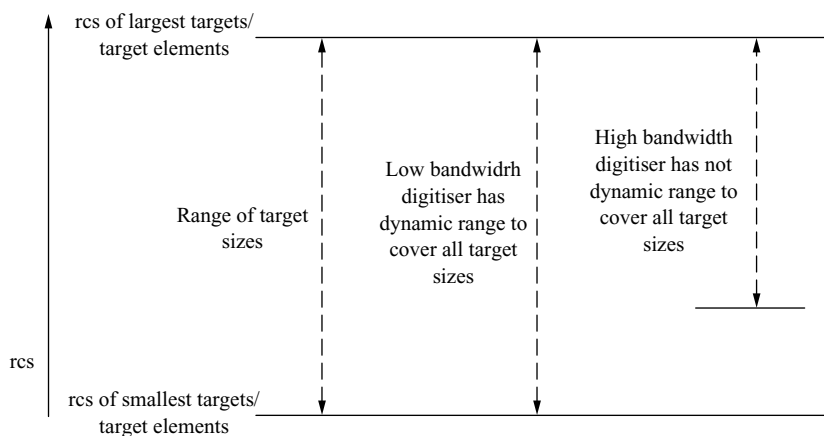
Figure 3.32   Low-speed digitiser used in stretch provides considerable dynamic range advantages

best utilised in applications with the targets of interest being relatively closely spaced. The actual parameters selected are highly dependent upon the application.

3.8 Bandwidth segmentation

3.8.1 Concept

The key advantage of using stepped frequency techniques for synthesising a high-range resolution pulse in frequency increments is the ability to achieve this with a radar, which has a narrow instantaneous bandwidth. The major disadvantage is the range ambiguities, which appear at the inverse of the frequency stepping rate, as discussed in Section 3.5. In some radar target recognition applications, it is not possible to accept the degraded performance associated with these techniques or it is not practical to modify the radar to support wideband waveforms, to overcome the ambiguities.

Various techniques have been investigated for using stepped frequency techniques for synthesising a wideband waveform, whilst minimising the effects of the range ambiguities. These techniques have been labelled here as 'bandwidth segmentation', which is taken to mean the dividing of the bandwidth of a wideband waveform into spectral segments. This is actually different from conventional stepped frequency techniques, in which frequency samples are taken across the frequency band of interest at specific points rather than synthesising the whole bandwidth. The concept of bandwidth segmentation is shown in Figure 3.33 and the main aspects of the technique are introduced in this section.

The spectrum of a wideband rectangular pulse is of the form $\sin x/x$. The stepped frequency techniques are attempting to synthesise this in order to obtain the benefits of a high-range resolution pulse. The stepped frequency technique presented in Section 3.5 earlier measures the reflected signal from the target at discrete frequencies, using long unmodulated pulses. The ambiguities in range arise as a result of the
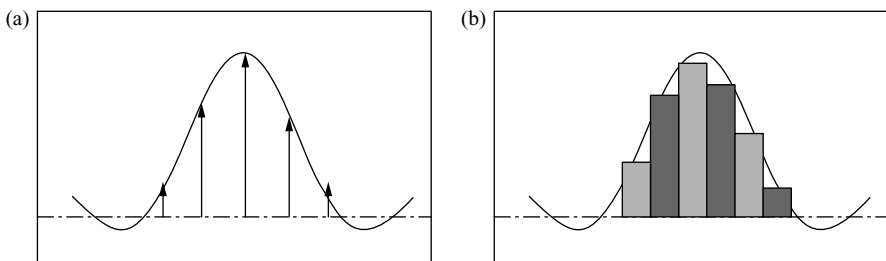
Figure 3.33   Synthesis of wideband pulse for stepped frequency and bandwidth segmentation techniques: (a) stepped frequency technique: spectrum of wideband pulse sampled at frequency intervals; (b) bandwidth segmentation technique: full spectrum of wideband pulse synthesised in frequency segments

spectrum, which is synthesised, but with gaps. This is shown in the auto-correlation function for this waveform in the appendix. The bandwidth segmentation techniques attempt to fill the spectrum, so that the gaps are minimised and that the auto-correlation function at the output of the matched filter for this waveform is much closer to that of the wideband pulse. If a spectrum, as shown in Figure 3.33(b), is transformed back into the time domain, as an amplitude against time series waveform, it is close to that of the wideband pulse, provided the phases of the various spectral components are correct.

3.8.2 Chirp segmentation

One bandwidth segmentation technique is called 'frequency-jumped burst', in which chirps are generated at each frequency step and 'sewed together' to generate a wideband spectrum, as part of the pulse compression process [23,24]. The concept of bandwidth segmentation is shown in Figure 3.34. In (a), a wideband linear chirp can be seen, which is the waveform to be synthesised. The segmented version of this chirp is shown in (b), which consists of five individual chirps, each with one-fifth of the frequency coverage of the wideband chirp. The actual frequency coverage of the two waveforms is exactly the same, so the same nominal range resolution should be achieved. The segmented waveform is transmitted as a series of individual pulses and the returns from targets are collected over the burst.

The data from the five chirp segments, in this example, are then compressed together so as to synthesise the spectrum of a high-resolution wideband pulse. One way of performing the pulse compression process using the data from a segmented waveform is to transform the returns from each pulse into the frequency domain, to represent the target's spectrum over its respective bandwidth.
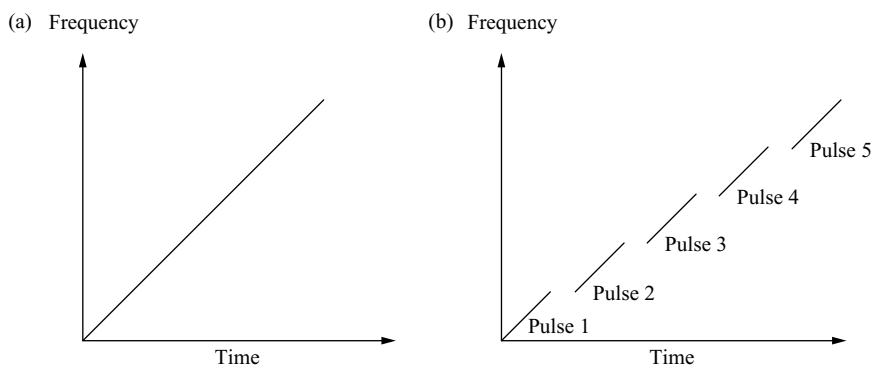
Figure 3.34 *Bandwidth segmentation concept: chirp segments are transmitted sequentially as individual pulses: (a) wideband chirp, and (b) wideband chirp divided into segments, which are transmitted as separate pulses*

(a)

(b)

Power

Frequency

Power

Frequency
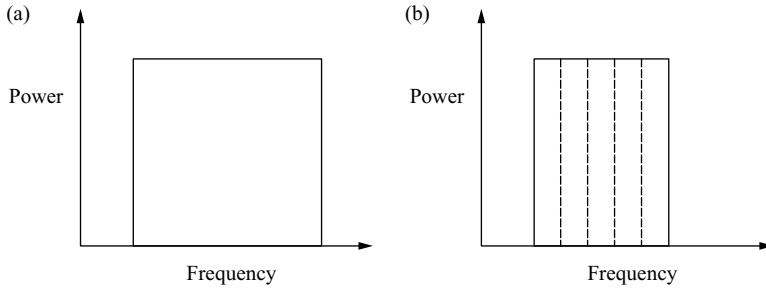
Figure 3.35   Synthesis of the spectrum of a wideband chirp in segments of lower bandwidth chirps: (a) idealised power spectrum of a wideband chirp and (b) synthesis of power spectrum by combining lower bandwidth chirps

The spectra from the individual pulses are then combined to form a composite spectrum synthesising the wideband pulse, which is then transformed back into the time domain to provide high-range resolution data.

Figure 3.35 illustrates how the spectrum of an idealised chirp, which would have a very high pulse compression ratio, could be synthesised in segments of lower bandwidth chirps occupying the same frequency range. The spectrum of a linear FM chirp, as the pulse compression ratio increases, becomes progressively more rectangular in shape, with the width be equal to the frequency interval over which the chirp sweeps. The individual spectra of the chirp segments also closely approximate rectangular functions, so can be integrated together to form a reasonable approximation to the wideband chirp spectrum. The output of the matched filter, which was seen earlier to be the auto-correlation function of the power spectrum, is the $\sin x/x$ characteristic for the chirp, as is shown in Figure 3.23.

The effects of Fresnel ripples, which are characteristic of chirps and appear as amplitude ripples in the frequency spectrum, have not been included in the discussion for clarity purposes. In practice, these types of effects complicate the signal processing, but do not significantly affect the concepts presented.

3.8.3   Combining segmented waveforms

A critical aspect of sewing together segmented waveforms is to apply the correct relative phase to each of the segments, particularly for moving targets. The segmented technique, in transmitting with gaps in time between the various contributing waveforms, has associated time delays between the end of one waveform segment and the beginning of the next. This contrasts with the long wideband chirp waveform, which has no gaps in time or phase discontinuities, as it is a single continuous pulse. Hence, within the pulse compression process, the time between the waveform segments being transmitted has to be known very accurately and also the target velocity, so that appropriate phase corrections can be made to construct the required spectrum with high integrity. The effectiveness of this high-range resolution technique is dependent

upon the radar hardware providing precise timing and required phase of the respective waveform segments and the ability to provide phase corrections associated with target motion.

3.8.4   Bandwidth segmentation techniques

Two types of segmentation technique are used for the compression of segmented chirp waveforms. The first involves the digitisation or analogue compression of each segment appropriate to its bandwidth. The second uses a stretch technique at each bandwidth, so that a lower bandwidth digitiser can be used, but the range coverage is then limited.

3.8.5   Bandwidth segmentations conclusions

The key advantages of bandwidth segmentation are the minimisation of range ambiguities at the equivalent of the inverse of the frequency stepping interval and the reduction in digitiser bandwidth required. The main disadvantage of bandwidth segmentation is that it tends to take longer to acquire the high-range resolution target data than with a single wideband chirp.

3.9   Summary of high-range resolution waveforms

The selection of the waveform for supporting high-range resolution radar functions is dependent upon the characteristics of the target, the environment and the design constraints associated with the host radar. In this section the main characteristics of the waveforms presented earlier in the chapter for supporting high-range resolution modes are summarised. The short duration high peak power radar pulse is ideal from the theoretical viewpoint of obtaining high-integrity target range profiles, but generally is not practical to implement in real systems.

The stepped frequency techniques, which synthesise a wideband waveform in a series of frequency increments, have the advantage of being reasonably straightforward to implement in the many radars available with restricted instantaneous bandwidths. However, they suffer the shortcomings associated with range ambiguities appearing in the vicinity of the target. It can also take longer to transmit a long sequence of frequency stepped waveforms than techniques with higher instantaneous bandwidths.

Noise-like waveforms can be useful in test ranges or short-range covert applications, but are generally not suitable for applications in the presence of high levels of clutter.

The bi-phase family of waveforms can provide high bandwidths with good time sidelobe performance. However, these waveforms are not Doppler tolerant, so more complex signal processing is required. Another disadvantage is that the spectrum produced is not rectangular in shape, but tends to be of the $\sin x/x$ shape, so the spectrum is not being utilised efficiently.

The linear FM chirp is probably the most popular high-range resolution waveform. It has good time sidelobes, moderate signal processing losses and is Doppler tolerant.

Table 3.2   High-range resolution waveform summary

Technique	Restricted range window	Time on target	Range ambiguities	Operation in clutter	Comments
Short high-level peak pulse	OK	OK	OK	OK	Not practical in most applications
Wideband chirp	OK	OK	OK	OK	Popular waveform for target recognition
Stepped frequency	Weakness	Weakness	Weakness	OK	Only requires low bandwidth components
Bandwidth segmentation	OK	Weakness	OK	Yes	Complex signal processing required
Noise-like waveform	OK	OK	OK	Weakness	Not used in main stream applications
Stretch	Weakness	OK	OK	OK	Only requires low bandwidth digitiser
Bi-phase codes	OK	OK	OK	OK	Not Doppler tolerant; Radar bandwidth not optimally used: poorer range resolution obtained

The stretch technique is a variation on the theme of the linear FM chirp, with the advantage that a lower higher dynamic range digitiser can be used, so higher integrity range profiles can be obtained. The major disadvantage is that the range coverage of the technique is limited.

The bandwidth segmentation techniques are a compromise between the classical stepped frequency techniques and the wideband chirp techniques. They can overcome the range ambiguities in the vicinity of the target, but more complex signal processing techniques are required to stitch together the various contributing waveform segments for moving targets. The waveform sequence can also take longer to transmit than wideband pulses.

The characteristics associated with the various high-range resolution waveforms are summarised in Table 3.2.

It can be seen that the various techniques each have their respective performance advantages, drawbacks and levels of implementation complexity. Although the

stepped frequency technique is identified as having most weaknesses, it is interesting to note that this was the first waveform that could be supported by conventionally designed radars to provide HRRPs of targets.

References

1 SWERLING, P. 'Detection of Fluctuating Pulsed Signals in the Presence of Noise' *IRE Transactions*, September 1957, Vol **IT-3**, pp. 175–8

2 RIHACZEK, A.W., and HERSCHOWITZ, S.J.: 'Theory and Practice of Radar Target Identification' (Artech House, Boston, MA, 2000) pp. 182–99

3 SKOLNIK, M.I.:'Introduction to Radar Systems' (McGraw Hill, New York, 1985) Chapter 9-2

4 PRAHBU, K.M.M., 'Generalised Families of Windows for Use in Signal Processing', *Journal of the Institution of Electronic and Radio Engineers*, 1987, **57**(4), pp. 174–7

5 BARTON, D.K. (Ed.): 'Pulse Compression' (Artech House, Boston, MA, 1975)

6 BACKUS, P.: 'Evolution of Pulse Compression in Radar'. *Microwave Journal*, November 1979, pp. 38–40

7 FULLER, H.W.: 'Broadband Microwave Pulse Compression', *Microwave Journal*, April 1980, pp. 52–61

8 DANIELS, W.D., CHURCHMAN, M., and SKUDERA, W.: 'Compressive Receiver Technology', *Microwave Journal*, April 1986, pp. 175–85

9 ARTHUR, J.W.: 'SAW Pulse Compression in Modern Multi-Channel Radar Applications', *Microwave Journal*, January 1986, pp. 159–69

10 ARTHUR, J.W.: 'Modern SAW-Based Pulse Compression Systems for Radar Applications, Part 1: SAW Matched Filters', *Electronics and Communication Journal,* December 1995, pp. 236–46

11 ARTHUR, J.W.: 'Modern SAW-Based Pulse Compression Systems for Radar Applications, Part 2: Practical Systems', *Electronics and Communication Journal,* April 1996, pp. 57–78

12 BARKER, R.H.: 'Group Synchronising of Binary Systems' (Academic Press, London, 1958), JACKSON, W. Editor

13 MASSEY, J.: 'Uniform Codes', *IEEE Transactions on Information Theory*, April 1966, **12** (2), pp. 132–4

14 TAYLOR, J.W., and BLINKIKOFF, H.J.: 'Quadriphase Code-A Radar Pulse Compression Signal with Unique Characteristics', *IEEE Transactions on Aerospace and Electronic Systems*, 24 (2), pp. 156–70

15 FRANK, R.L.: 'Polyphase Codes with Good Non-Periodic Correlation Properties', *IEEE Transactions on Information Theory*, January 1963, **IT-9**, pp. 43–5

16 LEWIS, B.L., and KRETSCHMER, F.F.: 'A new Class of Polyphase Compression Codes and Techniques', *IEEE Transactions on Aerospace and Electronic Systems*, May 1981, **AES-17**, pp. 364–72

17 LUKIN, K.A.: 'Millimetre Wave Noise Radar Applications: Theory and Experiment'. The Fourth International Kharkov Symposium on *Physics and Engineering of Millimeter and Sub-Millimetre Waves,* 2001. **1**, 4–9 June 2001, pp. 68–73

18 AXELSSON, S.R.J.: 'Noise Radar Using Random Phase and Frequency Modulation', *IEEE Transactions on Geoscience and Remote Sensing*, 2004, **42** (11), pp. 2370–84

19 WILLIAMS, F.C., and RADANT, M.E.: 'Airborne Radar and the Three PRFs', *Microwave Journal,* July 1983, pp. 129–35

20 KULPA, K.S., and CZEKALA, Z.: 'Ground Clutter Suppression in Noise Radar'. *Radar 2004*, Toulouse, France. Paper no. 211

21 GUOLIN WANG, RONGQING XU, and ZHIDAO CAO: 'System Compensation for Inverse Synthetic Aperture Radar'. *IEEE Conference,1994*

22 BLANTON, J.L.: 'Cued Medium PRF Air-to-Air Radar Using Stretch Range Compression'. *1996 IEEE National Radar Conference*

23 MARON, D.E.: 'Frequency Jumped Burst Waveforms with Stretch Processing'. *IEEE International Radar Conference, 1990*

24 SCHIMPF, H., WAHLEN, A., and ESSEN, H.: 'High Range Resolution by means of Synthetic Bandwidth generated by Frequency-stepped Chirps'. *Electronic Letters*, 2003, **39**(18), pp. 1346–48

Chapter 4

High cross-range resolution techniques

4.1 Introduction

In Chapter 3, the high-range resolution techniques discussed were appropriate to down range of the radar, along its radial vector. The range resolution obtained depended upon the bandwidth of the waveform transmitted. In this chapter, techniques for providing high cross-range resolution are presented, which correspond to the direction perpendicular to the radar's radial vector. As was briefly presented in Section 2.2.4, cross-range resolution is basically dependent upon the aperture of the antenna employed or the aperture that is synthesised by virtue of the motion of either the radar or the target. In some circumstances, when both the radar and the target are in motion, the synthesised aperture is dependent upon both of these motions.

In Section 4.2, Doppler beam sharpening is discussed. This is a high cross-range resolution technique, which is dependent upon the radar being located on a moving platform and utilising a coherent pulse Doppler waveform for providing increased cross-range resolution using the Doppler effect. It can contribute to target recognition by isolating individual targets in azimuth, but the actual cross-range resolution obtained would not normally be sufficiently high to resolve individual target scatterers.

In Section 4.3, SAR is presented, which provides high cross-range resolution by synthesising a large antenna aperture, due to the motion of the radar. This effectively decreases the beamwidth of the radar and a very narrow beam is synthesised, which provides high cross-range resolution and varies with target range for a fixed integration time. Various types of SARs are presented, which are dependent upon the look angle of the radar in relation to the associated platform's velocity vector, which is the same as its direction of motion. SAR is used for high-resolution mapping of the ground and for providing high-range resolution two-dimensional images of ground targets, when employed in conjunction with a high-range resolution waveform. The signature measured can then be used for target recognition purposes.

In Section 4.4, ISAR is discussed. This uses the target motion itself to generate a synthetic aperture to provide high cross-range resolution. When this is employed with a high-range resolution waveform, a two-dimensional target signature is obtained, which can then be used for target recognition.

4.2   Doppler beam sharpening

4.2.1   Real beam map

Before considering Doppler beam sharpening, as a means of introduction, real beam aperture mapping is first discussed. This technique generates the most basic radar map that can be obtained from a radar mounted on either a stationary or a moving platform. The cross-range resolution is equal to the antenna beamwidth, θ, multiplied by the range, R, and the down-range resolution, ΔR, is equal to $c\Delta t/2$, where Δt is the compressed pulse length, as presented in Chapter 2. This is illustrated in Figure 4.1. As the antenna scans, cells of size $R\theta \times \Delta R$ are generated to form a map of fairly coarse resolution. The size of the cells varies with range and usually the down-range resolution is far higher than the cross-range resolution. For example, a radar operating with 5 MHz bandwidth has a range resolution of about 30 m. If it has a 3° beamwidth the cross-range resolution at 20 km range is about 1000 m. Hence, the down-range resolution is about two orders of magnitude higher than the cross-range resolution. Real beam aperture mapping can provide some basic terrain features, but improved cross-range resolution is needed to provide a more useful map with similar range resolution in both dimensions. The cross-range resolution, ΔR_{c} is independent of the beam pointing angle. In the real beam map illustrated in the figure, the tone of the colour represents the amplitude of the signal received from each respective cell.
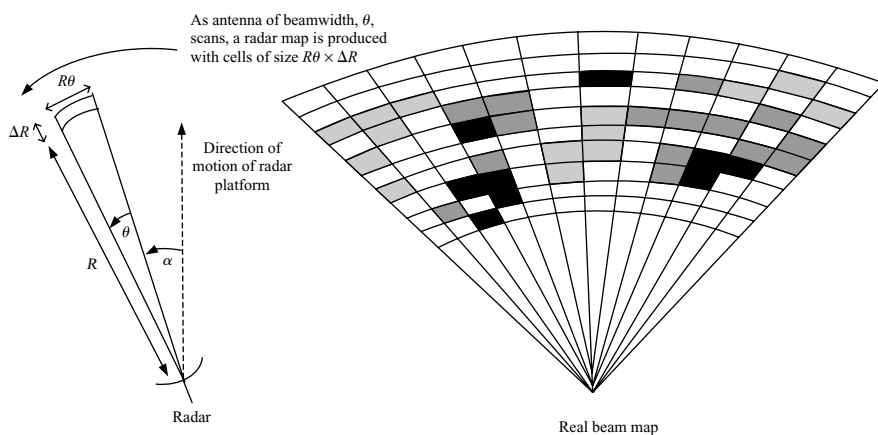
Figure 4.1   Real beam mapping

4.2.2 Doppler beam sharpening concept

Doppler beam sharpening [1] is the next stage towards providing higher cross-range resolution. This technique is employed in airborne and sometimes spaceborne radars to provide higher resolution maps of the terrain than can be achieved by using the cross-range resolution available from the antenna beamwidth alone. The increase in cross-range resolution achieved is dependent upon the differential Doppler velocities that can be instantaneously measured.

The Doppler beam sharpening concept is shown in Figure 4.2 for a radar moving with a velocity, v. The principle of the technique is based upon the fact that the relative velocity of a point on the ground is equal to the velocity vector of the radar multiplied by the cosine of the angle between the direction of motion of the radar and the line
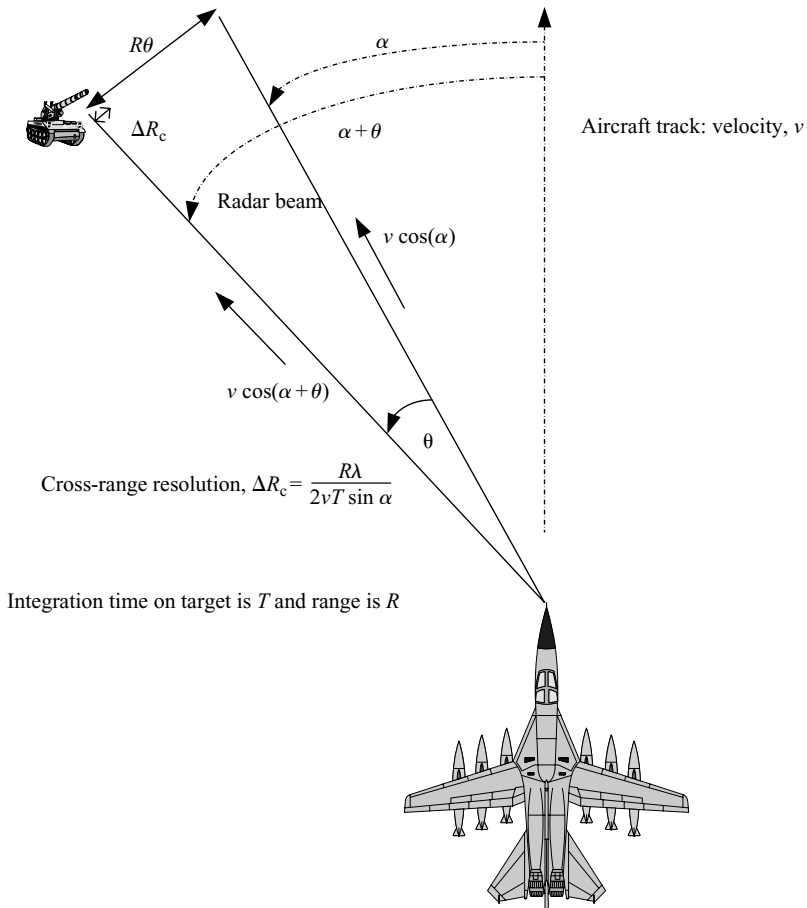
Figure 4.2   Doppler beam sharpening: the Doppler effect is used to improve cross-range resolution of objects within the radar beam

joining the radar to the position of interest on the ground. For different positions on the ground, within the radar beam, at the same range from the radar, different relative velocities and hence different Doppler frequencies are obtained.

For the example shown, with the radar beam covering offset angles between α and $\alpha + \theta$, the relative velocity vectors for points on the ground vary from $v \cos(\alpha)$ to $v \cos(\alpha + \theta)$. For a radar operating at a frequency of f Hz, the corresponding Doppler frequencies measured are $2vf \cos(\alpha)/c$ and $2vf \cos(\alpha + \theta)/c$, respectively. The frequency resolution for a measurement period, T, is given by $1/T$. The number of Doppler filters equates to the differential Doppler frequency across the beam, which is $(2vf \cos(\alpha)/c) - (2vf \cos(\alpha + \theta)/c)$ divided by the frequency resolution $1/T$. Hence, the cross-range resolution, ΔR_c is approximately equal to the cross-range resolution of the real antenna aperture, $R\theta$, divided by the number of Doppler filters associated with the measurement.

Hence the cross-range resolution, ΔR_c is given by:

$$\Delta R_c = \frac{cR\theta}{2vf(\cos(\alpha) - \cos(\alpha + \theta))T}$$

$$= \frac{cR\theta}{2vfT(\cos\alpha - (\cos\alpha\cos\theta - \sin\alpha\sin\theta))}$$

$$\approx \frac{cR\theta}{2vfT(\cos\alpha - (\cos\alpha + \theta\sin\alpha))}$$

$$\approx \frac{R\lambda}{2vT\sin\alpha} \tag{4.1}$$

For small values of beamwidth, θ and using $v = f\lambda$.

In practice, the value of cross-range resolution achievable is limited by the integration time, T. Over the integration period, the relative velocity of any point on the ground continuously varies, as the aircraft is moving. The limit occurs when the change of Doppler frequency over the integration period becomes close in value to the basic frequency resolution of the measurement, $1/T$. This change of Doppler frequency with time can actually be compensated for and is the basis of SAR, which will be discussed in the next section. The fundamental difference between Doppler beam sharpening and SAR is that the former processes the radar data for standard Doppler filters and the latter actually processes the data for a variable Doppler frequency against time characteristic. For Doppler beam sharpening, with reference to Equation (4.1), as the look angle of the radar increases from head on, $\sin(\alpha)$ increases, so the cross-range resolution improves. Around head on, the cross-range resolution is relatively poor and is close to that provided by the real antenna aperture, as discussed in the previous section.

Doppler beam sharpening can be considered to provide an intermediate map resolution between that determined by the real antenna aperture and the resolution obtained from SAR. Doppler beam sharpening is effectively an unfocused SAR mode.

4.3   Synthetic aperture radar

4.3.1   Concept

The concept of synthetic aperture radar or SAR [23], as it is known among the radar community, is shown in Figure 4.3. The radar is pointed in a direction that is at right angles to its motion vector. Conventional SAR is sideways looking, but a squint or spotlight mode is also possible and is discussed in Section 4.4. The radar is not rotating and is nominally fixed with respect to the platform.

   The idealised case is shown with an aircraft flying along a straight line track with the aircraft and the target in the same plane. The closest point of approach to the target is at range, R_{min}. The aircraft is flying at a velocity, v, and the integration period over which the synthetic aperture is generated is a time, T. Hence, the distance travelled by the aircraft over this period, D, is equal to vT. The angle between the direction of flight and the line joining the radar to the target is α. Over this period of time the radar is operating coherently and transmitting and receiver radar pulses.

   The relative velocity between the aircraft and the target is given by the velocity component of the aircraft's motion in the target's direction, which is $v \cos \alpha$. Over the radar integration period this varies from an initial closing velocity, to zero relative velocity at the closest point of approach, R_{min}, to a progressively increasing receding velocity.

4.3.2   SAR Doppler frequency shift

Consider the geometry of Figure 4.3 to calculate the value of Doppler frequency obtained. At time $t = 0$, the integration period for the SAR measurement begins.
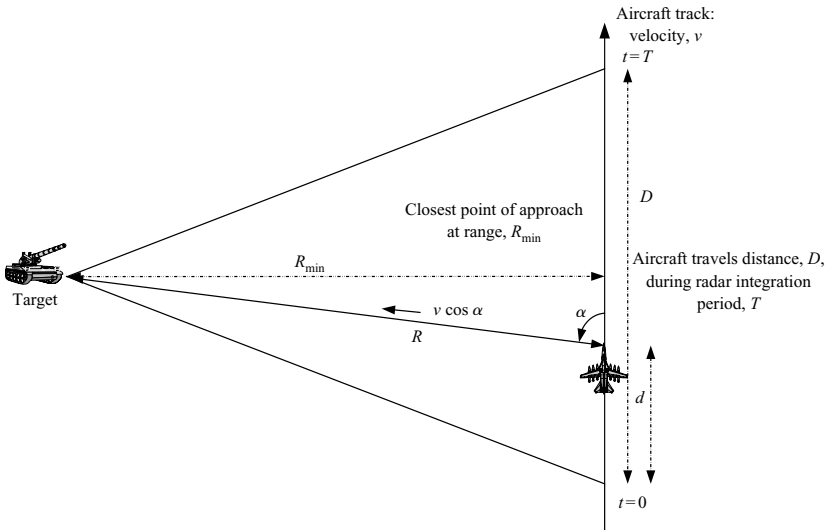
Figure 4.3   Synthetic aperture radar

At any other general time, t, the aircraft is at a position d, along the track, with reference to $t = 0$. In order to calculate the value of the Doppler frequency component of interest between the radar and the target, it is first necessary to calculate the associated Doppler frequency component, $v \cos \alpha$ as a function of time:

$$v \cos \alpha = \frac{v((D/2) - d)}{R} = \frac{v((D/2) - vt)}{\sqrt{(R_{min}^2 + ((D/2) - vt)^2)}} \tag{4.2}$$

As the value of the range, R_{min}, to the target is generally very much larger than the values of vt, d and D in practical SAR systems, then Equation (4.2) can be approximated to:

$$v \cos \alpha = \frac{v((D/2) - vt)}{R_{min}} \tag{4.3}$$

The corresponding Doppler frequency is

$$\frac{2vf \cos \alpha}{c} = \frac{2vf((D/2) - vt)}{R_{min}c} \tag{4.4}$$

Figure 4.4 shows the characteristic SAR Doppler frequency against time profile for the target perpendicular to bore-sight at the closest point of approach. The frequency can be seen to vary linearly with time as the radar sweeps past the target. This is a type of chirp waveform characteristic, which was discussed in a somewhat different
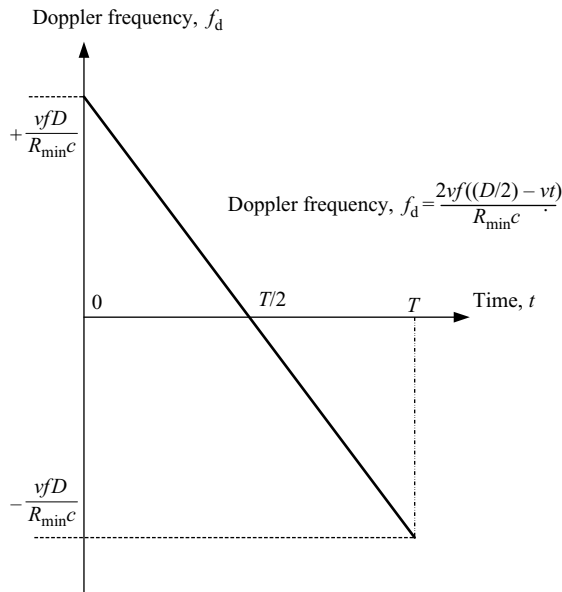
Figure 4.4   Doppler frequency versus time characteristic for SAR measurement of Figure 4.3

context in Chapter 3, but mathematically is the same. This waveform can be seen to vary with range to the target and velocity and transmission frequency of the radar. At the start of the integration period the target is closing relative to the radar and has a positive Doppler frequency of $+(vfD/R_{min}c)$. This reduces progressively, goes through zero at the closest point of approach at range, R_{min}, and becomes a negative Doppler frequency peaking at $-(vfD/R_{min}c)$ at the end of the integration time, T.

At any given time, targets at different ranges and look-angles simultaneously return to the radar with different Doppler frequencies. Targets at different ranges each have a different shape of time-Doppler frequency profile, as can be seen by examining Equation (4.4). Targets at the same closest point of approach to the radar, have the same time–frequency characteristic, but at different times. It is the function of the radar's signal processor to collect all these data samples from the targets, appropriately order them and perform the mathematical operations on them to provide high-range resolution data in the correct position and to form a radar map. This operation performs the matched filter function appropriate to each possible target location of interest.

4.3.3   SAR cross-range resolution

The cross-range resolution obtained is calculated using the chirp function shown in Figure 4.5. The total spread in Doppler frequency for the SAR integration period is $(2vfD/R_{min}c)$. This chirp waveform is compressed in the SAR receiver, using the appropriate matched filter, which is a multiplication by the complex conjugate of this waveform. The time resolution obtained is the inverse of the chirp bandwidth, $(2vfD/R_{min}c)$, which is $(R_{min}c/2vfD)$. This is shown in Figure 4.5.

This is equivalent to the same mathematical operation as the compression of the linear chirp for providing high down-range resolution. This value is the minimum time delay between two SAR time–frequency chirp characteristics, for two adjacent scatterers, which can be separated in time. It also represents the closest distance between
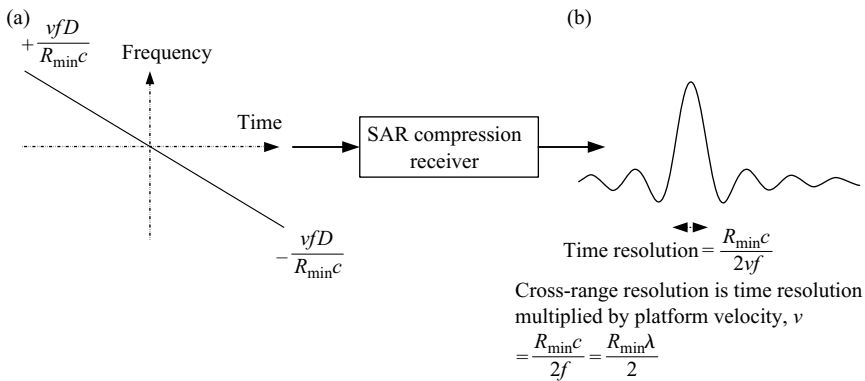
Figure 4.5   Cross-range resolution for SAR: (a) frequency against time and (b) amplitude against time (weighting function normally used, but not shown)

two scatterers, at the same values of R_{min}, which can be resolved in the cross-range dimension and is the value of the time resolution multiplied by the platform velocity.

The value $(R_{min}c/2vfD)$ can also be written in terms of wavelength, λ (using $c = f\lambda$) and equals $(R_{min}\lambda/2vD)$, so the cross-range resolution for SAR is:

$$\Delta R_c = \left(\frac{R_{min}\lambda}{2vD} \right) v = \frac{R_{min}\lambda}{2D} \tag{4.5}$$

For an antenna, the angular resolution, $\theta_a \sim (\lambda/D_a)$, where D_a is its aperture. The cross-range resolution at range R_{min} for a conventional radar is ΔR_a and is given by $\Delta R_a = R_{min}\theta_a = (R_{min}\lambda/D_a)$. The conventional cross-range resolution is:

$$\Delta R_a = \frac{R_{min}\lambda}{D_a} \tag{4.6}$$

By comparing Equations (4.5) and (4.6), the effective antenna aperture for the SAR system can be determined. In order to achieve the same cross-range resolution with a conventional aperture, such that $\Delta R_c = \Delta R_a$, then:

$$D_a = 2D \tag{4.7}$$

This equation states that the effective aperture synthesised is twice the value of the path length utilised for the SAR integration period. Hence, the synthesised antenna length, which provides $(R_{min}\lambda/2D)$ cross-range resolution is $2D$. The SAR range resolution is therefore twice the value obtained from a conventional antenna of the same length. Consider a conventional antenna, whereby the transmitted signal is generated across the whole aperture simultaneously and received by the whole aperture simultaneously. On transmission the simultaneous phase contributions of all the antenna elements across the aperture generate the phase front and the one-way beamshape (from Equation (2.20)) is a $(\sin x/x)$ function. The wavefront and beamshape function are shown in Figure 4.6(a). The two-way beamshape, which includes the effects on receiving the signal, is also shown in the figure and is a $(\sin x/x)^2$ function. The variable x is proportional to the aperture length.

In the SAR process, the transmitted and received signals from the target are effectively generated sequentially from each individual element of an array, or part of the antenna. The first pulse is transmitted and received by the first element and the second pulse is transmitted by the second element, etc. Each element of the antenna aperture effectively generates it own two-way beam pattern individually and sequentially and the net beam shape from all the antenna elements is formed by integrating their individual contributions.

The phase contribution of one antenna array element to the two-way antenna pattern is $2y \sin \alpha$, as shown in Figure 4.6(b), which is equivalent to the two-way distance to the wavefront being synthesised. The net two-way antenna beam pattern formed is the integration of all the antenna element contributions, which is a $(\sin 2x/2x)$ distribution. Hence, the conventional antenna has a $(\sin x/x)^2$ two-way beamshape compared to a $(\sin 2x/2x)$ antenna pattern for SAR.

(a)

One-way antenna pattern is: $f(\alpha) = \dfrac{[\sin \pi \, (D/\lambda) \sin \alpha]}{(\pi D/\lambda) \sin \alpha}$

Two-way antenna pattern is: $f(\alpha) = \dfrac{[\sin \pi \, (D/\lambda) \sin \alpha]^2}{(\pi D/\lambda)^2 \sin^2 \alpha}$

(b)

Contribution of phase of each element to two-way antenna pattern is: $(2y \sin \alpha)(2\pi/\lambda)$

Two-way antenna pattern is integrated value of all contributing elements:

$$\int_{-D/2}^{D/2} e^{(2\pi i/\lambda \times 2y \sin \alpha)} dy = \frac{[\sin \pi \, (2D/\lambda) \sin \alpha]}{\pi(2D/\lambda) \sin \alpha}$$
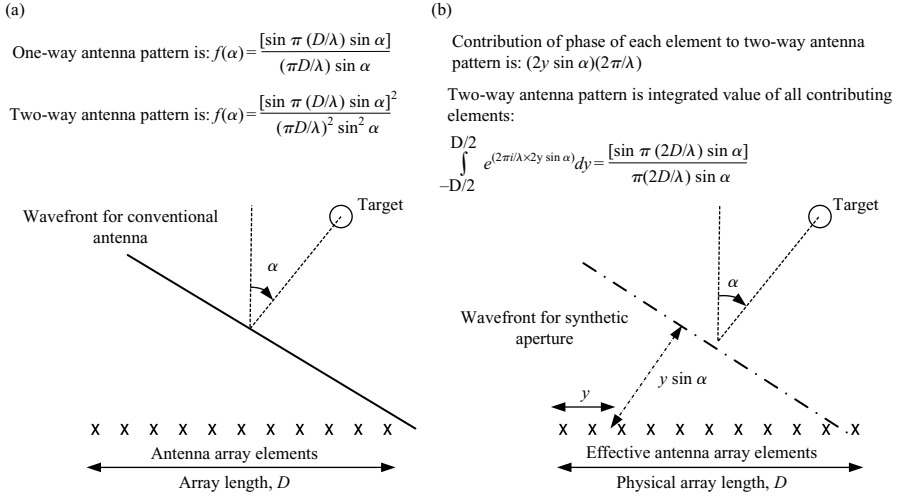
Figure 4.6   SAR can be considered to be a phased array with sequential sampling at the array elements as the radar moves, but has twice the cross-range resolution of the equivalent real aperture radar: (a) for conventional real aperture radar all elements of antenna simultaneously contribute to wavefront and simultaneously receive reflected signal (also see Figure 2.22 and Equation (2.20)); (b) for synthetic aperture radar only one element of effective antenna aperture contributes to wavefront at any one time and receives reflected signal: this improves cross-range resolution in relation to real aperture radar as transmitted and reflected signal is localised to single antenna element

The first null of the $(\sin 2x/2x)$ function occurs at an angle of $\pi/2$, whereas the first null of the $(\sin x/x)^2$ function occurs at π and approximates to double the former's beamwidth. The value of x for the real aperture antenna represents the physical length of the aperture and the associated beamwidth is inversely proportional to x. In contrast, the value of $2x$ represents twice the physical length of the synthetic aperture generated and the cross-range resolution obtained [4] is inversely proportional to $2x$.

4.3.4   Real beam illumination

An important point to note in SAR imaging is that the target must remain in the real antenna beam for the duration of the radar integration period, as shown in Figure 4.7.

If the target is not in the beam for the whole integration period, cross-range resolution and sensitivity are degraded.

4.3.5   Target Doppler frequencies and cross-range resolution

Figure 4.4 shows the Doppler frequency obtained from a single target during the SAR integration period. The characteristics of the Doppler frequencies with time for targets at different positions are shown in Figure 4.8.
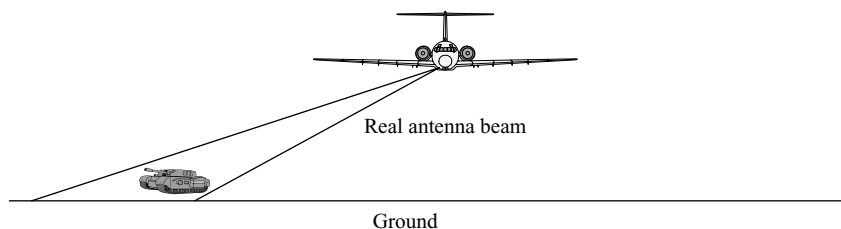
Figure 4.7   Target must remain in real beam during radar integration period to obtain required cross-range resolution
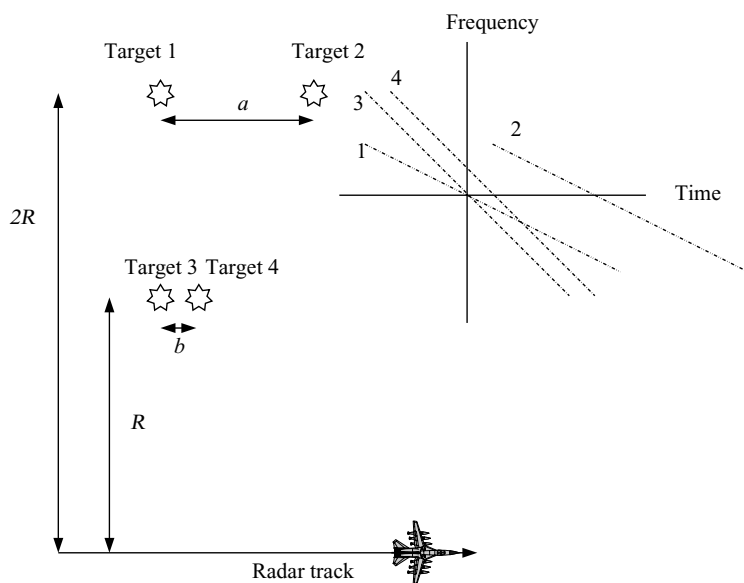
Figure 4.8   Typical frequency–time characteristics of targets at different ranges

Targets 1 and 2 are at the same distance of closest approach to the radar, $2R$, but separated by distance a along the track direction. Targets 3 and 4 are both at the minimum range of R and are separated by b. The frequency against time characteristics for targets 1 and 2 are identical apart from the time offset, which is a/v. Similarly targets 3 and 4 have identical frequency against time slopes, offset by b/v. As one pair of targets is at twice the minimum range of the other, the frequency–time characteristic of 1 and 2 has half the slope of that of 3 and 4. Also as 1 and 3 are at the same azimuth angle at the closest point of approach, they both have zero relative Doppler frequencies at the same time.

This simple example illustrates that the frequency–time slope and its position in time is specific to each target range and position along the aircraft track.

Hence, the cross-range signal processing has to provide a selection of matched filters appropriate to the frequency–time characteristics of targets of interest.

In Section 4.3.4 it was shown that for a synthesised antenna length of $2D$ the cross-range resolution obtained is $(R\lambda/2D)$. Hence, for the same integration period, the cross-range resolution obtained is proportional to the range at closest approach, R. With reference to Figure 4.8, this means that for the same integration period, targets at positions 1 and 2 have poorer cross-range resolution by a factor of two in comparison to targets 3 and 4. However, if double the integration time is used for 1 and 2, all four targets can be measured with the same cross-range resolution. It can be seen that to obtain constant cross-range resolution for targets at all ranges, an integration time proportional to the target's range is required. This is clearly far more complex to implement, as the signal processing is more complex. The actual mission requirements and signal processing power available determine the level to which range dependent SAR integration periods are required.

4.3.6   SAR range cells and target images

The SAR signal processing, which provides high down-range and cross-range resolution is presented as a two-dimensional map, as shown in Figure 4.9, in contrast to the high-range resolution techniques presented in Chapter 3, which produce one-dimensional range profiles of targets.

SAR produces an image, which consists of cells comprising a down-range against a cross-range grid. Each cell is called a 'pixel', which is a derivation of the term 'picture element'. An aircraft outline is shown in Figure 4.9(a) against the high-range resolution grid. This target is assumed to be stationary on the ground. An equivalent representation of a SAR image is shown in Figure 4.9(b). It is assumed that this aircraft is being viewed by the radar from a flight path, which is almost in the same horizontal plane as the aircraft and is following a track, which is orthogonal
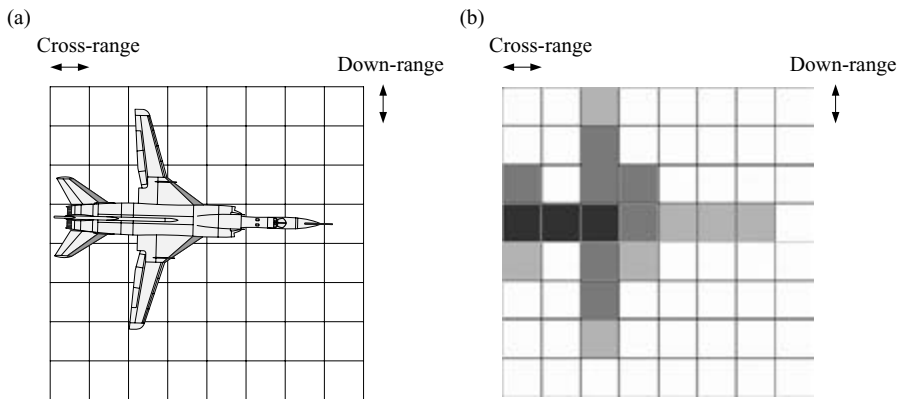
Figure 4.9   Representation of target and SAR image: (a) aircraft on grid and (b) SAR image

to the axis of symmetry of the target shown. In each pixel the energy from the target scatterers at the appropriate time delays is effectively integrated to provide a net amplitude and phase return for the cell. Each individual pixel corresponds to a unique Doppler frequency against time characteristic as the radar moves past, as was shown in Figure 4.8.

As explained above, the down-range resolution is dependent on the bandwidth of the waveform used and the cross-range resolution depends upon the aperture synthesised over the radar integration period. The application determines the range resolution requirements for the radar. In this example, the resolution used is sufficient to determine that an aircraft target has been detected and that the general outline can be discerned.

Nearby clutter tends to obscure the target's features at this range resolution. It is normally considered that optimum detection and recognition of targets with SAR are performed if the cross- and down-range resolutions chosen are similar.

Intuitively, it can be seen that the SAR image should provide better information for target recognition purposes as the radar signatures generated look more like the physical object than a range profile. As the cross-range scatterers are localised in SAR and are not confined to single-range gates as in range profiling, this other dimension provides considerably more information. Whatever techniques are used for recognising targets from their radar signatures, in terms of the quality of image produced, SAR outperforms range profiling. Interestingly, range profiles can also be obtained by suitably processing the raw SAR data. Effectively by collapsing the SAR image into one-dimension, a range profile is obtained. A range profile can be thought of as a sub-set of a SAR image.

4.3.7   SAR motion compensation

A critical issue for SAR, particularly for airborne platforms flying under turbulent weather conditions, is compensation for the motion of the platform on which the radar is mounted, when the track deviates from the ideal straight horizontal line [5,6]. All the SAR theory and techniques discussed to date in this chapter have assumed that the SAR platform is on a straight and level track, at constant speed and that the radar is firmly fixed to it, with no relative motion.

In a real application, an aircraft is not flying in an absolutely straight line and it is not staying at exactly the same altitude at the same speed. In many airborne systems vibration effects are present, so that the radar itself is vibrating relative to the host airframe. The concept of SAR involves measuring the Doppler frequencies of various targets on the ground with high precision. As has been discussed earlier in the chapter, this is performed by measuring the amplitude and phase of each reflected radar pulse and the Doppler frequency is obtained from measuring the rate of change of phase over a series of radar pulses. As the measurement of the phase [7] is the key factor, it has to generally be performed with an accuracy of much better than a wavelength and is clearly dependent upon the requirements of the application and upon the radar system parameters. If, for example, the measurement accuracy of phase was determined to be one-tenth of a wavelength or 30°, for a radar operating at

Deviation from ideal track

Ideal track — · — · — · —

Actual track
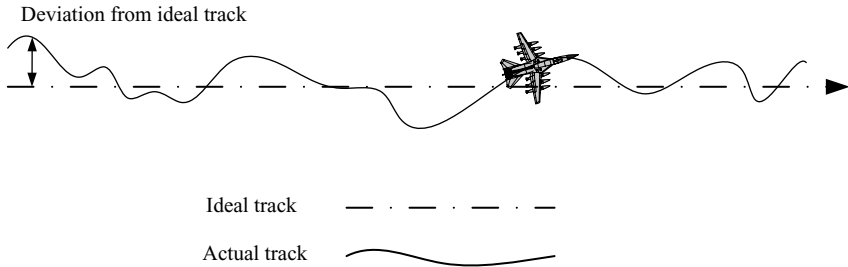
*Figure 4.10   Real motion of radar platform deviates from ideal straight horizontal
track and must be compensated for SAR*

a wavelength of 3 cm, then the corresponding motion compensation accuracy would
be 3 mm. This means that over the radar integration period the position of the radar
must be known within 3 mm of its true radar track. As aircraft cannot normally fly
with this accuracy, techniques must be used to compensate for the motion effects.
This concept of platform deviation from the ideal track is shown in Figure 4.10 [8].

The motion is a combination of effects occurring with different timescales. These
can vary from rapid high-frequency deviations to a slow long-term drift in the position
of the track. These effects contribute to various levels of distortion to the SAR image
and need to be compensated for [9]. Along the track the deviation from the ideal
motion can be compensated for using a number of techniques. By measuring the
deviation directly using various instruments on board the aircraft, the amount of
phase required to offset the motion effects can be determined on a pulse by pulse
basis and is fed directly into the SAR processor as an appropriate phase offset. For
very severe non-linear motion, whereby offsets from the ideal track are near to or
exceed the range resolution requirements of the radar, time or range compensation
may also be necessary to be applied to the data.

Sensors such as the platform inertial navigation system [10–13] can be used, which
measures position in three dimensions. The critical position is the phase centre of the
antenna, as that is the reference point within the radar for measuring the phases of
returning pulses. It is the variation of the distance between this position and points of
interest on the ground over the radar integration period, which must be established.
Another technique used is called SAR Auto-focus [14–17]. This method initially
assumes that the platform is moving along the ideal track and the raw radar data is
processed normally. In fact, if motion distortion is present, the SAR image obtained
is out of focus. The compensation technique then involves examining the data and re-
processing it iteratively until the radar map or target image is sharpened up and
focused. This would be performed automatically with no operator intervention. One
method used is to identify likely point scatterers in the radar returns and to use them
as a reference for the platform's motion. Effectively, it is assumed that the deviations
in the phase of the returns of point scatterers from the ideal is due to the motion of the
platform and is then directly taken to be the phase error. This would then be used to
compensate all the SAR image pixels. Data from the inertial navigation system (INS)

can be used in conjunction with auto-focus motion compensation techniques. The INS equipment is generally used to compensate for the low-frequency motion errors with time constants of the order of seconds. These can be considered to be the slow components of motion, which cause the platform to drift from its ideal track. The INS is not usually designed to accommodate high-frequency fluctuations in motion. Accelerometers have much higher frequency responses which are in the region of several kHz and can provide compensation data for rapid fluctuations in the motion of the platform from the ideal linear track. They can be used in conjunction with the INS instruments.

4.3.8   SAR signal processing operations

4.3.8.1   Transmitting and receiving signal

In this section the main signal processing operations required to obtain a SAR image are summarised. The signal processing operations for SAR [18,19] tend to be linear, which means that theoretically they can be performed in any order. The sequence of operations described below is typical and representative, but is not unique.

As the SAR platform is flying along, radar pulses are being transmitted at a regular rate and data is continuously being acquired, stored and processed. Figure 4.11 shows the collecting of radar data. If a prf of value f_{prf} is being employed, over the radar integration period, T, then $f_{prf} \times T$ or n pulses are transmitted to provide the information to generate the single cell of the SAR image indicated.

In the figure each position along the track at which a pulse is transmitted and received is shown. For each radar pulse transmitted, returns are received corresponding to the range extent of radar data required and also allowing for the expanded length of the radar pulse, assuming wideband pulse compression is being used. In this example, data appropriate to the single cell shown is presented for explanatory purposes.

The data for generating the high-resolution cell required is captured at the delay appropriate to the range of this target cell. The data is held as amplitude and phase information. Pulse compression would typically be used for providing high down-range resolution. For normal SAR processing, the range data utilised would correspond to many range gates plus the length of the expanded pulse, to enable a large number of high-resolution target cells to be processed.

4.3.8.2   Down-range pulse compression

Down-range pulse compression is exactly the same operation as presented in Chapter 3 for providing high-resolution range profiles and is shown in Figure 4.12.

Expanded pulses of received data are shown corresponding to each pulse transmitted and each position along the aircraft track. The pulses are compressed in a matched filter with an appropriate weighting function to minimise time sidelobes. The output of the operation is a complex sample of the received signal for each pulse transmitted. The data corresponding to one range gate is shown in the figure. For the processing of several range gates and more than one high-resolution range cell, a pro rata increase in
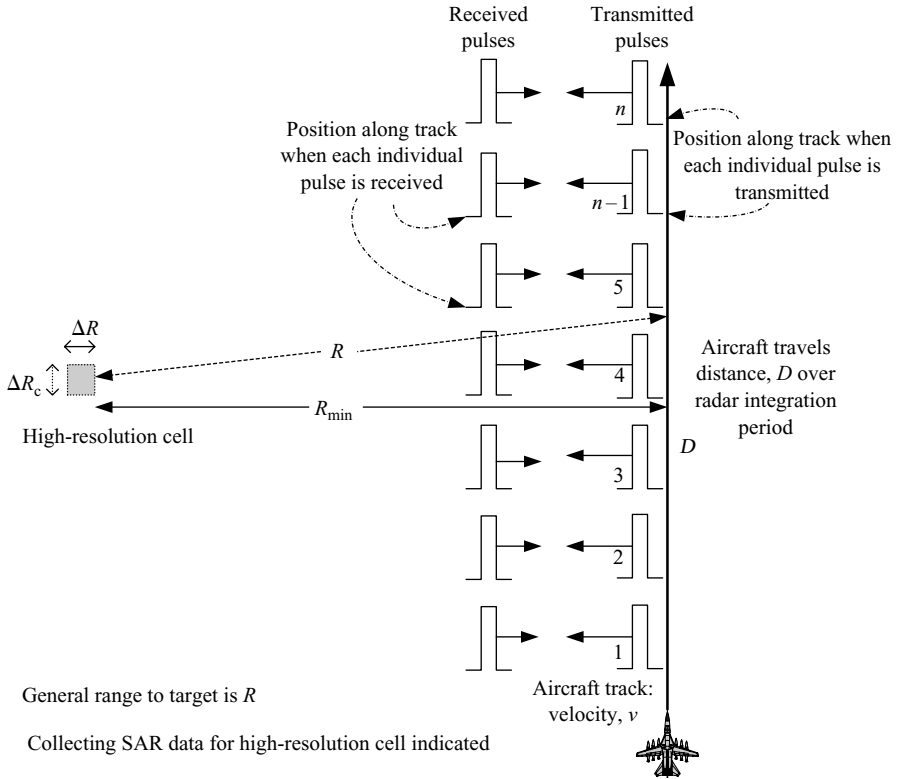
Figure 4.11   SAR data collected over radar integration period
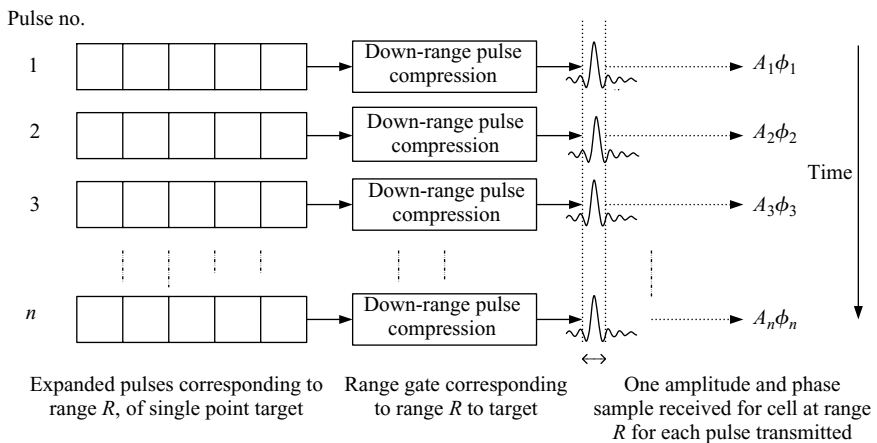
Figure 4.12   Down-range pulse compression

the number of samples of output data is obtained. Hence, for normal SAR processing a two-dimensional matrix of transmitted pulse number against range would be used.

4.3.8.3   Motion compensation

It is assumed that the aircraft is deviating from a straight-line track, so that corrections to the phases of the received signals are required as discussed in Section 4.3.8. In Figure 4.13 the inclusion of a phase correction factor for compensating for the non-linear radar platform is shown, as this is usually the most important aspect of motion compensation [20].

Using the measurements from the platform's sensors, the amount of deviation, Δl, of the distance from the straight-line track is calculated. From the geometry of the situation the difference between the actual range to the target, R_{Actual}, and the ideal

Range gate data for target cell shown below

Pulse no.	Output of down-range pulse compression	Path length correction for non-linear motion	Resulting motion-compensated data
1	$A_1\phi_1$	$\Delta\phi_1$	$A_1\phi_{1c}$
2	$A_2\phi_2$	$\Delta\phi_2$	$A_2\phi_{2c}$
3	$A_3\phi_3$	$\Delta\phi_3$	$A_3\phi_{3c}$
$\vdots$	$\vdots$	$\vdots$	$\vdots$
n	$A_n\phi_n$	$\Delta\phi_n$	$A_n\phi_{nc}$

Target cell

Range error due to motion is $R_{\text{Error}} = R_{\text{Actual}} - R_{\text{Ideal}}$

R_{Ideal}

R_{Actual} Two-way phase correction, $\Delta\phi = 4\pi R_{\text{Error}}/\lambda$

Δl

Phase correction $\Delta\phi$ is twice the difference in path length between actual range and ideal range for a straight line track

Figure 4.13   Motion compensating radar data by use of phase correction

range for the straight-line track, R_{Ideal}, is calculated as a range error, R_{Error}. Hence the equivalent two-way phase error, $\Delta\phi$, is then $4\pi R_{\text{Error}}/\lambda$.

This phase correction is an additive process, as the path length component of this deviation from the straight-line track in the direction of the target is directly manifested as a phase error. The phase correction components are simply added to the respective phase components of the output signals from the earlier pulse compression operation.

The motion compensation components actually vary for different high-resolution range cells in different locations, as the vectors joining the radar to the points on the ground will be in different directions. This means that the phase correction coefficients vary with location of the high-resolution cell and are particularly relevant to spotlight SAR, which is covered in Section 4.4.

Another factor affecting the motion compensation is a variable velocity along the platform track during the radar integration period. This means that the pulses are not transmitted at even intervals along the track. In order to compensate for this, interpolation of data between pulses can be performed to linearise the data in time. This would involve interpolating between the data points shown in Figure 4.13. Also for very large motion excursions, which are the same order as the size of a range cell, phase correction of the received pulses is not sufficient for compensation, as there is effectively range gate walk present. This means that received data from the same stationary target on the ground is effectively migrating from one time delay interval or range gate to its neighbour. This type of effect has to be compensated for by the use of time-shifting the received data, so that all signals from the same point on the ground are aligned in time.

Another effect which sometimes occurs even if the platform maintains a straight-level track at the same speed is range gate migration. This results from the geometry of the situation, such that the range is longer at the extremities of the aperture being synthesised than at the nearest point of approach to the target. This can be determined and corrected from knowledge of the parameters being employed for the measurements.

All these effects complicate the signal processing in real SAR systems, particularly for platforms with high non-linear motion characteristics. Motion compensation for SAR is generally considered to be a critical issue for generating high-integrity radar signatures.

4.3.8.4 Cross-range resolution processing

The signal data shown in the right-hand column of Figure 4.13 can now be processed to provide the high cross-resolution data for the cell of interest. Each data element still contains information from other cross-range cells, which are at the same down-range gate as the cell of interest. However, the other cells have different Doppler frequency against time characteristics, as was illustrated in Figure 4.8.

By using matched filter signal processing with an appropriate weighting function and multiplying the complex signal data by the complex conjugate of the required frequency against time characteristic of the cell of interest, cross-range cells with other frequency–time characteristics are filtered out and data from the required cell is obtained. The cross-range filtering is shown in Figure 4.14. This last operation is

Pulse no.	Radar data	Cross-range compression filter components		
1	$A_1\phi_{1c}$	$A_{1ref}\phi_{1ref}$		Synthetic aperture
2	$A_2\phi_{2c}$	$A_{2ref}\phi_{2ref}$		SAR processing provides high down-range cross-range cell
3	$A_3\phi_{3c}$	$A_{3ref}\phi_{3ref}$		
⋮	⋮	⋮		
n	$A_n\phi_{nc}$	$A_{nref}\phi_{nref}$		Cross-range pulse compression de-correlates other co-range cells

Radar data has previously been down-range compressed and motion compensated:
it is correlated in cross-range compression filter to provide output for cell required

Figure 4.14   Cross-range pulse compression

SAR compression, which synthesises the large aperture, which provides the very fine cross-range resolution.

4.3.8.5   SAR map

The sequence of operations discussed in this section has shown the signal processing functions that are required to generate a high down-range cross-range resolution cell from the received radar data. Exactly the same series of operations are required for each cell, which would comprise a high-range resolution radar map. The signal processing operations presented above then have to be performed for every high-resolution down-range gate, then for each high-resolution cross-range cell. These processing operations are required first to provide the down-range signal data and then motion compensate it. The data for each cross-range cell has then to be individually filtered with the appropriate Doppler frequency against time characteristics to provide a high-quality map.

If the map is to have the same range resolution throughout, as the cross-range resolution is proportional to target range (from 4.5), then it is necessary to generate a synthetic aperture, which is proportional to target range. This means that the number of pulses processed then varies linearly with range.

In practice, the operations can be streamlined to reduce the amount of data manipulation and mathematical operations involved. Some of the operations discussed do not have to be repeated for each new synthetic aperture that is generated, and some data obtained in synthesising the neighbouring cross-range resolution cell can be re-used.

4.3.9   SAR data

The data from the SAR is presented as a two-dimensional map and/or a two-dimensional target image. For target recognition applications, vehicles on the ground

<div align="center">Resolution = 1 m   Resolution = 1 foot   Resolution = 4 in</div>
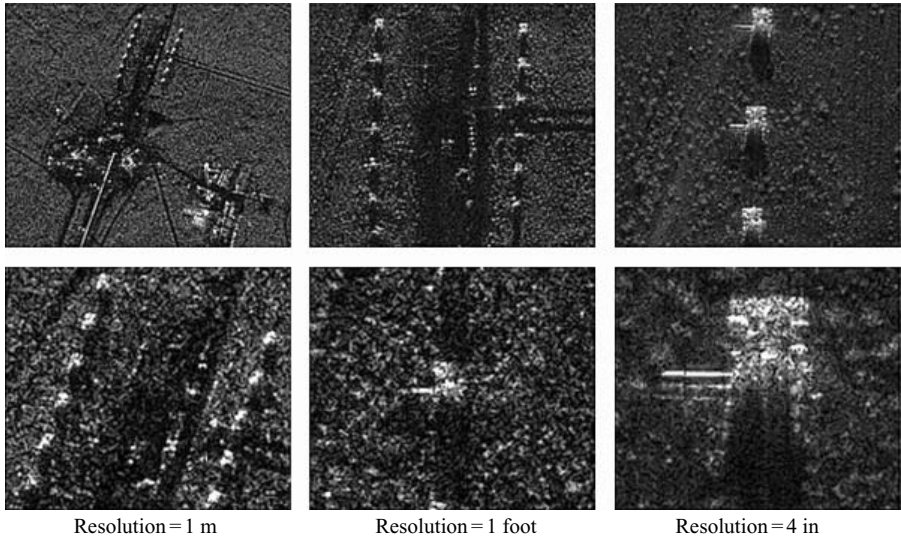
Figure 4.15   SAR images of tanks at various resolutions. The lower images are enlarged views of the upper SAR maps (Courtesy of Sandia National Laboratories, USA)

have first to be identified as vehicles and differentiated from objects on the ground, such as buildings, terrain or vegetation. In some circumstances vehicles of interest, such as tanks in military applications, could be close to or partially obscured by this clutter. An example of SAR images of tanks is shown in Figure 4.15. After identifying a potential target of interest as a vehicle, it is then necessary to identify whether it is a military vehicle, rather than perhaps a motor car or farm vehicle. It may also be necessary to identify it as a tank or armoured vehicle.

In order to perform these recognition functions, the output of the radar signal processing operations is now a picture, so image processing techniques are needed. The radar map data has to be manipulated in a computer and compared with reference data, and areas of the map with potential targets of interest are identified. These data points containing possible targets are clustered and features are extracted. In most cases the aspect angle of the target is not known, unlike in the case of range profiling discussed in Chapter 3, in which the track of the target could be used to provide an approximate aspect angle. Hence, any database or mathematical or feature model of the target has to be examined at all possible aspect angles for matching it to the measured SAR data. This is clearly made even more difficult in the presence of clutter in the target vicinity.

In some cases, very sophisticated applications techniques can be used to identify moving targets from SAR images, which makes the target recognition process easier [21–23]. The function is called ground moving target indication (GMTI). This enables moving targets to be localised, so that the process of finding the target is achieved and processing of the target's image for recognition purposes can then be performed.

If the received radar data is processed using conventional SAR operations, a moving target, which has a radial velocity component in relation to the ground, appears as a stationary target displaced in distance. Relative to a stationary target in the same position, the Doppler component adds an additional frequency component to the expected frequency–time characteristic. The SAR processing effectively range-Doppler couples the target. When SAR maps are viewed, which use conventional SAR processing, for example, cars travelling along a motorway are often seen to be displaced to a neighbouring field lined up in parallel to the motorway. However, with a GMTI mode, this effect is automatically corrected and the cars are positioned back into their correct positions on the motorway and would be displayed as moving targets.

There is now a wealth of image processing technology being developed for civil security applications, such as automatically recognising finger prints, signatures and eye characteristics. This can be used for the processing of SAR images and automatically recognising targets. This topic will be discussed in detail in Chapter 12.

4.4   Spotlight SAR

In the previous section, sideways looking SAR was presented, which is the most usual mode used for mapping purposes. However, in certain applications, such as in military operations, often it is a particular area that is of interest, rather than all the local terrain. It could be that military vehicles or a particular building are required to be engaged at a particular location and it is necessary to obtain a high-resolution radar image both to confirm the location and to identify the particular targets of interest there. A SAR mode has been specifically designed to address this type of mission and is called Spotlight SAR [24] and is shown in Figure 4.16.

As the aircraft progresses along its track, the radar beam is directed at the same area of interest on the ground. The name spotlight is quite appropriate as a small area of the ground is being continuously illuminated with a radar beam, which is analogous to an optical spotlight illuminating an area of interest. From the viewpoint of the aircraft the look angle of the antenna has to be changed continuously during the radar integration period. In this way a much longer synthetic aperture is obtained than in the case of the standard sideways looking SAR, so the cross-range resolution is improved. In addition, as the integration time is increased, more energy is received from the target, so better-quality target images are obtained. There is also the opportunity to obtain multiple looks at the target if the aspect angle is changing sufficiently over the period of the radar measurements allowing several images to be processed.

The principles of the signal processing operations employed are similar to sideways looking SAR. However, they tend to be more complex to implement to cover the flexibility required. The target range and start and stop look angle would normally be mission-dependent parameters, so the signal processing algorithms used would have to be programmable. Rather than in the case of normal SAR, which involves detecting chirp responses having a positive Doppler frequency going through zero
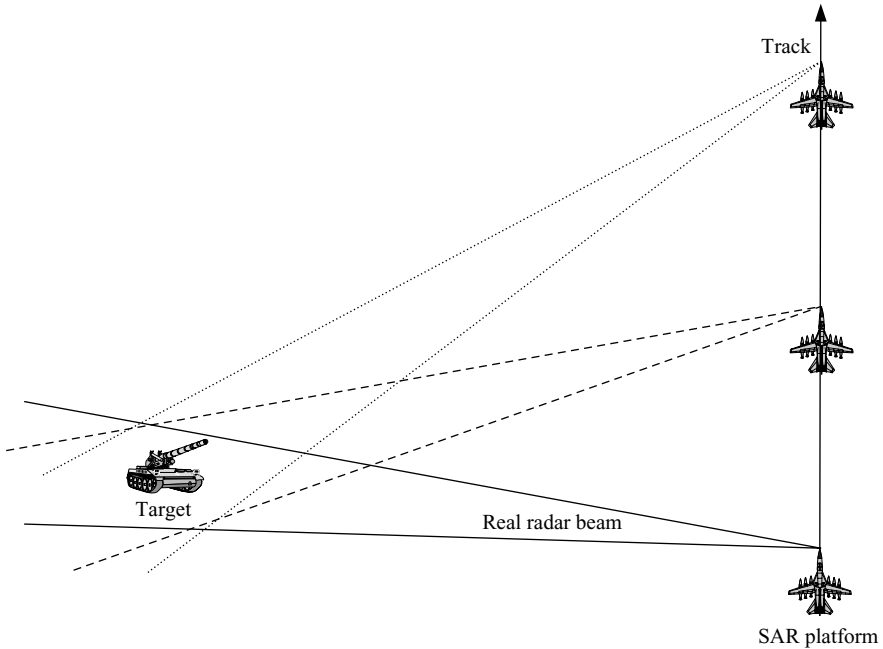
Figure 4.16   Spotlight SAR: as the aircraft flies along the look angle of the antenna is continuously changed to point at the same area on the ground

to the inverse Doppler frequency, any number of different frequency–time characteristics have to be allowed for. There is also the added complication of incorporating an antenna which has a large angular coverage and the associated control system to maintain both azimuth and elevation stabilisation over long integration periods. The pointing accuracy needed must be sufficient to maintain the target in the radar beam for the SAR integration period. However, one advantage is that spotlight modes normally process data for fewer range cells.

One application of Spotlight SAR is ground attack, whereby the aircraft on the mission would map the area of interest, prior to recognising the target and engaging it. For this type of mission the requirements on the radar's signal processing and recognition function are severe. It is necessary to rapidly provide a fully focused SAR image, localise and identify the target in near real time in the presence of surrounding clutter. This could also be under conditions of fire from the enemy.

4.5   Inverse SAR

4.5.1   Introduction

In this chapter so far, techniques for obtaining high cross-range resolution have been presented, which use the motion of the platform hosting the radar to synthesise a large

aperture as it travels along its track. Targets, which can be imaged using airborne and spaceborne platforms using SAR, are either stationary or are moving relatively slowly in a straight line. These targets do not have any significant rotational motion, so the differential Doppler frequencies used by the SAR platform are generated by virtue of the motion of the radar and not the target.

The SAR techniques presented are not suited to targets such as aircraft and ships, which tend to have their own rotational motion. The technique used to generate high cross-range resolution of a target due to the target's own rotational motion is called ISAR. The fundamental of the technique is to use the different Doppler frequencies from different parts of a rotating target to generate high cross-range resolution, in conjunction with using high down-range resolution to generate a two-dimensional radar image of the target. ISAR is completely dependent upon the target having a rotational motion component in relation to the radar. Unlike SAR, which has down-range and cross-range resolutions, which are totally dependent on the radar's parameters, platform motion and integration time, ISAR imaging is target motion dependent. The cross-range resolution obtained with ISAR images is determined by the target's motion.

4.5.2   ISAR cross-range resolution

In order to determine the cross-range resolution obtained with ISAR, consider Figure 4.17, in which an example is shown, in order to illustrate the concepts. Two points A and B are shown on an object rotating about a point, C. The radar is assumed

Scatterer, at position B, is at a cross-range distance, R_c, from the centre of rotation, C, and at a distance, d horizontally from, C.

The line AB is parallel to line of sight of radar

The instantaneous angle from the horizontal of the scatterer with respect to the centre of rotation is α and has velocity v

ϕ is the angle of rotation for the radar integration period

Cross-range resolution obtained is $\Delta R_c = \lambda/2\phi$

Figure 4.17   *ISAR uses target rotation to provide cross-range resolution*

to be stationary and is pointing towards the rotating object. The line AB is parallel to the line of sight of the radar.

The angular rotation of the scatterer at point B relative to the radar is of interest and can be used to determine the general expression for the cross-range resolution obtained using ISAR. The instantaneous velocity at point B is v and the instantaneous angular frequency is ω. As the target is rotating, these values are continuously varying. The angle between the lines joining the radar's line of sight and point B to the centre of rotation is α. The velocity vector is orthogonal to the line joining B to the centre of rotation, C. Point B is at a cross-range distance, R_c, from the centre of rotation, as the line AC is orthogonal to the line joining the target to the radar. The velocity, v, is given by the angular rotation rate, ω, multiplied by the distance from the centre of rotation, which is:

$$v = R_c\omega/\sin\alpha \tag{4.8}$$

The instantaneous velocity component of point B in the direction of the radar is $v\sin\alpha$ and the corresponding Doppler frequency component in the direction of the radar is:

$$f_d = 2v\sin\alpha/\lambda = 2R_c\omega/\lambda \tag{4.9a}$$

or

$$R_c = \lambda f_d/2\omega \tag{4.9b}$$

It can be seen that the Doppler frequency measured by the radar depends on the cross-range distance of the scatterer from the centre of rotation. Taking an example of constant angular frequency for illustrative purposes, then differentiating (4.9a) gives the relationship between an increment in Doppler frequency, Δf_d, and an increment in cross-range, ΔR_c:

$$\Delta f_d = 2\Delta R_c\omega/\lambda \tag{4.10}$$

Equation (4.10) means that the Doppler resolution is directly proportional to the cross-range resolution. If two scatterers are the distance ΔR_c apart in cross-range positions, they can be separated if the Doppler resolution Δf_d of the radar meets the requirements of (4.10).

The measurement period, T, corresponds to a frequency resolution of $1/T$, which also equates to the frequency resolution of the measurement, Δf_d. If the cross-range resolution is ΔR_c, then substituting these values into (4.10) gives:

$$1/T = 2\Delta R_c\omega/\lambda \tag{4.11a}$$

or

$$\Delta R_c = \lambda/2\omega T \tag{4.11b}$$

Hence, the cross-range resolution is proportional to the wavelength and inversely proportional to the angular frequency and the integration period. With reference to Figure 4.17, for small changes of angle over the radar integration period, the angular

rotation, ϕ, is given by the angular velocity, ω multiplied by the integration period, T. Equation (4.11) therefore becomes:

$$\Delta R_c = \lambda/2\phi \tag{4.12}$$

Equation (4.12) is general for ISAR and states that the cross-range resolution obtained is only dependent upon the rotational angle over the radar integration period and the wavelength of the radar signal. It actually applies equally well to motion with both variable and constant angular velocities. For each scatterer rotating about the centre of rotation, the associated range resolution obtained is independent of its position, so all scatterers associated with an angular rotation about a particular axis are measured with the same cross-range resolution.

Cross-range resolution improves with shorter wavelengths and over larger rotation angles. It is interesting that the cross-range resolution is independent of the range of the target, unlike SAR, in which the synthetic aperture has to be increased at long ranges to maintain range resolution.

4.5.3   Relationship between SAR and ISAR

Equation (4.12) is effectively the same physical phenomenon as the cross-range resolution obtained for SAR, which was discussed in Section 4.3.4. The equivalence between SAR and ISAR is illustrated in Figure 4.18.

In Figure 4.18(a), the radar is moving along a nominally straight track and views an aspect angle change of ϕ for stationary target on the ground. In Figure 4.18(b), the radar is stationary and the aircraft target, which is flying in a straight line, changes its relative aspect angle by ϕ during the radar integration period.

In SAR the change in aspect angle, ϕ, of the target over the radar integration period is D/R_{min}. For ISAR, using (4.12) for a change of aspect angle ϕ, the ISAR cross-range resolution is then $\lambda/2\phi$, which is $R_{min}\lambda/2D$. This is the cross-range resolution obtained using SAR, as in (4.5). The relative angular rotation of the target in SAR is brought about by the radar platform moving and is exactly equivalent to the target rotation as utilised in ISAR.

If two radars with exactly the same characteristics are used for the measurements and the radars and target are at the same altitude, for the same aspect angle change at the same range, the two images of the target obtained by ISAR and SAR, respectively, are theoretically exactly the same. In practice, different levels of distortion in the images occur due to noise and residual motion compensation errors, in one case due to radar motion and the other due to target motion.

4.5.4   Obtaining an ISAR image

4.5.4.1   Doppler frequency of rotating scatterers

It has been shown that ISAR is totally dependent upon the relative rotational motion of the target to the radar. The technique for obtaining an ISAR image of a ship is now shown. This simple example is used to demonstrate the concepts involved and it is

(a)

Aircraft track: velocity, v

Change of aspect angle during radar integration period for SAR measurement

ϕ

D

$\phi = D/R_{min}$

R_{min}

Target

Radar

(b)

ϕ

Change of aspect angle during radar integration period for ISAR measurement
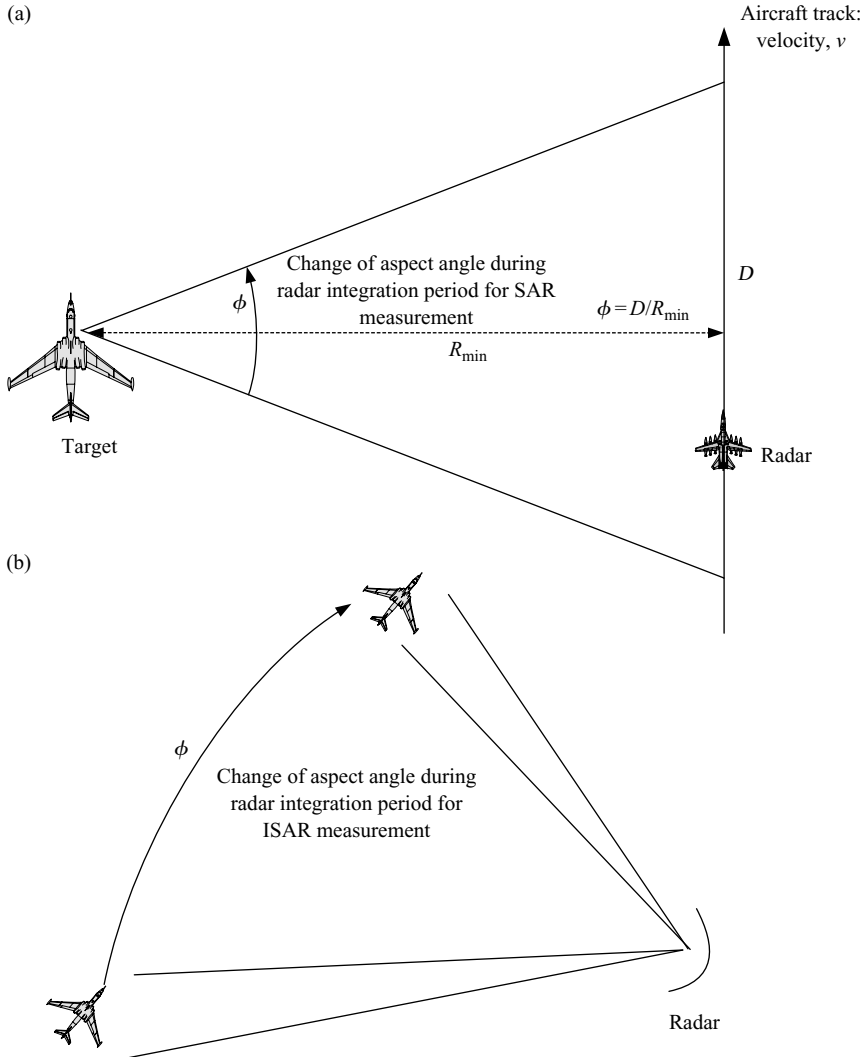
Radar

Figure 4.18   Equivalence of SAR and ISAR measurements: (a) SAR measurement: target stationary, radar moving; (b) ISAR measurement: relative target rotation, radar stationary

assumed that:

- The rotational motion of the target is such that the scatterers stay in each high-resolution down-range gate over the radar integration period.
- There is only a single component of rotational motion present.
- The axis of rotation is perpendicular to the radar's radial vector.
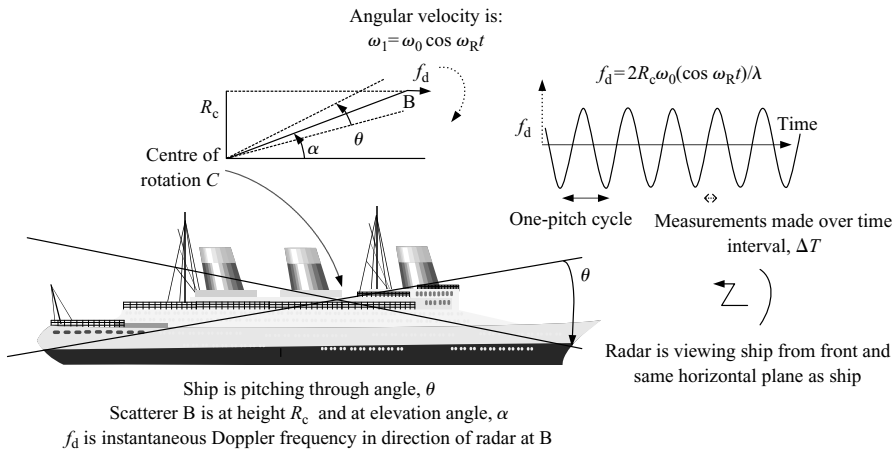
Figure 4.19   ISAR measurement for pitching ship

The more complex issues of motion compensation, ISAR scaling factor and scatterer migration are also discussed, but the detailed signal processing operations involved are not covered here and the interested reader is referred to the endnotes for further reading.

The ship in Figure 4.19 is pitching through an angle, θ, and is being viewed by the radar, which is in front of it and at the same height. The radar is initially considered to be stationary for the measurement.

The pitching of the ship means that scatterers on the ship lying within a vertical slice in the same high down-range resolution cell can be resolved in height in accordance with the cross-range resolution obtained using ISAR. In this case the cross-range resolution is in the vertical direction corresponding to the rotational motion of the ship. No resolution in the horizontal cross-range plane is possible in this example, as there is no appropriate rotational component available to provide the required information. If the rotational motion were yaw rather than pitch, the opposite would occur with high horizontal cross-range resolution obtained and no significant vertical resolution in each high down-range resolution slice.

The ship is rotating through an angle θ and a scatterer is at a height R_c above the centre of rotation. Assuming that the rotational motion is sinusoidal, then the instantaneous angular velocity ω_1 is varying sinusoidally with a peak value of ω_0 and at a frequency of ω_R as follows:

$$\omega_1 = \omega_0 \cos \omega_R t \tag{4.13}$$

For small angular excursions R_c can be considered to be constant over a rotational period. Using (4.9a), the Doppler frequency is then given by:

$$f_d = 2R_c\omega_1/\lambda = 2R_c\omega_0(\cos \omega_R t)/\lambda \tag{4.14}$$

Equation (4.14) states that the Doppler frequency of any rotating scatterer varies sinusoidally over the rotational period, which in this case is pitch motion. The Doppler frequency has a positive peak value when the ship is horizontal and is pitching towards the radar. Conversely, it has a negative peak frequency when pitching away from the radar. Zero values of f_d occur at the extremities of the pitch motion.

4.5.4.2   Radar measurements

Assume that the ISAR measurements are made over an interval ΔT. In each high-resolution down-range gate, amplitude and phase samples are taken from the target for every pulse transmitted, enabling a respective down-range profile to be generated. Over the radar integration period corresponding to the target's rotation through angle ϕ, which is less than θ, assume that N pulses are transmitted, so that N range profiles of the ship can be provided.

   Each scattering centre on the ship is constantly changing its aspect angle to the radar. The individual scatterers experience Doppler frequency against time characteristics, which are dependent of their locations with respect to the ship's centre of rotation, as stated in (4.14). For this pitching motion, the Doppler frequency is linearly dependent upon the distance of the scatterer to the centre of rotation.

   As the pitching motion is occurring sinusoidally rather than linearly, the aspect angle of the target to the radar is changing non-linearly. Hence, the synthetic aperture being synthesised varies in accordance with the part of the rotational cycle that is being used to perform ISAR. For the sinusoidal motion postulated in (4.13), the maximum change of aspect angle occurs when the ship is horizontal and is the best attitude for performing the measurements for obtaining the highest cross-range resolution.

4.5.4.3   Cross-range matched filters

In order to process this data to generate an ISAR image, it is necessary to provide filters with Doppler frequency against time characteristics, which match the respective target scatterer Doppler frequency against time histories for each of the positions on the ship. These should be good approximations to matched filters for the cross-range pulse compression process and follow the principles of the SAR processing previously discussed, but with different filters. Deviations in these filter characteristics from the actual scatterer Dopplers result in degraded cross-range resolution.

   In Figure 4.20 this process is shown. The range profiles of the ship are generated for each pulse transmitted and are aligned in time sequence. The amplitude and phase data from each range gate are now used to generate the scatterers' respective cross-range positions. There are several ways of generating a two-dimensional image for ISAR [25–30]. The key requirement is to determine the cross-range compression filter components, which best match the received radar data. The filter components would ideally be designed to be the complex conjugates of the received signals with a weighting function applied to reduce cross-range time sidelobes. The actual filter components are dependent upon the rotational motion of the ship, the position of

(a)

(b)

Time

Data from each high resolution
down-range gate is assembled
in time sequence

(c)

Time

Determine ISAR
cross-range
compression filters:
normally prominent
scatterers are
tracked across range
profiles to estimate
motion

(d)

ISAR cross-
range
compression
filters applied

Height of
cross-range cell:
scatterers with
largest Doppler
excursions are
furthest from
centre of rotation

Ship pitches

Radar

(e)

*Figure 4.20   Operations to generate an ISAR image: (a) radar data initially col-
lected in each high-resolution down-range gate; (b) a time series of
range profiles is obtained as ship pitches: (c) motion determined from
analysing data: (d) for each high down-range resolution gate, data is
applied to ISAR cross-range compression filters: (e) representation of
typical ISAR image of a ship*

the scatterers and the integration period of the radar. Although scatterers at different locations require different filters, they are all based on the same target motion characteristics and are related. With reference to Figure 4.19 and Equation (4.14), the Doppler frequency characteristics of a scatterer vary sinusoidally with time. Ideally, compression filters with these characteristics, for the part of the pitch cycle being used, would then be employed for the cross-range compression filter coefficients. The process for generating the two-dimensional image is now described functionally, which is dominated by the determination of the cross-range compression filters. In practice, there are several implementation techniques and they often utilise analysis of the actual range profile data and the tracking of prominent scatterers on a pulse-to-pulse basis. The phase history or Doppler against time characteristics of various scatterers can then be determined, which effectively provides measures of the rotational motion, allowing the cross-range compression filter characteristics to be synthesised. The determination of the cross-range compression coefficients is equivalent to utilising the radar data to characterise the target's rotational motion during the radar integration period.

The compression filter elements would be effectively sets of amplitude and phase data, for various scatterer positions, with each containing the number of data points appropriate to the number of pulses being received during a radar integration period. Figure 4.20 shows the cross-range compression function. After applying this filtering to each down-range resolution gate, the relative height of each scatterer above the centre of rotation is determined by its change in Doppler frequency over the radar integration period. Figure 4.20(e) shows a representation of an ISAR image of a ship. Each high down-range resolution gate is divided into high cross-range resolution cells arranged in order of height.

The two-dimensional image obtained would then be used as a basis for recognising the ship. Various operations are required to be applied to the image to condition it in order to enable automatic target recognition techniques to be used. These are discussed in Chapter 12. An ISAR image of a ship is shown in Figure 4.21.

(a)

(b)
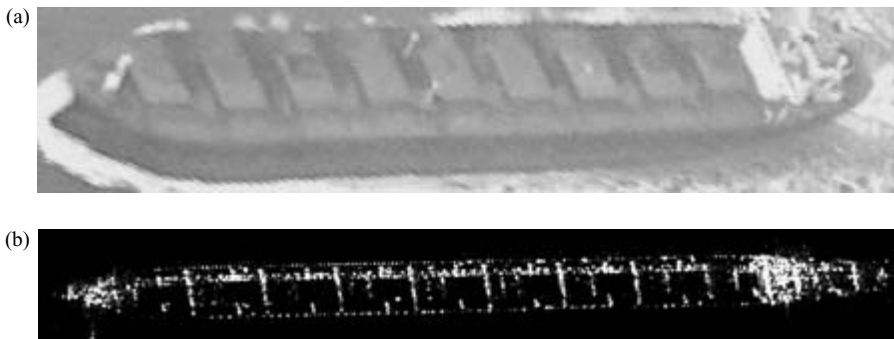
Figure 4.21   An ISAR image of a ship (Courtesy of QinetiQ) (a) photograph of bulk carier ship (b) ISAR image of bulk carrier in (a)

4.5.4.4   ISAR scaling factor

A major issue in ISAR is to determine the cross-range resolution scaling, in order to obtain an image with the same known linear dimensions in down- and cross-range. For the simple model used for ISAR in (4.9), corresponding to a measurement made over part of a rotational period, the Doppler frequency obtained is proportional to the angular velocity of the scatterer and its distance from the centre of rotation. These two factors are multiplied together in the equation and are not normally able to be decoupled for a single isolated measurement. For a single ISAR measurement, if the Doppler frequency against time characteristic is determined by matched filtering, as discussed in the previous section, and measurements are only made over part of a rotational cycle, then the absolute distance from the centre of rotation is not known. It could be due to a scatterer that is close to the centre of rotation and the ship has a high rotational rate or it could be located far from the centre of rotation with a low rotation rate.

However, if measurements are made over several rotational periods and the motion of the ship is regular, it is possible to determine the angle of rotation and the height of the scatterers. For regular rotational motion, the Doppler frequency and its rate of change with time both vary sinusoidally, but with a relative phase difference of 90°. It is necessary to measure the period of the rotational motion and the Doppler frequency and its derivative over at least one rotational cycle. The angle of rotation of a scatterer is then determined using the maximum value of the Doppler frequency, the maximum value of the rate of change of Doppler frequency and the rotational period [31].

For ISAR measurements of aircraft targets, which utilise yaw, pitch or roll motions, or ground targets, the motion is normally irregular and scaling issues are critical. This is a fundamental problem in ISAR, for a radar system observing a rotating target with complex motion. Unless *a priori* information is available or there is some other means of obtaining this data, the cross-range scaling is often unknown.

4.5.4.5   Other motion compensation issues

It is generally considered that ISAR processing is more difficult than SAR, as targets exhibit rotational motion in up to three axes and also can have translational motion in three dimensions. In addition, the radar platform can also be in motion. In ISAR applications, which rely on the target's rotational motions, the signal processing also has to take into account the motion of the radar platform. If the ISAR radar is on-board a moving aircraft platform and it is changing aspect angle by virtue of its own motion, as well as trying to measure target rotation for ISAR, both SAR and ISAR are present simultaneously. The techniques described in Section 4.3 on SAR then have to be integrated with the ISAR signal processing techniques discussed in Section 4.5. The signal processing then has to include both SAR and ISAR functions [32–34], which is extremely complex. As ships and aircraft have contributions of roll, pitch and yaw motions, the net rotational vector can be very complex.

The technique, which is often used in ISAR motion compensation, as described in Section 4.5.3.3, is to correlate successful range profiles from the returns from one pulse to the next to ensure that the down-range gate data is correctly aligned
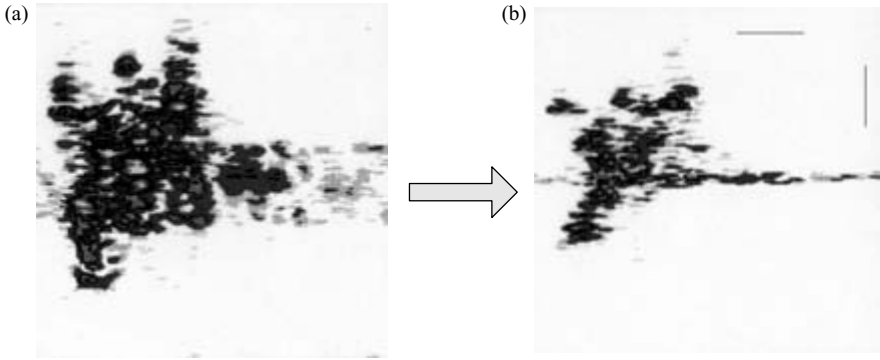
Figure 4.22   Focusing aircraft ISAR image (Courtesy of QinetiQ) (a) partially focused, (b) fully focused

before embarking on the full ISAR process. The auto-correlation peak would then provide the best match and the best alignment of the data. Range gate walk effects, whereby the returns from scatterers appear in incorrect range gates, usually occur when either the platform or the target or both is an aircraft. Over the radar integration period any errors in velocity estimates are manifested as range-gate misalignment.

Another problem that has to be overcome is range gate migration, which would normally occur when very high-range resolutions are being used. Over the radar integration period a scatterer moves out of one high-resolution range gate into neighbouring gates. If this effect is uncorrected the high-resolution cross-range data is distributed and range resolution is lost. Techniques, which track scatterers through range gates, are then required [35].

The ISAR images of an aircraft target before and after full motion compensation are shown in Figure 4.22.

4.6   Summary of cross-range resolution techniques

The cross-range resolution techniques discussed in this chapter are summarised in Table 4.1 with associated judgements on the achievable resolution and the relative implementation complexity.

As would be expected, improvements in range resolution performance place ever-increasing requirements on both the algorithms, on the radar hardware and on the motion compensation hardware. The algorithms encompass all the signal processing operations required to generate a high-resolution two-dimensional target image plus the image processing techniques required for recognising the target. The most complex applications occur when there is motion from both the target and the radar platform. For the air-to-air situation both linear and rotational motions can be present from both platforms, so there are four contributors to the net motion between the two platforms, which is a considerable challenge. Interestingly, for space applications

Table 4.1 Summary of cross-range resolution techniques

Technique	Targets/function	Platform	Resolution achievable	Implementation
Real beam map	Ground mapping	Aircraft	Relatively coarse	Straightforward
Doppler beam sharpening	Ground mapping	Aircraft	Reasonable	Straightforward

SAR	High precision ground mapping
	Recognition of:
	  Landmarks
	  Installations
	  Buildings
	Ground vehicles: stationary
	  and moving
		Aircraft (Space)	Very high	Complex:
				  Algorithms
				High down-range resolution waveforms
				Motion compensation hardware

ISAR	Recognition of:
	  Ships
	  Aircraft
	  Land vehicles
		Land ships (Space)	Very high	Complex:
				  Algorithms
				High down-range resolution waveforms

SAR/ISAR	Recognition of:
	  Ships
	  Aircraft
		Aircraft	Very high	Very complex algorithms
				Motion compensation hardware
				High down-range resolution waveforms

own platform motion compensation tends to be easier than for aircraft applications. The spacecraft orbit is well known and stable and there is no turbulence within the atmosphere, with which to contend, as is experienced by aircraft platforms. Although the orbit is curved and has to be compensated for and the earth's curvature and rotation also have to be taken into account, these effects are predictable [36].

References

1   LACOMME, P., HARDANGE, J.P., MARCHAIS, J.C., and NORMANT, E.: 'Air and Spaceborne Radar Systems' (Institution of Electrical Engineers, London, 2001) Chapter 15.4.1

2   GOJ, W.: 'Synthetic Aperture Radar and Electronic Warfare' (Artech House, Boston, MA, 1993)

3   KOVALY, J.: 'Synthetic Aperture Radar' (Artech House, Boston, MA, 1976)

4   SKOLNIK, M.: 'An Introduction to Radar Systems' (McGraw-Hill, 1970) pp. 519–20

5   MOREIRA, J.R.: 'A New Method of Aircraft Motion Error Extraction from Radar Raw Data for Real Time SAR Motion Compensation', *IEEE Transactions on Geoscience and Remote Sensing*, 1993, **28** (4), pp. 907–13

6   CROSS, M.G.: 'Millimetre S.A.R. Motion Compensation'. IEE Colloquium on *Synthetic Aperture Radar*, London, UK, 29 November 1989, pp. 6-1–6-4

7   FORNARO, G., SANSOSTI, E., FRANCESCHETTI, G., and PERNA, S.: 'Phase Accuracy of Motion Compensated Airborne SAR Images'. IEEE International Proceedings of *Geoscience and Remote Sensing Symposium, 2003. IGARSS'03*, vol. 6, 21–25 July 2003, pp. 4068–70

8   YONGMEI, G., WEN, H., and SHIYI, M.: 'The Geometric Distortion Correction in SAR Motion Compensation'. CIE International Proceedings on *Radar*, Beijing, China, 15–18 October 2001, pp. 943–6

9   DI FILLIPPO, D.J., and HASLAM, G.E.: 'Evaluation of a Kalman Filter for SAR Motion Compensation'. IEEE Symposium on *Position, Location and Navigation*, Orlando, FL, 1988, pp. 259–68

10   KENNEDY, T.A.: 'A Technique for Specifying Navigation System Performance Requirements in SAR Motion Compensation Applications'. IEEE Symposium on *Position, Location and Navigation*. Record 'The 1990's – A Decade of Excellence in the Navigation Sciences'. IEEE PLANS'90, Las Vegas, NV, March 1990, pp. 118–26

11   FUXIANG, C., and ZHENG, B.: 'Analysis and Simulation of GPS/SINU Integrated System for Airborne SAR Motion Compensation'. Proceedings of 2001 CIE International Conference on *Radar*, Beijing, China, 15–18 October 2001, pp. 1173–7

12   MAJURE, R.G.: 'Demonstration of a Ring Laser Gyro System for Pointing and Stabilisation Applications'. IEEE Symposium on *Position, Location and Navigation*. Record 'The 1990's – A Decade of Excellence in the Navigation Sciences', Las Vegas, NV, 20–23 March 1990, pp. 219–25

13   TITTERTON, D.H., and WESTON, J.L.: 'Strapdown Inertial Navigation Technology' (Institution of Electrical Engineers, London, 2005)

14   MOREIRA, A., MITTERMAYER, J., and SCHEIBER, R.: 'A SAR AutoFocus Technique Based on Azimuth Scaling'. IEEE Symposium on *Geoscience and Remote Sensing*, IGARSS '97, vol. 4, 3–8 August 1997, pp. 2028–30

15   BAMLER, R.: 'A Systematic Comparison of SAR Processing Algorithms'. International Symposium on *Geoscience and Remote Sensing*, IGARSS '91, Espoo, Finland, vol. 2, 3–6 June 1991, pp. 1005–9

16   WANG, J., and LIU, X.: 'SAR Autofocus using Entropy Minimisation'. *Radar* 2004, Toulouse, France, Paper no. 155

17   BLACKNELL, D., and QUEGAN, S.: 'Motion Compensation of Airborne Synthetic Aperture Radars using Autofocus', *GEC Journal of Research*, 1990, **7** (3)

18   OTTEN, M.P.G., GROOT, J.S., and WOUTERS, H.C.: 'Development of a Generic SAR Processor in the Netherlands'. International Symposium on *Geoscience and Remote Sensing*, vol. 2, IGARSS '94, 8–12 August 1994, pp. 903–5

19   GUO, W., and WANG, Y.: 'SAR Motion Compensation Based on Signal Processing Method'. Proceedings of the 2003 IEEE International Conference on *Robotics, Intelligent Systems and Signal Processing*, Changsha, China, October 2003

20   HEPBURN, J.S.A., and DOYLE, C.P.: 'Motion Compensation for Astor Long Range SAR'. IEEE Symposium on *Position, Location and Navigation*, IEEE PLANS '90, 20–23 March 1990, pp. 205–11

21   AXELSSON, S.R.J.: 'SAR/MTI Radar Mapping for Ships and Ground Based Vehicles'. International symposium on *Geoscience and Remote Sensing Symposium*, IGARSS '02, vol. 5, 24–28 June 2002, pp. 2738–41

22   AXELSSON, S.R.J., and NELANDER, J.: 'SAR/MTI from Helicopters'. IEEE International *Geoscience and Remote Sensing Symposium*, Toulouse, France, July 2003

23   MOATE, C.P., and LAWSON, A.J.: 'Formation of Focussed ISAR Imagery of Moving Ground Targets'. *Radar* 2004, Toulouse, France, Paper no. 7A-SAR-3

24   CARRARA, W.G., GOODMAN, R.S., and MAJEWSKI, R.M.: 'Spotlight Synthetic Aperture Radar Signal Processing Algorithms' (Artech House, Boston, MA, 1995)

25   NUTHALAPATI, R.M.: 'High Resolution Reconstruction of ISAR Images', *IEEE Transactions on Aerospace and Electronic Systems*, 1992, **28** (2), pp. 262–72

26   GOMBERT, G.: 'High Resolution 2-D Image Collection and Processing'. Proceedings of the IEEE *Aerospace and Electronics Conference*, NAECON 1994, vol. 1, 23–27 May 1994, pp. 371–7

27   FLORES, B.C., TARIQ, S., and SON, J.S.: 'Image-Focus Quality Indicators for Efficient Inverse Synthetic Aperture Radar Phase Correction'. SPIE Proceedings on *International Society for Optical Engineering*, vol. 2757, Paper no. 2757–01, pp. 2–13

28 THOMAS, G., CABRERA, S.G., and FLORES, B.J.: 'Selective Motion Compensation in ISAR Imagery using Time–Frequency Filtering'. SPIE Proceedings on *International Society for Optical Engineering*, vol. 2757, pp. 14–24

29 THAYAPPARAN, T., LAMPROPOULOS, G., WONG, S.K., and RISEBOROUGH, E.: 'Application of Joint Time–Frequency Algorithm for Focusing Distorted ISAR Images from Simulated and Measured Radar Data', *IEE Proceedings, Radar, Sonar and Navigation*, 2003, **150** (4)

30 TRINTINALIA, L.C., and LING, H.: 'Joint Time–Frequency ISAR using Adaptive Processing', *IEEE Transactions on Antennas and Propagation*, 1997, **45** (2), pp. 221–7

31 LACOMME, P., HARDANGE, J.P., MARCHAIS, J.C., and NORMAND, E.: 'Air and Spaceborne Radar Systems' (Institution of Electrical Engineers, London) Chapter 17.3

32 PORTER, N.J., and TOUGH, R.J.A.: 'Processing Schemes for Hybrid SAR/ISAR Imagery of Ships'. IEE Colloquium on *Radar and Microwave Imaging*, 16 November 1994, pp. 5/1–5/5

33 HE, C., and MOURA, J.M.F.: 'Detection in Unfocussed SAR/ISAR Images: A Geometric Approach'. IEEE National Conference on *Radar*, 13–15 May 1997, pp. 295–99

34 GIRET, R., MERIC, S., and CHASSAY, G.: 'Radar Images of Vehicles Based on SAR/ISAR Processing'. IEEE International Symposium on *Antennas and Propagation Society*, vol. 4 , 8–13 July 2001, pp. 277–80

35 XING, M., WU, R., LAN, J., and BAO, Z.: 'Migration Through Resolution Cell Compensation in ISAR Imaging', *IEEE Geoscience and Remote Sensing Letters*, 2004, **1** (2), pp. 141–4

36 BARBER, B.C.: 'Multi-Channel ATI-SAR with Application to the Adaptive Doppler Filtering of Ocean Swell Waves', *IEE Proceedings, Radar, Sonar and Navigation*, 2003, **150** (6), pp. 403–10

Chapter 5

Frequency and time domain analysis

5.1 Introduction

So far the high-resolution radar techniques used for target recognition described in the book have been associated with spatial attributes of the target. The high-resolution range profiling, the SAR and ISAR techniques all provide high-range resolution signatures of the target from reflections of the radar signal associated with scattering occurring from a particular area of the target. These methods have been based on the physical size and shape of the target remaining constant during the radar integration period, with SAR and ISAR being reliant on changes in aspect angle for a rigid target. The signal processing methods used to generate the SAR and ISAR images have assumed that the scatterer retains its relative position on the target over the period of the radar measurement. No moving parts of the target have been addressed and it has been assumed that range profiles and two-dimensional synthesised images have been derived from a target both with a stable geometry and stable scattering characteristics. Within this chapter a totally different approach is taken. The physically stable parts of the target are not used and it is the moving parts of the target that are utilised in the target recognition process. The moving parts of most interest are associated with the propulsion systems of the targets, particularly for aircraft. Any mechanical parts of the aircraft which are moving or rotating relative to the main body of the aircraft, and are illuminated by the radar signal, are potential candidates for providing attributes for target recognition purposes. Any moving or rotating parts of the aircraft, such as propellers, jet engine blades, rotors or rotor blades, interact with the radar signal to provide a constantly varying reflection with time. Most military and civil fixed-wing aircraft and helicopters have features associated with their propulsion systems, which are candidates for providing attributes for non-cooperative target recognition. 'Jet Engine Modulation', which is known as JEM, is a technique used to determine the characteristics of the engine from the radar returns. Helicopters can be recognised from returns from the rotor blades and from the rotor hub.

The radar and signal processing techniques required to extract the features associated with the propulsion systems tend to use low-range resolution waveforms and utilise time and frequency domain analysis methods. Fairly simple models are presented, which are representative of the techniques used for modelling the effects and performing the target recognition functions. References are provided for readers wishing to study papers following more complex approaches.

In relation to the high-range resolution techniques, different constraints apply in designing the waveforms and the radar integration period is dependent upon the characteristics of the propulsion systems and associated equipment. It is necessary that sufficient data are collected to extract the required features with the appropriate time or frequency resolution. The pulse repetition period has also to be carefully selected in order to sample the data at a fast-enough rate to capture specific transient events. The waveforms also have to be consistent with range and Doppler ambiguities and blind zones, which were discussed in Chapter 2.

In Section 5.2 the recognition of helicopters is discussed. The key radar returns of interest are those from the main and tail rotors and from the hub of the main rotor. In Section 5.3, the theory of JEM is presented and the measurements of the signatures of jet engines are discussed. The features, which are extracted from the data, and the recognition process, are presented. The subject of databases of targets is also covered. In the United Kingdom, much of the pioneering work on JEM research was led by Dr William Bardo at the Ministry of Defence Royal Signals and Radar Establishment at Malvern. This work was performed in the 1970s and was not published in the open technical literature as it was classified at that time.

5.2   Helicopter recognition

5.2.1   Introduction

In order to appreciate how radar measurements can be used for helicopter recognition, it is first necessary to summarise the basic theory of how helicopters fly. A conventional fixed-wing aircraft stays in the air by obtaining lift, by virtue of its wings. The air moving over its wings causes a difference in pressure between the upper and lower surfaces of the wings, which provides an upward force, which counteracts the weight of the aircraft under level flight conditions, so maintains its altitude.

However, in contrast to a fixed-wing aircraft, a helicopter is stated as having rotary wings.

The lift in a helicopter is provided by the main rotor blades [1], which rotate about a hub, as shown in Figure 5.1. The air flowing over the rotor blades causes differential pressure between the upper and lower surfaces of the blade and gives the helicopter lift. The blades are specially shaped in order to have these particular aerodynamic characteristics and to provide exactly the same function as is obtained in aircraft using fixed wings. The lift, which is obtained, compensates for the weight of the helicopter, enabling it to stay in the air. The rotation rate of main rotor blades is typically several hundred revolutions per minute. The main rotor blades are designed to have a maximum tip speed, which is less than the speed of sound, which is about 330 m/s.
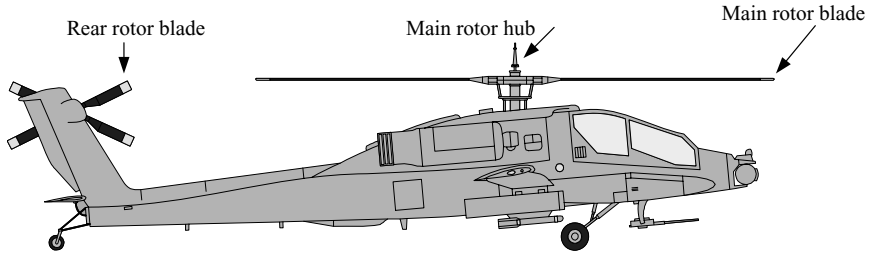
Figure 5.1   Helicopter with main and tail rotor blades

However, the main rotor is not sufficient for stable flight, as a single rotor generates a turning moment on the helicopter fuselage, which tries to rotate it in the direction opposite to the blades. This torque is overcome by the provision of a rear rotor. This is much smaller than the main rotor and generates a compensating turning moment for stabilising the helicopter to prevent rotation of the fuselage. The rear rotor is normally connected to the main rotor by a series of driveshafts and gear boxes and typically rotates at a rate of five times that of the main rotor. The rotors are normally driven by a jet engine, which is the main power source of the helicopter. The main and tail rotors can have different numbers of blades.

These moving parts of the helicopter provide the opportunity for helicopter recognition for the radar designer, which is discussed in the following sections.

5.2.2   Main rotor blades

5.2.2.1   Blade flash parameters

The main rotor blades of the helicopter rotate at several hundred revolutions per minute, which equates to a frequency of rotation of a single blade of typically a few hertz. The rotor blades are long and thin and can be represented in a very simple model as a long narrow plate to demonstrate its interaction with the radar signal. In Figure 5.2, a rotor blade is represented by a rectangular plate of length, L, and height, H. Although far more complex mathematical models of blades are available [2,3], the rudimentary model utilised here is sufficiently representative to illustrate the basic theory of helicopter blade detection.

Although real rotor blades have far more complex shapes, the long thin rectangular plate is a sufficiently good model to demonstrate the physical effects occurring and the effects on the detected radar signal. As was presented in Chapter 2, Table 2.3, a flat plate of length, L, and height, H, has a radar cross-section (rcs), σ_{LH}, which is:

$$\sigma_{LH} = \frac{4\pi L^2 H^2}{\lambda^2} \left[\frac{\sin((2\pi/\lambda)L\sin\theta)}{((2\pi/\lambda)L\sin\theta)} \right]^2 \cos^2\theta \tag{5.1}$$

where θ is the incident angle.

The modelled rcs of the rotor blade with angle of incidence or look angle, θ, is shown in Figure 5.3. It is assumed that the radar is in the same plane as the vector,
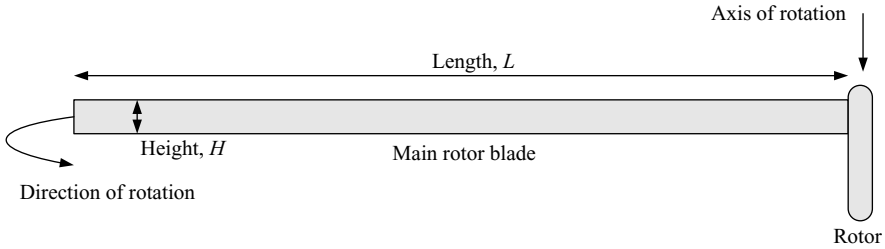
Figure 5.2   Representation of main rotor blade

Width of peak is approximately λ/L

rcs of rotor blade can be approximated as:

$$\frac{4\pi L^2 H^2}{\lambda^2}\left[\frac{\sin((2\pi/\lambda)L\sin\theta)}{(2\pi/\lambda)L\sin\theta}\right]\cos^2\theta$$
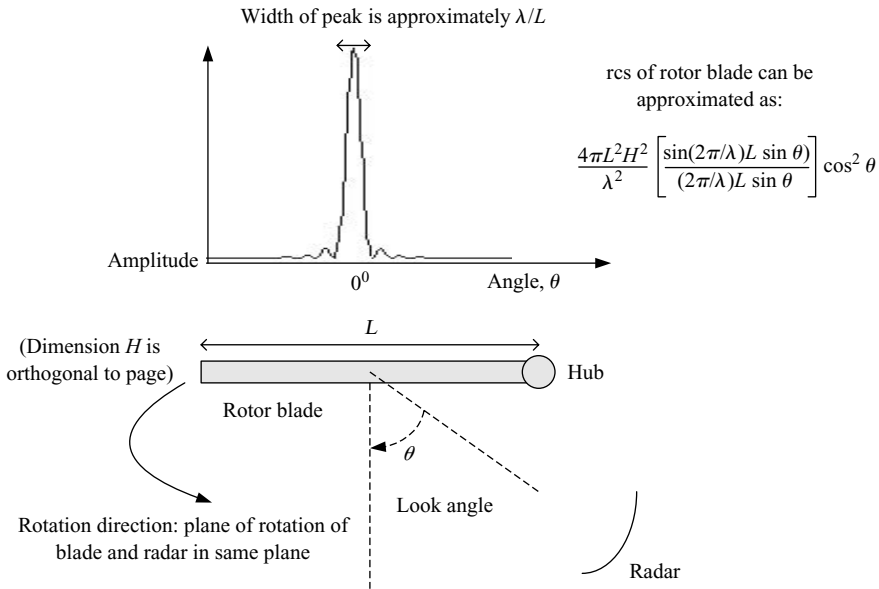
Figure 5.3   Modelling rcs of rotor blade: a peak signal is obtained when blade is at look angle of radar of $0°$

which is orthogonal to the plate, which is joined to the centre of the plate. For simplicity it is assumed that the plane swept through by the blade as it rotates and the radar are in the same horizontal plane. As the plate is narrow, there is far less angular dependence of rcs with vertical angle, so it is assumed to be constant as the blade rotates and no vertical angle rcs dependence is shown. In the horizontal plane the rcs follows a $(\sin x/x)^2$ function multiplied by $\cos^2$ factor. The former is effectively the diffraction pattern associated with an aperture, as discussed in Section 2.1.10. The latter term is due to the projection of this aperture in the direction given by θ. This means that the rcs is high for low values of angle, θ, and rapidly reduces for larger angles.

From the radar observation view point it can be seen that a peak in rcs is obtained when the radar is orthogonal to the blade and reduces either side of this peak by the $\sin x/x$ function shown. This means that generally sharp peak signals are detected when the blade is orthogonal to the radar, with relatively low-level signals measured at all the other angles. The ability to detect this signal, which is popularly known by radar engineers as 'blade flash', is therefore dependent upon the sharpness of the peak and the pulse parameters of the radar. It is necessary for the radar to be transmitting a pulse when the blade is near this orthogonal position. The angular width of this blade flash is approximately λ/L, which is analogous to the beamwidth obtained from an aperture of the same length, from antenna theory. For a typical helicopter rotor blade the length is several metres, so it can be seen that the angular width over which the blade flash is near its peak is proportional to the wavelength.

However, it can be seen from Equation (5.1) that there is also a $1/\lambda^2$ term, which means that the actual peak of the blade flash is inversely proportional to the wavelength squared, so that the value of the peak blade flash signal reduces as the wavelength of the radar signal increases. Hence, in order to detect blade flash there is a trade-off between the value of the peak signal obtained and the angular width of the peak, which are both dependent upon the wavelength used.

5.2.2.2 Detection of blade flash

The detection of the signal is also dependent upon the number of rotor blades on the helicopter. In Figure 5.4 a four-bladed helicopter is shown. Blade flashes occur when any blade is orthogonal to the radar's radial vector. For the four-bladed helicopter, flashes occur almost simultaneously from the rotor blade number 1, which is shown approaching the radar at position 'A' and the blade number 3, which is receding from the radar in position 'B'. Two opposite blades on the rotor do not quite remain rigidly opposite each other throughout the rotational cycle, due to aerodynamic drag effects. Slightly different forces are exerted on the blade, which is travelling in the direction of the helicopter's forward motion in comparison to the opposite blade, which is travelling in the opposite direction to the flight vector. However, these effects are slight and can usually be neglected. The result is that for a whole cycle of a single rotor blade, four flashes would be detected by the radar, as illustrated in Figure 5.5. Assume that the rotor blades are rotating at a frequency of R_0 cycles per second or R_0 Hz. Then the frequency of blade flashes occurring for an even-bladed helicopter is given by:

$$B_{\text{f}} = NR_0 \tag{5.2}$$

where B_{f} is the blade flash frequency, in Hz and N is the number of rotor blades.

As each rotor is expected to be almost identical both mechanically and as a radar target, the radar returns received would normally be expected to be almost identical for each blade passing a similarly timed radar pulse.

The time between blade flashes is therefore the inverse of this frequency, which is $1/B_{\text{f}}$. The duration of each blade flash is given by the angular width of the flash, which is λ/L, multiplied by the rotation rate, measured in radians per second, $2\pi R_0$,
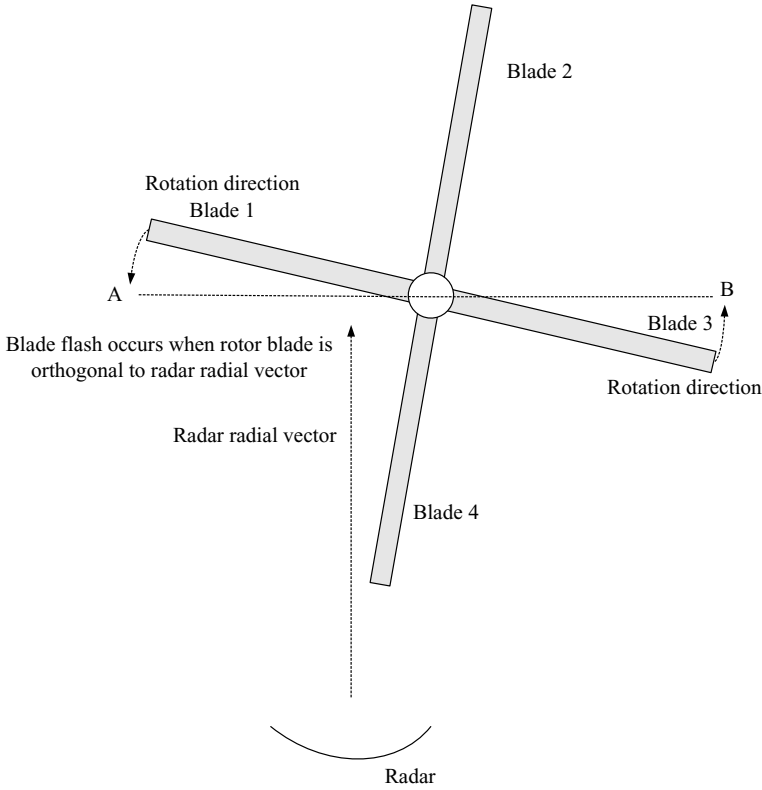
Figure 5.4   For helicopter with even number of blades, the flashes at 'A' and 'B' for approaching and receding blades occur almost simultaneously
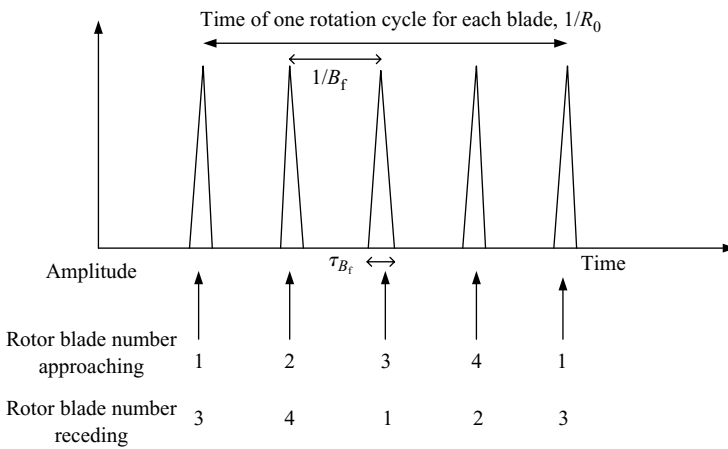
Figure 5.5   Blade flashes for helicopter with four blades
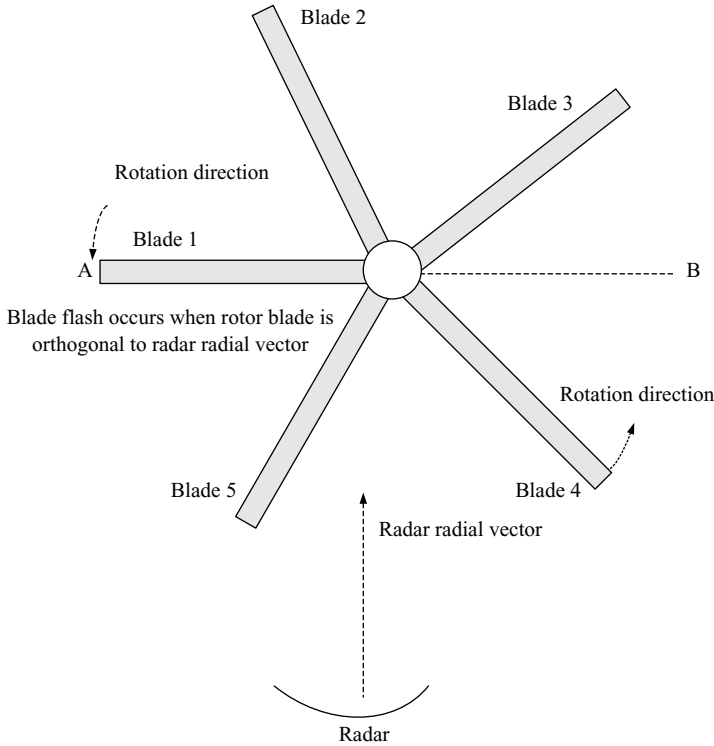
Figure 5.6   For helicopter with odd number of blades, the flashes at 'A' and 'B' for approaching and receding blades occur alternately

which is:

$$\tau_{B_f} = \frac{2\pi\lambda R_0}{L} \qquad (5.3)$$

where τ_{B_f} is the blade flash duration.

For helicopters with an odd number of blades the situation is somewhat different. A helicopter with five blades is shown in Figure 5.6. It can be seen that the approaching blade number 1 is positioned at A to provide the flash in the direction of the radar. However, in contrast to the even-bladed case, there is clearly no simultaneous flash from any other blade and the next flash occurs when the receding blade number 4 is in position B. However, the reflected signal is from the rear aspect angle of the blade as distinct from the forward blade aspect in position A. The next flash to occur is when blade number 2 is in position A, followed by blade number 5 in position B. It can be appreciated that the flashes occur alternately from the front and the rear of the blades. For aerodynamic reasons the blade shape is not mechanically symmetric for the forward and the rear, so it is not normally symmetric as a scatterer of microwave radar signals. This means that the amplitude of the reflected signal
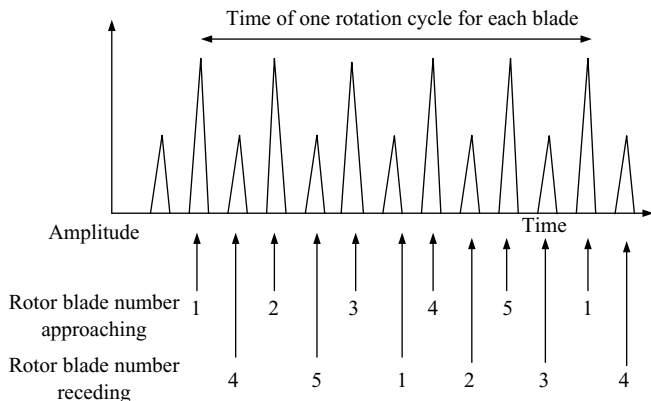
*Figure 5.7   Blade flashes for helicopter with five blades: flashes from the approach-
ing and receding blades alternate as they become orthogonal to radar
radial vector*

is expected to alternate between two different values as flashes from the rear and
front of the blades are alternately positioned orthogonally to the radar radial vector.
This is important, as it can be used as a discriminant between helicopters with odd
and even numbers of blades. Helicopters with odd numbers of blades also provide
a higher frequency of flashes than the even-bladed case, as each blade contributes
two independent flashes per revolution of the rotor. The blade flash sequence for the
five-bladed helicopter is shown in Figure 5.7.

As the rotor blades are rotating at a frequency of R_0 Hz, then the number of blade
flashes occurring for an odd-bladed helicopter is given by:

$$B_f = 2NR_0 \tag{5.4}$$

where B_f is the blade flash frequency, in Hz and N is the number of rotor blades.

In order to detect at least a single blade flash, it is necessary to use a pulse
repetition frequency which is sufficiently high so that the flash is not missed between
radar pulses. With reference to Figure 5.8, it can be seen that the pulse repetition
period, τ_{prp}, must be shorter than the flash duration in order to guarantee at least part
of one pulse hitting the blade. If the pulse repetition interval between transmitted
pulses is longer than the flash duration, the detection of the flash is not reliable and
dependent upon the timing of the transmitted pulse with respect to that of the blade
flash.

To ensure that at least one complete pulse can then illuminate the blade as it is
positioned to provide the flash, a slightly shorter pulse repetition period is required,
which is given by:

$$\tau_{prp} + \tau \leq \tau_{B_f} \tag{5.5}$$

where τ is the duration of the pulse.

To detect blade flash:

$$\tau_i \geq \frac{1}{B_f}$$

$$\tau_{\text{prp}} + \tau \leq \tau_{B_f}$$
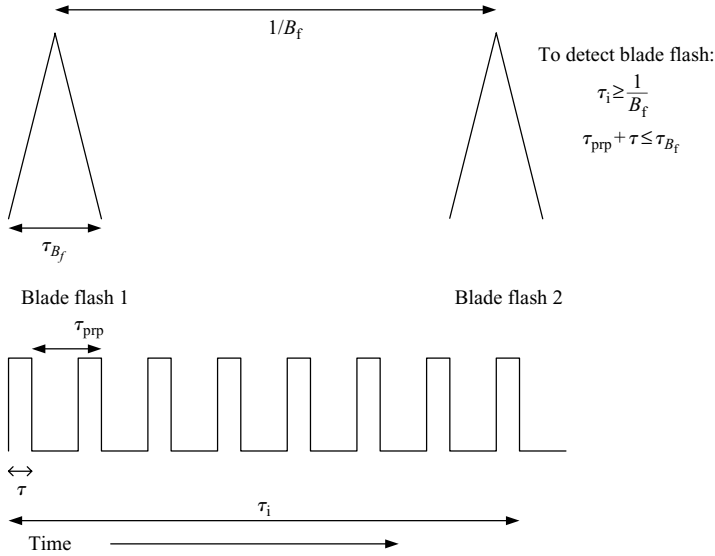
Figure 5.8   Selection of radar pulse parameters to detect blade flashes

Hence, in order to guarantee that at least one complete single pulse detects the blade flash, the length of the pulse plus the pulse repetition period must be less than the duration of the blade flash.

The duration of the radar integration period must also be considered. It is necessary that the radar dwell period is sufficiently long to ensure that at least one blade becomes orthogonal to the radar radial vector over this period. With reference to Figure 5.8, it can be seen that the radar integration period, τ_i, must be longer than the blade flash interval, $1/B_f$:

$$\tau_i \geq \frac{1}{B_f} \tag{5.6}$$

This ensures that at least one blade flash occurs over the radar integration period. The inequalities shown in (5.5) and (5.6) specify the requirements for the radar pulse parameters to detect the blade flash assuming that the characteristics of the helicopter's main rotor blade are known. It is necessary that the rotation rate and the blade dimensions, which determine the flash duration can be determined. If these are not known precisely for specific helicopters, boundaries on these values have to be determined from the known mechanics of helicopter design and flight aerodynamics, so that radar parameters can be used for a variety of helicopters and associated operating conditions. More sophisticated models for Equations (5.1)–(5.3) would be developed to provide the polar diagram of the blade flash at the radar frequency of interest.

However, in some circumstances it may not be necessary to detect a blade flash at every look such as with a long range surveillance radar. If several short looks

are available and the helicopter is visible for a long-enough period and the timelines for any follow-on actions allow it, blade flashes can be detected with reasonable reliability from the cumulative detection probability.

5.2.2.3   Extraction of a blade flash from radar data

So far the ability to detect at least a single blade flash has been considered. A typical technique for extracting a blade flash from radar data is now addressed. As was discussed in Chapter 2, radar usually uses pulse Doppler techniques for the coherent detection of moving targets. This involves transmitting a pulse sequence and performing a Fourier transform to detect moving targets. If a helicopter is being tracked, this type of waveform is used and updates in velocity are provided from the Doppler filtering. However, a helicopter blade flash is a different type of signal to detect and needs a specific signal processing function to detect its presence. A helicopter blade flash appears as a large impulse signal to the radar and is detected by very few of the radar pulses. This is illustrated in Figure 5.9.

In this representative example only one radar pulse has detected the flash over the radar integration period. When the reflected radar signal is examined, only this single pulse conveys information associated with the blade flash. If conventional pulse-Doppler signal processing is performed, as would be implemented for normal
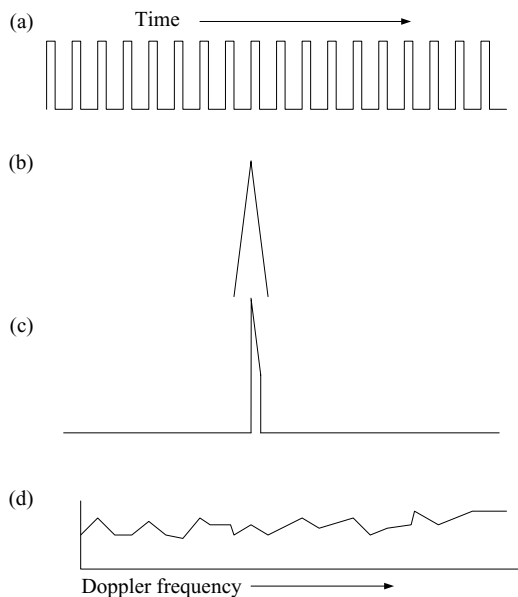
Figure 5.9   *Helicopter rotor blade flash in time and frequency domains: (a) transmitted waveform; (b) blade flash; (c) received signal tends to have large amplitude; (d) using conventional pulse Doppler signal processing, Fourier transform of received impulsive signal places energy across Doppler filters and it is not optimally detected*

radar detecting and tracking modes, this impulsive flash would transform into lower amplitude signals in each of the Doppler filters. This is because a short impulsive signal has a very broad spectrum. Although the helicopter blade is moving very rapidly and has a high Doppler frequency, the signal received cannot normally be detected by virtue of its Doppler frequency. It is not usually possible to perform coherent processing over several pulses to extract the pulse-to-pulse phase information required, using the methods discussed in Chapter 2, Section 2.1.18. In practice, the energy measured in each Doppler filter may be above the receiver noise floor for large impulses. However, detection using conventional Doppler signal processing techniques is not optimised for maximising detection sensitivity.

The recommended method used is to analyse the data in the time domain, as the pulse seen in Figure 5.9(b) is of high amplitude and much higher than the returns obtained over the rest of the dwell. Hence, in order to detect helicopter blade flash, while simultaneously searching for and tracking all targets of interest using pulse Doppler techniques, the same waveform can be used, but two different signal processing channels are required, as shown in Figure 5.10. After digitisation, the radar data would be directed into two separate signal processing channels. In the channel shown on the left of the diagram, the received data can be processed for moving targets and range-Doppler maps are generated. In the right-hand channel, a helicopter blade flash would be detected by comparing the returns from a single range gate and detecting isolated high levels of signal amplitude. The range at which the blade flash is detected can be determined from the associated time delay, as is used for any radar target. For a moving helicopter target, the left-hand signal processing chain also is able to obtain a detection, as the skin of the helicopter is moving and exhibits the normal Doppler effect. The result is that this skin return is positioned on the range-Doppler map and is identified as a moving target. For the same radar burst, if an impulse from the blade flash has also been measured from the other signal processing chain, it is positioned at the same range as the target detected in the range-Doppler map. The results from the two signal processing operations can then be associated with each other and the detected target would be tentatively classified as a helicopter. The degree of confidence associated with this decision is dependent upon the amplitude of the impulse received and the relative level of the receiver noise floor. This target can then be labelled as probably being a helicopter for subsequent tracking. If further impulses are detected during future dwells, the level of confidence in its being a helicopter becomes very high.

This method provides a means for detecting, tracking and recognising helicopters, as well as being able to detect and track other targets, such as land vehicles and fixed-wing aircraft. However, all the requirements presented earlier in this section on the radar pulse parameters have to be met for ensuring that the blade flash is detected.

5.2.2.4   Helicopter classification using blade flash

The detection of a single blade flash has just been considered for categorising the target as a helicopter [4]. In order to determine more information about the main rotor blade characteristics, it is necessary to dwell sufficiently long to be able to detect
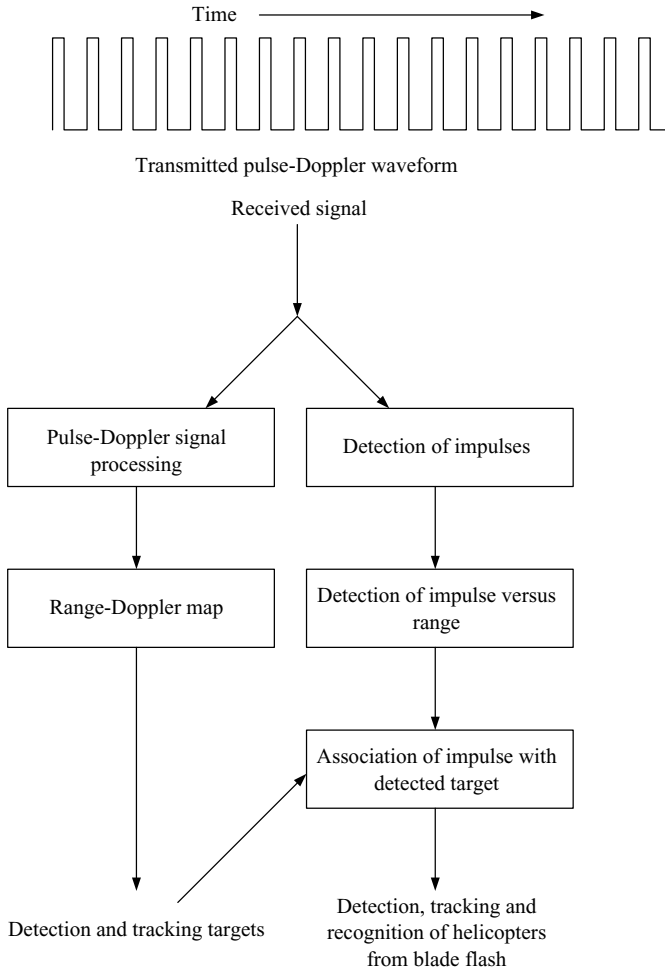
Figure 5.10   *Signal processing functions for recognition of helicopters from detection of blade flash*

a sequence of blade flashes. In Figure 5.11, a sequence of blade flashes is shown for a relatively long radar dwell period on the helicopter target. The typical speed of the tip of a main rotor blade is just below the velocity of sound, at about 300 m/s.

This tip velocity of each blade is given by:

$$V_T = 2\pi L R_0 \tag{5.7}$$

For a blade of 5 m in length, the rotation rate is about 10 Hz. It is recommended that in order to ensure that the characteristics of the blades are extracted for recognition purposes, one full cycle of rotation is detected. This should ensure that sufficient flashes are detected such that the relative amplitudes can be compared for even or odd

(a)

Time for one rotation cycle for each blade, $1/R_0$

Amplitude

Time

Time between blade flashes

(d)

(c)

Rotation rate, R_0 Hz

Rotor hub

Blade tip velocity $= 2\pi L R_0$

Blade

L
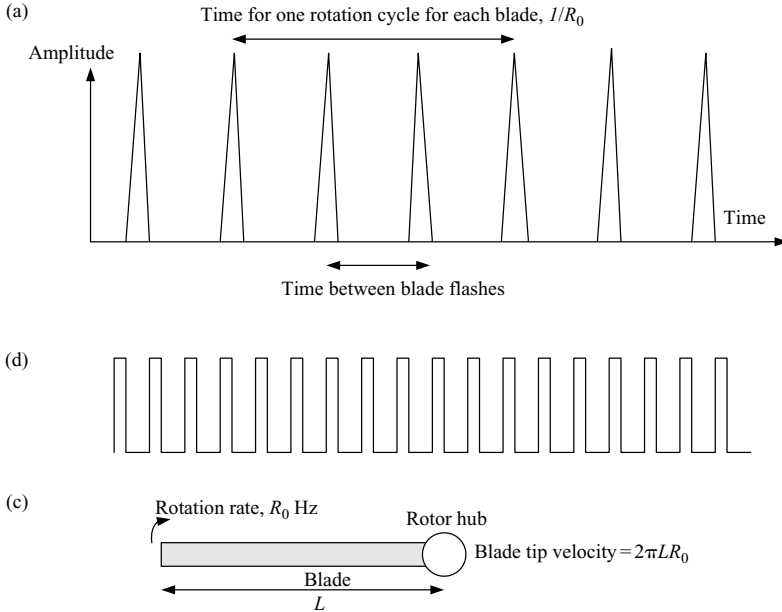
Figure 5.11   *Detection of several main rotor blade flashes for extracting helicopter features: (a) sequence of blade flashes; (b) radar waveform required to detect two full rotation cycles; (c) calculation of rotor blade tip velocity*

blade counts. Hence, for our example, this would require a dwell period of about 100 ms. This is much longer than conventional detection integration periods, so a specific measurement would be required to implement this function.

Over this period the time between blade flashes would be measured. Helicopters tend to operate at a constant main rotor period and alter the pitch of the blades to adjust the lift in accordance with the requirements of the flight, such as load, speed, altitude, acceleration and attitude. Hence, a specific helicopter has a particular blade rotation rate. This means that the time between blade flashes can be determined from knowledge of the number of blades present and the length of the rotor blades. The time measured between blade flashes could then be related to the characteristics of known helicopters. In addition, as was discussed earlier in this section on helicopters, the relative amplitudes of alternate blade flashes can be used to determine whether the helicopter has an even or odd number of blades.

It is clear that with *a priori* knowledge of specific helicopters' characteristics, the measurement of the main rotor blade flash characteristics can be used for recognition purposes.

5.2.3   *Rear rotor blades*

The rear rotor blades can also provide discriminants, which can be used for recognising and identifying helicopters. With reference to Figure 5.1, the main and tail rotors

Rear rotor blade flashes can be represented by fundamental frequency component at flash rate and its harmonics
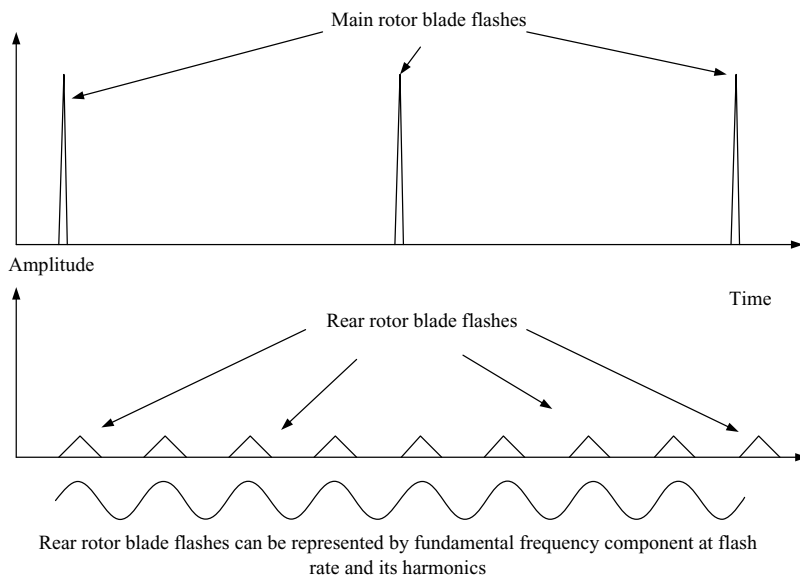
Figure 5.12   Comparison of 'flashes' from main and rear rotor blades: rear rotor blade returns can be analysed in the frequency domain

are shown. The main rotor is much larger than the tail rotor and the two are normally driven together via a mechanical gearing system. The gear ratio is typically of the order of three to six, with the rear rotor rotating faster. As the rear rotor blades are shorter, they can rotate much faster than the main rotor blades, while still maintaining their maximum speed at the blade tips below the speed of sound. As with the main rotor, the number of blades on the tail rotor varies from helicopter to helicopter.

As the tail rotor blades are much smaller than the main rotor blades, their corresponding rcs's are much less, so the signal received by the radar is relatively low. The smaller blades have a broader peak of blade flash, as the radar look angle varies with rotation. However, the rotation rate is faster than the main rotor. The same simple mathematical model used to derive the rcs of the main rotor blades, as shown in Figure 5.3, can be applied to the rear rotor blades. This provides very general guidance on the returns expected, but far deeper analysis [5] is required to generate accurate representations of the reflected signals. The rear blade flashes are illustrated in Figure 5.12 and are compared with the main blade flashes.

A typical example of parameters of main and rear rotors is shown in Table 5.1. The rotation rate of the rear rotor is given as 40 Hz and provides a modulation frequency, due to the presence of the four blades and a gear ratio of four, B_{rr}, of 160 Hz. In contrast to the main rotor blade flash, in which the impulsive response is spread over the Doppler frequency filters, as shown in Figure 5.12, the energy from the rear rotor tends to be more detectable as a frequency component, rather than an impulse.

It was stated earlier that, in order to obtain sufficient data for the analysis of the main rotor blade returns, a dwell period of about 100 ms was proposed. Over this

Table 5.1   *Typical parameters for main and rear rotor blades with gear ratio of four*

	Main rotor	Rear rotor
Rotation rate	10 Hz	40 Hz
No. of blades	4	4
Blade flash rate	40 Hz	160 Hz (B_{rr})

f_d is 'Skin' Doppler frequency of helicopter

B_{rr} is fundamental modulation frequency of rear rotor blades
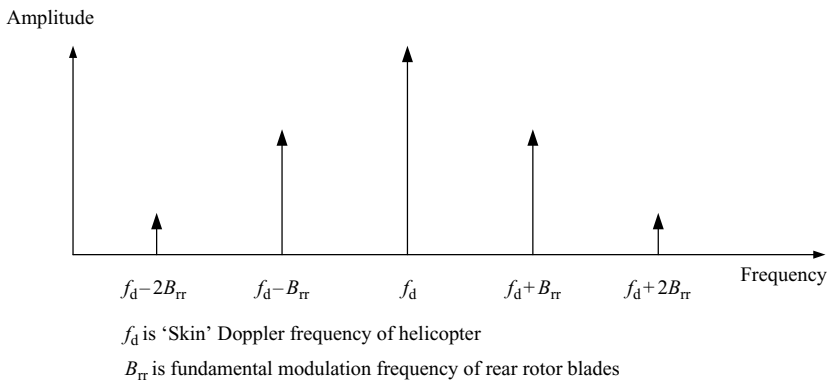
Figure 5.13   *Spectrum obtained from rear rotor blades of helicopter*

period the frequency resolution of the measurement, which is the inverse of 0.1 s, is 10 Hz. The rear rotor frequency periodicity of 160 Hz should be able to be measured as spectral components. The analysis of the spectrum generated by moving engine blades is dealt with in more detail in the section on Jet Engine Modulation. This theory can also be applied to the rear rotor blades, which results in the fundamental modulation frequency and its harmonics generating a spectrum about the Doppler frequency of the moving helicopter. A typical spectrum obtained from the rear rotor blades is shown in Figure 5.13.

The Doppler frequency of the helicopter is shown, due to its motion relative to the radar. The upper and lower modulation sidebands shown are due to the fundamental modulation frequency of the rear rotor blades and their second harmonics.

As the rear rotor blade returns are at a low level, they are frequently not measurable. However, if the radar has sufficient sensitivity and fundamental modulation frequency of the rear rotor blade modulation can be measured, it is another discriminant that can be used to classify the helicopter. The fundamental frequency of modulation of the rear rotor is mathematically related to the main rotor blade flash rate periodicity by the relative numbers of blades on the two rotors and the gearing ratio between them. Hence, knowledge of the main and rear blade numbers and

Figure 5.14   Main helicopter rotor

gearing characteristics of helicopters can be used in the analysis of the radar returns for establishing the classification of the helicopter.

5.2.4   *Main rotor spectrum*

The main rotor of the helicopter also provides information that can discriminate the detected target as a helicopter and can contribute to classifying it [6,7]. Figure 5.14 is a photograph, which shows the main rotor of a helicopter attached to the four rotor blades.

As the rotor rotates, its motion exhibits the Doppler effect. The rotor can be considered to be a right circular cylinder, as shown in Figure 5.15. If the surface is rotating with a velocity, v, then the velocity component in the direction of the radar is $v \sin \theta$, where θ is the angle between the line joining the point on the surface of the rotor to its centre and the radial vector of the radar. Only points on the rotor having values of θ between $+90°$ and $-90°$ reflect the signal back towards the radar. Hence, at any one time, there is a spread of velocity components from $v \sin(+90°)$ to $v \sin(-90°)$ reflected back towards the radar, that is, from $+v$ to $-v$.

This velocity spread for this idealised model is shown in Figure 5.16, where f is the transmission frequency.

The range of Doppler frequencies surrounding the helicopter's skin velocity is shown. The spread is plus and minus the Doppler frequency of the surface of the rotor. This 'plateau' type of spectrum is typical of that of a helicopter. The rotor velocity is given by the angular velocity of the rotor multiplied by its radius. Hence, from *a priori* knowledge of the rotation rate and radius of the rotor, the rotor's Doppler frequency

Rotation

θ

Velocity, v

Radar

Velocity at surface of rotor is v

At angle, θ, velocity component in direction
of radar is $v \sin \theta$

Points on the surface of rotor with values
of θ between +/– 90° reflect
energy back to the radar
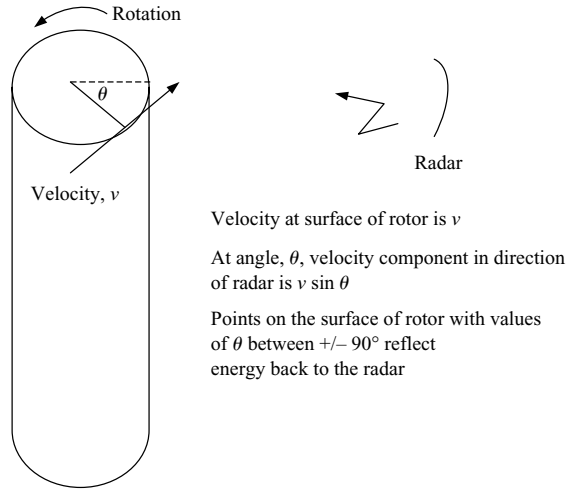
Figure 5.15   Velocity of points on the surface of rotor

Amplitude

Skin Doppler of
helicopter

Skin Doppler of helicopter
minus Doppler velocity of rotor

Skin Doppler of helicopter
plus Doppler velocity of rotor

$f_d - 2vf/c$ f_d $f_d - 2vf/c$ Frequency
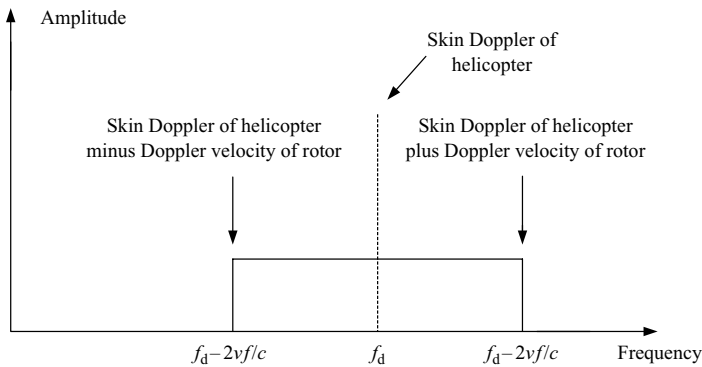
Figure 5.16   Doppler frequency spread from main rotor

spread can be predicted. If a particular velocity spread is measured, the reverse of
this process can be performed to classify the helicopter. From the measured value of
velocity spread, helicopters with the values of the rotor radius and angular velocity
that generate this spectrum are the candidate helicopter types. However, in practice,
the detection of this helicopter engine rotor modulation (HERM) is dependent upon
the rotor having some surface roughness. Otherwise, the HERM spectrum cannot be
measured with the same amplitude and phase information detected every pulse.

5.2.5   Helicopter recognition summary

There are several potential discriminants, which can be used to recognise helicopters.
The main feature differentiating helicopters from other airborne targets is the main

Table 5.2   Helicopter features measured

Measurement	Features
High-amplitude short duration flash	Presence of a helicopter
Time between blade flashes	Candidate helicopters listed
Relative amplitude of flashes	Even or odd blades
Rear rotor blade spectrum	Candidate helicopters listed
Main rotor spectrum	Candidate helicopters listed
Combining features from the above measurements	Short-list of candidate helicopters

rotor blade flash. This is a very short duration signal of high amplitude in relation to the helicopter's skin return. The measurement of the time between flashes and whether the amplitude of the flashes alternates between different values can provide estimates of the target's class or identity.

The rear rotor blades modulate the radar signal with characteristics related to the main rotor rotation rate, the number of blades on the rear rotor and the gear ratio between the main and rear rotors. However, these blades are relatively small and may not be detectable. The spread of Doppler frequencies from the main rotor also provides discriminants for categorising the helicopter. The measurements that can be used to recognise helicopters are summarised in Table 5.2.

As the data from the measurements is combined and analysed, the number of types of helicopter that match this data is reduced. The recognition process then provides a list of candidate helicopters, which are consistent with the measurements performed. The level of precision obtained in recognising the helicopter depends on how well the mechanical characteristics of individual types of helicopter propulsion system are known, the signal-to-noise ratio associated with the radar measurements and the level of mechanical similarity between different types of helicopters, which are required to be differentiated.

Bayesian networks can be used to determine the best estimate of the helicopter type from the different values of the features measured. They provide the best theoretical estimate of the relative probabilities from the options available and are discussed in Chapter 13.

5.3   Jet engine recognition

5.3.1   Introduction

5.3.1.1   Jet engine mechanics

In order to appreciate how the analysis of the spectrum obtained by illuminating a jet engine with a radar signal is performed to provide an estimate of its identity, it is first necessary to understand a little about the mechanics of a jet engine [8,9].
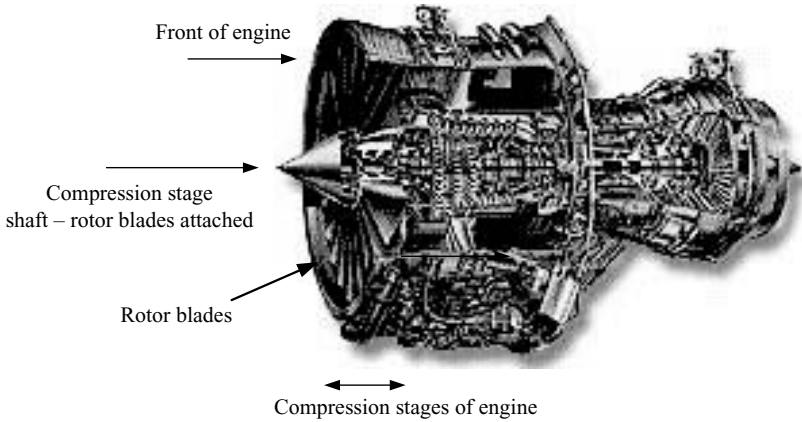
Figure 5.17   A jet engine: the front of the engine contains the compression stage blades, which generate the JEM spectrum when illuminated by radar (Photograph courtesy of Rolls Royce plc)

A typical jet engine is shown in Figure 5.17. Although there are many variations on the basic design of the jet engine, the principles with respect to the measurement of JEM with radar are generally similar. The air flowing into the front of a jet engine is compressed by a series of blades attached to a shaft, which normally rotates at several thousand revolutions per minute. There are a number of individual compression stages at the front of the engine, each with a set of rotor blades attached to the shaft and normally there is a different number of rotor blades on each stage. The blade sizes tend to reduce with distance into the compression stage, as the air is compressed into a progressively smaller volume. The distance between the compression stage blades also tends to reduce with distance into the compression section. The air is compressed to high pressure and mixed with the fuel and is forced into the ignition section. The fuel is then ignited, burns and is forced out through the exhaust via turbines and thrust is thereby generated, which propels the aircraft. The turbine blades at the rear of the engine tend to be small and are not easily observable with most radars at detection ranges of interest.

5.3.1.2   Interaction of radar signal with engine blades

A very simple representation of four compression blade stages at the front of a jet engine is shown in Figure 5.18. As the shaft is normally common to the first few stages of the compressor, each rotor stage rotates at the same angular velocity. Each rotor stage normally has a different number of blades.

As the radar signal progresses through an engine rotor stage, some energy is reflected by the rotor blades and the remainder propagates through to the next rotor stage. As the signal gets deeper into the engine, as the blades tend to become smaller and the gaps between them also become smaller, less energy propagates to the next
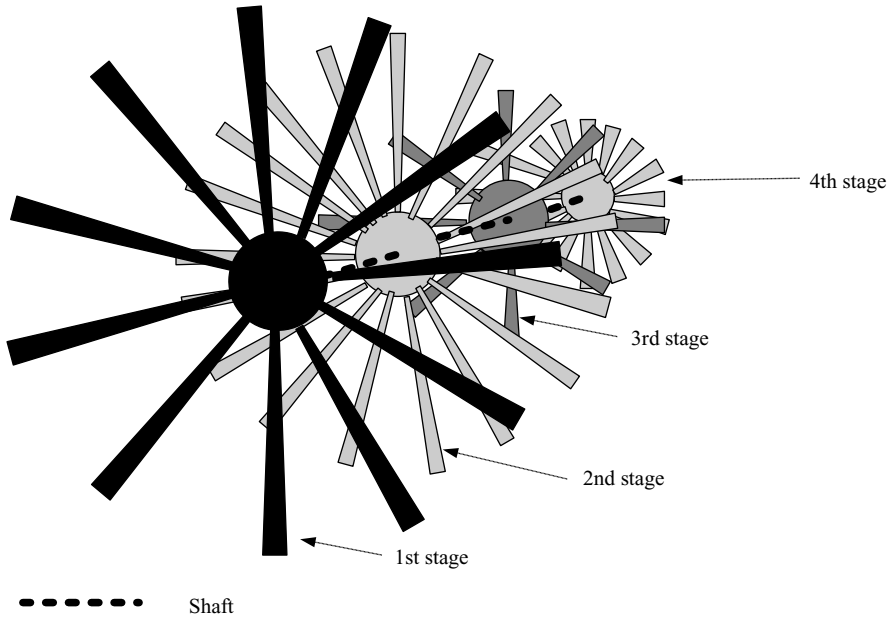
Figure 5.18   Rotor blade stages at the front of a jet engine: interaction of radar signal with compression stage rotor blades generates JEM spectrum used for engine recognition

rotor stage, as more is progressively reflected by the blades. This means that the energy that is reflected back towards the radar tends to come from the reflections associated with the first few rotor stages of the compressor, so these compressor stages are the ones of interest for engine recognition purposes.

Radar signals at the higher frequencies penetrate further into the engine than lower frequencies, as the wavelengths are shorter and the signal can propagate more effectively through the smaller gaps between the blades. Hence, radars operating at the higher frequencies penetrate deeper into the engine, so the signals received have a far higher content of returns from the deeper stages than radars operating at the longer wavelengths. The sizes of the rotor blades and associated gaps between them relative to the signal's wavelength determine the potential of the radar to provide a JEM spectrum, which has sufficient information for analysis for recognition of the engine. Normally, frequencies of 10 GHz and above have been found to be good for JEM measurements, as wavelengths of around 3 cm can propagate through a few rotor stages of typical civil and military jet engines. JEM measurements can be made on civil airliner engines down to 3 GHz and below, as they very often have large engines and a very short air in-take section, which support high signal levels arriving at the rotor blades. Military aircraft tend to have smaller engines and relatively long air in-take sections, making JEM measurements difficult at the longer wavelengths.
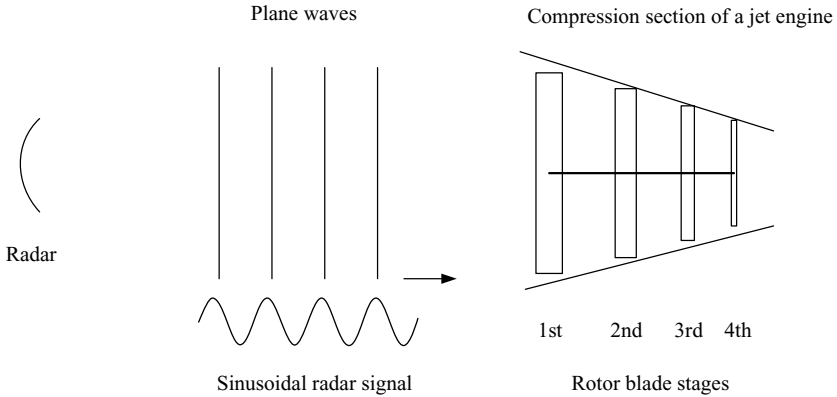
Figure 5.19   Illumination of jet engine with radar signal

5.3.2   JEM spectrum

5.3.2.1   Engine spool rate spectral components

The JEM spectrum obtained when illuminating a jet engine with an electromagnetic signal is dependent upon the frequency of the radar signal, the rotation rate of the engine and the mechanical construction of the engine. There are various papers in the technical literature, which explain JEM to the specialist, but are unlikely to be comprehensible to the general reader. These can be found in the references. In this section a theory is developed, which is based on fairly simple principles and has the objective of providing an explanation of JEM in less complex mathematical terms.

The illumination of a jet engine with a radar signal is shown in Figure 5.19. As the basis of the JEM technique is spectral analysis, the most straightforward waveform to employ for the purposes of demonstrating the technique is a sinusoidal signal.

The scattering effects, which occur as the electromagnetic wave interacts with the engine, are extremely complex. The radar signal initially encounters the first rotor blade stage. Some of the energy is reflected from the blades, some propagates through to the second rotor and some is reflected from the static casing of the compressor. Each element of each blade contributes an amplitude and a phase to the reflected wave. The contributions from all the parts of each blade and all the individual blades generate very complex wavefronts. At the second rotor stage some energy is reflected back towards the first stage, of which a proportion is reflected from the first blade stage and some propagates through the first stage blades out of the engine. These reflection and 're-reflection' effects occur as the radar signal penetrates through the engine. The net effect is that a proportion of the initial incident signal is reflected from the engine and a small proportion of this propagates back towards the radar. These multiple reflections are so complex that the provision of a high-integrity mathematical model to describe them is not generally considered feasible.

Superficially it may not seem technically achievable to understand and utilise effects which cannot realistically be fully modelled. However, by analysing the

(a)

Amplitude

τ

Phase

τ

(b)

τ

τ_i

(c)

Radar signal frequency line

$1/\tau$

$1/\tau_i$

f_{prf}
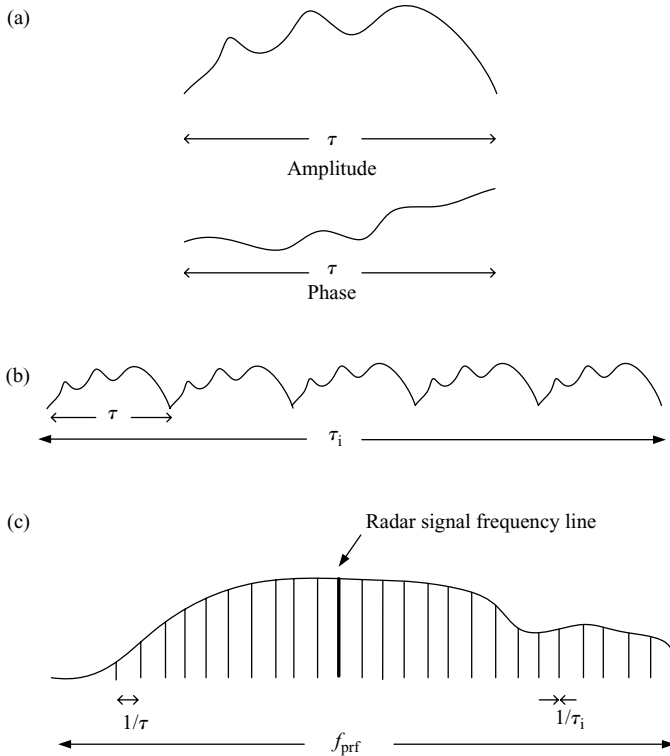
Figure 5.20   *JEM spectrum constructed from time domain signal received by radar from single rotation cycle of whole engine. All spectral lines are at harmonics of engine spool rate: (a) representation of amplitude and phase of signal from jet engine reflected back towards radar over one cycle of engine rotation; (b) representation of amplitude of signal from jet engine reflected back towards radar over several cycles of engine rotation comprising radar integration period; (c) JEM spectrum is Fourier transform of time domain signal, shown in (b) above*

periodicity and symmetry of the effects and extracting the most important elements of the scattering, a useful representation of JEM can be generated, which is sufficiently good to enable different engines to be recognised.

The rotation of the whole of the front compressor stage on its shaft is now considered. Some engines have different stages of the compressor on different shafts, which is even more complex. This will not be dealt with here, but the concepts derived can be applied to the front of the compressor, which is on a single shaft.

The rotation rate of the compressor is called the shaft rate or spool rate. If the engine is running at a constant speed and the aspect angle of the engine to the radar is not changing, then the signal received by the radar for each cycle of the engine is the same. This is illustrated in Figure 5.20 and is discussed later in this section.

Figure 5.21 area text:

Spool

Blade

Rotation

α

Plane of blade
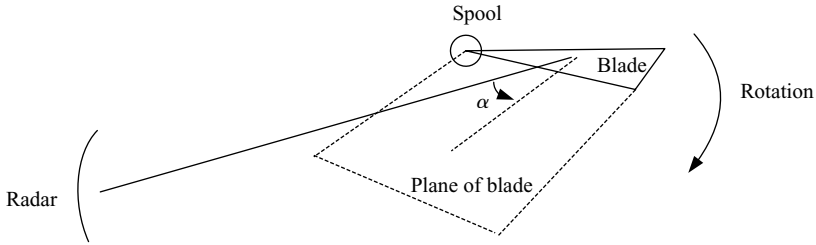
Radar

If blade is pitched, then as it rotates on the spool, the orientation of its plane continuously varies over engine cycle relative to the radar

Glancing angle α varies as blade rotates on the spool, so the amplitude and the phase of the reflected signal also vary at the radar

As the velocity component of moving blade in the direction of the radar varies over the engine cycle, Doppler effect is present, so gives rise to phase variation at radar

Figure 5.21   Reflected signal from blade varies over rotation cycle of engine

The amplitude characteristics are due to the net effect of all the contributions of all the blades in the direction of the radar. Each blade individually can be considered to be a reflector and for the incident electromagnetic wave generates a reflected wave with amplitude and phase components, which are dependent upon the look angle. All the components from all the blades then contribute to the wavefront generated in the direction of the radar. In Chapter 2, Figure 2.81, the amplitude of a signal reflected from a flat plate is presented. For jet engine blades with complex shapes, a far more complex variation of reflection amplitude with angle occurs. A single blade is shown on the spool in Figure 5.21.

Normally blades are pitched for aerodynamic reasons, which means that the plane of the blade is not the same as the plane of rotation of the blade about the spool. The blade is angled with respect to the plane perpendicular to the spool axis. This means that as the blade rotates on the spool, it is continuously presenting a different aspect angle to the radar, so that the amplitude measured at the radar varies over a cycle of the engine and repeats during the next cycle. This occurs for all the blades, so the net amplitude at the radar is the sum of all the amplitude contributions from all the blades. In addition, as the blade is moving and during certain parts of the rotation cycle is approaching the radar and is receding at other times, there is also a Doppler effect. This is manifested in a continuously varying phase change for each blade during the rotation cycle. Hence, both the amplitude and phase contributions from each blade are varying continuously and the net effect at the radar is the vector summation of all the contributions.

Although the time domain signal received by the radar from the jet engine is not known, it is known to be periodic repeating every cycle of the engine, τ. For the moment an arbitrary amplitude against time characteristic and an arbitrary phase against time characteristic representing the signal received by the radar is shown in Figure 5.20(a). Over the radar integration period, τ_i, this is repeated continuously,

as shown in Figure 5.20(b). This is the total time domain data that is received by the radar for performing JEM analysis over a single burst.

This JEM spectrum is the Fourier transform of this time domain sequence of data and is derived in Appendix 2 and is shown in Figure 5.20(c). The envelope of the spectrum is the Fourier transform of the signal received from a single cycle of the engine's rotation. The maximum spectral component frequency is actually due to the highest Doppler frequency of the blades' motion relative to the radar. Spectral lines can be seen appearing at intervals of the inverse of the rotation period of the engine, which is the engine rotation frequency. The lines are harmonics of the engine spool rate and have individual bandwidths of the inverse of the radar integration period. The spectrum shown in Figure 5.20(c) is general for an engine rotating on a single shaft. Without knowing anything about the number of blades on each rotor stage, it is possible to generate a generalised spectrum. It is assumed that the value of the prf is sufficiently high so that the spectrum obtained is unambiguous and free from frequency ambiguities. The amount of energy associated with each JEM line is dependent upon the number of rotor blades on each stage and many other factors and will now be discussed.

5.3.2.2   Front rotor stage spectrum

In the previous section, a general model was provided for the JEM spectrum obtained from several rotor blade stages, with all the lines being at offsets from the radar signal frequency of harmonics corresponding to the engine spool rate. However, there was no indication of the relative amplitudes of the individual lines. The approach taken is to study the JEM effects of individual rotor stages, which will identify the major spectral lines.

Consider a single rotor stage as shown in Figure 5.22(a). The engine has N blades on a single rotor stage. It can be seen that the engine is symmetric about the spool and that every time it undergoes a rotation of $1/N$ of a cycle, the mechanical action is repeated. From the radar view point it is assumed that each of the blades is identical. As the radar illuminates the engine, at any particular time, energy is reflected from all the blades simultaneously. The amplitude and phase measured by the radar receiver result from the contributions from all the blades. The analytical calculation of the returned signal is dependent upon the detailed mechanics of each blade's dimensions and positions and the radar wavelength.

However, the key factor, which is independent of the precise details and is general, is that the reflected radar signal is repeated every $1/N$ cycles of the engine, in synchronisation with the mechanical motion of the engine. In Figure 5.22(b) a simplified representation of a repeated amplitude characteristic is shown. Although the actual amplitude and phase characteristics are very complex in practice, the important fact is that they repeat at a rate that equal to the time taken for a single blade to move to the position of its neighbour. The example in Figure 5.22(a) shows adjacent blades at positions A and B.

The radar signal repeats at a time interval, which corresponds to the rotation period, τ, divided by the number of blades, N, which is τ/N.

(a)

N rotor blades on the spool

Rotation rate is R Hz

Rotation period, τ

Position A

Time for blade to move
from A to B is τ/N

Position B

Rotation

Radar

(b) Amplitude

τ/N

Time

τ/N is the time for the blade to go from position A to position B

(c) Amplitude

Spacing between
lines is N/τ

Frequency

$f-2N/\tau$ $f-N/\tau$ f $f+N/\tau$ $f+2N/\tau$
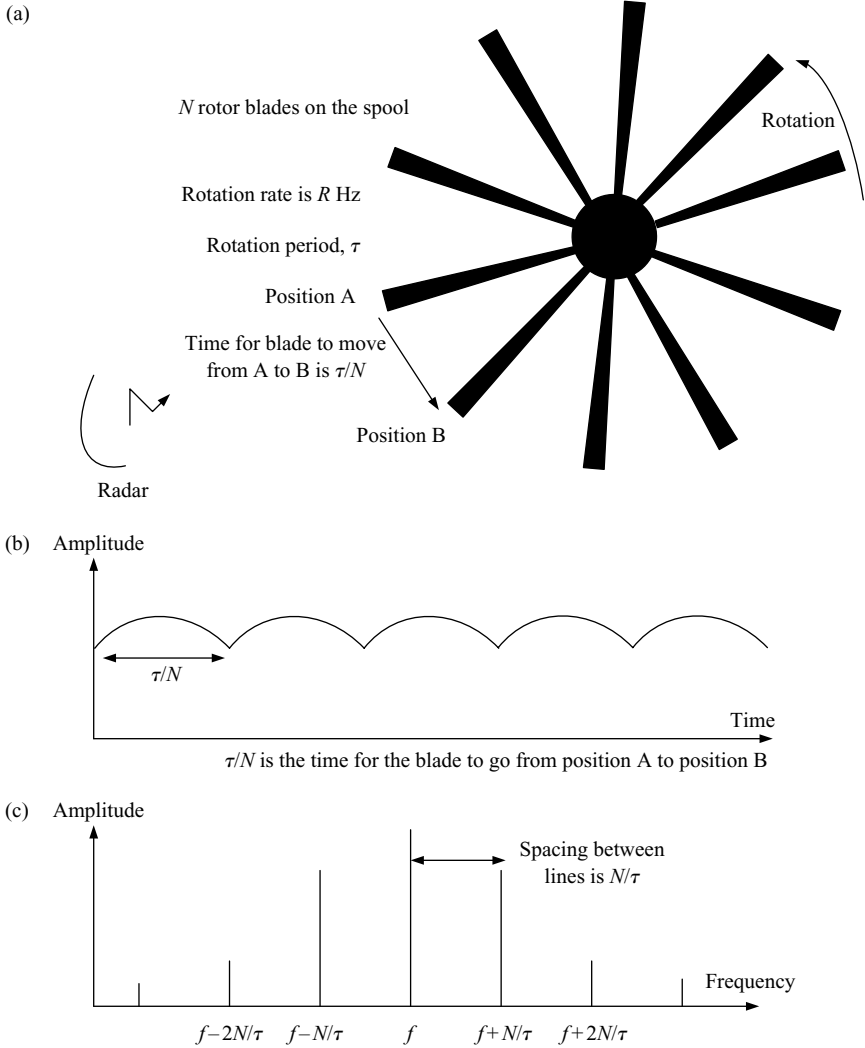
Figure 5.22   *Simple representation of time domain characteristics and typical JEM spectrum obtained from front rotor stage of engine with N blades: (a) single rotor stage at front of engine with N blades; (b) simplified amplitude against time characteristics of rotor stage with N blades: due to symmetry of engine, amplitude and phase characteristics repeat every τ/N; (c) JEM spectrum is frequency transform of time domain characteristics measured by the radar: most of the modulation energy is in the blade chopping rate sidebands at frequency offset of N/τ from transmission frequency, f*

It is the Fourier transform of this time domain data that is the JEM spectrum for a single rotor stage with N blades. The Fourier transform of this type of detected signal is derived in the Appendix. This spectrum is characterised by lines spaced at frequency intervals of N/τ from the radar signal transmission frequency and has a frequency span equal to the radar's pulse repetition frequency. The actual spectrum obtained and the amount of energy apportioned to each line is dependent upon the detailed time domain amplitude and phase characteristics received by the radar. The length, width and pitch of each blade determines the width of the spectrum, due to the first rotor stage. In practice, from experimental results from the real engines at microwave radar frequencies, most of the JEM energy resides in the main 'chopping' sidebands, which are at a frequency of N/τ, followed by the sidebands at twice the chopping frequency, $2N/\tau$. The spectrum from the single front rotor stage only contains frequencies that are offset at multiples of the chopping frequency. Hence, although the details of the time domain response signal received by the radar are not generally feasible to predict, the corresponding frequency domain signal measured is composed of discrete spectral components, which have values, which are related to each other very simply mathematically. This is a key aspect of JEM for target recognition and it is the mathematical relationships between various spectral lines, rather than an understanding and quantification of the scattering mechanisms associated with the rotor blades, spool and engine casing, that is important.

It should also be noted that the chopping sidebands identified at harmonics of N/τ are all each individually also harmonics of the spool rate, $1/\tau$. Hence, with reference to the spectrum shown in Figure 5.20(c), every Nth spool rate line harmonic is a blade chopping rate harmonic. For real engines, these chopping rate lines tend to have much higher amplitudes than the family of spool rate lines.

A more complex model for the electromagnetic scattering from rotor blades is found in References 10 and 11.

5.3.2.3 Subsequent rotor stage spectral contributions

The signal that is reflected back to the radar from the first rotor stage consists of the transmission frequency of the radar and modulation sidebands at the chopping rate harmonics. Signals with this same frequency content, but with differing amplitudes, are also propagated past the first rotor stage and encounter the second rotor stage, as shown diagramatically in Figure 5.23.

The main signals shown reflected from the front rotor stage are the unmodulated radar signal, f, and the first and second harmonics of the chopping frequency, N/τ. The most significant signals illuminating the second rotor stage are the unmodulated radar signal at frequency, f, and normally the first harmonics of the chopping frequency. The second harmonics are still propagated, but are at a relatively low level and are also reduced in amplitude on reflection from the second stage and on propagating back through the first stage.

The second stage has M rotor blades, so any signals are chopped at a rate of M/τ. As the main signals illuminating this stage are at frequencies, f, $f+N/\tau$ and $f-N/\tau$,

Signals reflected from the engine
shown in the upper half of the diagram

Compression section of a jet engine

$f-2N/\tau$
$f-N/\tau$
f
$f+N/\tau$
$f+2N/\tau$

$f+N/\tau+M/\tau$
$f-N/\tau+M/\tau$
f
$f+N/\tau-M/\tau$
$f-N/\tau+M/\tau$

$f-P/\tau$
f
$f+P/\tau$

$f-Q/\tau$
f
$f+Q/\tau$

$f-N/\tau$
f
$f+N/\tau$

$f-M/\tau$
f
$f+M/\tau$

f

Radar

Sinusoidal radar signal, frequency f

Signals transmitted into the engine
shown in the lower half of the diagram

4th: Q blades

3rd: P blades

2nd: M blades

1st: N blades

Rotor blade stages

At each rotor blade stage the main spectral components generated are shown

Figure 5.23   Typical JEM spectral components

the resultant dominating signals obtained are those chopped at M/τ. The resulting signals reflected back from the engine are:

1. $f, f+N/\tau$ and $f-N/\tau$ from reflecting from the first rotor stage.
2. $f+M/\tau, f+N/\tau+M/\tau$ and $f-N/\tau+M/\tau$, from reflecting from the second stage (upper frequency sideband).
3. $f-M/\tau, f+N/\tau-M/\tau$ and $f-N/\tau-M/\tau$, from reflecting from the second stage (lower frequency sideband).

The only strong signal normally expected to propagate through to the third stage is the unmodulated radar signal. When this encounters the third rotor stage with P blades, sidebands are again generated at the chopping rate of P/τ, giving sidebands at $f+P/\tau$ and $f-P/\tau, f+P/\tau$ and $f-P/\tau$. Similarly at the fourth rotor stage with Q blades, sidebands are generated at $f+Q/\tau$ and $f-Q/\tau$.

All these spectral components generated pass back through the front rotor stages, each undergoing further modulation due to the blades' chopping effects. The spectral components chosen are the ones that would be expected to be detected by the radar and would also be of most importance for JEM analysis. Clearly, every jet engine is different and has its own characteristic spectrum. However, the fundamentals of JEM and the key spectral components identified here are sufficiently general to be widely applicable. This should become clearer during the analysis section, which follows.

The harmonics of the fundamental blade chopping frequencies and the resulting frequencies from the mixing effects of various blade chopping frequency harmonics generate a large number of frequencies, all of which are multiples of the spool rate. Interestingly, each of the spool rate frequencies, as shown in Figure 5.20, can be viewed as having been generated by the complex mixing effects just described. The concept used to explain the family of spool line harmonics of Figure 5.20 is consistent with the approach taken for generating the JEM spectral components in Figure 5.23.

Main JEM lines are identified with respect to particular rotor stages, with blade numbers shown
Remaining lines are 'unclassified' and are labelled as spool line harmonics
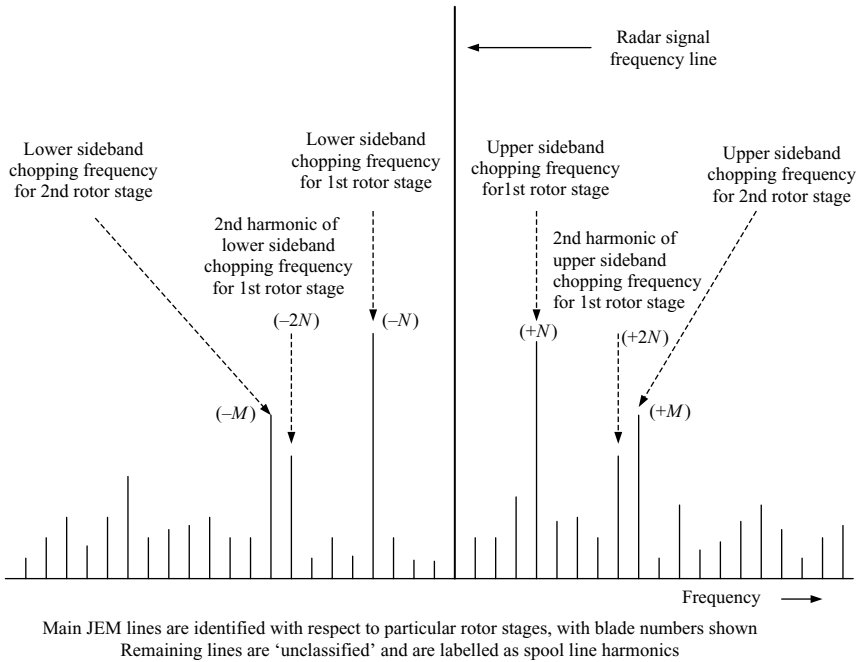
Figure 5.24   Typical JEM spectrum

The results of the concepts used here to describe JEM spectra are now consolidated into a typical JEM spectrum, which is shown in Figure 5.24

At the centre of the spectrum is the radar signal frequency and is due to the reflection component of the signal, which is not modulated by the engine. It also includes returns from the non-rotating parts of the engine and the skin of the aircraft. This component is always present and almost always is a much larger amplitude than that of any JEM lines. The most prominent lines are usually the upper and lower chopping rate frequencies of the first rotor stage. Providing the wavelength of the radar is sufficiently short and the electromagnetic wave propagates to the second stage, the second-stage chopping frequencies are normally detectable. Also shown are the second harmonics of the first rotor blade stage chopping frequency.

Some of the remaining lines can be identified as higher order harmonics of the first stages or the fundamental chopping frequencies of the stages, which are deeper in the engine. It can be seen that every frequency present is a multiple of the basic spool rate, which is the engine's physical rotation rate. The remaining lines, which are not specifically labelled as being associated with particular rotor blade stages, are the spool line harmonics.

The actual relative amplitudes of the JEM spectral lines are dependent upon the transmission frequency, engine mechanics and aspect angle. As the engine changes its speed all the lines move proportionately, as they are all multiples of the spool rate, so the engine speed effectively acts as a scaling factor for the JEM spectrum.

The next section discusses how the engine can be recognised from the measurement of the JEM spectrum.

5.3.3   Engine recognition from JEM spectrum

5.3.3.1   Waveform

The waveform is normally a train of unmodulated pulses, with each having a low bandwidth, as high-frequency resolution rather than high-range resolution is required for JEM. It is important to obtain high-frequency resolution to isolate the individual JEM lines. In order to be able to acquire the JEM spectral data necessary to recognise a jet engine, it should be obtained without ambiguities in the frequency domain. This means that all the time series data of interest from the engine should be sampled at a sufficiently high rate that the Nyquist Criterion [12] is satisfied.

The actual prf to be used cannot be specified universally for all radars and all engines. The JEM spectral content is dependent upon the transmission frequency of the radar, the maximum speed of the engine and the number of blades on the first few engine rotor stages. Some knowledge of the JEM spectra of engines that are to be recognised helps the decision to set the appropriate pulse repetition frequency of the radar. A criterion for the prf selection could be that the third harmonics of the fundamental chopping frequency can be unambiguously measured.

For a maximum engine speed of R Hz, the first-stage rotor chopping frequency is RN Hz, for N rotor blades. The associated third harmonics of this chopping frequency are at $+3NR$ and $-3NR$ Hz. Hence, in order to unambiguously measure these frequency components, the prf has to be greater than the spectral coverage required, which is $6NR$ Hz. This is shown in Figure 5.25. For example, for an engine with a maximum speed of 12 000 revolutions per minute (rpm), the maximum rotation rate and hence the maximum spool rate is 200 Hz. If the engine has 50 blades on the first rotor stage of the compressor, then the maximum chopping frequency is 10 kHz. The corresponding third harmonic frequencies are then ± 30 kHz, so the minimum prf to measure this spectrum unambiguously is 60 kHz.

Normally, the radar platform and the target aircraft would be expected to be moving relative to each other, so there is also an additional Doppler frequency component to take into account. The effect of this is to offset the whole of the JEM spectrum by this relative Doppler frequency, as is illustrated in Figure 5.26.

Two approaches can be taken to maintain an unambiguous JEM spectrum. Either a pulse repetition frequency is selected that is higher than the value calculated above by an additional amount equivalent to the maximum closing Doppler frequency between the two platforms. This is always a positive value for observing the compression section of almost all aircraft. (Exceptions are the very special cases of vertical take-off aircraft, such as the BAE SYSTEMS Harrier, which can fly backwards.)

The other approach is to use the original prf value, as calculated above, and to compensate for the measured spectrum by offsetting the target's relative Doppler frequency as a simple frequency shift. This method is preferred if it is desirable to minimise the prf for other radar equipment or clutter suppression considerations.

(a)

Maximum rotation rate $= R$ Hz

N blades on 1st
rotor stage

Radar

Chopping frequency for 1st blade stage is number
of blades $\times$ rotation rate $= NR$

3rd harmonic of 1st stage chopping frequency $= 3NR$

(b)

Bandwidth $= 6NR$

$-3NR$ $-2NR$ NR $+NR$ $+2NR$ $+3NR$

(c)
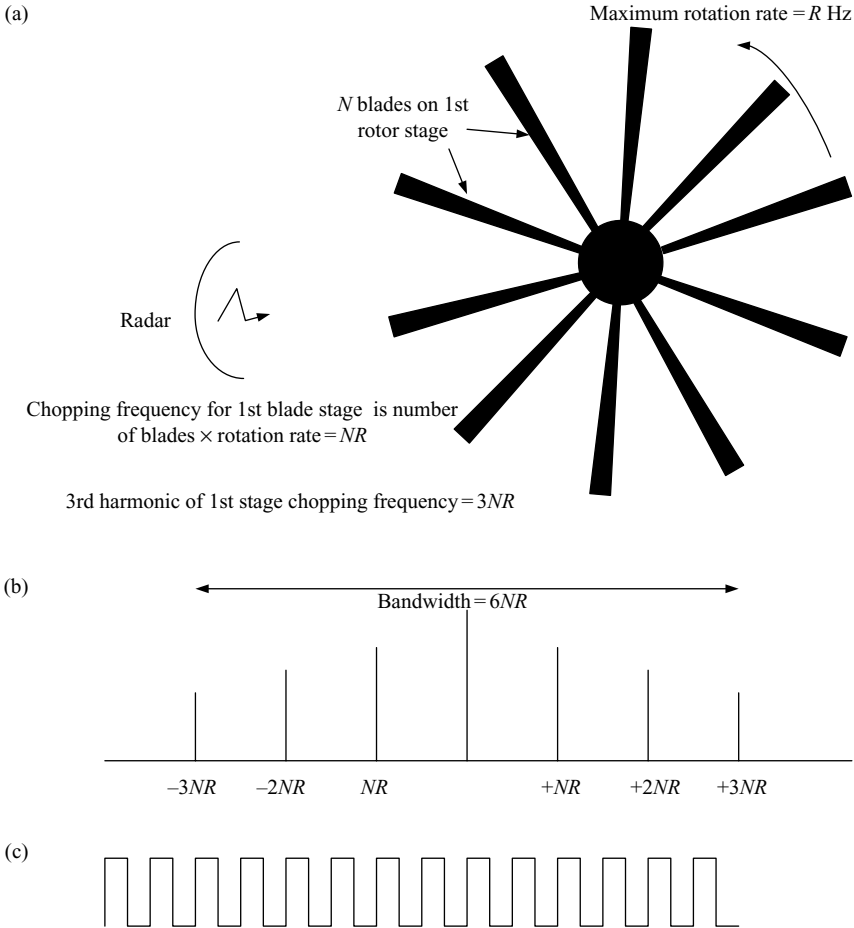
Figure 5.25   *Calculation of pulse repetition frequency required to unambiguously*
measure JEM spectral components: (a) calculating first-stage rotor
chopping frequency and third harmonics; (b) first three harmonics of
chopping frequency of first-stage rotor; (c) pulse repetition frequency
of radar must be greater than 6NR to measure spectral components
in (b) unambiguously

The dwell time for the JEM mode has to take into account various trade-offs.
If the dwell time is too long, the aircraft may have changed its engine speed or aspect
angle over the radar integration period, which has the effect of blurring the JEM lines.
This results in imprecise measurements of the spectral components and a degradation
in recognition performance. For example, for a dwell period of 200 ms, the frequency
resolution is 5 Hz, so if JEM lines at 25 kHz are to be accurately measured, they
should be stable to 5 Hz, which is one part in 5000. Hence, as the values of the
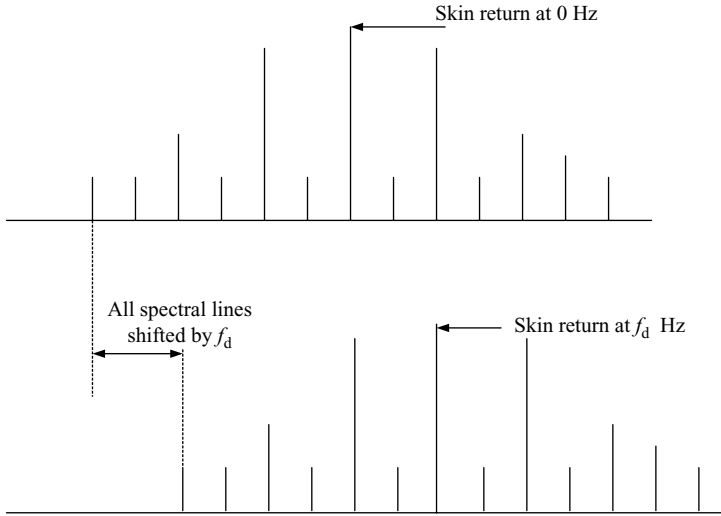
Figure 5.26   Effects of motion between radar platform and target on JEM spectrum: (a) JEM spectrum with no relative motion between target and radar platform; (b) JEM Spectrum in (a) shifted by Doppler frequency, f_d due to motion between platforms

spectral components are proportional to the engine speed, it has to be stable to this level, otherwise complex compensation techniques would be needed to try to 'focus' the lines, which would be categorised as very advanced target recognition techniques. Hence, JEM is best implemented for an aircraft moving at a constant engine speed and coming directly towards the radar, without any aspect angle change, allowing longer dwells to be utilised.

If the dwell time is too short, there is not sufficient frequency resolution to separate the spool lines. This is dependent upon the lowest likely engine speed, as the lines become closer as the engine speed drops. For example, if the minimum engine speed is 3000 rpm, then the minimum spool rate is 50 Hz. In order to separate lines as close as that, a measurement resolution of better than 25 Hz would be required. This corresponds to a minimum dwell time of 40 ms.

5.3.3.2   Sensitivity requirements for JEM measurement

Jet engine modulation involves the measurement and analysis of the radar returns from the jet engines of aircraft and utilises no other returns from the target. The engine has a rcs that is clearly less than that of the whole aircraft. Also as the JEM spectrum consists of a number spectral components, each one individually tends to be much lower in level than the sum of the JEM energy.

This means that the effective rcs associated with individual JEM lines is quite small in comparison to that of the whole aircraft, so detection of the individual JEM lines requires far more sensitivity than in detecting the whole target. A very simple

approach is now taken to show how low the effective rcs of the JEM line would be expected to be. A typical rotor blade on a fighter aircraft has a physical cross-section of about 4 cm × 25 cm in the plane perpendicular to the spool axis and in the direction of flight. This corresponds to an area of 100 cm^2 or 0.01 m^2. If there are 30 blades on the first stage then the total area of the first rotor blade stage is 0.3 m^2. If it is postulated that the average rcs of the rotor equates to its physical cross-section, as it is a metallic object, then the total rcs of the first rotor stage in 0.3 m^2. If 30 per cent of the energy reflected from this first rotor stage comprises each of the two fundamental chopping frequency harmonics, then the effective rcs of each of these is 0.1 m^2. This indicates that the main measurable JEM lines are about 20 dB or 1 per cent of the rcs of a conventional fighter aircraft, which would be expected to be about 10 m^2. Hence at least 20 dB extra sensitivity is needed to detect the main chopping lines in comparison to detection and tracking of the whole aircraft. In order to detect other harmonics of the main first-stage chopping frequencies, second-stage chopping frequencies or spool lines even more sensitivity is required, perhaps another 10 dB, depending upon the engine type, radar frequency and the aspect angle.

In order to improve the radar's sensitivity by 30 dB for performing JEM measurements, in comparison to normal detection and tracking, it can be obtained from a longer dwell period, by implementing it at a shorter range than the radar's detection range and by lowering the radar receiver's detection threshold. If, for example, the radar can detect a target with a 3 ms dwell period, for an extended dwell period of 300 ms for JEM, 20 dB of extra sensitivity is obtained. In order to gain a further 6 dB of sensitivity, the radar range at which JEM is implemented must be reduced, using the radar range equation, by the fourth root of 6 dB, which is about 71 per cent of the detection range. The additional 4 dB of sensitivity can be obtained by lowering the detection threshold in the receiver. As the target has been detected, there is no problem with detection false alarms, particularly as the sensitivity has been improved by 26 dB. The lowering of the threshold potentially gives rise to false JEM lines. However, if the false alarm rate has reduced to perhaps 10^{-4}, if 1000 frequency filters are present, then there is only a 10 per cent chance of one false line being generated over the whole of the JEM spectrum, which is considered to be acceptable.

Although the above analysis takes a fairly simple approach, it illustrates the key issues associated with the sensitivity required for making JEM measurements and provides techniques for achieving adequate range.

5.3.3.3   Spectral analysis and jet engine recognition

If the JEM measurement has been performed and a spectrum has been obtained with several spectral lines, as shown in Figure 5.26, analysis can now be performed [13]. Several approaches can be taken to establish the number of blades present on the various stages. The basis of all the techniques used is the analysis of the frequencies detected and the mathematical relationships between them. Analysis of JEM spectra can be considered to be a decoding activity, using principles based upon ratios between numbers, which are the blade counts on the rotor stages [14–16]. The method described here is a typical technique used and is summarised in Figure 5.27.

(a)

(b)

(c)

$f_1 f_2$ .... f_n

(d) f_1 f_2 .... f_n——▶ Determine common denominator, R, of frequencies

(e) $\dfrac{f_1}{R}$ $\dfrac{f_2}{R}$ .... $\dfrac{f_n}{R}$

(f)

$-2NR$ $-NR$ $+NR$ $+2NR$

Lower sideband chopping   Radar signal   Upper sideband chopping
frequency and harmonics   frequency   frequency and harmonics
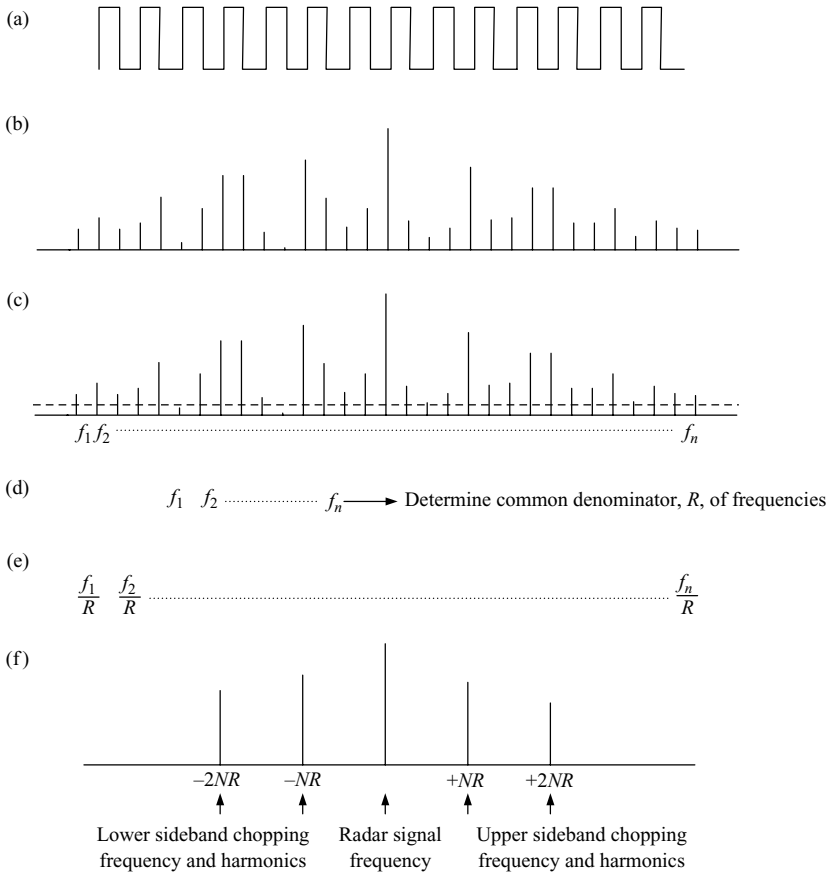
Figure 5.27   *Using JEM to extract number of blades on the rotor stage: (a) perform measurement of JEM spectrum with high prf waveform; (b) obtain unthresholded JEM spectrum; (c) threshold JEM spectrum end measure values of frequencies; (d) analyse values of frequencies and extract spool rate, R; (e) calculate ratio of each frequency to spool rate, R to give whole number; (f) chopping frequency components and harmonics of first rotor stage generally are among the highest signal amplitudes, enabling frequency NR and blade count N to be determined*

The first task is to extract the actual frequencies of the JEM spectral components. After thresholding, the frequencies of each of the spectral lines present are determined. The key frequencies to identify are the spool rate and the chopping rates of the rotor stages. As all the JEM lines detected are harmonics of the engine spool rate, the spool rate is found as it is the highest common factor that divides into all the JEM line frequencies.

After establishing the spool rate, all the spectral lines are divided by this quantity and should all be close to whole numbers. In practice, due to some JEM lines straddling

frequency filters, the change of engine speed over the radar integration period and the effects of noise, some calculated ratios deviate from whole numbers. Account has to be taken of these effects. The numbers can be rounded to the nearest whole number, or the nearest candidate whole numbers have to be considered and provide different blade count options.

In order to identify the chopping lines associated with the rotor stages, which are normally of a higher amplitude than the spool line harmonics, the larger signals should first be selected. As the chopping frequency components are grouped into upper and lower sideband pairs for each respective rotor stage and also have their associated chopping frequency harmonics, the larger amplitude spectral components meeting these criteria are the main candidates for chopping rotor components. Each of the higher amplitude spectral components has to be analysed for its potential to be one of the contributors to the main rotor stage chopping frequencies. If spectral components meet these criteria, the ratio of the fundamental chopping frequency to the spool rate gives an estimate of the blade count for the rotor stage. If other sets of frequency values meet these criteria, the ratios extracted provide further blade count values. However, as the signal is progressively reduced in amplitude, as it penetrates the engine, this analysis becomes much more difficult for stages beyond the first rotor. Perhaps only the upper and lower fundamental chopping frequency sidebands can be extracted, with the harmonics being at similar levels to the other spool rate lines. Any other large amplitude lines detected are likely to be mixing products associated with chopping frequencies of two different stages.

The estimates of the blade counts are then compared to the number of blades on known engines and the degree of correlation with one type of engine, and lack of correlation with others provides a measure of confidence of having identified the engine correctly. A database of blade counts of different engines would be structured as is shown in Table 5.3.

5.3.4   JEM summary

The basic theory of the use of JEM to analyse the spectral signatures of jet engines for recognition purposes has been presented. The measurements require a waveform with a high pulse repetition frequency and sufficient sensitivity must be available from the radar to analyse the spectral components of interest.

Table 5.3   Database of engine blade counts

Engine	Rotor stage 1	Rotor stage 2	Rotor stage 3
1	N_1	M_1	P_1
2	N_2	M_2	P_2
3	N_3	M_3	P_3
4	N_4	M_4	P_4

The frequency spectrum obtained is dependent upon the mechanical aspects of the engine's design, as well as considerations associated with the radar measurements. The signature measured depends on the factors which include the engine's rotation rate, the number of blades on the various compression rotor stages, the sizes and pitch of the blades, the air in-take to the engine and the radar wavelength.

The spectrum is analysed to extract components derived from the number of blades on the compression rotor stages of the engine and its rotation rate. Estimates are made of the numbers of blades on the various rotor stages and compared to the number of blades on the stages of known engines. The engine is recognised on the basis of the best match of the estimated parameters to those of the real engine.

In practice, additional complications are present, which make the task harder. If the aircraft is manoeuvring or accelerating the spectrum obtained can become blurred, making analysis of the spectral lines far more difficult. Many aircraft have more than one engine, so the spectra of multiple engines, which often run at different speeds, can get confused. Some engines have more than one shaft in the compression stage, which makes it more difficult to extract the spool rate, as there are different rotation rates present. The techniques described here have to be developed and extended for these complex situations, but the fundamental principles can still be followed.

Some engines have long air in-takes, which can reduce the level of signal both entering and emanating from the engine. Stealth technology is developing and the JEM signatures of military aircraft are expected to progressively reduce as measures are taken to reduce the level of signals reflected from the compression blades being emitted from the aircraft. It can be appreciated that there is considerable scope for the development of advanced JEM techniques to meet these increasingly difficult challenges.

It is also necessary to have an up-to-date database of the numbers of blades on the compression blade rotor stages on all engines of interest and the associated aircraft on which they are fitted. However, as the same engine can also be fitted to different aircraft, the recognition of the engine does not always determine the exact type of aircraft. Hence, other information has to be used to obtain a more precise estimate of the aircraft's identity. The other techniques described in this book such as range profiling or ISAR or the more advanced techniques to be covered in Chapter 6 can contribute to solving this problem.

5.4   Helicopter and jet engine recognition summary

Within this chapter, high-frequency resolution techniques, which do not require any high-range resolution measurement capability, have been described for recognising helicopters and jet engines. The radar signal frequencies and waveforms used for measuring the attributes of helicopters and jet engines have to be carefully designed from a knowledge of the target's general characteristics. The recognition of specific targets can only be performed if an up-to-date database is available, which includes all the target attributes of interest.

The recognition techniques rely upon the key mechanical aspects of the propulsion systems being known, such as dimensions of main rotating parts and rotation rates. By careful design it is possible to utilise the same waveforms and dwell times for both helicopters and jet engines, as fairly long dwell times with high pulse repetition waveforms are common to both measurement requirements.

The signal processing functions, feature extraction techniques and recognition methods are quite different for helicopters and jet engines, so parallel processing chains are needed for the two target sets.

References

1 BARNARD, R.H., and PHILPOT, D.R.: 'Aircraft Flight' (Longman Scientific and Technical, 1991) pp. 29–35
2 POULIGUEN, P., LUCAS, L., MULLER, F., QUETE, S., and TERRET, C.: 'Calculation and Analysis of Electromagnetic Scattering by Helicopter Blades', *IEEE Transactions on Antennas and Propagation*, 2002, **50** (10), pp. 1396–408
3 MISIUREWICK, J., KULPA, K., and CZEKALA, Z.: 'Analysis of Recorded Helicopter Echo'. *Radar 97*, 14–16 October 1997, IEE Publication no. 449
4 YOON, S.-H., KIM, B., and KIM, Y. S.: 'Helicopter Classification Using Time–Frequency Analysis', *Electronics Letters*, 2000, **36** (22), pp. 1871–2
5 GUOMING, Z., and RUIMING, Y.: 'New Method for Identifying Armed Helicopters'. Proceedings of *CIE International Radar Conference*, 8–10 October 1996, pp. 139–42
6 MISIUREWICZ, J., KULPA, K., and CZEKALA, Z.: 'Analysis of Radar Echo from Helicopter Rotor Hub'. Proceedings of the 12th International Conference on *Microwaves and Radar*, MIKON '98, Krakow, Poland, vol. 3, 20–22 May 1998, pp. 866–70
7 GREEN, H.E.: 'Electromagnetic Backscattering from a Helicopter Rotor in the Decametric Waveband Regime', *IEEE Transactions on Antennas and Propagation*, 1994, **42** (4), pp. 501–9
8 BARNARD, R.H., and PHILPOT, D.R.: 'Aircraft Flight' (Longman Scientific and Technical, 1991) pp. 163–7
9 ROLL ROYCE plc: 'The Jet Engine' (Rolls Royce plc, Derby UK, 1986)
10 MARTIN, J., and MULGREW, B.: 'Analysis of the Theoretical Return Signal from Aircraft Propeller Blades'. IEEE International *Radar Conference*, Brighton, UK, 1990
11 MARTIN, J., and MULGREW, B.: 'Analysis of the Effect of Blade Pitch on the Return Signal from Rotating Aircraft Blades'. IEE *Radar* 92 International Conference, Brighton, UK, 1992, pp. 446–9
12 http://mathworld.wolfram.com/SamplingTheorem.html
13 BELL, M.R., and GRUBBS, R.A.: 'JEM Modelling and Measurement for Radar Target Identification', *IEEE Transactions on Aerospace and Electronic Systems*, 1993, **29** (1), pp. 73–87

14   PARDINI, S., PELLEGRINI, P.F., and PICCINI, P.: 'Use of Target Spectrum for Detection Enhancement and Identification'. AGARD Conference, Ottawa, Canada, 1994

15   SCHNEIDER, H. 'Application of an Autoregressive Reflection Model for the Signal from Analysis of Radar Echoes from Rotating Objects'. IEE International *Radar* Conference, RADAR-87, London, UK, 1987, pp. 279–82

16   CUOMO, S., PELLIGRINI, P.F., and PIAZZA, E.: 'Model Validation for Jet Engine Modulation Phenomenon', *Electronics Letters*, 1994, **30** (24), pp. 2073–4

Chapter 6

Other high-resolution techniques

6.1   Introduction

Within this chapter other high-resolution radar techniques are presented, which can either supplement the techniques discussed in the earlier chapters of the book or are particular extensions or applications of these techniques.

The 'super resolution' techniques trade signal-to-noise ratio for resolution and can achieve much higher resolution than the limits defined by the Rayleigh criterion. Super resolution techniques are discussed in Section 6.2 and can theoretically improve any high-range resolution measurement performed using radar, providing sufficient signal-to-noise ratio is available. However, in most radar applications it is not the case, as signal-to-noise ratio tends to be a critical issue in its own right, so it is used only in particular situations. The effectiveness of super resolution techniques in radar target recognition is application-dependent and is very much under investigation, as the subject continues to develop.

Monopulse could be classed as a type of super resolution technique, which provides high cross-range resolution using a real aperture, rather than the synthetic aperture techniques previously described. It utilises a high signal-to-noise ratio to significantly improve on the cross-range resolution, which would normally be obtained at lower power signal levels using the Rayleigh criterion for determining resolution. Monopulse techniques for enhancing cross-range resolution are presented in Section 6.3.

Polarisation techniques can provide additional 'dimensions' of data gathered using high-range and high-frequency resolution techniques. Some particular shapes of object have specific reflection characteristics, which are dependent upon the polarisation direction of the incident electric field vector. The received signals can be analysed for polarisation vector content and provide estimates of the object shape, which can be used in the target recognition process. The application of polarisation techniques in radar target recognition is discussed in Section 6.4.

An extension of both high-range and high-frequency resolution techniques, which were described separately previously, is to perform these measurements simultaneously. The combined high-range and high-frequency resolution method provides signature data presented in a two-dimensional target matrix, which can provide more data than with the measurements performed separately. This high-resolution technique is described in Section 6.5.

Impulse and ultra high-range resolution radar methods are both types of high-range resolution technique, which utilise very large bandwidths of typically several giga hertz. They would normally only be permitted to transmit at very low power levels, as they would interfere with other electronic systems in the same frequency bands, such as telephones, communications or emergency services. For this reason they are limited to very short-range applications, such as the detection of abandoned landmines. These techniques are presented in Section 6.6.

6.2   Super resolution techniques

6.2.1   Conventional resolution

Before presenting super resolution, conventional resolution techniques are recapitulated. An example of the normal resolution criterion used in radar for separating two point targets in angle is shown in Figure 6.1. If two point targets are separated in angle by two antenna beamwidths, with each located at the centre of the antenna beam pattern, they can just be resolved as individual targets or scatterers. The radar detects two distinct point targets for the two outer-beam positions, A and C, with no
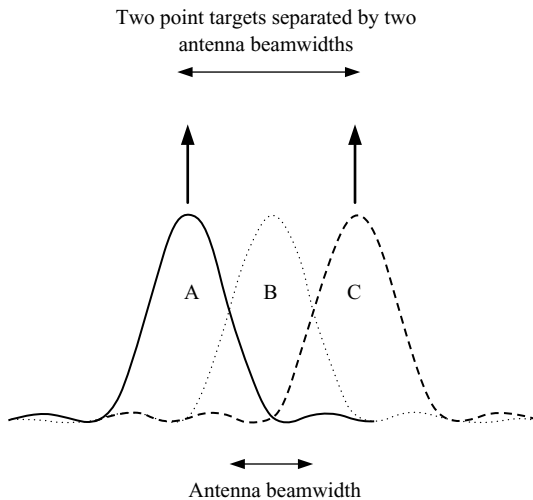
Figure 6.1   Conventional resolution criterion: two point targets, which are two antenna beamwidths apart can just be separated in angle

Targets are located at centres of range gate 2 and range gate 3, respectively
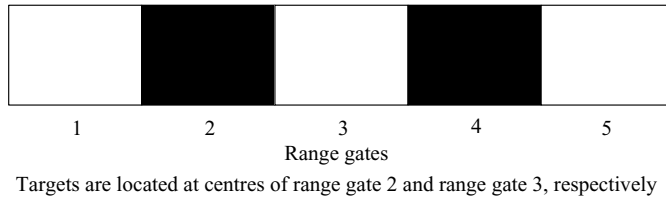
Figure 6.2   Conventional resolution criterion: returns from range gates 2 and 4 separated if no returns detected in range gate 3

detection for the central beam position, B. When the antenna is at position B, the gain at angles corresponding to the two targets is too low to detect them. This is a somewhat idealised situation and would represent a radar transmitting signals sequentially at positions A, B and C, as the antenna scans.

These resolution criteria can be applied to any type of radar measurement. For example, for resolving two scatterers in range, for target recognition applications, a criterion of one range gate with no detections between two neighbouring range gates having detections is a typical criterion used, as illustrated in Figure 6.2. The resolution is determined solely by the bandwidth of the pulse employed. Two scatterers centred in range gates, which are two range gates apart, are at the closest differential range, at which they can be separated and represent the resolution limit achievable, using conventional techniques.

Similar criteria can be used for cross-range resolution and spectral resolution in JEM for separating detection contributions, such as one clear Doppler filter between frequency returns.

6.2.2   Closely spaced targets

Consider three targets separated in angle over one antenna beamwidth, as shown in Figure 6.3. In this example it is assumed that only the amplitudes of the signals are used to illustrate super resolution for explanatory purposes. Super resolution techniques discussed below are readily applicable to targets with different phases, but the inclusion of interference effects here between different targets would overcomplicate the explanation. For the three consecutive radar dwells, the antenna beam positions are shown. If all the other radar parameters measured are the same for the three targets shown, which are very close in angle, they would not normally be resolved by the radar using conventional detection and signal processing techniques. They are within about one beamwidth of each other and the radar returns in angle would follow the envelope of the composite signal comprising contributions from the three targets.

As the radar samples at discrete positions as it rotates, it would detect returns from target 1 only in position A, as returns from targets 2 and 3 would be at a very low level, due to the low antenna gain at those angles.

At position B the highest radar signal would normally be detected, unless the returns from the three targets destructively interfered with one another, which is
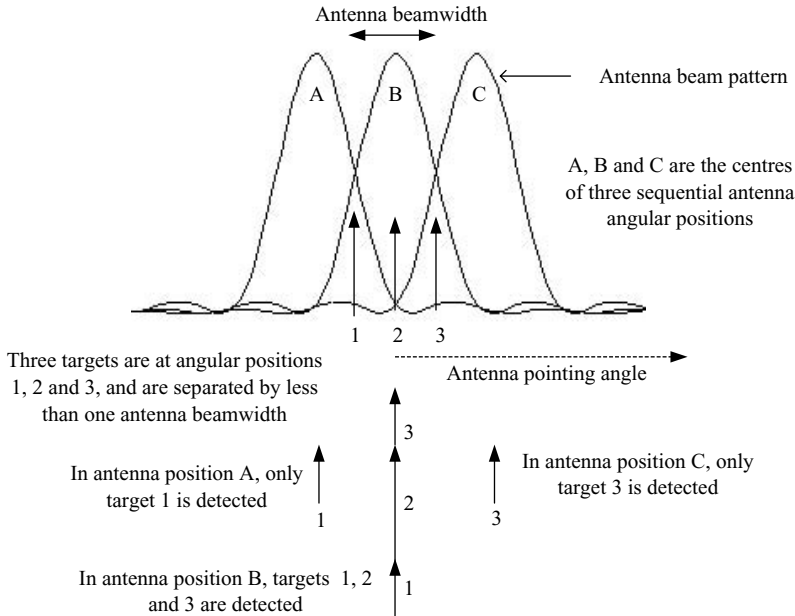
Figure 6.3   Three targets within one beamwidth are not resolved using conventional techniques. Three sequential beam positions are shown

rather unlikely. All three targets are in the antenna beam at position B. Target 2 is at the beam centre and targets 1 and 3 are also in the beam, albeit at lower gain levels.

In position C, only returns from target 3 are detected, as the antenna has very low gain at the positions corresponding to targets 1 and 2.

Hence, the returns, as viewed by the radar at the three consecutive beam positions, would be continuous. It would not be possible to determine how many targets were present. It could be a long continuous target or one or more discrete targets. Hence, using conventional resolution criteria, the three targets would not be separated.

6.2.3   Application of super resolution techniques

Super resolution is now discussed and is used to obtain higher resolution than with using the conventional radar techniques just described. The basis of the super resolution techniques is to sample the target data more rapidly and to utilise knowledge of the characteristics of the antenna gain with angle, for example.

In Figure 6.4, the composite returns of the three targets of Figure 6.3 are shown, as the antenna sweeps through them. This characteristic is actually a convolution of the antenna pattern through the targets. This is represented mathematically as $G*T$:

$$G*T = \int T(\theta)G(\phi - \theta)d\theta \tag{6.1}$$
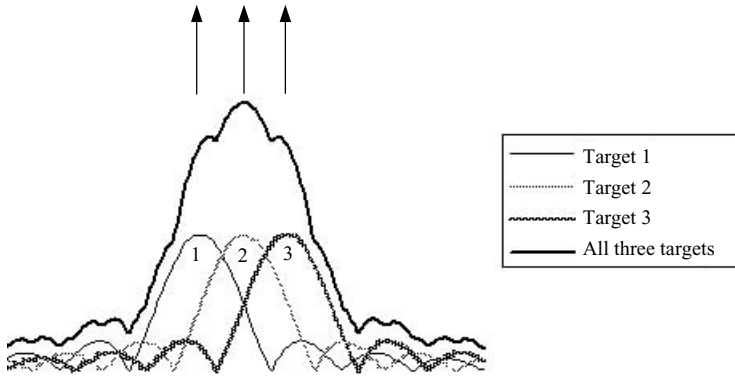
Figure 6.4   Composite radar return versus angle for three point targets (of Figure 6.3) positioned within one beamwidth

where $G(\theta)$ is the antenna gain as a function of angle and $T(\theta)$ is the complex target reflection coefficient with angle.

This is a continuous mathematical function, but in practice the signal is sampled discretely. The discrete amplitude characteristic for this example is shown in Figure 6.5. The phase characteristics are also normally utilised, but are not shown in this simple example. The sample points shown in the figure are at the antenna pointing angles when measurements are taken. It can be seen that in comparison to conventional radar sample with antenna angle, far more antenna angular pointing positions are utilised. The absolute minimum sample rate for an antenna would normally be in steps of one-half of a beamwidth to ensure that all targets can be detected. For super resolution this would be increased by one or two orders of magnitude.

With reference to Figure 6.5, the antenna pattern is known, which is shown in Figure 6.5(b), and a complex characteristic of the targets has been measured. Equation (6.1) states that the result shown in Figure 6.5(a) is the convolution of the target returns with the antenna pattern. If this resultant characteristic is designated, $R(\theta)$, then the actual target characteristics $T(\theta)$, relate to the antenna pattern and $R(\theta)$, as $R(\theta) = G(\theta){*}T(\theta)$. In order to determine the value of the target characteristic, $T(\theta)$ involves a 'de-convolution' operation. Effectively, the function $T(\theta)$ has to be estimated as the unknown function, which when convolved with the known function $G(\theta)$ produces $R(\theta)$. As the antenna characteristics are known and radar returns from targets have been measured, the de-convolution operation calculates the target characteristics, which when convolved with the antenna characteristics generate the radar returns, which have been measured. The reference function, which is analogous to the reference antenna characteristic, for general applications, is called the point spread function.

In practice, de-convolution is not perfect and distortion occurs in the resulting target image. This occurs because noise is present in the received data and would be included in the samples shown in Figure 6.5(a). The de-convolution process de-convolves the noise as well as the target data and causes distortion to the resulting target image.

(a)

(b)

(c)
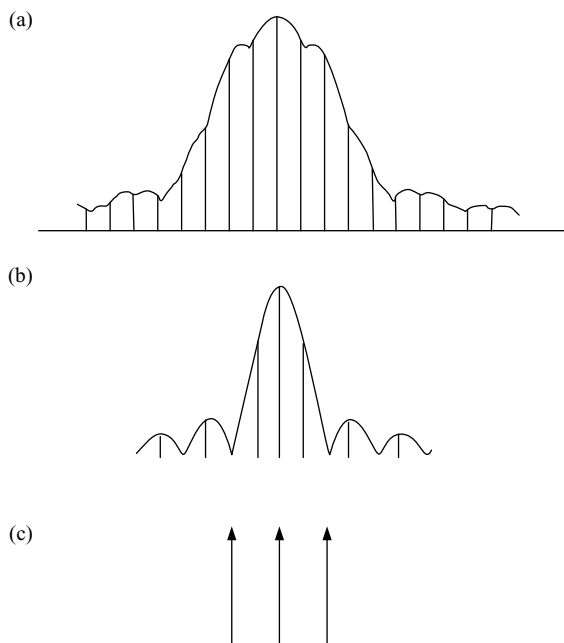
*Figure 6.5   Discrete samples of radar returns and reference characteristics, such
as antenna patterns, are used in super resolution. Example shown
is discretely sampled version of Figure 6.4: (a) amplitude char-
acteristic is discretely sampled as antenna sweeps through targets;
(b) discretely sampled amplitude characteristic of antenna versus angle;
(c) if de-convolution operation is successful, amplitude and phase
characteristics of targets versus angle are obtained*

Various mathematical methods are available to perform de-convolution [1,2].
They rely upon data being oversampled, as discussed above, or by combining several
low-resolution data sets. In qualitative terms, the higher the level of oversampling, the
greater the amount of data obtained and the higher the level of improved resolution
can be obtained. The techniques also require relatively high signal-to-noise ratios in
comparison to those normally needed for target detection, for example.

Two very popular super resolution techniques used in image processing are the
MUSIC [3,4] (MUlti SIgnal Classification Method) and CLEAN algorithms. The
CLEAN method was originally developed by Hogbom [5] for improving radio-
astronomy images obtained using radio telescopes and various improvements have
subsequently been implemented [6,7]. With reference to the amplitude characteristic
shown in Figure 6.5(a) the operations for the most basic function of the CLEAN
algorithm follow and are shown in Figure 6.6. It is assumed that point sources are
present in the data although the algorithm can work well with extended sources.
Figure 6.6(a) is known as the dirty map, which is $R(\theta)$ in this example. The CLEAN
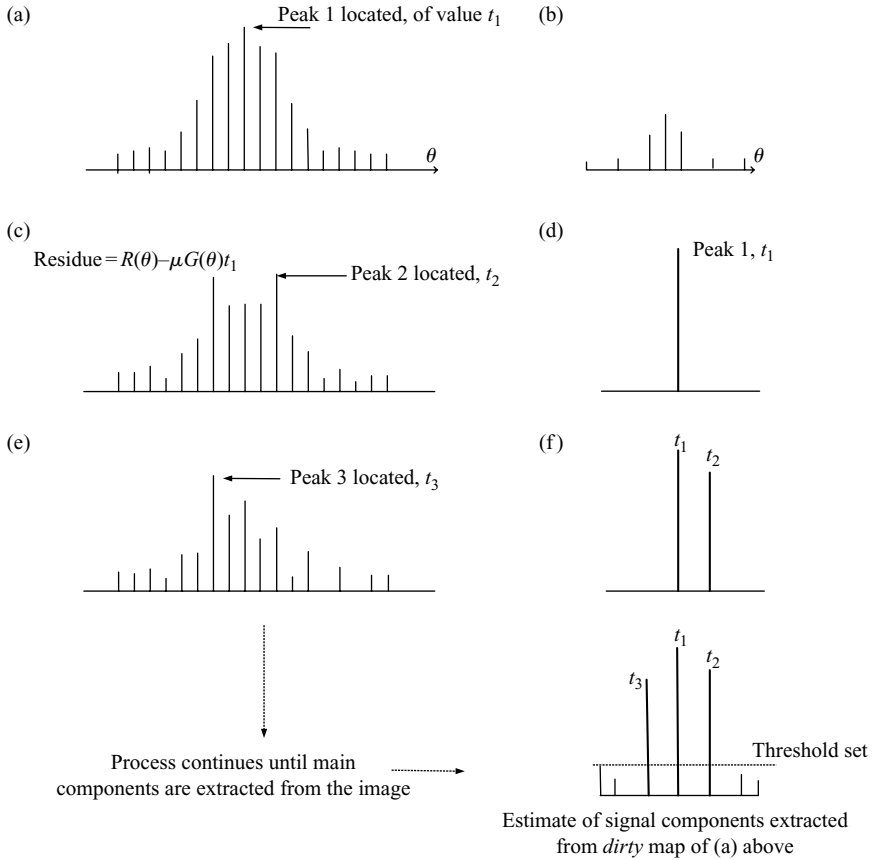
Figure 6.6 CLEAN algorithm operations: (a) dirty map, $R(\theta)$: discretely sampled characteristics of signal. Peak amplitude is located; (b) discretely sampled reference antenna pattern, $G(\theta)$. It is multiplied by μ and t_1, and then is subtracted from (a); (c) residual pattern after multiplying (b) by μ and t_1 and subtracting from (a); (d) first component of CLEAN image, t_1, following identification and positioning of peak in (a); (e) residual pattern after multiplying (b) by μ and t_2 and subtracting from (c); (f) first and second components of CLEAN image following identification of peaks and their locations in (a) and (c)

algorithm constructs discrete approximations $T_n(\theta)$ to the CLEAN map required, from the convolution:

$$G(\theta) * T_n(\theta) = R(\theta)$$

The CLEAN algorithm starts with an initial value of $n = 0$ corresponding to $T_0(\theta) = 0$, which means that no peaks have yet been extracted from the dirty map.

At the nth iteration, it then searches for the highest value in the residual map:

$$R(\theta) - \mu G(\theta) * T_{n-1}(\theta)$$

where $T_n(\theta) = t_n(\theta) + t_{n-1}(\theta) + \cdots + t_1(\theta)$ are the values of the extracted peaks after n iterations. μ is a number less than 1 and is called the loop gain or damping factor. $T_n(\theta)$ is the estimate of the CLEAN map after n iterations.

Initially the position of the peak amplitude is identified and its associated amplitude, t_1, is measured as in Figure 6.6(a). The antenna array pattern of Figure 6.6(b), $G(\theta)$, is now taken and multiplied by μ. It is then multiplied by the value of the peak signal, t_1. This is positioned at the location of the peak amplitude identified at the appropriate angle, θ, and is subtracted from the pattern in Figure 6.6(a).

The residue, $R(\theta) - \mu G(\theta)t_1$, from these operations is shown in Figure 6.6(c) results. This operation identifies the estimated largest contributor to the image and subtracts its effect in a first iteration. Its position and amplitude are shown in Figure 6.6(d), in which the new CLEAN image is being constructed. The operation is repeated on the residual image in Figure 6.6(c) and the largest peak is again identified and positioned. The antenna reference pattern from Figure 6.6(b) is multiplied by μ and t_2 and then is subtracted from Figure 6.6(c) to form the next residual image shown in Figure 6.6(e). The position and amplitude of the second peak are now shown in Figure 6.6(f) with the first peak, and the CLEAN image is beginning to form. These operations continue until all the residue amplitudes lie below a specified level which would normally be related to the noise level in the image. In this example the three peaks of Figure 6.4 should eventually appear as the main point source images and a threshold level is also shown.

This process is not perfect and the effects of noise present in the data result in errors in the resultant image, so the actual values of the signal components vary from their real values.

6.2.4 Discussion on super resolution

Down-range, cross-range and JEM frequency measurements can all be improved using super resolution techniques. If super resolution techniques are being applied to a high-resolution range profile, in very general terms, improvements in range resolution would be dependent upon individual scatterers having sufficient signal-to-noise ratio. For improving high-range resolution, the oversampling can be regarded as trying to synthesise a larger bandwidth on receiving the radar returns. The super resolution techniques also tend to rely upon there being a limited number of radar scatterers present. If noise were not present, as with most aspects of radar, de-convolution would be far simpler. When noise is present there can be large numbers of possible mathematical solutions. Usually the lowest number of targets or scatterers that provides a consistent solution to the problem would be used. It will be seen in the references that the improvements in image quality obtained with super resolution are very dependent upon the actual target of interest. For general guidance [8], when high precision measurements are made on point scatterers, for example, accuracy tends to improve as the square root of the signal-to-noise ratio utilised. Similar considerations apply to

super resolution for targets with only a few scatterers. Although for high-resolution radar imaging applications, such as SAR, super resolution techniques are being investigated for improving range resolution, there is some concern about its effectiveness. Other references of super resolution techniques are provided at the end of the chapter [9–17]. Reference 18 is particularly critical about its benefits for target recognition purposes.

One type of super resolution technique, which has been used in radar for several decades and is undeniably most successful, is monopulse, which is covered in the next section.

6.3   Monopulse

6.3.1   Introduction

Monopulse radar techniques are so called as they can obtain the angle of arrival of a signal from measurements on a single detected pulse. They are used in tracking radars for measuring the angle of a target relative to the radar antenna's bore-sight, normally in both azimuth and elevation. This information is then used in a control loop to feed back the error signal to the antenna servo controls to maintain the target as close as possible to the antenna bore-sight. In addition, the target range and range rate are also tracked and the target is said to be in lock.

Monopulse techniques are generally used in weapons systems, in which the radar locks onto the target. Several types of weapon system architectures can be used. The radar can be located on land, on a ship or aircraft and acts as the fire control radar to maintain track on the target and this information is communicated to the missile for guidance and homing purposes. It could be located on-board the missile in a fire and forget mode, so that all the tracking of the target is performed on the missile with error signals from the monopulse being used by the missile's guidance system to maintain course to intercept the target.

For target recognition purposes, the angular information available from the monopulse can be used to obtain cross-range information on the target scatterers.

6.3.2   Background to monopulse techniques

6.3.2.1   Introduction

Monopulse radar techniques are used for obtaining angular information on the target's position with relatively high precision. Two main types of techniques have been employed, amplitude and phase comparison monopulse [19–23].

6.3.2.2   Phase comparison monopulse

The basis of the phase comparison monopulse techniques is to divide the antenna into four quadrants, enabling measurements of angle to be made in both azimuth and elevation. The four quadrants of the antenna have gain patterns, which are nominally identical. The amplitudes of the signals received in each quadrant are the same and
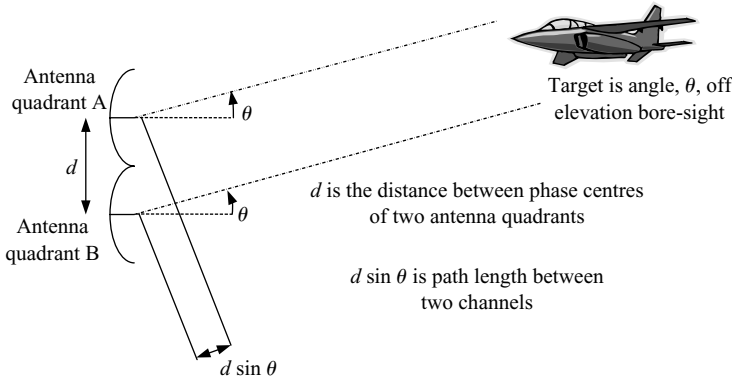
Figure 6.7   Phase comparison monopulse. Two quadrants of the antenna are shown for obtaining the target's elevation angle

are independent of the target's angular position. However, for off bore-sight targets, the phases of the signals at each quadrant differ. The monopulse phase comparator techniques determine these phase differences and use them to calculate the azimuth and elevation angles of the target. The monopulse concept is shown in Figure 6.7 for two quadrants of the antenna.

The phase difference measured between the two antennas is dependent upon the angular offset, θ, of the target from bore-sight. For antennas with their respective phase centres separated by a distance, d, the electrical path length difference is $d \sin \theta$, which is a phase difference of $2\pi d \sin \theta / \lambda$. For the small offset angles, θ, which are of interest, the phase difference between the two channels is approximately $2\pi d\theta / \lambda$. Hence, the phase difference between the channels is proportional to the angle of the target from bore-sight and this is the error signal, which is used in the servo control loop for tracking the target. Different receiver channels are used to extract this phase information. Phase comparison monopulse techniques can also form the basis for high-resolution cross-range measurements, which will be discussed later in this section.

6.3.2.3   Amplitude comparison monopulse

The amplitude comparison monopulse techniques use separate antenna beams, which have phase centres, which are nominally colocated. For obtaining azimuth and elevation angular data on the target, four antenna beams are used, each of which is slightly offset from bore-sight by the same angle with their beam patterns normally being symmetric about bore-sight. A four-horn monopulse system is shown in Figure 6.8.

Each horn, in the cluster shown at the focus of the antenna, generates an antenna beam pattern, which is centred slightly off the antenna's bore-sight. A microwave signal combining network is connected to the horn cluster to provide three signal channels, which facilitates the generation of the transmitted signal and the receiving channels needed for conditioning and processing the signals for extracting the target's
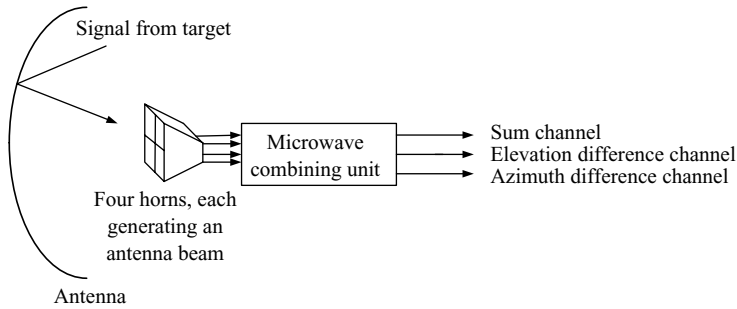
Figure 6.8 *Amplitude monopulse comparator antenna concept. Four antenna beams are formed to generate the sum and two difference beams on receive*
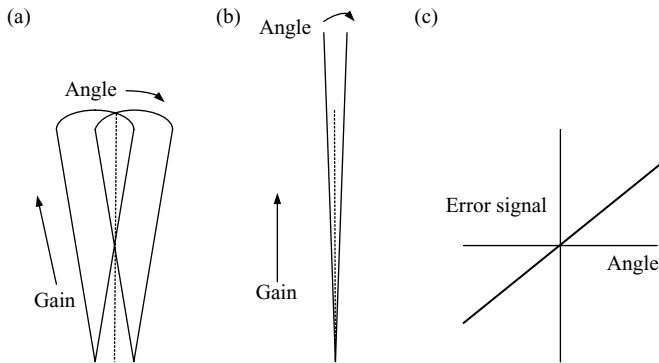
Figure 6.9 *Amplitude monopulse antenna beam characteristics: (a) overlapping beam patterns from two pairs of horns; (b) sum beam pattern of two beams in (b) has higher gain and narrower beamwidth than (a); (c) difference beam pattern of two beams in (a) near bore-sight*

range and angular data. The sum pattern is used on both transmitting and receiving and is a summation of the contributions of the four beams. As the four horns are in close proximity, there is negligible phase difference to the target between the four beams. The elevation difference channel is formed by subtracting the sum of the outputs of the two lower horns from the sum of the upper two. Similarly, the azimuth difference channel is formed by subtracting the sum of the two left horn outputs from the right horn outputs.

The antenna beam patterns utilised in amplitude monopulse are shown in Figure 6.9. In Figure 6.9(a) are the beam patterns from two pairs of horns and they can be seen to partially overlap. In addition to the pattern shown, which could be the elevation characteristics, for example, there would be the azimuth beam characteristics. In Figure 6.9(b) is the sum beam pattern, formed by combining the two beams in Figure 6.9(a). As amplitude monopulse does not use phase information, this beam

pattern is the sum of the amplitude patterns of the contributing beams. In Figure 6.9(c) the difference pattern for the two beams in Figure 6.9(a) is shown. This is the result of subtracting one of the beam patterns in Figure 6.9(a) from the other one. Although amplitude monopulse does not specifically employ phase information, it can be seen that the difference characteristics can have a positive or negative value, depending upon which side of bore-sight the target is located. This has to be taken into account in the processing of the signal data, to ensure that the error signal, which is used to track the target, has the correct polarity.

The essence of the amplitude monopulse techniques is to measure the amplitudes of the signals in the sum channel and in the difference channels. The ratio and polarity of these values enable the point on the beam characteristic shown in Figure 6.9(a) to be determined, and hence the angle offset from the antenna's bore-sight. At bore-sight, the highest level of sum channel signal is received and theoretically no signal in the difference channel is received, apart from noise contributions. The accuracy of the measurement of target angle is typically the antenna beamwidth divided by the square root of the signal-to-noise ratio. For the higher values of difference channel signal-to-noise, which are obtained off-bore-sight, the corresponding angular accuracies are higher than those measured close to bore-sight. The beamwidth of the sum channel is less than for the two horn patterns in Figure 6.9(a) and has higher gain. The difference beam characteristic shown in Figure 6.9(c) is linear near bore-sight.

The functions employed in the radar receiver to extract the target's range, azimuth and elevation angles are summarised in Figure 6.10. The sum channel signal undergoes conventional down-conversion and digitisation and signal processing, enabling the target's range to be measured. If several pulses are coherently integrated, the Doppler frequency can also be extracted.
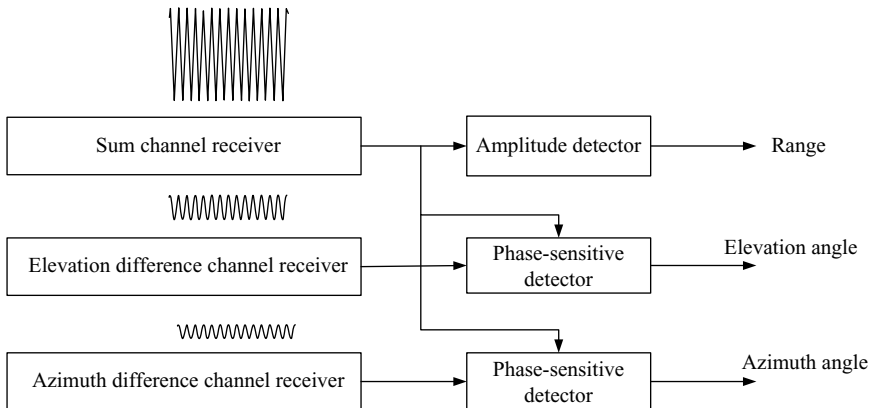
Figure 6.10   Extracting target range, elevation and azimuth angles from amplitude monopulse comparator. Phase-sensitive detector measures amplitude of difference channel signal relative to sum channel signal and determines relative polarity of signals

The difference channel signals are also down-converted and are used, in conjunction with a sample of the sum channel signal, for extraction of the target's angular position [24]. The phase detector determines the relative amplitude and polarity of the sum and difference signals, enabling the point on the monopulse characteristic of Figure 6.9, corresponding to the target's angle, to be established. This is performed on both the azimuth and elevation difference data, so that the target's angles, range and Doppler frequency can be measured. In order to correlate the data from a single target in the three receiver channels, the common time delay is used.

For conventional low-range resolution radar tracking applications, a low bandwidth waveform is used and the target signature details would not be resolved, with most of the energy appearing in a single range gate. The azimuth and elevation angles measured would normally be approximate averages of the target's position. (Sometimes interference between returns from different scatterers occurs and errors in angle result, which is a condition known as glint [25].)

The application of monopulse techniques for target recognition is discussed in the next section.

6.3.3 Application of monopulse techniques to target recognition

The monopulse techniques described above have been designed to track a single target and to hold it close to the antenna bore-sight (Figure 6.11). This process has traditionally been a relatively low-range resolution radar application and has not generally
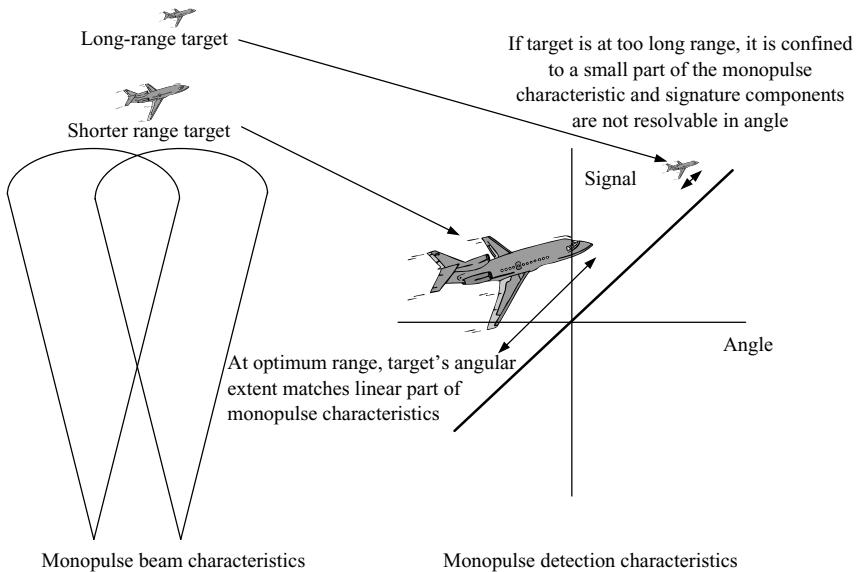

Figure 6.11   Applying monopulse techniques for target imaging: dimensions of target must be similar to overlap between antenna beams for optimum imaging

been used as a target recognition function. The ability to measure the angles of targets very accurately provides an opportunity to develop these techniques for target recognition. This basic design concept for monopulse has to be developed to enable high-resolution target signatures to be obtained and can use either the amplitude or the phase comparator monopulse technique. The first requirement is to employ a high-range resolution waveform, which can provide a high-resolution range profile of the target. The monopulse radar has to be designed to generate wideband waveforms and to digitise and process them. By applying the standard monopulse signal conditioning and processing operations to this wideband waveform, a high-resolution range profile is generated in the sum channel.

In order to optimally apply monopulse to a single target, the cross-range width of the target must be similar to the angular extent of the overlap between the monopulse beams at the ranges of interest, and the signals received are on the linear part of the monopulse characteristic. If the angle of the target subtended at the radar is too small, it is then confined to a small part of the monopulse angle characteristics and components of the target signature are not resolvable. Amplitude comparison monopulse is now used to illustrate the technique.

For target imaging, it is the rcs of each target element in the range profile, which determines the sensitivity of the measurements, rather than the whole rcs of the target, as in normal tracking monopulse. Each high-resolution gate range of the target's range profile undergoes the monopulse comparison of sum and difference channels, as shown in Figure 6.12. For each range gate the amplitudes and polarities of the signals in the sum and the difference channels are compared and mapped onto the monopulse angle characteristics. For each range gate, single values of signal amplitude, elevation angle and azimuth angle are obtained respectively.

From a knowledge of the target's range, the elevation and azimuth angles for each range gate can then be used to provide the range scaling required to generate
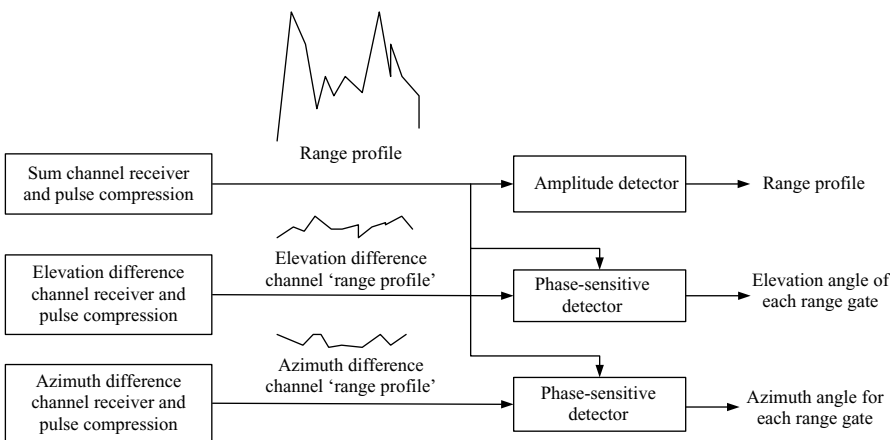
Figure 6.12   Application of monopulse to high-resolution target imaging
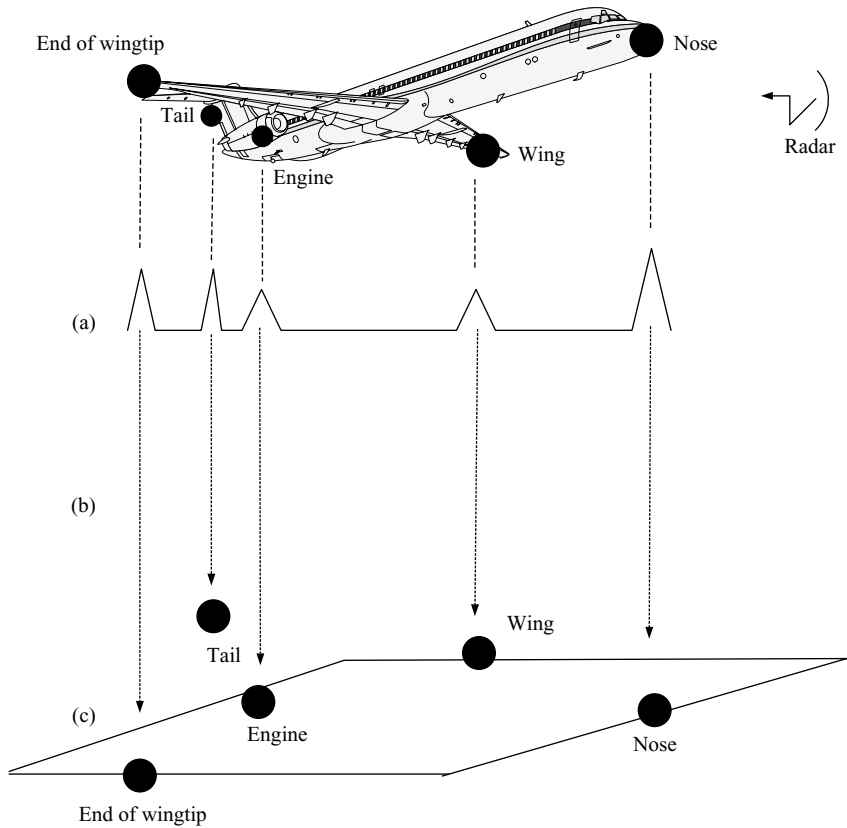
*Figure 6.13   Obtaining a three-dimensional target image using high-range res-
olution monopulse. Five scatterers are shown: (a) range profile;
(b) monopulse process: elevation and azimuth position of each range
gate identified; (c) construction of three-dimensional target image*

a three-dimensional image of the target. This process is summarised in Figure 6.13
using a simple example. The high-resolution range profile of the aircraft is first
obtained from the monopulse sum channel.

Five scatterers have been identified for illustrative purposes. The monopulse
process is performed for each scatterer and its position in azimuth and elevation is
estimated. The three-dimensional target image is then constructed. Image processing
techniques can then be used for recognising the target.

6.3.4   Discussion on application of monopulse to target recognition

The employment of monopulse techniques in radar target recognition is very much in
its infancy. There are several critical issues, which have to be addressed for practical
applications.

A key point presented earlier was the application range. From both the angular resolution and the signal-to-noise ratio requirements, application ranges are likely to be restricted to several hundred metres or possibly a few kilometres for typical radars. For example, a radar with a 1 m aperture, operating at 10 GHz, has a beamwidth of about 2° and would have a range of several tens of kilometres on small aircraft targets. A typical monopulse comparator can probably achieve an angular resolution of one hundredth of a beamwidth under the most favourable conditions. If cross-range resolution of one half of 1 m is required, this would then be obtained at a maximum range of about 3 km. This is very short in comparison with the radar's normal application range.

Another important issue is multiple scattterers being in the same range gate of the range profile. The monopulse process described only has the capability to assign the received signal in one range gate to one elevation angle and one azimuth angle. If more than one scatterer is present an averaging effect would occur and the contributing signature data would be placed at a single elevation angle and a single azimuth angle, so would distort the three-dimensional target image. If sufficient range resolution is present, these effects can be reduced. Individual scatterers are more likely to be isolated and localised to separate range gates as range resolution improves.

6.4   Polarisation

6.4.1   Introduction

The polarisation of a radar signal is defined as the direction of the electric field vector of the electromagnetic wave, as it propagates. In Chapter 2, the propagation of radar signals was discussed with the electric and magnetic field vectors shown to be in a plane orthogonal to the direction of propagation of the wave. The electric and magnetic field vectors are also orthogonal. For radar signals propagating under normal conditions through the earth's atmosphere or through space, these three vectors remain mutually orthogonal. Radar signals are normally transmitted with the electric field vector either in the horizontal or vertical plane, as shown in Figure 6.14. These electromagnetic waves are defined as having linear polarisation. The electric (and magnetic) field of the wave is varying with time and distance, as it propagates, in accordance with Equation (2.3). For a linearly polarised wave the direction of the electric field vector remains in the same plane as the wave propagates.

The reflection characteristics of targets, when subjected to signals with different polarisations, are of interest for target recognition and are discussed in the next section.

6.4.2   Polarisation matrix

The polarised signals shown in Figure 6.1 of both horizontally and vertically polarised signals, which do not necessarily have the same amplitudes. Some examples are shown in Figure 6.15. The resulting polarisation is due to the amplitudes of the vertical and horizontal components and their relative phases. The respective 'pure' horizontal and vertical polarisations in Figure 6.15(a) and (b) are due to just one component of the
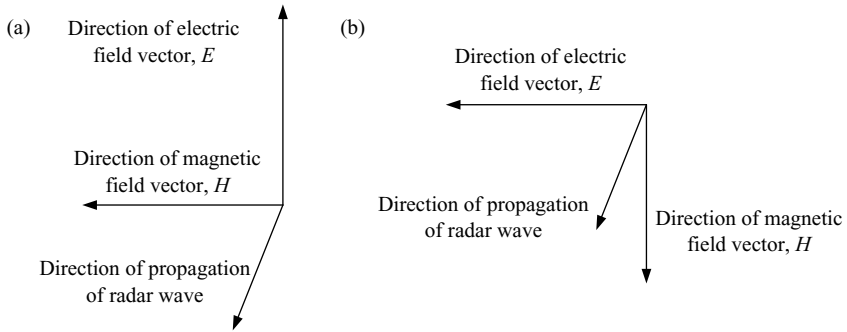
E and H vectors are in plane of page. Direction of propagation is out of page.

Figure 6.14   *Radar waves with vertical and horizontal polarisation: (a) vertical polarisation: electric field has vertical directionality; (b) horizontal polarisation: electric field has horizontal directionality*
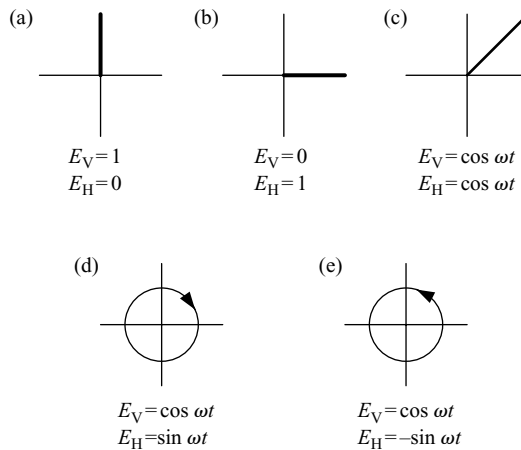
Figure 6.15   *Polarisation of typical radar signals: (a) vertical polarisation, (b) horizontal polarisation, (c) linear polarisation at 45°, (d) left-hand circular polarisation and (e) right-hand circular polarisation*

electric field having an amplitude. If the horizontal and vertical components are equal and are in phase, the linearly polarised signal shown in Figure 6.15(c), at 45° results. When the components are equal in amplitude, but are 90° out of phase, circularly polarised signals result, as shown in Figure 6.15(d) and (e). The combination of the sine signal and the cosine signal from the respective vertical and horizontal axes generates an electric signal vector which has a direction that varies continuously at

the signal's frequency. The electric field vector rotates around in a circle, so is named a circularly polarised signal. Depending upon the relative phasing between the sine and cosine signals, the resulting electric field vector can go around in the two separate directions, which are defined by convention as left- and right-hand polarisation.

The circularly polarised signal is therefore composed of two orthogonal linearly polarised signals.

In order to provide a measure of how targets, or component parts of targets, reflect radar signals with different polarisations, a concept called a polarisation matrix, is defined. All polarised signals can be resolved into vertical and horizontal components. In addition, as circularly polarised signals are also composed of vertical and horizontal electric field components, any polarised signal can also be resolved into right- and left-hand circular components.

Hence, in order to study a target's polarisation characteristics, it is necessary to sequentially illuminate it with signals having the two different polarisation vectors. These can be either the vertically and horizontally polarised signals or the two circularly polarised signals. The signal reflected from a target, when illuminated by a signal with a single polarisation component, can have components of both polarisations.

A target has two reflection components for each of the two polarisations, which can be applied to it. Hence, there is a total of four polarisation components, which are needed to fully describe a target's polarisation characteristics, which is called the target's polarisation matrix. This is illustrated in Figure 6.16. In Figure 6.16(a) a vertically polarised signal is applied to the target and both vertically and horizontally
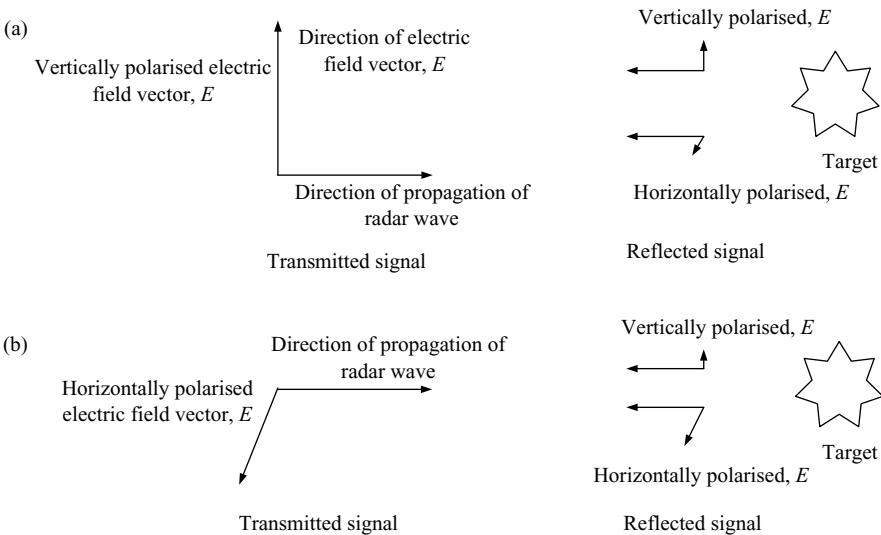
Figure 6.16 *Polarisation matrix components reflected from target: (a) transmitting in vertical polarisation and receiving in vertical and horizontal polarisation; (b) transmitting in horizontal polarisation and receiving in vertical and horizontal polarisation*

polarised components of the reflected signal are generated. Figure 6.16(b) shows the equivalent reflected components for a horizontally polarised incident signal.

Mathematically the polarisation matrix is defined as:

$$E_H^R = S_{11}E_H^T + S_{12}E_V^T$$
$$E_V^R = S_{21}E_H^T + S_{22}E_V^T$$

(6.2)

where E_H^R is the reflected horizontal polarisation component of the electric field, E_H^T is the transmitted horizontal polarisation component of the electric field, E_V^T is the transmitted vertical polarisation component of the electric field, E_V^R is the reflected horizontal component of the electric field and S_{11}, S_{12}, S_{21} and S_{22} are the polarisation matrix components.

The matrix is stated as:

$$\begin{bmatrix} S_{11} & S_{12} \\ S_{21} & S_{22} \end{bmatrix}$$

The values, S_{11} and S_{22} are designated the co-polar scattering coefficients, whereas the values S_{12} and S_{21} are designated the cross-polar scattering matrix coefficients. As well as being defined in terms of linear polarisation, a matrix with circularly polarised components is equally valid. The polarisation matrix can be applied to a whole target or elements of a target, which can be resolved using a high-range resolution waveform, for example.

6.4.3 Polarisation characteristics of targets

6.4.3.1 Introduction

Targets with certain geometrical shapes and sizes have polarisation matrices, which are well defined. They can be used as potential discriminants for recognising certain targets or structures associated with specific targets. The scattering matrix components, for metallic objects with some well-known shapes, are now presented.

6.4.3.2 Sphere

When a sphere is illuminated with a circularly polarised signal, the sense of the polarisation is changed, from left to right or vice versa. This is illustrated in Figure 6.17. For a linearly polarised signal the plane of polarisation is maintained and there are no cross-polar components [26]. There is 180° phase change on reflecting from the sphere, but this really does not have much practical significance as far as radar measurements are concerned.

The matrix for linear polarisation is:

$$\begin{bmatrix} 1 & 0 \\ 0 & 1 \end{bmatrix}$$

For circular polarisation, the sense is changed on reflection from a sphere with respect to the direction of propagation, so that the co-polar value is zero and the cross-polar value is one.
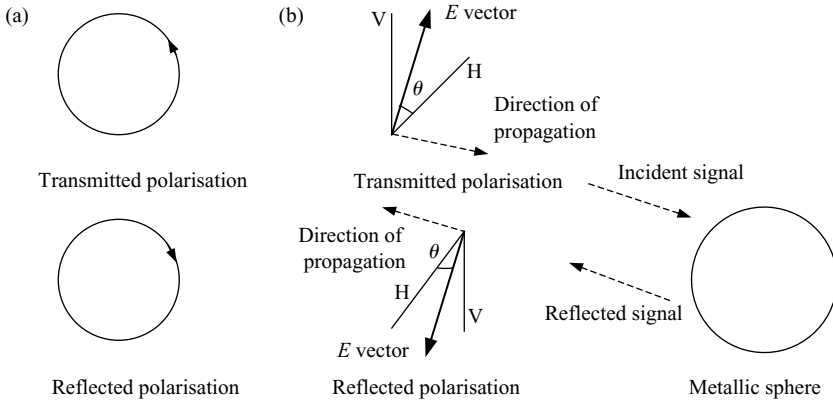
Figure 6.17   *Polarisation characteristics of a sphere (or flat plate): (a) circular polarisation: sense of polarisation reversed relative to propagation direction; (b) linear polarisation: plane of polarisation maintained*

The matrix for circular polarisation is:

$$\begin{bmatrix} 0 & 1 \\ 1 & 0 \end{bmatrix}$$

6.4.3.3   Flat plate

There is only a very narrow angle over which returns are reflected back in the direction of the radar (Chapter 2, Table 2.3). For circular polarisation, the sense is reversed and for linear polarisation it is maintained in the same direction. These are the same polarisation matrix components as for the sphere in Figure 6.17. However, the difference is that the sphere reflection components are constant with aspect angle, in comparison to the rapidly varying reflections from the flat plate with changes of aspect angle.

6.4.3.4   Dihedral corner reflector

This consists of two flat plates orthogonal to each other, as shown in Figure 6.18(a). Incident signals propagating in a plane orthogonal to the line joining the two plates undergo two reflections. For conducting plates the incident and reflected angles are the same, as is also the case of geometric optics, resulting in the signal being reflected back towards the radar following the two reflections. For circular polarisation the sense is changed at each reflection, so that the resulting signal maintains its polarisation.

The co-polar component is one and the cross-polar component is zero.

The matrix for circular polarisation is:

$$\begin{bmatrix} 1 & 0 \\ 0 & 1 \end{bmatrix}$$

Similarly for linear polarisation, the plane of polarisation is maintained.
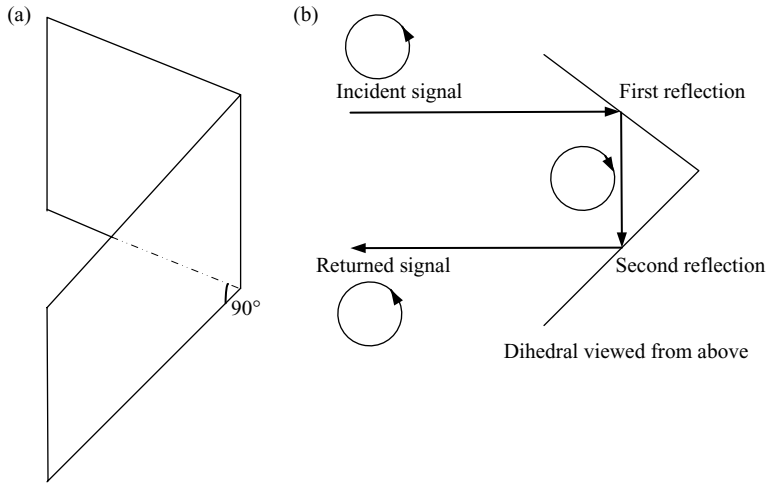
Figure 6.18   Polarisation characteristics of dihedral corner reflector: (a) dihedral corner reflector and (b) circular polarisation changes sense at each reflection
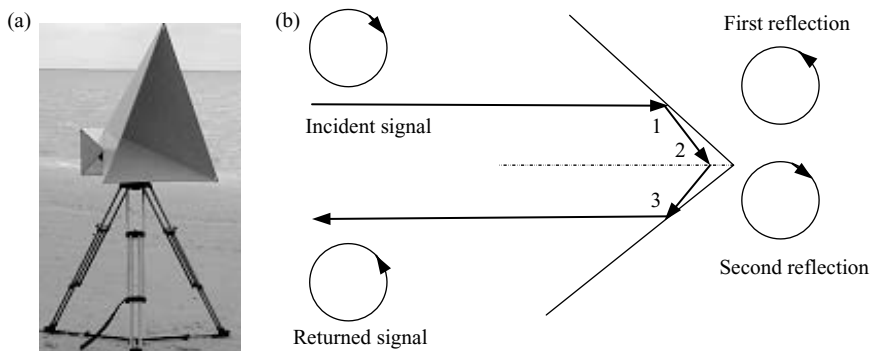
Figure 6.19   Trihedral corner reflector and circular polarisation characteristics. (Photograph courtesy of BAE Systems Insyte): (a) trihedral corner reflector and (b) representation of circularly polarised signal undergoing these reflections

6.4.3.5   Trihedral corner reflector

This consists of three mutually orthogonal reflecting surfaces as shown in Figure 6.19(a).

The principle of operation of the trihedral corner reflector is the three-dimensional equivalent of the dihedral, which reflects signals back to the radar in a single plane. The trihedral reflects signals arriving in a cone of approximately 15° half angle, about its axis of symmetry, back in the direction of the radar [27]. The signal undergoes
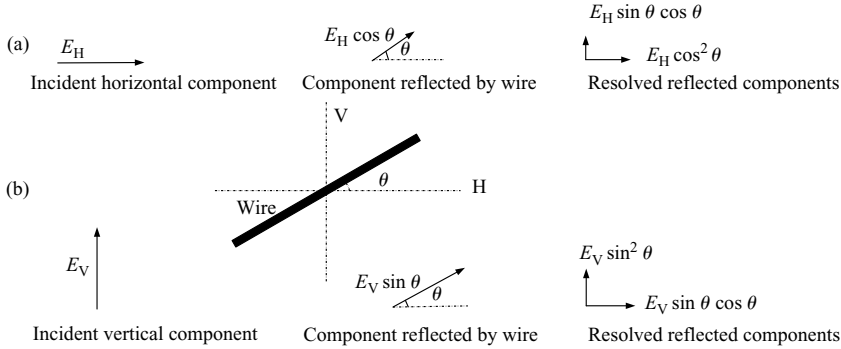
Figure 6.20   Polarisation effects for a length of wire: (a) effects on horizontal electric field component and (b) effect on vertical electric field component

three reflections, with the sense of the circularly polarised signal changed at each reflection. The resulting signal has a changed polarisation. For linearly polarised signals, the polarisation direction is maintained.

The matrix for circular polarisation is:

$$\begin{bmatrix} 0 & 1 \\ 1 & 0 \end{bmatrix}$$

6.4.3.6   Straight length of wire

The polarisation effects resulting from a wire inclined at an angle, θ, to the horizontal are shown in Figure 6.20 for incident horizontal and vertical electric field components.

The wire reflects the component of the electric field, which is parallel to its axis. The resulting matrix for linear polarisation is:

$$\begin{bmatrix} \cos^2 \theta & \sin \theta \cos \theta \\ \sin \theta \cos \theta & \sin^2 \theta \end{bmatrix}$$

6.4.4   *Radar design for supporting polarisation measurements*

In order to obtain the full polarisation matrix, it is necessary to transmit either two linear orthogonal polarisations or the two circular polarisations and to receive two polarisations. Generally, the two orthogonal polarisations are transmitted sequentially. From the relationships shown in Figure 6.15, the transmitted polarisation can be either linear or circular. The mathematical relationships between the two can be used to convert one set of measurements (e.g. linear) into the second set (e.g. circular), as different shapes are more easily characterised by certain polarisations. A typical radar design [28] for generating and receiving polarised signals is shown in Figure 6.21.

The transmitter design is exactly the same as for a conventional single-channel high-resolution radar, which utilises one polarisation, as is discussed in Chapter 7,
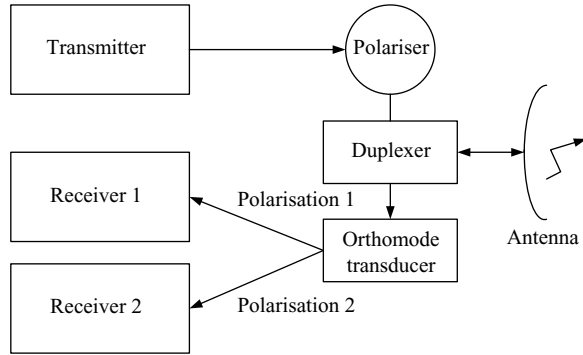
Figure 6.21   Design concept for radar measuring target polarisation matrix

Section 7.5. The polariser controls the polarisation of the transmitted signal on a pulse-by-pulse basis. On receiving the signal, it passes through a device, which is called an orthomode transducer, which separates the two polarisations reflected from the target. These are then directed into two receivers, which are exactly the same as a conventional single-channel high-range resolution receiver. Additional signal processing is needed to extract the polarisation matrices using the receivers' output data.

6.4.5   Using polarisation for target recognition

In Section 6.4.2, the polarisation matrices of metal objects having some standard geometrical shapes were discussed. The basis of using polarisation in radar target recognition is to determine the polarisation matrices of targets or part of targets of interest, and then to reverse the process discussed above to establish the shape corresponding to the matrix, which has been measured. This process is illustrated in Figure 6.22 for a high-resolution range profile [29].

In each high-resolution range gate the polarisation matrix parameters are determined [30]. These are compared to a database of polarisation matrix parameters of known geometrical objects. The nearest matches then provide an estimate of the shape of a particular part of the target. As a high-resolution range profile (HRRP) contains data from all the cross-range target returns, for complex targets with several scatterers in each range gate, the polarisation matrix is a combination of the matrices of all the contributing scatterers. Hence, the localisation of an individual matrix for a particular target feature is not reliable for targets with many scatterers in each range gate using only HRRP, such as a large ship.

However, if SAR [31,32] or ISAR is used, and if the down-range and cross-range resolutions are sufficiently high to isolate the scatterers of interest, the polarisation matrices of the individual target pixels are more readily isolated. This should enable estimates to be made of the geometrical shapes of the target associated with the respective polarisation matrices in each pixel. By studying the shapes of the elements comprising the target, an estimate of the target type can be made.

S_{11}

S_{12}

S_{21}

S_{22}

High-resolution range gates
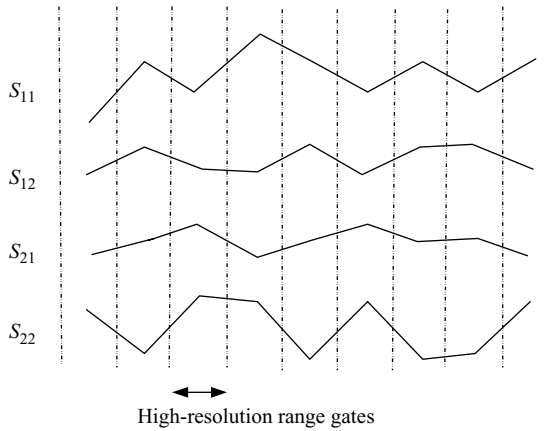
Figure 6.22   Polarisation matrix parameter values are measured in each high resolution range gate to determine object shape

6.5   Impulse radar

6.5.1   Introduction

An impulse radar is a type of high-range resolution radar. The impulse radar design, the technology used to generate the signal and the applications are sufficiently different from the techniques described earlier, which are based upon modulated pulse-Doppler waveforms and transmitters utilising travelling wave tube and solid-state amplifiers, to merit its own section [32,33].

Impulse radars normally operate at baseband and do not have a specific carrier frequency. The ideal impulse is a 'Dirac' delta function, which has infinite amplitude and zero time duration [34]. In practice, this is not physically achievable and one to three cycles of amplitude variation have been defined as being an impulsive waveform [35]. The target recognition applications cover two main classes of target. The first class is targets buried below the surface of the ground. These can be buried ordnance including landmines, archaeological objects, pipes and cables of interest to utility companies and items, which are of interest to police, forensic and customs investigators. Also included for prospecting applications are mineral seams and rock strata. Small targets, such as plastic landmines can be detected at a depth of a few centimetres, whereas large metallic targets, such as pipes, can be detected at depths of up to several metres.

The other class of objects is associated with the recognition of vehicle targets and fixed installations, which are the main subject of this book. The baseband impulse radar signal can penetrate through foliage, giving it the potential to recognise targets that are hidden from the higher frequency radars. For the frequency bands of up to several hundred MHz, signals have far less attenuation than in the traditionally used microwave bands, which utilise signals with frequencies of Giga Hertz.
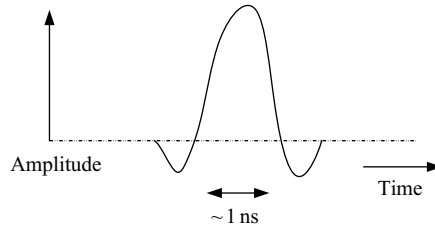
Figure 6.23   Typical pulse generated by impulse radar
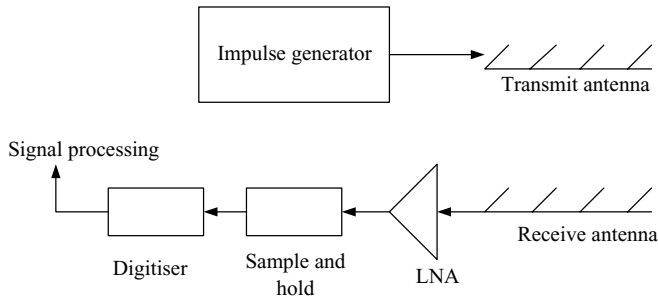
Figure 6.24   Block diagram of typical impulse radar

6.5.2   *Impulse radar pulse characteristics*

An impulse radar is designed to generate a very short duration pulse and an example is shown in Figure 6.23.

   The duration of the pulse is typically 1 ns, which corresponds to a half power bandwidth of about 1 GHz and provides a range resolution in air of about 20 cm. As there is no carrier frequency present, all of the energy resides at the baseband, so the pulse has most of its spectral content from a few tens of MHz to several hundred MHz. As the attenuation in soil and through foliage tends to rise with frequency, a signal with this type of spectrum is well suited for penetrating soil or foliage. As the pulse also has good range resolution, it has the potential to recognise buried objects and targets hidden by foliage using range profiling or SAR techniques.

6.5.3   *Impulse radar system design*

The block diagram of a typical impulse radar is shown in Figure 6.24. The radar signal is produced in the impulse generator and is transmitted via the antenna. It should be noted that normally an impulse radar has separate antennas used for transmitting and receiving the signal. The main reason is that for subsurface applications the isolation achieved between the transmitter and the receiver is higher with the two antennas, particularly as the targets of interest are at such short ranges. Duplexers or fast switches for isolating the transmitted and received signals have not been generally available in these frequency bands.

After receiving the signal, it is amplified in the LNA to establish a low noise figure; various techniques can then be used for sampling the signal. In Figure 6.24, a high-speed sample and hold circuit is shown, followed by a high-speed digitiser. This type of design enables high-speed samples to be taken of single or multiple received pulses, so that the complete profile of the returned signal can be measured and then digitised.

Another technique involves correlation. A replica of the transmitted impulse is delayed and correlated with the received signal, which acts as a matched filter of the transmitted signal for a single range. To build up a succession of returns from different range gates, the time delay of the reference impulse can be sequentially varied to cover the range bracket of interest as many impulses are transmitted. Another technique is to use a bank of correlators, each set for different time delays. After correlation or digitisation the signal can be analysed.

6.5.4   Applications

The ground probing application of impulse radars is illustrated in Figure 6.25. The separate transmit and receive antennas are shown. The time delay of the object provides its depth. In order to localise the object in three dimensions the radar can be moved in a grid pattern horizontally. The returns at the different horizontal positions can then be used to generate a three-dimensional map of the ground [36].

The concept of using an impulse radar for detecting objects hidden by foliage from an airborne platform is shown in Figure 6.26.

The low-frequency impulse signal is reflected less from the trees [37–39] than for signals at microwave frequencies and so can illuminate targets which are hidden beneath the foliage. As the impulse signal is wideband, it has high-range resolution and has the potential to recognise these targets. Experimental impulse radars have been used to perform SAR [40].
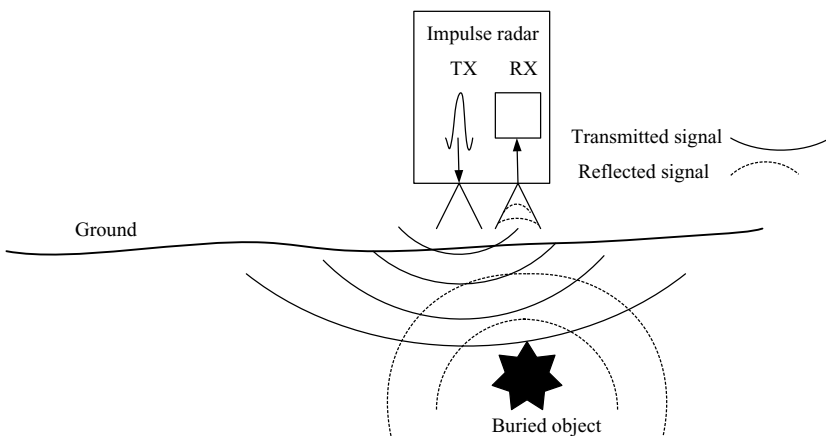
Figure 6.25   Application of impulse radar to ground probing

Figure 6.26   Impulse radar can be used to detect and recognise targets hidden beneath foliage

6.5.5   Challenges for applications of impulse radar for target recognition

The possibilities for employing SAR to recognise targets have been presented above. However, for practically realisable systems there are various challenges that have to be overcome.

Generally impulse radars use high peak powers, so have a relatively poor detection performance in comparison with conventional microwave radars. An example is given in Reference 40, which states that 10 km range is obtained with an impulse radar, which has a peak power of 10 MW.

Another problem is that the gain of an antenna with a given aperture varies with frequency and the impulse radar's band could include frequencies with ratios of up to five to one. The sensitivity of the radar could therefore vary by at least an order of magnitude over the impulse radar's band, which would be inefficient for the detection of targets. Another associated difficulty is that the beamwidth of the antenna also varies with frequency, so some targets may be detected by the lower frequency components of the waveform, which are not detectable by the higher frequency components, which have a narrower beamwidth.

Another issue is electromagnetic interference between the impulse radars and other systems, such as television and radio broadcasts in the UHF and VHF bands. The impulse with its very high peak output can interfere with other systems, and operating procedures restricting their use may be required [41]. Also the level of man-made noise and interference from other systems can desensitise the impulse radar, as the local noise floor can be raised [42].

6.6   Ultra-wideband/ultra high-resolution radar

6.6.1   Introduction

Ultra-wideband radar is another class of high-range resolution radar and is included in this book for completeness. Impulse radar, which was described in the previous section, is also a subset of ultra-wideband radar. Ultra-wideband radar has been defined as having a bandwidth that is at least 25 per cent of its operating frequency [43]. The actual waveforms used in ultra-wideband radar systems are not limited and can be generated by any technique. These can include both impulses and techniques based on those utilised by conventional lower bandwidth radars and are developed for larger bandwidths and higher range resolutions. The associated range resolution can also be defined as ultra high-range resolution.

The waveforms utilised can be based on modulated carrier frequencies, impulses at baseband or a hybrid between an impulsive waveform and pulse on a microwave carrier frequency, which is a very short pulse on a carrier.

6.6.2   Coherent ultra high-range resolution

The techniques used to generate ultra-wideband coherent waveforms can be based on pulse-Doppler techniques. An example of a design is provided in Reference 44. The ultra-wideband waveform is generated by a combination of analogue and digital techniques and bandwidth multiplier circuits are used to increase the bandwidth of the modulation to several giga hertz. The technique is summarised functionally in Figure 6.27 and uses solid-state components to generate a waveform with a few centimetres range resolution.

The quadrature up-converter can employ in-phase and quadrature signals at its input with bandwidths of a few hundred mega hertz. The bandwidth of the output signal is then multiplied in a number of stages until several giga hertz of bandwidth is then obtained. As solid-state techniques can be used to generate these wideband waveforms, a few watts of peak power can provide the same detection sensitivity as impulse radars with many orders of magnitude more peak power. This should generate significantly less interference than in an equivalent impulse radar.

These techniques have been employed to detect buried plastic landmines [45]. The techniques are coherent and use pulse compression. Doppler filtering and the coherent
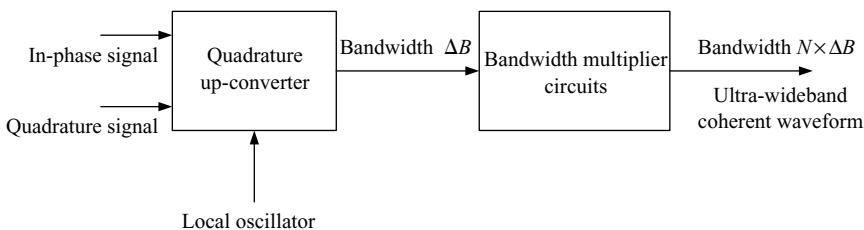

Figure 6.27   Ultra-wideband signals can be generated using solid-state techniques

integration of pulses can be performed in a very similar manner to the methods used in conventional pulse-Doppler radars with much lower bandwidth systems. Antennas are also being designed to cover these very large bandwidths [46].

6.6.3 Conclusion

Ultra-wideband signals can be in the form of impulses or as the ultra-wideband equivalent of conventional modulated radar waveforms. Impulse radars have been employed successfully for many years for ground probing. The former monopoly of impulse radars in being able to generate ultra high-resolution waveforms is now being challenged by the development of solid-state techniques evolving from conventional radar designs. Although these techniques have not been very widely employed yet in the recognition of military vehicle targets, some systems are now under development [47].

6.7 Combined high-range and high-frequency resolution

6.7.1 Introduction

In Chapter 3, high-range resolution techniques were presented and in Chapter 5 frequency and time domain analysis techniques were discussed. The high-range resolution techniques are dependent upon generating a high bandwidth waveform and high-frequency resolution is provided with a long coherent integration period.

In some ways the waveform requirements of these two high-resolution methods are conflicting. In order to generate a high-quality range profile of a moving target, as the integration period is increased the target can exhibit range gate walk effects and the range profile can be decorrelated if the aspect angle changes. The range gate walk effects have to be corrected to focus the range profile. If the aspect angle changes over the integration period, and ISAR is not specifically being performed, defocusing of the range profile can also occur, which is effectively a decorrelation of the target's signature. Hence, in order to reduce these effects, the radar integration period should be minimised. In contrast, for measuring the frequency content of reflected returns from a target, resolution theoretically improves with integration time.

There are interesting parallels in radar measurements with the 'Heisenberg Uncertainty Principle' of quantum mechanics. With radar, range or time delay are to be measured simultaneously with frequency. In quantum mechanics there is a limit to the accuracy by which the position and velocity of a particle can be simultaneously measured. The radar and quantum mechanical measurements are not absolutely equivalent and the reader is referred to the discussion in Reference 48.

6.7.2 Waveforms

In order to measure simultaneously the range profile and JEM signatures of a target or the range profile and helicopter blade flash and HERM, the requirements for both sets of measurements have to be assessed to establish whether a common waveform can

be utilised. A key issue is the type of target of interest and its motion during the radar integration period. For range profiling the maximum tolerable integration time has to be determined. For measuring JEM spectra, helicopter blade flash and the rotor modulation spectrum, there are constraints on pulse lengths and integration times, which were discussed in Chapter 5.

In order to obtain high-resolution frequency domain data, a waveform, which is repeated many times, is required, so a significant number of pulses are needed. This would be a pulse-Doppler waveform. For example, if 64 pulses are transmitted and processed using Fourier transforms, 64 cells are obtained in the frequency domain, for analysis. This then precludes the employment of stepped frequency waveforms for most applications for maximising performance, for example. The stepped frequency waveform transmitted is not the same for every pulse and cannot be defined as a standard pulse-Doppler waveform over the radar integration period, so does not optimise frequency resolution. In Chapter 8, Section 8.2 is a discussion of waveforms for supporting stepped frequency techniques.

The waveforms that are recommended are repeated pulses, which could be wideband chirps or even impulses. These wideband pulses provide high-range resolution and their repetition over the radar integration period enables high-frequency resolution to be performed. However, stretch waveforms, for example, exhibit range-Doppler coupling effects, as discussed in Chapter 3, and have to be compensated.

Other constraints are the integration time available within the radar's mode scheduling for the high-resolution function to be performed and the signal-to-noise ratio requirements for obtaining the target signature.

6.7.3   Two-dimensional range-frequency signature

If the various integration time issues, which were discussed above, can be overcome, and the radar design can support the coherent wideband waveforms required, high-quality target images can be obtained. Even if a reduced dwell period is available, reasonable target images can be obtained, which can contribute to target recognition. An example is shown in Figure 6.28, which utilised a relatively short dwell time. A high-resolution signature of a helicopter has been obtained. A high-range resolution waveform has been employed, which provides the range profile of the helicopter. In each high-resolution range gate, the data have also been Doppler-processed for frequency analysis. The helicopter aspect angle for the measurement is as shown in the figure and the bulk motion has been compensated for, so that the range profile returns are along the '0 Hz' Doppler filter. The length of the helicopter, as viewed by the radar, is its radar length multiplied by the cosine of its aspect angle to the radar. In any range gate in which there is motion of a mechanical part of the helicopter relative to the helicopter's skin echo, this is manifested as a return in the same range cell, but in another Doppler filter. For example, the rear rotor blades are moving and exhibit the Doppler effect. When the returns are Doppler-filtered for their associated range gates, the measured Doppler frequency components are located in the appropriate filters. These returns include the effects discussed in Chapter 5 associated with the rear blade flashes and the spectra associated with the blades modulating the radar signal.
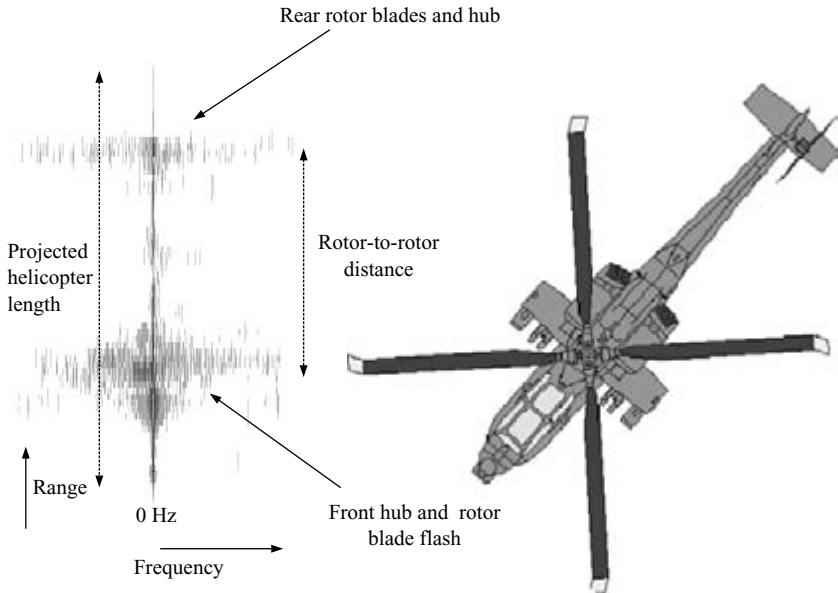
Figure 6.28   Two-dimensional range-frequency signature of helicopter (Courtesy of BAE Systems Insyte)

The rear rotor of the helicopter has been localised in range and its spectrum has been measured.

Similarly, the front rotor and part of a rotor blade flash have also been detected and localised in range and the spectral components have also been measured. Hence, the discriminants extracted for target recognition using this two-dimensional technique are: the projected helicopter length and range profile; the spectrum of the front rotor, the front blade flash and rotor position along the range profile; the spectrum of the rear rotor and its location along the range profile. A wealth of information is obtained in relation to either an individual range profile or frequency analysis measurement being made. These features would be used to develop recognition algorithms to classify the target.

The short time available for this measurement would not have been sufficient for blade flash analysis for helicopter recognition, as discussed in Chapter 5, as a series of blade flashes would be needed, rather than the single flash detected. However, the information provided by this type of measurement can make a major contribution to recognising the target even if no blade flash is detected. Clearly, for long dwell periods, signatures of this type can also be supplemented by blade flash analysis, so all these signal processing and analysis techniques can be used to maximise recognition performance.

Similarly, for targets with jet engines, each engine can be localised in range, so its position along the range profile can be used as a target feature.

6.7.4 Conclusion

It is concluded that the two-dimensional range-frequency analysis technique can provide high-quality target images, which are significantly superior to individual high-range or high-frequency measurements being made. In providing more target discriminants, this technique also has the potential to provide a higher reliability target recognition function than the individual techniques.

However, the effective employment of this technique is dependent upon the actual targets of interest, their range, the ability of the radar to support the waveform and the time available for implementation of this type of target recognition mode. This technique is expected to still be reasonably effective, even when only short integration periods are available for the target recognition function.

6.8 Summary of other high-resolution techniques

The high-resolution techniques presented in this chapter can be considered to be extensions of the main target recognition methods discussed earlier in the book. The super resolution and monopulse techniques effectively improve the resolution of radar measurements by utilising relatively high signal-to-noise ratios. However, for the practical implementation of these methods, the radar must operate at higher than normal sensitivities, which means that the target range is short or there is time available for long integration periods.

The polarisation techniques are directly compatible with, and would be used in conjunction with, other high-resolution methods. Relatively high signal-to-noise ratios are required to extract all the polarisation matrix components.

The impulse and ultra-wideband techniques are extensions of high-range resolution methods and tend to have niche applications.

The combined high-range resolution and high-frequency resolution techniques are based on the respective individual techniques and can be applied to targets with mechanical propulsion systems. Components such as rotors, rotor blades and jet engines can be detected, recognised and localise in range, to supplement range profile data.

References

1　JANSSON, P.A. (Ed.): 'De-Convolution of Images and Spectra' (Academic Press, London, UK; San Diego, CA, 1996)
2　MENDEL, J.M., and BURRUS, C.S.: 'Maximum Likelihood-Deconvolution: A Journey into Model-Based Signal Processing' (Springer-Verlag, New York, 1990)
3　BENITZ, G.R.: 'High-Definition Vector Imaging', *Lincoln Laboratory Journal*, 1997, **10** (2), pp. 147–69
4　ZHANG, Q.T.: 'Probability of Resolution of the MUSIC Algorithm', *IEEE Transactions on Signal Processing*, 1995, **43** (4), pp. 978–7

5 HOGBOM, J.A.: 'Aperture Synthesis with a Non-Regular Distribution of Inter-ferometric Baselines', *Astronomy Astrophysics*, 1974, (Suppl. 15), pp. 417–26

6 CLARK, B.G.: 'An Efficient Implementation of the Algorithm *CLEAN*', *Astronomy Astrophysics*, 1980, **89**, pp. 377–8

7 CORNWELL, T.G.: 'A Method of Stabilizing the CLEAN Algorithm', *Astronomy Astrophysics*, 1983, **121**, pp. 281–5

8 SKOLNIK, M.I.: 'An Introduction to Radar Systems' (McGraw-Hill, New York, 1970) Chapter 10.5

9 BAKER, S., and KANADE, T.: 'Limits on Super-Resolution and How to Break Them', *IEEE Transactions on Pattern Analysis and Machine Intelligence*, 2002, **24** (9), pp. 1167–81

10 LUTTRELL, S.P.: 'Bayesian Auto-Focus Super-Resolution Theory'. IEE Colloquium on *Role of Image Processing in Defence and Military Electronics*, 9 April 1990, pp. 1/1–1/6

11 FREEMAN, W.T., JONES, T.R., and PASZTOR, E.C.: 'Example-Based Super-Resolution', *IEEE Computer Graphics and Applications*, March/April 2002, **22** (2), pp. 56–65

12 CALLE, D., and MONTANVERT, A.: 'Super-Resolution Inducing of an Image'. Proceedings of International Conference on *Image Processing*, ICIP 98, Chicago, IL, vol. 3, 4–7 October 1998, pp. 232–6

13 SALE, D., SCHULTZ, R.R., and SZCZERBA, R.J.: 'Super-Resolution Enhancement of Night Vision Sequences'. IEEE International Conference on *Systems, Man, and Cybernetics*, Nashville, TN, vol. 3 , 8–11 October 2000, pp. 1633–8

14 BI, Z., and LIU, S.-H.: 'Super Resolution SAR Imaging via Parametric Spectral Estimation Methods', *IEEE Transactions on Aerospace and Electronic Systems*, 1999, **35** (1), pp. 267–81

15 LI, J., STOICA, P., BI, Z., WU, R., and ZELNIO, E.G.: 'A Robust Hybrid Spectral Estimation Algorithm for SAR Imaging'. Proceedings of the 32nd Asilomar Conference on *Signals, Systems and Computers*, Monterey, CA, vol. 2, 1–4 November 1998, pp. 1322–6

16 WU, R., and LI, J.: 'Autofocus and Super-Resolution Synthetic Aperture Radar Image Formation', *IEE Proceedings, Radar, Sonar and Navigation*, 2000, **147** (5), pp. 217–23

17 DICKEY, F.A., ROMERO, L.A., DE LAURENTIS, J.M., and DOERRY, A.W.: 'Super-Resolution Degrees of Freedom and Synthetic Aperture Radar', *IEE Proceedings, Radar, Sonar and Navigation*, 2003, **150** (6), pp. 419–29

18 RIHACZEK, A.W., and HERSCHKOWITZ, S.J.: 'Theory and Practice of Radar Target Identification' (Artech House, Boston, MA, 2000) pp. 96–7

19 SKOLNIK, M.I.: 'An Introduction to Radar Systems' (McGraw-Hill, New York, 1970) Chapter 5-4

20 STIMSON, G.W.: 'Introduction to Airborne Radar' (Scitech Publishing Incorporated, 1998) p. 103

21 SHERMAN, S.M.: 'Monopulse Principles and Techniques' (Artech House, Boston, MA, 1984)

22   RHODES, D.R.: 'Introduction to Monopulse' (Artech House, Boston, MA, 1980)

23   CHAUMETTE, E., SAULAIS, P., and COLIN, N.: 'Modern Monopulse Tracking'. *Radar* 2004, Toulouse, France, Paper no. 9B-TRACK-1

24   STONE, T.W.: 'Monopulse Receiver Design Depends on IF Processor Success', *Microwave Systems News*, August 1983, pp. 53–63

25   SKOLNIK, M.I.: 'An Introduction to Radar Systems' (McGraw-Hill, New York, 1970) Chapter 5.5

26   CLOUDE, S.R.: 'Polarimetric Techniques in Radar Signal Processing', *Microwave Journal*, July 1983, pp. 119–27

27   SKOLNIK, M.I.: 'Radar Handbook' (McGraw-Hill, New York, 1970) Chapter 27-16

28   EFURD, R., COHEN, M., and SJOERG, E.: 'Advanced Intrapulse Polarisation Radar Nears Deployment', *Microwave Systems News*, February 1984, pp. 67–76

29   WANG, Y., CHEN, J., and LIU, Z.: 'High Resolution Fully Polarised Radar Target Identification Using One-Dimensional Scattering Centres'. *Radar* 2004, Toulouse, France, Paper no. 127

30   BERIZZI, F., DALLE MESSE, E., CANTINI, L., and CALUGI, D.: 'Polarimetric Feature Extraction for Wideband Radar Systems'. *Radar* 2004, Toulouse, France, Paper no. 207

31   FERRO-FAMIL, L., and POTTIER, E.: 'Unsupervised Classification of Complex Scenes Using Polarimetric Interferometric SAR Data'. *Radar* 2004, Toulouse, France, Paper no. 8A-IFPOL-2

32   DANIELS, D.: 'Applications of Impulse Radar Technology'. *Radar* 97, IEE publication no. 449, Edinburgh, 14–16 October 1997, pp. 667–72

33   DANIELS, D., GUNTON, D.J., and SCOTT, H.F.: 'Introduction to Subsurface Radar', *IEE Proceedings*, (1988), 135

34   BLACK, D.L.: 'An Overview of Impulse Radar Phenomenon', *IEEE AES Magazine*, December 1992, pp. 6–11

35   SKOLNIK, M.I.: 'An Introduction to Impulse Radar', US Naval Research Laboratory, Washington, November 1990, Memorandum report no. 6755

36   DANIELS, D., GUNTON, D.J., and SCOTT, H.F.: 'Introduction to Subsurface Radar', *IEE Proceedings on Radar and Signal Processing*, (1988), 135, pp. 278–320

37   LE PALUD, M.: 'Modelling of Radar Wave Propagation Inside Forest'. *Radar* 2004, Toulouse, France, Paper no. 104

38   TAMIR, T.: 'Radio Wave Propagation Along Mixed Paths in Forest Environments', *IEEE Transactions on Antennas and Propagation*, 1997, **25** (4), pp. 471–7

39   DUBOIS, C., CHAUVET, V., DIOT, J.C., LABORDE, S., VAUCHAMP, S., BERTRAND, V. *et al*.: 'Analysis of Foliage Penetration Properties by Using a Transient Ultra Wide Band Measurement System'. *Radar* 2004, Toulouse, France, Paper no. 204

40 VICKERS, R.S.: 'Ultra-Wideband Radar-Potential and Limitations', *IEEE MTT-S Digest*, 1991, **1**, pp. 371–4
41 FISHER, J. *et al*.: 'Ultra-Wideband and Radar Co-Existence'. Proceedings of the 1st EMRS DTC Technical Conference, Edinburgh, 2004
42 VICKERS, R.S.: 'Ultra-Wideband Radar-Potential and Limitations', *IEEE MTT-S Digest*, 1991, p. 372
43 NOEL, B.W. (Ed.): 'Abstracts of Papers Presented at the First Los Alamos Symposium on Ultra Wideband Radar' (CRC Press, Florida, March 1990)
44 FFRENCH, T.E., GUNTON, D.J., and TAIT, P.D.F.: 'Coherent Ultra High Range Resolution Radar'. World International Intellectual Property Organisation, ref WO 98/13704, April 1998
45 FFRENCH, T.E., GUNTON, D.J., and TAIT, P.D.F.: 'Anti-Personnel Landmine Detection Using Ultra High Resolution Radar Technique'. IEE *Detection of Abandoned Landmines Conference*, Edinburgh, October 1998
46 DELMOTE, P., DUBOIS, C., ANDRIEU, J., LALANDE, M., BERTRAND, V., BEILLARD, B. *et al*.: 'Two Original UWB Antennas'. *Radar* 2004, Toulouse, France, Paper no. 166
47 LYNCH, D., GENELLO, G., and WICKS, M.: 'Ultra Wideband Perimeter Surveillance'. *Radar* 2004, Toulouse, France, Paper no. 138
48 SKOLNIK, M.I.: 'An Introduction to Radar Systems' (McGraw-Hill, New York, 1970) Chapter 10-6

Chapter 7

System issues

7.1 Introduction

Earlier in the book the various high-resolution radar techniques employed for target recognition were presented. Within this chapter the design issues at the radar system level associated with integrating target recognition functions are discussed. The implications on components, antenna design and operational aspects are discussed in subsequent chapters.

There are design issues associated with sensitivity, dynamic range and calibration, which are generally common to most target recognition functions, which are more stressing than for the design of the conventional radar modes. One key issue in target recognition is that the target is divided into small elements by the high-resolution waveform, each of which has a much lower radar cross-section (rcs) than the whole target. Hence, the sensitivity of the target recognition mode has to be related to the target constituents measured and the 'Radar Range Equation' has to be modified accordingly. These are discussed in Section 7.2. In addition, as clutter is still present, so that the radar is required to instantaneously cope with clutter and the small target elements of interest, dynamic range is a critical issue and is discussed in Section 7.3.

Another key issue is the distortion of the signal within the radar itself, particularly for the wideband high-range resolution target recognition techniques. This is not usually an issue for the lower resolution target detection and tracking modes, as there is generally very little distortion occurring over the associated relatively narrow bandwidths used. A specific 'calibration' or 'distortion compensation' function is required in high-range resolution applications, which measures the distortion of the signal and provides compensation for this and is presented in Section 7.4.

Most radar systems are designed to support the normal target detection and tracking functions as their primary requirements. Target recognition modes would normally utilise the existing architecture of the radar's design as much as possible, with modifications for target recognition being minimised, on the grounds of cost and complexity. In contrast, air- and space-based surveillance systems, for example, utilising SAR

modes, may not necessarily have primary target detection modes and be specifically designed for high-resolution modes, to support target recognition. The radar system design issues for supporting the various high-resolution techniques are discussed in Section 7.5.

7.2   Sensitivity

7.2.1   Radar range equation for target detection

In Chapter 2, the radar range equation (Equation (2.55)) was discussed for conventional radar modes and is

$$R^4 = \frac{PA^2\eta^2\sigma\tau n}{4\pi\lambda^2 L_t L_r SkT_0(NF)} \tag{7.1}$$

The key parameter of interest, which differs for the high-resolution modes, is the rcs, σ.

7.2.2   High-resolution radar range equation

For the detection and tracking of targets, conventional waveforms have a lower range resolution than the target dimensions, so that all of the energy reflected from the target, which is detected by the radar, is confined to one or at most two range gates. This is illustrated in Figure 7.1, in which the range gate is longer than the target range extent.

  For the higher range resolution, frequency and time domain analysis modes used for target recognition, the value of the rcs used for sensitivity calculations is only a small fraction of the rcs of the whole target.

  In Figure 7.2, the range profile of a target is represented. The total rcs of the target is now divided into small elements corresponding to returns from the individual range gates. These have values of σ_e, which are usually much smaller than the total rcs of the target.

  Similarly, for a JEM spectrum, each spectral line has an effective rcs at a particular radar frequency, for a given set of engine parameters and aspect angle. Each spectral line of interest can be considered to be a target element (Figure 7.3).
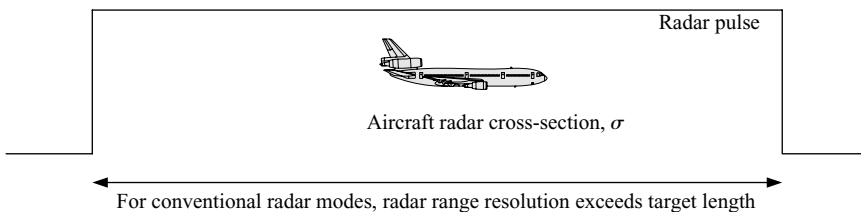

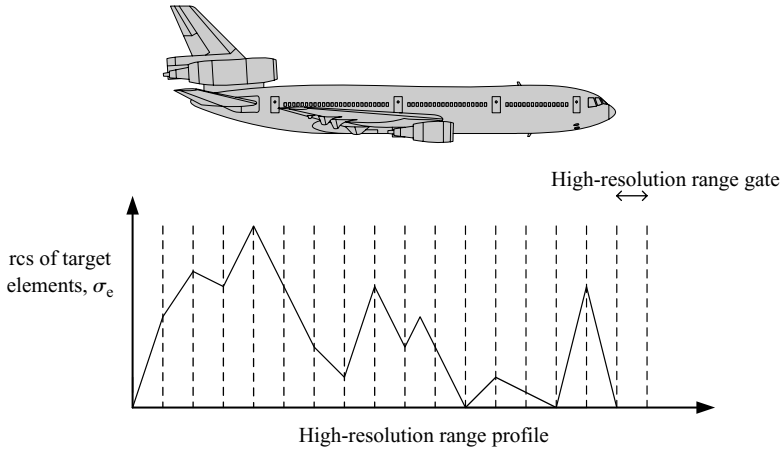*Figure 7.1   Conventional radar modes detect complete rcs of target*

Figure 7.2   For high-resolution range profiling sensitivity is dependent upon rcs of each target element, σ_e
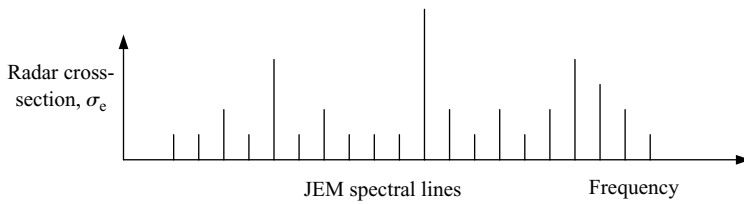

Figure 7.3   Each JEM spectral line has an effective rcs

For SAR and ISAR the target signature consists of two range dimensions, and is also divided into small elements of relatively low rcs, so detection sensitivity and range are again dependent upon the lowest value of target rcs of interest. The SAR radar range equation determines the sensitivity obtained [1].

For real aperture radars, in order to calculate the range for the detection of the target elements, the radar range equation is modified to substitute the value, σ_e, for the *traditional* value, σ, used for detecting the whole target:

$$R^4 = \frac{PA^2 \eta^2 \sigma_e \tau N}{4\pi \lambda^2 L_t L_r S k T_0 (NF)} \tag{7.2}$$

Clearly, as the rcs of the target elements are much smaller than that of the whole target, the range for the application of the high-resolution mode is reduced in comparison to that of target detection, if all the other parameters remain the same. The value of the pulse length, τ, used in the equation needs an explanation. For the high-resolution mode, if pulse compression is being employed and the same expanded pulse length is being used, the total amount of energy transmitted in both cases is exactly the same. Although τ is reduced, the pulse compression ratio effectively compensates for this,

(a)

Peak power $= P$

τ

(c)

(b)

Peak power $= P$

Peak power $= P\,P_C$

τ

$1/P_C\tau$
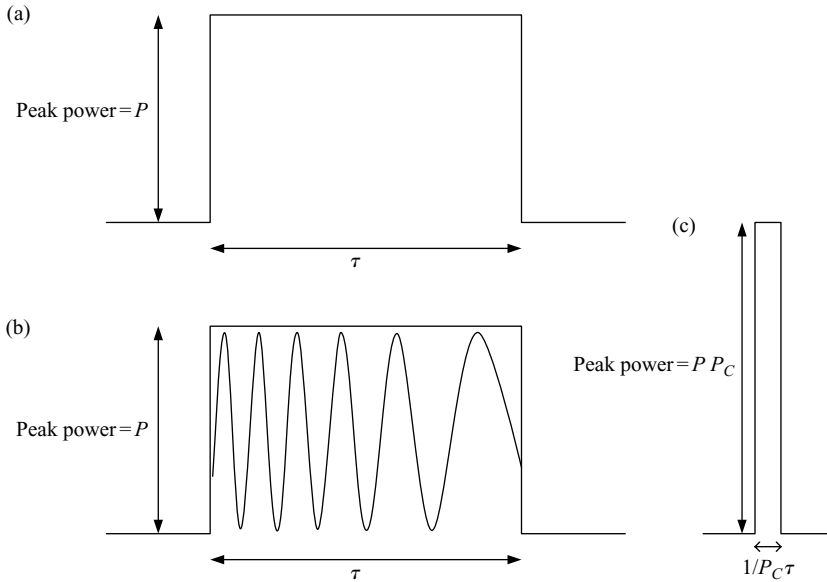
Figure 7.4 *For the same expanded pulse length employed, receiver noise bandwidth is effectively unchanged in high-range resolution mode: (a) low resolution pulse: noise bandwidth $= 1/\tau$; (b) high-resolution pulse with pulse compression: pulse compression ratio $= P_c$, noise bandwidth $= P_c/\tau$ and (c) compressed output signal has power level of PP_c. For the same peak power employed and the same number of pulses transmitted in detection and high-range resolution modes, the effective receiver bandwidth remains the same. The larger bandwidth target recognition waveform corresponds to a larger noise bandwidth, but is compensated for by the increased level of the signal due to the pulse compression ratio*

so that the value of τ used in the equation can be maintained. This is illustrated in Figure 7.4.

The value of the pulse compression ratio used for the high-range resolution mode is the same as the increase in bandwidth of the received signal. Hence, with reference to (7.2), the increase in peak power by a factor of P_C, which is the pulse compression ratio for the high-resolution mode, compensates exactly for the pulse length reduction by a factor of P_C.

With reference to (7.2), if the rcs of the smallest target element of interest for recognition is 20 dB, or one hundredth of the value of the rcs of the whole aircraft, then the range at which the same signal-to-noise ratio is obtained is the fourth root of one hundred, which is about three. This means that the target recognition mode can only be applied at one-third of the range of the target detection mode, if all other parameters are maintained. This is a key aspect of designing a high-resolution mode, the overcoming of this ratio between the detection of the target and the application of the target recognition mode.

7.2.3   *Maximising application range for target recognition mode*

It is necessary to examine Equation (7.2), in order to identify any system parameters, which the radar designer can employ, in order to redress this range balance. The peak transmitter power, P, can sometimes be increased for short periods of time for a specific mode, but is unlikely to be more than one or possibly 2 dB. The antenna aperture, A, is a fixed value for most radars, so it cannot be changed. However, for some types of phased arrays, which use multiple beams for surveillance, there are opportunities for concentrating the transmitted power into a single beam, to utilise the full aperture available. The rcs, σ_e and effective pulse length, τ, have been discussed. The number of pulses integrated, N, is a good candidate for improving radar sensitivity. By coherently integrating more pulses on the target, the sensitivity and radar range are increased. This can be achieved by increasing the pulse repetition frequency (prf) of the waveform, which is generally dependent upon the transmitter design, or by dwelling for a longer period on the target. An extended dwell period can have operational and practical difficulties, which will be explored in Chapter 10.

The radar wavelength employed, the system losses and the noise figure of the radar cannot realistically be improved for the high-resolution mode. However, the value of the threshold, S, has potential to be reduced. As the target has generally been detected before the application of the high-resolution mode or several detected scatterers are clustered together and some are well above the system noise floor, there is scope to reduce the detection threshold. The statistics used for target detection and the establishment of detection probabilities and false alarm rates are not really applicable to high-resolution modes in the same way. For target recognition, it is not a question of whether the target has been detected, but more a question of whether the level of noise affects the reliability of the whole target recognition process. This is again dependent upon the actual type of target recognition technique being employed, the precision with which the mode is required to perform and the number of different types of target, which have to be differentiated. This is a very complex issue and cannot easily be generalised. However, it would normally be considered that the thresholds used in detection of typically 14 dB would be too high for target recognition and could be lowered by several decibels.

Hence, when these various measures for maximising the range for the application of the target recognition mode are taken, it is possible to approach the primary detection range of the radar. The radar can then apply the recognition function to most targets over most of the ranges of interest after performing initial detection and the establishment of a confirmed track.

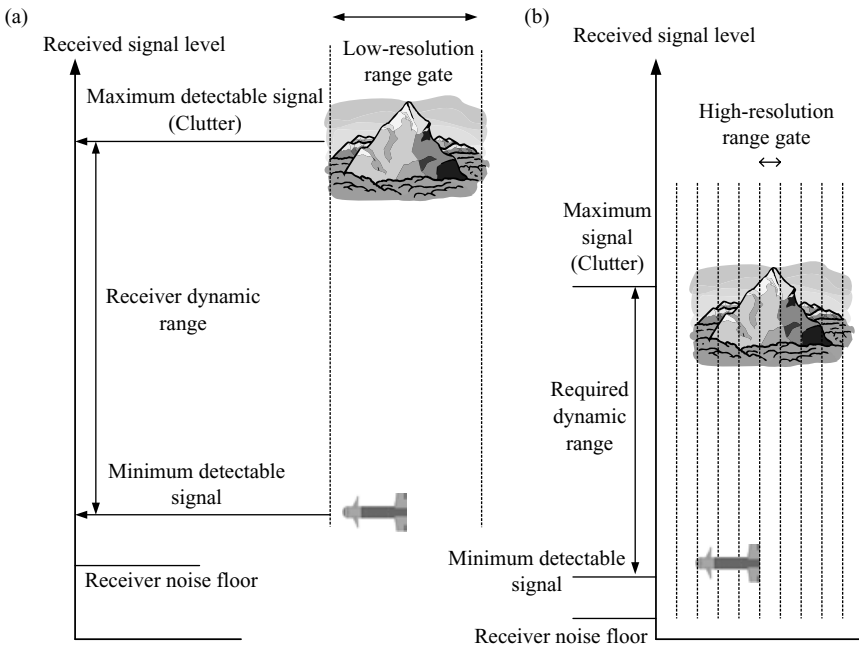## 7.3   Dynamic range

7.3.1   *Introduction*

In the design of most radar systems clutter is usually a significant factor, which has to be taken into account. The levels of reflected returns from ground and sea clutter can be many orders of magnitude larger than the desired signals from targets, which

are required to be detected. In order to efficiently detect targets simultaneously with clutter entering the radar, it is necessary that all the radar receiver components remain within their linear operating regions so that distortion does not occur. If the receiver is driven into the non-linear part of its operating characteristic by high levels of clutter, it can result in spurious signals being generated, which raise the radar's false alarm rate and can obscure the returns from targets of interest.

7.3.2   High-resolution applications

In target recognition applications the dynamic range requirements are even more stringent than for conventional target detection and tracking modes. As discussed earlier, the high-resolution waveform dissects the target into small elements, so rather than the clutter returns competing with the whole target's rcs in the receiver for being detected, each target element now has to compete with the clutter.

However, when employing a high-range resolution mode, for clutter that is distributed in range, it too is dissected by the waveform and is shown in Figure 7.5. For the conventional radar mode in Figure 7.5(a), the whole return from the missile target is detected simultaneously with the clutter return from the mountain, which is set at the maximum amplitude that the receiver can linearly detect, for this example.
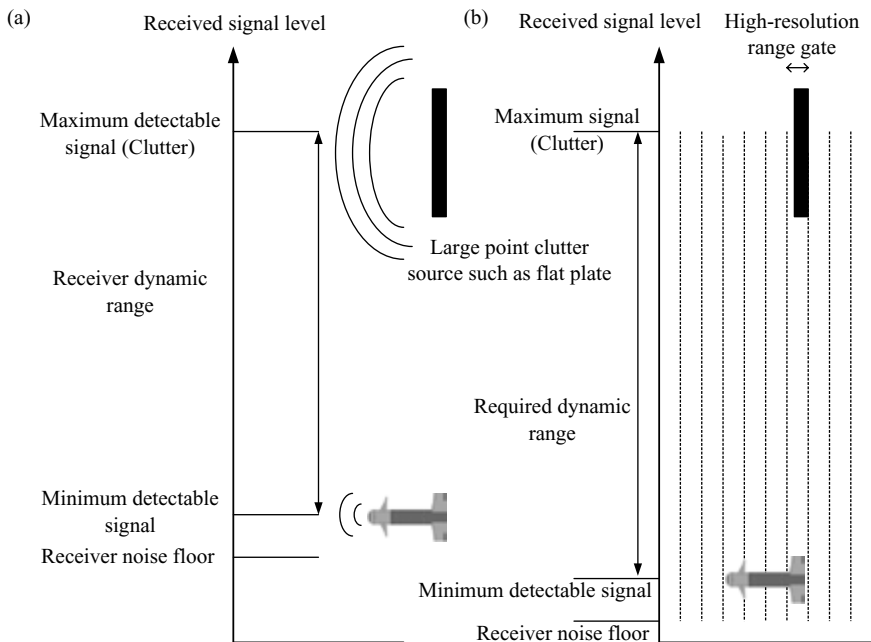

Figure 7.5   Dynamic range for distributed clutter: high-resolution waveform divides target and clutter signals into smaller elements: (a) conventional radar modes and (b) high-range resolution mode

The level of the signal entering the receiver from the missile is set to be the minimum amplitude that can be detected with the conventional waveform. For the high-range resolution mode, shown in Figure 7.5(b), assuming that more pulses are integrated than for the conventional mode, the receiver sensitivity is improved, so the noise floor drops and the small target elements of the missile can be detected. The clutter returns from the mountain are assumed to be distributed in range and are also dissected by the high-resolution waveform, so the maximum signal level in each range gate is reduced, in comparison with the conventional mode.

The actual dynamic range requirements for the radar are determined by the high-resolution characteristics of both the target of interest and the clutter.

For large point clutter returns, such as those from objects containing flat plates or corner reflectors, the situation is much more difficult. With the high-resolution waveform the radar has to receive and process the clutter signals, which are still of very high amplitudes, simultaneously with the small target elements. This is illustrated in Figure 7.6. It can be seen that the radar system has a more severe dynamic range requirement in the high-resolution case, than for conventional modes. Although the target is divided into small elements by the high-resolution waveform, the point clutter, which is localised in range, is confined to a single range gate. Hence, the elements

Figure 7.6   Dynamic range for point clutter: high-resolution waveform divides target into small elements, which have to be simultaneously detected with large point clutter returns, which are not divided into small elements: (a) conventional radar modes and (b) high-range resolution mode

of the target have to be simultaneously detected with the large point clutter source. Although the noise floor is reduced by integrating radar pulses, for example, so that smaller targets or parts of targets can be detected, the point clutter source remains at the same level. This contrasts with the distributed clutter case previously discussed, in which the target, clutter and noise floor are all effectively lowered by use of the high-resolution waveform and the integration of more pulses.

Most high-resolution radars would encounter both distributed and point clutter. The radar design has to address the level of the signals from the target and the clutter entering the receiver and requirements on the digitiser and signal processing functions for extracting the target signature data. The design has clearly to accommodate the requirements of both the radar's conventional and high-resolution modes. The component implications of the dynamic range requirements are discussed in the next chapter.

7.4   Calibration and compensation for system distortion

7.4.1   Introduction

For designing and operating radars with conventional low-resolution modes, requirements very rarely arise for compensating for distortions in the radar occurring over the bandwidth of the transmitted pulse. Over a few MHz of bandwidth, corresponding to several tens of metres of range resolution, radar components generally have relatively linear amplitude and phase characteristics, so compensation for associated distortion is not required. However, for high-range resolution applications, in particular, the signal is often distorted by the non-linear characteristics of radar components and compensation is required. Within this section, a summary of typical distortion effects [2,3] is provided and techniques used to compensate [4] for the distortion are presented.

7.4.2   System distortion effects

A major issue for high-range resolution radar systems, which operate over large bandwidths, is the distortion, which occurs due to non-ideal amplitude and phase characteristics of the components comprising the radar system. The actual waveform generated can undergo distortion in the transmitter, antenna and the receiver components. This results in the signal that is effectively transmitted and received by the radar deviating from the signal which was intended to be transmitted. In the absence of any method for compensating for the distortion, the range resolution and time sidelobe performance of the radar can be significantly degraded.

Amplitude distortion occurs as a result of the amplitude versus frequency characteristics of any component deviating from constant gain or loss across the bandwidth of the waveform and is illustrated in Figure 7.7.

The amplitude of the signal for a typical radar component varies across its bandwidth. Distortions due to amplitude variations can occur in active components, such as
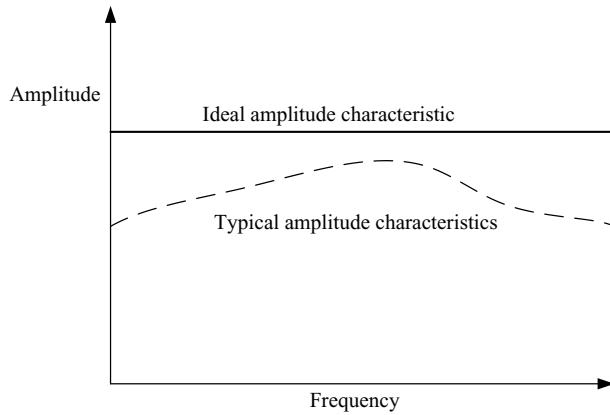
Figure 7.7   Amplitude characteristics of radar components, which vary across fre-quency band, can distort signal and degrade high-range resolution performance
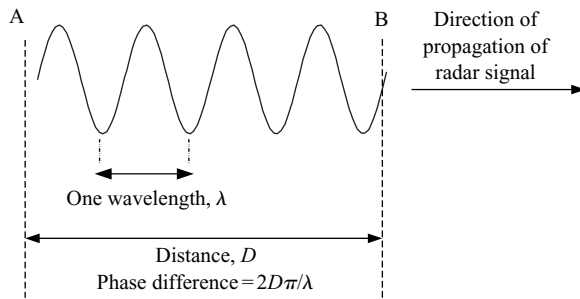

Figure 7.8   In freespace, group delay, τ_d, between positions A and B, is time delay of waveform, which is distance, D, divided by c

amplifiers, passive components, such as filters and frequency conversion components, such as mixers.

In practice, the major contributor to distortion of the radar signal is phase rather than amplitude. The distortion of the radar signal due to phase distortion is actually an effect associated with the time delay of the signal through the component. The time delay of a signal through a component is called the group delay, τ_d, and is defined as:

$$\tau_d = \frac{d\varphi}{(2\pi)df} \tag{7.3}$$

where φ is the phase and f is the frequency. It can be seen that group delay is defined as the rate of change of phase with frequency. For free space propagation of a sinusoidal radar signal, consider, for example, Figure 7.8. Over a distance, D,
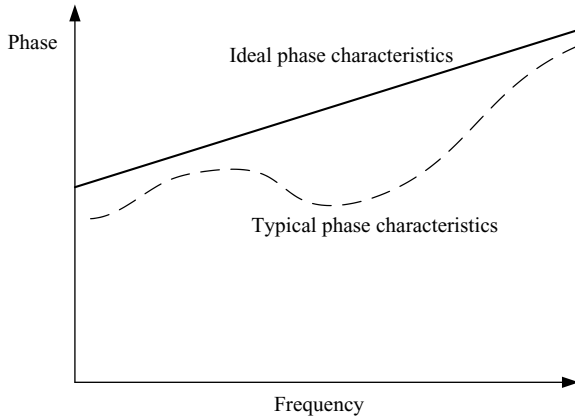
Figure 7.9   In typical radar components, the phase departs from the ideal linear characteristics of freespace

the actual phase difference at wavelength, λ, between the positions A and B, is $2D\pi/\lambda$, measured in radians. As $c = f\lambda$, for freespace, then this phase difference can also be expressed as $2d\pi f/c$. Using Equation (7.3), the differential of this phase with respect to frequency is:

$$\tau_d = \frac{d\varphi}{(2\pi)df} = \frac{d}{(2\pi)df}\left(\frac{-2D\pi f}{c}\right) = \frac{D}{c} \tag{7.4}$$

(D/c) is the group delay and is the time taken for the radar wave to propagate from positions A to B, τ_d, in freespace. The group delay is the time delay through a component or series of components, at a particular frequency.

A non-linear group delay characteristic is exactly equivalent to phase characteristics, which deviate from a linear slope over the radar's bandwidth. This is illustrated in Figure 7.9. For ideal components the phase length is proportional to frequency and is a linear characteristic. The phase length through a linear component is proportional to its frequency, as in freespace propagation. In practice, components have some degree of non-linearity and have characteristics which deviate from the straight line.

The main components, which exhibit group delay distortion from the high-range resolution perspective, are travelling wavetube amplifiers and waveguide components, such as couplers and filters. Waveguide components are inherently dispersive [5], due to the nature of electromagnetic wave propagation. The net effect is that the phase characteristic of the waveform against time deviates from the theoretical signal that was supposed to be transmitted. Components of the signal at different frequencies effectively experience different time delays through the radar.

In order to overcome both the amplitude and group delay effects, it is first necessary to characterise them throughout the complete transmit and receive paths of the radar.

7.4.3   *Measurement of distortion of wideband signal through radar*

7.4.3.1   **Distortion of waveform**

In order to illustrate the effect of amplitude and phase distortion over a large band-width, the utilisation of the stepped frequency technique for providing high-range resolution is used as an example, which is shown in Figure 7.10. At each frequency step, the amplitude and phase of the target are measured. However, at each step assume that there are both amplitude and phase errors occurring due to distortions in the radar. If these are not corrected for, the range profile obtained is distorted, as the measured data includes these errors. The phase errors effectively add different time delay errors to each respective measurement. It is equivalent to the target moving a random number of degrees between each frequency step measurement.
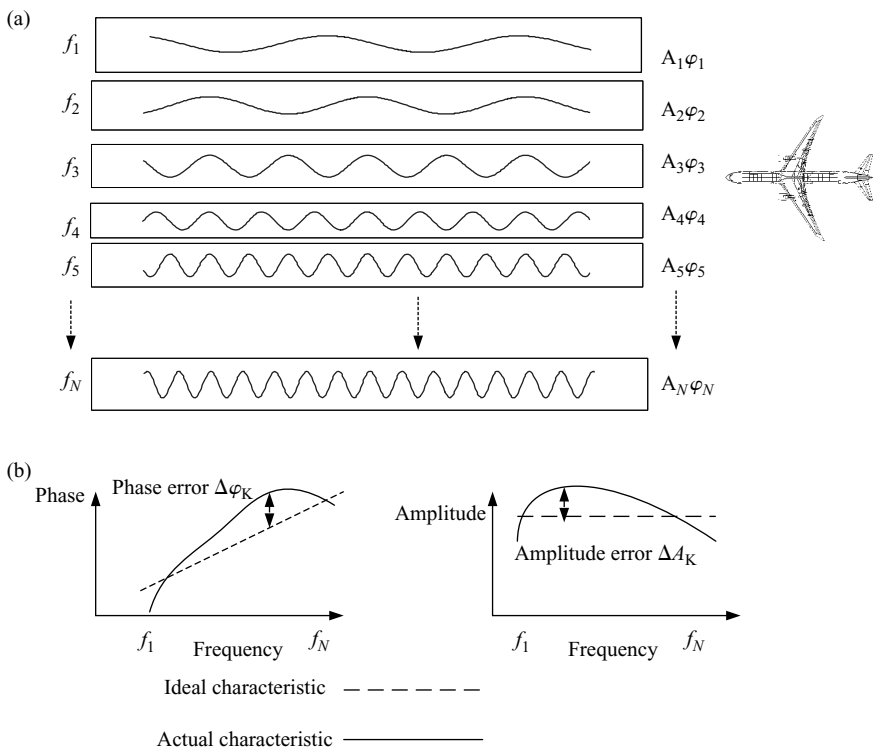
Figure 7.10   Example of distortions caused by radar components to high-range reso-lution measurement using stepped frequency techniques: (a) amplitude and phase characteristics of target are measured at each frequency and (b) errors in amplitude and phase measurements due to non-linearities in radar. Each measurement of amplitude, A_N and phase ϕ_N, in (a) must be compensated for by distortion in radar, ΔA_N and $\Delta \phi_N$

Hence, at each frequency step, it is necessary to measure the amplitude and phase distortions.

7.4.3.2   Characterisation of signal distortion

It is best to measure the amplitude and phase distortions in the radar with exactly the same waveform as utilised for the actual high-range resolution measurements and at a power level that is in the linear region of the radar's dynamic range. This means that the operating conditions for characterising the distortion are as close as possible to those of the operational high-resolution mode, so maximising the calibration function's effectiveness.

In addition, the maximum number of the radar's components should be included in the characterisation measurement, while minimising the use of extraneous components to support the measurement, as they too can contribute to distortion. Two types of techniques can be used: closed loop and the employment of an external test target.

7.4.3.3   Closed loop measurement

The closed loop calibration method is shown in Figure 7.11. The high-resolution radar signal is generated normally, up-converted and amplified in the transmitter. A sample of the signal is shown to be coupled from the output of the transmitter and coupled into the receiver. The amplitude and phase characteristics of the received waveform are then measured. As the output power of the transmitter is very much greater than the input power, which the receiver can safely accommodate, it is necessary to reduce the level of this reference signal. This would only be an extremely small proportion of the total power transmitted and be reduced by perhaps 90 dB or a factor of one thousand million. The coupler is a passive power splitter, which allows the rest of the power to either be transmitted normally via the duplexer and antenna or to be absorbed into a matched load. The latter approach obviates the need to transmit the signal into freespace, so does not require a test site.

The coupler may be a permanent feature of the radar design, which can be used for general testing of the radar system and not just for the high-resolution mode. If a coupler were not normally installed, it would have to be specially fitted for this
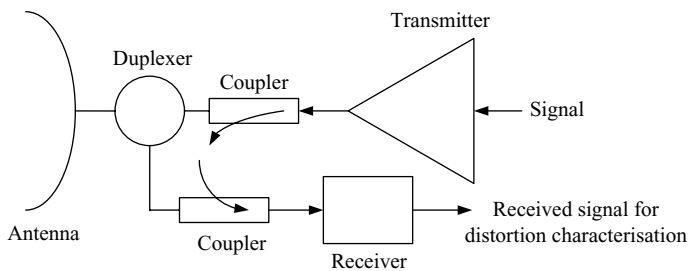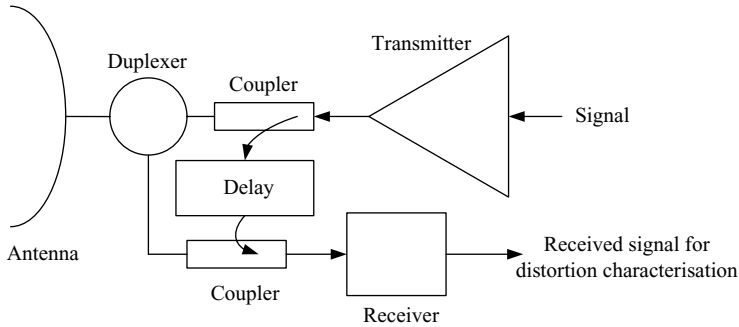

Figure 7.11   Characterisation of radar distortion using closed loop calibration method: a sample of the transmitted signal is directed into the receiver

Figure 7.12   Characterisation of radar distortion using closed loop calibration method and delay of sampled reference signal

measurement. This means that the radar would have to undergo some modifications from its build state when being used operationally. Also as the signal is coupled directly into the receiver, the duplexer, the antenna and the receiver protection switch are not included in the calibration measurement.

This reference signal appears to the radar receiver as a target at almost zero range. As close in clutter can reflect large amounts of power back into the receiver, it is normally turned off (Chapter 2, Section 2.1.14) for short-range targets. The receiver must be isolated from the transmitter power reflected from the duplexer, by either disconnecting it or by using attenuators connected to the duplexer to prevent leakage to the receiver. Also there could be other leakage paths from the transmitter to the receiver via general 'pick up', which can be experienced with high-power transmitters.

It can be seen that there are several practical problems with this closed loop approach for measuring the distortion characteristics of the relevant components. A technique for improving this measurement is to delay the reference signal after being coupled from the transmitter's output, prior to be coupled into the receiver, as shown in Figure 7.12. The delay would be provided by a device, which is called a transponder, which would ideally delay the signal, but not contribute any distortion. The delay of the signal would have to be sufficiently long to overcome the transmitter leakage breaking through into the receiver during the pulse and to allow time for recovery from any associated overloads in the receiver.

It is not normally practical to delay radar pulses at the microwave transmission frequency as the delay time required represents at least tens of metres of line length. This would have to be in microwave cable or waveguide, which would be rather bulky and lossy and would also need to be measured for group delay distortion. Techniques used involve converting the microwave signal to either an acoustic [6] or an optical [7] signal. Time delays can be achieved with the more compact and practical hardware involved such as with Surface Acoustic Wave delay lines and optical delay line transponders, the latter of which employ fibre-optic cables [8] to obtain the delay. After conversion to the delay line frequency the signal is delayed then converted back to the microwave radar frequency. It can be appreciated that the conversion and
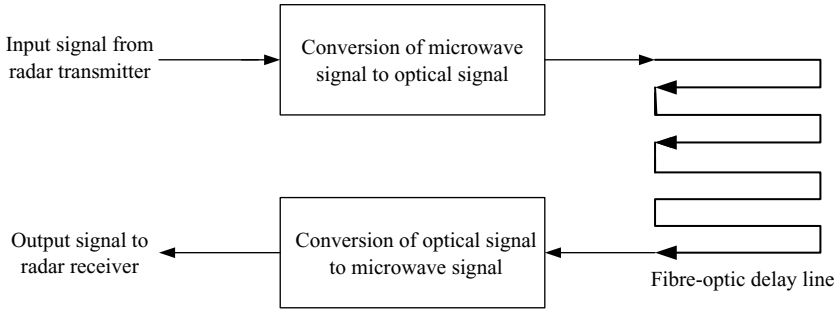
Figure 7.13   Functional block diagram of optical delay line transponder

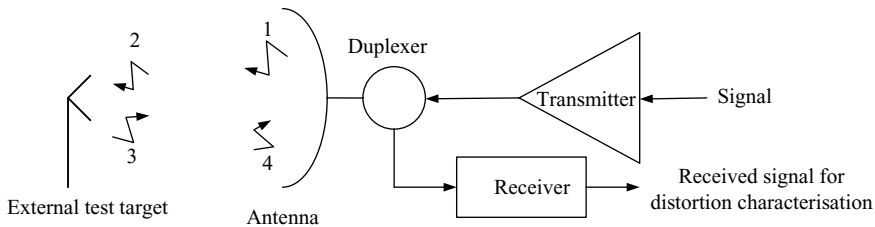*Figure 7.14   Characterisation of radar distortion using an external test target*

delay processes must be both wideband and linear in order to ensure that additional distortions from the delay line transponder do not affect the measurement. Hence, it is necessary to ensure that the transponder is operating in its linear region and that its output signal is at an appropriate power level for the radar receiver. A functional diagram of an optical delay line transponder is shown in Figure 7.13.

However, this method of characterising the radar still excludes the duplexer and antenna and includes couplers, which may not be part of the standard radar build. A major advantage is that it does not require a test site and an external test target for radiating signals and performing the measurements.

7.4.3.4   Employment of external test target

In order to ensure that all of the radar components that could contribute to the distortion of the radar signal are included in the measurement, the use of an external test target is required, as shown in Figure 7.14.

It can be seen that the complete radar system is being used in the measurements and no modifications to the radar are required. The key issues are the range to the test target, the local clutter conditions and the type of test target employed.

A large trihedral corner reflector located on the ground, with a physical area of about $1\,\mathrm{m}^2$, has a reasonably high rcs at most microwave radar frequencies. If there is negligible clutter in the vicinity and the radar pulse length utilised enables it to be
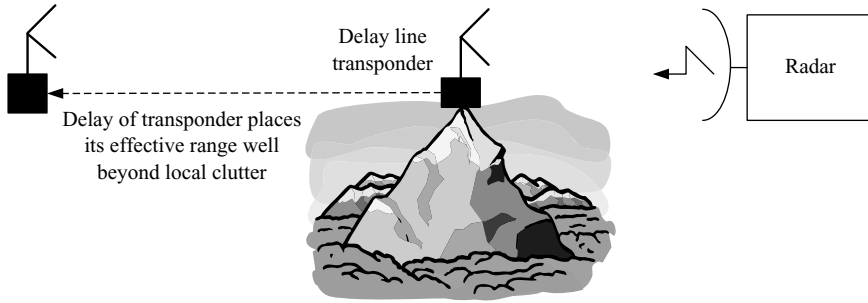
Figure 7.15   *External delay line transponder places test target at range that is well beyond local clutter, so characterisation of the radar system distortions can be performed*

placed at a few hundred metres range from the radar, then satisfactory measurements can be made.

In many cases the above criteria cannot be met and the level of clutter in the vicinity of the test target is too high, so that the positioning of a corner reflector on the ground is not the solution. In the past, schemes involving targets, such as metallic spheres being towed by inflated balloons have been used, so that the test target was in the air and clear of the antenna's mainbeam clutter. However, they tended to be logistically difficult to organise, costly and not possible to check on a regular basis.

The current approach is to utilise the delay line transponder described above as the remote test target. Provided its internal time delay is set such that it is placed much further in range than local clutter, it is an effective characterisation technique. This concept is shown in Figure 7.15.

If clutter is still troublesome, a frequency offset can be introduced in the transponder, so that it appears to be moving, so that if a coherent pulse Doppler waveform is being used, clutter can then be rejected by Doppler filtering. This technique is dependent upon the Doppler modulation process in the transponder not distorting the signal.

7.4.4   Compensation for signal distortion

The ideal or theoretical high-range resolution signal that is aimed to be transmitted is represented in the time domain as $f_{sig}(t)$. The Fourier transform of this signal provides its spectrum in the frequency domain:

$$f_{sig}(f) = \int\limits_{-\infty}^{\infty} f_{sig}(t)e^{-2\pi i f t} dt \tag{7.5}$$

where f is its frequency.

Using the process described above for characterising the radar signal, which is actually transmitted and received from a point target, let this time domain signal

be $f_{\text{actual}}(t)$. The spectrum of this signal is

$$f_{\text{actual}}(f) = \int_{-\infty}^{\infty} f_{\text{actual}}(t)e^{-2\pi ift}\,dt \tag{7.6}$$

$f_{\text{actual}}(f)$ is the spectrum of the signal, which is effectively the waveform used by the radar and includes the distortion effects. As the variations of group delay across the signal's bandwidth cause the most distortion effects and they are frequency dependent, it is easier to work in the frequency domain for determining and compensating for them. With reference to Equations (7.5) and (7.6), the values of the spectra defined are those of the theoretical and measured waveforms. As both of these values are available from the Fourier transforms of the time domain signals, the ratio of the two spectra is the distortion of the waveform across the frequency band, $f_{\text{dist}}(f)$ and is defined as:

$$f_{\text{dist}}(f) = \frac{f_{\text{actual}}(f)}{f_{\text{sig}}(f)} = \frac{\int_{-\infty}^{\infty} f_{\text{actual}}(t)e^{-2\pi ift}\,dt}{\int_{-\infty}^{\infty} f_{\text{sig}}(t)e^{-2\pi ift}\,dt} \tag{7.7}$$

Equation (7.7) represents the amplitude and phase error coefficients of the signal across its frequency band for a point target.

The process for compensating data obtained from real high-resolution targets is now discussed. It is necessary to compensate radar signals from each high-resolution range gate with the distortion coefficients, which were measured in the characterisation activity. If the received radar signal from a target is represented in the time domain as $F_{\text{target}}(t)$, then in the frequency domain it is:

$$F_{\text{target}}(f) = \int_{-\infty}^{\infty} F_{\text{target}}(t)e^{-2\pi ift}\,dt \tag{7.8}$$

This is the distorted spectrum of the target. The compensated spectrum, $F_{\text{comp}}(f)$, is obtained by dividing it by the coefficients in Equation (7.7):

$$F_{\text{comp}}(f) = \frac{F_{\text{target}}(f)}{f_{\text{dist}}(f)} \tag{7.9}$$

Hence, the compensated range profile of the target, $F_{\text{comp}}(t)$ is the Fourier transform of Equation (7.9) and is:

$$F_{\text{comp}}(t) = \int_{-\infty}^{\infty} F_{\text{comp}}(f)e^{2\pi ift}\,dt \tag{7.10}$$

The measured distortion characteristics of the radar can then the used to compensate for any high-resolution range profiles of targets measured by that particular radar over that bandwidth.

7.5 System design issues

7.5.1 Introduction

The key issues for including high-resolution modes into radar systems with conventional detection and tracking modes are minimising the additional components needed and minimising any effects on the performance of the standard modes. It would not normally be tolerable to degrade the performance of essential radar functions in order to support a target recognition mode.

The implications on the overall system design are presented here for typical target recognition modes. Apart from SAR applications, they are also required to operate with the conventional lower resolution tracking and detection modes. The issues associated with components for supporting high-resolution modes are discussed in Chapter 8.

7.5.2 Implementation

7.5.2.1 Introduction

The components needed for the standard radar modes are shown in Figure 7.16. The dotted components are ones which may be required to be modified, supplemented by or replaced to support the high-resolution modes, and are dependent on the actual waveform employed and its application.

In the following sections, the system level design issues are discussed for the most commonly used high-resolution techniques. It can be seen that the basic system
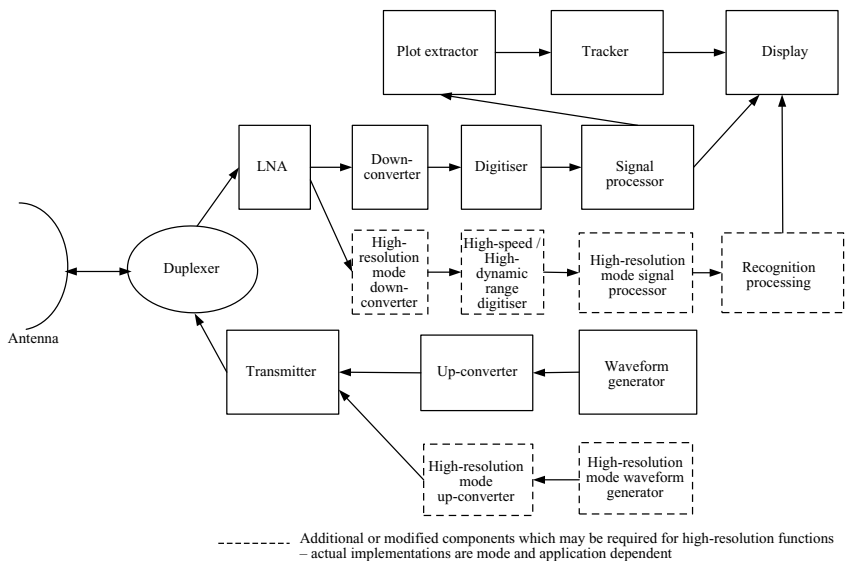

Figure 7.16 *System design architecture for supporting standard modes and high-resolution modes*

architectures are the same. Normally the transmitter, duplexer, mechanically scanning antenna and LNA can support all modes. Issues specifically relevant to phased array implementations are discussed in the Chapter 9, Section 9.3.

For upgrading existing systems or designing new systems with high-resolution modes, parallel signal channels are recommended and electronic switches would also be needed to route the signal through the appropriate components for the mode selected.

An additional signal processor is shown being used for the high-resolution modes. A processor for performing the target recognition function is also shown and its output can be seen to be displayed with the radar track data. This could be just a label on each track displaying the best estimate of the target's identity or a target signature for the radar operator's interpretation.

7.5.2.2   JEM

For JEM implementations it may be feasible to use all the existing components and upgrade the software for the signal processing and recognition functions. As only narrowband components are used throughout the system for JEM, there is no requirement for wideband components or high-speed digitisers. It may be necessary to upgrade the waveform generator and digitiser for dynamic range reasons, as discussed in Section 7.2. The requirements for the signal processor are dependent upon whether there is sufficient capacity to accommodate the conventional and high-resolution modes.

A major issue is whether the transmitter can support the high prf waveform needed for unambiguous JEM measurements. It can be the main factor that determines the practicality of including a JEM mode in the system.

Provided the transmitter has a high prf capability, overall the system design changes for supporting JEM are small in comparison with most of the other target recognition techniques.

7.5.2.3   Wideband high-range resolution

In order to support wideband high-range resolution modes, signals with large bandwidths have to be accommodated throughout the radar. The waveform generator, up-converter, down-converter and digitiser are all required to operate with bandwidths that are perhaps one or two orders of magnitude higher than for the conventional modes. Hence, designs specific to wideband waveforms are required. Separate channels for the signal path are recommended up to the transmitter input and after the LNA in the receiver.

For the signal processing and recognition algorithm processing, the implementation is again dependent upon available signal processing capacity. This is also the case for the other high-range resolution techniques discussed later.

7.5.2.4   Stretch

As was seen in Chapter 3, Section 3.7, the objective of the 'Stretch' design technique is to implement a high-range resolution mode by using a low-bandwidth digitiser.

The waveform used in a wideband chirp has a much larger bandwidth than is required for conventional modes, so a waveform generator with a large output bandwidth is required. The up- and down-converter are needed to accommodate this wideband chirp. The latter is also required to mix the received signal with the wideband reference chirp to provide the low-bandwidth signal into the low-speed digitiser.

7.5.2.5 'Classical' stepped frequency techniques

In synthesising a wideband waveform in frequency increments, the major advantage of the stepped frequency technique is that only relatively narrowband components are needed throughout the radar. This means that the basic design of the system for the conventional and high-range resolution mode are very similar.

However, it is necessary for the up- and down-converters to include a local oscillator (LO), which is stepped in frequency across the required band. This is discussed in more detail in Chapter 8.

7.5.2.6 Bandwidth segmentation techniques

These were discussed in Chapter 3, Section 3.8, and are effectively a compromise between wideband waveforms and stepped frequency techniques. The actual implementation is very much application dependent. It certainly requires a LO, which can be stepped over the bandwidth to be synthesised. The requirements for the bandwidths of the waveform generator, up- and down-converters and digitiser are generally more than needed for the 'classical' stepped frequency techniques, but less than for the wideband within pulse modulation method.

7.5.2.7 ISAR

For ISAR, the high-range resolution waveform used determines the system design, and the points just discussed in the previous sections apply. The only additional aspects are that the signal processing load is heavier for the longer dwell periods than for the range profiling modes and that motion compensation sensors and techniques are also needed, as discussed in Chapter 4, Section 4.5.

7.5.2.8 SAR

For the particular case of SAR applications, the low-resolution components can usually be excluded leaving the wideband high-range resolution components required for ground mapping and target identification. Motion compensation equipment may also be required, as discussed in Chapter 4, Section 4.3.

7.6 Summary of system issues

High-resolution modes for recognising targets have more stressing system design and performance requirements than for conventional radar modes. As high-resolution waveforms dissect the target into small elements, the sensitivity and dynamic range

of the radar have to accommodate the processing of these relatively low power returns from the constituent parts of the target, as well as clutter and frequently at long ranges.

Wideband radar signals are required to provide high-range resolution signatures of targets. However, some active and passive components used in radars are non-linear and can substantially distort the signal. In order to overcome the potentially serious degradation to the high-range resolution performance, the distortion of the system has to be characterised and then used to compensate the received signal. Techniques for characterising radar system distortion can involve closed loop measurements on the radar or external tests using a remote test target. Delay line transponders are often used for the test target, as they can overcome the problems of short-range clutter affecting the characterisation measurements.

For upgrading current systems with high-resolution modes or designing systems that can support conventional and high-resolution modes, parallel signal channels are often required to accommodate the specialist mode requirements. There are trade-offs between the complexity of the design and the performance of the high-resolution mode. Additional signal processing capacity is needed for the signal data and for the recognition functions.

References

1   SKOLNIK, M.I.: 'An Introduction to Radar Systems' (McGraw-Hill, New York, 1970) Chapter 14
2   http://www.microwaves101.com/encyclopedia/groupdelay.cfm
3   VUOLEVI, J., and RAHKONEN, T.: 'Distortion in RF Power Amplifiers' (Artech House, Boston, MA, 2003)
4   TAIT, P.D.F., and SHEPHARD, D.J.: 'Radar System'. UK Patent no. 2 300 989. Application date 20/11/96
5   REITZ, J.R., and MILFORD, F.J.: 'Foundations of Electromagnetic Theory' (Addison-Wesley Publishing Co., Reading, MA, 1971) Chapter 16.5
6   MORGAN, D.P.: 'History of SAW Devices'. IEEE *International Frequency Control Symposium*, Pasadena, May 1998
7   YOFFE, G.W., ARKWRIGHT, J.W., TOWN, G.E., and SMITH, B.G.: 'Tunable Optical Delay Line Based on a Fibre Bragg Grating', *Electronics Letters*, 1998, **34** (17), pp. 1688–90
8   SYMS, R., and COZENS, J.: 'Optical Guided Waves and Devices' (McGraw-Hill, New York, 1992)

Chapter 8

Component implications

8.1 Introduction

The detailed requirements for the radar components needed to support target recognition functions are dependent upon several factors. The key ones are the type of high-resolution mode being employed, the range and the type of target, the level and the reliability of the target recognition capability required and the clutter environment. Although requirements for individual applications vary considerably from recognising ships with ISAR at short range, to discriminating the warhead at a range of several hundred or even thousands of kilometres in ballistic missile defence, general guidelines can be provided.

The implications on the design of the waveform generator and reference frequencies, the up-converters, the transmitter, the receiver, the digitiser and the signal processor are discussed for the various high-resolution techniques. As a design reference, the high-resolution mode requirements for the radar components and system are compared with the requirements for lower resolution modes for the detection and tracking of the target with the same radar. As many radars that are used for conventional radar modes can be potentially upgraded to provide target recognition modes, this is considered to be a reasonable basis for comparison.

8.2 Waveform generation

8.2.1 Introduction

The function of the waveform generator is to provide highly stable baseband signals, at the correct frequency, at the correct time and with the required modulation. Also included are reference and local oscillator (LO) frequencies, which are used throughout the radar. The term frequency synthesiser can also be used to describe this function.

The two types of applications covered are high-range resolution and high-frequency resolution.

8.2.2   High-range resolution

8.2.2.1   Stepped frequency techniques

The key design requirement for stepped frequency techniques is the generation of a series of frequencies [1], which are normally evenly spaced and are very close to their nominal frequencies. As the phase to the target is measured at each step, an error of a few degrees, due to the inaccuracy of transmitted frequency, can degrade the range profile. For example, for a radar operating at 10 GHz and making high-resolution measurements of a target at 100 km range, the error in the set frequency will now be calculated for an allowable phase error of 3°. This has been selected as being a reasonable assumption to scope the frequency accuracy requirement. The number of degrees to the target and back is given by twice the target's range divided by the wavelength, which is 3 cm, and multiplied by 360°, which gives 2 400 000 000°. An error of 3° corresponds to a wavelength error of one part in 800 000 000 and corresponds to 12.5 Hz at a transmission frequency of 10 GHz. Hence, it can be seen that the transmitted frequencies must be very precise. As the radar is switching frequencies sequentially across the band, they must each be at the required frequency very rapidly and the frequency must be maintained over the duration of the measurement period at each step. The accuracy requirement is illustrated in Figure 8.1. The LO frequencies used in up-conversion and in the receiver also need to be very accurately set. It is recommended that each frequency is generated from a common reference frequency, by direct digital synthesis, for example, so that all the frequencies can be precisely mathematically related.

In order to operate in an environment with clutter present, for applying the high-range resolution mode to moving targets and to reject the clutter, a pulse-Doppler variant of the stepped frequency technique, which was described in Chapter 3, Section 3.5, is required. By applying one pulse at each frequency, clutter cannot be rejected. Essentially clutter has to be rejected at each frequency step, so several
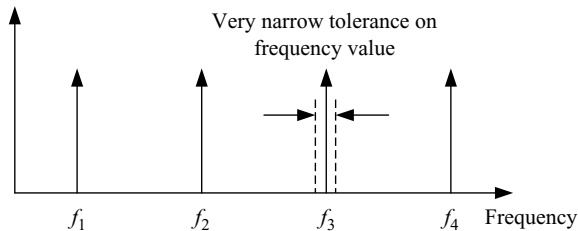

Figure 8.1   Stepped frequency waveforms have a very narrow tolerance on the value of each frequency
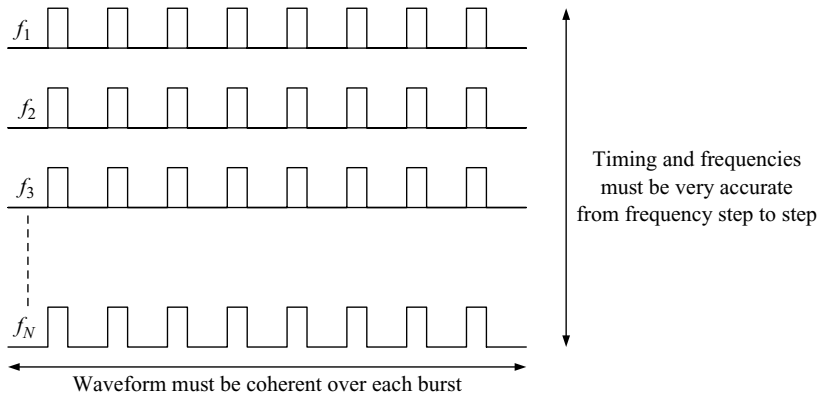
Figure 8.2 Stepped frequency waveform is required to transmit a burst of pulses at each step for clutter rejection

pulses at each frequency have to be repeated, so that coherent pulse-Doppler processing can filter out the clutter. The stepped frequency waveform is now effectively being adapted to be a pulse-Doppler waveform for a burst of repeated pulses at each step. The Doppler filter with the target energy then provides the contribution to the range profile from that particular frequency step. The range profile is then generated from all the frequency steps, using the target energy in the appropriate Doppler filter. The waveform generator must also provide high accuracy timing between the frequency steps so that when motion compensation is applied for moving targets, the phase correction can be made at the correct time. This waveform is shown in Figure 8.2.

As the signal at each frequency is now a burst of radar pulses, it is necessary for the waveform generator to provide this function. However, it would normally be expected to be incorporated in the basic design for the waveform generator, as the conventional radar modes would normally use a pulse-Doppler waveform burst for detection and tracking. The high-resolution mode would then sequentially step through several of these bursts as the signal frequency incrementing each burst.

Under these conditions, very good phase noise performance is required. It is determined by the maximum level of co-range point clutter, which is likely to be encountered. As was discussed in Chapter 7, Section 7.3, on system dynamic range requirements, high levels of point clutter stress the design, as small target elements, rather than the whole target, are now competing with the large clutter return. In comparison with standard radar modes, the phase noise requirements for operating in the presence of large point clutter returns is increased by the ratio of the whole target radar cross-section (rcs) to that of the smallest target element of interest, so would be expected to be a few orders of magnitude more stringent. If only distributed clutter is experienced, the requirement would not be expected to be different from the normal radar mode. Any spurious signals produced in the waveform generator can potentially degrade the high-range resolution performance, so should be filtered out.

The level of precision of the timing of the individual frequency steps is not considered to be more severe than normal radar modes. However, step-to-step timing is important, as compensation for moving targets is required. The range at each step must be known to within a few degrees, so the timing accuracy for each burst must also be consistent with this requirement.

8.2.2.2   Wideband waveforms

The main requirements for the waveform generator for wideband within pulse waveforms [2] are to provide a waveform close to the theoretical design, with low levels of spurious signals and phase noise, and repeated every pulse, so that coherent integration can be performed. Clutter can then be rejected and the sensitivity benefits of coherent pulse integration are obtained.

The synthesis of the waveform is normally now performed digitally in either in-phase and quadrature channels or directly in a single channel. The fidelity of the actual waveform with respect to the theoretical waveform is dependent upon the number of bits in the digital to analogue converter (DAC) used. Eight bits are readily available for up to several hundred MHz of bandwidth and are not considered to be a limitation.

The level of any spurious signals generated must be such that it does not degrade either the time sidelobe or the Doppler noise floor performance of the radar.

For moving targets the time sidelobe requirements are dependent upon the dynamic range of the scatterers of the targets of interest. For example, if scatterers within the measured range profiles, with power amplitude variations of 30 dB, were to be encountered, the effects of any spurious signals generated at 40 dB below the peak return, would not generally present a problem. For stationary targets, which compete against ground clutter, more severe requirements would be expected.

The type of spurious signal generated and whether it is coherently integrated over the pulse train or if it experiences compression gain within the pulse compression process, determine the effect on the range profile.

The Doppler noise floor is dependent upon phase noise considerations, as discussed in the previous section. The DAC clock, which generates the amplitude coefficients of the transmitted signal, has to be specified for phase noise performance. Phase noise on the transmitted signal translates into noise in the frequency domain when the returned signal from the target is processed in the receiver. As wideband waveforms are being employed, the phase noise performance has to be specified over a much wider band than for the conventional modes. However, in practice, the level of phase noise reduces for higher modulation frequencies, so it does not tend to be a problem.

The considerations discussed so far in the section are applicable to wideband waveforms, which are digitised appropriate to the bandwidth employed and to stretch techniques. One critical issue for the implementation of stretch techniques was until recently the linearity of the frequency modulated waveform ramp. The employment of digital modulation techniques and the high-quality frequency sources now available have eliminated this problem for most applications.

8.2.3   JEM waveforms

The key issue for high-frequency resolution waveforms is again phase noise. As the JEM lines have low rcs in comparison to clutter, the requirements are more stressing than for the detection and tracking modes. Each JEM line has to be resolved and detected in the presence of potentially high levels of returns from clutter. As the JEM waveform is usually low bandwidth, it has large range gates, so all co-range clutter has to be rejected by the Doppler filtering, as it cannot be differentiated in range. As JEM waveforms have high pulse repetition frequencies (prfs) to provide unambiguous frequency returns for JEM analysis, the range is highly ambiguous. Short-range clutter can reflect very large returns to the radar, and they appear in the same range gate as JEM lines, which are at a much longer range. This exacerbates the phase noise problem, so high-quality reference oscillators are needed for performing JEM in these circumstances.

8.3   Up-conversion

The main issues for up-conversion are for wideband waveforms. If in-phase and quadrature up-conversion techniques are being used, maintaining the amplitude and phase balance over the large signal bandwidth is important. Imbalance is manifested as time sidelobes in the target's range profile. Although signal processing techniques can be used to quantify and compensate for these mismatches, it is generally better to use wideband components with inherently good channel balance. LO breakthrough can also be a problem for wideband systems utilising in-phase and quadrature up-conversion. It can also contribute to degradation of the range profile. The selection of mixers, which have low levels of breakthrough, is recommended. Good frequency filtering is needed during the up-conversion stages, as wideband signals can generate large numbers of harmonics and intermodulation products, which can mix and generate unwanted spurious signals. Normal microwave design techniques are usually adequate.

8.4   Transmitter

The key issue for the transmitter, whether it is a vacuum tube or solid-state device, is that it generates sufficiently high power over the required bandwidth. If the power falls off too rapidly with frequency, the range resolution obtained is degraded.

Added phase noise can be a key issue for some travelling wave-tube designs, whereby the amplification process itself generates phase noise [3] and is not related to reference oscillator stability, as is generally the case in radar. Although the phase noise performance may be adequate for conventional radar modes, the increased dynamic range requirements of high-resolution modes are more stringent. Travelling wave tubes also tend to generate higher levels of spurious output signals than solid-state devices, so this has to be taken into account in the design and also remedial filtering may be needed.

8.5   Receiver

The dynamic range, spurious signals and phase noise are the most critical issues for a radar receiver supporting high-resolution target recognition functions. The analogue component limiting the dynamic range is generally the low noise amplifier, which has to establish the radar's noise figure and to also linearly amplify high-level clutter signals. However, the requirement is not normally more severe than for the conventional modes, as the actual levels of power received are similar for the two types of modes for the same expanded pulse lengths and transmitted power.

The effects of generating spurious signals are more severe than for the conventional modes as they compete with the required returns from the small target elements used for recognition. Hence, the generation and filtering of spurious signals must be more tightly controlled for high-resolution modes.

Phase noise is again a critical issue and depends upon the performance of the reference oscillator used in the radar and on the up-conversion techniques used to synthesise the RF signal and LOs. JEM is the high-resolution mode, which is likely to be most affected by phase noise and has the most stringent requirements. It is generally good practice in high-resolution applications for a single reference oscillator to be used to generate all the RF signals, clocks for digital to analogue and analogue to digital conversion and for all the timing signals for the radar pulse lengths and prfs. This approach ensures that all components in the radar are well synchronised and that any drifting in the master oscillator frequency is common to all components and functions. It is not absolutely essential but is recommended.

The quadrature down-converter should be well balanced in amplitude and phase to minimise 'image frequencies' being generated in wideband applications, to maintain low time sidelobes. Quadrature down-converters can also have relatively high levels of dc voltage at the output for some configurations of mixers used. These levels should be minimised, by using ac coupling, for example, as this voltage can adversely affect the following analogue to digital converter's (ADC) dynamic range. A large dc offset lowers the 'headroom' for large signals, so non-linear effects occur for lower level signals if the offset is left uncorrected.

8.6   Analogue to digital converter

8.6.1   High-range resolution

For many high-resolution radar applications the ADC is the weakest link. If the radar is transmitting signals with similar power levels, duty cycles and pulse lengths to the low-range resolution mode, the digitiser also has to accommodate the larger bandwidth signals for the high-range resolution mode. It is required to digitise the signal at a faster rate and also have a higher spurious free dynamic range for the smaller target elements to be detected in the presence of high levels of point clutter, as shown in Figure 7.6. The requirement for the increased dynamic range is shown, which usually means that more pulses must be coherently integrated and the level of any spurious signals generated in the digitiser must be kept below the lowest signal level.

As both pulse compression and coherent pulse integration are normally performed digitally, any spurious signals generated in the digitiser potentially compete with the small signals detected from the elements of the target. As the bandwidth increases, digitisers tend to have less effective bits, so that issues of setting the noise floor for detecting the smallest signals of interest and linearly processing the peak signal levels are crucial. The performance of the radar's high-range resolution mode, particularly in the presence of clutter, is often dependent upon a high-performance digitiser being employed and optimally used. As higher and higher range resolution is needed to detect finer target details, the requirements for the performance of the digitiser are also constantly increasing. However, this is balanced by the rapid development in digitiser technology [4].

Another requirement on the digitiser is in-phase and quadrature channel balance for the same reasons as for the down-converter. If the basic design does not meet the requirements, they can be achieved by using a built-in calibration function. Test signals are generated over the frequency band and the output amplitude and phase are measured and are used to compensate for the imbalance as part of the signal processing functions.

8.6.2   JEM

Jet engine modulation has the advantage of having a requirement of digitising at a relatively slow rate of perhaps 100 kHz, in comparison with high-range resolution modes having requirements of perhaps several hundred MHz. However, as JEM is highly ambiguous in range and small elements of targets at longer range compete with short-range clutter in relatively large-range gates, the dynamic requirements on the digitiser can be quite severe. As lower bandwidth digitisers tend to have more effective bits and a higher spurious free dynamic range than higher speed digitisers, these requirements are not quite so daunting, but are still challenging.

8.7   Signal and data processor

In target recognition applications high-resolution radar techniques are used to identify unknown targets, which are potentially a threat. In both the military and civil situations, the target is being recognised in order to make a decision about the next course of action. For an aircraft intruding into airspace, it could be an interception by an air defence aircraft or a missile engagement, if the target is particularly threatening. In the case of a small ship, for example, moving into an unauthorised area, the reaction could be an interception by a coastal patrol boat.

In most cases, decisions have to be made rapidly, using up-to-date and reliable information. The requirement is then for the radar to provide both target signature data and estimates of the target's identity in real time. The other components previously discussed in this chapter are able to continuously generate, transmit, receive and digitise radar data, on an almost indefinite basis in real time. It is also necessary for the signal and data processing functions to operate in real time.

For the synthetic and inverse synthetic aperture radar modes, the requirements are probably the most exacting. For high-resolution mapping modes, a continuous stream of radar data is required to be processed, to provide a map of the ground and images of targets of interest in real time. The data rate is appropriate to the radar signal's bandwidth, so up to perhaps hundreds of millions of signal samples are obtained every second. The interface from the digitiser to the signal processor is crucial, in that this data must continuously feed into the processor, without any significant delay. It must then be processed rapidly to provide the high-resolution map. Targets must then be detected on the map and recognition algorithms be used to establish the potential level of threat.

The signal and data processing functions can be performed by dedicated digital signal processors (DSP) [5,6], by field programmable gate arrays (FPGA) [7] or using powerful general-purpose processors [8–10].

8.8   Summary of component implications

The requirements on the performance of the radar components to support target recognition modes, excluding the antenna, which is dealt with in the next chapter, are fundamentally extensions of those required for supporting the implementation of conventional radar modes. The improvements required tend to be evolutionary. The basic design architectures to support the high-resolution modes are similar and are often compatible with upgrading conventional radars. The parameters most affected are phase noise, dynamic range, bandwidth and processing speed. The performance and application range of the target recognition function are dependent upon each of the components in the radar being designed to meet the detection requirements of the target elements, which are used as discrimination features by the recognition algorithms employed.

References

1   MICHAEL, B., MENZEL, W., and GRONAU, A.: 'A Real-Time Close-Range Imaging System with Fixed Antennas', IEEE *Transactions on Microwave Theory and Techniques*, 2000, **48** (12), pp. 2736–41

2   BALDANZI, M., TORTOLI, P., and ATZENI, C.: 'Programmable Wideband Signal Generation and Matched Filtering through a full Digital Approach'. Proceedings of the IEEE 4th International Symposium on *Spread Spectrum Techniques and Applications*, Volume: 1, 22–25 September 1996, pp. 42–6

3   GILMOUR, A.S., 'Principles of Travelling Wave Tubes' (Artech House, Boston, MA, 1994) Chapter 15

4   PACE, P.E.: 'Advanced Techniques for Digital Receivers' (Artech House, Boston, MA, 2000) Chapters 5–9

5   ANALOG DEVICES; http:// www.analog.com/processors

6   TEXAS INSTRUMENTS: http://dspvillage.ti.com

7   UNIVERSITY OF IDAHO, Microelectronics Research and Communications Institute, USA: http:// www.mrc.uidaho.edu/fpga/index.php

8   HU, Y.H. (Ed.): 'Programmable Digital Signal Processors: Architecture, Programming and Applications' (Marcel Dekker Inc., New York, 2001)

9   DAHNOUN, N.: 'Digital Signal Processing Implementation: Using the TMS320C6X Processors' (Prentice Hall, New York, 2000)

10 GAN, W.-S., and KUO, S.N.: 'Digital Signal Processors: Architectures, Implementations, and Applications' (Prentice Hall, New York, 2004)

Chapter 9

Antenna design issues

9.1 Introduction

In the previous chapter, the implications on the design of radar components required to support target recognition functions, were discussed. In this chapter the design issues for supporting high-range resolution modes, using two important classes of antenna, the traditional parabolic dish and the more modern phased array radars, are presented. The topics raised are representative of most types of antenna employed in target recognition. There are no critical issues for JEM associated with the antenna, as it is a narrow bandwidth mode.

In Section 9.2, parabolic dish antennas are discussed followed by phased arrays in Section 9.3. More details on antenna design can be obtained from Reference 1.

9.2 Parabolic dish antennas

The parabolic dish is well suited to high-range resolution applications. Parabolic dishes have been one of the most popular designs for radar antennas over many years. The design is inherently broadband, so it can accommodate the application of wideband signals, for high-range resolution modes, without any design modifications. Radars designed for conventional radar modes usually have some frequency agility [2], in order to overcome deliberate jamming or interference within the band. The part of the frequency band that is in 'the clear' is selected and used for transmitting the signal. The design of the antenna enables the electromagnetic wave to propagate in the same direction, without the need to perform any tuning or adjustments to the antenna when the frequency transmitted changes. Generally, parabolic dishes can provide at least 10 per cent bandwidth, with respect to the centre frequency of the band. An antenna, which has an appropriately designed feed and can launch an electromagnetic wave in the same direction, over a wide frequency range, is said to be *squintless*. This is illustrated in Figure 9.1.
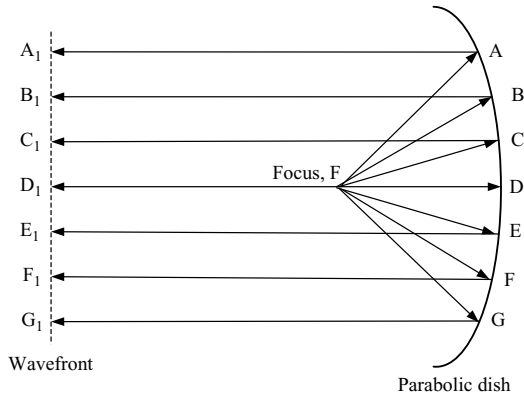
Figure 9.1   Squintless antenna supports high-range resolution modes. For ideal squintless antennas: (a) the distance from the focus to the wavefront, $FAA_1, FBB_1, \ldots, FGG_1$ is constant for all frequencies within the band and (b) the direction of propagation is constant with frequency

The parabolic dish can accommodate all the frequencies in its band of operation, both independently for frequency agility and simultaneously for wideband within pulse modulation for target recognition. The first important implication for high-range resolution is that when a wideband waveform is employed, it propagates in the same direction with frequency, so that all the frequency components of the signal illuminate the target. The same process occurs in reverse on collecting the signal from the antenna aperture. All the signal's frequency components are received. The second important implication is that the time delay of the components of the signal, as shown by the equivalent distances FAA_1, FBB_1 through to FGG_1, are all the same and are constant with frequency. This means that the various frequency components comprising the wavefront do not experience any dispersive effects, so that the integrity of the waveform is maintained as it passes through the antenna. In practice, most antennas are not quite squintless, but any minor distortion effects can be measured and compensated for using the calibration techniques discussed in Chapter 7.

Hence, a radar which utilises a parabolic antenna and can support a high bandwidth signal, can be used for high-range resolution modes without any modification required. This is significant both in the design of new high-range resolution radar systems and for the upgrading of existing radars with high-range resolution modes. This applies to high-resolution range profiling, SAR and ISAR. Other types of antenna can be used provided the same design constraints are met.

9.3   Phased arrays

9.3.1   Introduction

It is ironic that the key strength of phased arrays, which is the essence of their function and provides considerable performance benefits, is the control of the beam position by

adjusting the phase of the array elements. This is also their Achilles' heel (Achilles was the great Greek hero of the Trojan war, who was invulnerable apart from his heel) when the application of wideband waveforms is required. The problem is the fundamental narrow bandwidth of the phased array technique, which is a result of the physics of the technique and is not a technology limitation. Typically, phased arrays have instantaneous bandwidths of about 1 per cent of the signal frequency.

The bandwidth limitation can be viewed in two ways, which are really equivalent physical effects. The first is antenna squint in which the wavefront formed by the phased array changes angle with frequency. This means that the peak antenna gain varies with frequency and at a given look angle for the antenna, peak gain is only obtained over a narrow bandwidth, which limits the range resolution that can be supported. The second way of regarding the bandwidth limitation is in terms of the time delay across the array. If the antenna beam is required to be pointed away from boresight to support a wideband high-range resolution pulse, the contributing elements of the wavefront, have actually to result from wave contributions, which have relative time delays from each other. The elements arising from parts of the antenna furthest away from the wavefront experience an additional time delay compared with those close to the wavefront at the other end of the antenna. This differential time delay can also be considered to be a range resolution degradation, as a wavefront, which is required to be formed by contributions extended over tens of centimetres or metres, for example, is actually spread out in range.

Squint is discussed in the next section and its effect as a differential time delay are then presented in Section 9.3.3.

9.3.2   Squint

The theory of phased array beamforming was discussed in Chapter 2, Section 2.1.23. Squint is the direction of the wavefront formed by an antenna varying with wavelength, as shown in Figure 9.2. For the wavelengths λ_1 and λ_2, the wavefronts are formed at angles θ_1 and θ_2, respectively.

From Section 2.1.23.3 Equation (2.56), the relationship between the phase difference set between the phase shifters, ϕ, the spacing between them, d, the wavelength and the propagation direction is $\phi = (2\pi d \sin \theta)/\lambda$. Hence, for a constant setting of the phase shifters, ϕ, and the distance, d, is fixed, so $\lambda = \sin \theta (2\pi d/\phi)$, which means that the sine of the angle of the direction of propagation is proportional to the wavelength. If it is attempted to transmit a wideband chirp from the array, it would change the direction of propagation with the frequency sweep. In any particular direction only a small fraction of the bandwidth available would illuminate the target, so little benefit would be obtained from the high-range resolution waveform for target recognition purposes.

The maximum percentage bandwidth of a phased array is equal to its beamwidth measured in degrees [3]. Hence:

$$\frac{\Delta f}{f} = 0.57 \Delta \theta \qquad (9.1)$$
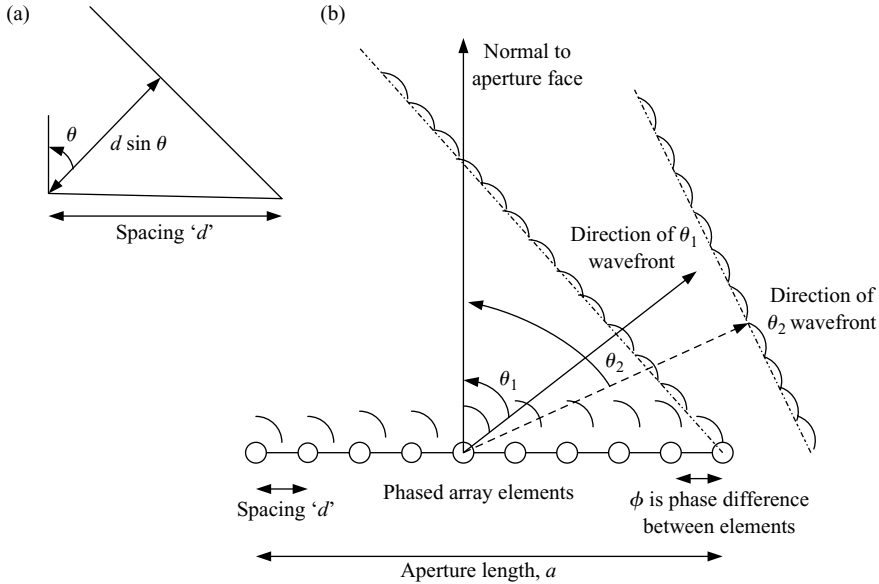
(a)   (b)

Figure 9.2   Antenna squint: the direction of the transmitted wavefront varies with wavelength: (a) beamforming when contributions of two elements are in phase and (b) at wavelengths λ_1 and λ_2 elements on array face form wavefronts at angles θ_1 and θ_2, respectively

where Δf is the bandwidth of the phased array, f is transmission frequency and $\Delta\theta$ is the beamwidth. From (2.22), the antenna beamwidth $\Delta\theta$ is $\sim \lambda/a$ where a is the array aperture.

Equating (2.22) and (9.1) and using the range resolution, $\Delta R = c/(2\Delta f)$:

$$\Delta R \sim 0.9a \tag{9.2}$$

The range resolution, which can be obtained by using the maximum bandwidth available from a phased array, is approximately the length of the array aperture. This is discussed in more detail in the next section.

9.3.3   Time delay effects

In Figure 9.3, the effects of squint are illustrated in terms of differential time delays for forming a wavefront off bore-sight for a wideband chirp waveform. A simple model, which is a representative of the differential time delay, or dispersive effects, is presented here. A more detailed model, which addresses the relationships between dispersive loss, bandwidth and time sidelobes, appears in Reference 4. Three phased array elements have been selected at positions A, B and C on the array face. It is assumed that the signal reaches each of these in phase and is synchronised in time, such that the beginning of the chirp is transmitted from each simultaneously. For beamforming off bore-sight, the respective distances to the wavefront to be formed, AA_1,
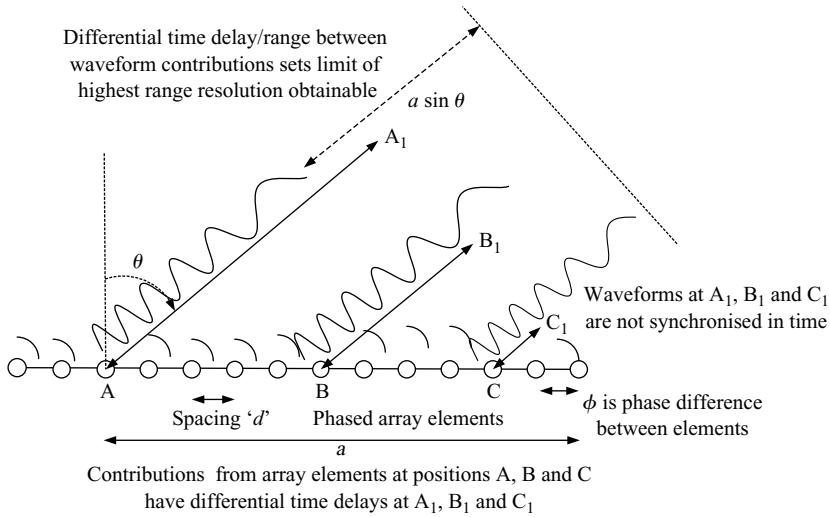
Figure 9.3 Differential time delays across phased array for wideband chirp waveform

BB$_1$ and CC$_1$, can be seen to differ and for this example it is assumed that these differential time delays are of the same order as the range resolution required. This effect is also shown at positions A$_1$, B$_1$ and C$_1$, with the respective chirp contributions being out of time synchronisation. These must be in-phase and in time synchronisation for a wavefront to form. Even if the phase shifters at each array element are set at specific values, the contributions to the chirp continue to be out of time synchronisation and a high-range resolution wavefront cannot form normally in this direction. Although the individual wavefront contributions do propagate towards the target, they are not focused. Any targets illuminated have their returns smered by these differential time delays, so the range resolution is degraded. A point target would have returns spread over this time delay interval, which is equivalent to a distance of $a \sin \theta$. These effects occur on both transmission and reception of the signal, so the received waveform actually spreads over a distance of $2a \sin \theta$. This two-way distance is equivalent to a differential time delay of $2a \sin \theta / c$, which is a range spread of $a \sin \theta$. For narrow scan angles, this value is small and corresponds to close to bore-sight operation and is not limited by these dispersive effects. As the scan angle increases, the differential time delay in the direction of the target also increases and the corresponding range resolution obtainable decreases. In the limit, for scan angles approaching $90°$, the range resolution degradation approaches the length of the array aperture a. This sets the limit for the highest range resolution obtainable for the array and is in reasonable agreement with Equation (9.2).

This illustrates that with phased array beamforming, waveforms with large bandwidths cannot form a beam in a particular off-bore-sight direction by using standard techniques for controlling the phases at each element. The effects of squint,
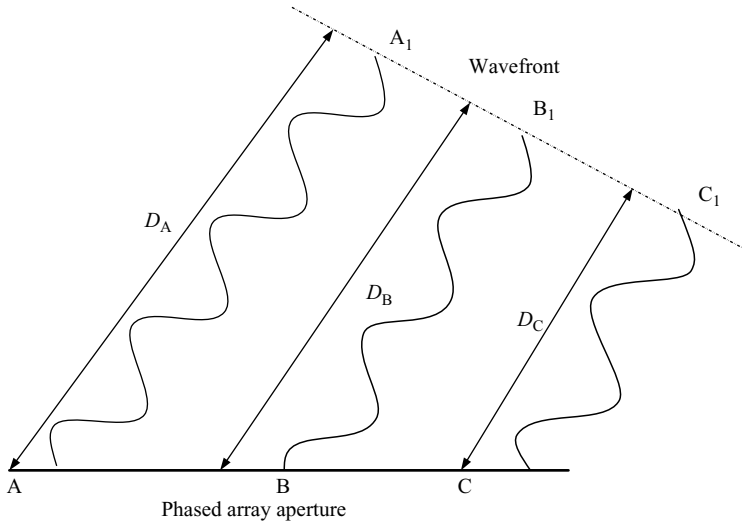
Figure 9.4   Stepped frequency techniques are well suited to phased arrays. As stepped frequency technique uses sine waves, the differential time delays at A_1, B_1 and C_1 are not significant as in-phase sine waves are identical

shown in Figure 9.2 and differential time delay in Figure 9.3 are manifestations of the same physical effect. It is controlling the differential time delay that provides a solution to the narrowband phased array problem. It is presented in Section 9.3.5 and is based on true time delay beamforming techniques.

9.3.4   Stepped frequency techniques

Phased array radars are well suited to classical stepped frequency waveforms for obtaining high-range resolution, as the effects of squint can be readily overcome. As the waveform at each frequency step is essentially a long pulse, compared with the dimensions of the antenna, there are no issues associated with differential time delay across the array.

As the pulses are effectively continuous sinusoidal signals, the wavefront is constructed by identical waveforms, which are in phase. Even if there are differential time delays for the energy to reach the wavefront from the various array elements, the effects can be neglected. The signal generated then has a very slight amplitude weighting with time, which has a negligible effect on the pulse. These effects are illustrated in Figures 9.4 and 9.5.

The sinusoidal waveform at positions A_1, B_1 and C_1 is in phase and effectively identical along the wavefront, so that there are no differential time delay effects, which degrade the range resolution obtained.

Figure 9.5 illustrates the very slight effects associated with the sinusoids at the different array elements being generated slightly out of time synchronisation. As each radar pulse is likely to be orders of magnitude longer than these 'edge effects', and

Differential time delays apply very
slight weighting function to waveform

All components of
wavefront in phase

Radar pulse very long compared to end of pulse effects
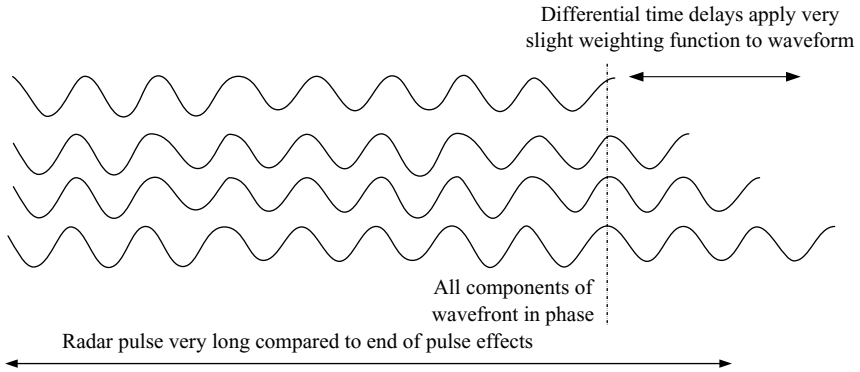
Figure 9.5   Sinusoidal waveforms have negligible end effects on forming signal

they also provide a slight weighting function anyway, time delay errors for the stepped frequency technique for phased array applications are eliminated.

9.3.5   True time delay

In order to overcome the inherent bandwidth limitations of conventional phased array designs, which are the squint and dispersion effects, true time delay techniques have been invented to support the use of wideband waveforms. The objective of the techniques is to use time synchronisation for beamforming, rather than phase. These techniques provide time as the parameter for the unambiguous control of the waveform, in contrast to phase, which has ambiguities repeated for every wavelength and gives rise to the low instantaneous bandwidth.

In order to support true time delay, it is necessary to provide the technology plus the integration of these techniques into the phased array type of architecture. True time delay is shown functionally in Figure 9.6. The wideband signal is distributed to various true time delay units (TDUs), each one of which is programmed to provide the appropriate time delay for the required beam pointing position. As the antenna receives a command to apply the high-range resolution mode for particular azimuth and elevation angles, the time delay settings for TDUs are rapidly calculated and implemented.

In practice, TDUs feed sets of antenna sub-arrays, rather than each individual array element. The bulk of the time delay required is set in the TDU and phase shifters are used to provide the fine tuning. This design concept is used to minimise complexity and cost. In the example provided, the time delay setting for TDU 1 is shown to be zero, as this particular sub-array has the longest electrical path length, D_A, to the wavefront at A_1 from the middle of the sub-array A. There is no point in delaying the signal.

For TDU 2, the time delay is set to be the difference of the path lengths between the centre of sub-array 1 to the wavefront and the centre of sub-array 2 to the wavefront for phase array element positions A and B, respectively. This is the distance $D_A - D_B$
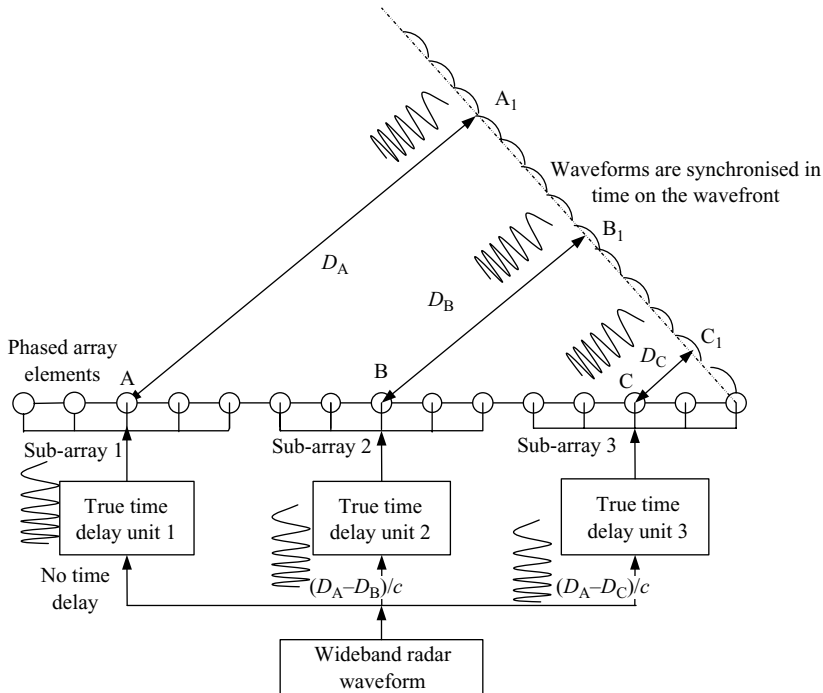
Figure 9.6   *True time delay for wideband phased array radar: (a) true time delay units feed sub-arrays of antenna, (b) each time delay unit is programmed for required delay at each beam position and (c) for this example: true time delay unit 1 has no delay, true time delay unit 2 has time delay of $(D_A - D_B)/c$, true time delay unit 3 has time delay of $(D_A - D_C)/c$*

and corresponds to the time $(D_A - D_B)/c$. Similarly for TDU 3, the time delay setting required to synchronise the waveform for sub-array 3 with those of sub-array 1 and sub-array is to provide a compensation for the differential path length $D_A - D_C$, which is a time delay of $(D_A - D_C)/c$.

Hence, the waveforms that have been transmitted from the three sub-arrays arrive at the required wavefront in exact time synchronisation, so the phases are also the same. The waveform has no theoretical restriction on the bandwidth, which can be transmitted using true time delay techniques.

On receiving the signal, the equivalent process is also followed, otherwise the uncorrected time of arrival of the wavefront reflected from the target would considerably degrade the range resolution. The signal is again delayed for sub-array 3 and sub-array 2 relative to sub-array 1 by exactly the same values as on transmission. These constituents of the signal are then combined in time synchronisation to maintain the integrity of the received waveform. The signal is then processed to provide the high-resolution range profile.

There are different techniques available for providing true time delay. The first to emerge was the simple concept of switching in different lengths of microwave cables or waveguide to provide a set of time delays. This involved the use of complex switching networks and a selection of line lengths, based upon binary addition, to provide the required delay with the minimum use of components. However, for most applications this approach is rather costly and cumbersome, so other techniques have been developed. Rather than using microwave components for providing the time delay, modern systems are using optical delay line components, as they are much smaller and lighter. These techniques involve converting the microwave radar signal to an optical signal, providing the delay in terms of switched in lengths of fibre-optic cable, then converting the signal back to the microwave band [5].

Other techniques involve the application of very different concepts, such as using the phase shifters as modulators of the signal during the pulse to generate the wideband pulse. This is performed by appropriately timing the modulation of the phase shifters to form the wavefront in the required direction.

Some designs involve no TDUs on reception, but utilise the outputs of the digitisers from the sub-arrays to provide the true time delay function as a signal processing operation. The outputs from the sub-arrays are combined with the required delays being generated digitally in the signal processor. A number of papers describing true time delay appear in References 6–10.

9.4 Summary of antenna design issues

The type of antenna used by a radar has a significant impact on the types of high-range resolution waveform that can be used, and the subsequent target recognition performance, which can be achieved. Two general types of antenna have been discussed and have been used as examples to illustrate the key issues for their applications for high-range resolution modes. From the target recognition viewpoint wideband waveforms are straightforward to transmit and receive from the traditional parabolic dish antenna and there are no dispersion issues.

For phased arrays, which are inherently narrowband, dispersion effects and the cost and complexity of employing true time delay make it much more difficult to provide high-performance high-range resolution modes. The standard stepped frequency techniques are readily employed, but in applications in which the target range extent, range ambiguities and time-on-target issues are acceptable. True time delay techniques provide the technical solution to support any wideband waveform and await the reduction in the costs of integrating the true time delay components before they are universally applied.

References

1   KRAUS, J., and MARHEFKA, R.: 'Antennas', McGraw-Hill Series in Electrical Engineering (McGraw-Hill, New York, 2001)

2   BARTON, D.K. (Ed.): 'Frequency, Agility and Diversity' (Artech House Books, Boston, MA, 1977)

3   SKOLNIK, M.I.: 'Radar Handbook' (McGraw-Hill, New York, 1970) Chapter 11-3

4   HOWARD, R.L., COREY, L.E., and WILLIAMS, S.P.: 'The Relationships between Dispersion Loss, Sidelobe Levels and Bandwidth with Subarrayed Antennas'. International Symposium on *Antennas and Propagation Society*, AP-S. Digest, 6–10 June 1988, Syracuse, vol. 1, pp. 184–7

5   KUMAR, A.: 'Antenna Design with Fiber Optics' (Artech House Books, Boston, MA, 1996)

6   AICKLEN, G.H.: 'Wideband Planar Array Antenna'. IEEE *Military Communications Conference,* MILCOM '95, 5–8 November 1995, vol. 3, pp. 1056–60

7   TARRAN, C., MITCHELL, M., and HOWARD, R.: 'Wideband Phased Array Radar with Digital Adaptive Beamforming'. IEE *High Resolution Radar and Sonar* Colloquium (Ref. No. 1999/051), 11 May 1999, pp. 1/1–1/7

8   RABIDEAU, D.J.: 'Improved Wideband Time Delay Beamsteering'. Thirty-Fifth Asilomar Conference on *Signals, Systems and Computers*, 4–7 November 2001, vol. 2, pp. 1385–90

9   CORBIN, J., and HOWARD, R.L.: 'TDU Quantisation Error Impact on Wideband Phased Array Performance'. Proceedings of IEEE International Conference on *Phased Array Systems and Technology*, 21–25 May 2000, pp. 457–60

10 SARCIONE, M., MULCAHEY, J., SCHMIDT, D., CHANG, K., RUSSELL, M., ENZMANN, R. *et al.*: 'The Design and Testing of the THAAD (Theatre High Altitude Area Defence) Solid State Phase Array (Formerly Ground Based Radar)'. IEEE International Symposium on *Phased Array Systems and Technology*, 15–18 October 1996, pp. 260–5

Chapter 10

Operational issues

10.1   Introduction

So far in this book the target recognition techniques and associated technology for supporting them have been presented. In this chapter operational issues are discussed, which involve how the techniques are applied for real systems, how they link in with the other functions of the radar and how and when decisions on the target's identity are made. As will be seen, some of the operating characteristics of certain types of radars constrain the target recognition functions that can be supported and the performance that can be achieved. Three generic types of radars have been selected to illustrate the key issues: a mechanically scanning tracker radar, a passive-phased array and an active-phased array radar. The active array is divided into two categories, arrays with fixed faces and rotating arrays. Although some radars are actually combinations of these selected types, the general principles discussed still apply.

Tracking radars will be described in Section 10.2 and it will be shown that they are very well suited to provide high-performance target recognition functions, whilst still meeting the requirements of tracking targets.

Passive- and active-phased array radars, which can be used in surveillance, tracking and multi-functional roles, are also discussed in Sections 10.3 and 10.4, respectively. These types of radars have many tasks to perform and generally have little time available for performing target recognition functions. The constraints affecting their potential to support radar target recognition modes are presented.

The role of the operator in making decisions about the target's identity and issues concerning automatic recognition by the computer are discussed for the respective types of radar system.

However, in some environments in which target recognition functions are absolutely essential, it is not practical to implement them using surveillance and multi-function radars, which either do not have the time available or have technical

shortcomings. In these situations radars specifically dedicated to target recognition are beginning to be developed and these are also discussed in Section 10.5.

10.2   Tracking radars

10.2.1   Introduction

The function of tracking radars is to support the associated weapon system during an engagement. The tracker is initially required to acquire the target, which is normally obtained from a cue from the surveillance sensor. It is then required to obtain a track on the target and to maintain it until the weapon, which is usually a missile, intercepts and destroys the target. The target parameters tracked are normally elevation and azimuth angles, range and range rate. Weapons systems use the tracking information in different ways. The Sparrow missile [1] and its European variants, Sky Flash [2] and Aspide [3], use the tracker as an illuminator of the target. This air-to-air missile operates in a semi-active mode and locks onto the reflected signal from the target, provided by the tracker, and homes in on it by operating in a receive mode. The UK Rapier [4] ground-to-air missile system operates in a different way. The tracking radar tracks both the outgoing missile and the target. It uses the track information on both to provide command to line of sight data to the missile via a communication link. The main function of the tracking radar is shown in Figure 10.1. The missile is guided to the target by the radar.

10.2.2   Tracking radars for target recognition

A tracking radar spends most of its operational life not being used, but in a stand-by mode. It awaits the cue from a surveillance sensor, which has previously detected a potentially hostile target for missile engagement. Traditionally, tracking radars have not been required to contribute to the identification of the target that is being engaged.
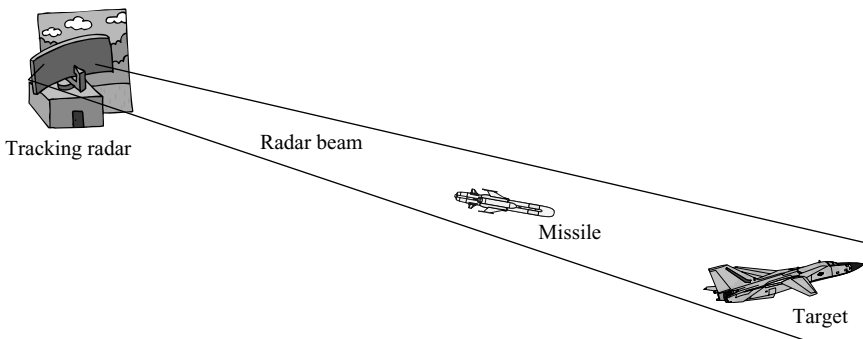
Figure 10.1   Tracking radar guiding missile to target

If the target is appearing to be a real threat, there is very little time, for a naval close in weapons systems defending a sizeable asset, for example, for a decision to be made about the threat and its intentions. As was discussed in Chapter 1, if the threat is real and there is reluctance to engage it, in case it were a civil airliner, the ship could be destroyed. On the other hand, if it really is a civil airliner and it is thought to be a missile, and is shot down, there are severe political and diplomatic implications, as well as the associated human tragedy.

The normal function of the tracker is to lock onto a single target and to guide the missile to it over several seconds or even tens of seconds. The radar is only illuminating the target, and possibly also the outgoing missile, which would generally be in the same radar beam, with no other tasks to perform. Under these conditions, in terms of radar resource time, there is considerable time available for target recognition modes to be applied. Even if only a small percentage of time is spent implementing target recognition modes, significant information can be obtained from the measured signature, while the tracking function can still be maintained. As tracking radars are designed to operate in conditions under which the target is temporarily lost, such as in clutter or when the target is obscured, they can tolerate short periods when tracker data is unavailable. They can then 'coast' until the next tracking data is obtained. The track can then be readily re-acquired when the blanked out period has passed. This means that there is potentially time available, which can be used for the target recognition function, to be applied while the radar is continuing to track the target.

These concepts are shown in Figure 10.2. In (a) a sequence of tracking measurements is shown and includes a target 'fade', when no track update data is obtained. If the fade does not last too long, the next tracking measurement made is readily utilised to maintain the target track. In (b) the ability of the radar to maintain tracking, when a tracking measurement is omitted, is utilised for applying a high-resolution target recognition measurement.

Interestingly, as the high-resolution measurement can be more precise than the basic tracking measurement that it replaces, it is possible for tracking to actually be improved using the high-resolution range or radial velocity data from the target.

It is not absolutely necessary to recognise the target before the missile is launched, although it is clearly preferred. High-resolution measurements can be made as the missile is approaching the target and if the measurements strongly indicate that the target is no threat, the engagement can be aborted and with the missile being steered away from the target.

The target recognition techniques used in this type of application would be JEM, high-resolution range profiling, ISAR and polarisation. The actual techniques would be specific to the time available from a particular tracker to make the high-resolution measurements, the engagement timelines, the types of target encountered and the mode that the radar can readily support.

There are no issues associated with the radar having to find the target for applying the high-resolution mode, as the tracker is designed to lock onto the target after being cued and to keep it within its radar beam. The tracker radars supporting the UK's Seawolf missile system are shown in Figure 10.3.

(a)

Tracking
measurement

Target 'Fade'

Time

(b)

Tracking
measurement

High-resolution
measurement

Time
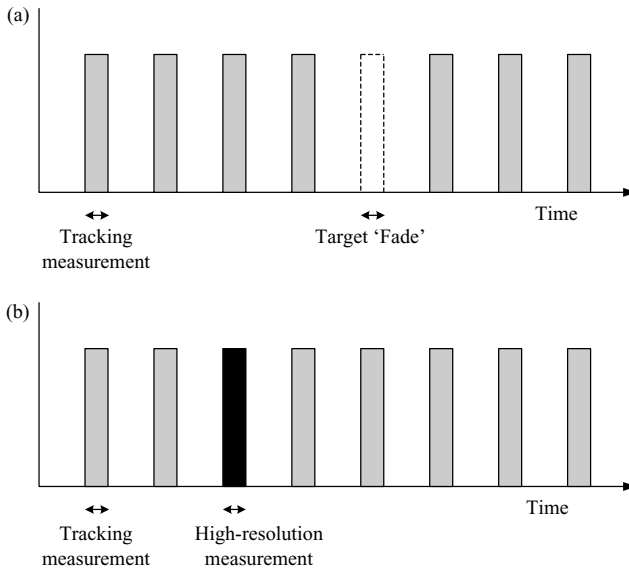
Figure 10.2 Target recognition modes for tracker radars utilise ability of radar to maintain track during periods when tracking data is unavailable: (a) tracker radars are designed to tolerate short periods of target 'fading' and can still maintain track and (b) tracker radars have time available to perform high-resolution measurements and still maintain track

Figure 10.3 Seawolf tracker radars (Courtesy of BAE Systems Insyte)

For tracking radars, which support missile systems, the engagement timelines are usually short. If there are only a few seconds available from threat detection to interception, it is unlikely that an operator could be accommodated in the decision making loop. The time taken for he/she to study target signature and feature data for

making the decision on the threat's identity would to too long. It would be necessary to rely on the automatic process.

   If engagement time lines were longer, the operator would have the opportunity to study the signature data and the computer's recommendations and make the final decision on whether to abort the interception of the target.

10.3   Passive-phased array radars

10.3.1   Introduction

This type of radar was discussed in Chapter 2, Section 2.1.23. Normally, these are surveillance radars, which rotate at a constant rate. The passive beamforming is usually used to determine the altitude of targets by generating several beams in elevation. The dwell period on a particular target is usually fixed, as azimuth scanning is not usually employed. However, certain specialist designs do incorporate an azimuthal squint effect, which can be utilised to lengthen the dwell period, if a special waveform is used. This is discussed in the next section.

10.3.2   Passive-phased array radars for target recognition

A passive array used as a surveillance radar is shown in Figure 10.4. The radar is rotating continuously and illuminates each target for the same time, as it scans around 360°. For a fixed illumination period on the target, which would normally have been designed to provide sufficient signal-to-noise ratio for detection, there is normally no additional energy available from the radar to increase this for the high-resolution mode. This type of radar cannot realistically be slowed down to increase the dwell time and the target's signal-to-noise ratio for the high-resolution mode. Its primary
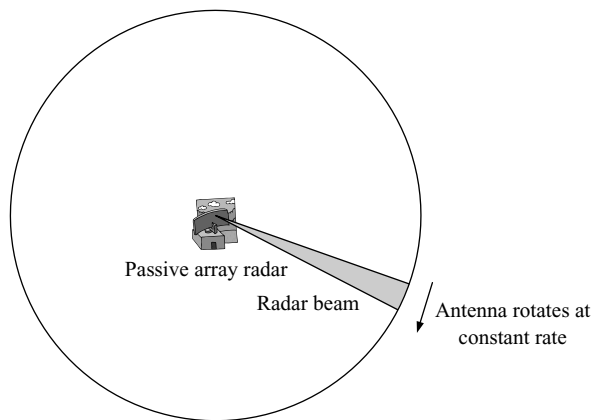
Figure 10.4   *Passive-phased array radar rotates at constant rate and has normally little flexibility in altering dwell time on target*

function is surveillance and it has to maintain its scanning rate to observe targets in its coverage area. One means of increasing the signal-to-noise ratio is to implement the target recognition mode at shorter range. However, it may mean that a hostile target has penetrated defences by then and it could be too late.

It can be seen that this type of radar is not readily suited to target recognition applications unless the design can support an increase in dwell period on the target, without altering the rotation rate. One method of achieving this is to utilise an antenna with azimuthal squint, such that the antenna beam points in a different direction as the transmission frequency changes. By careful synchronisation of the rotation rate with the frequency to be transmitted, a far longer dwell period can be obtained. Effectively the antenna has a look back and a look forward capability. It can illuminate targets off its centre frequency bore-sight. This is illustrated in Figure 10.5. It can be seen that at frequencies f_1, f_2 and f_3, the beam is pointing in different directions.

The waveform used would be a stepped frequency sequence. f_1 is transmitted when the target is at the antenna's bore-sight for this frequency; f_2 is then transmitted when the target is at the bore-sight at this frequency and so on. The range resolution obtained is then dependent upon the bandwidth covered by the stepped frequency sequence, which is related to the antenna's squint characteristics. Operating in this way, with the energy concentrated in the target's direction, is at the expense of neighbouring azimuthal directions, which would not be illuminated by the radar. Surveillance and tracking functions on any targets in these directions would then be 'on hold' for the duration of the high-resolution mode and would have to be resumed on the next rotation period.

Before applying the high-resolution mode, the target would normally be initially detected and the track would be established. Targets with tracks, altitudes and ranges, which are of interest, would then be the subject of the high-resolution mode. The
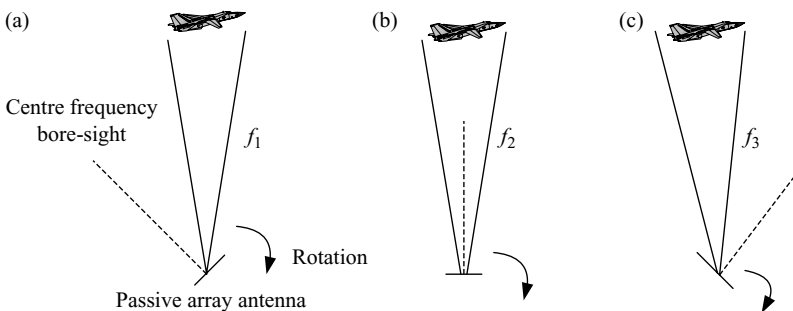
Figure 10.5   *Squinting antenna can be utilised for increasing dwell period on target with rotating antenna: (a) antenna beam utilises squint by selecting frequency f_1 to look ahead, (b) frequency f_2 selected for on bore-sight target and (c) antenna beam utilises squint by selecting frequency f_3 to look back*

track parameters would be used to estimate the azimuth of the target for the scan during which the high-resolution mode is to be applied. The range and the velocity of the target would be used to calculate an appropriate prf, such that the target is not in a blind velocity or range zone.

This type of radar is not suited to JEM or ISAR modes as the time required to implement these is too long for the dwell period available, while maintaining its primary functions.

10.4 Active-phased array radars

10.4.1 Introduction

The design concepts of active-phased array radars were discussed in Chapter 2, Section 2.18.3. The main advantage of the active array, in comparison with the passive array just described, is that it is normally designed to form beams in any azimuth and elevation direction. This provides it with much more flexibility for supporting target recognition modes.

Active-phased array radars are designed to either have fixed faces, which do not rotate, or a single or two back-to-back faces, which do rotate. An example of a fixed face phased array is the US Ballistic Missile Early Warning System [5] radars (BMEWS), which have either two or three fixed faces. An example of a phased array radar that rotates is the UK's Sampson radar, which utilises two back-to-back radiating faces and is shown in Figure 10.6.
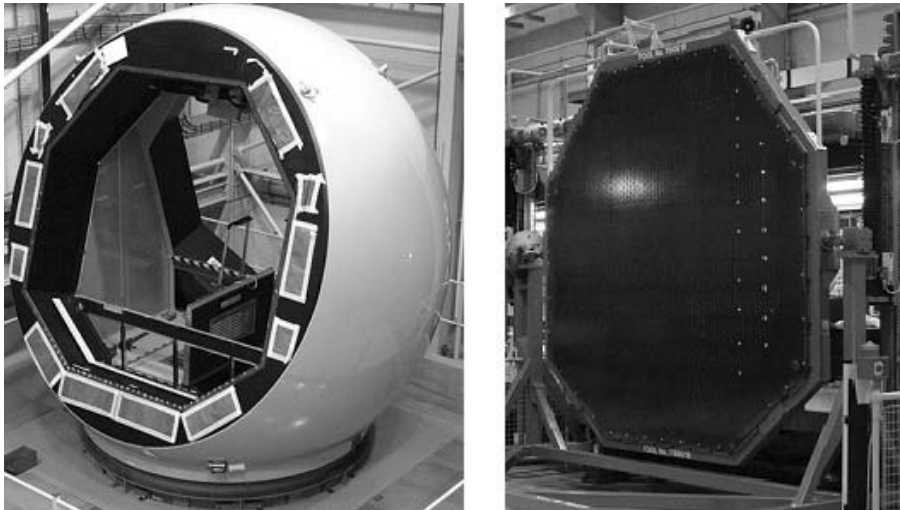
Figure 10.6   Sampson phased array radar: antenna housing (left) and single array aperture (right) (Courtesy of BAE Systems Insyte)

10.4.2   *Active-phased array radars for target recognition*

For either the fixed face or rotating face designs, the key advantage for supporting target recognition modes is the available time on target. For the fixed face design, the beam can be pointed in the appropriate direction as long as it is necessary to obtain the high-resolution signature of the target of interest. The only constraint is that the radar is using this resource time for target recognition and not surveillance or tracking, which are essential functions. The time utilised for target recognition would be dependent upon the resource scheduling philosophy and the mission of the specific radar system. The important point is that the radar can provide a target recognition function while maintaining its other functions. The actual recognition mode to be employed is dependent upon the radar's basic architecture and frequency of operation. For radars with narrow instantaneous bandwidths stepped frequency techniques are the best option for providing high-range resolution. At the higher microwave frequencies JEM modes can be applied. If the radar can support true time delay beamforming, high-range resolution modes can be employed, which do not have the constraints and performance limitations of the stepped frequency techniques, as discussed in Chapter 3, Section 3.5. ISAR modes can also be applied at the higher microwave frequencies, which give better frequency and hence cross-range resolution.

Rotating active arrays do not provide as much flexibility as the static array face, as they are constrained by the rotation rate of the antenna array. However, as the beam can be steered by either using phased shifters in conventional active array designs or by true delay techniques for the more advanced systems, a satisfactory dwell time can be obtained for range profile and JEM modes. This concept is shown in Figure 10.7. The time available for the radar to implement the target recognition mode is again a crucial issue, as multi-function phased array radars have many functions to perform. As ISAR tends to require dwells of several hundred milliseconds to seconds, it is not generally feasible to use it for the rotating array, as this time cannot be made available even with beam steering.

(a)   Bore-sight (1)   Rotation   Active array antenna
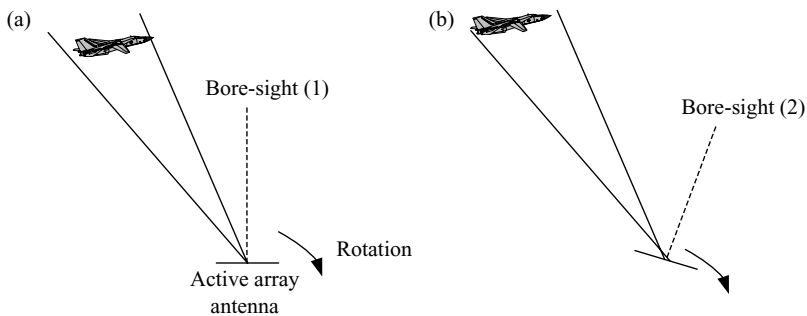
(b)   Bore-sight (2)

Figure 10.7   Rotating active array radars can steer beam to maintain target in beam for high-resolution mode: (a) antenna bore-sight pointing in direction 1 and (b) antenna bore-sight pointing in direction 2

For active-phased arrays, which are normally long-range systems, there would normally be sufficient time available for the operator to study the target signature data and the computer identity estimate and make the final decision on the identity and the appropriate response.

10.5 Dedicated target recognition radars

If high-resolution modes are to be employed at a rapid rate, so that large numbers of detected targets are to be routinely recognised, radars specifically dedicated to target recognition are required. The surveillance and multi-function radars discussed previously only have the time available to apply high-resolution modes to a small proportion of all targets detected and tracked. In the United States the first radars that are specifically to be used for target recognition are under development. In order to support the Aegis surveillance and tracking radar, an X-band discriminator radar is under development [6]. For ballistic missile defence applications, the sea-based X-band radar is stated as being the sensor used for discriminating the threatening warhead [7]. In the United Kingdom, the use of an upgraded tracker radar dedicated for target recognition, to support the surveillance radar, has been proposed [8].

10.6 Summary

From the operational viewpoint tracking radars are considered to be well suited for incorporating high-performance target recognition modes, while maintaining the main tracking function.

Active-phased array radars can also support high-resolution modes, but are more constrained by design architecture issues than the trackers. Active arrays with fixed faces have more time available than the rotating designs, so can support modes with longer dwell periods. The passive-phased array radars are the most difficult for incorporating a target recognition function, while maintaining the key operating functions of the radar. However, passive array designs, which include an azimuthal squint capability, provide potential for increasing the dwell period for implementing stepped frequency high-range resolution modes. Phased array radars have surveillance and tracking functions to perform, so target recognition modes have to be implemented within already tight resourcing budgets.

For environments with large numbers of targets to be recognised, radars are under development that are to be specifically used for target recognition.

For systems, such as tracker radars, that can operate with very short engagement timelines, the target identity decisions would be made automatically. For longer range surveillance and multi-function radars, there would normally be sufficient time for the operator to study the signature data and the computer's recommendations and make the final decision on the target's identity and the appropriate response to the threat.

References

1 UNITED STATES NAVY WEBSITE. www.chinfo.navy.mil/navpalib/factfile/missiles/wep-spro.html

2 UNITED KINGDOM ROYAL AIR FORCE WEBSITE. www.raf.mod.uk/equipment/airtoair.html#skyflash

3 FEDERATION OF AMERICAN SCIENTISTS WEBSITE. www.fas.org/man/dod-101/sys/missile/row/aspide.htm

4 UNITED KINGDOM ROYAL AIR FORCE WEBSITE. www.raf.mod.uk/equipment/surfacetoair.html#rapier

5 US MISSILE DEFENCE AGENCY WEBSITE. http://www.acq.osd.mil/mda/mdalink/html/mdalink.html

6 FEDERATION OF AMERICAN SCIENTISTS WEBSITE. www.fas.org/man/dod-101/sys/ship/docs/cg_14-93.html

7 www.aviationnow.com/avnow/news/channel_aerospacedaily_story.jsp?id=news/mda04083.xml

8 TAIT, P.D.F.: 'Upgrading Tracker Radars to Provide Non Co-operative Target Identification'. Xth European Air Defence Symposium, Shrivenham, United Kingdom, March 2002

Chapter 11

Applications

11.1 Introduction

A variety of radar target recognition methods have been discussed. Various constraints and critical issues have been identified for the technology required to support them and for associated operational aspects. In this chapter, the radar target recognition techniques currently most appropriate to the different types of targets and applications likely to be encountered are presented, taking into account these afore-mentioned issues.

In some cases, such as JEM and helicopter engine rotor modulation (HERM), the techniques previously presented are specific to particular types of target and have already been covered in depth. These applications are included here for completeness. The objective of this chapter is to provide a consolidated view of the techniques recommended for the recognition of different targets for radars installed on various platforms. Aircraft targets are discussed in Section 11.2 followed by ships in Section 11.3 and land vehicles in Section 11.4. Air breathing and ballistic missiles are discussed in Sections 11.5 and 11.6, respectively. In Section 11.7, the recommended techniques are summarised and are presented in tabular form.

11.2 Aircraft

11.2.1 Introduction

The recognition of three different types of aircraft is discussed: fixed wing aircraft with jet engines, fixed wing aircraft with propellers and helicopters.

11.2.2 Fixed wing aircraft with jet engines

11.2.2.1 Airborne platforms

In order to recognise aircraft from another airborne platform, a major factor is the relative speed of the two aircraft, which can be very high for closing targets. Under

these conditions the timelines tend to be quite short, so that high-resolution modes, which can be implemented rapidly and reliably, are required. The two most appropriate modes are JEM and high-resolution range profiling. As was seen in Chapter 3, the wideband within pulse modulation modes can cope much better with multiple targets than the stepped frequency techniques, so the former are much preferred. For some radar designs, it is also possible to employ these two modes simultaneously, so that the engine positions are localised in range, as well as obtaining JEM and range profile data [1].

The complexities of motion compensation for both the radar platform and the target mean that the implementation of ISAR for aircraft imaging is a challenging requirement. It is considered to be feasible, but there is little application information available in the public domain at present and is generally considered to be in the realms of research.

11.2.2.2   Surface-based platforms

The most straightforward mode to implement is high-resolution range profiling and if possible, using wideband waveforms rather than with stepped frequency techniques. JEM is more difficult to implement for surface platforms, on account of the high prf requirements, which then result in highly ambiguous range operation. A very high dynamic range radar would be needed to cope with short-range land clutter, particularly from hills and buildings for targets at low altitude.

Surface-based systems have the advantage that when illuminating airborne targets, they have far less or none of their own motions to contend with, compared with the airborne sensor discussed in the previous section. Hence, ISAR modes are more readily employed, particularly by a radar dedicated to target recognition. This technology is still under development.

11.2.3   *Propeller driven aircraft*

For propeller driven aircraft, the most significant discriminant for target recognition is the propeller's modulation of the radar signal. The theory of the associated modulation is very similar to that for JEM, as discussed in Chapter 5, but is much simpler. There is normally only one single stage having blades and the number of blades is very low. The resulting spectrum is composed of harmonics of the blade chopping rate, which again is the engine speed multiplied by the number of blades installed. The fundamental frequency is usually a few tens of hertz, which can be detected by spectral analysis, as for JEM, or by time domain analysis, as in helicopter rotor blade flash detection. As the propeller spectrum has a much lower frequency content than JEM spectra a much lower prf can be used, so the problems of ambiguous range operation are either far less severe or non-existent. Therefore, the issues of ground clutter, which affect surface-based JEM measurements, do not apply. Range profiling can also be used. If the radar can support a waveform that can simultaneously measure the range profile and the propeller characteristics, the propeller's position on the range profile can be localised [2]. Developments could provide an ISAR capability, but it is considered that the information available for the propeller modulation and

range profiling should be sufficient to provide a good indication of the presence of a propeller driven aircraft and its main scattering centres.

11.2.4   Helicopters

The techniques for recognising helicopters were discussed extensively in Chapter 5. It was concluded that time domain analysis was required to detect the main rotor blade flash. Spectral analysis was required for the detection of the Doppler frequencies from the main rotor and for the spectral components generated from the rear rotor blade chopping frequencies. The prfs required tend to be lower than for measuring JEM spectra, so the problems of close-in ambiguous clutter should not arise.

High-range resolution waveforms can generate the range profile of the helicopter and if applied simultaneously with the measurement of the spectral components, can localise the front and rear rotors along the range profile [2]. Also, if the high-range resolution waveform can be applied simultaneously to provide time domain blade flash measurements, the position along the range profile at which the blade flash occurs can be identified. ISAR is not currently considered necessary for helicopter recognition, as the techniques identified provide considerable discriminants. The same helicopter recognition techniques can be employed for both surface and airborne platforms.

11.3   Ships

11.3.1   Surface-based platforms

The techniques used for recognising ships from surface-based platforms are high-resolution range profiling and ISAR. For land-based systems using fixed installations, the platform clearly needs no motion compensation for ISAR, which is a major advantage. Ideally, the radar should be located well above sea level, with nothing obscuring its view for detecting targets at sea for this coastal surveillance application. For naval platforms, the range for applying high-resolution modes is limited by the relatively short distance to the horizon, so the radar should again be installed as high as possible on the ship. The main targets to be recognised would be small boats, which are potentially threatening, such as patrol and rubber inflatable boats. If the platform is exhibiting rotational and linear motions these have to be compensated for in order to provide a focused high-resolution target signature.

11.3.2   Airborne platforms

For airborne platforms SAR and ISAR modes can be employed plus combinations of both of these, as discussed in Chapter 4. The actual mode employed depends upon the integration time of the radar and the motion of the ship of interest. For less sophisticated applications high-range resolution can obviously be used. Motion compensation is again a critical issue.

11.4　Land vehicles and people

11.4.1　Surface platforms

The key factors limiting the detection of targets on the ground using a ground-based platform are terrain obscuration and clutter. Direct line-of-sight between the radar and target is generally difficult to achieve. For a sensor installed on high ground, which is overlooking flat terrain and for short ranges targets, the detection and tracking of targets is the most feasible.

For sensors based near the ground and with obscuration from terrain and buildings, most targets are likely to only be in view spasmodically, so short duration dwell periods often have to be used. High-resolution range profiling and the use of spectral analysis for the detection of the Doppler frequencies from wheels or tracks are recommended [3,4]. If possible, these techniques should be employed simultaneously, so that the tracks or wheels can be localised in range.

ISAR could be used in certain circumstances, but would not be expected to be a standard target recognition mode employed. In order to measure the signatures of vehicles moving along a road, the sensor would need to be located so as to observe a sufficient change in aspect angle over the radar integration period. In order to measure signatures of vehicles moving across bumpy terrain, the effects of random motion variations and associated flexing which change the vehicle geometry have to be overcome. The ISAR signal processing algorithms would be required to process non-periodic motion occurring at irregular intervals, which is quite different from the techniques described in Chapter 4 for which the motion was more predictable. They would be classed as advanced target recognition techniques.

For naval platforms attempting to recognise land targets, terrain obscuration is considered to be even more of a problem than from a land-based platform. In principle, similar modes for land-based systems could be used.

If the target is not moving, ISAR and the spectral analysis technique are not applicable. High-resolution range profiling modes have target returns competing with all the co-range clutter within the radar beam. Hence, the use of these modes for stationary targets is considered to be challenging.

Frequency analysis techniques are also being investigated for the detection of intruders and infantry [5]. The bulk Doppler velocity measured from a moving person indicates that a moving target has been detected. The leg and arm motions of a person who is walking or running also give rise to associated Doppler frequency characteristics. The use of these frequency domain attributes is being investigated to establish the feasibility of detecting moving people and to discriminate them from false alarms and vehicles.

11.4.2　Airborne platforms

Airborne platforms overcome many of the terrain obscuration and clutter difficulties discussed earlier for surface deployed sensors, but can still have significant problems in obtaining high-quality signatures, which can be recognised. For stationary

land targets, SAR modes can be employed. High-range resolution modes are one-dimensional and are clearly not as effective as SAR for stationary targets. For moving targets spectral analysis can again be employed for wheel or track detection provided they are visible to the sensor. In combination with high-range resolution, the moving parts can be localised on the range profile.

MTI SAR techniques are under development, which can reduce many of the clutter related problems experienced with stationary targets by Doppler filtering, enabling two-dimensional SAR images to be isolated from nearby clutter. For vehicles exhibiting rotational motion characteristics on uneven farm tracks, for example, there are also ISAR effects which also have to be taken into account. These tend to degrade SAR images [6]. Complex signal processing is required to unravel the SAR and ISAR contributions to the image and is currently the subject of research.

11.5   Air breathing missiles

11.5.1   Introduction

In comparison to the other targets discussed so far in this chapter, air breathing missiles have less constituent parts and have less complex radar scattering characteristics. They are almost always unitary objects, of cylindrical shape, with a nose cone, some control surfaces and a propulsion system. They are normally a few metres long and have a diameter measured in tens of centimetres.

As long thin objects, they have range profile characteristics. Owing to the relatively short control surfaces and wings, there is only limited cross-range information potentially available, which is orthogonal to the missile's axis of symmetry. However, the lack of cross-range signature data actually provides a discriminant for missile recognition.

Air breathing missiles use oxygen to ignite a fuel, which generates thrust to propel the missile. Their engines and mechanical propulsion mechanisms are not known to have any measurable discriminants, such as JEM lines. The engines tend to be small, with small air in-takes, so little penetration by a microwave radar signal is expected.

11.5.2   Air breathing missile recognition techniques

From above discussion, high-resolution range profiling is the only technique that can realistically be applied to recognising air breathing missiles at present. There have been no reports that spectral analysis techniques have any discriminants that can be detected.

The main issues affecting the application of the high-range resolution waveform from the different platforms are motion compensation, ground clutter and dynamic range. As a missiles can exhibit extremely high acceleration turns, the aspect angle is rapidly changing, as well as the velocity component in the radar's direction. These are considerable challenges for generating high-quality range profiles. However, the high levels of acceleration and rapid changes of direction, would be key attributes of

a missile and in most cases its identity would not have to be known in order to take appropriate action. These types of decision, which involve using other available information, which is not obtained from the radar signature, are discussed in Chapter 13.

The airborne platform tends to have the best visibility of the missile, but also has high clutter returns, especially in relation to a missile with a low rcs. For low altitude missiles, ground-based systems can also experience high clutter levels and can suffer from terrain obscuration. For higher altitude missiles, which can be tracked by a surface-based radar in a 'look-up' mode, clutter levels are less severe and detection is easier.

11.6   Ballistic missiles

11.6.1   Introduction

Superficially it may be considered that the radar techniques and requirements for recognising ballistic missiles have similarities with the techniques discussed in the previous section on air breathing missiles. However, the cases are very different, particularly for missiles with multiple booster stages. The key objective is to detect the warhead associated with the re-entry vehicle in ballistic missile defence, in the presence of various booster stages, separation debris and even countermeasures. Also the velocities of the ballistic missile threat cloud objects, can be up to several thousand metres per second and have to be detected and destroyed at hundreds and even thousands of kilometres of range from the radar [7]. The detection, tracking and recognition of the warhead under these situations is probably one of the most challenging requirements radar engineers have ever had to face.

11.6.2   Techniques for recognising ballistic missiles

In order to differentiate the various objects in the ballistic missile threat cloud, the obvious initial radar measurement to make is high-resolution range profiling, using as much range resolution as possible. The booster stages are normally much longer than the re-entry vehicle, which in turn, is longer than the separation debris, such as bolts. This target set is illustrated in Figure 11.1.

If as a result of the natural physical forces associated with the separation of objects in space [8], rotational motion is imparted to the objects, this can also be used to support a recognition function. Rotating objects are continuously changing their

Re-entry vehicle   Separation debris   Booster
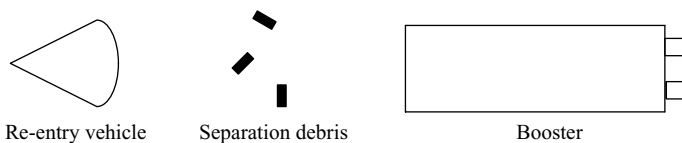
Figure 11.1   Typical objects in ballistic missile threat cloud

Table 11.1   Summary of radar recognition techniques for aircraft targets

Target	Radar platform	Recommended NCTR techniques	Comment
Fixed wing jet	Airborne	JEM HRR HRR/JEM	ISAR research
Fixed wing jet	Surface-based	JEM HRR HRR/JEM	ISAR under development
Propeller aircraft	Airborne and surface	Spectral/time domain analysis HRR HRR/spectral analysis	ISAR not considered necessary
Helicopters	Airborne and surface	Spectral analysis Time domain analysis HRR/spectral analysis HRR/time domain analysis	HRR and ISAR not considered necessary

Table 11.2   Summary of radar recognition techniques for ship targets

Radar platform	Recommended NCTR techniques	Comment
Land-based	HRR ISAR	
Sea-based	HRR ISAR	Own ship motion requires compensation
Airborne	HRR ISAR SAR SAR/ISAR	Own platform motion requires compensation

aspect angles to the radar, which is a pre-requisite for performing ISAR measurements. Hence, by employing high-range resolution waveforms in conjunction with obtaining the high-resolution Doppler data from the rotating object and using ISAR signal processing techniques, both down-range and high cross-range resolution target images can be formed. These can then be used to determine the general shape and size of the various objects for discrimination purposes.

Table 11.3   Summary of radar recognition techniques for land vehicles

Radar platform	Recommended NCTR techniques	Comment
Land-based	HRR Spectral analysis HRR/spectral analysis	Techniques mostly applicable to moving targets ISAR could be used in some circumstances
Sea-based	HRR Spectral analysis HRR/spectral analysis	Terrain obscuration is major problem Techniques mostly applicable to moving targets to reject clutter
Airborne	HRR SAR/MTI SAR Spectral analysis Combined HRR/spectral analysis SAR/ISAR	Detection and recognition of stationary targets difficult with nearby clutter Moving targets can exhibit complex motion

Table 11.4   Summary of radar recognition techniques for missiles

Target	Radar platform	Recommended NCTR techniques	Comment
Air breathing missiles	Airborne, land and naval	HRR	Motion compensation difficult for highly manoeuvring missiles Dynamics parameters can be used for recognition
Ballistic missiles	Land and naval	HRR ISAR	Radars required generally are too large for airborne platforms

As ballistic missiles are at long distances from the radar, normally surface-based radars are used for detecting, tracking and discrimination, as high power radars with large antennas are needed. Airborne radars can only be used for the relatively short-range missiles.

For threat clouds with several objects in close proximity, it is necessary to employ a high-range resolution waveform with the best performance, such as wideband within pulse modulation or stretch techniques. These are also suitable for ISAR modes. Stepped frequency techniques are at a disadvantage for these applications, as they

have range ambiguities in the vicinity of the target, which cause insurmountable problems for complex threat clouds. They also take far too long to perform ISAR, as several pulses are needed at each step to provide the required Doppler resolution.

11.7   Summary

Within this chapter the main radar recognition techniques for various types of targets have been discussed. In each case, if the radar has the scheduling time available and the hardware is installed, polarisation measurements can also be made. This is particularly true for the high-range resolution measurements. The target recognition techniques are summarised in Tables 11.1–11.4 for the different classes of target for radars installed on ground, naval and airborne platforms.

References

1   TAIT, P.D.F., and SHEPHARD, S.J.: 'Radar Systems'. United Kingdom patent no. 2 298 330 A, filed 28-2-90

2   TAIT, P.D.F.: 'Developments in Target Recognition Technology for Tracker Radars'. XIth Air Defence Conference, Shrivenham, United Kingdom. June 2004

3   STOVE, A.G., and SYKES, S.R.: 'A Doppler-Based Automatic Target Classifier for a Battlefield Surveillance Radar'. Proceedings of IEE International Radar Conference *Radar 2002*. IEE Conference Publ 490, pp. 419–21

4   STOVE, A.G., and SYKES, S.R.: 'A Doppler-Based Target Classifier Using Linear Discriminants and Principal Components'. Proceedings of IEEE International Radar Conference, Adelaide, September 2003, pp. 171–6

5   VAN DORP, P.: 'Measuring Human Behaviour with Radar'. Proceedings of Geman Radar Symposium, GRS 2000, 11–12 October 2000, Berlin, pp. 423–9

6   RIHACZEK, A.W., and HERSCHKOWITZ, S.J.: 'Theory and Practice of Radar Target Identification' (Artech House, 2000) pp. 294–6

7   US MISSILE DEFENCE AGENCY WEBSITE: www.acq.osd.mil/mda/mdalink/html/mdalink.html

8   SIDI, M.J.: 'Spacecraft Dynamics and Control: A Practical Engineering Approach', Cambridge Aerospace Series, (Cambridge University Press, Cambridge), Chapter 4

Chapter 12

Target recognition process

12.1 Introduction

Within this chapter the various processes which are required to provide a radar target recognition function are brought together and build on the concepts that have been discussed earlier in the book. Key radar measurements issues, which were extensively presented earlier, are reviewed and include a discussion on target signature distortion in Section 12.2.

  The general requirements for and the description of target signature databases are presented in Section 12.3 for the various target recognition techniques. The methods used for assembling the target signature databases are discussed in Section 12.4. Techniques used for the modelling of target signatures are presented in Section 12.5. Two distinct classes of recognition algorithm approaches employed are presented in Section 12.6, which are template matching and feature extraction. The sequence of operations required from the signature measurement and the extraction of the target signature data to applying the recognition algorithms and reference templates to estimate the target's identity are presented in Section 12.7.

12.2 Radar measurements

12.2.1 Introduction

In the various chapters of this book, the measurement techniques appropriate to the different types of target recognition techniques were presented. They are each matched to particular target attributes, which are to be measured in the time and/or the frequency domains. The main requirement from the measurement is to provide a high-quality target signature, which is compatible with the recognition algorithms and reference signature templates or target features being used.

12.2.2   Measurement issues

For a particular application, decisions have to be made on the measurement resolution needed to provide the target signatures with sufficient resolution, so that the target types, which are to be differentiated, can be recognised with the required reliability. This includes, for example, considering the number of pixels in SAR image or the number of Doppler filters for spectral analysis techniques, which will be needed to provide sufficient information from the signature. It may also be necessary to consider the use of super resolution techniques and the associated high sampling rates to ensure that the measured scatterers are well isolated and localised.

Normally an extensive data collection, modelling and analysis campaign is required to provide the information needed to address the above issues.

12.2.3   Measurement quality

The quality of the radar measurement clearly affects the recognition performance obtained. Measurements made under conditions of poor signal-to-noise ratio are obviously inferior to those made with very strong signals received from the target. The presence of clutter, electrical interference or jamming, for example, all contribute to degrading the radar's target recognition probability. In order to determine the reliability of a target recognition measurement and to provide a realistic probability of the target type, a measure of the quality of the signature data obtained has to be made. Algorithms are required, for example, to determine the signal-to-noise ratio and how the reliability of the recognition process varies with signal-to-noise ratio. The effects of clutter and electrical interference have to be taken into account. Ideally, the radar's signal processing operations can filter out these unwanted signals. Otherwise some measure of recognition probability degradation with residual unfiltered clutter or interference is required. If this is not feasible, it may then be necessary to determine whether an interfering signal was present and ignore the measurement and try to repeat it.

Other effects, which are internal to the radar, such as a defocused target profile, resulting from the incorrect compensation of the target's motion over the radar integration period, degrade the range resolution and consequently the recognition performance. The degradation of a range profile is illustrated in Figure 12.1.

12.2.4   Correlation times

12.2.4.1   Multiple measurements

If time is available, the use of multiple measurements can provide a series of target signatures, which can be used to improve the recognition performance, by increasing the cumulative recognition probability. However, if the measurements are made at too rapid intervals and are correlated, misleading results can be obtained as they are not statistically independent. If two measurements are highly correlated it means that they are very similar and that the second measurement provides little additional information, which was not provided by the first measurement. Correlation times are dependent upon the target aspect angle changes over the period in which

Undistorted range profile

Distorted range profile
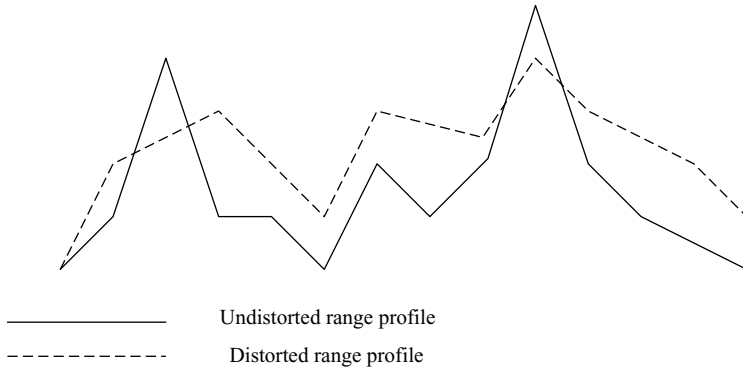
Figure 12.1   A distorted range profile

the radar measurements are made, which are in turn dependent upon the target's motion and on the robustness of the target signature with aspect angle. This is applicable to the measurement of range profiles and JEM lines. In both these cases the signature characteristics can have significant dependencies with look angle.

Knowledge of the high-resolution characteristics of signatures and their angular correlation properties is required in order to assess the level of independence of two sequential measurements. This information can also be used to determine the optimum update rate of a series of measurements, if time is available, to maximise the cumulative recognition probability.

12.2.4.2   De-correlated measurements

The reverse effect can also occur over a single radar measurement, in which the aspect angle of a manoeuvring target, for example, is changing rapidly. The target is effectively de-correlating over the radar measurement period. The range profile would then be a complex combination of range profiles of the target at the various aspect angles swept through over the dwell period and a degraded recognition performance would be expected. An ISAR mode would probably be best suited to a target changing its aspect angle, provided the radar can support this function.

12.3   Target signature database

12.3.1   Introduction

An up-to-date and representative target signature database is required to support the reliable recognition of targets using radar. It should include both civil and military targets for friendly, neutral and potential adversaries and also include variations with aspect angle, stores fits and operational conditions. Variants of each type of target associated with different build states, appropriate to evolving designs and different

missions, are also ideally included. A civil aircraft example is the Boeing 737 airliner, which has been extended in length over several years, with a number of different variants being in service.

Theoretically, it is feasible to have access to the characteristics of targets belonging to, or manufactured by, allies, but a real problem is obtaining the signature characteristics of targets manufactured elsewhere. This question is addressed later in the chapter, and solutions are proposed. The contents of the target signature databases for the various target recognition techniques are presented in the following sections.

12.3.2   Range profiles

12.3.2.1   Database constituents

The initial concepts for assembling a target signature database were presented in Section 3.3.3. Template matching and feature extraction methods can both be used for recognising targets from range profiles and are presented in Section 12.6. Whatever algorithmic technique is being used, it is necessary to assemble a database of range profiles or range profile attributes appropriate to the range resolution, frequency and polarisation of the radar being used to perform this function. The actual constituents of the database are closely related to the recognition algorithm (or classifier) being employed.

Both techniques involve storing either a library of reference target signature templates or extracted target feature attributes, each entry of which covers a range of target aspect angles. The actual range of angles over which this reference data is robust is a critical issue and is discussed in the next section.

Templates for range profiles are stored as amplitude data against range, corresponding to the target's electrical length. Target feature data is stored in a format appropriate to the features being used by the classifier. These can be a combination of the relative amplitudes of scatterers and the distances between key scatterers, so can be stored as a series of numbers, which represent the range profile's attributes for each respective target aspect angle.

Superficially, the dynamic range of the reference range profile data would be considered to be ideally as high as possible, as the higher its information content, the closer it represents the real target and hence the recognition performance would be thought to be maximised. However, in practice, too high a dynamic range adds little to the target recognition performance. It makes the assembling of the database more complex and increases the computational requirements on the recognition data processing, as more bits are needed. One approach to establishing the range profile dynamic range required is to consider the radar measurements that will be performed operationally for recognising the targets. The distance from the radar to the targets of interest, their rcs values and the radar parameters determine the signal-to-noise ratio of the target signatures obtained. As a reasonable guideline, it is proposed that only the range profile elements above the noise floor are included, as it is not considered that parts of the range profile, which are below the noise level, have any significant contribution to make to the performance of the target recognition function.

For target attributes equivalent considerations can apply. Any target features, which are reliably measured, would be associated with target signature characteristics being above the noise floor.

12.3.2.2   Angular dependency

A key issue for the target database is how many reference range profiles or sets of features are required to represent the signature of a particular target at all aspect angles of interest and their associated angular separations. This is dependent upon the radar's high-range resolution measurements, the types of targets included in the database and the recognition performance required. For a particular target, its range profile varies with the aspect angle of the illuminating radar. The variation of the target's range profile with aspect angle is a measure of the robustness of the target's signature with aspect angle and can be quantified by correlating range profiles. The angles over which the range profiles are well correlated can employ the same reference template. The angle over which other targets are rejected and are not correlated with the 'true' target also has to be taken into account. In certain applications, if only relatively dissimilar targets are to be differentiated, it can be appreciated that the angular tolerances on the templates can be looser than in situations in which more similar targets have to be differentiated. The same considerations apply to target features extracted.

The range profiles of real targets vary very rapidly with aspect angle. The angular stability or robustness of a target's range profile is determined by the interference between scatterers at its cross-range extremities. Consider the aircraft target shown in Figure 12.2 with two hypothetical identical isotropic scatterers located at the ends of the wings, which are separated by a distance, D.

For a change in aspect angle, θ, the two-way path length of the reflected signals from these two scatterers also varies. It is zero when the aircraft is initially on
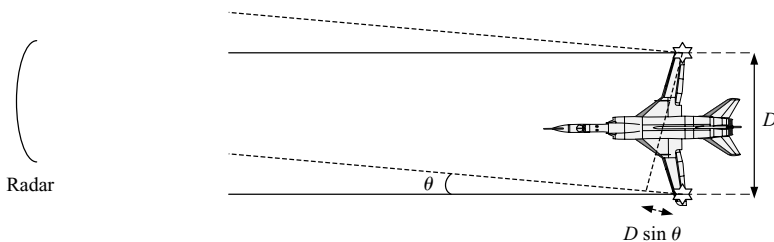
Figure 12.2   *Range profile of target is robust over only narrow aspect angle: (a) interference between scatterers varies with radar aspect angle; (b) for hypothetical scatterers on ends of wings, for change of aspect angle, θ, two-way path difference of signals to radar is $2D \sin \theta$; (c) to avoid significant changes in interference effects between scatterers, $2D \sin \theta$ must be fraction of wavelength and $\frac{1}{4}$ wavelength is selected as maximum tolerable; (d) range profile of target then robust when $\theta \sim (\lambda/8D)$*

the radar's bore-sight, and $2D \sin \theta$ at the off bore-sight aspect angle, θ. If this path length is a half wavelength, the contribution of these scatterers to the range profile changes from constructive interference on bore-sight to destructive interference at θ, which is the worst case change. It is postulated that the interference effects between these scatterers should be fairly constant for path lengths of less than one quarter of a wavelength, so that the range profile should remain stable over the corresponding angle. Hence, with these assumptions, the maximum value of θ is suggested to be $\lambda/(8D)$ for maintaining a robust range profile. As an example, consider an aircraft with a wingspan of 6 m and a radar wavelength of 3 cm. The angle of which the range profile is stable is about 0.04°. This shows that the range profile is only fairly constant over a very small angle. Hence, in order to provide range profile templates over a full 360°, thousands are required. In addition, if similar considerations apply to the elevation angle, at least several hundred would be required for each azimuth angle, resulting in perhaps hundreds of thousands being required in total, for all combinations of azimuth and elevation angles for a single target.

In practice, it is not feasible to provide so many templates, so they are provided at angular intervals, which cover a wider than optimum range of aspect angles. Hence, a typical range profile template is not a perfect representation of the target, so this is a limitation of this technique.

For template matching the reference signatures used are derived from measurements, and/or modelling, with perhaps some 'averaging' being performed over a particular range of angles. No judgements are made on including, rejecting or weighting any particular contributors to the template apart from thresholding and only including the higher amplitude scatterers.

For feature extraction techniques, the range profile attributes have to be analysed to determine their robustness and the number required from measurements and modelling of target signatures. The provision of templates or features for one aspect angle of an aircraft target is illustrated in Figure 12.3. A representation of a target signature database is shown in Figure 3.7 in the introductory section on range profiling.
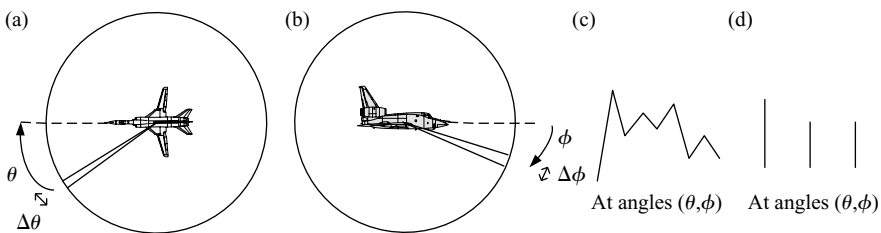
Figure 12.3   *Template or target attribute database covers all azimuth and elevation aspect angles of interest: (a) templates for each angle θ cover azimuth angle range $\Delta\theta$; (b) templates for each angle ϕ cover elevation angle range $\Delta\phi$; (c) range profile template; (d) representation of target attributes*

12.3.2.3 Signature variability

Stores configurations on aircraft targets, for example, modify the high-range resolution signature and the reference template may need to take this into account. At any aspect angle, the correlation between the range profiles of a single target with different stores fits can be used to assess whether a single template can be employed or whether several are needed. Again, the variation of the signature of one target with different stores fits and the correlation with other targets to be differentiated determines the relative similarity of the targets and the number of reference templates needed in the database. Similarly, targets that can change their range profiles with changes in flight configuration, such as the multi-national swing wing Tornado aircraft, also have to be assessed for the robustness of the signature with these variations.

If there are variants of some types of target, assessments have to be made on the relative similarity of features within the type, in comparison to the other target types. The determination of the similarity and dissimilarity of target signatures or features is discussed later in the chapter in the recognition algorithm section. These considerations apply to the range profiles of land, naval and airborne targets.

12.3.2.4 Ballistic missiles

For ballistic missile defence different considerations apply for the target signature database in comparison to other targets. The key issue is to identify the warhead and differentiate it from the other threat cloud objects. Unlike the other targets discussed above, the type of warhead is not necessarily of much interest.

Generic characteristics of warheads would be expected to be held in the database, for likely aspect angles. One method of populating the database would be to provide estimates of the tolerance limits on all the expected threat cloud object parameters, which would then be held as features. Range profile measurements would be used for feature extraction to measure target length, for example.

12.3.2.5 Conclusion

The requirements for the assembly of a target signature database for range profiling involve many complex issues for surface and airborne targets. From trials, modelling and analysis, sufficient information has to be known about the signatures of the targets of interest, under a variety of conditions, to determine which type of classifier should be used.

For feature-based techniques, the actual features used, which are needed to differentiate the targets, and their robustness with aspect angle, have to be determined. Similarly, for template matching, the robustness of the range profiles of individual targets with aspect angle, and their variation from target to target, need to be established. The number of entries in the database for each target and the associated angular coverage for each entry can then be determined.

For ballistic missiles, the critical issue is developing a generic database for all possible threat cloud objects, in order to discriminate the warhead.

12.3.3   Two-dimensional target signatures

For SAR and ISAR imaging, similar approaches to those presented for range profiling are used for storing the reference signature data from targets. They can be based either on representing the whole target at all aspect angles of interest, in a similar way to the range profile templates discussed previously, or in the form of target features.

The issues associated with the templates are very similar to those discussed for the range profiles. These are the number of reference signatures needed and their robustness and tolerance to different variants of the same target type and variations in the target's configuration, such as the rotation of the turret of a tank. One difference is that the target signatures are two-dimensional, so an order of magnitude increase in the data storage requirements is expected. This approach involves a very large database.

The use of feature extraction techniques for representing the target and for applying the recognition algorithms should reduce the data storage requirements in comparison to the reference signature template techniques.

For systems utilising manual, rather than techniques, computational for target recognition, photographs and also reference radar signature data of the targets of interest can be used to train the operators. The two-dimensional radar image measured can then be presented to the operator for the recognition function to be performed.

The assembly of two-dimensional target signature databases and features for target recognition applies to airborne, ground and naval targets.

12.3.4   Helicopters

The recognition of helicopters was discussed extensively in Chapter 5. The parameters, that are required to be known for recognising helicopters are discussed here and this information is used for determining which parameters are incorporated into the database.

For each helicopter the tolerance range of the rotation rate of the main rotor and the number of associated blades must be known, as they determine the blade flash rate. The length of these blades and the effective reflecting area for both the approaching and receding cases are required, as these determine duration of the blade flash and the radar parameters necessary to detect it reliably. However, it is considered that using the duration of the blade flash as a discriminating feature in the database is not likely to be useful, as only very high prf radars are able to measure it.

The diameter of the main rotor hub is needed, which when used with the rotation rate provides the Doppler frequency parameters and would be included in the database.

The number of blades on the rear rotor and its rotation rate are required to be known for analysis of associated spectral information. The information could be stored in the database as the number of blades and the main to rear rotor gear ratio.

For radars that can measure the above parameters simultaneously with high-range resolution, the distance between the rotors would also be included in the database.

It can be seen that several helicopter features can be measured by radar and compared with the reference database. The recognition algorithm techniques used to combine these different radar features are discussed in Chapter 13.

12.3.5 Jet engines

Jet engine modulation was discussed in Chapter 5. As JEM recognises engines rather than a particular type of aircraft, it is necessary to list the number of engines on individual types of aircraft and the types of engines that are fitted to them, as some aircraft are able to accommodate different engines.

For each type of engine, and any significant variants of the main design, it is necessary to know the number of blades on the first few stages of the compressor. It is also necessary to know if all the compressor stages are on the same shaft.

The tolerance range on the rotation rate of the engine is required, as this determines the limits on the spool rate and its harmonics.

For radars that can simultaneously measure JEM and the high-resolution range profile, the position of the engines with reference to a datum point on the aircraft, such as its nose, is required.

12.4 Assembling a database

12.4.1 Introduction

For the various targets to be recognised and the different types of target recognition techniques employed, the requirements on the types of data to be included in the database vary considerably, as was seen in the previous section. In this section, the techniques used to assemble a database are presented. The difficult problem of assembling data on targets of potential adversaries and neutrals, who do not wish to provide it, is also discussed.

12.4.2 Database assembly techniques

12.4.2.1 High-range resolution

For the high-range and high cross-range measurements, databases are required, which are potentially quite complex in having to represent each target's characteristics over many aspect angles. Up to four main types of techniques are used to assemble a database and are now discussed. The most obvious method is to measure the range profiles and cross-range characteristics of all targets of interest at all appropriate aspect angles. This is theoretically possible for available targets, but tends to be very costly. Real measurements have a very important role to play in assembling a database and verifying other models, but it is generally not considered practical to perform every possible measurement.

Real measurements can be performed on ground targets mounted on a rotating turntable. The rotational motion enables ISAR measurements to be performed, so that both down-range and cross-range resolutions can be obtained, enabling ISAR

images to be generated and the main target scatterers to be identified. Measurements
are made at a number of elevation angles and can be compared with airborne SAR
measurements. However, differences occur due to a DC line appearing along the
centre of an ISAR turntable image, due to nearby clutter returns, which does not
occur with airborne SAR measurements of the same target. The near-field measure-
ments obtained from turntable data can also differ from the far-field measurements
obtained from the air. These effects have been analysed, understood and compensated
for to gain confidence that the ground measurements are representative of airborne
measurements.

Ships would normally be measured at sea.

Aircraft targets can be measured both in flight and on turntables which also result
in differences in the measured signatures. The effects of ground clutter for the turntable
measurements and the near-field/far-field effects as discussed earlier for ground tar-
gets have to be taken into account. In addition, the orientation of the aircraft in flight
and its associated aspect angle to the radar have to be established accurately.

The next technique widely employed is the electromagnetic modelling of the
target, which is discussed in more detail later in this chapter. This tends to be compu-
tationally intensive and depends upon the physical characteristics of the target being
modelled with very high integrity.

The third approach is to use scale models and to measure the signatures at a
correspondingly scaled higher frequency in a specially built test facility [1]. This again
depends upon knowing the target's physical characteristics in great detail, which also
includes the use of representative materials. This technique is clearly dependent upon
the available physical modelling skills. Scale modelling is less costly than making
measurements on real targets and an example of a scale model of an aircraft and the
associated signature are shown in Figure 12.4.

The key issue with the mathematical and scale modelling techniques is whether
they agree with the measured data from real targets. This means that it is still necessary
to measure real target signatures, so the various techniques can be compared.
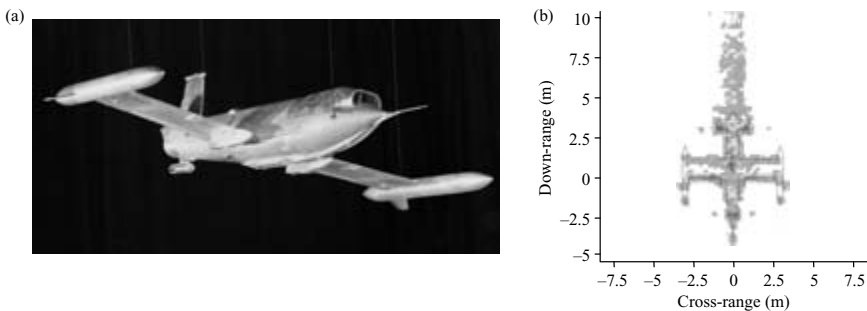
*Figure 12.4   Scale model of an aircraft and its signature. (Courtesy of Thales
Defence Systems UK): (a) scale model of aircraft target; (b) signature
of scale model*

The objective is to obtain good agreement between the different measurement and modelling methods and to use the mathematical and physical modelling methods for providing most of the database. Checks of real and modelled measurements need to be made at regular intervals to maintain confidence in the agreement between the methods.

12.4.2.2 Helicopters and jet engines

These databases are a collection of fairly simple parameters and were discussed in Section 12.3.4.

12.4.3 Unknown targets

In radar target recognition one of the most difficult challenges is dealing with unknown targets. If the manufacturers of particular types of target are unwilling to provide any data on their targets or if the existence of a particular type of target is kept secret, covert techniques are required to obtain the data. Within this section some approaches to assembling target signature data on targets that are not readily available for characterisation are discussed.

It would be expected that one way of obtaining information on the characteristics of unknown targets would be to use intelligence agencies. If the target dimensions can be established with good accuracy and estimates can be made of the target materials, a three-dimensional mathematical model of the target can be generated. This can then be used to develop an electromagnetic model of the target, as is described in Section 12.5, and the high down-range and high cross-resolution images of the target can be modelled. This would enable a target signature database for range profiling, SAR and ISAR measurements to be established.

Photographs from satellites of targets on the ground, for example, can also be used to provide information. If high-resolution SAR data is also available for the same target, it can be correlated with the photographic data. A mathematical model of the mechanics of the target dimensions can then be developed. This can then be used in conjunction with the measured radar data to develop an electromagnetic model of the target. However, it would be expected that many radar measurements and photographs over a wide range of viewing angles would be required to generate the data for a high-integrity three-dimensional model of the target to be established.

For ships, photographs of the targets at sea supplemented by SAR/ISAR measurements from satellites and aircraft can be used to build the signature database.

For aircraft, measurements can be made of the targets in flight to supplement the mathematical modelling of the signatures.

Most of these methods are unlikely to provide the comprehensive database required on unknown targets in practice. There is also the problem of targets for which there has never been any prior knowledge. However, if any of these unknown targets are detected operationally and the signature can be measured, there are still situations in which decisions on the target class and threat potential can be made. For moving targets their signatures can normally be clearly differentiated from the background clutter using Doppler filtering. The measured signature and any extracted

features can be compared to signatures of known targets in the database. Assuming that the signature database includes all possible known targets, then the probabilities that the characteristics of the unknown target match those of known targets can be determined. (Recognition probabilities are discussed in Section 12.6.) As the high-resolution radars can measure features and profiles, any new values that do not equate to existing types are immediately classed as unknown and the measured features can provide an estimate of the target class. One proposed technique is to store generic features associated with different types of target. For aircraft: fighters, helicopters, civil airliners and missiles, each have sets of potentially generic discriminating features: spectral, rcs, range profile, width, length, speed, altitude and manoeuvre envelope. This information can also be supplemented by any intelligence obtained to provide additional confidence.

Hence, although there are difficulties with new targets appearing, with unknown characteristics, which are not in the signature database, it is considered that in practice radar target recognition techniques in conjunction with other available data, can be employed to provide operationally useful information. For example, the following scenario is postulated. An unknown airborne target is moving rapidly, has no JEM, HERM or propeller signature, has a low rcs, manoeuvres rapidly and has a range profile which does not match any target in the database. The lack of any modulation associated with the propulsion system would strongly indicate that the target is military, either a stealthed fighter or a missile. The low rcs and rapid manoeuvres and speed would also be consistent with these target types. It would then be concluded that a neutral or foe stealth fighter or missile has been detected. If it were approaching a large naval asset, it would be recognised as hostile and would be expected to be engaged by the ship's weapon system.

The most difficult challenge is unknown stationary ground targets. Unknown ground targets can be mistaken for ground clutter and may not even be detected as a target and certainly not identified. The techniques for recognising them are considered to be immature and are not widely reported in the open technical literature. If the radar data is insufficient to detect and identify the target, the use of other sensors is required. Other sensor techniques to supplement radar are described in Chapter 13.

12.4.4   Critical database issues

The number of different types of targets required in the database and the number of stored templates or features representing each target and their complexity are critical issues. If the number of entries is so large that accessing the data takes longer than the operational timelines allow, it is clearly unacceptable. In contrast, if the database is too small and the targets encountered are not adequately represented and leads to high levels of incorrect identification occurring, it is equally unacceptable.

The operational requirements for the target recognition system determine the requirements for the target signature database. For a particular application, limits can be defined on the types of target normally encountered. For a particular scenario or operation, the targets available to friends, foes and neutrals are usually known

or can be determined by intelligence. The number of target types to be stored in the database should then be constrained.

The number of reference signatures required for each target and the associated complexity are determined by the similarity of targets to be differentiated and the reliability specified for the recognition function. There is no general solution, which can be provided, as it is determined solely by the application. If the system is only required to differentiate civil airliners from military aircraft, for example, the database requirements would normally be far less stressing than for a system required to reliably identify each aircraft to type.

In order to address unknown targets, generic characteristics of different types of targets can be stored in the database, particularly aircraft, as discussed in the previous section. This would not be expected to be a large database. This then enables any measured target signatures to be categorised to target type and differentiated from known targets of the same class.

12.5 Target signature models

12.5.1 Introduction

A pre-requisite for the mathematical modelling of a target's signature is the provision of a detailed physical description of the target's geometry. The mathematical representation of the shape and size of the target is a three-dimensional surface, which should be in a format that is consistent with computer-aided design techniques.

In addition, it is necessary that the dielectric constant and electrical conductivity of the constituting materials, are defined and are also included in this physical model. In some cases magnetic permeability is also required. The degree to which this mathematical model represents the real target's physical features is one of the factors that determines the accuracy of the electromagnetic model of the target and hence the accuracy of the modelled high-resolution radar characteristics. Target features, such as discontinuities, gaps and cavities, should be modelled. The 'shadowing' of one part of the target by another should also be taken into account.

The techniques used to determine the radar scattering characteristics of the target are based on various approaches to solving Maxwell's equations for incident signals, in order to calculate the reflected signals. These methods are generally very complex and the most popular will be summarised in the following sections, with references being provided for readers who would like to study them in more detail.

Software is commercially available for modelling radar targets and any particular package generally uses a variety of techniques to accommodate the various scattering and propagation effects which occur, as they all have an impact on the target's signature.

12.5.2 Geometrical and physical optics

The most straightforward method that is appropriate to high-frequency signals, which have wavelengths that are much shorter than any of the dimensions of the target

features, is geometrical optics. The scattering mechanism is represented by 'ray tracing', which is widely used for modelling the propagation of light through an optical system. The classical optical reflection law is used to determine the direction of the returned signal. The propagation of the signal is along straight lines and no interference effects are modelled.

In contrast, in order to accommodate any diffraction effects, which occur when the dimensions of the target features are of a similar size to the signal's wavelength, physical optical techniques are used. These model the signal as an electromagnetic wave and allow interference effects to occur between different contributions to the wavefront. A popular method used is to divide the target into a mesh of geometrical shapes, whose shape and size are dependent upon the wavelength of the signal and the curvature of the local surface of the target. The effects of illuminating each of these individual shapes by the radar signal, in the appropriate propagation direction, is then modelled and is used to determine its contribution to the net scattered radar signal. The reflected signal is then the complex sum of the individual amplitude and phase components.

A combination of geometrical and physical optics can be used, whereby the geometrical optics are first used to determine the incident electromagnetic field strength on every part of the object. The object is then divided into a number of flat plates and the electric field, which is calculated at each plate, is then used to determine the reflected signals from each of the plates. The contributions of each of these plates are integrated to provide the net reflected signal in the direction of interest [2–4]. This procedure is shown in Figure 12.5.

In order to model the high-range resolution characteristics of a target using these techniques, the scattering parameters are measured at a series of frequency steps, as discussed in Chapter 3, Section 3.5. The complex data is then frequency-transformed to generate the range profile.

In order to model the SAR or ISAR characteristics of a target, these techniques can be used to simulate the rotation of the target relative to the radar. The amplitude and phase characteristics are modelled over a series of target angles at each frequency step. Range profiles can be modelled at the various aspect angles and then used to generate the ISAR images.

12.5.3 Finite difference time domain method

The Finite Difference Time Domain (FDTD) method divides the target into a three-dimensional mesh, which is then used to solve Maxwell's equations numerically [5–7]. It is particularly appropriate for targets with internal structure. The target's values of electrical conductivity, dielectric constant and magnetic permeability are assigned to each of the respective points on the grid. This concept is shown in Figure 12.6. Initially the equations are solved in free-space in time increments, as the wave propagates from the signal source, representing the radar. Time increments continue to be applied as the electromagnetic wave spreads out and interacts with the target. The values of the electric and magnetic fields are determined for each target and free-space grid position at each time increment.
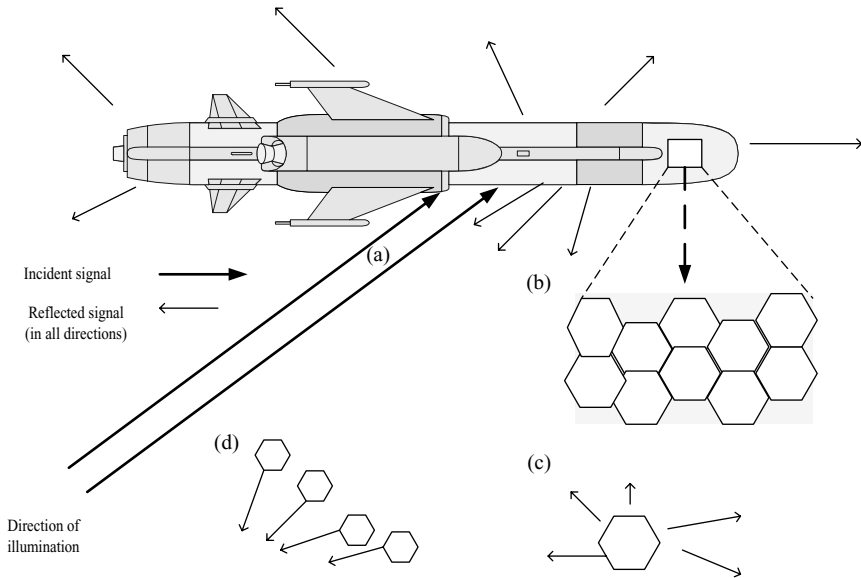
Figure 12.5   Application of geometrical and physical optics to model target reflection characteristics: (a) geometrical optics used to determine electric field strength at target (ray tracing), (b) target surface divided into flat plates, (c) physical optics used to determine reflected field strength of signal from each plate with angle and distance and (d) contributions from each plate integrated to provide resultant electric field strength

As the wave is reflected from the target, the wave propagating back in the direction of the source is of interest, as it represents the monostatic radar characteristics of the target. Under steady-state conditions, when the field strength amplitudes have stabilised and any target transient effects have decayed, the resultant fields modelled, which are propagating back to the source, are those initially required. However, these ranges are normally, in radar range terms, very close to the target, so these 'near-field' values have to be compensated to be appropriate to the 'far-field'.

Using the modelled amplitude and phase values, similar techniques can be used to generate range profiles, SAR and ISAR models, using stepped frequency methods as discussed in the previous section. However, wideband techniques have also been investigated to minimise the computer running time associated with many stepped frequency increments [7].

12.5.4   Method of moments

Another technique used for modelling target signatures is the Method of Moments. It is briefly summarised here and references are provided for further reading. It is a boundary element method and divides the surface of the target into geometrical shapes,

Signal source
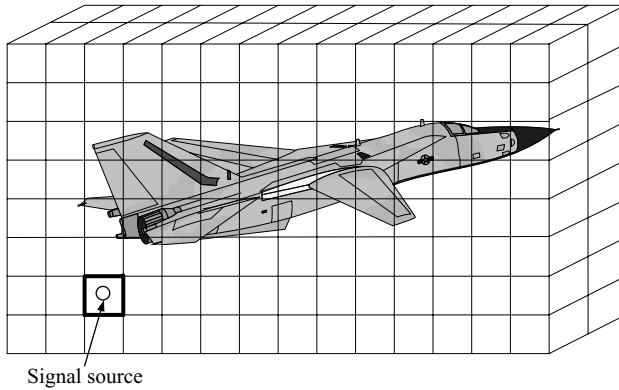
Figure 12.6   *FDTD method for determining target's scattering characteristics: (a) target space is divided into three-dimensional grid; (b) each element of target is assigned values of conductivity, permeability and dielectric constant (c) maxwell's equations are progressively solved in time increments as the signal propagates through grid and illuminates target; (d) resultant field strength reflected back at source represents target rcs*
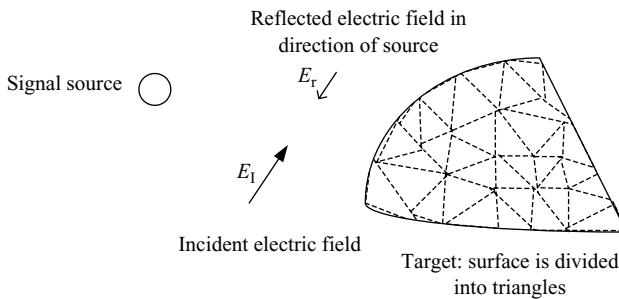
Figure 12.7   *Method of Moments used to calculate target scattering characteristics: (a) using Maxwell's equations, surface currents are determined for each triangular sub-domain for incident electric field; (b) integrated effect of all surface currents generates reflected signal; (c) amplitude and phase of electric field reflected towards radar used to calculate target scattering characteristics*

such as triangles [8–10], which are called sub-domains. It uses the Electric Field Integral Equation to determine the surface currents for each of the sub-domains for an incident electric field. These currents are then used to calculate the resultant reflected electric field generated, by integrating the contributions from the sub-domains (Figure 12.7).

12.5.5 Summary of target signature modelling

Several types of techniques have been developed for modelling radar target signatures and the most suitable technique for a particular application is dependent upon both the target characteristics and the radar wavelength. Factors such as whether cavities or discontinuities are present in the target and the wavelength in comparison to target features are important. The material composition of the target is also significant. In practice, most commercially available software for the prediction of radar scattering from targets involves a combination of the techniques [12,13].

12.6 Recognition algorithms

12.6.1 Introduction

There are two general classes of techniques that are used to recognise images, which includes high-resolution radar signatures: template matching and feature extraction. The concept of comparing a measured range profile with a library of reference range profile signatures is called template matching. The best match provides the best estimate of the target type. In Chapter 5, frequency and time domain techniques were described for recognising jet engines and helicopters from their mechanical attributes, such as blade counts, which are examples of extracting features from targets.

In this section the target classification process is discussed in more detail. The 'Confusion Matrix' is presented, which is a well-known way of representing target recognition probabilities. The use of range profile template matching is reviewed and the general process of using feature extraction techniques for target recognition is discussed.

12.6.2 Target recognition confusion matrix

A simple way of representing the degree to which the 'true' target is reliably recognised and false targets are incorrectly recognised by a target recognition system is by constructing a 'confusion matrix', an example of which is shown in Table 12.1. It is a measure of the performance of the whole target recognition process. It starts with physical measurements of the targets, which may be supported by modelling, in order to extract the targets' discriminating features or the development of signature templates, which are then used as mathematical representations of the targets. The next element in the chain is the development of target recognition algorithms, which operate on a measured target signature data for comparison with the previously derived mathematical representations of the targets, to provide an estimate of the target's identity.

The performance of the recognition system is represented by the confusion matrix. In the left-hand column of Table 12.1 the true identity of the target is stated. In this simple example, it is assumed that it is an idealised 'closed world' of only three types of targets and that the probabilities of correct identification and misidentification have been quantified in the trials measurements using these targets. The three

Table 12.1   Closed world 'Confusion Matrix' presents
probabilities of identifying and misidenti-
fying targets with no unknown column

Actual target identity	Target identity probability		
	Target A (%)	Target B (%)	Target C (%)
Target A	92	6	2
Target B	5	83	16
Target C	3	11	84

right-hand columns represent the probabilities of correctly and incorrectly identifying the target. Target A is stated as having a 92 per cent probability of being correctly identified, with it being misidentified as Target B on 6 per cent and Target C on 2 per cent of occasions. Similarly, the percentages are stated for estimating the identities of Targets B and C in the table's lower two rows. The values of the probabilities should add up to 100 per cent in each row, but this is very rarely the case for each column. For this simple closed world case it is assumed that the classifier is forced into deciding which of the three possible targets is correct.

A figure of merit for the overall performance of the recognition system uses the probabilities from the whole confusion matrix and is the ratio of the sum of the values appearing in the diagonal to the sum of all the other values. This should be as high a value as possible, which is infinite for a perfect algorithm and is clearly never achievable in the real world.

The recognition process is never perfect, as it is limited by noise in the radar measurements, errors in the generation of the signature reference data and the use of classifiers, which usually involve design compromises. This results in some measurements of Target B, for example, appearing to be more similar to Target A reference data than its own, so the algorithm is 'confused' and selects the wrong target.

The simple representation shown in Table 12.1 does not take into account targets of unknown type or known targets, of which there are incomplete signature data sets. The recognition algorithms have to be given the option of concluding that the measured target signature is a poor match with anything in the database and that its identity is unknown. If it forced into making a decision using only existing data, it could result in a major error. A criterion can be established for declaring an unknown target. A threshold value could be set at the output of the classifier which could be a correlation coefficient or probability value. If this is not exceeded the target would be declared as being an unknown.

As will be seen in a later section in this chapter on feature extraction and associated probabilities, there are techniques for dealing with incomplete signature data sets and unknown targets.

12.6.3 Template matching using correlation techniques

12.6.3.1 Introduction

Template matching is a method that compares different sets of data for their similarity and is one of the simplest forms of image or pattern recognition techniques. A set of stored patterns or reference templates is used to identify the data acquired by determining which reference template is the closest match to the data. This is performed by passing the measured data, such as a range profile, to a comparator, which performs a similarity measure between it and each of the set of pre-stored reference template patterns. The comparison, which provides the best match, is the best estimate of the identity of the acquired radar signature data. This comparator is the recognition algorithm for the template matching technique.

12.6.3.2 Euclidean distance measure and cross-correlation

The comparison between a reference range profile template and a measured range profile is expressed mathematically as a distance measure. There are several distance measures, which can be applied. Consider the two range profiles shown in Figure 12.8, which is a simple example in which they have the same number of range gates and they have also been aligned in range. The Euclidean distance between the two is defined as $\sqrt{\sum_{i=1}^{N}(x_i - y_i)^2}$. When this is zero the two range profiles are identical [13].

When comparing a measured radar signature with a set of reference templates, the template that minimises the value of the Euclidean distance is the best match and provides the best estimate of the target type [14–16]. In order to perform this type of function the data first has to be conditioned. To provide a common mathematical
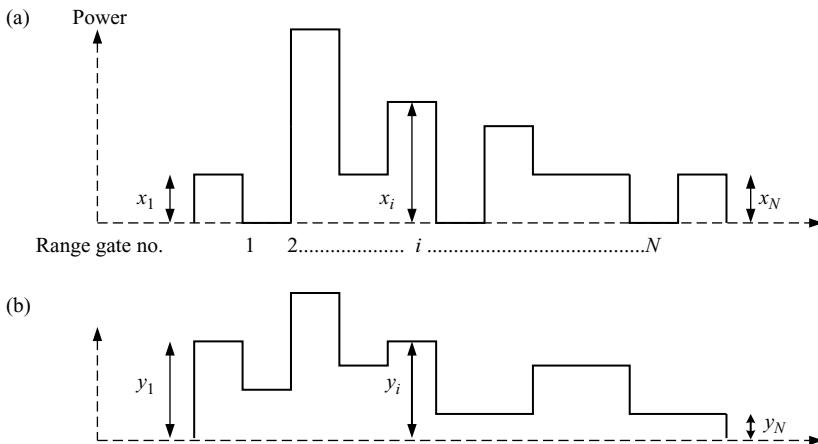
Figure 12.8 *Similarity between two range profiles can be defined by Euclidean distance: (a) range profile with N range gates: amplitudes, x_i; (b) range profile with N range gates: amplitudes, y_i.*

basis for assessing the distance measure between different radar measurements and stored templates of different targets, it is necessary for the data to be normalised. This involves multiplying the amplitudes of each of the constituting range gates of a given range profile by a factor, so that the total energy contained is the same value. This means that individual measurements of range profiles made at different ranges can have a common basis for the comparison with the reference templates, which would also be normalised. Also, thresholding with respect to noise is normally required. Unlike Figure 12.8, which is an idealised example of matching two range profiles, in practice they would be of different lengths and not be aligned in range. The actual algorithm used has to measure the Euclidean distance for any potential combination of relative time shifts. The full number of samples from each profile has to be used, so that the shorter profile effectively contains amplitudes of zero value in some of the range gates.

Another way of expressing the Euclidean distance measure is as a cross-correlation between two sets of values, which is given by:

$$C(t) = \int_{-\infty}^{\infty} x(\tau)y(t+\tau)d\tau \tag{12.1}$$

where $C(t)$ is the cross-correlation between range profile $x(\tau)$ and range profile $y(\tau)$.

The best match of sets of data being cross-correlated occurs when the maximum value is obtained. The reference template, which provides this value, corresponds to the best estimate of target type. The maximum cross-correlation value occurs when the reference template and the measured range profile are identical [17,18]. Template matching techniques are included in a class of pattern recognition techniques called nearest neighbour.

A range profile can be defined as a one-dimensional feature vector. In not measuring any features, template matching does not provide any information on why a particular template match is a more likely candidate for the target's identity than another reference template with a poorer value. For targets that are unknown and have not been seen previously, template matching on its own provides little useful information on the characteristics of the target. If it is a good match to an existing target in the library, it would probably be mistaken for it. If it were not a good match to anything in the template library, it would be concluded that it was of unknown origin. Template matching can also be applied to two- or three-dimensional images. In order to provide more information on the characteristics of the target from the measured radar data, than from using simple template matching, feature extraction techniques are required, which are discussed in the following section.

12.6.4   Feature extraction

12.6.4.1   Introduction

It was seen in the previous section that simple template matching determines little of the characteristics of an unknown target from measurements, other than whether it matches anything in the reference database. Statistical pattern recognition techniques
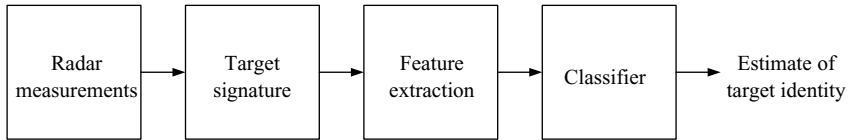
Figure 12.9   Target recognition process using feature extraction

determine the class or identity of a measured object by means of the features extracted from the measured pattern or signature. Feature extraction techniques for recognising targets from radar signatures are discussed in this section.

12.6.4.2   Feature extraction process

The feature extraction process is shown in Figure 12.9. The main parts are the feature extractor and the classifier.

The measured radar signature may initially be thresholded and is then fed into the feature extractor. The discriminating features used for classification are extracted and are called feature vectors. This information is then passed into the classifier and the features are used to make a decision about the identity of the target.

Feature extraction techniques tend to be more tolerant to noise and random variations in target characteristics than template matching methods. The whole of the target signature is not used in the classifier and the extracted features are generally more resilient to variations in the measured signatures. Examples of resilient features are JEM lines, helicopter blade flash frequency and scatterers which can be detected over large angles.

12.6.4.3   Feature space

In some cases, such as engine blade count, the features can have a physical meaning, which can be readily understood. However, features do not always have a physical meaning and their selection is dependent upon the statistics of real target characteristics. They can also be multi-dimensional, which can include range, cross-range in azimuth and elevation, polarisation and engine propulsion parameters. A simple one-dimensional example of feature space is shown in Figure 12.10(a) for JEM for a single engine blade count, whereas Figure 12.10(b) shows the two-dimensional feature space for two blade stages. For the case in which only the single blade count is obtained, only engine type D can be uniquely identified, with A, B and C, and E and F, respectively, not uniquely identified. However, when the second-stage blade count can also be made, the individual engines can be individually identified.

A blade count is a very robust feature and it can seen that in this example, as the dimensionality of the JEM analysis increases, the unique blade count features associated with the respective engines to be recognised are isolated in feature space. It is generally not possible to have such clear distinctions between classes of features, such as those extracted from range profiles or SAR images, as there is more potential of overlap between the signatures of different targets. However, the objective is
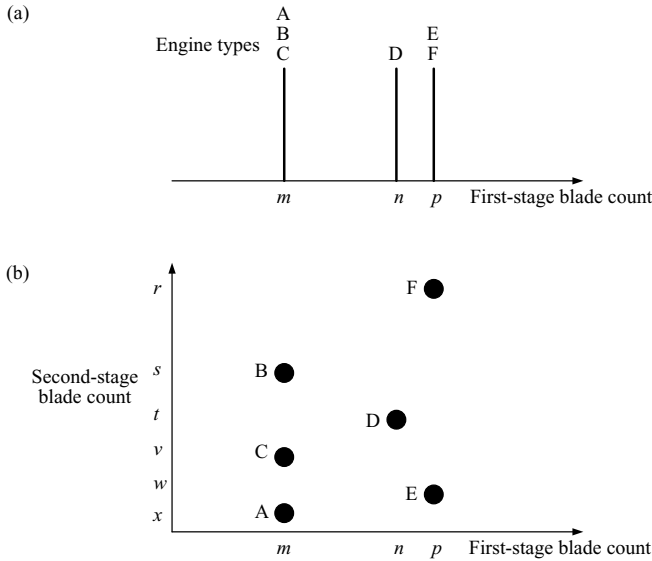
Figure 12.10   One- and two-dimensional features used for JEM: (a) one-dimensional features: for single-stage blade count for JEM, only engine D can be uniquely identified; (b) two-dimensional features: with first- and second-stage blade counts obtained all six engines can be uniquely identified
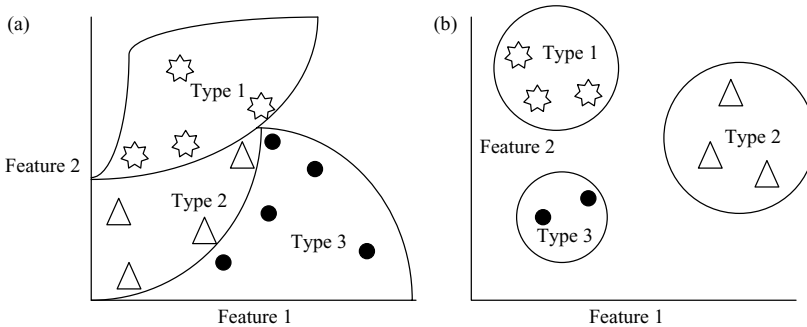
Figure 12.11   Clustering of target features: (a) types of target with features which are close in value are prone to wrong decisions due to noise or measurement errors; (b) types of target with features which are well-clustered are ideal for reliable recognition

to have a sufficient number of robust features, which can reliably be isolated in feature space. Rather than the discrete features of blade counts, a more typical feature map would have less precise boundaries between classes of target. A two-dimensional feature map is shown in Figure 12.11(a). Receiver noise or errors in the signature
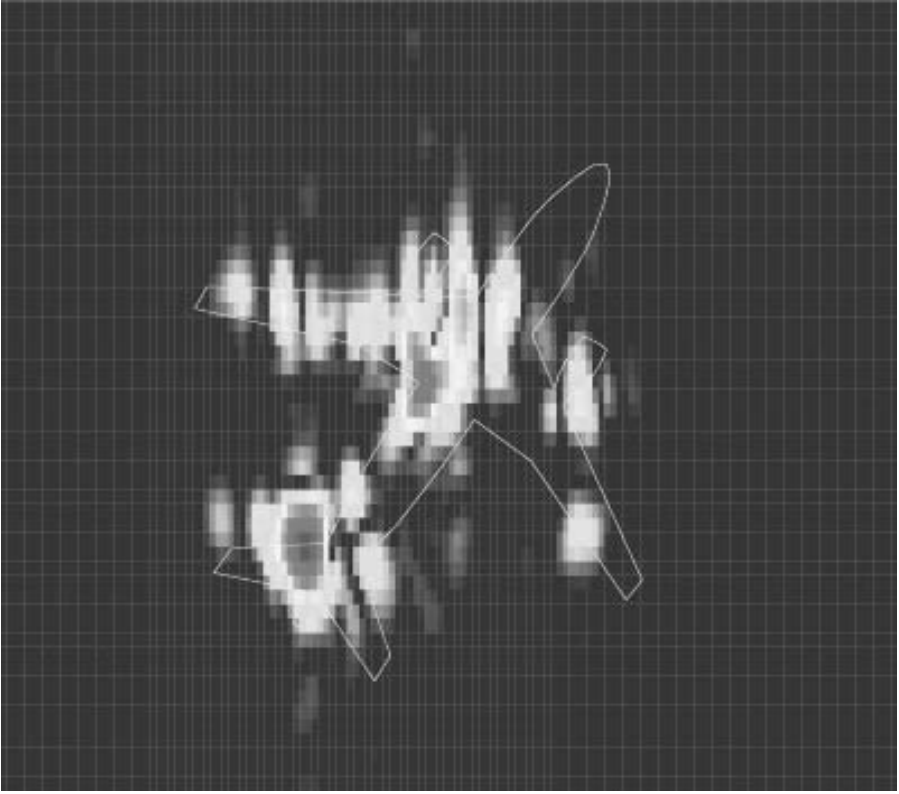
*Figure 12.12   Two-dimensinal ISAR image measured with the TNO FUCAS radar
(Reproduced with permission from Reference 16. Radar data courtesy
of the TNO Physics and Electronics Laboratory, the Netherlands)*

measurement can give rise to targets being assigned to the wrong class, particularly
for feature values, which are close to the boundary between classes. If features can be
found, which are clustered, as shown in Figure 12.11(b), so that there is space between
the target classes, reliable recognition should be obtained.

12.6.4.4   Extraction of target features

Target signatures are arrays of numbers, which are required to have various mathe-
matical operations to be performed on them, in order to extract the features of interest
[19–22]. The first task is usually to threshold the measured data with respect to the
noise, which then localises the signature data. This is often followed by normalisation
of the data by dividing each pixel by the total power in the whole image.

Mathematical operators are then used to extract features from the signature,
such as that shown in Figure 12.12. An edge detection algorithm is used to locate the
extremities of the target. Large scatterers in a target image are identified using a ridge
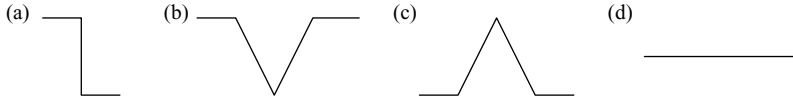
Figure 12.13   *Operators used to extract features from target signatures: (a) edge detector, (b) valley detector, (c) ridge detector and (d) line detector*

detection algorithm. Troughs in the signature are found using a valley detection operator. Straight lines are identified using a Hough transform [23]. These operators are illustrated in Figure 12.13.

The main characteristics of the target should then be extracted, such as its length and the main scattering centres for range profiles [24–30]. For SAR and ISAR images, shape and size can also be extracted.

Initially, in order to identify robust features, which are maintained over a wide range of look angles and measurement conditions, a large amount of data has to be collected for analysis, which is called the training data. Figure 12.14 shows an example of an aircraft target at four different aspect angles with the corresponding range profiles. In Figure 12.14(a) and (b) the main scatterers are shown and can be associated with physical features of the aircraft. Several scatterers are robust over the 20° of aspect angle change for the closing target. Taking the aircraft symmetry into account this would correspond to at least 40° in total. The engines, the front of the wing, cockpit and tail are considered to be the robust scattering areas for this aircraft.

In contrast, for the crossing target in Figure 12.14(c) and (d), the returns of much of the aircraft merge as the main scattering areas become very close in range to those of the fuselage and are not readily differentiated. However, by comparing the range profiles in Figure 12.14(c) and (d), it can be seen that there are some similarities which indicate that it may be possible to extract some robust features. The recognition of aircraft using range profiling for across range tracks tends to be more challenging than for the closing targets.

In general for assembling a database using target features, each robust scatterer's position would be stored in the database and localised in three dimensions corresponding to its location on the target. The angular coverages of each would also be included.

When the robust features have been identified, using the training data, the recognition algorithms can be developed. In practice, the identification and characterisation of target features is a major undertaking requiring considerable data collection and analysis.

12.6.4.5   Recognition algorithms for features

Reference features for each target of interest would be stored in a database. After each high-resolution measurement is performed on a target, the features are extracted for comparison with the reference feature data. The requirements for the recognition algorithms used are to determine the level of similarity of the features measured with the features stored.

(a)

Radar

Cockpit

Engines

Tail

Front of wing

(b)

Nose

Engines

Front of wing

Cockpit

Tail

For aircraft approaching radar, several scatterers are identified and are robust over wide range of angles

(c)

Wing tip

(d)

Wing tip

As aircraft aspect angle changes from approaching to crossing, some scatterers isolated in (a) and (b) merge in (c) and (d), while the wing tip scatterer becomes isolated

Figure 12.14 Robust scatterers from the range profile can be used as recognition features: (Courtesy of BAE Systems Insyte): (a) aircraft approaching radar at 20° *from head-on; (b) aircraft approaching radar head-on; (c) aircraft approaching radar at* 70° *from head-on; (d) aircraft crossing radar at* 90° *from head-on*

The techniques used for recognising the target from the measured features are based upon various scoring methods for the candidate targets. Rule-based techniques utilise features such as the number of scatterers present and their respective distances apart, their relative amplitudes and the widths of the peaks [31,32]. These can be very strict rules defining absolute limits for each feature for each target, at a given aspect angle, or can be based on probability distributions derived from the statistics
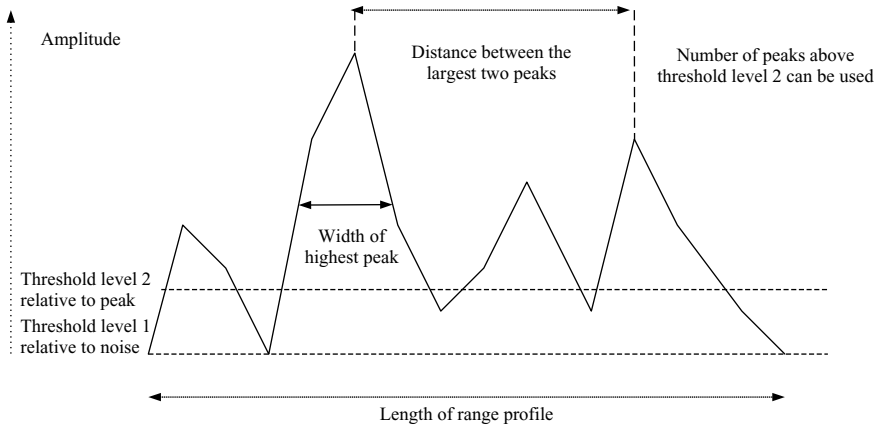
Figure 12.15   Range profile with features that can be used for recognition

of the features. An example of features obtainable from a range profile is illustrated in Figure 12.15. Euclidean distance measures can also be used for comparing features, such as the target length. For each feature measured, the Euclidean distance can be calculated with respect to the reference features. If some of the features measured are considered to have different levels of importance to the overall decision being made, they can be weighted in accordance with their respective perceived values.

The sum of all the distance measures for all the features is then determined and the minimum distance measure is the best assessment of the target's identity. Automatic neural network methods [33] and techniques based on support vector machines [34] and Markov [35,36] models are being studied to perform the feature extnaction and classifier functions [37,38].

12.6.4.6   Bayesian techniques

A very important group of classifiers are based upon Bayes' theorem [39–44], which is discussed in the Appendix. Bayesian classifiers are based upon knowing the statistics of each of the target features. If the statistics of each feature comprising the target is known, the probability of determining the identity of the target can be found from integrating the statistical contributions from each of the features. The composite probability that each of the measured features constitutes a particular target is then quantified. A very simple example of this concept is shown in Figure 12.16, in which a single length measurement is the discriminating feature. For each of the two aircraft, under a given set of measurement conditions, the probabilities of obtaining particular lengths are shown as probability distributions.

For the measurement made of length, L, the respective probabilities of each aircraft having this dimension are $P(L|\text{Type A})$ and $P(L|\text{Type B})$, as shown in the figure. These probabilities mean that if the actual target identity is known, the length measured has this probability distribution. The probabilities of the targets being types A and B are defined as $P(\text{Type A}|L)$ and $P(\text{Type B}|L)$, respectively. Using

Probability

Measured length, *L*

P(*L*|Type A)→

P(*L*|Type B)

Target length
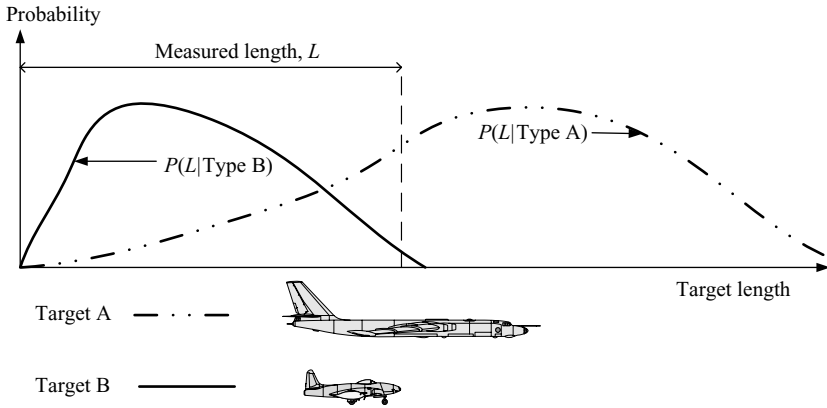
Target A — · · —

Target B ———

Figure 12.16 Bayesian classifier uses probability functions of measured features to determine identity of target. Length is feature shown in this example

Bayes' Formula from Equation (A.23), and assuming that there is equal likelihood of targets A and B being detected, then the actual probabilities of the target being type A or type B are:

$$P(\text{Type A}|L) = \frac{P(L|\text{Type A})}{P(L|\text{Type A}) + P(L|\text{Type B})} \quad (12.2a)$$

$$P(\text{Type B}|L) = \frac{P(L|\text{Type B})}{P(L|\text{Type A}) + P(L|\text{Type B})} \quad (12.2b)$$

It can be seen that the identity of the target is much more likely to be type A as the respective probabilities are directly proportional to the probabilities of the two targets having the length, *L*, as illustrated in Figure 12.16. This means that if the probability density functions of a target feature are known for various targets, by measuring the values of the features, the probability that the target is a certain type can be determined.

In order to show how the Bayesian recognition process operates, an example is now provided. Assume that the length of target measured in Figure 12.16 is 20 m. *P*(*L*|Type A) is the probability that target A has particular length and in this example a value of 0.2 is assigned as the probability that its length lies between 15 and 25 m.

For target B a value of 0.01 is assigned as the probability that its length lies between 15 and 25 m.

From the measured value of length and these *a priori* probability values, Equation (12.2) is now used to assess the probability of the target type.

Hence, the value of *P*(Type A|*L*), which means the probability the target is type A, given that the length has been measured as 15 m, is 0.952.

The value of *P*(Type B|*L*), which means the probability the target is type B, given that the length has been measured as 15 m, is 0.048.

Hence, there is a much higher probability that the target was type A.

If other target features were to be measured, such as the distances between major scatterers, and their probability statistics are known, the overall probabilities of the target being declared as the various classes are determined by combining the contributing probability density functions [45,46]. Bayesian classifiers provide the theoretically best estimate of the target's identity from the measured data and the available information on the feature detection probabilities. The techniques provide the target identification equivalent of the matched filter for radar detection. However, if these probabilities are not known, the applicability of the Bayesian techniques is limited.

In the above example, a closed world of two target types was given and no allowance was made for unknown targets. Bayesian techniques can be used to classify the target as unknown if the probability of the measured target feature does not exceed a defined threshold. For the aircraft example discussed above, assume a length measurement of 60 m had been made and the respective probabilities of the two target types having a length over 50 m were 10^{-5} and 10^{-6}. If a probability threshold had been set at 10^{-4}, then the decision on the target would be an unknown type.

12.6.5   *Recognition algorithm summary*

Examples of classifiers used for radar target recognition have been provided. They are representative of the methods used, but are not an exhaustive list of those available.

- Template matching: Euclidean distance measure between the measured signature and the reference templates, with the lowest value obtained being the closest match. (Mathematically equivalent to correlation.)

For the feature extraction techniques, the main classes of methods used are:

- Rule-based, utilising defined limits of the values of the features, in order to determine the reference template, which matches the most features.
- Euclidean distance measure, based upon determining the minimum sum of the Euclidean distances of the features measured with those of the reference features.
- Bayesian techniques, which utilise the probability statistics of each feature to determine the reference target features, which maximise the recognition probability.
- Combinations of the above three methods can be used.

Feature extraction techniques tend to be much more useful than template matching, particularly for unknown targets. Whereas template matching provides a score of how well the measured signature matches the reference templates, it does not provide information on the matching attributes. Feature extraction can provide much more information about the unknown target. For example, even if a JEM mode cannot identify the target from the estimated blade count, the fact that the JEM spectrum has been measured means that an unknown jet aircraft has been detected. From other attributes, such as its length, rcs and speed, some conclusions about its identity can be drawn.

(a)

(b)
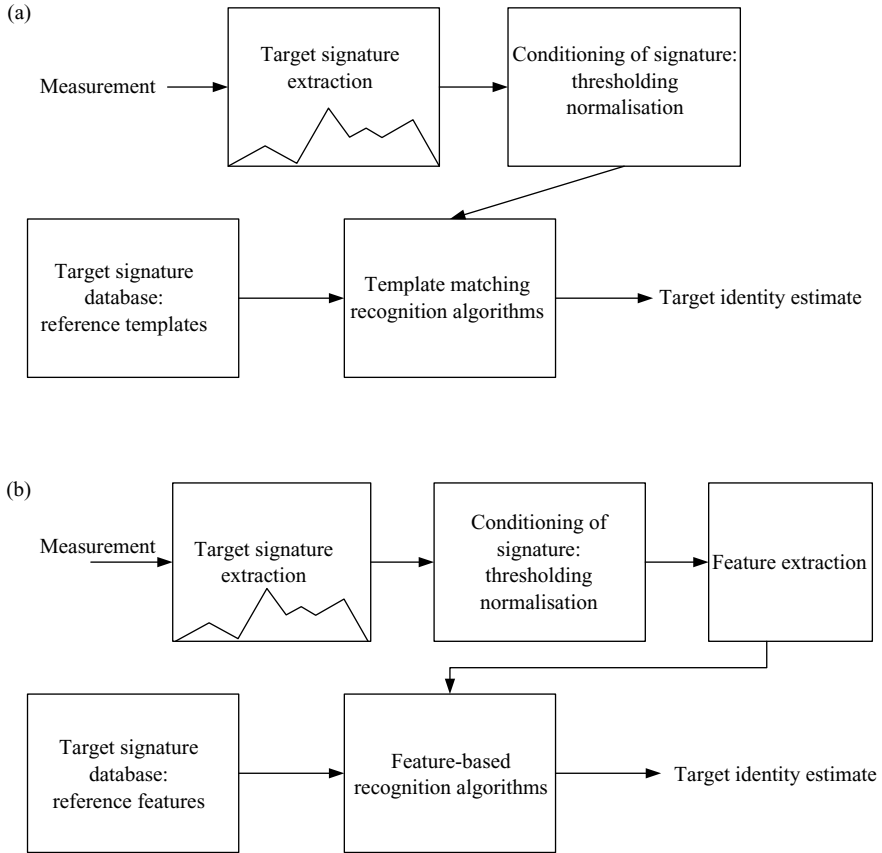
Figure 12.17   *Data processing functions for target recognition: (a) template matching; (b) feature-based recognition*

12.7   Data processing functions

12.7.1   Introduction

The measured radar signature undergoes a series of operations in the data processor, to provide the estimate of the target's identity. The main processes involved for recognition algorithms based upon both template matching and feature extraction techniques are shown in Figure 12.17.

12.7.2   Extraction of target signature data

After the signature of the target is measured or a high-resolution SAR map is produced, it then has to undergo various conditioning processes prior to the application of the recognition algorithm. Initially, algorithms are needed that determine the parts of the

received radar data that contain the target signature of interest. They would normally be expected to utilise any previous data from the initial detection or tracking of the target. For SAR, a type of constant false alarm rate (CFAR) process is required to identify features in the target map that may correspond to potential targets.

Algorithms are then applied for determining the centroid and the extent of the target signature data for each potential target. This function localises the target signature data and is aimed to reject noise and clutter in neighbouring cells, which could be range, cross-range or frequency. This operation tends to be more complex for air-to-ground modes for stationary targets, as each pixcel of the image is a potential constituent of the target, so the target data has to be extracted from the background clutter.

12.7.3　Conditioning of signature data

The processing operations then continue with the signature data being thresholded and normalised. These operations provide the scaling functions required for measurements performed under different conditions of sensitivity.

12.7.4　Feature extraction

Features are then extracted from the target signature data for algorithms using feature-based recognition techniques. There is no equivalent process for the template matching techniques.

12.7.5　Recognition algorithms

It is assumed that the target recognition algorithms are applied automatically and a computer performs these functions with no operator intervention, for the purposes of this discussion. For both feature-based and template matching techniques, the respective reference features or target templates are extracted for the candidate targets, from the database. Only reference signatures or features appropriate to the estimated range of elevation and azimuth aspect angles of the target would be used. They are then used with the recognition algorithms to provide an estimate of the target's identity. A series of probabilities or other measures of match between the measured signature data and reference data, such as cross-correlation coefficient, for the candidate targets are then provided as the output of this process.

For ballistic missile defence applications the target signature data would be used in conjunction with the generic features of threat cloud objects stored in the database. The recognition algorithms would then provide the best estimate of the object being the warhead, by comparison of expected warhead characteristics with the measured signature data.

12.7.6　Data processor

The data processor is more of a function than a specific item of computing hardware and its physical realisation is dependent upon the level of complexity involved

in implementing the recognition process. For the target recognition modes, which require large target databases and many operations, such as range profiling, a specific processor would normally be expected to be dedicated to the task. For the less processing intensive NCTR modes, such as helicopter blade flash detection, the radar signal processor should be readily able to accommodate this function.

As target recognition is often required in real time, the data processor has to perform the functions very rapidly, so the more complex the algorithms and the more extensive the database, the longer it takes to provide the target identity estimate.

12.8   Summary of target recognition process

Within this chapter the sequence of operations required to provide an estimate of the identity of a target from radar measurements has been discussed. Initially, the issues associated with performing a high-quality high-resolution radar measurement to acquire the target signature were discussed.

The critical issue of the assembly of target databases has been presented for both high-range resolution based techniques and for methods based upon measuring the characteristics of aircraft propulsion systems, such as blade counts. The use of measurements of real targets, mathematical modelling and scale modelling has been presented. The employment of geometrical and physical optics, the finite difference time domain technique and the method of moments for the modelling target signatures have been outlined.

The two main classes of recognition algorithms, or classifiers, based on template matching and feature extraction have been discussed. The advantages of utilising target features for recognition, which reduces the requirements on the size of reference target databases, have been presented. Rule-based, Euclidean distance and Bayesian techniques have been summarised, the latter of which provide a mathematical framework, based on probability theory, for maximising the target recognition performance.

A summary of the data processing operations required to support the target recognition functions for providing an estimate of the target's identity has been presented.

References

1   BIRD, D.: 'Target RCS Modelling'. IEEE National *Radar* Conference, IEEE Aerospace and Electronic Systems, New York, March 1994, pp. 74–9
2   BRAND, M.G.E., VAN EWIJK, L.J., KLINKER, F., and SCIPPERS, H.: 'Comparison of RCS Prediction Techniques, Computations and Measurements'. International Conference on *Computation in Electromagnetics*, IEE, London, 25–27 November 1991, pp. 39–42
3   WANG, S.Y., and JANG S.K.: 'A Deterministic Method for Generating a Scattering-Center Model to Reconstruct the RCS Pattern of Complex Radar

Targets', *IEEE Transactions on Electromagnetic Compatibility*, 1997, **39** (4), pp. 315–23

4   LEES, P.A., and DAVIES, M.R.: 'Computer Prediction of RCS for Military Targets', *IEE Proceedings of Radar and Signal Processing*, 1990, **137** (4), pp. 229–36

5   YEE, K.S., TAFLOVE, A., and BODWIN, M.E.: 'Numerical Solution of Steady-State Scattering Problems Using the Time-Dependent Maxwell's Equations', *IEEE Transactions, Microwave Theory and Techniques*, 1975, **23**, pp. 623–30

6   JOHNSON, J.M., and SAMII, Y.R.: 'Multiple Region FDTD (MR/FDTD) and its Application to Microwave Analysis and Modelling', *IEEE MTT-S Digest*, 1996, **3**, pp. 1475–8

7   LUEBBERS, R., STEICH, D., HUNSBERGER, F., KUNZ, K., and CABLE, V.: 'Wideband FDTD Scattering from Dispersive Targets'. Antennas and Propagation Society International Symposium, AP-S. *Merging Technologies for the 90's'. Digest*, 7–11 May 1990, **2**, pp. 994–6

8   DESCHANDE, M.D., COCKRELL, C.R., BECK, E.F.B., VEDELER, E., and KOCK, M.B.: 'Analysis of Electromagnetic Scattering from Irregularly Shaped Thin, Metallic Flat Plates'. NASA Paper 3361, September 1993

9   REDDY, C.J., and DESCHANDE, M.D.: 'Application of AWE for RCS Frequency Response Calculations Using Method of Moments'. NASA Contract no. 4758, October 1996

10 BRAND, M.G.E., VAN EWIJK, L.J., KLINKER, F., and SCIPPERS, H.: 'Comparison of RCS Prediction Techniques, Computations and Measurements'. International Conference on *Computation in Electromagnetics*, IEE, London, 25–27 November 1991, pp. 39–42

11 Roke Manor Website: www.roke.co.uk/sensors/epsilon

12 PRITCHARD, A., RINGROSE, R., and CLARE, M.: 'Prediction of SAR Images of Ships'. IEE Colloquium on *Radar System and Modelling*, London, October 1998, ref 98/459, pp. 2/1–2/5

13 PEARSON, D. (Ed.): 'Image Processing' (McGraw-Hill Book Company Ltd, 1991) Chapter 5.3

14 NOVAK, L.M., OWIRKA, G.J., and BROWER, W.S.: 'Performance of 10- and 20-Target MSE Classifiers', *IEEE Transactions on Aerospace and Electronic Systems*, 2000, **6** (24), pp. 1279–89

15 VAN DER HEIDEN, R.: 'Aircraft Recognition Using Range Profiles'. Ph.D. thesis, University of Amsterdam, October 1998, Chapter 5

16 VAN DER HEIDEN, R., and GROEN, F.C.A.: 'Distance Based Range Profile Based Classification Techniques for Aircraft Recognition by Radar–A Comparison on Real Radar Data'. Agard Conference Proceedings on *Tactical Aerospace C3I in Coming Years*, Lisbon, May 1995, pp. 17/1–17

17 HUDSON, S., and PSULTIS, D.: 'Correlation Filters for Aircraft Identification from Radar Range Profiles', *IEEE Transactions on Aerospace and Electronic Systems*, 1993, **20** (3), pp. 741–8

18 JINSONG TANG, and ZHAODA ZHU: 'Comparison Study on High Resolution Radar Target Recognition'. Proceedings of the IEEE 1996 *National Aerospace and Electronics* Conference, NAECON, vol. 1, 20–23 May 1996, pp. 250–3

19 BOYLE , R., and THOMAS, R.: 'Computer Vision: A First Course' (Blackwell Scientific Publications, Oxford, UK, 1988)

20 DAVIES, E.: 'Machine Vision: Theory Algorithms and Practicalities' (Academic Press, San Diego, CA, 1990)

21 ROBERTS, L.: 'Machine Perception of 3-D Solids' (Optical and Electro-optic Information Processing, MIT Press, Cambridge, MA, 1965)

22 VERNON. D.; 'Machine Vision' (Prentice-Hall, Old Tappan, NJ, 1991)

23 JAIN, A.: 'Fundamentals of Digital Image Processing' (Prentice-Hall, Old Tappan, NJ, 1989)

24 ROSENBACH, Kh., and SCHILLER, J.: 'Identification of Aircraft on the Basis of 2-D Radar Images'. IEEE International *Radar* Conference, Alexandria, VA, 1995, pp. 405–9

25 ZERNIKE, F.: Beugungstheorie des schneidenverfahrens und seiner verbesserten form, der phasenkontrast methode, *Physica*, 1934, **1**, p. 689

26 KOHONEN, T.: 'Self Organising Maps' (Springer Verlag, New York, 1997, 2nd edn)

27 HU, R., and ZHU, Z.: 'Research on Radar Target Classification Based on High Resolution Range Profiles'. Proceedings of the IEEE 1997 *National Aerospace and Electronics* Conference, NAECON 1997, vol. 2, 14–17 July 1997, (IEEE Press, September 1997), pp. 951–5

28 PEI, B., and BAO, Z.: 'Radar Target Recognition Based on Peak Location of HRR Profile and HMMs Classifiers'. *Radar* 2002, IEE conference publication no. 490, London, Edinburgh, UK, 15–17 October 2002, pp. 414–8

29 MAKI, A., FUKUI, K., KAWAWADA, Y., and KIYA, M.: 'Automatic Ship Identification in ISAR Imagery: An On-line System using CMSM'. Proceedings of the IEEE *Radar* Conference, 2002, 22–25 April 2002, pp. 206–11

30 CASSABAUM, M.L., RODRIGUEZ, J.J., RIDDLE, J.G., and WAAGEN, D.E.: 'Feature Analysis Using Millimetre-Wave Real Beam and Doppler Beam Sharpening Techniques'. IEEE 5th South West Symposium on *Image Analysis and Interpretation*, 2003, pp. 101–5

31 HE, S., ZHANG, W., and GUO, G.: 'High Range Resolution MMW Radar Target Recognition Approaches with Application'. Proceedings of the IEEE 1996 *National Aerospace and Electronics* Conference, NAECON 1996, vol. 1 20–23 May 1996, pp. 192–5

32 NIEUWOUDT, C., and BOTHA, E.C.: 'Relative Performance of Correlation-Based and Feature-Based Classifiers of Aircraft Using Radar Range Profiles'. Proceedings of 14th International Conference on *Pattern Recognition*, vol. 2, 16–20 August 1998, pp. 1828–32

33 NANDAGOPAL, D., MARTIN, N.M., JOHNSON, R.P., LOZO, P., and PALANISWAMI, M.: 'Performance of Radar Target Recognition Schemes Using Neural Networks – A Comparative Study'. IEEE International Conference

on *Acoustics, Speech, and Signal Processing*, ICASSP-94, vol. 2, 19–22 April 1994, pp. II/641–4

34 LI, Z., WEIDA, Z., and LICHENG, J.: 'Radar Target Recognition Based on Support Vector Machines'. Proceedings of the 5th International Conference on *Signal Processing* WCCC-ICSP 2000, vol. 3, 21–25 August 2000, pp. 1453–6

35 BHARADWAY, P., RUNKLE, P., CARIN, L., BERRIE, J.A., and HUGHES, J.A.: 'Multiaspect Classification of Airborne Targets via Physics-Based HMMs and Matching Pursuits', *IEEE Transactions on Aerospace and Electronic Systems*, 2001, **37** (2), pp. 595–606

36 JAHANGIR, M., PONTING, K.M., and O'LOGHLEN, J.W.: 'Correction to "Robust Doppler Classification Technique Based on Hidden Markov Models" ', *IEE Proceedings on Radar, Sonar and Navigation*, 2003, **150** (5), p. 387

37 COOKE, T., REDDING, N.J., SCHROEDER, J., and ZHANG, J.: 'Target Discrimination in Complex Synthetic Aperture Radar Imagery'. Conference Record of the 34th Asilomar Conference on *Signals, Systems and Computers*, vol. 2, 29 October–1 November 2000, pp. 1540–4

38 HAN, P., WU, R., WANG, Y., and WANG, Z.: 'An Efficient SAR ATR Approach'. Proceedings of IEEE International Conference on *Acoustics, Speech, and Signal Processing*, ICASSP '03, vol. 2, 2003, 6–10 April 2003, pp. II-429–32

39 BAYES, T.: 'An Essay Toward Solving a Problem in the Doctrine of Chances', *Physical Transactions of the Royal Society of London*, 1794, **53**, pp. 370–415

40 DEGROOT, M.: 'Optimal Statistical Decisions' (John Wiley & Sons)

41 SIVIA, D.S.: 'Data Analysis: A Bayesian Tutorial' (Clarendon Press, Oxford University, UK, July 1996)

42 GELMAN, A.: 'Bayesian Data Analysis' (CRC Press, Florida, FL, 2003)

43 LEE, P.M.: 'Bayesian Statistics: An Introduction' (Hodder Arnold H&S, London, UK, September 1997)

44 D'AGOSTINI, G.: 'Bayesian Reasoning in Data Analysis: A Critical Introduction' (World Scientific Publishing, Hackensack, NJ, August 2003)

45 YAN, J., FENG, X., and HUANG, P.: 'Bayes-Optimally Based Feature Transform for High Resolution Range Profile Identification'. Proceeding of the 6th International Conference on *Signal Processing*, vol. 2, 26–30 August 2002, pp. 1396–8

46 ZHOU, D., WU, L., and LIU, G.: 'Bayesian Classifier Based on Discretized Continues Feature Space'. Proceedings of the 4th International Conference on *Signal Processing*, ICSP '98, vol. 2, 12–16 October 1998, pp. 1225–8

Chapter 13

Combining radar signature and other data

13.1   Introduction

The measurement of radar signatures has been extensively discussed in this book so far. Although radar is a very powerful technique for providing high-quality signature data for recognising the target, and is generally more reliable than any other technique for beyond visual range identification, other available information can enhance the performance of the recognition function. This chapter discusses other available data and information, which can support and improve radar target recognition, and methods for combining it with radar signature data for maximising performance. These data fusion concepts are currently (in 2005) under development for operational systems and are not expected to be fielded for several years.

All the target recognition techniques presented in the previous chapters have almost exclusively been concerned with identifying the target using the attributes of the radar signature. Other measurements associated with the radar can also support the target recognition function and will be discussed in Section 13.2.

Only a single radar sensor has been discussed for recognising targets. Measurements from other radars can also provide useful information, which can improve the recognition performance. In addition, data from other sensors, such as optical, infrared and electronic surveillance receivers can be of considerable benefit in certain circumstances. Data from the IFF system can also be used as supporting information. Other available sensor data is discussed in Section 13.3.

Techniques for combining data from different sensors, which can be in a variety of locations, are based upon extending the Bayesian techniques, which were outlined in Chapter 12 for a classifier for a single radar sensor. The concept of using Bayesian networks for combining data is described in Section 13.4 and their application to the classifier function is developed in Section 13.5. A simulated example is provided for illustrative purposes in Section 13.6. The targets can be associated with land, naval, airborne or space environments. The chapter is summarised in Section 13.7.

13.2   Other radar data

13.2.1   Introduction

As well as the radar signature data, the radar provides other measurement information, both directly and indirectly, which can be used in the target recognition process. A single radar can provide track data, which includes altitude, velocity and manoeuvre information. Additionally, the rcs of the target can be measured and the fluctuation statistics analysed over a series of measurements.

13.2.2   Track data

Some examples of the use of track data are provided within this section. This is not an exhaustive list, but should show how some of the available information, or in some cases, the lack of it, can be used to support the target recognition process and threat assessment.

The track provides the location of the target, so any intrusion into an exclusion zone, which could be air or sea, military, coastal surveillance or economic, requires further investigation.

The radar track provides various levels of evidence of the origin of the target and its projected destination. Clearly, the track originating from a potentially hostile location requires attention. If the target is heading towards a sensitive location or an exclusion zone, this also needs immediate action.

If separate clustered targets are detected on the same or very similar tracks, particularly aircraft, this is a very strong indication that they are military, as civil targets very rarely exhibit this type of behaviour.

If the track parameters do not correspond to an expected target at a particular location or time, they are grounds for further investigation. Similarly, if an aircraft target is squawking in response to a secondary surveillance radar's interrogation signal, but the response does not equate to an expected target with that particular track, the situation requires further investigation.

13.2.3   Altitude, velocity and manoeuvres

Each type of airborne target has an envelope of flight parameters, such as altitude and speed. These can be used as discriminants for supporting the radar target recognition measurements.

The acceleration and manoeuvre capabilities of both airborne and naval targets can also be used as recognition attributes. Civil airliners, for example, are not capable of the very high accelerations of many military aircraft or missiles. Small rapidly moving and manoeuvring navals targets could be rubber inflatable boats, which could pose a military or terrorist threat.

All this information on general target motion characteristics can be stored in a database.

13.2.4   Radar cross-section

The measurement of the average rcs of a target and the statistical variation can be obtained from the low-range resolution waveform, which performs the detection and tracking functions. These parameters can be compared with a database of known targets' rcs values and can be used in the recognition decision. They would only be expected to provide fairly coarse information on target size, but can contribute to the jigsaw of information for estimating the target type.

13.2.5   Radar data summary

It can be appreciated that the combination of the low-resolution radar data discussed above can provide very useful inputs to target recognition. The past, present and projected future location of the target, and whether it is supposed to be there, give strong indications as to its intentions and if it is likely to be a threat of some sort. The altitude, velocity, manoeuvre and rcs data provide good estimates of the likely class of target, but not its type.

   If it is not possible to perform a high-quality high-resolution radar measurement, due to a poor signal-to-noise ratio, for example, evidence of the presence of JEM, HERM, helicopter blade flash or propeller blades can also be useful for decision making on an unknown target's class.

   However, if high-quality target recognition measurements can be performed, in addition to utilising this other supporting data, and it can all be combined effectively, the target recognition performance is maximised for a single radar sensor [1]. It is employing all the high- and low-resolution measured radar data available, obtained when implementing detecting, tracking and high-resolution modes.

13.3   Other sensor data

13.3.1   Electronic surveillance receivers

13.3.1.1   Introduction

Passive electronic surveillance receivers support military operations by detecting and analysing signals emitted in the electromagnetic spectrum [2]. The characteristics of the intercepted signals are measured and are used to isolate, identify and locate the emitter. This information is then used to assess the nature of the platform emitting the signal and provides inputs into threat assessment and decisions on any actions to be taken.

   Electronic surveillance receivers are normally installed on important military assets, such as aircraft and ships.

13.3.1.2   Emitter bearing

Electronic surveillance receivers can measure the waveform of the emitter, its direction and the time at which the signals are received [3]. The direction of the emitted signal is obtained by utilising two receiving channels. The outputs are compared and

(a)

Aircraft emitting signals

(b)

θ

A   B

$c\Delta\tau$

θ

A   B

d

Surveillance platform
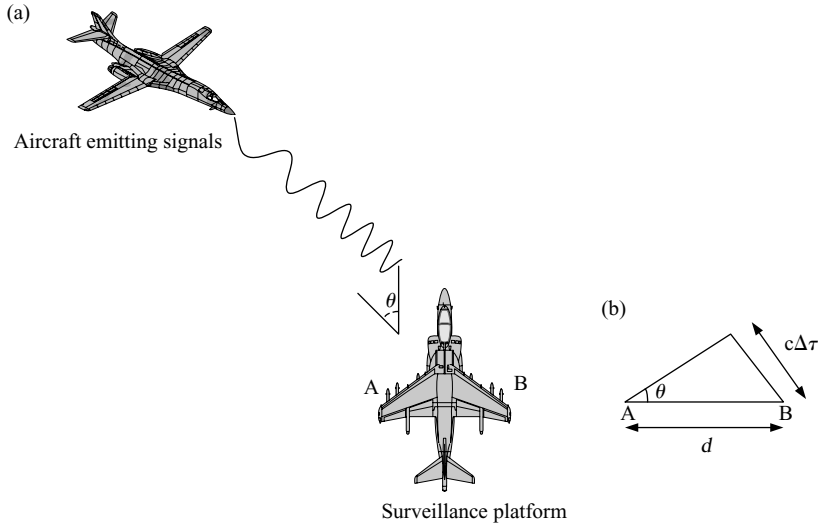
Figure 13.1   Electronic surveillance receiver determines bearing of emitter from difference of time of arrival of signal between two antennas: (a) electronic surveillance receiver antennas located at ends of each wing, at A and B, separated by distance, d; receiver measures time of arrival difference, Δt, between A and B; (b) emitter bearing calculated using: $\sin\theta = c\Delta t/d$

techniques, such as the time on arrival of the signals at the respective receivers, are used to determine the direction of the signal source. This concept is illustrated in Figure 13.1.

The outputs from the two antennas are compared, using cross-correlation for example, and the time of arrival difference is determined. As the distance between the antennas is known, the relationship between the bearing and time difference measured is given by $\sin\theta = c\Delta\tau/d$. Generally, time of arrival measurements are performed in the horizontal plane only, so elevation angles of targets are not usually available using these techniques.

If the emitter is assumed to be on a straight-line track, a technique called kinematic tracking [4,5] can be used to determine its range in addition to its bearing.

13.3.1.3   Waveform measurements

The electronic surveillance receiver measures the main waveform parameters, and algorithms for recognising the modulation are employed. A library of reference emissions [6] of targets of interest is held and the type of signal and the associated platform candidates are estimated. Classes of emissions include radar, communications and jamming. This function is illustrated in Figure 13.2.

Techniques employed for recognising the measured waveform parameters by comparing them with a library of reference signals utilise the same general principles
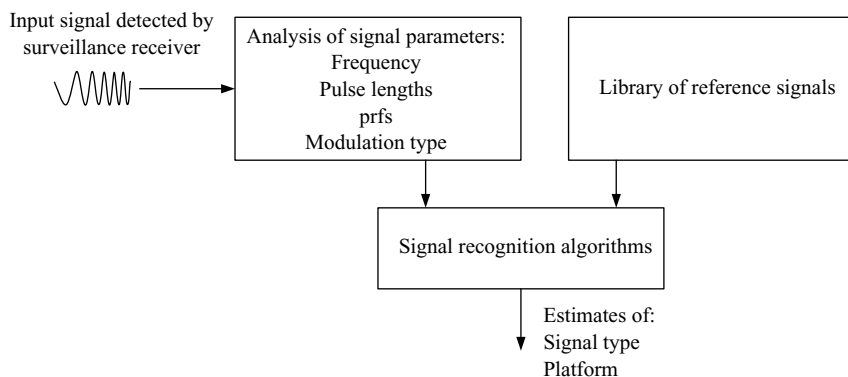
Figure 13.2   Determining emitter characteristics

as those discussed earlier for recognising targets from their radar signatures. The
waveform library would be required to contain information on any civil or military
emitter in the frequency bands of interest for friends, potential foes and neutrals.

13.3.1.4   Electronic surveillance receiver summary

For signals within the coverage of its frequency band and sensitivity limits, the elec-
tronic surveillance receiver has the potential to detect target emissions, localise them
in bearing, possibly also in range, and recognise them and their associated platforms.

13.3.2   *Optical and infrared detection systems*

13.3.2.1   Introduction

Optical detection systems are familiar to us all, as seeing is one of the key human
senses. Electronic systems using optics for surveillance, tracking and recognition,
usually have a telescope to improve sensitivity over that obtained from the eye. The
light captured by the system's objective lens undergoes focusing and is converted into
electrical signals, using components, such as charge coupled devices [7].

Infrared sensing systems detect the heat generated by targets [8,9] and provide
images, which have similarities to the optical images. The main difference is that
infrared detection systems can function in the day and night and do not require any
external illumination of the target. The sensitivity obtained is dependent upon the
temperature and other thermal characteristics of the target in relation to those of
the background clutter. Infrared systems use components, such as thermoelectric
detectors [10], for converting the infrared signal to an electronic signal.

Although optical and infrared techniques are limited by weather effects, such as
rain and fog, and by atmospheric attenuation, they can provide a useful contribution
to target recognition under some circumstances. Any good data obtained should be
included in the overall decision-making process on the target's identity. Radar and

optical sensors also tend to be complementary, as radar is active and is strong on providing high-range resolution and moving target indication, whereas optical systems provide high-resolution cross-range information.

13.3.2.2   Recognition techniques

Optical and infrared systems use image processing and pattern recognition techniques for extracting target features and recognising them. The theory of the techniques is similar to that discussed for radar signatures earlier in this book, but the nature of the optical and infrared images are different.

The essence of the recognition techniques is again to identify robust target features and develop reliable techniques for extracting them from the target images. Recognition algorithms have to be developed and libraries of target features have to be assembled. Some of the methods used are discussed in References 11–19.

13.3.3   *Acoustic sensors*

Acoustic sensors [20] are normally best used for short-range surveillance operations to detect human speech for intelligence gathering, rather than for the detection and recognition of vehicle targets. Applications are in law enforcement agencies' surveillance of criminals and in counter-terrorism.

Acoustic sensors are limited in performance by the slow speed of sound in air and in sensitivity for sensors of a manageable size, which limits range. As bullets and supersonic missiles travel faster than the speed of sound, the acoustic wave reaches the target after the time of impact. They would only be able to contribute to this type of scenario if they were forward based and used a high-speed data link.

In some circumstances, acoustics can contribute, providing the timelines for reaction can be sufficiently long. For hovering helicopters, the acoustic data can be useful for localisation and possibly recognition. For ships and land vehicles, the passive acoustic sensors can provide target location and recognition data.

Acoustic sensors are affected by atmospheric propagation effects [21]. For most target detection and recognition applications, acoustic sensors are inferior to radar, optical, infrared and electronic support measure receiver sensors.

13.4   **Bayesian networks**

13.4.1   *Introduction*

In this chapter so far, the measurements of various attributes of targets have been discussed, using different types of sensors, which employ active and passive techniques in different parts of the electromagnetic spectrum. Operationally, measurements on an unknown target can be made using sensors on a common platform or from a variety of platforms. In order to determine an estimate of the type of target detected, from the various characteristics measured using the different sensors, a method has to be developed for combining this data.
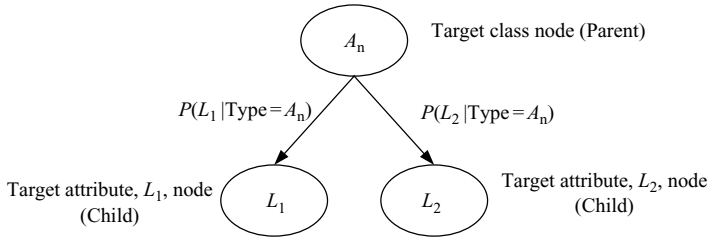
Figure 13.3   Bayesian network concept

In Chapter 12, Bayesian techniques were discussed for recognising a target from a single type of radar measurement using probability functions. Bayes' Theorem is also presented in Appendix 3. In the remainder of this chapter, the extension of Bayesian techniques is presented to include both different types of radar measurements and to utilise data from different sensors, for estimating target identity. These techniques described are known as Bayesian networks.

13.4.2   Bayesian network description

Bayesian networks [22–25] can be used for a vast variety of applications from target recognition, to medical diagnoses [26] to financial modelling [27]. The common factor is the optimum use of all the information available to make decisions, taking into account *a priori* knowledge. In general, Bayesian networks are used to solve problems by generating probabilistic models that represent a set of random variables and the probabilistic relations between them. They are based upon applying Bayes' Formula, Equation (A.22), as presented in the Appendix.

In a Bayesian network, each variable is conventionally represented by an ellipse and this representation is called a 'node', as shown in Figure 13.3. The relationship between this variable, A_n, and another variable, which it influences, is described by a line, with an arrowhead, which points in the direction of the influenced variable. In normal terminology, the influencing variable is called the 'parent' and the influenced variable, the 'child'. The line connecting each parent to each child has an *a priori* probability assigned to it.

The target class, A_n, is the parent node and the two target attributes, which can be measured, L_1 and L_2, are the child nodes. The probability linking the target to the child, $P(L_1|\text{Type} = A_n)$ is the *a priori* probability that the target type A_n has a particular value of attribute L_1. There is a separate *a priori* probability function for each target, A_n, linking each attribute, L_m. From Equation (A.22), Bayes' Formula, the *a posterior* probability that the target is type A_n from a measurement of the attribute L_1 is given by:

$$P(\text{Type} = A_n|L_1) = \{P(L_1|\text{Type} = A_n)P(\text{Type} = A_n)\}\{P(L_1|\text{Type} = A_1)$$
$$\times P(\text{Type} = A_1) + P(L_1|\text{Type} = A_2)P(\text{Type} = A_2) + \cdots$$
$$+ P(L_1|\text{Type} = A_N)P(\text{Type} = A_N)\}^{-1} \tag{13.1}$$

Similar equations describe the respective *a posterior* probabilities for each attribute and target type. Equation (13.1) is used to calculate the *a posterior* probability that the target is a particular type for each attribute measured. It uses the measured value of attribute L_1 for each possible target type, A_n, by applying the probability functions $P(L_1|\text{Type} = A_n)$ and the *a priori* probabilities, $P(\text{Type} = A_n)$, of detecting the various types of targets, A_n.

The probability function for a particular attribute could be the probability that a particular aircraft engine has a certain number of jet engine blades on a particular compressor stage or that the length is between two defined limits. In practice, there would be far more nodes than the three shown in this example.

Each of the values of the *a priori* probabilities assigned is unique to each respective type of target. When several target attributes are measured the overall probability that the target is a particular type is obtained by combining the individual probability functions and is described in Sections 13.5 and 13.6.

13.5   Bayesian classifier

13.5.1   *Introduction*

In order to design a classifier for recognising targets, from knowledge of the sensor measurements being performed, it is necessary to determine the nodes in the Bayesian network [28–31]. The different target categories, which are to be used for assigning the target type, must be defined and comprise parent nodes. The parameters, which the various sensors measure, determine the attributes extracted from the targets and form the child nodes.

In addition, other influences must be taken into account, which affect the measurements. For example, the range of the target determines the signal received and hence the reliability of the measurement performed, so must be taken into account. The aspect angle of the target affects the signature measured, so must also be addressed in the network. As these two factors are influences on the target attributes measured, they are parent nodes and connect to the attribute nodes in the network via arrowheads.

A major task is the assignment of the *a priori* probabilities of each of the target categories having particular target attributes. These values have to be quantified to complete the network.

13.5.2   *Design*

An example of some basic elements of a Bayesian network classifier architecture for a sensor platform comprising a radar, an infrared sensor and an electronic surveillance receiver is shown in Figure 13.4 for one of the possible target categories.

The radar is assumed to be able to measure the JEM spectrum, range profile, altitude and speed. The infrared sensor measures a target signature, which can be a high-resolution image at the shorter ranges, but perhaps only provides an estimate
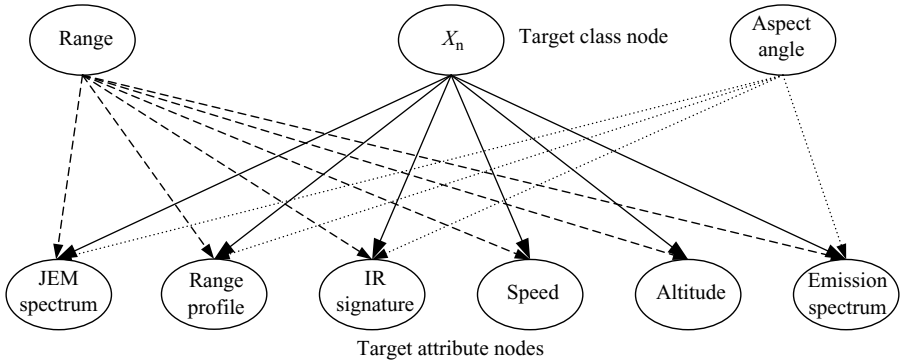
Figure 13.4   Example of Bayesian network classifier architecture for radar, infrared and electronic surveillance sensors

of the energy emitted in the infrared spectrum at the longer ranges. The electronic surveillance receiver measures the waveform parameters of any emissions and relates them to a type of platform.

For each of the attributes, a probability function linking the attribute value to the target category is assigned. This could be on the basis of measurements or mathematical modelling. The range and aspect angle are also shown to influence the measurements being made, so that the *a priori* probabilities defined for the sensors measuring particular values of target attributes can include these influences.

Consider the measurements made of particular target attributes. The *a priori* probabilities of an aircraft target A_n having particular JEM spectrum characteristics, JEM_j, and a particular range profile, Range Profile$_{rp}$ at aspect angle, θ, and Range, R, are defined as:

$$P(\text{JEM}_j(\theta, R)|\text{Type } A_n) \text{ and } P(\text{Range Profile}_{rp}(\theta, R)|\text{Type } A_n), \text{ respectively.}$$

In order to determine the *a posterior* probability that the characteristics of the target obtained from a single measurement were from a particular target type, Bayes' Formula has to be applied.

For all the candidate targets, the *a priori* probabilities for each set of measured characteristics are used to determine $P(\text{Type } A_n|(\text{JEM}_j(\theta, R)))$, for example, which is the *a posterior* probability that the aircraft detected at aspect angle, θ, and range, R, is type A_n for the JEM measurement only. Hence, the *a posterior* probabilities are determined for each candidate target.

Similarly for each measurement made by each sensor, the *a posterior* probabilities are calculated for each attribute measured to determine the respective probabilities for each target. The *a posterior* probabilities for the individual target attribute nodes are then combined to determine the overall *a posterior* probability of the target type from all the sensor information available. This sequence of functions is summarised as

follows:

1. Determine the *a priori* probability that each type of target can be detected.
2. For each target attribute, which each sensor can measure, specify the *a priori* probability function for the attribute value, for each target category.
3. For each attribute measured by the sensors, use Bayes' rule to determine the *a posterior* probability for each target having this attribute value. This is performed separately for each attribute.
4. Combine the individual *a posterior* probabilities for the respective attributes measured by the various sensors to provide the overall *a posterior* probabilities of the detected target being in each category.

A worked example is provided in the next section, to show how this type of classifier functions in practice.

13.6 Bayesian classifier simulation

13.6.1 *Assumptions*

In order to illustrate the operation of a Bayesian network classifier for target recognition, without overcomplicating the explanation, a number of assumptions are made. The essence of how the classifier functions is still maintained.

A closed world is postulated, in which two types of aircraft target, *A* and *B*, can be detected with equal likelihoods. No other targets can be detected and no unknown target categories can be assigned at any point within the process. The *a priori* probabilities for the targets' having particular JEM spectra, range profiles, infrared signatures and emission spectra are specified for the particular set of measurement conditions of range and target aspect angle.

It is also assumed that each of these four target attributes is independent, so that the respective probability functions can be treated separately. The sensor measurements are taken simultaneously with only one measurement being made for each sensor. The measurements are all taken to be of equal value, so there is no relative weighting between them. Perfect data association from the target is assumed, which means that all the sensor data available from the single target is obtained and that there are no other targets in the vicinity with which it can be confused.

13.6.2 A priori *probabilities*

When the sensor measurements are made, a JEM spectrum, a range profile, an infrared signature and an emission spectrum from the target are obtained, as shown in Figure 13.5. For each of these target signatures, the respective a *priori* probabilities for both targets are determined. At this stage, the probabilities stated only relate to the probability distributions for the respective targets having the appropriate attribute values.

For the JEM spectrum measured, its position on the probability density function for attributes extracted for target *A* is determined and the associated probability,
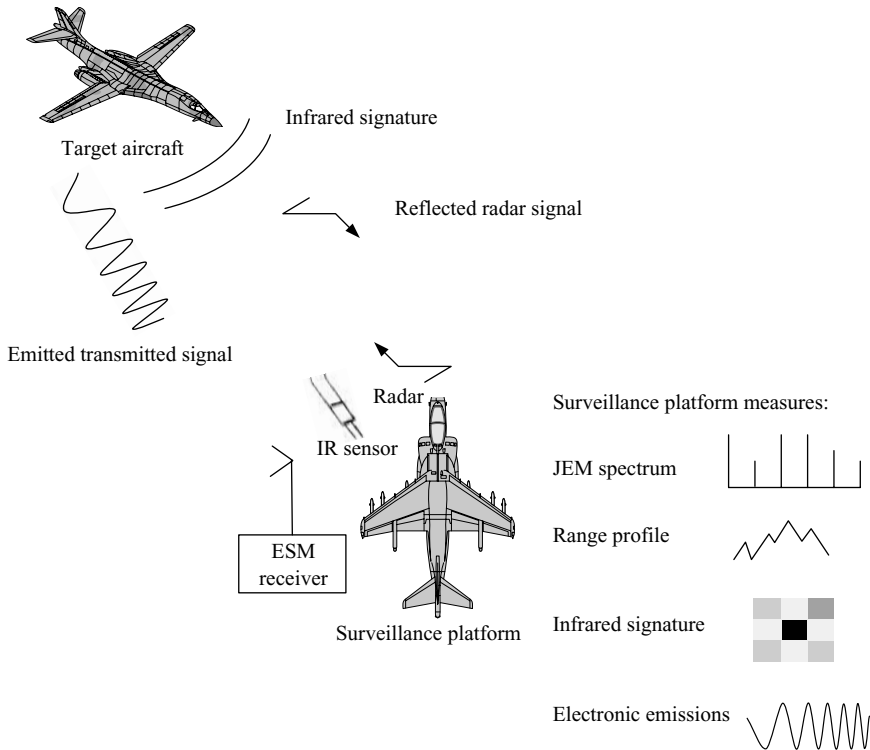
Figure 13.5   Bayesian network combines data from several sensors for recognising target

Table 13.1   A priori probabilities for target attributes measured

Target attribute measured	Probability that target A has attribute measured	Probability that target B has attribute measured
JEM spectrum	$P(\text{JEM}|A) = 0.6$	$P(\text{JEM}|B) = 0.2$
Range profile	$P(\text{Range profile}|A) = 0.8$	$P(\text{Range profile}|B) = 0.4$
Infrared signature	$P(\text{IR}|A) = 0.7$	$P(\text{IR}|B) = 0.2$
Emission spectrum	$P(\text{ES}|A) = 0.3$	$P(\text{ES}|B) = 0.1$

$P(\text{JEM}|A)$, is obtained. The general values of the *a priori* probabilities for the attributes are shown in Table 13.1 with numerical values selected for this example. $P(\text{JEM}|A)$ is taken to be 0.6, which means that target A has an *a priori* probability of 0.6 of having the JEM spectrum obtained at the target's range and aspect angle. Target B has only a low probability of having this JEM spectrum.

Table 13.2   A posterior probabilities for target attributes measured

Target attribute measured	Probability that target A has attribute measured	Probability that target B has attribute measured
JEM spectrum	$P(A|\text{JEM}) = 0.75$	$P(B|\text{JEM}) = 0.25$
Range profile	$P(A|\text{RP}) = 0.67$	$P(B|\text{RP}) = 0.33$
Infrared signature	$P(A|\text{IR}) = 0.78$	$P(B|\text{IR}) = 0.22$
Emission spectrum	$P(A|\text{ES}) = 0.75$	$P(B|\text{ES}) = 0.25$

Similarly for the other target attributes measured, the probabilities are shown.

13.6.3   Applying Bayes' Formula

In order to determine the *a posterior* probabilities, Bayes' Formula Equation (13.1) is applied for the individual attributes and each target type to the data in Table 13.1. For the emission spectrum it is as follows:

$$P(A|\text{ES}) = \frac{P(\text{ES}|A)}{P(S|A) + P(\text{ES}|B)} = \frac{0.3}{0.3 + 0.1} = 0.75$$

$$P(B|\text{ES}) = \frac{P(\text{ES}|B)}{P(\text{ES}|A) + P(\text{ES}|B)} = \frac{0.1}{0.3 + 0.1} = 0.25$$

where $P(A|\text{ES})$ and $P(B|\text{ES})$ are the respective *a posterior* probabilities for the emission spectral data to be assigned to target types A and B. In the absence of any other measurements being made, these figures would provide the best estimates available for the target type. As there are defined to be only two possible types of target, the sum of their probabilities of having the measured emission spectrum is one. The same procedure is adopted to determine the *a posterior* probabilities for the other attributes measured. These have been calculated and appear in Table 13.2.

In order to determine the overall estimate of the target type, using all of the data from the individual attributes, it is necessary to combine the probabilities of Table 13.2.

$$P(A|\text{Overall}) = \{P(A|\text{JEM})P(A|\text{RP})P(A|\text{IR})P(A|\text{ES})\}$$
$$\times \{[P(A|\text{JEM})P(A|\text{RP})P(A|\text{IR})P(A|\text{ES})]$$
$$+ [P(B|\text{JEM})P(B|\text{RP})P(B|\text{IR})P(B|\text{ES})]\}^{-1}$$

and similarly:

$$P(B|\text{Overall}) = \{P(B|\text{JEM})P(B|\text{RP})P(B|\text{IR})P(B|\text{ES})\}$$
$$\times \{[P(A|\text{JEM})P(A|\text{RP})P(A|\text{IR})P(A|\text{ES})]$$
$$+ [P(B|\text{JEM})P(B|\text{RP})P(B|\text{IR})P(B|\text{ES})]\}^{-1}$$

By inserting the values from Table 13.2, the respective probabilities that the target is type *A* or *B* are:

$$P(A|\text{Overall}) = 0.985$$

$$P(B|\text{Overall}) = 0.015$$

Hence, it can be seen that the result of utilising the data from several sensors provides a much higher probability of recognising the target than by using data from a single measurement.

13.7 Summary

In addition to high-resolution signature data being obtained from the radar, other information from the radar, such as target speed, manoeuvres and altitude, can provide indications of the target type. Data from other sensors, which include infrared, and optical devices and surveillance receivers, can also provide useful information for recognising the target.

The Bayesian network provides the framework and the mathematical means for integrating the outputs of each of the individual sensor estimates of target type, to provide the best overall estimate of target type from the information available. The target recognition performance is expected to be considerably enhanced by the efficient utilisation of all the sensor data. The techniques can be used with sensor data obtained from single platforms or from platforms that are separated. They can also utilise data measured at different times.

However, although the theoretical basis for the design and function of the Bayesian Network for classifying targets is very sound, the key challenge for real systems is the definition of the probability distributions for the various network nodes. This means that for every possible target that can be detected, and for every sensor measurement that can be performed, the probability distribution functions for the attributes used for recognition have to be determined.

If there is any correlation of the probability functions for different sensors, which could relate to a particular property of the target being utilised by them, this must be taken into account within the network.

Data association with the appropriate target is a critical issue. Targets in close proximity would be the most likely to have their measured attributes misassociated. If measured target attributes are assigned to the wrong target, major recognition errors can easily occur.

References

1   MORUZZIS, M., SAULAIS, P., TAT, T.H., and HUEI, T.C.: 'Automatic Target Classification for Naval Radars'. *Radar* 2004, Toulouse, France, Paper no. 8B-NCTR-2

2   WILEY, R.: 'Electronic Intelligence' (Artech House, Boston, MA, 1995, 2nd edn)

3   POISEL, R.: 'Electronic Warfare Target Location Methods' (Artech House, Boston, MA, 2005)

4   MONFORT, B., PAQUELET, S., and DELABBAYE, J.-Y.: 'A Fast Method for Target Motion Analysis'. *Radar* 2004, Toulouse, France, Paper no. 110

5   LE CADRE, J.P., and JAUFFRET, C.: 'On the Convergence of Iterative Methods for Bearings-Only Tracking', *IEEE Transactions on Aerospace and Electronic Systems,* 1999, **AES-35**, pp. 801–17

6   GUAN, X., YI, X., and HE, Y.: 'Radar Emitter Recognition Approach of Gray Correlation Analysis Based on D-S Reasoning'. *Radar* 2004, Toulouse, France, Paper no. 216

7   HOLST, G.C.: 'CCD Arrays, Cameras and Displays' (SPIE, May 1999, 2nd edn)

8   HENINI, M., and RAZEGHI, M.: 'Handbook of Infra-red Detection Technologies' (Elsevier Advanced Technology, Massachusetts, USA, 2002)

9   SELEX SENSORS WEBSITE (Formerly BAE Systems Avionics Website: www.infrared-detectors.com/)

10   UNIVERSITY OF LEICESTER SPACE RESEARCH CENTRE WEBSITE: www.src.le.ac.uk/instrumentation/solid_state/infrared

11   SHAIK, J.S., and IFTEKHARUDDIN, K.M.: 'Automated Tracking and Classification of Infrared Images'. Proceedings of the International Joint Conference on *Neural Networks*, vol. 2, 2003, 20–24 July, pp. 1201–6

12   KAGESAWA, M., IKEUCHI, K., and KASHIWAGI, H.: 'Local Feature Based Vehicle Recognition in Infra-Red Images Using Parallel Vision Board'. IEEE International Conference on *Intelligent Robots and Systems*, Kyongju, 1999, pp. 1828–33

13   MCLAUGHLIN, R.A., and ALDER, M.D.: 'Recognition of Infra Red Images of Aircraft Rotated in Three Dimensions'. Proceedings of the 3rd Australian and New Zealand Conference on *Intelligent Information Systems*, ANZIIS-95, Orlando, FL, 27 November 1995, pp. 82–7

14   SADJADI, F.A., and CHUN, C.S.L.: 'Passive Polarimetric IR Target Classification', *IEEE Transactions on Aerospace and Electronic Systems*, 2001, **37** (2), pp. 740–51

15   ANDREONE, L., ANTONELLO, P.C., BERTOZZI, M., BROGGI, A., FASCIOLI, A., and RANZATO, D.: 'Vehicle Detection and Localisation in Infra-Red Images'. Proceedings of the IEEE 5th International Conference on *Intelligent Transportation*, Singapore, September 2002, pp. 141–6

16   KAGESAWA, M., UENO, S., IKEUCHI, K., and KASHIWAGI, H.: 'Recognizing Vehicle in Infra-Red Images Using IMAP Parallel Vision Board', *IEEE Transactions on Intelligent Transportation Systems*, 2001, **2** (1), pp. 10–17

17   POHLIG, S.C.: 'An Algorithm for Detection of Moving Optical Targets', *IEEE Transactions on Aerospace and Electronic Systems*, 1989, **AES-25** (1), pp. 56–63

18 PIATER, J.H., and GRUPEN, R.A.: 'Feature Learning for Recognition with Bayesian Networks'. Proceedings of the 15th International Conference on *Pattern Recognition*, Barcelona, Spain, vol. 1, 3–7 September 2000, pp. 17–20

19 SHAIK, J.S., and IFTEKHARUDDIN, K.M.: 'Automated Tracking and Classification of Infra-Red Images'. Proceedings of the International Joint Conference on *Neural Networks*, Portland, OR, vol. 2, 20–24 July 2003, pp. 1201–6

20 QUACH, A., and LO, K.: 'Automatic Target Detection Using a Ground-Based Passive Acoustic Sensor'. Proceedings of *Information, Decision and Control*, IDC 99, Adelaide, Australia, 8–10 February 1999, pp. 187–92

21 BLACKSTOCK, D.T.: 'Fundamentals of Physical Acoustics' (John Wiley & Sons, New Jersey, NJ, 2000)

22 'Basics of Bayesian Inference and Belief Networks'. www.Research. microsoft.com/adapt/MSBNx

23 JENSEN, F.V.: 'An Introduction to Bayesian Networks' (Springer-Verlag, New York, 1996)

24 PAN, H.: 'Learning Bayesian Networks 1 – A Theory Based on MAP-MDL Criteria'. Proceedings of the 5th International Conference on *Information Fusion*, Annapolis, USA, vol. 2, 8–11 July 2002, pp. 769–76

25 HADDAWY, P., JACOBSON, J., and KAHN, C.E.: 'An Educational Tool for High-Level Interaction with Bayesian Networks'. Proceedings of the 6th International Conference on *Tools with Artificial Intelligence*, New Orleans, LA, 6–9 November 1994, pp. 578–84

26 ANTAL, P., MESZAROS, T., DE MOOR, B., and DOBROWIECKI, T.: 'Annotated Bayesian Networks: A Tool to Integrate Textual and Probabilistic Medical Knowledge'. Proceedings of the 14th IEEE Symposium on *Computer-Based Medical Systems*, CBMS 2001, 26–27 July 2001, pp. 177–82

27 GOLDSZMID, M., and DARWICHE, A.: 'Plan Simulation Using Bayesian Networks'. Proceedings of the 11th Conference on *Artificial Intelligence for Applications*, Los Angeles, CA, 20–23 February 1995, pp. 155–61

28 EL-MATOUAT, F., COLOT, O., VANNOORENBERGHE, P., and LABICHE J.: 'Using Optimal Variables for Bayesian Network Classifiers'. Proceedings of the 3rd International Conference on *Information Fusion*, FUSION 2000, Paris, France, vol. 1, 10–13 July 2000, pp. MOD1/18–MOD1/23

29 LASKEY, K.B.: 'Sensitivity Analysis for Probability Assessments in Bayesian Networks', *IEEE Transactions on Systems, Man and Cybernetics*, 1995, **25** (6), pp. 901–9

30 PIATER, J.H., and GRUPEN, R.A.: 'Feature Learning for Recognition Using Bayesian Networks'. Proceedings of the 15th International Conference on *Pattern Recognition*, vol. 1, 3–7 September 2000, pp. 17–20

31 PAVLOVIC, V., FREY, B.J., and HUANG, T.S.: 'Time Series Classification Using Mixed-State Dynamic Bayesian Networks'. IEEE Computer Society Conference on *Computer Vision and Pattern Recognition*, vol. 2, 23–25 June 1999, p. 615

Chapter 14

Summary and conclusions

14.1 Introduction

The humanitarian, political and military implications of errors made by armed forces in identifying targets, which result in the destruction of friendly, neutral, unthreatening or civil targets, with the associated loss of innocent lives, are unacceptable. In former times incidents of this type were not widely reported so their existence was largely unknown to the general public. However, the availability of news reports around the clock from the media from many countries, who have immediate access to mobile satellite links to their bases, means that news of any incidents occurring throughout the world can be broadcast worldwide almost instantly. In contrast, any deficiencies of armed forces or law enforcement agencies to detect, identify and deal with any infiltrating adversaries or terrorists, which result in the loss of life or of major economic assets, are equally unacceptable. In order to minimise the frequency of these types of situations, the ability to reliably and rapidly recognise air-borne, naval and land targets provides an important contribution towards solving this problem.

Radar is the key sensor for providing a long-range, all weather, day and night, non-cooperative target recognition capability. In this final chapter, the main radar techniques employed for recognising targets and the key technical and implementation issues are summarised. In Section 14.2 is a general discussion on the developments in radar technology which are making radar target recognition a reality. The main radar target recognition techniques are summarised in Sections 14.3–14.6. System design issues, the implications on the requirements for radar components and antenna design issues are addressed in Sections 14.7, 14.8 and 14.9, respectively. The operational issues associated with employing a radar target recognition function are summarised in Section 14.10. The target recognition process is covered in Section 14.11, followed by techniques for combining high-resolution radar data with other available data, to maximise target recognition performance in Section 14.12. Future challenges for all the parties associated with specifying, developing and using

a radar with a target recognition mode are covered in Section 14.13. The outlook for radar target recognition is discussed in Section 14.14.

14.2   Developments in radar technology

Radar technology is developing to meet the target recognition requirements, which are mainly military, and to a lesser extent civil, that procurement agencies are, and will be, placing on radar manufacturing companies. By the year 2015, it is expected that most of the major radar manufacturing companies will have introduced products which can support target recognition functions. The basic techniques required to support the rudimentary target recognition modes have now migrated from the research laboratory to product development.

The two areas of technological development that are enabling target recognition modes to be supported are semi-conductor technology and pattern recognition techniques. The developments in device technology enable wideband high-range resolution signals and high-frequency resolution signals to be generated, conditioned, transmitted, received, digitised and processed. This includes microwave and baseband components, in addition to personal computer (PC)-based signal processors. The latter enable radar signature data to be rapidly provided and then processed for recognising the target.

Image processing and pattern recognition technologies that have been developed for other applications, such as finger print and car number plate recognition for police forces, are now being developed for radar target recognition. The basic functions involved in recognising an image, from whatever source, extracting its features and applying recognition algorithms, or correlating it with a database of reference images, are fundamentally the same processes, enabling the techniques developed in other fields to be transferred and adapted for radar target recognition.

14.3   High-resolution range profiling

High-resolution range profiling is the one-dimensional imaging technique, which dissects the target into down-range cells. The range profile is obtained using a waveform, which covers a large bandwidth. This can be generated in various ways and the actual waveform used is dependent upon the technology that can be incorporated into the radar system. The best practical, and a very popular, waveform tends to be a wideband linear frequency modulated signal. This is a pulse compression technique for obtaining the high-range resolution required, while maximising the power available from the radar transmitter and hence the sensitivity of this high-resolution function. This waveform has a good ambiguity diagram for minimising time sidelobes and is compatible with coherent pulse-Doppler techniques.

Other techniques, such as stepped frequency waveforms and coded waveforms, can also be employed, but tend to be limited by time sidelobe or ambiguity effects.

A major issue with range profiling is the requirement to assemble databases or mathematical models of the characteristics of targets of interest, over a variety of

aspect angles. Recognition algorithms are also needed to provide the estimate of target identity from the measured target signature.

High-resolution range profiling can be used for land, naval, airborne and ballistic missile targets from surface and airborne platforms.

14.4   High cross-range resolution techniques

High cross-range resolution techniques generate a two-dimensional image of the target using high down-range resolution and high cross-range resolution. The former is obtained using a high-range resolution waveform, as in range profiling. The cross-range resolution is obtained by generating a very large synthetic aperture, which effectively increases the aperture of the antenna by virtue of the relative angular motion between the target and the radar platform.

Synthetic aperture radar (SAR) uses a nominal straight-line track of a moving platform, which would typically be an aircraft, to image a stationary target on the ground. The aperture generated is directly proportional to the integration period over which the radar pulses are processed and the range resolution obtained is inversely proportional to this synthetic aperture. The critical issue with SAR is the motion compensation of the radar platform for deviations from the straight track.

SAR is used by airborne and spaced-based platforms for imaging the terrain, land and naval targets. It can be used to image both stationary and moving targets.

Inverse synthetic aperture radar (ISAR) uses the rotational motion of the target relative to the radar platform to generate the synthetic aperture. The angle through which the target rotates over the radar integration period determines the cross-range resolution obtained and is totally dependent upon the target's rotational motion. The actual cross-range data obtained is dependent upon the axis of rotation of the target. The radar platform is often moving for ISAR imaging, so it can also be required to undergo motion compensation in order to ensure that a high-integrity target image is obtained. ISAR can be performed by land, naval and airborne platforms for aircraft, land vehicles and ship targets. It can also be used by surface-based platforms to image ballistic missile targets. When the target and the radar platform are both moving, a combination of SAR and ISAR signal processing is needed, which tends to be rather complex, such as an airborne platform imaging a moving ground vehicle.

As SAR and ISAR images are two-dimensional and usually look far more like an image of the target, than a range profile, which is more abstract, image processing techniques can be used to extract target features for recognition purposes. It is again necessary to have a database of stored features of targets of interest.

14.5   Jet engine and helicopter recognition techniques

Within this book, time and frequency analysis techniques have been described for the recognition of the propulsion systems of fixed and rotary wing aircraft. Rotating

machinery, which is used as the power plant of an aircraft, has a radar signature that varies in time at a rate determined by the periodicity of the rotational motion. These effects can be detected from jet engines, helicopter rotors and rotor blades. They can either be measured as spectral components or as impulses detected in the time domain. The periodicity of the effect and the radar integration time available largely determine the actual technique used. The radar techniques employed for recognising propulsion systems generally are high-frequency resolution modes with low-range resolution.

The spectrum received from illuminating a jet engine is determined by its rotation rate and the number of blades on its compressor stages for a closing aircraft target. The JEM analysis process extracts the measured frequency components and uses them to estimate the number of blades on various stages of the compressor. These are then compared with a library containing blade counts on known engines, to estimate the engine type. Spectral analysis techniques can also be used for recognising propeller-driven aircraft.

For helicopters the Doppler frequency spread associated with the rotation of the main rotor hub is determined by the rotation rate and hub diameter. This measured Doppler spectrum is then compared with a library of Doppler spreads from known helicopters to provide an estimate of the helicopter type.

A 'flash' from a main rotor blade of the helicopter occurs when the blade is optimally placed to maximise the reflected signal back to the radar. This usually occurs twice every rotational cycle of the hub. The time interval between main rotor blade flashes is determined by the number of blades on the helicopter and the hub rotation rate. Helicopters with even and odd blade counts tend to have different blade flash characteristics. These time domain analysis techniques can also be applied to propeller-driven aircraft. Another discriminant for recognising the helicopter is the spectrum obtained from the rear rotor blades. This is again determined by the number of blades on the rear rotor and the rotation rate. All these various features extracted from the helicopter and their relationships can build-up confidence for recognising it. However, in practice, the various spectral components associated with the specific mechanical features, which can be measured, cannot always be isolated, as the respective spectral components can overlap.

14.6   Other high-resolution techniques

The mainstream target recognition techniques have been covered in the previous sections of this chapter. Techniques, which are being investigated or have specialist applications, are summarised here.

Super resolution is a class of techniques that can improve the resolution of any radar parameter measured, by using a high signal-to-noise ratio. The extra resolution obtained is at the expense of requiring the radar to operate under high signal-to-noise ratio conditions and limits the opportunities to practically employ these techniques. They can be used to improve down-range resolution and cross-range resolution for range profiling and target imaging. JEM and other spectral and time domain

measurements can be used to extract target features with higher precision at high signal-to-noise ratios. Super resolution techniques would normally be employed in systems with high signal-to-noise ratios available, but which are not practical or economic to upgrade with higher resolution waveforms and techniques.

Monopulse target imaging is a super resolution technique, which can provide high cross-range resolution. It uses the monopulse comparator, which is normally employed for target tracking, for obtaining high cross-range information on target scatterers. It is used in conjunction with high down-range resolution to provide either a two-dimensional target image if monopulse in one angle is used, or a three-dimensional image if elevation and azimuth monopulse are employed.

Its application is limited to short ranges and its effectiveness is dependent upon each down-range cell having only a single scatterer.

Radar signals can be 'polarised' horizontally, vertically or with left or right circular polarisation, which are descriptions of the electric field direction. Geometrical objects of different shapes and materials have different responses to polarised signals. The components of the reflected polarised signals received by the radar are called the object's polarisation matrix. Some simple geometrical objects acting as radar targets can be characterised by their polarisation matrices and hence recognised as objects of a particular shape. Polarisation analysis can also be applied to a complete target if the high-range resolution radar technique employed can isolate individual scatterers of the target and measure their associated polarisation matrices. The polarisation matrices of some of the scatterers can then be matched to those known for particular geometrical shapes. The isolation of most target scatterers can generally be achieved by using SAR or ISAR techniques to provide a two-dimensional signature. With high-range resolution alone it is less effective as there are often several scatterers in each high-resolution range gate and the polarisation matrix of each scatterer cannot be isolated. However, the presence of large dominating reflectors such as di-hedral objects can be determined from a range profile using the polarisation matrix components. Hence, if the shapes of certain parts of the target can be determined and localised on the target signature using the properties of the scatterers' polarisation matrices, they can be included with other extracted features identified to recognise the target.

Impulse radar is a type of high-resolution radar, which is normally used for ground penetration for detecting buried objects. The transmitted signal has spectral components from about 100 MHz to 3 GHz and can propagate through the ground.

Impulse radars have found few applications for the detection of surface and above-surface targets to date. However, an interesting development is in the detection and recognition of vehicles under foliage. The same characteristics, which allow it to penetrate through the ground, are used to propagate through foliage.

Ultra-wideband and ultra high-resolution radars are high-range resolution radars, which have much higher range resolution than normal radars. Impulse radars can be categorised as a subset of this class. However, very wideband modulation techniques using solid-state components can now be used to provide radar waveforms with a few centimetres range resolution.

These types of techniques are employed in systems that require the best range resolutions available. Landmine detection and ballistic missile defence are the main

applications currently being considered for these techniques. However, they have not yet been widely employed.

Some radar systems are able to support high-range resolution and high Doppler resolution waveforms simultaneously. If the design parameters are optimised, target recognition performance can be maximised.

The ability to simultaneously provide a high-range resolution and high-frequency resolution waveform, for example, supports obtaining the range profile, the JEM spectrum and the localisation of the engine positions along the range profile of an aircraft target, the latter of which is an additional target feature. In addition, it also reduces the time available for implementing the mode or effectively increases the sensitivity of the combined measurement by using all the time available.

14.7   System design issues

Although the designs of radars with a target recognition capability can be considered as being evolutionary, with reference to conventional radar designs, at the system design level there are crucial differences. In addition to requirements for supporting high-resolution waveforms, there are implications on the sensitivity, dynamic range and distortion characterisation of the radar system.

In providing a high-resolution capability in the radar, the target is effectively dissected into components by the high-resolution waveform. This means that rather than the whole of the target's rcs being used in the radar range equation for establishing sensitivity, the rcs of the smallest target element of interest determines the sensitivity. Generally, one or two orders of magnitude of improved sensitivity are required for target recognition modes.

The dynamic range of the radar is also stressed with the high-resolution modes. The most difficult situation is to simultaneously deal with a high rcs clutter point target while obtaining a high-resolution target signature.

For low-range resolution waveforms supporting conventional radar modes, there is generally little variation in the radar's characteristics over the relatively narrow signal bandwidth. However, over tens and hundreds of MHz of bandwidth needed for high-range resolution modes, the characteristics of the radar components vary, such that without any compensation applied, target recognition performance can be degraded. It is necessary to characterise the radar using a test target, so that the amplitude and phase distortions over the signal's bandwidth can be measured. Algorithms employing these distortion coefficients are then used in the signal processing of received signals to minimise these effects.

14.8   Component implications

Target recognition modes require wider band and/or higher frequency resolution waveforms, higher dynamic range and higher system sensitivity than the conventional detection and tracking waveforms. These requirements all increase the severity of the performance specifications of the radar components employed.

For the waveform generator the bandwidth, spectral purity, spurious outputs and phase noise of the reference master oscillator performance requirements all tend to be more stringent than for the traditional radar modes. For high-range resolution waveforms, the rejection of inter-modulation products, harmonics and spurious mixing products over the high bandwidths used, is important and requires high-performance filters and good design practice for up-conversion.

For high-range resolution modes the transmitter has to supply sufficient power over a large bandwidth. For travelling wave tube amplifiers, the levels of added phase noise and the generation of spurious output signals are critical issues.

The dynamic range is the most critical issue for the receiver. The mixers and amplifiers employed need to have high third-order intercept points and good phase noise performance. The analogue to digital converter has often been the most critical item in the entire radar for supporting target recognition modes. The target recognition requirements for high dynamic range and high digitiser speed imply that the digitiser needs a large number of effective bits and a high spurious free dynamic range.

With the advent of very high speed commercially available and affordable signal processing technology, the signal and data processing functions required to support target recognition should not be critical issues, as progressively higher power PCs are produced [1,2].

14.9   Antenna design issues

The classes of antenna used in current radar designs are mechanically rotating dishes, electronically scanning phased array radars and in some cases combinations of both of these. The implementation issues of high-range resolution modes in these types of systems are quite different.

Parabolic dish antennas generally have a bandwidth of at least 10 per cent of the signal's frequency. They also tend to be 'squintless', such that the beam points in the same direction as the frequency varies. For these reasons they can support wideband high-range resolution waveforms.

Phased array radars have a sufficiently large bandwidth to support detection and tracking waveforms. Normal designs do not support wideband waveforms, so stepped frequency techniques tend to be used for providing high-range resolution, but inferior target recognition performance is usually obtained.

In order to support wideband waveforms, phase arrays have to incorporate true time delay beam steering, which is becoming available, but is complex and expensive.

14.10   Operational issues

Key issues for operating a target recognition function are how and when decisions on the target's identity are made and whether it is a manual or automatic process or a combination of both. The implementation and operation of target recognition modes are largely determined by the type of radar employed and its function.

These issues are summarised here for mechanically scanning tracker radars, active and phased array radars and typical approaches are presented.

Tracking radars support weapons systems and are very good candidates for introducing a target recognition mode. For military engagements the tracker is normally cued-in by a surveillance sensor to track the outgoing missile towards the threatening target. The operational concept is that tracking and target recognition modes are interleaved during the missile fly-out.

Initial target signature data may even be able to be obtained prior to missile launch, as the tracker acquires initial lock on the target, but this is dependent upon the engagement timelines for the associated missile system.

The operational need involves obtaining as much target recognition data as possible, to maximise the probability of correct recognition, while still maintaining the target and missile tracks. If possible, contiguous high-resolution measurements should be performed as the missile flies out. This data is processed and continuous estimates of the target identity are made and refined. A command link to the missile would then abort the intercept if the target were deemed to be non-threatening with high confidence.

If the timelines for the engagement were only a few seconds, automatic recognition would be required, as the tasks involved for an operator to make a decision would take too long. For longer engagements, the operator would have time to observe measured target signatures or feature data extracted from the signature and apply his/her own judgement and over-ride the computer's recognition decision. In some cases the automatic process could advise recognition probability estimates with the operator being required to make the decision to pass the information on to a commander.

Passive phased arrays are normally used as surveillance radars and generally rotate at a constant rate to provide target detection and track data. They can beamform in azimuth, elevation or both, and this is dependent upon the design. The key issue for implementing a target recognition function is how to obtain sufficient signal-to-noise ratio at operational ranges to provide a useful mode.

For passive arrays with elevation beamforming only, with no azimuth scanning capability, it is not normally feasible to meet these requirements. It is not generally practical to slow-down the antenna rotation rate, without degrading the primary operational functions of obtaining target detections and tracks at particular ranges, which would then occur at slower update rates.

If azimuth scanning is available, the dwell time on the target of interest can be increased by keeping the beam pointed at the target as the antenna rotates, to provide the additional signal-to-noise ratio required. For surveillance radars, which operate at long ranges, there would normally be sufficient time for the radar operator to study target signatures and extracted features to review the computer's recognition estimate and make the final decision and implement an appropriate response.

Active phased array radars can be both surveillance and multi-function radars and can scan the beam in elevation and azimuth, whether or not they have fixed faces or rotate. They should have no problems in obtaining sufficient signal-to-noise ratio for target recognition. They should also be able to include the target recognition modes into their resourcing schedule without degrading their other functions. These radars

normally have relatively long ranges and there should be adequate time available for the operator to study the target identity data and conclusions made by the computer, and make the final decision or communicate the information and respond accordingly.

14.11   Target recognition process

The processes involved in providing the radar target recognition function are summarised in this section. In order to provide a useful target recognition function it is clearly necessary for the radar being used to obtain high-quality target signature data. The waveform parameters used must support the acquisition of signature data, which minimises distortion effects, such as ambiguities. The characteristics of the radar components must either contribute little to distort the measured target signature or the effects of the distortion must be characterised and compensated.

The signal-to-noise ratio must be sufficiently high and the effects of interference, clutter and jammers should be suppressed.

In order to be able to perform a target recognition function, it is necessary that measured signatures can be compared to a reference set of known target signatures, so that a comparison can be made and an estimate of the target type can be provided. The assembly and arrangement of a set of reference target signatures or attributes of targets forms a target signature database. Every type of radar target recognition mode would have an associated signature database. The collection of signature data from allies, neutrals and potential adversaries is a critical issue in target recognition.

Campaigns are normally required involving measurements, modelling and analysis for generating the signature database. Targets that have not been previously seen and do not appear in the database can be a problem, but approaches can be taken for overcoming the difficulties. Any unknown target would have its various attributes measured by the high-resolution modes and its behaviour would be observed. If the attributes were indicative of its being a fighter aircraft or missile, for example, and the behaviour were threatening, then it would be considered to be a high-priority threat and would have to be dealt with using force.

As it is generally not practical or affordable to measure the signature of every target of interest at every aspect angle under all conditions, a common approach is to model the signature mathematically.

The size, shape and materials comprising the target have to be defined first in three dimensions. A mathematical model is then developed to determine the reflection characteristics of the target at the appropriate frequency range of interest. Techniques based upon electromagnetic modelling, geometrical and physical optics can be used. Computer power is then applied to generate the signatures for the aspect angles and conditions of interest.

Scale modelling is also used to provide target signatures. High-integrity miniature targets are manufactured and have their signatures measured at the appropriate scaled frequency. This data can also be used to populate the target signature database. In order to have confidence that the mathematical modelling and scale modelling are

representative, they are compared with real signature measurements under different sets of conditions.

The target recognition algorithms or classifiers provide the means by which the target signature measured is compared with the signature database, enabling a decision on the target's identity to be made. There are two general types of recognition algorithms used, template matching and feature extraction.

Template matching correlates measured range profiles with a reference signature. The highest value of correlation is then deemed to be the best match and the corresponding reference signature is the best estimate of target type.

An example of extracting target attributes and using them for target recognition is JEM. The spectrum measured is analysed and the main spectral components are extracted and are used to determine the blade counts on the compression stage rotors. The numbers of blades are compared to those in the database and the jet engine providing the match is recognised. The blade counts are the jet engine's target features.

If the probability of each target having particular attribute values can be quantified, Bayesian classifier techniques provide the best possible estimate of the target's identity from the available information.

For most radar target recognition applications the estimated identity of the target is required rapidly and reliably. A decision on whether to engage a target, which is potentially threatening to imminently destroy assets and endanger life, has to be taken quickly. It is therefore essential that all the operations associated with processing the signature data must be performed in real time. These functions are the conditioning of the signature data, the extraction of features, the accessing of the signature database and the operation of the recognition algorithms.

Fortunately, the speed of processing data continues to increase, as available computer power progressively rises, so that real-time target recognition is feasible.

14.12   Combining radar signature and other data

In addition to radar signature data, other information is available from the radar. Other radars and other types of sensors on different platforms can also contribute to target recognition. A summary of the types of sensors available for supporting radar target recognition and techniques for combining this multifarious data follows.

Radars can provide altitude, track, velocity, manoeuvre and rcs data. The origin and projected destination of a target can also be useful information for determining its intentions. These characteristics measured by radar vary with different types of targets, so can be used as target recognition discriminants.

Other data, such as the presence of JEM lines, can contribute to the identification process, even though a full JEM target recognition capability may not be supported by a particular radar.

Electronic surveillance receivers, optical and infrared detection systems can provide very useful data from the target for supporting target recognition.

Electronic surveillance receivers detect radio frequency emissions from targets and can measure the angle of arrival of the signal. The waveform, which could be

a radar, communication or navigation signal, is analysed and recognised by means of comparison with a reference library of known emissions. The emitter can be localised by triangulation and by combining data from two or more receivers and can be tracked by using the single receiver and employing kinematic tracking.

Although optical and infrared sensors are dependent upon good weather conditions, they can provide two-dimensional target images. The infrared sensors can also measure the effective temperature of the target. The features measured by these sensors are compared with a database of target characteristics for recognising the target. Data from IFF signals can clearly also be included.

Bayesian networks can be used in target recognition to combine data from a multitude of sources in order to make a decision on the target's identity. They rely on knowing the probability statistics of the attributes measured by each sensor for each possible target that can be detected. They link together all the statistics for the individual sensors. Mathematically, the Bayesian network provides the best decision from the available sensor data. The outputs of the Bayesian network are the respective probabilities of the detected target being certain types. In practice, there are considerable challenges in determining the statistics that are used.

14.13   Future challenges

The introduction of target recognition functions into operational radars is probably one of the most difficult challenges the radar community is facing today. In addition to the technical requirements placed upon the radar engineers, the sponsoring agencies, procurement authorities and users of the target recognition systems also have challenging tasks. They have to ensure that the recognition functions are correctly specified, implemented in the systems and are operationally effective.

The implementation of these functions into real systems is relatively recent and most nations have little practical experience to date. For most of the stakeholders in target recognition systems there will be a learning curve associated with the new technical concepts, implementation and operational aspects. The key issues for these various participants in radar target recognition systems are summarised below and some approaches are proposed for addressing them.

The issues for the engineers developing the technology are considerably more stressing than for the conventional radar modes. The sensitivity and dynamic range of the radar and the high-resolution waveforms used have to meet the requirements for detecting elements of the target, rather than detecting a complete target, as in conventional modes. These drive component specifications, subsystem and systems designs.

The harmonious integration and scheduling of NCTR modes with the other radar functions have to be addressed. The performance of the basic radar modes should not be significantly affected.

Radar is evolving from its traditional detection and tracking roles to becoming an imaging and identification sensor. Technologies that have previously not

been employed in radar are now required. Pattern recognition and image processing technologies, which are being used in other fields, are being studied, adapted and developed for radar target recognition.

Target signatures have to be measured, modelled and analysed, to enable the attributes used for recognition to be identified. The techniques for reliably extracting these attributes from the target have to be determined. Libraries of target data have to be assembled, ordered, managed and updated as new targets emerge and more target signature data becomes available.

The development of reliable recognition algorithms is clearly critical for developing a high-performance target recognition capability.

The issues for procurement agencies also have to be addressed. The standard radar functions are generally much easier to specify with defined performance limits than a target recognition function. A typical radar is specified to detect a target of a given rcs, at a particular range, with a defined probability and false alarm rate [3]. Trials can usually provide confidence that the specification can be met.

The challenges for the agency procuring a target recognition system are how to specify it and demonstrate its performance. The concept of correctly recognising a target from a given set of known targets, with a particular probability, can be clearly understood. However, for a given system, a decision has to be made on an acceptable level of recognition probability. This will depend upon the type of system, the implications of incorrect recognition, whether the process is automatic or manual, and who takes responsibility for the decision. The types of target to be categorised and the level of recognition required, such as to class, subclass, type or variant, also have to be defined.

The task would involve defining the level of target recognition performance required operationally for the system for the targets of interest. In order to establish whether this requirement could be achieved in practice and whether it would be acceptable to a radar supplier as a contractual commitment, a programme of work, which is normally referred to in the United Kingdom as a Technology Demonstrator Programme, would be needed. This would encompass signature measurement, analysis, modelling and recognition algorithm development, so as to build up the level of technical confidence needed to proceed with the programme.

In order to demonstrate performance, the high-resolution radar system would be expected to measure the signatures of a given set of targets and to recognise them with the specified probability, under a given set of conditions. As it is likely to be only practically feasible to perform measurements over a limited number of conditions, simulation and modelling could provide justification for performance for the other conditions, providing there was sufficient validation of the models used.

As the time to make a decision on a target's identity is also a critical issue, this should also be specified and demonstrated.

The users of radar systems with a target recognition capability should liaise closely with both the procurement authority and the engineers during the development phase to ensure that their operational requirements are addressed. The areas that are of most importance to the user are the method, timing, frequency and priorities for implementing the high-resolution mode, the level of operator control, the

interpretation of the output of the recognition function and associated decisions on any action required.

The procedure for implementing the target recognition mode is dependent upon the timelines of the application, whether the operator makes the decision, whether the radar alerts the operator when it recommends implementation or whether it is a totally automatic process.

The method of presentation of the outputs of the whole target recognition process to the operator has to be decided. It could be in the form of probabilities of the main candidate targets, including supporting information such as key target signature attributes and altitude, velocity and track data. It could also include the target signature or extracted features, if the mission or engagement timelines permit its study by the operator. Reference signatures or attributes from the target library could be displayed to the operator for comparison purposes.

Decisions on future action, such as whether to fire a missile or to guide fighter aircraft to intercept the target or to take no action, are dependent upon the confidence level obtained from the target recognition process and whether there is time for more information to be gathered. There are also issues involving who makes the decision, which would be the operator or a commander and the associated communication for procedures.

Most radar operators would not yet have seen high-resolution images of targets, extracted attributes, libraries of reference signatures or probabilities of targets being particular identities. Training, experience and understanding of the target recognition function and process are essential for its successful application.

However, it is anticipated that with experience, as often happens in radar, the operators would be able to make significant contributions to improve this function. It is expected that with experience they would be able to provide recommendations on the balance between manual and automatic operation, the displaying of information and may even become adept in reliably recognising targets from their signatures.

14.14   Outlook

In some ways the introduction of target recognition modes into radar is a minor revolution. Using radar as a more intelligent sensor, which can use the measured target characteristics to determine its identity, will take time to become fully accepted, particularly for those who are more familiar with the traditional radar functions. As radar designers, procurement agencies and users gain experience with the development and application of radar target recognition techniques, confidence will be built up and the techniques will migrate from being interesting new technology to mainstream radar techniques and designs. Rather than being a novelty they will be accepted as standard requirements and will be demanded by users.

It is hoped that with the introduction of radar target recognition, the tragic friendly-fire incidents and the shooting down of civil aircraft in error can be largely eliminated. It should also be making its contribution in coastal defence, for countering terrorism, illegal immigration and the control of economic exclusion zones. The effective use of

both civil and military resources should also improve as targets become more reliably identified and assets are employed to directly match the threat being posed.

The utilisation of other sensor data to support radar target recognition measurements should provide excellent overall performance and confidence that automatic target recognition can be implemented and relied upon.

References

1　MOORE, G.M.: 'Cramming More Components onto Integrated Circuits' (Electronics, 9 April 1965) www.intel.com/research/silicon/mooreslaw.htm
2　Intel Website: http://www.intel.com/research/silicon/mooreslaw.htm
3　WATTS, S., GRIFFITHS, H.D., HOLLOWAY, J.R., KINGHORN, A.M., MONEY, D.G. *et al*.: 'The Specification and Measurement of Radar Performance'. *Radar* 2002 Conference, Edinburgh, Scotland, 15–17 October 2002, pp. 542, IEE Publication no. 490

Appendices

Appendix 1   'Classical' stepped frequency technique

A1.1   Introduction

In this appendix, the output of the matched filter for the classical stepped frequency technique is derived. This is required to determine the various properties of the wave-form, which affect its applications in target recognition. Initially, in this and the following section, the properties of a basic pulse are presented (Figure A.1). The frequency transform of a pulse on a carrier frequency, f_c, of width, $\Delta\tau$, is:

$$F(f, f_c) = \int_{-\infty}^{\infty} e^{-2\pi i f t} e^{2\pi i f_c t} dt \tag{A.1}$$

where $F(f, f_c)$ is the frequency transform of time domain signal.

 This frequency domain signal is:

$$F(f, f_c) = \left\{ \frac{(\sin(f - f_c)\pi \Delta\tau)}{(f - f_c)\pi} \right\} \tag{A.2}$$

 The power spectrum of a pulse of duration $\Delta\tau$ and frequency f_c is the square of Equation (A.2):

$$\{F(f, f_c)\}^2 = \left\{ \frac{(\sin(f - f_c)\pi \Delta\tau)}{(f - f_c)\pi} \right\}^2 \tag{A.3}$$

which is now defined to be a function $= \{F(f - f_c)\}^2$.
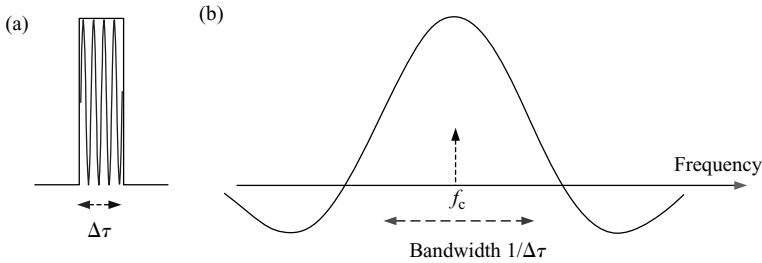
Figure A.1   Time and frequency domain representations of a sinusoidal signal of frequency, f_C, modulated by a pulse of duration Δτ: (a) time and (b) spectrum
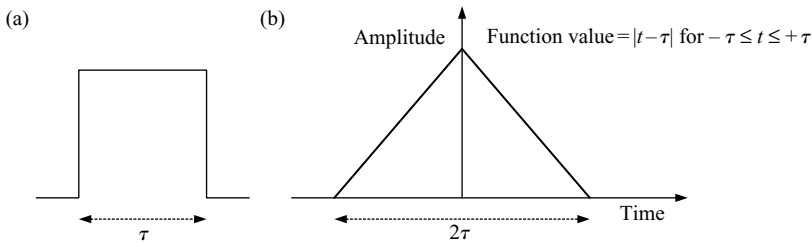
Figure A.2   The auto-correlation function of a pulse of width τ: (a) pulse and (b) auto-correlation function

A1.2   Auto-correlation function of a single pulse

The output of the matched filter is the auto-correlation [1] of the time domain signal:

$$C(t) = \int_{-\infty}^{\infty} F_{sig}(\tau)^* F_{sig}(t + \tau) d\tau \tag{A.4}$$

where $C(t)$ is the waveform's auto-correlation function, $F_{sig}(\tau)^*$ is the complex conjugate of the signal and $F_{sig}(t + \tau)$ is the signal shifted in time by t (Figure A.2).

For a single pulse, with an amplitude of unity, it is the function shown in Equation (A.2). This is also the Fourier transform of Equation (A.3) and has the value $|t - \tau|$ for $-\tau \leq t \leq +\tau$, which is the numerical value of the difference between a reference time and the duration of the pulse. This is discussed in Chapter 2 and is illustrated in Figures 2.65 and 2.66.

A1.3   Synthesing a wideband pulse

The basis of the stepped frequency high-range resolution technique is to synthesise a high-range resolution pulse in increments of low bandwidth signals. Consider

(a) Amplitude   (b)

Frequency

f_1················· f_N

f_C

f_1··············· f_N
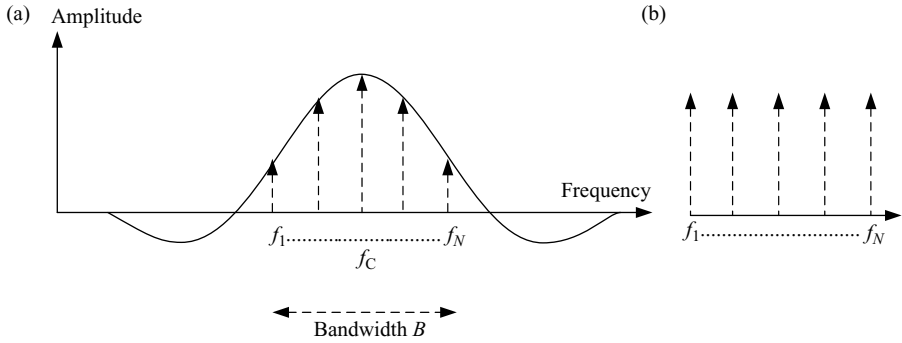
Bandwidth B

Figure A.3   Bandwidth, B, of signal is sampled at N frequencies, spaced at intervals of B/(N − 1): (a) spectrum of a pulse sampled at constant frequency increments; (b) sequence of frequencies actually used have constant amplitudes

providing a set of sampled frequencies to cover the bandwidth of the pulse shown in Figure A.3. The signal to be synthesised is a pulse of duration, τ, with carrier frequency, f_c. The bandwidth, B, of the signal is sampled at N frequencies, spaced at intervals of $B/(N − 1)$. The frequencies are each continuous wave (CW) sinusoids of duration, τ, and are of low bandwidth.

The frequency of the radar steps from f_1 to f_N. Each frequency is sequentially transmitted, with a pulse length $\Delta\tau$, and it is assumed that the amplitudes at each frequency increment are the same. The power spectrum of the waveform sequence shown in Figure A.3(b) is the sum of the power spectra of each contributing frequency, each of which has a power spectrum as defined in Equation (A.3).

Power spectrum of waveform sequence, $P(f, N)$ is:

$$= \sum_{n=1}^{N} \{F(f - f_n)\}^2$$

$$= \sum_{n=1}^{N} \frac{\sin^2(\pi \Delta\tau (f - f_1 - (Bn/(N - 1))))}{(\pi(f - f_1 - (Bn/(N - 1))))^2} \tag{A.5}$$

The power spectrum is shown in Figure A.4 for positive values of frequency increment.

This power spectrum can also be expressed as a convolution:

$$P(f, N) = \frac{\sin^2(\pi f \Delta\tau)}{(\pi f)^2} * \sum_{n=1}^{N} \delta\left(f - f_1 - \left(\frac{Bn}{N - 1}\right)\right) \tag{A.6}$$

where the left-hand term is the power spectrum of a single pulse and the right-hand term is a series of N *delta* functions representing the periodicity of the waveform in the frequency domain.
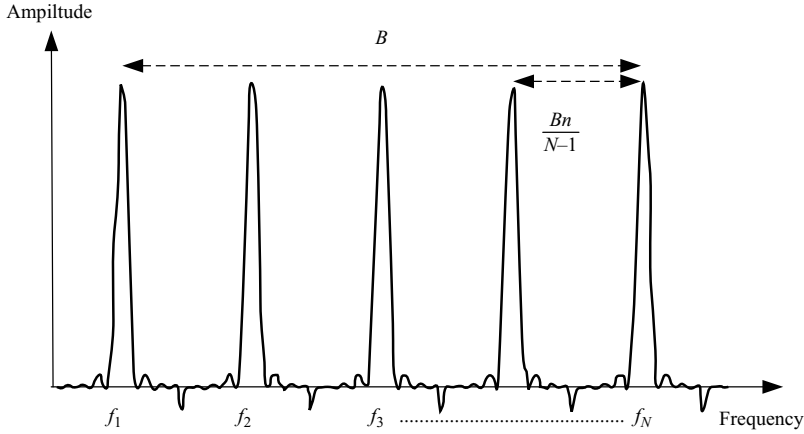
Figure A.4   Power spectrum P(f, N) *of stepped frequency waveform sequence (Equation (A.5))*

A1.4   Auto-correlation function of stepped frequency pulse sequence

In order to establish the effects of this stepped frequency waveform on a target, the output of the matched filter, which is the auto-correlation function of the input signal, has to be calculated. The characteristics of the matched filter output signal will now be determined for a stationary target. If the target is moving range-Doppler coupling effects occur, but the fundamental conclusions are the same.

From the Wiener–Khinchine Theorem [2] the auto-correlation function of a signal is the Fourier Transform of its power spectrum, as shown in Equation (A.3) above for a single frequency component. For a stationary target, the output of the matched filter for the whole sequence of N frequency steps is the Fourier transform of the sum of the individual frequency components, which is expressed in Equation (A.6).

The convolution theorem [3] states that 'The Fourier transform of the product of two variables is equal to the convolution of the Fourier transform of one of the variables with the Fourier transform of the other'. The Fourier transform of Equation (A.6) is required, and by applying the convolution theorem, becomes the product of the Fourier transforms of the two terms of Equation (A.6).

Defining the Fourier transform of P(f, N) as $C(f, N)$, which is the waveform's auto-correlation function, then

$$C(f, N) = \left[\int_{-\infty}^{\infty} \frac{\sin^2(\pi f \Delta \tau)}{(\pi f)^2} e^{-2\pi i f t} dt \right]$$

$$\times \left[\int_{-\infty}^{\infty} \sum_{n=1}^{N} \delta \left(f - f_1 - \left(\frac{Bn}{N-1} \right) \right) e^{-2\pi i f t} dt \right] \tag{A.7}$$

(a)

(b)

(c)

Delta functions in (a)=rectangular function in (b) multiplied by delta functions in (c)
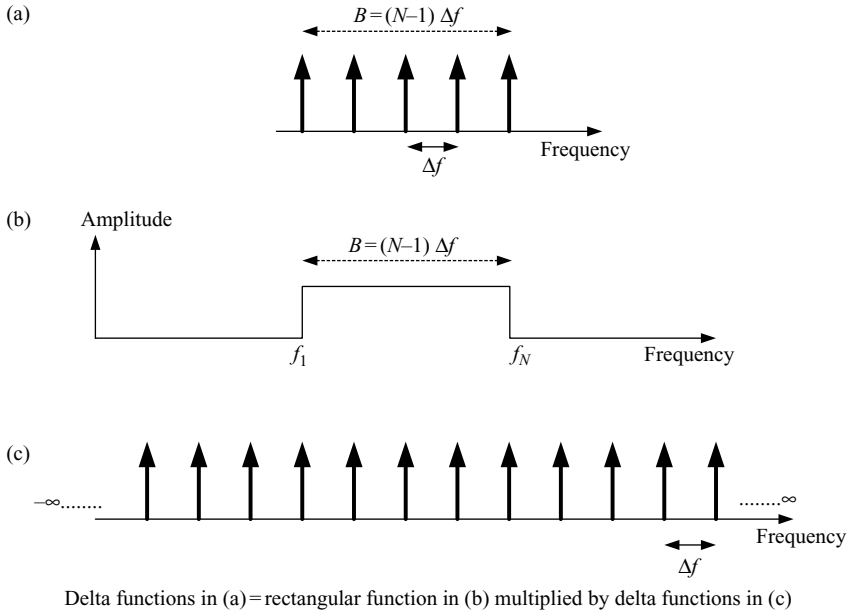
Figure A.5   *Representation of finite set of delta functions by an infinite set multi-plied by a rectangular function: (a) N delta functions of spacing Δf; (b) rectangular function of width $B = (N-1)\Delta f$; (c) infinite set of delta functions spaced at Δf*

The left-hand term in Equation (A.7) is the Fourier transform of the left-hand term in Equation (A.6) and is the auto-correlation of a single pulse. This is shown in Equation (A.2) and Figure A.2.

The right-hand side of Equation (A.7) is the Fourier transform of the right-hand term of Equation (A.6) and is the Fourier transform of N delta functions, spaced at the frequency stepping interval, $B/(N-1)$, which is defined as Δf. This Fourier transform is now to be evaluated.

This function can also be expressed as an infinite set of delta functions of separation, Δf, multiplied by a rectangular function of width $(N-1)\Delta f$. This is shown in Figure A.5.

Using the convolution theorem, the frequency transform of the product of these two variables is the convolution of the frequency transform of the delta functions with the transform of the rectangular function.

The transform of an infinite set of delta functions, of frequency spacing Δf, is an infinite series of delta functions of spacing $1/\Delta f$ as shown in Figure A.6.

The δ functions in Figure A.6 are expressed as:

$$D_\infty(t) = \sum_{n=-\infty}^{\infty} \delta\left(t - \frac{n}{\Delta f}\right) \tag{A.8}$$
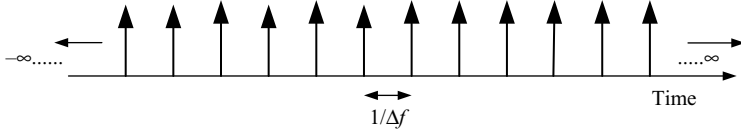
*Figure A.6   Fourier transform of infinite set of delta functions of frequency spacing,
Δf, is an infinite set of delta functions of spacing 1/Δf in time*
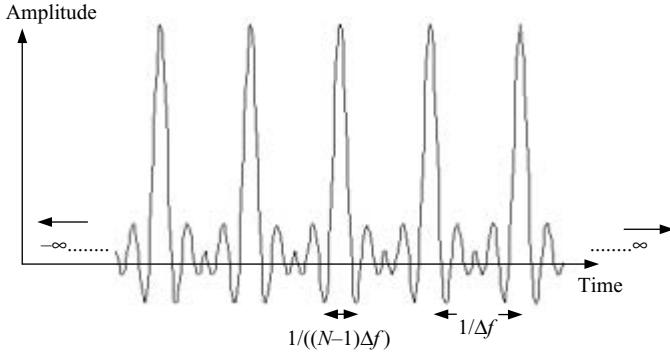
Figure A.7   Fourier transform of a set of N delta functions separated by Δf

The Fourier transform of the rectangular function of width $(N-1)\Delta f$ is:

$$f(t) = \frac{\sin\{(N-1)\pi\,\Delta ft\}}{\pi t} \tag{A.9}$$

The right-hand term in Equation (A.7) is therefore the convolution of the functions appearing in Equations (A.8) and (A.9), as follows:

$$D_\infty(t) * f(t) = \sum_{n=-\infty}^{\infty} \frac{\sin\{(t-(n/\Delta f))((N-1)\pi\,\Delta f)\}}{(t-(n/\Delta f))(\pi)} \tag{A.10}$$

The function defined in Equation (A.10) is shown in Figure A.7. The time domain function shown is a series of 'sin x/x' components extending to infinity, each of bandwidth $1/((N-1)\Delta f)$.

The Fourier transform of the power spectrum of the stepped waveform is then the product of the two terms of Equation (A.7), which are:

- The auto-correlation function of a single pulse shown in Figure A.2 and Equation (A.3)
- The function shown in Equation (A.10) and Figure A.7.
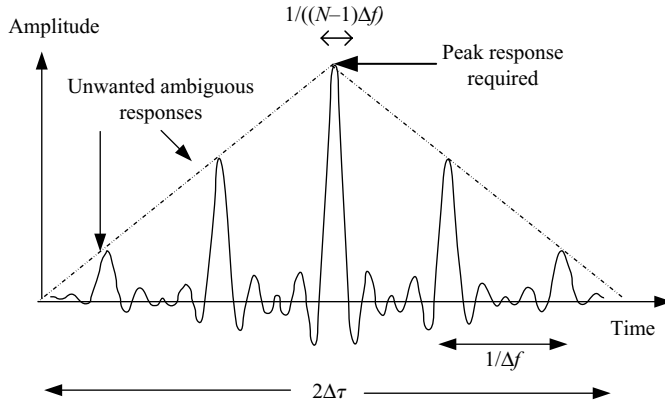
Figure A.8   Output of matched filter for unweighted stepped frequency waveform sequence is product of functions in Figures A.2(b) and A.7

Hence, auto-correlation function of stepped frequency waveform is:

$$= |t - \tau| \sum_{n=-\infty}^{\infty} \frac{\sin\{(t - (n/\Delta f))(N - 1)\pi \Delta f\}}{(t - (n/\Delta f))(\pi)}$$

$$\text{for} -\tau \le t \le +\tau \tag{A.11}$$

This is the triangular function of width, 2τ of Figure A.2 multiplied by the function in Figure A.7 and is shown in Figure A.8. This is the auto-correlation function of the whole stepped frequency waveform sequence of the N pulses at the output of the matched filter.

If a weighting function is applied across the rectangular pulse in Figure A.2, the effect is to sharpen each of the matched filter peaks, which have the $\sin x/x$ form of Equation (A.10) and Figure A.7. The resulting modified matched filter output is shown in Figure A.9. This function describes the processed signal obtained using the stepped frequency waveform and is used in Chapter 3, Section 3.5, to explain the design constraints associated with its applications.

Weighting or window functions, as they are sometimes known, reduce sidelobes arising from the Fourier transform process [4]. A weighting function, such as a raised cosine function, changes the Fourier transform of the rectangular function from the $\sin x/x$ function of Equation (A.11) to reduce the sidelobes between the main peaks of Figure A.8. This is illustrated in Figure A.10, in which an unweighted rectangular function is transformed into a $\sin x/x$ function and is compared to the weighted function.

This in turn has the effect of reducing the sidelobes in Figure A.10. It is important to minimise these sidelobes as they have the effect of distorting the range profile of the target.
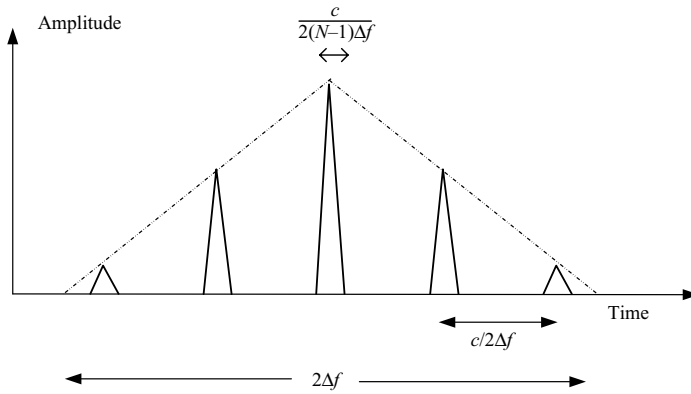
Figure A.9   Output of matched filter for stepped frequency waveform using weighting function
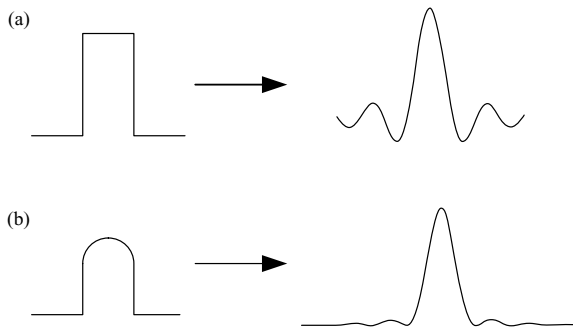
Figure A.10   Weighting function reduces time sidelobes: (a) rectangular pulse transforms to $\sin x/x$ *function and (b) weighted pulse transforms with reduced sidelobes*

Appendix 2   Derivation of JEM spectrum

A2.1   Introduction

Within this section the general spectrum for a rotating engine is derived. Initially, the spectral components associated with the harmonics of the engine's rotation rate are covered, followed by the contributions due to the blades of the first stage of the compressor. It is assumed that the engine is on a single shaft.

A2.2   Engine rotational rate harmonics

Over a single cycle of the engine, the radar measures the reflected signal providing unique amplitude and phase characteristics, which are dependent upon the engine
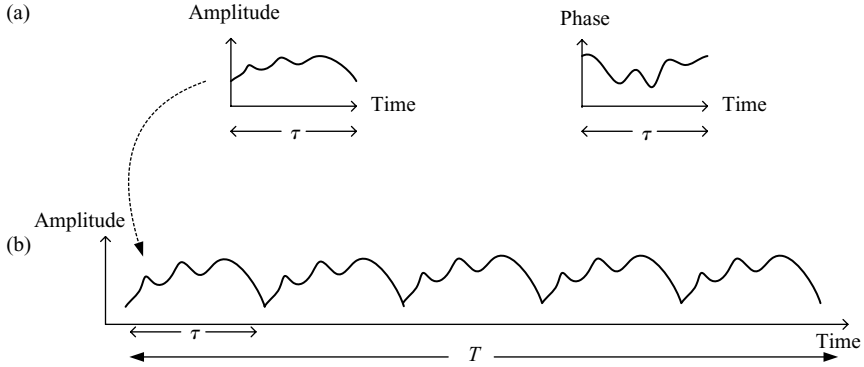
Figure A.11   Amplitude and phase characteristics of jet engine over single rotation period and over radar integration period: (a) representation of amplitude and phase of jet engine over single rotation cycle and (b) time domain signal over N_R cycles of engine comprising radar integration period, T: amplitude shown

design, the radar frequency and parameters and the aspect angle. It is assumed that the mechanical characteristics of the engine are repeated exactly from cycle to cycle of the engine. It is also assumed that the signal detected over one engine cycle is repeated over the integration period, for analysis purposes. This concept is shown in Figure A.11.

The amplitude and phase characteristics detected by the radar over a single engine rotational period are shown in Figure A.11(a) and over the integration period for N_R cycles, the amplitude is shown in Figure A.11(b). In order to establish the JEM spectrum, the complex radar signal in the time domain must be transformed into the frequency domain and the associated mathematics will now be established. The time domain signal repeats every rotational period, τ, and can be represented as a convolution of two functions.

Let the complex signal detected over a single engine rotation cycle, τ, be designated as $a(t)$. For N_R cycles of the engine the detected time domain signal is:

$$a(t) * D_{NR}(t) = \int a(t')D_{NR}(t - t')dt' \tag{A.12}$$

where the sum of N_R delta functions

$$D_{NR}(t) = \sum_{n=1}^{N_R} \delta(n\tau) \tag{A.13}$$

The convolution Equation (A.12) states that the signal from N_R cycles of a rotating engine is the convolution of N_R delta functions, separated by τ, as shown in Figure A.12.

The convolution theorem is now applied to Equation (A.12) to determine the JEM spectrum. The convolution of the Fourier transform of $a(t)$ with the Fourier transform

Time domain returns from N_R engine cycles, as shown in Figure A.11(b), are convolution of returns from single engine period with N_R delta functions separated by rotation period
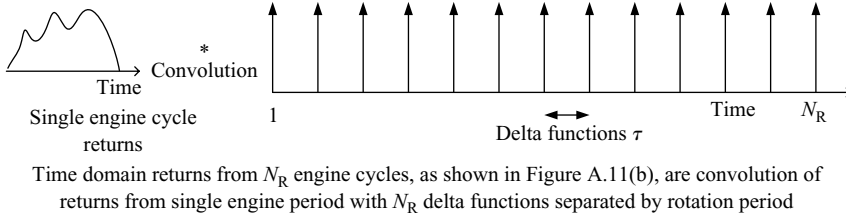
Figure A.12   *Time domain returns over radar integration period are convolution of two functions*
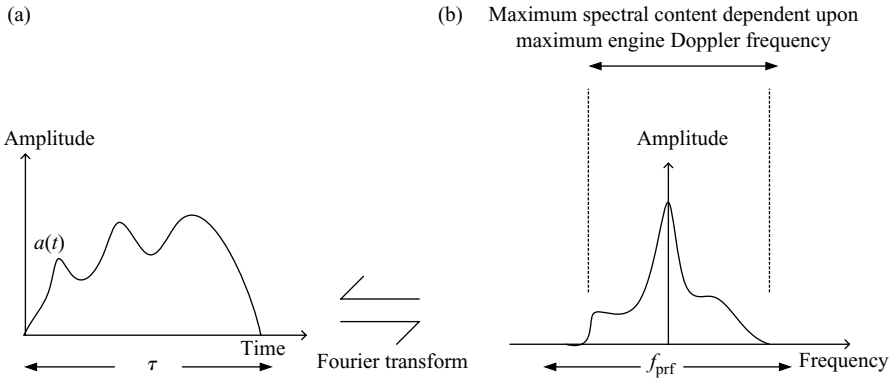
Figure A.13   *Spectrum generated from one engine rotation cycle: (a) time domain signal from one engine rotation and (b) frequency domain signal from one engine rotation*

of $D_{NR}(t)$ is the Fourier transform of the product of the Fourier transform of $a(t)$ with the Fourier transform of $D_{NR}(t)$.

Hence, the JEM spectrum is the product of the Fourier transform of $a(t)$ with the Fourier transform of $D_{NR}(t)$, which is:

$$\text{JEM spectrum} = \int_{-\infty}^{\infty} a(t)e^{-2\pi ift}dt \int_{-\infty}^{\infty} D_{NR}(t)e^{-2\pi ift}dt \tag{A.14}$$

The function, $\int_{-\infty}^{\infty} a(t)e^{-2\pi ift}dt$ is the Fourier transform of the time domain signal over one single rotation period. This is a continuous function and its spectral content is dependent upon the actual frequency components associated with a particular engine and the radar parameters. Its maximum frequency component is actually the maximum Doppler frequency of the engine by virtue of its maximum motion with respect to the radar. However, it is not necessary to know the actual detail of this function, as it acts as an envelope for the second integral of Equation (A.14). The function $\int_{-\infty}^{\infty} a(t)e^{-2\pi ift}dt$ is shown in Figure A.13 with its Fourier transform.
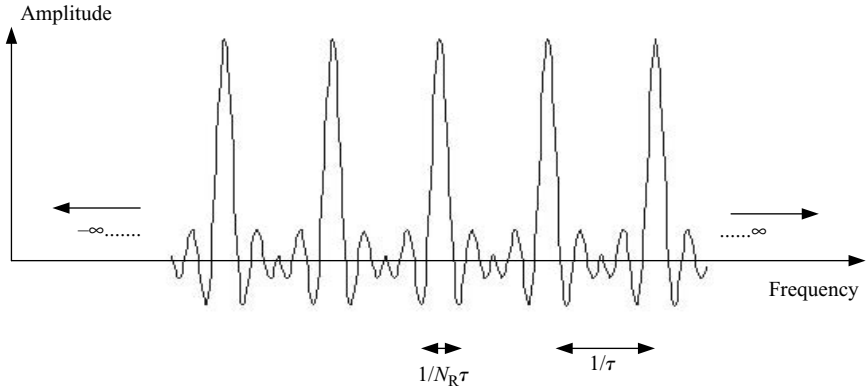
Figure A.14   Spectral components generated from periodicity of engine spool rate

The function $\int_{-\infty}^{\infty} D_{NR}(t)e^{-2\pi ift}dt$ is the Fourier transform of the delta function in Figure A.12 and Equation (A.14). It represents the periodicity at the engine's spool rate. This transform was covered in Section A1.4 earlier and is shown in Equation (A.10) and has been used to develop Equation (A.15). It is shown in Figure A.14.

$$\int_{-\infty}^{\infty} D_{NR}(t)e^{-2\pi ift}dt = \sum_{n=-\infty}^{\infty} \frac{\sin\{(f-(n/\tau))(N_R\pi\tau)\}}{(f-(n/\tau))(\pi)} \tag{A.15}$$

This spectrum consists of an infinite series of '$\sin x/x$' functions, each having a width equivalent to the inverse of the integration time. The peaks are separated at intervals of the inverse of the engine rotation period.

The resultant JEM spectrum is obtained by using Equation (A.14) and multiplying the two contributions, which are shown in Figures A.13 and A.14, to obtain the result shown in Figure A.15. Only the amplitude components are shown. Using Equations (A.14) and (A.15) the JEM spectrum is:

$$= \int_{-\infty}^{\infty} a(t)e^{-2\pi ift}dt \sum_{n=-\infty}^{\infty} \frac{\sin\{(f-(n/\tau))(N_R\pi\tau)\}}{(f-(n/\tau))(\pi)} \tag{A.16}$$

All of the lines are at harmonics of the engine rotational rate (or spool rate) and result from the engine having repeated characteristics every cycle. The envelope is the Fourier transform of the signal received from a single engine rotation. The maximum positive and negative JEM frequencies correspond to the highest respective closing and receding Doppler frequencies of the engine relative to the radar. The width of each spectral line is the inverse of the radar integration period, T.
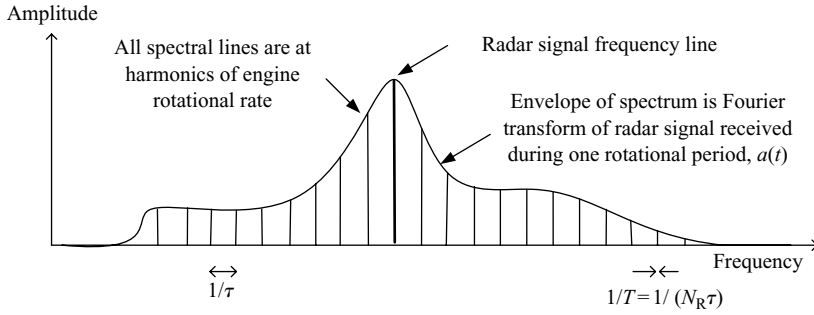
Figure A.15   JEM spectrum for N_R cycles of engine of period τ

A2.3   Spectral lines due to first-stage blades

The mathematical approach employed in the previous section, to develop a model of the components of the JEM spectrum due to the effects associated with complete cycles of the whole engine, is identical to that required for determining the contributions of the first blade stage.

The model developed above considered the repetitive nature of the time domain signal, which had a frequency of the engine rotation rate. For the first blade stage, assuming all the blades are identical, the repetition period is the engine rotational rate divided by the number of blades, as shown in Figure A.16(b).

Let the complex signal detected over the period, τ/N, in which a single blade moves to the next corresponding blade position be $b(t)$.

For N_R cycles of the engine detected time domain signal is:

$$b(t)^* D_{NNR}(t) = \int b(t') D_{NNR}(t - t') dt' \tag{A.17}$$

where the sum of NN_R delta functions

$$D_{NNR}(t) = \sum_{n=1}^{NN_R} \delta \left(\frac{n\tau}{N} \right) \tag{A.18}$$

The JEM spectrum due to the first blade stage is the Fourier transform of Equation (A.17) and following the same mathematical procedure as in Section A2.2 is:

$$= \int_{-\infty}^{\infty} b(t) e^{-2\pi i f t} dt \sum_{n=-\infty}^{\infty} \frac{\sin\{(f - (nN/\tau))(N_R \pi \tau)\}}{(f - (nN/\tau))(\pi)} \tag{A.19}$$

This spectrum is shown in Figure A.17. The left-hand term of Equation (A.19) is the Fourier transform of the time domain signal occurring in the period in which one blade moves to the next corresponding position and forms the envelope of the spectrum. The right-hand term is a series of 'sin x/x' characteristics, each of which is centred at harmonics of the rotational rate of the engine multiplied by the number of blades, N,

(a)

N rotor blades on spool
Rotation rate is R Hz
Rotation period, τ

Position A

1/N of one
rotation cycle

Position B

Rotation

Radar

(b) Amplitude

τ/N

Time

τ/N is time for blade to go from position A to position B
Precise amplitude and phase characteristics are not known. However, due to
symmetry of engine, amplitude and phase characteristics repeat every τ/N
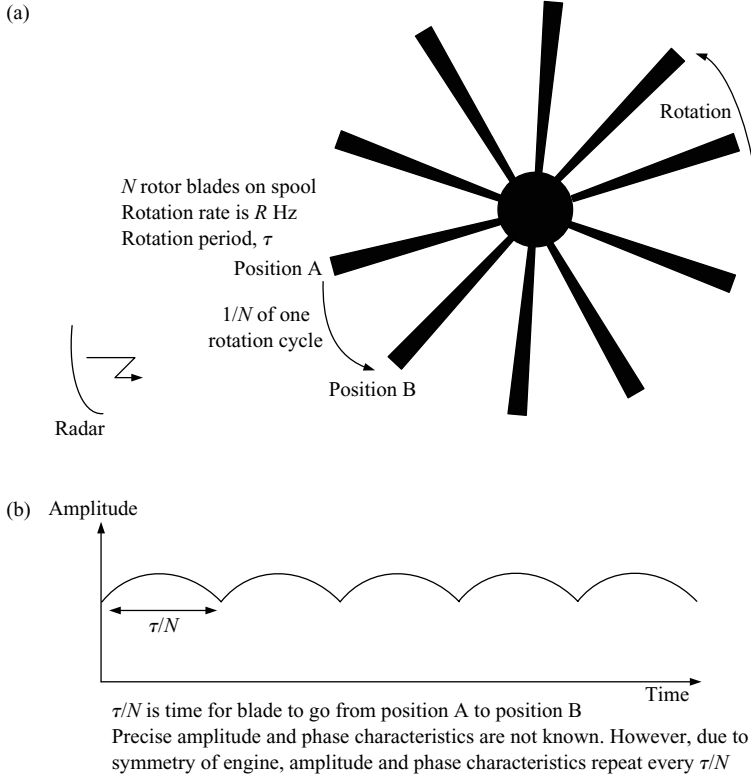
*Figure A.16   Time domain characteristics due to first-stage blades: (a) single
rotor blade stage at front of engine and (b) amplitude and phase
characteristics repeat at fundamental frequency of N/τ*

on the rotor stage, which is called the blade chopping frequency. The width of each
spectral line is the inverse of the radar integration period.

Appendix 3   Bayes' theorem

A3.1   Introduction

Bayes' theorem [5] is concerned with updating the hypothesis associated with an
event when new evidence becomes available. It states:

> The probability of a hypothesis A_k conditional on a given body of data L is
> the ratio of the unconditional probability of the conjunction of the hypothesis
> with the data to the unconditional probability of the data alone.

This means that the probability of an event A_k occurring as a result of an event L
having occurred, $P(A_k|L)$, is the probability of event L occurring given that event A_k

Envelope of spectrum is Fourier transform of radar signal received during 1/*N* of rotational period, *b*(*t*)

Radar signal frequency

All spectral lines are at harmonics of engine rotational rate multiplied by the number of blades: *N*/τ

Amplitude

Spacing between lines is *N*/τ

Frequency

$f-2N/\tau \quad f-N/\tau \quad f \quad f+N/\tau \quad f+2N/\tau \quad \longrightarrow \longleftarrow$

$1/T = 1(N_R\tau)$

JEM spectrum is frequency transform of time domain characteristics measured by radar: most of the modulation energy is in the blade chopping rate sidebands at frequency offset of *N*/τ from transmission frequency, *F*

Figure A.17   JEM spectral lines due to single stage with N blades

has occurred, $P(L|A_k)$, multiplied by the probability of event A_k occurring, $P(A_k)$, divided by the probability of event L occurring, $P(L)$:

$$P(A_k|L) = \frac{P(L|A_k)P(A_k)}{P(L)} \tag{A.20}$$

From probability theory, the probability of event L occurring resulting from separate events A_1 to A_N occurring is:

$$P(L) = P(A_1)P(L|A_1) + P(A_2)P(L|A_2) + P(A_3)P(L|A_3) + \cdots$$
$$+ P(A_N)P(L|A_N) \tag{A.21}$$

Equation (A.21) then becomes:

$$P(A_k|L) = \{P(L|A_k)P(A_k)\}\{P(A_1)P(L|A_1) + P(A_2)P(L|A_2)$$
$$+ P(A_3)P(L|A_3) + \cdots + P(A_N)P(L|A_N)\}^{-1} \tag{A.22}$$

This is called Bayes' Formula.

From the viewpoint of radar target recognition, it is used to estimate the identity of a particular target from a set of possible targets from measurements of features. An example is provided here to demonstrate how this theorem is used.

A3.1.1   Example

For illustrative purposes of Bayes' theorem, as applied to radar target recognition, assume there are only two types of targets, type A and type B, which can be detected by the radar. The *a priori* probability of detecting either type of target depends upon the number of targets of each type, which are potentially available to be detected and on the relative detection sensitivity of the radar for the two targets. For a given set of conditions, if a target detection is made, assume that the *a priori* probabilities of detecting the type A and type B targets are $P(\text{Type} = A)$ and $P(\text{Type} = B)$,

respectively. These probabilities which represent the *unconditional probability of the data alone*, $P(A_k)$ as stated in Bayes' Theorem and shown in Equation (A.20). As this scenario is a 'closed world' of two types of targets, a detected target must be one of the two types, then $P(\text{Type} = \text{A}) + P(\text{Type} = \text{B}) = 1$.

Although false alarms are neglected here, as they over-complicate this simple example, Bayesian techniques can also include them.

Hence, in the absence of any other knowledge, if a single target is detected, these probabilities provide the best estimate of the target's identity. However, assume a target attribute, such as the length of the target, is measured and that for both targets the probability density function for length is known. These are defined as $P(\text{Length}|\text{Type} = \text{A})$ and $P(\text{Length}|\text{Type} = \text{B})$, respectively, and are distributions as shown in Figure 12.15 and are equivalent to $P(L|A_k)$ in Bayes' theorem. These distributions mean that if the target identity is known, the length, which is equivalent to the body of data, L, in Bayes' theorem, has this probability distribution.

This new information on target length is used in the Bayesian method to work back to the probabilities of the two types of targets having this length. In order to calculate the respective probabilities of the target being type A, $P(\text{Type} = \text{A}|\text{Length})$, or type B, $P(\text{Type} = \text{B}|\text{Length})$ from the measurement of the length of the target, applying Bayes' Formula:

$$P(\text{Type} = \text{A}|\text{Length}) = \{P(\text{Length}|\text{Type} = \text{A})P(\text{Type} = \text{A})\}$$
$$\times \{P(\text{Length}|\text{Type} = \text{A})P(\text{Type} = \text{A})$$
$$+ P(\text{Length}|\text{Type} = \text{B})P(\text{Type} = \text{B})\}^{-1} \qquad \text{(A.23)}$$

A similar equation states the probability for target B and $P(\text{Type} = \text{A}|\text{Length})$ is the *a posterior* probability of the target being type A, following the measurement, which is required. Hence, from knowledge of the probabilities of detection of the two types of targets and the probability distributions for a measured feature, this information is used to determine the probability of the target's identity. The *a priori* probability of the target being type A, $P(\text{Type} = \text{A})$, has been updated by the measurement to give the *a posterior* probability, $P(\text{Type} = \text{A}|\text{Length})$ and similarly for target B.

A3.1.2 Conclusions

Bayesian techniques use all the available statistical information and provide the mathematically best estimate of hypotheses from the evidence. This is only a simple example of the use of Bayesian techniques. Large numbers of targets and features can be accommodated by the natural extension of the techniques discussed here.

References

1   KINGSLEY, S., and QUEGAN, S.: 'Understanding Radar Systems' (McGraw-Hill Book Company, Maidenhead, UK, 1992) Chapters 4.7-4.8

2   Wolfram Research
     website: http:/mathworld.wolfram.com/Wiener-KhinchinTheorem.htl
3   Wolfram Research
     website: http:/mathworld.wolfram.com/ ConvolutionTheorem.htl
4   PRABHU, K.M.M.: 'Generalised Families of Windows Used in Signal Processing', *Journal of the Institution of Electronic and Radio Engineers*, 1987, **57**, pp. 174–7
5   BAYES, T.: 'An Essay Toward Solving a Problem in the Doctrine of Chances', *Physical Transactions of the Royal Society of London*, 1794, **53**, pp. 370–415

Index

Introduction to Radar Target Recognition

This new text provides an overview of the radar target recognition process and covers the key techniques being developed for operational systems. It is based on the fundamental scientific principles of high resolution radar, and explains how the underlying techniques can be used in real systems, taking into account the characteristics of practical radar system designs and component limitations. It also addresses operational aspects, such as how high resolution modes would fit in with other functions such as detection and tracking.

Peter Tait is currently Head of High Resolution Radar and Non Co-operative Target Recognition at BAE Systems Integrated System Technologies. He joined the Marconi Research Laboratories in 1974 after graduating in Physics from Imperial College, London University with first class honours. He initially worked in the field of radar and communications receiver research. From 1986 he led the core target recognition research programme in GEC-Marconi and the group developing the technology for high resolution modes for company radars including Captor for the Typhoon fighter aircraft. He then spent two years on the Captor programme as Technical Adviser to the Euroradar Board of Directors and in 1997 became Chief Engineer of Sensors Division. In 2000 he joined the predecessor company to BAE Systems in his current post to develop target recognition technology for naval and land-based surveillance, tracking and phased array radars. He is a member of NATO air and ground target recognition working groups and is a reviewer for IEE journals. He has been granted several UK and worldwide patents, has presented papers at several international conferences and is known internationally for his expertise in target recognition. In 2001 he won the BAE Systems Chairman's Silver Innovation Award for inventing techniques for detecting plastic land mines. In 2004 he was presented by the United Kingdom Government Minister for Technology and Innovation with a world class company innovation award for his work in target recognition technology.